BIOGEOCHEMISTRY AND GENOMICS OF SILICIFICATION AND SILICIFIERS

EDITED BY: Marion Gehlen, Stephen Baines, Brivaëla Moriceau and Paul Tréguer
PUBLISHED IN: Frontiers in Marine Science and Frontiers in Earth Science

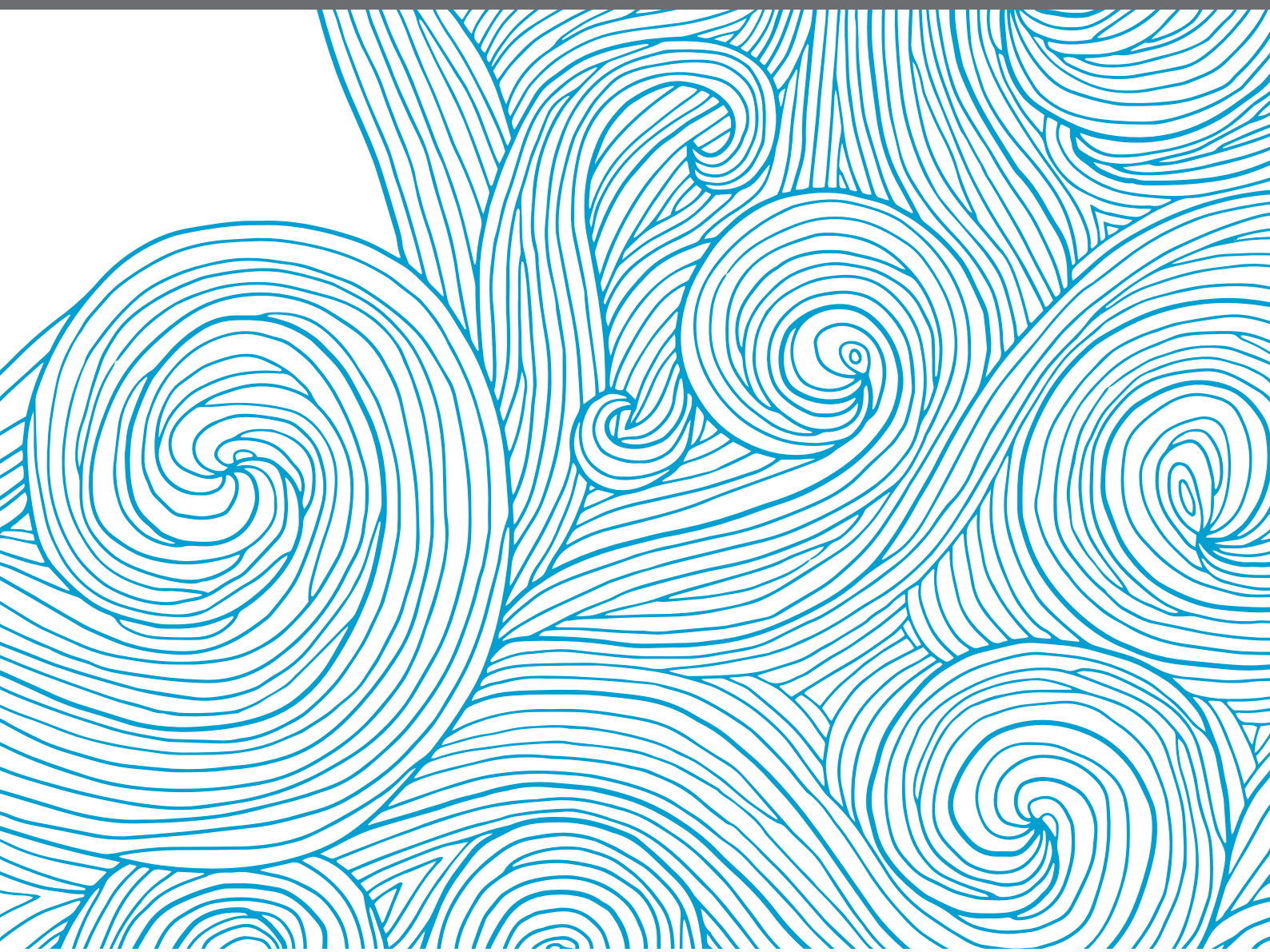

frontiers Research Topics

frontiers

Frontiers Copyright Statement

© Copyright 2007-2019 Frontiers Media SA. All rights reserved.

All content included on this site, such as text, graphics, logos, button icons, images, video/audio clips, downloads, data compilations and software, is the property of or is licensed to Frontiers Media SA ("Frontiers") or its licensees and/or subcontractors. The copyright in the text of individual articles is the property of their respective authors, subject to a license granted to Frontiers.

The compilation of articles constituting this e-book, wherever published, as well as the compilation of all other content on this site, is the exclusive property of Frontiers. For the conditions for downloading and copying of e-books from Frontiers' website, please see the Terms for Website Use. If purchasing Frontiers e-books from other websites or sources, the conditions of the website concerned apply.

Images and graphics not forming part of user-contributed materials may not be downloaded or copied without permission.

Individual articles may be downloaded and reproduced in accordance with the principles of the CC-BY licence subject to any copyright or other notices. They may not be re-sold as an e-book.

As author or other contributor you grant a CC-BY licence to others to reproduce your articles, including any graphics and third-party materials supplied by you, in accordance with the Conditions for Website Use and subject to any copyright notices which you include in connection with your articles and materials.

All copyright, and all rights therein, are protected by national and international copyright laws.

The above represents a summary only. For the full conditions see the Conditions for Authors and the Conditions for Website Use.

ISSN 1664-8714
ISBN 978-2-88963-085-1
DOI 10.3389/978-2-88963-085-1

About Frontiers

Frontiers is more than just an open-access publisher of scholarly articles: it is a pioneering approach to the world of academia, radically improving the way scholarly research is managed. The grand vision of Frontiers is a world where all people have an equal opportunity to seek, share and generate knowledge. Frontiers provides immediate and permanent online open access to all its publications, but this alone is not enough to realize our grand goals.

Frontiers Journal Series

The Frontiers Journal Series is a multi-tier and interdisciplinary set of open-access, online journals, promising a paradigm shift from the current review, selection and dissemination processes in academic publishing. All Frontiers journals are driven by researchers for researchers; therefore, they constitute a service to the scholarly community. At the same time, the Frontiers Journal Series operates on a revolutionary invention, the tiered publishing system, initially addressing specific communities of scholars, and gradually climbing up to broader public understanding, thus serving the interests of the lay society, too.

Dedication to Quality

Each Frontiers article is a landmark of the highest quality, thanks to genuinely collaborative interactions between authors and review editors, who include some of the world's best academicians. Research must be certified by peers before entering a stream of knowledge that may eventually reach the public - and shape society; therefore, Frontiers only applies the most rigorous and unbiased reviews.
Frontiers revolutionizes research publishing by freely delivering the most outstanding research, evaluated with no bias from both the academic and social point of view. By applying the most advanced information technologies, Frontiers is catapulting scholarly publishing into a new generation.

What are Frontiers Research Topics?

Frontiers Research Topics are very popular trademarks of the Frontiers Journals Series: they are collections of at least ten articles, all centered on a particular subject. With their unique mix of varied contributions from Original Research to Review Articles, Frontiers Research Topics unify the most influential researchers, the latest key findings and historical advances in a hot research area! Find out more on how to host your own Frontiers Research Topic or contribute to one as an author by contacting the Frontiers Editorial Office: researchtopics@frontiersin.org

BIOGEOCHEMISTRY AND GENOMICS OF SILICIFICATION AND SILICIFIERS

Topic Editors:
Marion Gehlen, Laboratoire des Sciences du Climat et de l'Environnement
Stephen Baines, Stony Brook University, United States
Brivaëla Moriceau, Université de Bretagne Occidentale (UBO), France
Paul Tréguer, Université de Bretagne Occidentale (UBO), France

Citation: Gehlen, M., Baines, S., Moriceau, B., Tréguer, P., eds. (2019). Biogeochemistry and Genomics of Silicification and Silicifiers. Lausanne: Frontiers Media. doi: 10.3389/978-2-88963-085-1

Table of Contents

frontiers in Marine Science

EDITORIAL
published: 19 March 2019
doi: 10.3389/fmars.2019.00057

Editorial: Biogeochemistry and Genomics of Silicification and Silicifiers

Brivaëla Moriceau[1], Marion Gehlen[1], Paul Tréguer[1], Stephen Baines[2], Jacques Livage[3] and Luc André[4]*

[1] CNRS, IRD, Ifremer, LEMAR, Univ. Brest, Plouzane, France, [2] Department of Ecology and Evolution, Stony Brook University, Stony Brook, NY, United States, [3] Chimie de la Matière Condensée, CNRS-UMR 7574, UPMC, Paris, France, [4] Royal Museum for Central Africa, Tervuren, Belgium

Keywords: silicon cycle, biogenic silica, diatom, isotope, Bolidophycae, sponge (Porifera), nanostructured silica, anthropogenic pressure

Editorial on the Research Topic

Biogeochemistry and Genomics of Silicification and Silicifiers

Silicon (Si) is continuously created in the universe by the thermonuclear fusion of oxygen atoms, mainly in massive stars (Woosley et al., 1973). Although silicon and carbon have similar electron configurations, life on Earth is based on carbon and not on silicon. The high stability of Si-O bound under the oxidizing conditions of the Earth's atmosphere and seas means that solid mineral SiO_2 is the end product of most chemical reactions involving Si. The discovery of the oldest putative evidence for life in SiO_2-rich chert deposits, stimulated a debate about the role of silica (SiO_2) in the emergence of life (e.g., Derenne et al., 2008). Nowadays, silica is present in most lineages of living organisms, often conferring some defensive advantage (Hodson et al., 2005; Exley, 2015). The main biologically available form of Si is also the most common species of dissolved Si (DSi), silicic acid ($Si(OH)_4$). Silicic acid was present at very high concentrations in natural waters during Earth's early history, which promoted the formation of mineral silica that was then deposited on to the seafloor. Some organisms eventually evolved the ability to biosynthesize organized silica skeletons through a condensation reaction between a silanol group of silicic acids and the hydroxyl group of silaffins, silacidins, and silicateins which act as scaffolds (e.g., Kröger et al., 1999). In the marine realm, 240 Tmol of silica are produced each year (Tréguer et al., 1995) as compared to 84 Tmol of Si in the terrestrial realm (Conley and Carey, 2015). Si is required for the growth of diatoms and some sponges. It is also utilized by radiolarians, silicoflagellates, several species of choanoflagellates, and can accumulate in some picocyanobacteria (Baines et al., 2012).

Over the past 550 years, different silicifiers in the marine realm have successively dominated (Conley et al. this issue). Most recently, diatoms have dominated the Si cycle owing to their great abundance, fast growth rate and high affinity for silicic acid. Over this period, they have stripped the ocean of silicic acid, bringing concentrations down to an average of 73 μM in the deep sea and <10 μM in surface waters, as indicated by the tendency for their frustules to become less silicified over geological time (i.e., lower Si/C, Si/N ratios) (Tréguer et al., 1995). Despite the reduced levels of available Si, diatoms are responsible for about 1/4th of the primary production of planet Earth and half of the carbon flux to the deep ocean via the "biological pump" (review in Tréguer et al., 2018). Since 2004, the genomes of several diatom species have been deciphered. Differences to those of terrestrial plants reflect the complex evolution/adaptation of diatoms

OPEN ACCESS

Edited and reviewed by:
Eric 'Pieter Achterberg, GEOMAR Helmholtz Center for Ocean Research Kiel, Germany

****Correspondence:***
Brivaëla Moriceau
moriceau@univ-brest.fr

Specialty section:
This article was submitted to Marine Biogeochemistry, a section of the journal Frontiers in Marine Science

Received: *30 November 2018*
Accepted: *01 February 2019*
Published: *19 March 2019*

Citation:
Moriceau B, Gehlen M, Tréguer P, Baines S, Livage J and André L (2019) Editorial: Biogeochemistry and Genomics of Silicification and Silicifiers. Front. Mar. Sci. 6:57. doi: 10.3389/fmars.2019.00057

in response to the drastic variations of the ocean composition since the early Jurassic period (Armbrust et al., 2004). Development of genomic tools in the last few years, may strongly augment traditional biogeochemistry and biological approaches, and enhance our understanding of the Si cycle, silicification processes and the role of silicifiers in ecosystems.

For this reason, the first SILICAMICS conference was held near Brest (France) in September 2015. This conference, endorsed by European institutions, included researchers from multiple disciplines (including chemistry, biogeochemistry, biochemistry, physiology, genomics) and reviewed extant knowledge on silicification and silicifiers, underlining the importance of working across disciplines, as well as considering all silicifiers and their respective roles in the ecosystem and the Si cycle. The following questions were addressed:

1-What processes drive the variations of silicic acid and of its isotopes in the oceans through geologic time and in the present time?

Conley et al. combine genomic and geological data to suggest that biological processes have influenced oceanic silicic acid concentrations (DSi) ever since oxygenic photosynthesis first evolved. They show that a spectacular decrease in DSi in the global ocean was initiated first by bacterial Si related metabolism, followed by the evolution of different eukaryotic lineages capable of converting DSi into mineralized structures. Sutton et al. discuss the geochemical tools that are available for studying the Si cycle and highlight our present understanding of the marine, freshwater and terrestrial systems. They discuss challenges associated with the development of environmental proxies for the global Si cycle, and how each system within the global Si cycle might change over time. Meyerink et al. show how iron availability influences silicon isotope fractionation in two typical Southern diatoms. They describe how variations in the Si isotope enrichment factor can be explained by the adaptations of diatoms to the nutrient status of their environments.

2-What explains the success of silicifiers in the living world?

Hendry et al. examine fossils, sediments, and isotopic geochemistry to show the emergence and expansion of silica biomineralization in the ocean through geological time. Taking metagenomics data into account, they also discuss the competition between silicifiers and non-silicifiers as it has influenced evolutionary trajectories in the past, and how it affects the biogeochemical cycles of Si, C, and other nutrients in the present day. Among silicifiers, diatoms are one of the most efficient competitors, which allows them to build their silica frustules in only a few hours under unfavorable temperature and silicic acid conditions. Because the properties of biogenic silica have important technological applications, this unique capacity of diatoms has been scrutinized by the scientific community over the past 20 years. Hildebrand et al. recall that over this period, approaches used to characterize the molecular components involved in cell wall silicification have evolved, revealing that the diatom cell wall formation is highly dynamic. Mcheik et al. describe optical properties of nanostructured silica structures from marine organisms, and highlight interesting optical properties, such as light waveguiding, diffraction, focusing, and photoluminescence.

3-Which organisms play a major role in the control of the silicon cycle?

Kuwata et al. summarize the current information on taxonomy, phylogeny, ecology, and physiology obtained by recent studies using a range of approaches including metabarcoding of Bolidophycae, a sister picoplanktonic group of diatoms that contain species with cells surrounded by silica plates. Toullec and Moriceau show for the first time that transparent exopolymer particles (TEP) selectively increase biogenic silica dissolution from fossil diatoms compared to fresh diatoms. In line with results by Akagi (2013) they suggest that diatom excretion of TEP may accelerate the dissolution of refractory silica and provide an alternative source of DSi when limitations arise. Alvarez et al. extracted data from over 320,000 records of Porifera from the Global Biodiversity Information Facility (GBIF) to describe the overall distribution of sponge orders and families along DSi gradients and depth. They conclude that the use of sponge taxa assemblages as a proxy for DSi concentration or depth must be treated with caution as these animals are adapted to a great range of DSi conditions, as well as other unspecified variables that are also related to depth.

4-Silicifiers in a changing world

Diatoms are important drivers of the biological carbon pump, but their efficiency may be modulated by interactions with other organisms. In the mesocosm study described in Moriceau et al. an increase of copepod abundance boosts phytoplankton production through trophic cascade, but reduces the sinking flux of particulate organic carbon when diatoms dominate the phytoplankton community. Ragueneau et al.'s article, using a long-term research effort devoted to study the Si cycle of the bay of Brest, illustrates how human activity may impact and be affected by the competition between silicifiers and non-silicifying phytoplankton. They describe how the succession between diatom and toxic algal bloom may be controlled by invasive benthic organisms and diversity. Building on the strength of an interdisciplinary approach linking natural and social sciences, they propose a method for the improved use of the ecosystem while ensuring its sustainability.

AUTHOR CONTRIBUTIONS

BM and PT wrote the manuscript. MG, SB, JL, and LA corrected the manuscript.

ACKNOWLEDGMENTS

This research topic results from a collaborative effort initiated during the first international conference SILICAMICS, held in the Aber Wrac'h near Brest (France). This conference, that had the ambitious objective to better understand silicification processes and the role of silicifiers in the marine ecosystems, has been supported by Labex-Mer, EuroMarine, the University of Western Brittany, and Local Authorities from the région Bretagne.

REFERENCES

Akagi, T. (2013). Rare earth element (REE)–silicic acid complexes in seawater to explain the incorporation of REEs in opal and the "leftover" REEs in surface water: new interpretation of dissolved REE distribution profiles. *Geochim. Cosmochim. Acta* 113, 174–192. doi: 10.1016/j.gca.2013.03.014

Armbrust, E. V., Berges, J. A., Bowler, C., Green, B. R., Martinez, D., Putnam, N. H., et al. (2004). The genome of the diatom *Thalassiosira pseudonana*: ecology, evolution, and metabolism. *Science* 306, 79–86. doi: 10.1126/science.1101156

Baines, S. B., Twining, B. S., Brzezinski, M. A., Krause, J. W., Vogt, S., Assael, D., et al. (2012). Significant silicon accumulation by marine picocyanobacteria. *Nat. Geosci.* 5, 886–891. doi: 10.1038/ngeo1641

Conley, D. J., and Carey, J. C. (2015). Biogeochemistry: Silica cycling over geologic time. *Nat. Geosci.* 8, 431. doi: 10.1038/ngeo2454

Derenne, S., Robert, F., Skrzypczak-Bonduelle, A., Gourier, D., Binet, L., and Rouzaud, J.-N. (2008). Molecular evidence for life in the 3.5 billion year old Warrawoona chert. *Earth Planet. Sci. Lett.* 272, 476–480. doi: 10.1016/j.epsl.2008.05.014

Exley, C. (2015). A possible mechanism of biological silicification in plants. *Front. Plant Sci.* 6:853. doi: 10.3389/fpls.2015.00853

Hodson, M. J., White, P. J., Mead, A., and Broadley, M. R. (2005). Phylogenetic variation in the silicon composition of plants. *Ann. Bot.* 96, 1027–1046. doi: 10.1093/aob/mci255

Kröger, N., Deutzmann, R., and Sumper, M. (1999). Polycationic peptides from diatom biosilica that direct silica nanosphere formation. *Science* 286, 1129–1132.

Tréguer, P., Bowler, C., Moriceau, B., Dutkiewicz, S., Gehlen, M., Aumont, O., et al. (2018). Influence of diatom diversity on the ocean biological carbon pump. *Nat. Geosci.* 11, 27–37. doi: 10.1038/s41561-017-0028-x

Tréguer, P., Nelson, D. M., Bennekom, A. J. V., Demaster, D. J., Leynaert, A., and Quéguiner, B. (1995). The silica Balance in the World Ocean: a Reestimate. *Science* 268, 375–379.

Woosley, S. E., Arnett, W. D., and Clayton, D. D. (1973). The explosive burning of oxygen and silicon. *Astrophys. J. Suppl.* 26:231. doi: 10.1086/190282

Conflict of Interest Statement: The authors declare that the research was conducted in the absence of any commercial or financial relationships that could be construed as a potential conflict of interest.

Copyright © 2019 Moriceau, Gehlen, Tréguer, Baines, Livage and André. This is an open-access article distributed under the terms of the Creative Commons Attribution License (CC BY). The use, distribution or reproduction in other forums is permitted, provided the original author(s) and the copyright owner(s) are credited and that the original publication in this journal is cited, in accordance with accepted academic practice. No use, distribution or reproduction is permitted which does not comply with these terms.

frontiers in Marine Science

REVIEW
published: 29 October 2018
doi: 10.3389/fmars.2018.00370

Bolidophyceae, a Sister Picoplanktonic Group of Diatoms – A Review

Akira Kuwata[1], Kazumasa Yamada[2], Mutsuo Ichinomiya[2], Shinya Yoshikawa[3], Margot Tragin[4], Daniel Vaulot[4] and Adriana Lopes dos Santos[4,5,6]*

[1] Tohoku National Fisheries Research Institute, Japan Fisheries Research and Education Agency, Shiogama, Japan, [2] Faculty of Environmental & Symbiotic Sciences, Prefectural University of Kumamoto, Kumamoto, Japan, [3] Faculty of Marine Bioscience, Fukui Prefectural University, Obama, Japan, [4] UMR7144, Station Biologique de Roscoff, CNRS – Sorbonne Université, Roscoff, France, [5] GEMA Center for Genomics, Ecology and Environment, Universidad Mayor, Huechuraba, Chile, [6] Asian School of the Environment, Nanyang Technological University, Singapore, Singapore

OPEN ACCESS

Edited by:
Brivaela Moriceau, UMR6539 Laboratoire des Sciences de L'environnement Marin (LEMAR), France

Reviewed by:
Jun Sun, Tianjin University of Science and Technology, China
Yantao Liang, Qingdao Institute of Bioenergy and Bioprocess Technology (CAS), China

***Correspondence:**
Akira Kuwata
akuwata@affrc.go.jp

Specialty section:
This article was submitted to Marine Biogeochemistry, a section of the journal Frontiers in Marine Science

Received: *05 December 2017*
Accepted: *25 September 2018*
Published: *29 October 2018*

Citation:
Kuwata A, Yamada K, Ichinomiya M, Yoshikawa S, Tragin M, Vaulot D and Lopes dos Santos A (2018) Bolidophyceae, a Sister Picoplanktonic Group of Diatoms – A Review. Front. Mar. Sci. 5:370. doi: 10.3389/fmars.2018.00370

Pico- and nano-phytoplankton (respectively, 0.2–2 and 2–20 μm in cell size) play a key role in many marine ecosystems. In this size range, Bolidophyceae is a group of eukaryotes that contains species with cells surrounded by 5 or 8 silica plates (Parmales) as well as naked flagellated species (formerly Bolidomonadales). Bolidophyceae share a common ancestor with diatoms, one of the most successful groups of phytoplankton. This review summarizes the current information on taxonomy, phylogeny, ecology, and physiology obtained by recent studies using a range of approaches including metabarcoding. Despite their rather small contribution to the phytoplankton communities (on average less than 0.1%), Bolidophyceae are very widespread throughout marine systems from the tropics to the pole. This review concludes by discussing similarities and differences between Bolidophyceae and diatoms.

Keywords: bolidophyceae, parmales, diatoms, genetic diversity, mitosis, geographical distribution, seasonal dynamics and silicification

INTRODUCTION

Following the appearance of oxygenic photosynthesis in the ancestors of cyanobacteria, this complex process was distributed across all eukaryotic lineages via permanent primary, secondary, and tertiary endosymbioses (Not et al., 2012). Ocean photosynthesis is dominated by phytoplankton, a functional group of single cell organisms including prokaryotes and eukaryotes. In the late 70's, early 80's the work of Waterbury et al. (1979) and Johnson and Sieburth (1982) revealed the importance of very small cells, some below one micron in size, for primary productivity, which importance was formalized with the concept of the microbial loop by Azam et al. (1983). However, it was only in the mid 90′s, when researchers began to investigate the eukaryotic compartment of picophytoplankton, and realized that while cyanobacteria are

very little diversified, at the least at the genus level with a couple of taxa (*Prochlorococcus*, *Synechococcus*) dominating, eukaryotes turned out to be very diverse with picoplankton taxa distributed widely across several branches of eukaryotic tree of life (Vaulot et al., 2008).

Microphytoplankton such as diatoms, dinoflagellates or coccolithophorids that produce short lived blooms such as *Emiliania huxleyi*, have been extensively investigated, in contrast to other members of the picoplanktonic community. A large number of photosynthetic picoeukaryotes species (and clades) described to date belong to Stramenopiles (also called Heterokonts), which are characterized by flagellated cells, produced at least at some point of their life cycles, with two unequal flagella (heterokont), one being ornamented with hair-like structures called mastigonemes. Their plastids are thought to have been acquired through secondary endosymbiosis and typically contain chlorophylls *a* and *c*. Stramenopiles besides include diatoms, a very successful lineage which cells are encased in ornamented silica structures, Dictyochophyceae, also called silicoflagellates, and Pelagophyceae, well known because of the toxic algal blooms of the brown tide species *Aureococcus anophagefferens* and *Aureoumbra lagunensis* (Gobler and Sunda, 2012) or *Pelagomonas calceolata*, frequently isolated from sea water. Although often seen as less diverse, some of these groups play important ecological roles in marine ecosystems are fundamental for our understanding of the evolution of algae.

Bolidophyceae, a class created by Guillou et al. (1999a) is the Stramenopiles group phylogenetically nearest to the diatoms. They are often detected in molecular surveys, although in low abundance. We now know that they can occur as two distinct forms, either silicified pico-sized (2–5 μm) or non-silicified flagellated (1–1.7 μm) cells (Guillou et al., 1999a; Ichinomiya et al., 2011, 2016) and cultures from both forms have been isolated from the marine environment. This review summarizes the discovery of Bolidophyceae and current information of phylogeny, ecology, and physiology obtained by recent studies using a range of approaches. We discuss similarities and differences between Bolidophyceae and diatoms to explore the evolutionary link between these silicified algal groups.

DISCOVERY AND TAXONOMY

Well before the creation of the class Bolidophyceae, their silicified forms (**Figure 1**) were first reported from scanning electron microscopy (SEM) images in oceanic samples from the North Pacific (Iwai and Nishida, 1976). Initially, they were thought to be resting cysts of silicified loricate choanoflagellates (Silver et al., 1980). However, the observation of red auto fluorescence indicating the presence of chlorophyll and the existence of a chloroplast in sectioned cells observed by transmission electron microscopy revealed that they were active phytoplankton cells

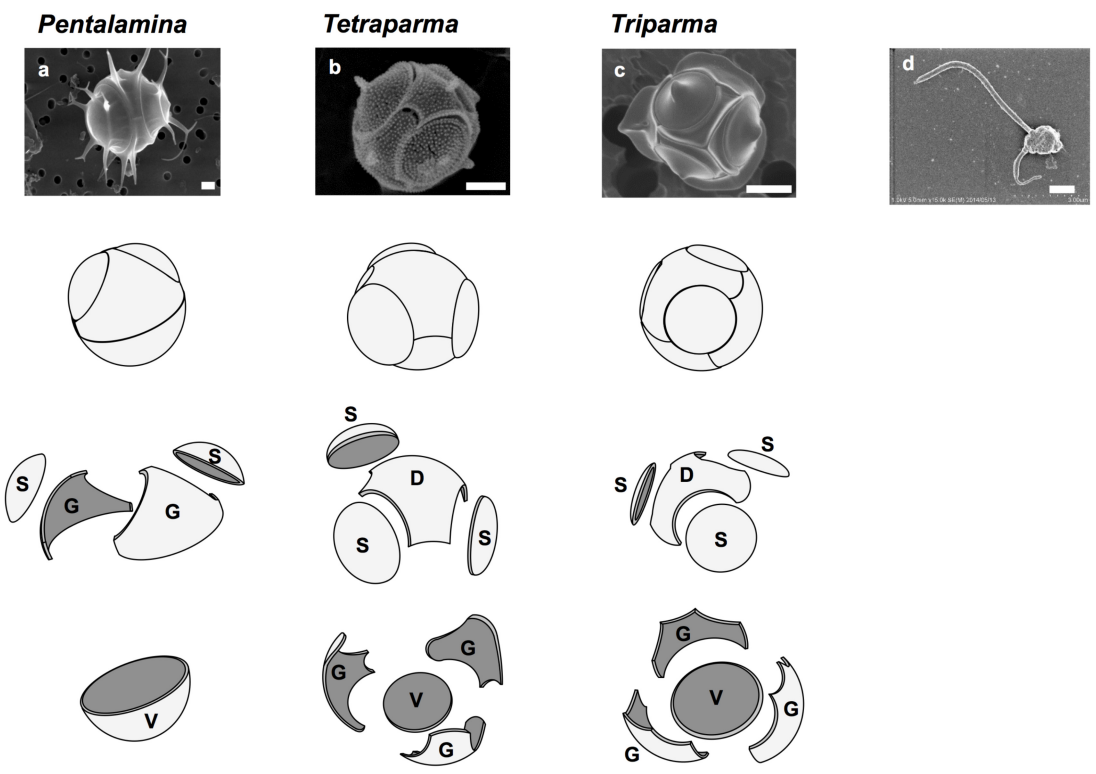

FIGURE 1 | Silicified and flagellated species of Bolidophyceae. **(a)** *Pentalamina corona*, **(b)** *Tetraparma pelagica*, **(c)** *Triparma laevis* f. *inornata*, and **(d)** *Triparma eleuthera*. Scale bars = 1 μm. Diagrams of silica plates in the three genera of silicified species (Parmales); D, dorsal plate; G, girdle plate; S, shield plate; and V, ventral plate. Redrawn from Booth and Marchant (1987) with permission.

(Marchant and McEldowney, 1986). Marchant and McEldowney (1986) could not establish their taxonomic position, although they suggested some morphological similarities with other algae groups such as Bacillariophyceae and Chrysophyceae.

Booth and Marchant (1987) tentatively established Parmales (Latin: small round shields) as a new order within Chrysophyceae. The taxonomy of Parmales was based on the morphological features of silica plates that can only be observed with SEM. Two families and three genera were established: Pentalaminaceae with one genus *Pentalamina* (Latin: five plates) and Triparmaceae with two genera, *Tetraparma* (Latin: four small round shields) and *Triparma* (Latin: three small round shields) (**Figures 1a–c**). *Pentalamina* has 2 circular shield plates of equal size, a larger ventral plate and 2 triradiate girdle plates. *Tetraparma* has 3 shield plates of equal size, a smaller ventral plate, a triradiate dorsal plate and 3 girdle plates. *Triparma* has 3 shield plates of equal size, a larger ventral plate, a triradiate dorsal plate and 3 girdle plates (Booth and Marchant, 1987, 1988; Kosman et al., 1993; Bravo-Sierra and Hernández-Becerril, 2003; Konno and Jordan, 2007; Konno et al., 2007).

The flagellated forms of Bolidophyceae (**Figure 1d**) were originally isolated from the Pacific Ocean and Mediterranean Sea, and described as two flagellated species, *Bolidomonas pacifica* and *B. mediterranea*, differing in the angle of the insertion of the two flagellum, swimming patterns as well as in 18S rRNA gene signatures (Guillou et al., 1999a). The name "*Bolidomonas*" refers to the rapid swimming behavior of the cells remembering a racing car. A variety, *B. pacifica* var. *eleuthera*, was later proposed based on both cultures and environmental sequences (Guillou et al., 1999b). Analyses of photosynthetic pigments as well as nuclear 18S rRNA and plastid RubisCO large subunit (*rbcL*) sequences (Guillou et al., 1999a; Daugbjerg and Guillou, 2001) demonstrated the sister relationship between *Bolidomonas* and diatoms, although *Bolidomonas* are flagellates and lack the siliceous frustule characteristic of diatoms. Bolidophyceae were thus proposed to be an intermediate group between diatoms and all other Stramenopiles (Guillou et al., 1999a).

For more than 24 years, Parmales escaped isolation. These silicified cells are small and difficult to distinguish them from other small phytoplankton in field samples under the light microscope. To overcome this problem, Ichinomiya et al. (2011) used the fluorescence dye PDMPO (2-(4-pyridyl)-5-((4-(2-dimethylaminoethylaminocarbamoyl) methoxy)phenyl) oxazole) (Shimizu et al., 2001), which is co-deposited with silicon into the solid silica matrix of the newly produced cell walls and fluoresces under UV excitation whenever silicic acid is polymerized forming biogenic silica. Using PDMPO staining and a serial dilution technique, the first Parmales strain was established from Oyashio region of the western North Pacific (Ichinomiya et al., 2011).

Scanning electron microscopy established that this strain belonged to the species *Triparma laevis* and transmission electron microscope observations showed the typical ultrastructure of photosynthetic Stramenopiles, with two endoplasmic reticulate membranes surrounding the chloroplast, a girdle and two to three thylakoid lamellae as well as a mitochondrion with tubular cristae. Phylogenetic analyses based on 18S ribosomal rRNA sequences from the new strain demonstrated that *T. laevis* was closely related to Bolidophyceae (Ichinomiya et al., 2011), rather than part of Chrysophyceae as hypothesized initially (Booth and Marchant, 1987). Phylogenetic analyses using plastidial and mitochondrial encoded genes from *T. laevis* also confirmed its sistership with Bolidophyceae and diatoms (Tajima et al., 2016).

Recent phylogenetic analyses using nuclear, plastidial, and mitochondrial genes from several novel strains, including a flagellate form very closely related to the silicified strains, led to a taxonomic revision (**Table 1**) in which the order Parmales was included within the class Bolidophyceae and *Bolidomonas* species were transferred to the genus *Triparma* (Ichinomiya et al., 2016).

GENETIC DIVERSITY

Clade Diversity

The analysis of full-length nuclear 18S rRNA gene sequences from public databases revealed the existence of two environmental clades (Env. clade I and II) in addition to the group corresponding to the genus *Triparma* (Ichinomiya et al., 2016). These clades are only formed by environmental sequences and no sequences from cultures or isolates are available. Within the *Triparma* group, sub-clades formed by sequences from strains and the environment corresponded to the species *Triparma eleuthera*, *Triparma pacifica,* and *Triparma mediterranea*. The "*T. laevis*" sub-clade, including the species *T. laevis* f. *inornata*, *T. laevis* f. *longispina*, *Triparma strigata*, *Triparma* aff. *verrucosa* and the flagellated strain *Triparma* sp. RCC1657. Other molecular markers (plastid 16S rRNA and rbcL, nuclear ITS rRNA and mitochondrial *nad1*) revealed the presence of two distinct sub-clades within the "*T. laevis*" sub-clade, hereafter called for convenience *Triparma* clade I with the two forms of *T. laevis* (f. *inornata*, and *longispina*) and *Triparma* clade II with *T. strigata*, *T.* aff. *verrucosa* and the flagellated strain RCC1657.

In order to review the current state of the diversity of Bolidophyceae, we analyzed existing GenBank sequences as well as metabarcodes obtained from a range of recent studies (**Table 2**) focusing on the V4 region of the 18S rRNA gene (see **Supplementary Material** for Methodology). The phylogenetic analysis of the newly obtained V4 sequences (**Figure 2**) recovered the two major environmental clades previously described (Env. clade I and II, Ichinomiya et al., 2016), but also revealed the existence of a third environmental clade (called Env. clade III) within which two sub-clades IIIA and IIIB can be clearly separated. Each environmental clade contained sequences from clone libraries (GenBank) as well as identical or nearly identical metabarcode sequences from different surveys suggesting that these environmental clades are not artefactual. These environmental clades may, for some of them, correspond to species of Parmales (e.g., from genera *Tetraparma*

TABLE 1 | Current taxonomy of Bolidophyceae.

class, order, family, genus, species, subspecies, forma (= synonym, basyonym)	Reference
Class Bolidophyceae Guillou et Chrétiennot-Dinet emend. Ichinomiya et Lopes dos Santos	Guillou et al., 1999a ; Ichinomiya et al., 2016
Order Parmales Booth et Marchant emend. Konno et Jordan emend. Ichinomiya et Lopes dos Santos	Booth and Marchant, 1987; Konno and Jordan, 2007; Ichinomiya et al., 2016
Family Pentalaminaceae Marchant emend. Konno et Jordan	Booth and Marchant, 1987; Konno and Jordan, 2007
Genus *Pentalamina* Marchant	Booth and Marchant, 1987
Pentalamina corona Marchant	Booth and Marchant, 1987
Family Triparmaceae Booth et Marchant emend. Konno et Jordan emend. Ichinomiya et Lopes dos Santos (= "Octolaminaceae" Booth et Marchant)	Booth and Marchant, 1987; Booth and Marchant, 1988; Konno and Jordan, 2007; Ichinomiya et al., 2016
Genus *Tetraparma* Booth emend. Konno et Jordan	Booth and Marchant, 1987; Konno and Jordan, 2007
Tetraparma catinifera Konno et al.	Konno et al., 2007
Tetraparma gracilis Konno et al.	Konno et al., 2007
Tetraparma insecta Bravo-Sierra et Hernández-Becerril emend. Fujita et Jordan	Bravo-Sierra and Hernández-Becerril, 2003; Fujita and Jordan, 2017
Tetraparma pelagica Booth et Marchant	Booth and Marchant, 1987
Tetraparma silverae Fujita et Jordan	Fujita and Jordan, 2017
Tetraparma trullifera Fujita et Jordan	Fujita and Jordan, 2017
Genus *Triparma* Booth et Marchant emend. Konno et Jordan emend. Ichinomiya et Lopes dos Santos (= *Bolidomonas* Guillou et Chrétiennot-Dinet)	Booth and Marchant, 1987; Guillou et al., 1999a ; Konno and Jordan, 2007; Ichinomiya et al., 2016
Triparma columacea Booth	Booth and Marchant, 1987
Triparma columacea f. *convexa* Konno et al.	Konno et al., 2007
Triparma columacea f. *fimbriata* Konno et al.	Konno et al., 2007
Triparma columacea f. *longiseta* Fujita et Jordan	Fujita and Jordan, 2017
Triparma columacea subsp. *alata* Marchant	
Triparma eleuthera Ichinomiya et Lopes dos Santos (= "*Bolidomonas pacifica* var. *eleuthera*")	Ichinomiya et al., 2016
Triparma laevis Booth	Booth and Marchant, 1987
Triparma laevis f. *fusiformins* Fujita et Jordan	Fujita and Jordan, 2017
Triparma. laevis f. *inornata* Konno et al.	Konno et al., 2007
Triparma laevis f. *longispina* Konno et al.	Konno et al., 2007
Triparma laevis f. *mexicana* (Kosman) Bravo-Sierra et Hernández-Becerril (=*Triparma laevis* subsp. *mexicana* Kosman)	Kosman et al., 1993; Bravo-Sierra and Hernández-Becerril, 2003
Triparma laevis subsp. *pinnatilobata* Marchant	Booth and Marchant, 1987
Triparma laevis subsp. *ramispina* Marchant	Booth and Marchant, 1987
Triparma mediterranea (Guillou et Chrétiennot-Dinet) Ichinomiya et Lopes dos Santos (= *Bolidomonas mediterranea* Guillou et Chrétiennot-Dinet)	Guillou et al., 1999a ; Ichinomiya et al., 2016
Triparma pacifica (Guillou et Chrétiennot-Dinet) Ichinomiya et Lopes dos Santos (= *Bolidomonas pacifica* Guillou et Chrétiennot-Dinet)	Guillou et al., 1999a ; Ichinomiya et al., 2016
Triparma retinervis Booth	Booth and Marchant, 1987
Triparma retinervis f. *tortispina* Fujita et Jordan	Fujita and Jordan, 2017
Triparma retinervis subsp. *crenata* Booth	Booth and Marchant, 1987
Triparma strigata Booth	Booth and Marchant, 1987
Triparma verrucosa Booth	Booth and Marchant, 1987

Adapted from Ichinomiya and Kuwata (2017) with permission.

or *Pentalamina*) that have not yet been isolated in cultures.

Diversity Within the Genus *Triparma*

We explored the level of inter- and intra-clade diversity within the genus *Triparma* by analyzing the folding pattern of the ITS2 (see **Supplementary Material** for Methodology) from 14 strains previously described in Ichinomiya et al. (2016). The general ITS2 secondary structure of Bolidophyceae proposed contains the four-helices domains known in many eukaryotic taxa in addition to helix B9 (**Figure 3**). We located in Helices II and III the universal hallmarks proposed by Mai and Coleman (1997) and Müller et al. (2007): the pyrimidine–pyrimidine (Y–Y) mismatch in helix II and YRRY (pyrimidine – purine – pyrimidine) motif on the 5′ side of Helix III, respectively, at alignment positions 95 and 148 and between nucleotides 205 and 208 (**Figures 3**, **4**). In all strains analyzed, the Y–Y mismatch was represented by the pair U x C, with the exception of *T. pacifica* strains (U x U), and the YRRY motif of helix III by the sequence UGGU (**Figure 3**).

TABLE 2 | List of metabarcoding studies using the V4 region of the 18S rRNA genes that have been used for the phylogenetic (**Figure 2**) and the biogeography analyses (**Figures 6**, **7**).

Data set	Region	Samples #	Bioproject	Sequencer	Clustering	Reference
OSD – LGC – 2014	Ocean	157	PRJEB8682	Illumina	0.97	Kopf et al., 2015
MALINA – Monier 2014	Arctic Ocean	24	PRJNA202104	454	0.98	Monier et al., 2013, 2014
ACME – Comeau – 2011	Arctic Ocean	11	SRA029114	454	0.98	Comeau et al., 2011
Nansen Basin – Metfies – 2016	Arctic Ocean	17	PRJEB11449	454	0.97	Metfies et al., 2016
Southern Ocean – Wolf – 2014	Southern Ocean	6	PRJNA176875	454	0.97	Wolf et al., 2014
Fieldes Bay – Luo – 2016	Southern Ocean	10	PRJNA254097	Illumina	0.97	Luo et al., 2015
Fram Strait – Kilias – 2013	Arctic Ocean	5	454	454	0.97	Kilias et al., 2013

*See **Supplementary Material** for details.*

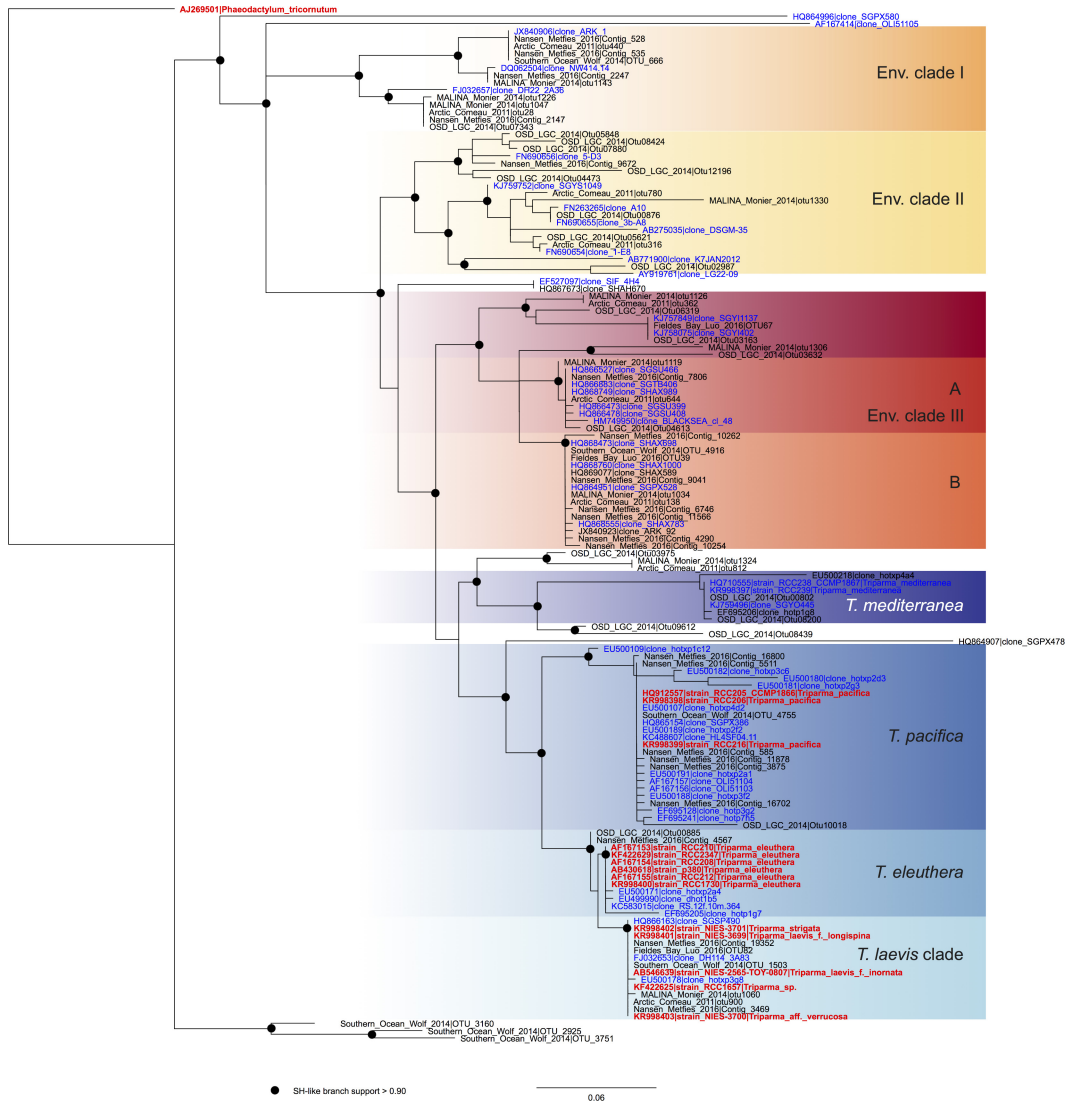

FIGURE 2 | ML phylogenetic tree based on the V4 region of the 18S rRNA gene based both on GenBank sequences available from the PR^2 database (Guillou et al., 2013) and on metabarcodes OTUs obtained from the studies listed in **Table 2** (see Methodology in **Supplementary Material**). The tree was constructed with phyML and dots correspond to nodes with SH-like branch support >0.90. GenBank sequences from environmental samples are colored in blue and those from cultures, in red.

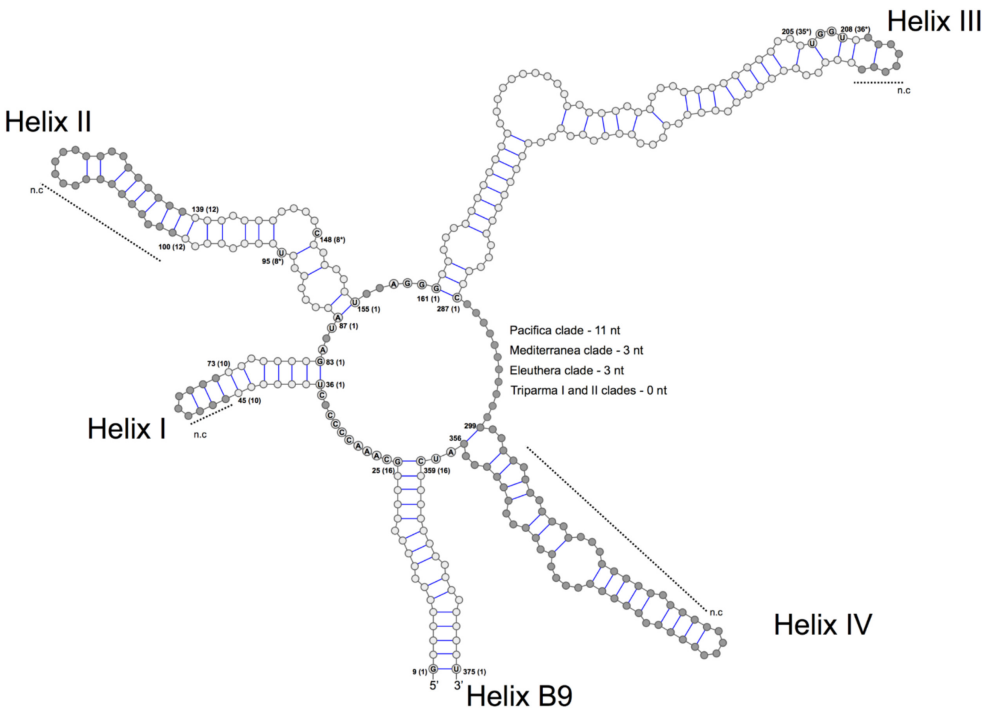

FIGURE 3 | General structure model of the ITS2 molecule of the *Triparma* clades. The four major helices are labeled as Helix I – Helix IV and the interaction region of 5.8S and 28S rRNA as B9. Numbers refer to the alignment positions and those between brackets to the compared positions in each helix. The nucleotides that are 100% conserved in the helices spacers, hallmarks positions in helices II and III and first two base pairs of the helices are shown. The gray dots represent segments that display length and sequence variation (see Methodology in **Supplementary Material**).

The spacers between helices B9 and I, I and II, II and III, and IV and B9 were conserved in length and sequence among the clades (**Figure 3**), as well as the first two base pairs of helices I, II, and III. In contrast, the spacer between helices III and IV showed greater variation between Bolidophyceae clades but it was conserved at the intra-clade level (**Figure 3**). Helices B9 (a region of the 5.8S and 28S rRNA interaction) and III showed good intra and inter-clade conservation (**Figure 3** and **Supplementary Figure 1**). The ITS2 sequence from *T.* aff. *verrucosa* is incomplete and the 3′side arm of helix B9 could not be determined (**Supplementary Figure 1**).

The identification of CBCs in Bolidophyceae ITS2 secondary structure was based on the phenetic approach which relies on a base pair sequence comparison of all CBCs between two sequences without direct reference to their evolutionary origin (Müller et al., 2007; Coleman, 2009). The phylogenetic approach method which considers the status of a given base pair in the ancestor of two sister taxon could not be applied for Bolidophyceae given the conflicting branching pattern among phylogenies (for more details see Ichinomiya et al., 2016).

Putative CBCs, hCBCs, and non-CBCs type changes were identified in the conserved regions of the helices B9, I, II, and III within each clade and between clades (**Figure 4** and **Supplementary Figure 1**). Helix IV (**Figure 4**) was not included in the inter-clade analysis given its known variable nature (Coleman, 2007). Several CBCs and hCBCs were identified at inter-clade level suggesting that each clade within *Triparma* genus (*T. pacifica, T. mediterranea, T. eleuthera*, *Triparma* I and II, *sensu* Ichinomiya et al., 2016) is composed by at least one species (**Figure 4**).

At the intra -clade level, no CBC, nor hCBCs were identified between the two forms of *T. laevis*, f. *inornata* and f. *longispina* (*Triparma* clade I), that differ by the plate morphology, suggesting that these two forms may belong to the same species, although the absence of CBCs is not an absolute indicator that two organisms belong to the same species (Müller et al., 2007; Caisová et al., 2011, 2013). However, at least one CBC is a good indicator (93.1% of confidence for plants and fungi) that in most of the cases, two organisms represent distinct species (Müller et al., 2007). For *Triparma* clade II (*T.* aff. *verrucosa*, *T. strigata,* and *Triparma sp.* RCC1657), no CBC or hCBCs were identified between the morpho species *T.* aff. *verrucosa* and *T. strigata*. The ITS operon sequences from these two strains, including the two internal transcribed spacers and 5.8S rRNA, are nearly identical (99.1%) differing only by six nucleotides. Although three of these substitutions are within the ITS2, none correspond to a nucleotide pair in the ITS2 secondary structure (**Figure 4**). However, between *Triparma sp.* RCC1657 on the one side and *T.* aff. *verrucosa* plus *T. strigata* on the other side, 1 hCBC (helix B9, position 6, **Supplementary Figure 1**) and 1 CBC (helix IV, box, **Supplementary Figure 1**) were identified, suggesting that *Triparma* clade II is composed by at least two species, one corresponding to *Triparma sp.* RCC1657 and the other by *T.* aff. *verrucosa* and *T. strigata*.

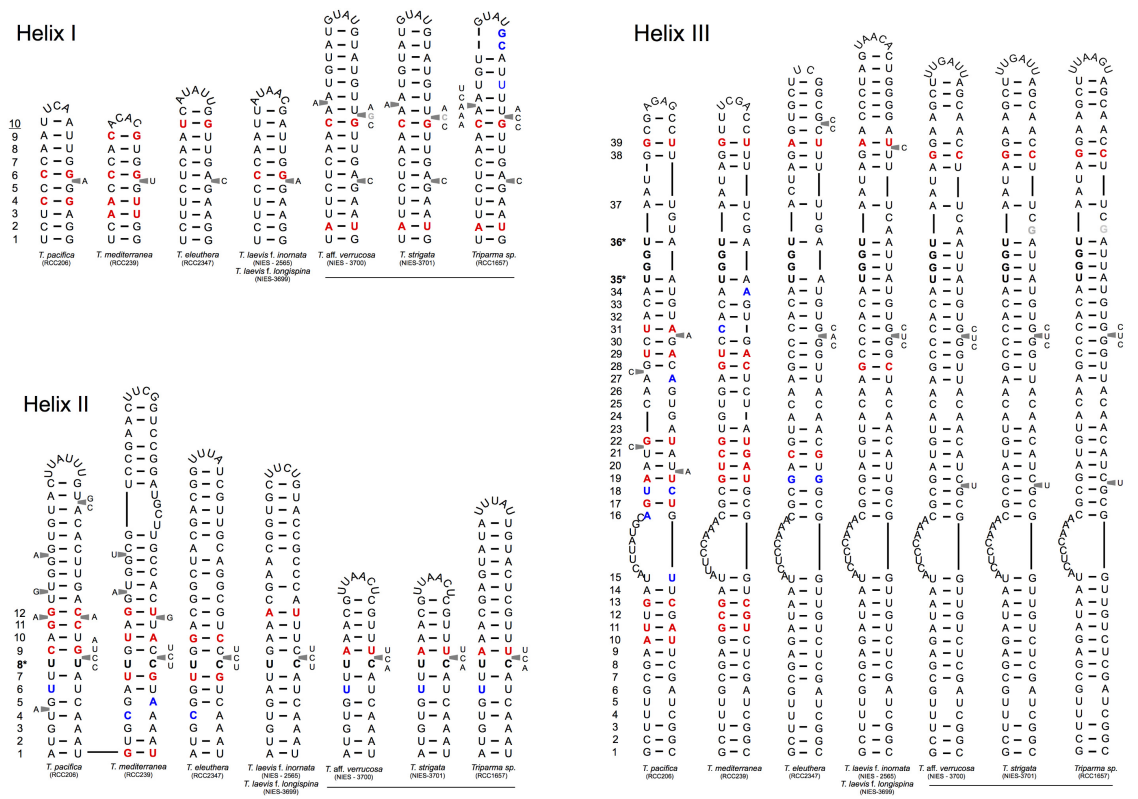

FIGURE 4 | Simplified secondary structural diagram of helices I, II, and III among the different *Triparma* clades. The conserved base pair among the different clades are numbered. Double-sided CBCs (compensatory base changes) and hemi-CBCs are highlighted by bold red nucleotides. Non-CBCs (N – N ↔ N × N) are represented by bold blue nucleotides. The pyrimidine-pyrimidine (Y–Y) mismatch in helix II and the YRRY (pyrimidine – purine – pyrimidine) motif on the 5′ side arm of the helix III are showed by bold nucleotides and by * positions. Single nucleotide substitution between *T.* aff. *verrucosa* and *T. strigata* is showed by gray nucleotides (see Methodology in **Supplementary Material**).

ECOLOGY

Oceanic Distribution

We explored the distribution of Bolidophyceae in the ocean using data obtained by SEM observation, environmental sequencing and metabarcoding. By compiling available records of observed silicified morphological species of Bolidophyceae in natural waters (**Supplementary Table 1**), we mapped the geographical and specific distribution pattern of each morphological species (**Figure 5**). *Tetraparma pelagica,* and the *Triparma* species, *T. laevis, T. columnacea, T. retinervis, and T. strigata* are widely distributed from polar to subtropical regions. In contrast, *Pentalamina corona*, *Tetraparma gracilis*, *Tetraparma catinifera,* and *Triparma verrucosa* are restricted to polar or subpolar regions. *T. gracilis* was observed in both, Arctic and Antarctic regions while *P. corona* seems endemic to the Antarctic and, *T. verrucosa* and *T. catinifera* to the subarctic region. *Tetraparma insecta* and the recently described species *Tetraparma silverae* and *Tetraparma trullifera* seem to be restricted so-far to subtropical regions.

Using both available environmental GenBank sequences and 18S rRNA V9 metabarcodes acquired during the Tara *Oceans* expedition, Ichinomiya et al. (2016) established the oceanic distribution of the major *Triparma* species and of environmental clades. *T. mediterranea* metabarcodes dominated in the Mediterranean Sea while *T. pacifica* and *T. eleuthera* were co-dominant in the tropical and sub-tropical oceans. The *T. laevis* clade was clearly associated with cold Antarctic waters but was also found near the Costa Rica dome. Bolidophyceae sequences were most abundant in the picoplanktonic fraction (0.8–5 μm) of the Tara *Oceans* samples and represented at most 4% of the photosynthetic reads and less than 1% on average (Ichinomiya et al., 2016).

In order to obtain a more complete image of the Bolidophyceae distribution, we used the large data set of 18S rRNA V4 metabarcodes described above. This data set includes a range of studies (**Table 2**) including OSD (Ocean Sampling Day) that sampled an extensive set of coastal stations (Kopf et al., 2015) and several from Arctic and Antarctic waters that were not covered by the Tara expedition.

Among these metabarcodes, the *Triparma* clade was slightly dominating in terms of total reads followed by the three environmental clades III, I, and II, respectively, in this order (**Figure 6A**). Within *Triparma*, *T. pacifica* was most abundant followed by *T. mediterranea*. One environmental subclade (IIIA) was also particularly abundant. The relative contribution of

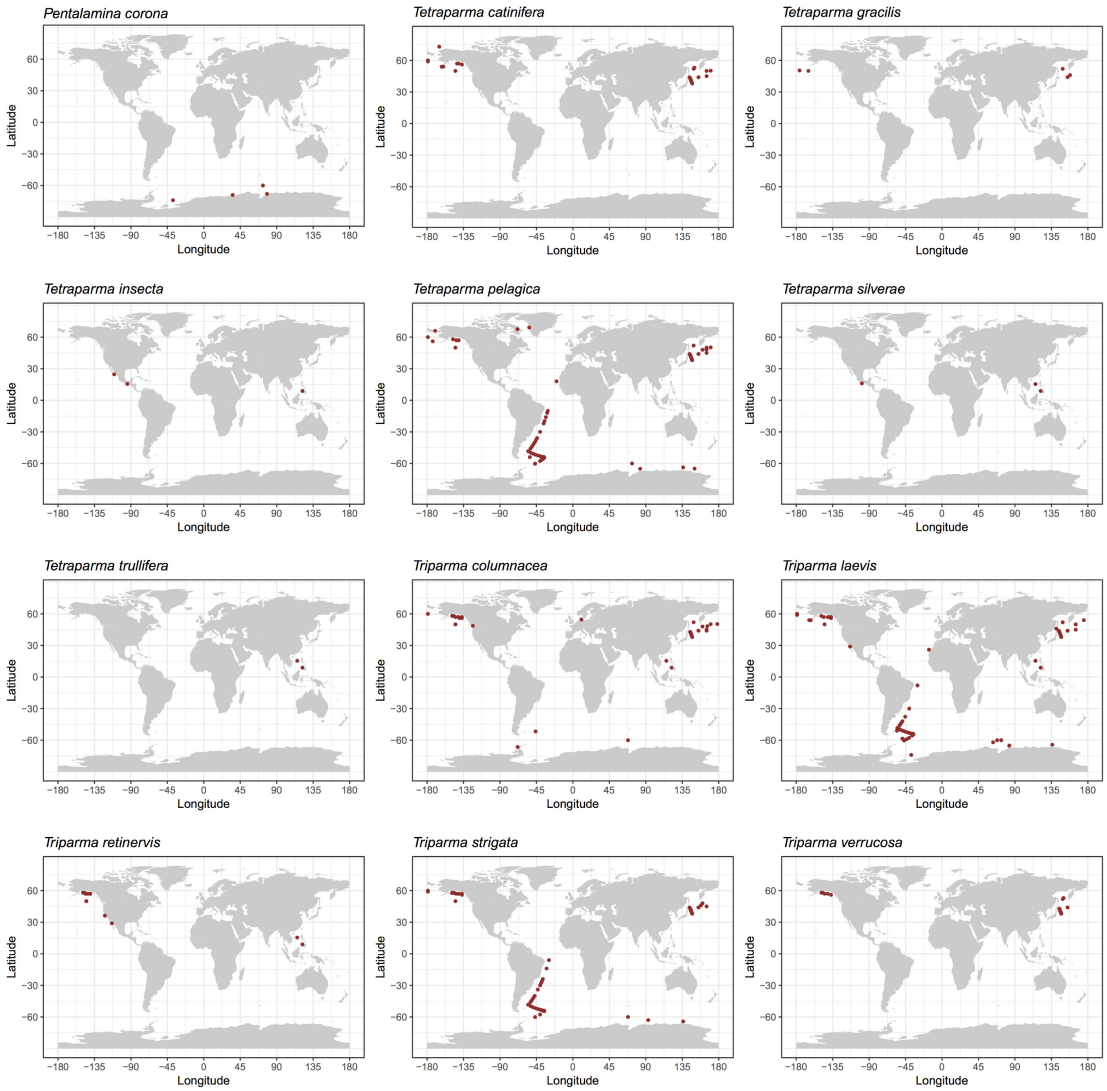

FIGURE 5 | Distribution of silicified Bolidophyceae species based on literature records of SEM observations (see **Supplementary Table 1**).

Bolidophyceae to total metabarcodes at each station varied widely with an average of 0.23% (**Figure 6B**). It was highest, up to 12%, in both Arctic and Antarctic regions as well as around the European coast. In contrast Bolidophyceae were absent at several stations along the East coast of North America and in the Eastern Mediterranean Sea (**Figure 6C**).

The distribution of individual *Triparma* species and environmental clades confirmed some of the trends observed in the Tara *Oceans* data (Ichinomiya et al., 2016) but also revealed new features (**Figure 7**). Among the *Triparma* species, *T. eleuthera* and *T. pacifica* were the most ubiquitous and often co-occurred at the same stations, suggesting that their ecological niches are very close. They did not seem to be present though in really polar waters such as in the Beaufort Sea. In contrast, it was confirmed that *T. mediterranea* was indeed mostly restricted to the Mediterranean Sea while the *T. laevis* clade was only found at high latitudes both in the Arctic and Antarctic. Some environmental clades had clear biogeographic distributions such as clade IIIA found mostly in temperate latitudes and IIIB only in the Arctic and Antarctic regions. The latter clade seemed particularly prevalent in the high Arctic Ocean. Clade I was also mostly observed at high latitudes, although not restricted to polar waters, in contrast to clade II which was more widespread. These distribution patterns may reflect the genetic diversity within these clades. Clades IIIA and B have very low genetic diversity (**Figure 2**) in contrast clades I or II. The former may therefore correspond to a single species with a narrow niche and the latter to several species or even genera, explaining their wide distribution.

Seasonal Cycle

Ichinomiya and Kuwata (2015) investigated the seasonal influence in the abundance and vertical distribution of the

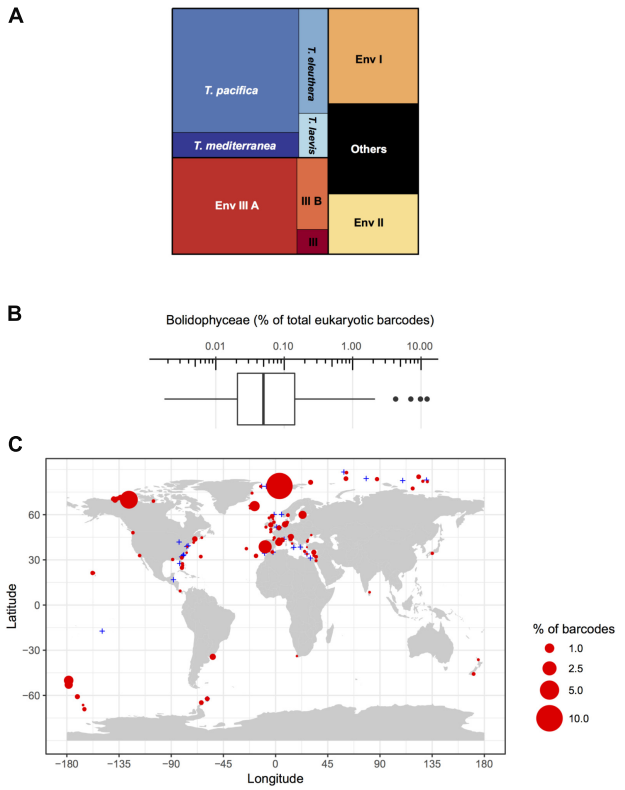

FIGURE 6 | (A) Distribution of read abundance among the different environmental Bolidophyceae clades and *Triparma* species in the metabarcoding studies based on the 18S rRNA V4 region listed in **Table 2**. **(B)** Overall statistics of the proportion of Bolidophyceae reads related to the total number of reads from studies listed in **Table 2**. Only surface samples were considered. **(C)** Oceanic distribution of Bolidophyceae. Circle size is proportional to the number of Bolidophyceae reads related to the total number of reads at a given station.

silicified forms of Bolidophyceae in the western North Pacific using SEM. The area investigated is surrounded by the cold Oyashio current with water temperature below 5–8°C at 100 m (Shimizu et al., 2009). The Bolidophyceae community was mainly composed of *T. laevis* (64 ± 22%) with only small regional and seasonal differences in contrast to diatoms that display clear seasonality patterns (Takahashi et al., 2008; Suzuki et al., 2011). The vertical distribution of the silicified Bolidophyceae community changed seasonally according to the hydrographic condition. Silicified Bolidophyceae had a wide vertical distribution between 0 and 100 m with high abundance of 10–10^2 cells mL^{-1} in March and May at stations where the water column was well mixed or weakly stratified (**Figure 8**). In contrast, from May to October at stations where the water was stratified Bolidophyceae were absent from the surface layer, but mainly distributed under the pycnocline from 20 to 50 m with lower abundance of <0.1–10 cells mL^{-1}. Komuro et al. (2005) also reported similar seasonal variations in depth distributions of the silicified form at Station KNOT (44°N, 155°E) in the western North Pacific. They extended from 0 to 100 m in January and May, but were restricted to the subsurface layer from 30 to 100 m in August. Silicified Bolidophyceae have optimal growth temperatures below 10°C, but do not grow above 15°C (see section "Cell Physiology"). These data suggest that silicified Bolidophyceae actively grow during the cold mixing season and maintain their population under the pycnocline during the warm stratified season (**Figure 9**). Flagellated forms of Bolidophyceae may also be present in the surface layer during stratification since they have been reported in the surface layer during the summer season in the English Channel (Not et al., 2002) and northern South China Sea (Wu et al., 2017) using 18S rRNA-targeted oligonucleotide probes specific of Bolidophyceae detected by *in situ* hybridization and tyramide signal amplification (FISH-TSA). 18S rDNA sequences of Bolidophyceae have also been detected using high-throughput sequencing (Kataoka et al., 2017) at 10 m in summer and autumn in the Oyashio region when silicified forms were absent.

Role in Food Webs

It is not clear how Bolidophyceae contribute to the microbial food web. Materials resembling silicified Bolidophyceae have been reported in fecal pellets of copepods (Booth et al., 1980; Urban et al., 1993) and Antarctic krill (Marchant and Nash, 1986), indicating that they can be grazed by larger predators (Kosman et al., 1993). Bolidophyceae main grazers are expected to be small protozoans, such as choanoflagellates (Taniguchi et al., 1995) although there is no evidence of their direct ingestion by protists.

CELL PHYSIOLOGY

Temperature

Ichinomiya et al. (2013) and Ichinomiya and Kuwata (2015) conducted growth experiments at various temperature ranging from 0 to 15°C, using three silicified strains: *T. laevis* f. *inornata*, *T. laevis* f. *longispina*, and *T. strigata*. These silicified Bolidophyceae species were able to grow at 0 to 10°C (*T. laevis* f. *inornata* and *T. strigata*) and 5 to 10°C (*T. laevis* f. *longispina*) but not over 15°C (**Figure 10**). The optimal growth temperatures were 5°C for *T. laevis* f. *inornata* and 10°C for *T. laevis* f. *longispina* and *T. strigata*, with growth rates of 0.35 d^{-1}, 0.50 d^{-1}, and 0.69 d^{-1}, respectively. In contrast, strains of naked flagellated forms have higher growth rates and grow at higher temperatures (**Figure 10**). *T. eleuthera* showed positive growth at 16–24°C with the maximum growth rate of 1.7 d^{-1} at 22°C (Stawiarski et al., 2016) while *T. pacifica* and *Triparma* sp. RCC201 had growth rates of 0.91 d^{-1} and 0.51 d^{-1} at 20°C, respectively (Jacquet et al., 2001; Thomas and Campbell, 2013).

Silica

The growth of diatoms is limited by dissolved silicate (Martin-Jézéquel et al., 2000; Sarthou et al., 2005). Diatoms cell cycle is controlled by silica and silica limitation arrests cells at the G_1–S boundary (Darley and Volcani, 1969; Okita and Volcani,

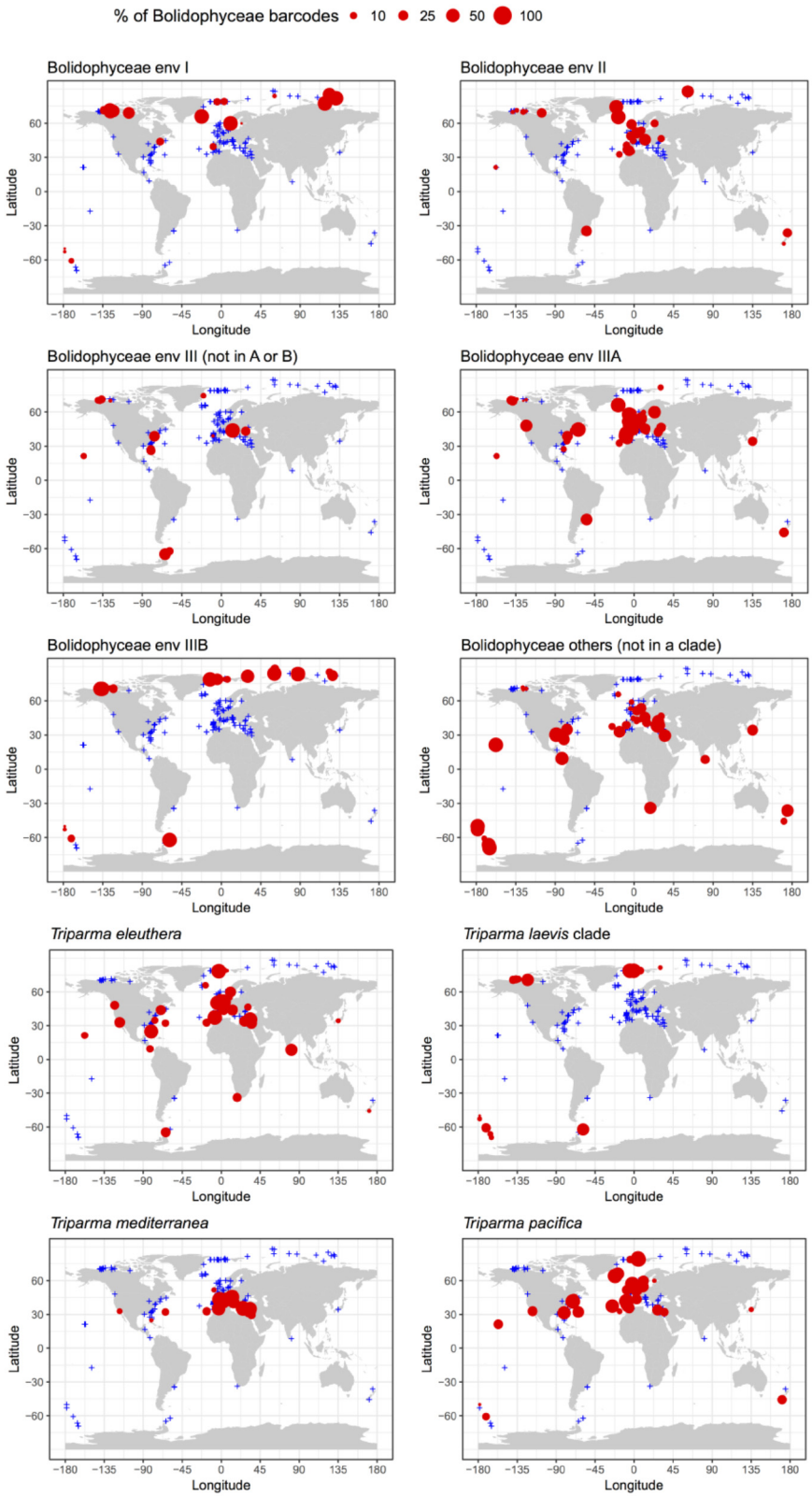

FIGURE 7 | Percentage relative to the total number of Bolidophyceae reads of the different environmental Bolidophyceae clades and *Triparma* species in the metabarcoding studies based on the 18S rRNA V4 region listed in **Table 2**. Only surface samples were considered.

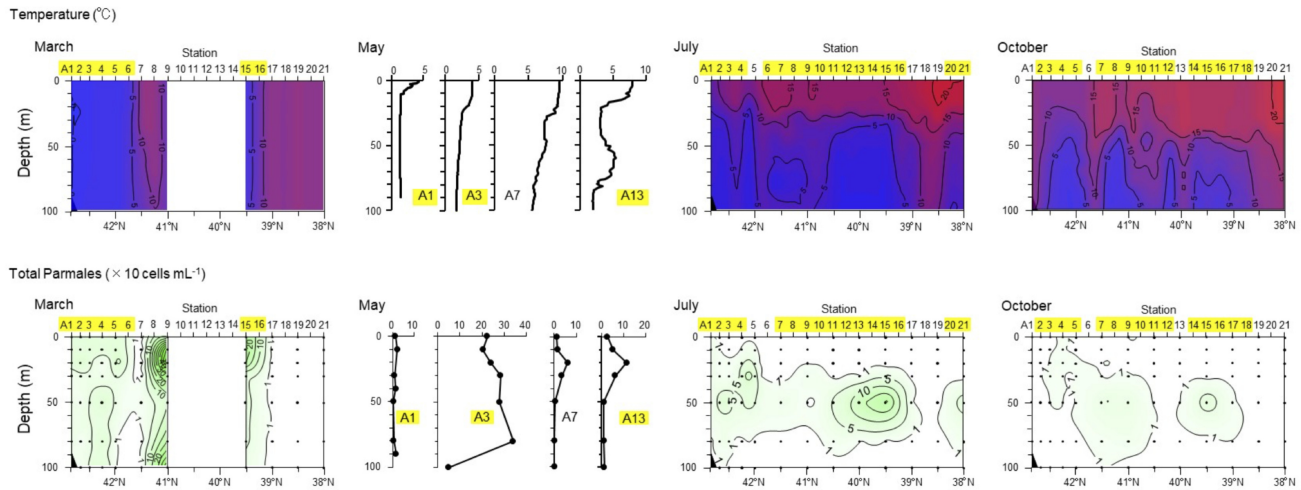

FIGURE 8 | Seasonal variation in vertical distributions of temperature and abundance of the Parmales community along the A-line in March, May, July, and October 2009. Station numbers shaded in yellow indicate the Oyashio region. Redrawn from Ichinomiya and Kuwata (2015) with permission.

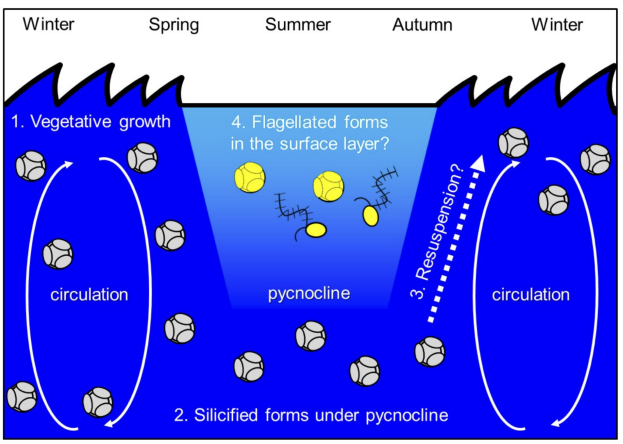

FIGURE 9 | A proposed life history of *T. laevis* (see text for details).

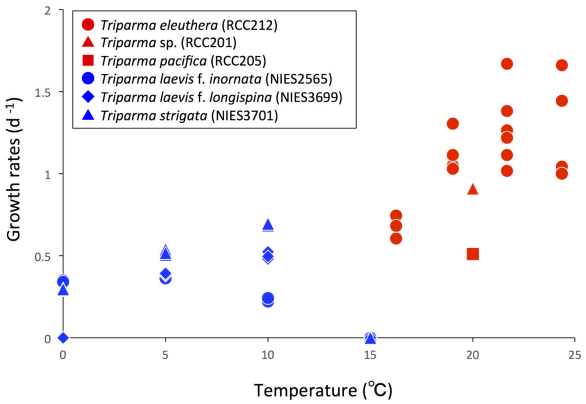

FIGURE 10 | Growth rates of the silicified (blue symbols) and naked flagellated (red symbols) *Triparma* strains. Data redrawn from Stawiarski et al. (2016) for *T. eleuthera* (RCC212), Jacquet et al. (2001) for *Triparma* sp. (RCC201), Thomas and Campbell (2013) for *T. pacifica* (RCC205) and Ichinomiya and Kuwata (2015) for *T. laevis* f. *inornata* (NIES-2565), *T. laevis* f. *longispina* (NIES-3699), and *T. strigata* (NIES-3701).

1978; Vaulot et al., 1987) and during the G2–M transition due to silica requirement for DNA replication and cell wall formation, respectively (Vaulot et al., 1987; Brzezinski et al., 1990).

In contrast, Bolidophyceae despite possessing silica plates can grow in the absence of silica (Yamada et al., 2014). *T. laevis* f. *inornata* cells growing under sufficient silicate (100 μM) are surrounded by eight plates, rounded shield and ventral plates, as well as non-rounded dorsal and girdle plates. However, plate formation becomes incomplete and the fraction of cells lacking dorsal and girdle plates increases at low silicate concentration (10 μM). Cells finally loose almost all plates at silicate concentrations lower than 1 μM (Yamada et al., 2014). Other silicified Bolidophyceae strains, *T. laevis* f. *longispina* and *T. strigata,* can also grow under silicate depletion without formation of a silica cell wall (unpublished data). Cell wall is restored within a day in about 40% of the naked cells after replenishment of silicate (Yamada et al., 2014). Direct observation of regeneration of the silica cell wall in naked cells after re-supply of silicate using transmission and SEM revealed that shield plates appear first, followed by ventral, dorsal, and girdle plates, in this order. The dorsal and girdle plates are inserted into the space between the previously secreted shield and ventral plates to complete cell wall (Yamada et al., 2016). Similar uncoupling between the formation of silica structures and cell growth has also been observed in other silicified Stramenopiles such as Dictyochales (Henriksen et al., 1993) and Synurales (Leadbeater and Barker, 1995; Sandgren et al., 1996).

TABLE 3 | Mitotic characters of Stramenopiles.

	Bolidophyceae*[1]	Diatoms	Pelagophyceae	Phaeophyceae	Xanthophyceae	Chrysophyceae/ Synurophyceae	Raphidophyceae	Eustigmatophyceae
Interphase microtubules focus	Centrioles	Microtubule center	No report	Centrioles	Centrioles	Centrioles	Centrioles	No report
Spindle pole	Centrioles	Polar plate	Centrioles	Centrioles	Centrioles	Rhizoplast	Golgi body	barrel/ boomerang-shaped nuclear pole body
Extranuclear spindle	+	+	+	−	−	−	−	−
Bundled spindle	+	+	+	−	−	−	−	−
References	Yamada et al., 2017	Pickett-Heaps et al., 1975; Pickett-Heaps, 1991	Vesk and Jeffrey, 1987	Markey and Wilce, 1975	Massalski et al., 2009	Slankis and Gibbs, 1972; Vesk et al., 1984, Brugerolle and Mignot, 2003	Heywood, 1978	Murakami and Hashimoto, 2009

*[1] *Reported in only silicified strain Triparma laevis NIES-2565.*

Rounded plates of silicified Bolidophyceae have a structure similar to the valves and scales of auxospores from centric diatoms (Mann and Marchant, 1989; Yamada et al., 2014). In other groups that display silica structures such as diatoms, chrysophytes, synurophytes, and dictyochophytes (Simpson and Volcani, 1981; Knoll and Kotrc, 2015; Finkel, 2016; Marron et al., 2016), silica formation takes place within a specialized membrane-bound compartment termed the Silica Deposition Vesicle (SDV) (Simpson and Volcani, 1981; Preisig, 1994). The origin and location of SDV differ among taxa. Diatoms SDVs for the development of valve, girdle bands of vegetative cells and auxospores scales are formed adjacent to the plasma membrane (Stoermer et al., 1965; Edgar and Pickett-Heaps, 1984; Lee and Li, 1992; Idei et al., 2012), possibly generated from the Golgi body (Lee and Li, 1992). Synurophytes and chrysophytes SDVs are located in the cytoplasmic or chloroplast endoplasmic reticulum. Bolidophyceae SDVs forming the shield and ventral plates are initially produced around the chloroplast and moving toward the plasma membrane like synurophytes and chrysophytes (Yamada et al., 2016). In contrast, SDVs for dorsal and girdle plates are formed adjacent to the plasma membrane like in diatoms. Such differentiation in the development site of SDVs depending on the type of silica plates within a single species has not been previously reported in other organisms (Yamada et al., 2016).

Mitotic Nuclear Division

In eukaryotes, cell division, mitotic process, and related apparatus are often well conserved within high phylogenetic levels (e.g., at the class or phylum levels, Heath, 1980; Schmit and Nick, 2008; De Martino et al., 2009). Among Stramenopiles, the organelles related to the focus of interphase microtubules and spindle poles are the centrioles, like recently observed in Bolidophyceae (Yamada et al., 2017, **Table 3**). However, some classes have unique organelles (**Table 3**), such as the Microtubule Center (MC) and Polar Plate (PP) in diatoms (Pickett-Heaps et al., 1975; Tippit and Pickett-Heaps, 1977; Edgar and Pickett-Heaps, 1984; Pickett-Heaps, 1991; De Martino et al., 2009), the rhizoplast in chrysophytes and synurophytes (Slankis and Gibbs, 1972; Vesk et al., 1984; Brugerolle and Mignot, 2003) or a barrel/boomerang-shaped nuclear pole body in eustigmatophytes (Murakami and Hashimoto, 2009).

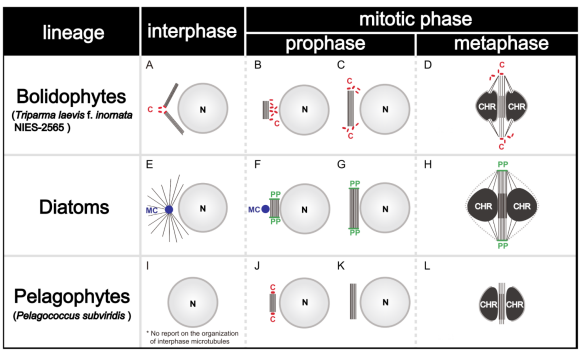

FIGURE 11 | Graphical scheme of the interphase microtubule nucleation and the spindle formation in bolidophytes **(A–D)**, diatoms **(E–H)**, and pelagophytes **(I–L)**. See text for details. Figures **(A–D)** and **(E–H)** are adapted from Yamada et al. (2017) and De Martino et al. (2009) with permission.

During the mitosis of *T. laevis* f. *inornata*, the interphase cell has more than four very short centrioles (ca. 80 nm in contrast to 150–500 nm of typical mature centrioles in other Stramenopiles, (**Figure 11A**). In prophase, the spindle bundle forms at in the extranuclear region (**Figure 11B**), the centrioles move to the spindle poles (**Figure 11C**) and then it moves to the cytoplasmic tunnel of the nucleus (**Figure 11D**). All along metaphase, the kinetochore microtubules elongate from the spindle poles to the condensed chromatin through the region of partially disintegrated nuclear envelope (**Figure 11D**). Finally, the chromatin is separated to both sides of the cell.

Spindle configuration and formation of *T. laevis* f. *inornata* are very similar to the process found among diatoms and pelagophytes (**Table 3**). They share two conspicuous characters: extranuclear spindle formation (**Figures 11B,C,F,G**) and the bundling of the interpolar microtubules (**Figures 11D,H**). However, the organelle serving as a Microtubule Organizing Center (MTOC) and its behavior differ. *T. laevis* f. *inornata* and pelagophytes have centrioles while diatoms have the specialized MC and PP (**Figures 11E–H**). The centrioles of pelagophytes (reported only in one species, *Pelagococcus subviridis*) appear

TABLE 4 | Comparison of selected characters between Bolidophyceae and diatoms.

Properties	Bolidophyceae		Diatoms
	Silicified species	**Flagellated species**	
Size (μm)	2–5	1–1.7	2–2000
Level of organization	Unicellular	Unicellular	Unicellular, often form colonies
Silicified cell wall	Yes	No	Yes
Flagellate form	Yes	Yes	Yes in male gametes of centric diatom
Chloroplasts	Lamellae with three thylakoids, girdle lamella		Lamellae with three thylakoids, girdle lamella
Major Pigments	Chl a, Chl c, fucoxanthin, diatoxanthin, diadinoxanthin, b-carotene		Chl a, Chl c, fucoxanthin, diatoxanthin, diadinoxanthin, b-carotene
Mitochondria	Tubular type		Tubular type
Si requirement for growth	No	No	Yes
Position of SDV	Chloroplast ER and plasma membrane	NA	Plasma membrane
Mitotic aparatus	Interphase microtubules focus:Centrioles	NA	Interphase microtubules focus:Microtubule center
	Spindle pole:Centrioles		Spindle pole:Polar plate
Number of species	12	3	30,000–100,000
Oceanic distribution	Ubiquitous, but minor		Ubiquitous, often dominant
Main habitat	Cold eutrophic water	Warm oligotrophic water	Eutrophic water
	(Polar and subpolar region)	(Tropical or subtropical)	(Polar, coastal, and upwelling region)

NA, not available.

only during the spindle initiation phase (Vesk and Jeffrey, 1987) while those of *T. laevis* f. *inornata* occur after central spindle formation in the extranuclear region. Since centriole is the most common organelle serving as MTOC in Stramenopiles (**Table 3**), the mitotic apparatus of *T. laevis* f. *inornata* shows more ancestral features than the diatoms.

CONCLUSION – THE EVOLUTIONARY RELATIONSHIPS BETWEEN DIATOMS AND BOLIDOPHYCEAE

Diatoms are highly diverse with 30,000 to 100,000 species (Mann and Vanormelingen, 2013) and constitute one of the top group of primary producers, contributing to about 20% of the photosynthesis on Earth, the equivalent of terrestrial rainforests (Nelson et al., 1995; Falkowski et al., 1998; Mann, 1999). They cover a wide size range from 2 μm to 2 mm and form large blooms in high-nutrient coastal and upwelling systems (Margalef, 1978; Hasle and Syvertsen, 1997). They are the main prey for zooplankton and the carbon that they fix through photosynthesis is efficiently transferred to higher trophic levels highlighted by their role in fish production (Ryther, 1969; Cushing, 1989). From an evolutionary point of view, the appearance of this highly productive group and the resulting increase in oceanic primary production may have driven the evolution of crustaceans, pelagic fish, and whales and shaped modern marine pelagic ecosystems (Parsons, 1979). Although, the origin and early evolution of diatoms remain controversial, the first well–preserved diatom fossils have been dated from ∼110 Myr ago, in the early Cretaceous (Gersonde and Harwood, 1990; Harwood and Gersonde, 1990), while molecular-clock-based estimations suggest that the origin of diatoms may have occurred 180 – 250 Myr ago (Medlin, 2011).

Recent multigene phylogenetic analyses suggest that bolidophytes, diatoms, pelagophytes, and dictyochophytes form a monophyletic lineage (Riisberg et al., 2009; Yang et al., 2012; Ševèíková et al., 2015; Derelle et al., 2016). This lineage, called Diatomiista (Derelle et al., 2016) or Khakista (Riisberg et al., 2009), originally only included diatoms and bolidophytes (Cavalier-Smith and Chao, 2006).

Recent success in the isolation of strains of both silicified and naked flagellated Bolidophyceae species allow detailed phylogenetic studies, clarifying the taxonomic position of this group as a sister group of diatoms and revealing the close relationship between silicified and naked strains. Cell wall formation and mitotic division in the silicified species *T. laevis* f. *inornata* have intermediate features between diatom and more ancient stramenopiles (**Figure 11** and **Tables 3**, **4**). Analysis of organellar genomes of this species also suggested that it displays more ancestral characteristics than diatoms (Tajima et al., 2016). Gene contents of the plastid and mitochondrial genomes are similar between *T. laevis* f. *inornata* and diatoms whereas the gene order of the mitochondrial genome is different. The structure of the mitochondrial genome is also more compact in *T. laevis* f. *inornata* than in diatoms since the latter species has no introns or repeat regions which are often observed in some diatoms species (Oudot-Le Secq and Green, 2011).

The phylogenetically close relationship between silicified and naked Bolidophyceae strains and recent occasional observation of flagellated cells in cultures of *T. laevis* f. *inornata* (Ichinomiya et al., 2016) suggest that bolidophytes may have a life cycle that switches between silicified non-flagellated and naked

flagellate stages. This hypothetical life cycle has similarities to centric diatoms for which the diploid vegetative stage produces haploid naked flagellated cells (male gametes or spermatozoa) during sexual reproduction (Drebes, 1977; Vaulot and Chisholm, 1987). The origin, early evolution and key processes for the acquisition of the silica cell wall are not yet been fully understood and Bolidophyceae could play a key role in answering these questions. More comprehensive analyses, including whole genome sequences, observations of the life-cycle, and fossil records, would lead a deeper understanding of the evolutionary relationships between Bolidophyceae and diatoms.

AUTHOR CONTRIBUTIONS

DV analyzed GenBank and metabarcode sequences and draw distribution maps. MT analyzed the OSD metabarcoding data. ALdS performed ITS secondary structure. MI and AK analyzed the distribution of silicified species. AK, KY, MI, SY, DV, and ALdS wrote the manuscript and contributed to the final editing.

FUNDING

Financial support for this work was provided by the following projects: Grants-in-Aid for Scientific Research 22657027, 23370046, 26291085, 15K14784, and 17H03724 from the Japan Society for the Promotion of Science (JSPS), the Canon Foundation, ANR PhytoPol (ANR-15-CE02-0007), ECCOS MicrAntar (C16B02), TaxMArc (Research Council of Norway, 268286/E40), and CONICYT/FONDECYT regular PiSCOSouth (1171802). MT was supported by a Ph.D. fellowship from the Université Pierre et Marie Curie and the Région Bretagne.

ACKNOWLEDGMENTS

We are thankful to Adam Monier, Katja Metfies, Estelle Kilias, and Wei Luo for communicating to us their raw metabarcoding data, and Mary-Hélène Noël for providing us with a SEM image of *T. eleuthera*. We would also like to thank the Ocean Sampling Day consortium for providing sequence data and the ABIMS platform in Roscoff for access to bioinformatics resources.

SUPPLEMENTARY MATERIAL

The Supplementary Material for this article can be found online at: https://www.frontiersin.org/articles/10.3389/fmars.2018.00370/full#supplementary-material and https://doi.org/10.6084/m9.figshare.5549638.

REFERENCES

Azam, F., Fenchel, T., Field, J., Gray, J., Meyer-Reil, L., and Thingstad, F. (1983). The ecological role of water-column microbes in the sea. *Mar. Ecol. Prog. Ser.* 10, 257–263. doi: 10.3354/meps010257

Booth, B. C., Lewin, J., and Norris, R. E. (1980). Siliceous nanoplankton I. Newly discovered cysts from the Gulf of Alaska. *Mar. Biol.* 58, 205–209. doi: 10.1007/BF00391877

Booth, B. C., and Marchant, H. J. (1987). Parmales, a new order of marine chrysophytes, with descriptions of three new genera and seven new species. *J. Phycol.* 23, 245–260. doi: 10.1111/j.1529-8817.1987.tb04132.x

Booth, B. C., and Marchant, H. J. (1988). Triparmaceae, a substitute name for a family in the order Parmales (Chrysophyceae). *J. Phycol.* 24:124. doi: 10.1111/j.1529-8817.1988.tb04467.x

Bravo-Sierra, E., and Hernández-Becerril, D. U. (2003). Parmales (Chrysophyceae) from the Gulf of Tehuantepec, Mexico, including the description of a new species, *Tetraparma insecta* sp Nov., and a proposal to the taxonomy of the group. *J. Phycol.* 39, 577–583. doi: 10.1046/j.1529-8817.2003.02181.x

Brugerolle, G., and Mignot, J. P. (2003). The rhizoplast of chrysomonads, a basal body-nucleus connector that polarises the dividing spindle. *Protoplasma* 222, 13–21. doi: 10.1007/s00709-003-0016-4

Brzezinski, M., Olson, R., and Chisholm, S. (1990). Silicon availability and cell-cycle progression in marine diatoms. *Mar. Ecol. Prog. Ser.* 67, 83–96. doi: 10.3354/meps067083

Caisová, L., Marin, B., and Melkonian, M. (2011). A close-up view on ITS2 evolution and speciation - a case study in the Ulvophyceae (Chlorophyta, Viridiplantae). *BMC Evol. Biol.* 11:262. doi: 10.1186/1471-2148-11-262

Caisová, L., Marin, B., and Melkonian, M. (2013). A consensus secondary structure of ITS2 in the Chlorophyta identified by phylogenetic reconstruction. *Protist* 164, 482–496. doi: 10.1016/j.protis.2013.04.005

Cavalier-Smith, T., and Chao, E. E. Y. (2006). Phylogeny and megasystematics of phagotrophic heterokonts (kingdom Chromista). *J. Mol. Evol.* 62, 388–420. doi: 10.1007/s00239-004-0353-8

Coleman, A. W. (2007). Pan-eukaryote ITS2 homologies revealed by RNA secondary structure. *Nucleic Acids Res.* 35, 3322–3329. doi: 10.1093/nar/gkm233

Coleman, A. W. (2009). Is there a molecular key to the level of "biological species" in eukaryotes? A DNA guide. *Mol. Phylogenet. Evol.* 50, 197–203. doi: 10.1016/j.ympev.2008.10.008

Comeau, A. M., Li, W. K. W., Tremblay, J. -É., Carmack, E. C., and Lovejoy, C. (2011). Arctic Ocean microbial community structure before and after the 2007 record sea ice minimum. *PLoS One* 6:e27492. doi: 10.1371/journal.pone.0027492

Cushing, D. H. (1989). A difference in structure between in strongly stratified waters and in those that are only weakly stratified. *J. Plankton. Res.* 11, 1–13. doi: 10.1093/plankt/11.1.1

Darley, W. M., and Volcani, B. E. (1969). Role of silicon in diatom metabolism: a silicon requirement for deoxyribonucleic acid synthesis in the diatom *Cylindrotheca fusiformis* Reimann and Lewin. *Exp. Cell Res.* 58, 334–342. doi: 10.1016/0014-4827(69)90514-x

Daugbjerg, N., and Guillou, L. (2001). Phylogenetic analyses of Bolidophyceae (Heterokontophyta) using rbcL gene sequences support their sister group relationship to diatoms. *Phycologia* 40, 153–161. doi: 10.2216/i0031-8884-40-2-153.1

De Martino, A., Amato, A., and Bowler, C. (2009). Mitosis in diatoms: rediscovering an old model for cell division. *Bioessays* 31, 874–884. doi: 10.1002/bies.200900007

Derelle, R., López-García, P., Timpano, H., and Moreira, D. (2016). A phylogenomic framework to study the diversity and evolution of stramenopiles (=Heterokonts). *Mol. Biol. Evol.* 33, 2890–2898. doi: 10.1093/molbev/msw168

Drebes, G. (1977). "Sexuality," in *The Biology of Diatoms*, ed. D. Werner (Oxford: Blackwell Scientific Publications), 250–283.

Edgar, L. A., and Pickett-Heaps, J. D. (1984). Valve morphogenesis in the pennate diatom *Navicula cuspidata*. *J. Phycol.* 20, 47–61. doi: 10.1111/j.0022-3646.1984.00047.x

Falkowski, P. G., Barber, R. T., and Smetacek, V. (1998). Biogeochemical controls and feedbacks on ocean primary production. *Science* 281, 200–206. doi: 10.1126/science.281.5374.200

Finkel, Z. V. (2016). "Silicification in the microalgae," in *The Physiology of Microalgae*, eds M. A. Borowitzka, J. Beardall, and J. A. Raven (Basel: Springer International Publishing), 289–300. doi: 10.1007/978-3-319-24945-2_13

Fujita, R., and Jordan, R. W. (2017). Tropical Parmales (Bolidophyceae) assemblages from the Sulu Sea and South China Sea, including the description of five new taxa. *Phycologia* 56, 499–509. doi: 10.2216/16-128.1

Gersonde, R., and Harwood, D. M. (1990). "Lower Cretaceous diatoms from ODP Leg 113 Site 693 (Weddell Sea). Part 1: vegetative cells," in *Proceedings of the Ocean Drilling Program, Scientific Results*, College Station, TX, 365–402.

Gobler, C. J., and Sunda, W. G. (2012). Ecosystem disruptive algal blooms of the brown tide species, *Aureococcus anophagefferens* and *Aureoumbra lagunensis*. *Harmful Algae* 14, 36–45. doi: 10.1016/j.hal.2011.10.013

Guillou, L., Bachar, D., Audic, S., Bass, D., Berney, C., Bittner, L., et al. (2013). The protist ribosomal reference database (PR2): a catalog of unicellular eukaryote Small SubUnit rRNA sequences with curated taxonomy. *Nucleic Acids Res.* 41, D597–D604. doi: 10.1093/nar/gks1160

Guillou, L., Chrétiennot-Dinet, M.-J., Medlin, L. K., Claustre, H., Loiseaux-de Goër, S., and Vaulot, D. (1999a). *Bolidomonas*: a new genus with two species belonging to a new algal class, the Bolidophyceae (Heterokonta). *J. Phycol.* 35, 368–381. doi: 10.1046/j.1529-8817.1999.3520368.x

Guillou, L., Moon-van der Staay, S. Y., Claustre, H., Partensky, F., and Vaulot, D. (1999b). Diversity and abundance of Bolidophyceae (Heterokonta) in two oceanic regions. *Appl. Environ. Microbiol.* 65, 4528–4536.

Harwood, D. M., and Gersonde, R. (1990). "Lower cretaceous diatoms from ODP Leg 113 site 693 (Weddell Sea). Part 2?: resting spores, chrysophycean cysts, an endoskeletal dinoflagellate, and notes on the origin of diatoms," in *Proceedings of the Ocean Drilling Program, Scientific Results*, Vol. 113, College Station, TX, 403–425. doi: 10.2973/odp.proc.sr.113.201.1990

Hasle, G. R., and Syvertsen, E. E. (1997). "Marine diatoms," in *Identifying Marine Phytoplankton*, ed. C. R. Tomas (San Diego, CA: Academic Press), 5–385.

Heath, I. B. (1980). Variant mitoses in lower eukaryotes: indicators of the evolution of mitosis? *Int. Rev. Cytol.* 64, 1–80. doi: 10.1016/S0074-7696(08)60235-1

Henriksen, P., Knipschildt, F., Moestrup, Ø., and Thomsen, H. A. (1993). Autecology, life history and toxicology of the silicoflagellate *Dictyocha speculum* (Silicoflagellata, Dictyochophyceae). *Phycologia* 32, 29–39. doi: 10.2216/i0031-8884-32-1-29.1

Heywood, P. (1978). Ultrastructure of mitosis in the chloromonadophycean alga *Vacuolaria virescens*. *J. Cell Sci.* 31, 37–51.

Ichinomiya, M., dos Santos, A. L., Gourvil, P., Yoshikawa, S., Kamiya, M., Ohki, K., et al. (2016). Diversity and oceanic distribution of the Parmales (Bolidophyceae), a picoplanktonic group closely related to diatoms. *ISME J.* 10, 2419–2434. doi: 10.1038/ismej.2016.38

Ichinomiya, M., and Kuwata, A. (2015). Seasonal variation in abundance and species composition of the Parmales community in the Oyashio region, western North Pacific. *Aquat. Microb. Ecol.* 75, 207–223. doi: 10.3354/ame01756

Ichinomiya, M., and Kuwata, A. (2017). Establishment of first ever culture revealed an unidentified algal taxa: the Parmales (in Japanese). *Jpn. J. Phycol.* 65, 153–158.

Ichinomiya, M., Nakamachi, M., Shimizu, Y., and Kuwata, A. (2013). Growth characteristics and vertical distribution of *Triparma laevis* (Parmales) during summer in the Oyashio region, western North Pacific. *Aquat. Microb. Ecol.* 68, 107–116. doi: 10.3354/ame01606

Ichinomiya, M., Yoshikawa, S., Kamiya, M., Ohki, K., Takaichi, S., and Kuwata, A. (2011). Isolation and characterization of Parmales (Heterokonta/Heterokontophyta/Stramenopiles) from the Oyashio region, Western North Pacific. *J. Phycol.* 47, 144–151. doi: 10.1111/j.1529-8817.2010.00926.x

Idei, M., Osada, K., Sato, S., Toyoda, K., Nagumo, T., and Mann, D. G. (2012). Gametogenesis and auxospore development in *Actinocyclus* (Bacillariophyta). *PLoS One* 7:e41890. doi: 10.1371/journal.pone.0041890

Iwai, T., and Nishida, S. (1976). The distribution of modern coccolithophores in the North Pacific. *News Osaka Micropaleontol.* 5, 1–11.

Jacquet, S., Partensky, F., Lennon, J. F., and Vaulot, D. (2001). Diel patterns of growth and division in marine picoplankton in culture. *J. Phycol.* 37, 357–369. doi: 10.1046/j.1529-8817.2001.037003357.x

Johnson, P. W., and Sieburth, J. M. N. (1982). *In-situ* morphology and occurrence of eucaryotic phototrophs of bacterial size in the picoplankton of estuarine and oceanic waters. *J. Phycol.* 18, 318–327. doi: 10.1111/j.1529-8817.1982.tb03190.x

Kataoka, T., Yamaguchi, H., Sato, M., Watanabe, T., Taniuchi, Y., Kuwata, A., et al. (2017). Seasonal and geographical distribution of near-surface small photosynthetic eukaryotes in the western North Pacific determined by pyrosequencing of 18S rDNA. *FEMS Microbiol. Ecol.* 93:fiw229. doi: 10.1093/femsec/fiw229

Kilias, E., Wolf, C., Nöthig, E.-M., Peeken, I., and Metfies, K. (2013). Protist distribution in the Western Fram Strait in summer 2010 based on 454-pyrosequencing of 18S rDNA. *J. Phycol.* 49, 996–1010. doi: 10.1111/jpy.12109

Knoll, A. H., and Kotrc, B. (2015). "Protistan skeletons: a geologic history of evolution and constraints," in *Evolution of Lightweight Structures*, ed. C. Hamm (Dordrecht: Springer), 1–16. doi: 10.1007/978-94-017-9398-8

Komuro, C., Narita, H., Imai, K., Nojiri, Y., and Jordan, R. W. (2005). Microplankton assemblages at Station KNOT in the subarctic western Pacific, 1999-2000. *Deep Sea Res. Part 2 Top. Stud. Oceanogr.* 52, 2206–2217. doi: 10.1016/j.dsr2.2005.08.006

Konno, S., and Jordan, R. W. (2007). An amended terminology for the Parmales (Chrysophyceae). *Phycologia* 46, 612–616. doi: 10.2216/07-29.1

Konno, S., Ohira, R., Harada, N., and Jordan, R. W. (2007). Six new taxa of subarctic Parmales (Chrysophyceae). *J. Nannoplankt. Res.* 29, 108–128.

Kopf, A., Bicak, M., Kottmann, R., Schnetzer, J., Kostadinov, I., Lehmann, K., et al. (2015). The ocean sampling day consortium. *Gigascience* 4:27. doi: 10.1186/s13742-015-0066-5

Kosman, C. A., Thomsen, H. A., and Østergaard, J. B. (1993). Parmales (Chrysophyceae) from Mexican, Californian, Baltic, Arctic and Antarctic waters with the description of a new subspecies and several new forms. *Phycologia* 32, 116–128. doi: 10.2216/i0031-8884-32-2-116.1

Leadbeater, B. S. C., and Barker, D. A. N. (1995). "Biomineralization and scale production in the Chrysophyta," in *Chrysophyte Algae: Ecology, Phylogeny and Development*, eds C. D. Sandgren, J. P. Smol, and J. Kristiansen (Cambridge: Cambridge University press), 141–164. doi: 10.1017/CBO9780511752292.008

Lee, M., and Li, C. W. (1992). The origin of the silica deposition vesicle of diatoms. *Bot. Bull. Acad. Sin.* 33, 317–325.

Luo, W., Li, H., Gao, S., Yu, Y., Lin, L., and Zeng, Y. (2015). Molecular diversity of microbial eukaryotes in sea water from Fildes Peninsula, King George Island, Antarctica. *Polar Biol.* 39, 605–616. doi: 10.1007/s00300-015-1815-8

Mai, J. C., and Coleman, A. W. (1997). The internal transcribed spacer 2 exhibits a common secondary structure in green algae and flowering plants. *J. Mol. Evol.* 44, 258–271. doi: 10.1007/PL00006143

Mann, D. G. (1999). The species concept in diatoms. *Phycologia* 38, 437–495. doi: 10.2216/i0031-8884-38-6-437.1

Mann, D. G., and Marchant, H. J. (1989). "The origins of the diatom and its life cycle," in *The Chromophyte Algae: Problems and Perspectives*, eds J. C. Green, B. S. C. Leadbeater, and W. L. Diver (Oxford: Clarendon Press), 307–323.

Mann, D. G., and Vanormelingen, P. (2013). An inordinate fondness? The number, distributions, and origins of diatom species. *J. Eukaryot. Microbiol.* 60, 414–420. doi: 10.1111/jeu.12047

Marchant, H., and Nash, G. (1986). Electron microscopy of gut contents and faeces of *Euphausia superba* Dana. *Mem. Natl. Inst. Polar Res. Spec. Issue* 40, 167–177.

Marchant, H. J., and McEldowney, A. (1986). Nanoplanktonic siliceous cysts from Antarctica are algae. *Mar. Biol.* 92, 53–57. doi: 10.1007/BF00392745

Margalef, R. (1978). Life-forms of phytoplankton as survival alternatives in an unstable environment. *Oceanol. Acta* 1, 493–509. doi: 10.1007/BF00202661

Markey, D. R., and Wilce, R. T. (1975). The ultrastructure of reproduction in the brown alga *Pylaiella littoralis*. *Protoplasma* 85, 219–241. doi: 10.1007/BF01567948

Marron, A. O., Ratcliffe, S., Wheeler, G. L., Goldstein, R. E., King, N., Not, F., et al. (2016). The evolution of silicon transport in eukaryotes. *Mol. Biol. Evol.* 33, 3226–3248. doi: 10.1093/molbev/msw209

Martin-Jézéquel, V., Hildebrand, M., and Brzezinski, M. A. (2000). Silicon metabolism in diatoms: implications for growth. *J. Phycol.* 36, 821–840. doi: 10.1046/j.1529-8817.2000.00019.x

Massalski, A., Kostikov, I., Olech, M., and Hoffmann, L. (2009). Mitosis, cytokinesis and multinuclearity in a *Xanthonema* (Xanthophyta) isolated from Antarctica. *Eur. J. Phycol.* 44, 263–275. doi: 10.1080/09670260802636274

Medlin, L. K. (2011). "A review of the evolution of the diatoms from the origin of the lineage to their populations," in *The Diatom World*, eds J. Seckbach and P. Kociolek (Dordrecht: Springer), 94–118. doi: 10.1007/978-94-007-1327-7_4

Metfies, K., von Appen, W.-J., Kilias, E., Nicolaus, A., and Nöthig, E.-M. (2016). Biogeography and photosynthetic biomass of arctic marine pico-eukaroytes during summer of the record sea ice minimum 2012. *PLoS One* 11: e0148512. doi: 10.1371/journal.pone.0148512

Monier, A., Comte, J., Babin, M., Forest, A., Matsuoka, A., and Lovejoy, C. (2014). Oceanographic structure drives the assembly processes of microbial eukaryotic communities. *ISME J.* 9, 990–1002. doi: 10.1038/ismej.2014.197

Monier, A., Terrado, R., Thaler, M., Comeau, A., Medrinal, E., and Lovejoy, C. (2013). Upper Arctic Ocean water masses harbor distinct communities of heterotrophic flagellates. *Biogeosciences* 10, 4273–4286. doi: 10.5194/bg-10-4273-2013

Müller, T., Philippi, N., Dandekar, T., Schultz, J., and Wolf, M. (2007). Distinguishing species. *RNA* 13, 1469–1472. doi: 10.1261/rna.617107

Murakami, R., and Hashimoto, H. (2009). Unusual nuclear division in *Nannochloropsis oculata* (Eustigmatophyceae, Heterokonta) which may ensure faithful transmission of secondary plastids. *Protist* 160, 41–49. doi: 10.1016/j.protis.2008.09.002

Nelson, D. M., Tréguer, P., Brzezinski, M. A., Leynaert, A., and Quéguiner, B. (1995). Production and dissolution of biogenic silica in the ocean: revised global estimates, comparison with regional data and relationship to biogenic sedimentation. *Glob. Biogeochem. Cycles* 9, 359–372. doi: 10.1029/95GB01070

Not, F., Siano, R., Kooistra, W. H. C. F., Simon, N., Vaulot, D., and Probert, I. (2012). Diversity and ecology of eukaryotic marine phytoplankton. *Adv. Bot. Res.* 64, 1–53. doi: 10.1016/B978-0-12-391499-6.00001-3

Not, F., Simon, N., Biegala, I., and Vaulot, D. (2002). Application of fluorescent in situ hybridization coupled with tyramide signal amplification (FISH-TSA) to assess eukaryotic picoplankton composition. *Aquat. Microb. Ecol.* 28, 157–166. doi: 10.3354/ame028157

Okita, T. W., and Volcani, B. E. (1978). Role of silicon in diatom metabolism IX. Differential synthesis of DNA polymerases and DNA-binding proteins during silicate starvation and recovery in *Cylindrotheca fusiformis*. *Biochem. Biophys. Acta* 519, 76–86.

Oudot-Le Secq, M. P., and Green, B. R. (2011). Complex repeat structures and novel features in the mitochondrial genomes of the diatoms *Phaeodactylum tricornutum* and *Thalassiosira pseudonana*. *Gene* 476, 20–26. doi: 10.1016/j.gene.2011.02.001

Parsons, T. R. (1979). Some ecological, experimental and evolutionary aspects of the upwelling ecosystem. *S. Afr. J. Sci.* 75, 536–540.

Pickett-Heaps, J. D. (1991). Cell division in diatoms. *Int. Rev. Cytol.* 128, 63–108. doi: 10.1016/S0074-7696(08)60497-0

Pickett-Heaps, J. D., McDonald, K. L., and Tippit, D. H. (1975). Cell division in the pennate diatom *Diatoma vulgare*. *Protoplasma* 86, 205–242. doi: 10.1007/BF01275633

Preisig, H. R. (1994). Siliceous structures and silicification in flagellated protists. *Protoplasma* 181, 29–42. doi: 10.1007/BF01666387

Riisberg, I., Orr, R. J. S., Kluge, R., Shalchian-Tabrizi, K., Bowers, H. A., Patil, V., et al. (2009). Seven gene phylogeny of Heterokonts. *Protist* 160, 191–204. doi: 10.1016/j.protis.2008.11.004

Ryther, J. H. (1969). Photosynthesis and fish production in the sea. *Science* 166, 72–76. doi: 10.1126/science.166.3901.72

Sandgren, C. D., Hall, S. A., and Barlow, S. B. (1996). Siliceous scale production in chrysophyte and synurophyte algae. I. Effects of silica-limited growth on cell silica content, scale morphology, and the construction of the scale layer of *Synura petersenii*. *J. Phycol.* 32, 675–692. doi: 10.1111/j.0022-3646.1996.00675.x

Sarthou, G., Timmermans, K. R., Blain, S., and Tréguer, P. (2005). Growth physiology and fate of diatoms in the ocean: a review. *J. Sea Res.* 53, 25–42. doi: 10.1016/j.seares.2004.01.007

Schmit, A. C., and Nick, P. (2008). Microtubules and the evolution of mitosis. *Plant Cell Monogr.* 11, 233–266. doi: 10.1007/7089_2007_161

Ševèíková, T., Horák, A., Klimeš, V., Zbránková, V., Demir-Hilton, E., Sudek, S., et al. (2015). Updating algal evolutionary relationships through plastid genome sequencing: did alveolate plastids emerge through endosymbiosis of an ochrophyte? *Sci. Rep.* 5:10134. doi: 10.1038/srep10134

Shimizu, K., Del Amo, Y., Brzezinski, M. A., Stucky, G. D., and Morse, D. E. (2001). A novel fluorescent silica tracer for biological silicification studies. *Chem. Biol.* 8, 1051–1060. doi: 10.1016/S1074-5521(01)00072-2

Shimizu, Y., Takahashi, K., Ito, S. I., Kakehi, S., Tatebe, H., Yasuda, I., et al. (2009). Transport of subarctic large copepods from the oyashio area to the mixed water region by the coastal oyashio intrusion. *Fish. Oceanogr.* 18, 312–327. doi: 10.1111/j.1365-2419.2009.00513.x

Silver, M. W., Mitchell, J. G., and Ringo, D. L. (1980). Siliceous nanoplankton. II. Newly discovered cysts and abundant choanoflagellates from the Weddell Sea, Antarctica. *Mar. Biol.* 58, 211–217. doi: 10.1007/BF00391878

Simpson, T. L., and Volcani, B. E. (1981). *Silicon and Siliceous Structures in Biological Systems*. Hamburg: Springer Verlag Gmbh, doi: 10.1017/CBO9781107415324.004

Slankis, T., and Gibbs, S. P. (1972). The fine structure of mitosis and cell division in the chrysophycean alga *Ochromonas danica*. *J. Phycol.* 8, 243–256. doi: 10.1111/j.1529-8817.1972.tb04035.x

Stawiarski, B., Buitenhuis, E. T., and Le Quéré, C. (2016). The physiological response of picophytoplankton to temperature and its model representation. *Front. Mar. Sci.* 3:164. doi: 10.3389/fmars.2016.00164

Stoermer, E. F., Pankratz, H. S., and Bowen, C. C. (1965). Fine structure of the diatom *Amphipleura pellucida*. II. Cytoplasmic fine structure and frustule formation. *Am. J. Bot.* 52, 1067–1078. doi: 10.1002/j.1537-2197.1965.tb07286.x

Suzuki, K., Kuwata, A., Yoshie, N., Shibata, A., Kawanobe, K., and Saito, H. (2011). Population dynamics of phytoplankton, heterotrophic bacteria, and viruses during the spring bloom in the western subarctic Pacific. *Deep Sea Res. Part 1 Oceanogr. Res. Pap.* 58, 575–589. doi: 10.1016/j.dsr.2011.03.003

Tajima, N., Saitoh, K., Sato, S., Maruyama, F., Ichinomiya, M., Yoshikawa, S., et al. (2016). Sequencing and analysis of the complete organellar genomes of Parmales, a closely related group to Bacillariophyta (diatoms). *Curr. Genet.* 62, 887–896. doi: 10.1007/s00294-016-0598-y

Takahashi, K., Kuwata, A., Saito, H., and Ide, K. (2008). Grazing impact of the copepod community in the Oyashio region of the western subarctic Pacific Ocean. *Prog. Oceanogr.* 78, 222–240. doi: 10.1016/j.pocean.2008.06.002

Taniguchi, A., Suzuki, T., and Shimada, S. (1995). Growth characteristics of Parmales (Chrysophyceae) observed in bag cultures. *Mar. Biol.* 123, 631–638. doi: 10.1007/BF00349241

Thomas, S. L., and Campbell, D. A. (2013). Photophysiology of *Bolidomonas pacifica*. *J. Plankton Res.* 35, 260–269. doi: 10.1093/plankt/fbs105

Tippit, D. H., and Pickett-Heaps, J. D. (1977). Mitosis in the pennate diatom *Surirella ovalis*. *J. Cell Biol.* 73, 705–727. doi: 10.1083/jcb.73.3.705

Urban, J. L., McKenzie, C. H., and Deibel, D. (1993). Nanoplankton found in fecal pellets of macrozooplankton in coastal Newfoundland waters. *Bot. Mar.* 36, 267–281. doi: 10.1515/botm.1993.36.4.267

Vaulot, D., and Chisholm, S. W. (1987). Flow cytometric analysis of spermatogenesis in the diatom *Thalassiosira weissflogii* (Bacillariophyceae). *J. Phycol.* 23, 132–137. doi: 10.1111/j.1529-8817.1987.tb04435.x

Vaulot, D., Eikrem, W., Viprey, M., and Moreau, H. (2008). The diversity of small eukaryotic phytoplankton ($\leq$ 3 μm) in marine ecosystems. *FEMS Microbiol. Rev.* 32, 795–820. doi: 10.1111/j.1574-6976.2008.00121.x

Vaulot, D., Olson, R. J., Merkel, S., and Chisholm, S. W. (1987). Cell-cycle response to nutrient starvation in two phytoplankton species, *Thalassiosira weissflogii* and *Hymenomonas carterae*. *Mar. Biol.* 95, 625–630. doi: 10.1007/BF00393106

Vesk, M., Hoffman, L. R., and Pickett-Heaps, J. D. (1984). Mitosis and cell division in *Hydrurus foetidus* (Chrysophyceae). *J. Phycol.* 20, 461–470. doi: 10.1111/j.0022-3646.1984.00461.x

Vesk, M., and Jeffrey, S. W. (1987). Ultrastructure and pigments of two strains of the picoplanktonic alga *Pelagococcus subviridis* (Chrysophyceae). *J. Phycol.* 23, 322–336. doi: 10.1111/j.1529-8817.1987.tb04141.x

Waterbury, J. B., Watson, S. W., Guillard, R. R. L., and Brand, L. E. (1979). Widespread occurrence of a unicellular, marine, planktonic, cyanobacterium. *Nature* 277, 293–294. doi: 10.1038/277293a0

Wolf, C., Frickenhaus, S., Kilias, E. S., Peeken, I., and Metfies, K. (2014). Protist community composition in the Pacific sector of the Southern Ocean during austral summer 2010. *Polar Biol.* 37, 375–389. doi: 10.1007/s00300-013-1438-x

Wu, W., Wang, L., Liao, Y., Xu, S., and Huang, B. (2017). Spatial and seasonal distributions of photosynthetic picoeukaryotes along an estuary to basin transect in the northern South China Sea. *J. Plankton Res.* 39, 423–435. doi: 10.1093/plankt/fbx017

Yamada, K., Nagasato, C., Motomura, T., Ichinomiya, M., Kuwata, A., Kamiya, M., et al. (2017). Mitotic spindle formation in *Triparma laevis* NIES-2565(Parmales, Heterokontophyta). *Protoplasma* 254, 461–471. doi: 10.1007/s00709-016-0967-x

Yamada, K., Yoshikawa, S., Ichinomiya, M., Kuwata, A., Kamiya, M., and Ohki, K. (2014). Effects of silicon-limitation on growth and morphology of *Triparma laevis* NIES-2565 (Parmales, Heterokontophyta). *PLoS One* 9:e103289. doi: 10.1371/journal.pone.0103289

Yamada, K., Yoshikawa, S., Ohki, K., Ichinomiya, M., Kuwata, A., Motomura, T., et al. (2016). Ultrastructural analysis of siliceous cell wall regeneration in the stramenopile *Triparma laevis* (Parmales, Bolidophyceae). *Phycologia* 55, 602–609. doi: 10.2216/16-32.1

Yang, E. C., Boo, G. H., Kim, H. J., Cho, S. M., Boo, S. M., Andersen, R. A., et al. (2012). Supermatrix data highlight the phylogenetic relationships of photosynthetic Stramenopiles. *Protist* 163, 217–231. doi: 10.1016/j.protis.2011.08.001

Conflict of Interest Statement: The authors declare that the research was conducted in the absence of any commercial or financial relationships that could be construed as a potential conflict of interest.

Copyright © 2018 Kuwata, Yamada, Ichinomiya, Yoshikawa, Tragin, Vaulot and Lopes dos Santos. This is an open-access article distributed under the terms of the Creative Commons Attribution License (CC BY). The use, distribution or reproduction in other forums is permitted, provided the original author(s) and the copyright owner(s) are credited and that the original publication in this journal is cited, in accordance with accepted academic practice. No use, distribution or reproduction is permitted which does not comply with these terms.

frontiers in Marine Science

ORIGINAL RESEARCH
published: 13 April 2018
doi: 10.3389/fmars.2018.00124

The Impossible Sustainability of the Bay of Brest? Fifty Years of Ecosystem Changes, Interdisciplinary Knowledge Construction and Key Questions at the Science-Policy-Community Interface

Olivier Ragueneau[1], Mélanie Raimonet[2], Camille Mazé[1], Jennifer Coston-Guarini[1], Laurent Chauvaud[1], Anatole Danto[1], Jacques Grall[1], Frédéric Jean[1], Yves-Marie Paulet[1] and Gérard Thouzeau[1]*

[1] UMR6539 Laboratoire des Sciences de L'environnement Marin, Plouzané, France, [2] UMR7619 Milieux Environnementaux, Transferts et Interactions dans les Hydrosystèmes et les Sols, Paris, France

OPEN ACCESS

Edited by:
Stephen B. Baines,
Stony Brook University, United States

Reviewed by:
Claire E. Reymond,
Leibniz Center for Tropical Marine Research, Germany
Maxime M. Grand,
University of Hawaii at Manoa, United States

***Correspondence:**
Olivier Ragueneau
olivier.ragueneau@univ-brest.fr

Specialty section:
This article was submitted to Marine Biogeochemistry, a section of the journal Frontiers in Marine Science

Received: 13 September 2017
Accepted: 23 March 2018
Published: 13 April 2018

Citation:
Ragueneau O, Raimonet M, Mazé C, Coston-Guarini J, Chauvaud L, Danto A, Grall J, Jean F, Paulet Y-M and Thouzeau G (2018) The Impossible Sustainability of the Bay of Brest? Fifty Years of Ecosystem Changes, Interdisciplinary Knowledge Construction and Key Questions at the Science-Policy-Community Interface. Front. Mar. Sci. 5:124. doi: 10.3389/fmars.2018.00124

In this contribution, the study of the Bay of Brest ecosystem changes over the past 50 years is used to explore the construction of interdisciplinary knowledge and raise key questions that now need to be tackled at the science-policy-communities interface. The Bay of Brest is subject to a combination of several aspects of global change, including excessive nutrient inputs from watersheds and the proliferation of invasive species. These perturbations strongly interact, affecting positively or negatively the ecosystem functioning, with important impacts on human activities. We first relate a cascade of events over these five decades, linking farming activities, nitrogen, and silicon biogeochemical cycles, hydrodynamics of the Bay, the proliferation of an exotic benthic suspension feeder, the development of the Great scallop fisheries and the high biodiversity in maerl beds. The cascade leads to today's situation where toxic phytoplankton blooms become recurrent in the Bay, preventing the fishery of the great scallop and forcing the fishermen community to switch pray and alter the maerl habitat and the benthic biodiversity it hosts, despite the many scientific alerts and the protection of this habitat. In the second section, we relate the construction of the interdisciplinary knowledge without which scientists would never have been able to describe these changes in the Bay. Interdisciplinarity construction is described, first among natural sciences (NS) and then, between natural sciences and human and social sciences (HSS). We finally ask key questions at the science-policy interface regarding this unsustainable trend of the Bay: How is this possible, despite decades of joint work between scientists and fishermen? Is adaptive co-management a sufficient condition for a sustainable management of an ecosystem? How do the different groups (i.e., farmers, fishermen, scientists, environmentalists), with their diverse interests, take charge of this situation? What is the role of power in this difficult transformation to sustainability? Combining

natural sciences with political science, anthropology, and the political sociology of science, we hope to improve the contribution of HSS to integrated studies of social-ecological systems, creating the conditions to address these key questions at the science-policy interface to facilitate the transformation of the Bay of Brest ecosystem toward sustainability.

Keywords: sustainability, land-ocean continuum, Bay of Brest, interdisciplinarity, science-policy-community interface

INTRODUCTION

From the first Earth Day in 1970 to the adoption of "sustainable development goals" in September 2015 at the UN Assembly, through the Brundtland Report (Brundtland, 1987) defining it, sustainable development has become a dominant paradigm of environmental public action, from the international level to national and more local scales. Accompanying these policy changes, new scientific fields and initiatives have emerged like the Resilience Alliance (Holling, 2001) or sustainability science (Kates et al., 2001; Kates, 2011), in which the concept of a social-ecological system is central (Liu et al., 2007; Ostrom, 2009; Collins et al., 2010; Binder et al., 2013). Whatever the conceptual diagrams used to reconnect the natural and social templates that have been disconnected in our modern societies, ecosystem services are most often the means to rationalize this reconnection (Daily, 1997; Millennium Ecosystem Assessment, 2005). To complement these trends, major international scientific programs addressing aspects of global change re-organized in 2012 as the Future Earth Initiative, with the aim to provide a single platform about "research for global sustainability." This is supposed to incentivize a more solution-oriented, interdisciplinary (especially between humanities and natural sciences but also with engineering sciences, Matson et al., 2016) and participatory community by involving policy-makers, funders, academics, business and industry, and other sectors of civil society in co-designing and co-producing research agendas.

One mode of social-ecological governance, called adaptive co-management (Armitage et al., 2009; Plummer et al., 2013), illustrates some of the ways knowledge produced by scientific research, experts and professional communities (e.g., fishermen, farmers) and policy-makers are being integrated. Co-management refers to the sharing of power and responsibility among local resource user communities and resource management agencies; the idea of adaptive management refers to the science of learning by doing (see Kofinas, 2009 and references therein). Such a move from science-based decision-making toward adaptive co-management in social-ecological governance is remarkable (see for example, Butler et al., 2015; Schultz et al., 2015), as it engages cultural diversity, integrated knowledge production, power sharing, social and adaptive learning, which in turns involves the integration of monitoring, research and policy making.

Different frameworks have been developed to overcome the difficulties frequently encountered when trying to put inter- or trans-disciplinary and participatory research into practice. Indeed, despite some very interesting success stories, it is important to acknowledge that in many places there are numerous barriers against interdisciplinary and participatory science. For example, Hart et al. (2015) discussed how the role of universities could be strengthened to address sustainability challenges, by requiring strong institutional changes regarding both how research and training are organized in order to overcome "disciplinary silos." "Disciplinary silos" is a figurative term referring to how the one-discipline/one-department structure of most higher education institutions reinforces and rewards single-discipline researchers and impedes inter- or trans-disciplinary initiatives and careers. One could also mention the difficulties in communication across disciplines or in combining scientific and other forms of knowledge (Kueffer et al., 2012; Lang et al., 2012); all these challenges require new frameworks to facilitate sustainability research. It is therefore important to examine how and where interdisciplinary collaborations and participatory science have been constructed, highlighting how barriers, and conflicts have been resolved during the process. The example we will focus on in this contribution concerns the origins of integrated research approaches within a coastal social-ecological system located in the Bay of Brest (northwestern France).

Ecosystems and habitats in coastal zones supply many valuable ecosystem services (recreation, food production, protection against the sea, nutrient cycling, carbon storage…), providing many benefits in terms of welfare and well-being to society (Turner, 2015). At the same time, they are also very vulnerable to anthropogenic environmental changes which are intensified in coastal zones where human populations are increasingly concentrated and where disturbances are driven not only by activities in the immediate area (e.g., fishing, aquaculture, introduction of alien species, waste disposal, coastline modifications, tourism, development of marine renewable energy), but also by activities upstream (inland) such as, agriculture, urbanization, and industrial production. The pace of change in the highly complex and dynamic coastal zones is much faster than what was anticipated a decade ago (Cloern et al., 2015), creating a daunting challenge to manage these areas in a sustainable way. New forms of management are replacing earlier policies driven solely by science, something that has been characterized as "a generally failed experiment" for coastal environments (Christie, 2011). According to Bremer and Glavovic (2013), the "science-policy interface" in the coastal zone should be framed as a "governance setting," reflecting the multiplication of stakeholders involved and the strong need for inter- and trans- disciplinary research in this area.

The Bay of Brest (France) is an example of coastal ecosystem subject to different aspects of global change, i.e., eutrophication, arrival and proliferation of alien species, and climatic trends (Cloern et al., 2015). The bay is considered a relatively well-studied ecosystem, but major environmental problems persist, such as increasing harmful algal blooms (HABs) (Chapelle et al., 2015) and biodiversity losses have become dramatic since the harvesting of the *Venus verrucosa* clam from maerl beds has begun within the bay (Dutertre et al., 2015).

In this article, we first recount the environmental changes observed in the Bay of Brest over the past five decades, focussing on links between eutrophication, the biogeochemical cycle of silicon (Si), the proliferation of invasive species and their combined effects on local fisheries. In the second section of this article, we relate how interdisciplinary collaborations arose amongst the community of researchers involved in studies of the Bay, emphasizing the importance of geographical proximity (Reckers and Hansen, 2015) and also of the creation of "boundary settings" between different research groups (Mollinga, 2010; Mattor et al., 2014) intended to stimulate long-term interactions among scientists from different disciplines, first within Natural Sciences (NS), then together with Human and Social Sciences (HSS). We close with a critical examination of the present-day unsustainable situation and key periods of strong interactions between scientists and communities of fishers and farmers over the last decades, raising a number of questions about the interactions between the scientific community and other policy and user communities involved. It is suggested that answering these questions now requires actively integrating the social sciences of politics (SSP) with environmental studies to facilitate transformations of coastal environments toward sustainability (Mazé et al., 2015, 2017).

THE BAY OF BREST ECOSYSTEM SINCE WWII

Agriculture and Phytoplankton Dynamics

The Bay of Brest has undergone two major anthropogenic perturbations following World War II: one originating from land, and one from the sea. The French government, faced with an urgent need to augment food production in the aftermath of WWII, promoted the widespread use of artificial fertilizers to increase arable land productivity and modernize (i.e., mechanize) farming. The agricultural system in Brittany underwent significant changes during the 1960's, moving toward intensive monoculture farms centered on vegetables and pigs. As a direct consequence, nitrate concentrations greatly increased in rivers and green tides of mainly *Ulvae* sp. developed along many coasts around Brittany. These episodes became a public nuisance and health problem, leading to 30 years of conflicts between environmental non-governmental organizations and the agricultural sector. They have also been the object of contentious exchanges between the French government and the European Commission in Brussels. In the Bay of Brest, nitrate concentrations in the Aulne and Elorn rivers doubled between the 1970's and the 1990's (Le Pape et al., 1996) reaching concentrations of up to 700 μM, which is more than five times the good water quality threshold defined by the European Water Framework Directive. However, because of the decoupling between nitrogen inputs (winter and spring) and the temperature optimum for the development of the macroalgae *Ulvae* sp. (summer), which leads to the export of 94% of dissolved inorganic nitrogen to coastal waters before spring (Le Pape et al., 1996), and because of the macrotidal character of the bay, these nitrate concentrations did not generate important green tides in the Bay of Brest, except for very localized areas near the mouth of the Elorn River (Le Pape and Menesguen, 1997).

Instead, the indirect consequences of increasing land-derived nitrogen (N) and phosphorus (P) inputs occur through the silicon (Si) cycle. Silicon arrives in the aquatic environment mostly in the form of dissolved silicic acid (dSi), following the natural weathering of silicate rocks (Meybeck, 1982), and as amorphous silica (Conley, 1997), which can also be perturbed by anthropogenic processes (see review in Ragueneau et al., 2010). Constant Si inputs, associated with increasing N and P loads from human activities inland, have decreased Si:N and Si:P ratios in rivers, affecting phytoplankton dynamics in the receiving coastal waters (Officer and Ryther, 1980; Ragueneau et al., 1994, 2010; Billen and Garnier, 2007). Since the review of Smayda (1990), documenting several examples of similar decreasing nutrient ratios, many regions around the world have experienced switches from a diatom-based primary production to a primary production dominated by other phytoplankton groups, e.g., dinoflagellates, which include many toxic species (Conley et al., 1993; Ragueneau et al., 2006a,b and references therein). However, the Bay of Brest did not exhibit dramatic phytoplankton community shifts, despite strong decreases in the Si:N and Si:P ratios, well below the Redfield (1958) or Brzezinski (1985) ratios for diatoms growing under nutrient-rich conditions (Del Amo et al., 1997).

Explanations for the absence of such shifts were provided in the mid 1990's. The intensity of Si recycling both at the sediment-water interface and in the water column (Ragueneau et al., 1994; Beucher et al., 2004) modifies the properties of various diatom species (Roberts et al., 2003). For instance, their degree of silicification (Rousseau et al., 2002) ultimately favors the switch from diatom to non-diatom species when the dSi stress becomes too strong. The combination of Si recycling and macrotidal regime provided a reasonable explanation (Ragueneau et al., 1996) to account for the maintenance of the diatom succession observed throughout spring and summer since the 1980's (Quéguiner, 1982; Del Amo et al., 1997). And this was despite the apparent lack of dSi following the first spring diatom bloom (direct and indirect evidence of dSi limitation is discussed in Del Amo et al., 1997 and Ragueneau et al., 2002). It was proposed at that time that the Bay of Brest sediments could represent a coastal silicate pump (Del Amo et al., 1997), because they retain dSi within the ecosystem, allowing the dSi replenishment of coastal waters following the summer temperature increase and subsequent intensification of Si recycling at the sediment-water interface. As we shall see, the motor of that pump was biologically driven and had to do with the proliferation of a benthic invader in the bay environment.

Proliferation of Invasive Species and Environmental Impacts on the Ecosystem

In parallel with these increasing land-derived N and P concentrations and fluxes, the Bay of Brest experienced several introductions of non-indigenous species following WWII, including macroalgae (*Gracilaria vermiculophylla*), halophytes (*Spartina alterniflora*) and benthic mollusks such as the Pacific oyster *Crassostrea gigas* and the American slipper limpet *Crepidula fornicata* (see review in Stiger-Pouvreau and Thouzeau, 2015). Aquaculture practices and expanding international shipping both increase the opportunities for the translocation of fauna and flora (Carlton and Geller, 1993). Proliferation of introduced species has become a major issue in many areas with unanticipated linkages between terrestrial and marine components of coastal ecosystems being exposed (Van der Wal et al., 2008). Here, we will focus on the effects of one of these introduced species in the bay, the slipper limpet, *Crepidula fornicata* (**Figure 1**), because of its role in the silicate pump (Del Amo et al., 1997). *C. fornicata* is a filter-feeder that proliferates in bay and estuarine environments, and can reach several thousands of individuals per square meter because adults attach to each other in "chains" creating dense accumulations on the seafloor (Blanchard, 2009). *C. fornicata* arrived in the Bay of Brest in 1949; the invasion then progressed from south to north and there was a sharp increase in abundance between 1995 and 2000 when the estimated standing stocks increased by a factor of four (Guérin, 2004; Stiger-Pouvreau and Thouzeau, 2015).

Through these accumulations, the engineer gastropod modifies its local environment by adding new physical and biological substrates and modifying local hydrodynamics along with rates of particle erosion and sedimentation at the sediment-water interface (Moulin et al., 2007). Although suspension feeders have dominated benthic communities in the bay (Hily, 1984; Jean and Thouzeau, 1995; Grall and Glémarec, 1997), *C. fornicata* became the main suspension feeder by 2,000 (97% of total suspension feeder biomass; Thouzeau et al., 2000). Active filter feeders like *C. fornicata* produce a fraction of non-ingested material which is excreted and accumulates at the sediment surface as pseudo-feces (Norkko et al., 2001). This leads to local deposition rates that can exceed passive sedimentation rates in high density filter feeder beds (Dame, 1993), and creates carbon (C) and N enriched sediments (Kautsky and Evans, 1987).

In the Bay of Brest, the impacts of *C. fornicata* on hydrodynamics and transport properties of the benthic boundary layer (Moulin et al., 2007), as well as on benthic biodiversity, demonstrated a gradual shift toward smaller species with a higher turnover rate (Grall and Glémarec, 1997). Locally, biodiversity increased as new microhabitats for other benthic sessile and mobile fauna were created (Chauvaud et al., 2000); but at the scale of the entire bay, *C. fornicata* carpeted parts of the seafloor, homogenizing benthic surfaces, endangering the total biodiversity of the ecosystem (Chauvaud, 1998). It competed for space with the Great Scallop (**Figure 1**) (*Pecten maximus;* Thouzeau et al., 2000*),* threatening other economically important bivalve fisheries in the region (Frésard and Boncoeur, 2006).

Proliferation of *C. fornicata* and the Silicate Pump Hypothesis

The effects of this shift were studied on the benthic community respiration (Martin et al., 2006, 2007), as well as on the benthic cycling of carbon and several associated biogenic elements, such as N (Martin, 2005; Martin et al., 2006), P (Martin, 2005) and Si (Ragueneau et al., 2002). Combining the importance of Si recycling at the sediment-water interface in the maintenance of diatom blooms (silicate pump) with the major role being played by *C. fornicata* in the recycling of nutrients in the bay, Chauvaud et al. (2000) formulated a working hypothesis (**Figure 2**) about the possible effects of this combination on the ecosystem: when the silicate pump (mostly driven by *C. fornicata*) is active, filtration and biodeposition by benthic suspension feeders would lead to Si retention as Si-enriched sediment deposits. Then, dissolution would continuously replenish overlying surface waters with dSi, allowing diatom succession to take place even in summer. In contrast, when hydroclimatic conditions limit the filtration and biodeposition of benthic suspension feeders (e.g., because of excessive microalgal biomass, high sedimentation, gill clogging and/or hypoxia), Si would be exported out of the Bay, leading to dSi limitation and non-siliceous phytoplankton species during summer (see Chauvaud et al., 2000).

In the decade following the latter article, this hypothesis was tested extensively. Sediment core incubations (Ragueneau et al., 2002) and the deployment of benthic chambers (Martin, 2005) at sites exhibiting low and high densities of *C. fornicata* provided direct evidence of the role played by this organism in nutrient recycling - in particular for dSi. In addition, as this gastropod has no Si requirement, the feces became enriched in Si relative to C and other nutrients, reinforcing the silicate pump mechanism (Ragueneau et al., 2005). Silicon biogeochemical budgets were established at seasonal and annual scales (Ragueneau et al., 2002, 2005), clearly demonstrating the importance played by benthic recycling for diatom growth, particularly during summer. The feedback of enhanced benthic nutrient fluxes on phytoplankton dynamics was then studied with mesocosm experiments (Fouillaron et al., 2007; Claquin et al., 2010) and modeling (Laruelle et al., 2009). The dynamic 2-dimensional physical and biological model included an explicit representation of the benthic-pelagic coupling with *C. fornicata*. The model was used to simulate the effects of removing this gastropod on the ecosystem functioning because the local fishery committee had suggested this to reduce the pressure on the scallop stock (see section Construction of a Basis for Interdisciplinary Knowledge About the Bay of Brest). The modeling suggested that removal of *C. fornicata* would increase the probability for the development of HABs due to a dSi limitation during summer.

What Is the Present State of the Bay of Brest?

HABs have taken place in the Bay of Brest on some occasions but, as mentioned before, this ecosystem has long resisted to the development of dinoflagellate blooms. Since 2012 however, their frequency and magnitude have been increasing: HABs take place every summer in the Bay of Brest, mostly in its

FIGURE 1 | Images of *Crepidula fornicata* **(A)**, of *Pecten maximus,* the Great Scallop **(B)** and of competition for space between those two benthic suspension feeders **(C)**.

southern part with *Alexandrium minutum* (Chapelle et al., 2015). Many processes may contribute to the development of toxic phytoplankton blooms e.g., temperature, tides and the hydrodynamic regime, inorganic nutrients ratios, ratio between organic and inorganic nitrogen (Roberts et al., 2003; Chapelle et al., 2015), and it is difficult to attribute their occurrence to a single cause. Nonetheless, strong decreases in the total biomass of *C. fornicata* have also been reported in the central and southern basins of the bay based on extensive surveys conducted in 2013/2014 (data of A. Carlier as cited in Stiger-Pouvreau and Thouzeau, 2015). Whatever the precise reasons for this decline (which remain to be determined, see section Key questions at the science-policy-community interfaces), it provides plausible evidence for the silicate pump/*C. fornicata* hypothesis proposed in Chauvaud et al. (2000) and agrees with the development of HABs predicted during the modeling exercise, especially dinoflagellates which do not require Si (Laruelle et al., 2009).

The increasing frequency and magnitude of HABs in the Bay of Brest have many implications, especially for the lifecycle of benthic suspension feeders and the benthic ecosystem as a whole (Fabioux et al., 2015; Coquereau et al, 2017). Some benthic organisms, including those of commercial interest, accumulate toxins secreted by these microalgae preventing them from being sold (Belin et al., 2013). In the Bay of Brest, the *P. maximus* fishery has suffered greatly from this type of contamination. Detoxification is longer for the Great Scallop than for other bivalves, and the fishing community has had to find replacement species to maintain the Bay's fishery. One of those replacements has been the clam *V. verrucosa,* which is collected with dredges from the maerl beds of the southern basin (Pantalos, 2015). Maerl beds (**Figure 3**), including those of the Bay of Brest, have a high ecological importance and conservation value (Grall and Hall-Spencer, 2003). They are unique areas because of their high biodiversity, their role as a nursery for targeted species of fish and the Great Scallop, and the role of the bivalves living on/in maerl beds that serve as brood stock for the surrounding areas. Maerl beds are also commercially valuable as their calcium carbonate makes them an excellent soil amendment and waste-water filter. As noted by Pantalos (2015), maerl extraction is mostly a thing of the past in Europe and has been banned since January 1st 2013 under the European Union Habitats Directive (92/43/EEC; 1992 May 21). But both dredging and trawling continue in some regions of the world, despite numerous calls for protection in scientific publications (e.g., Hall-Spencer et al., 2003), and despite the laws and directives already enacted that apply specifically to maerl beds (Amice et al., 2007). This is the case in the Bay of Brest (**Figure 3**), where recurrent dredging activities have affected 50% of the maerl banks (Grall et al., 2009).

To summarize this first section dedicated to the study of the Bay of Brest ecosystem changes over the last 50 years, we have constructed a schematic diagram, or sequence, of this chain of events (**Figure 4**), that will help guide us in the last section Key questions at the science-policy-community interfaces as we ask important questions related to the social-ecological system. The ecosystem apparently initially absorbed the excessive N and P inputs from land, and resisted decreasing Si:N and Si:P ratios, maintaining diatoms in the system probably due to a very active silicate pump. However, if the pelagic ecosystem seemed to remain relatively unchanged, the less visible benthic ecosystem was experiencing important modifications due to high population abundances of *C. fornicata*. While this species' abundance was having negative impacts on the Bay's biodiversity and causing trouble to the Great Scallop fishing community to the point that they wanted to eradicate it by the mid 2000's (see section Construction of a Basis for Interdisciplinary Knowledge About the Bay of Brest), it was also suggested that the presence of *C. fornicata* was helping maintain diatoms in the ecosystem, through its impact on the Si biogeochemical cycle (**Figure 2**) and possibly preventing or slowing down the development of HABs. Following the unexplained drastic diminution of *C. fornicata* abundances in the Bay, HABs have started to develop. Even if this is consistent with the silicate pump/*C. fornicata* hypothesis, it has had important ecological and socio-economic consequences, such as the on-going destruction of the Bay's maerl banks as the fishermen community switched prey and started dredging for *V. verrucosa*.

Obviously, the Bay of Brest is not following a sustainable path, despite decades of strong interdisciplinary studies of the ecosystem and regular interactions between scientists and

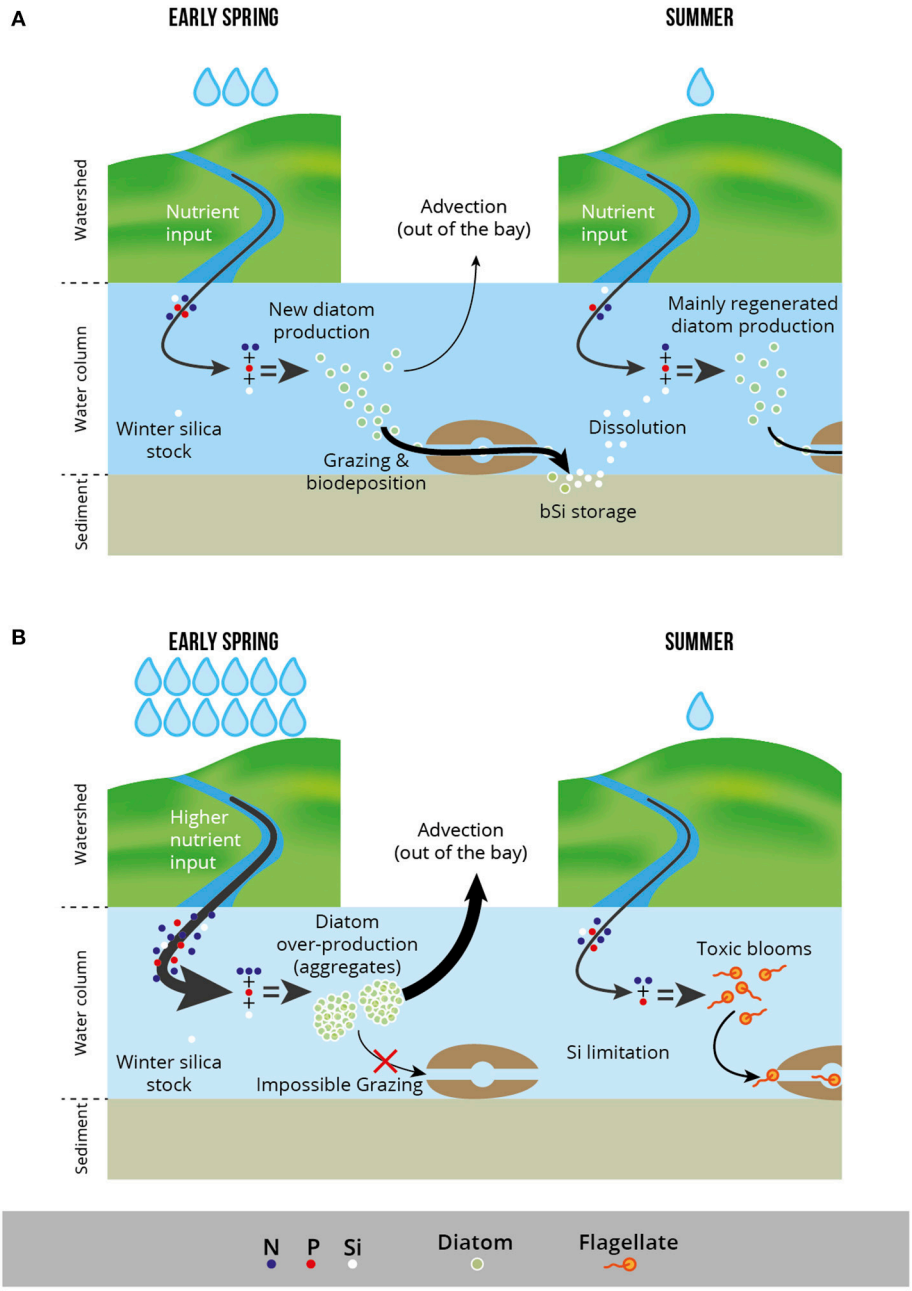

FIGURE 2 | The Crepidula/Si working hypothesis (redrawn from Chauvaud et al., 2000). Two contrasting situations are displayed. On top **(A)**, under "normal" climatic conditions, the diatom spring production is being grazed by benthic suspension feeders, dominated by *Crepidula*; the Si is being stored in the sediment and slowly released as silicic acid during summer, allowing the maintenance of diatoms in the system. At the bottom **(B)**, the spring diatom production cannot be grazed and most of the diatom production is exported out of the Bay, depleting the system in silicic acid and favoring a summer production of dinoflagellates. In this figure, reasons for the impossible grazing are linked to excessive nutrient inputs under heavy rains, and the formation of diatom aggregates, that sediment massively to the bottom and cannot be as easily grazed. Other situations may lead to the prevention of such grazing and biodeposition activities. See text for more details.

communities of farmers and fishers. This raises important questions at the science-community and science-policy interfaces, as we discuss in the last section of this contribution (III). Before that (II), we examine how the interdisciplinary knowledge necessary to understand the ecosystem changes and present the cascade of events (**Figure 4**) was built, first in natural sciences studies of ecosystem complexity; we then show how social scientists have entered into collaborative research programs with NS during the last 10 years to start addressing questions raised concerning the sustainability of the social-ecological system of the Bay of Brest.

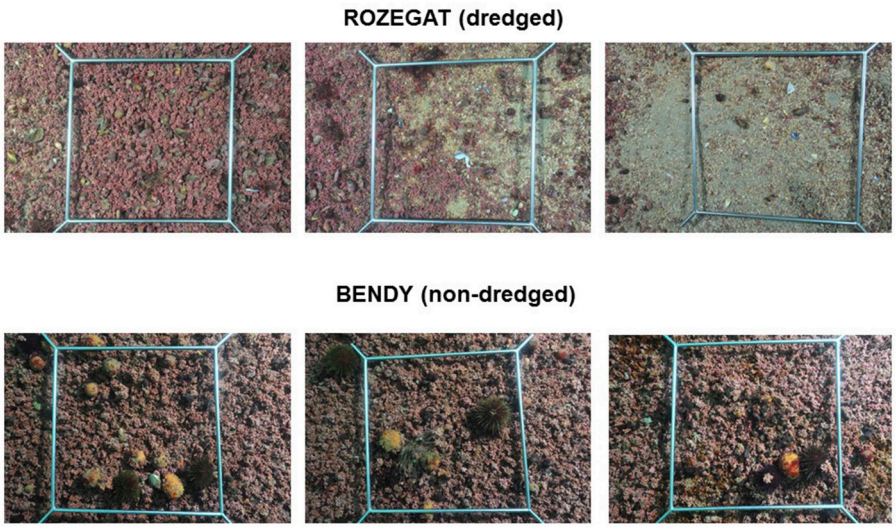

FIGURE 3 | Photographs of 0.1 m^2 quadrats taken on the fished maerl bed (Rozegat) and on the unfished maerl bed (Bendy) in March 2011. Note the differences in habitat structure, live maerl distribution as well as in the presence or absence of associated benthic megafauna.

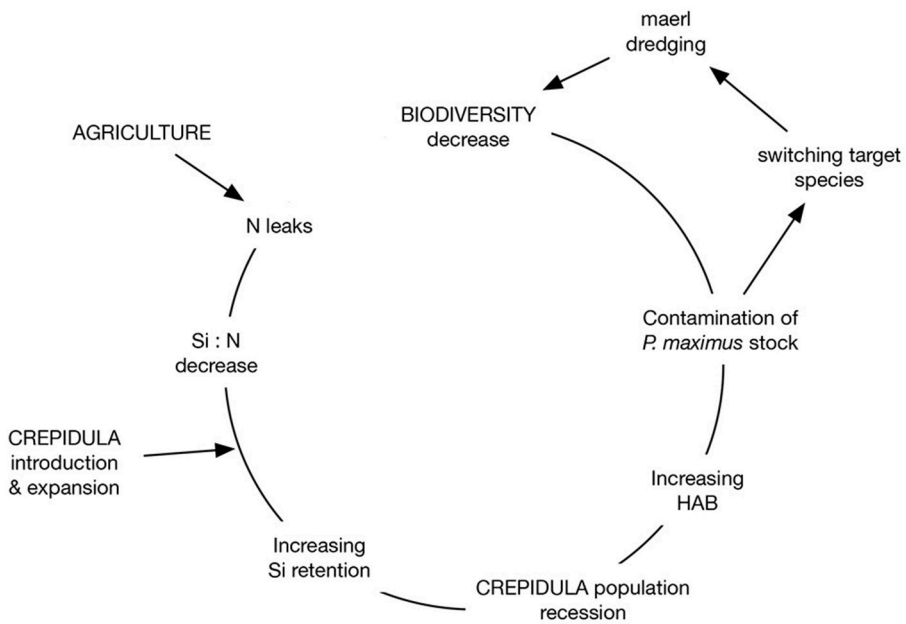

FIGURE 4 | Schematic description of a cascade of events over the last 50 years in the Bay of Brest, from changes in agricultural practices after world war II to present-day threats on biodiversity, including interactions between changing nutrient ratios and the proliferation of *Crepidula fornicata* (see text) and their impacts on the Great Scallop fishery.

CONSTRUCTION OF A BASIS FOR INTERDISCIPLINARY KNOWLEDGE ABOUT THE BAY OF BREST

All the studies described above were led by groups associated with research infrastructures in the Brest region, in particular with the IUEM (*Institut Universitaire Européen de la Mer*, a component of the *Université de Bretagne Occidentale* or 'UBO') and the IFREMER which conducts research on the exploitation of marine resources. We review in the next paragraphs how geographical proximity led to the emergence of interdisciplinary approaches to the environmental issues faced by the larger community discussed earlier. From a science studies viewpoint, it is important to distinguish two main periods: before and after

the creation of the IUEM in 1997. Relating the circumstances of the origin of this structure contributes to an on-going debate as to whether interdisciplinarity is orchestrated by funding agencies (Kwa, 2006), is a bottom-up process and "unlikely to be successfully planned" (Rosenberg, 2009), or a combination of both.

When Pelagic and Benthic Scientists First Meet

During the late 1970's and the 1980's, researchers in the pelagic and benthic realms were working almost independently in three different laboratories of UBO. Within the laboratory of chemical oceanography, under the leadership of Paul Tréguer, Professor of biogeochemistry, a group of physical, biogeochemical and biological oceanographers worked on biogeochemical cycles. This group developed a strong expertise on the Si biogeochemical cycle (Tréguer et al., 1995; Ragueneau et al., 2000), due to the importance of this element for the growth of diatoms and the role of diatoms in the functioning of coastal ecosystems (Ragueneau et al., 2006a,b) and in the austral biological pump (Pondaven et al., 2000). Taken altogether, the work produced by this group between 1980 and 2000 provided a description of the pelagic nutrients (Si, N, P) cycles and their relationships with phytoplankton dynamics in rivers, the bay and the adjacent Iroise Sea; it also provided empirical evidence of the benthic-pelagic coupling in the Bay of Brest (Ragueneau et al., 1994, 1996), that led to the suggestion of a coastal silicate pump as a major player in the resistance of the bay to the effects of decreasing Si:N and Si:P ratios (Del Amo et al., 1997).

At UBO, benthic marine biologists were spread between two laboratories: the laboratory of biological oceanography (head, Professor Michel Glémarec) and the laboratory of marine biology (head, Professor Albert Lucas). The most prominent research topic of this group initially concerned marine bivalve aquaculture, and in particular, they accomplished the first successful reproduction and larval rearing of *P. maximus*. By the early 1980's, the group was working on population ecology, larval recruitment, genetics and pathogens. For example, studies were undertaken to characterize, both qualitatively and quantitatively, the benthic macro- and mega-fauna of soft bottom sediments, the importance of benthic biodiversity and the role of hydrological conditions in determining spatial distributions. In addition, the functional roles of benthic species began to be investigated; this includes examining how benthic and pelagic systems were coupled (Hily, 1989; Jean and Thouzeau, 1995) and led to a renewed interest in the role of suspension feeders and their potential influence on phytoplankton biomass by the end of the 1990's (Grall and Glémarec, 1997).

By 1992, the three laboratories were already united under a single name ("*Flux de matière et réponses du vivant*") and led by Prof. Tréguer, but biogeochemists and benthic biologists remained in different buildings. New interactions between pelagic and benthic researchers appeared, such as the official opportunities during quarterly meetings of the "Laboratory Council," as well as additional chances for informal ones during shared cruises on the small research vessel (RV "*Sainte Anne,*" IFREMER). However, these interactions could probably not be characterized as co-construction of scientific questions, but they did contribute to pave the way for the creation of IUEM by the mid-1990's leaded by Prof. Tréguer. When the IUEM building was completed in 1997, the laboratory was renamed "*Laboratoire des sciences de l'environnement marin*" (LEMAR) and installed on one corridor, greatly increasing the opportunities for interdisciplinary exchange. These exchanges occurred both formally (e.g., organization of joint seminars, creation of annual laboratory meetings ("*Les Journées du LEMAR,*" 2001 - present) as well as informally through more regular discussions and debates. It is at this time that the Si/*C. fornicata* working hypothesis emerged.

Origin of the Silicate Pump/*C. fornicata* Hypothesis

Pelagic scientists had looked at the sediment-water interface as a means of replenishing surface waters with nutrients for phytoplankton growth. They suggested the possibility of an active silicate pump that could maintain the diatom populations within the ecosystem (Del Amo et al., 1997). At the same time, benthic scientists looked at pelagic waters and phytoplankton as environmental conditions and food resource influencing the physiology and life cycle of benthic mollusks and ecosystems. They aimed to calibrate shell growth parameters (Guarini et al., 2011) as proxies for environmental variables such as temperature (Chauvaud et al., 2005) or phytoplankton blooms (Lorrain et al., 2000).

Hence, several observations from benthic and pelagic studies led to the formulation of the Si/*C. fornicata* hypothesis. First, if the integrated chlorophyll *a* (Chl-*a*) concentrations did not exhibit major changes during the 1980's and 1990's, phytoplankton bloom compositions did evolve (Nézan et al., 2010, see Chauvaud et al., 2000, Figure 9) and the seasonality index dramatically decreased over the same period: the Chl-*a* annual cycle moved from a typical pattern characterized by a strong first spring bloom and small summer peaks to a succession of higher-frequency but smaller-amplitude blooms over the productive period (Chauvaud et al., 2000). Secondly, the shell daily growth rates of year 1 (1994) and year 2 (1995) cohorts of *P. maximus* exhibited strikingly different patterns between 1994 and 1995, with major growth "accidents" (rate decreases) occurring not only following summer toxic phytoplankton blooms, but also slightly earlier when the spring diatom bloom material sedimented (Chauvaud et al., 1998). The Si/*C. fornicata* hypothesis emerged from the observation of these curves of *P. maximus* shell daily growth rates and the numerous discussions of benthic biologists with phytoplankton experts and biogeochemists, that were facilitated by the new daily interactions among researchers (Chauvaud et al., 2000). The publication of this paper stimulated many studies in the following years, designed to test this hypothesis using experiments (Ragueneau et al., 2002), biogeochemical budgets (Ragueneau et al., 2005), or modeling (Laruelle et al., 2009) and all these studies involved both pelagic and benthic scientists, biogeochemists and benthic ecologists.

We suggest that the construction of the institute "IUEM" represents a good example of the importance of proximity to overcoming barriers to interdisciplinarity. Surprisingly, as noted by Reckers and Hansen (2015), few contributions in the literature on interdisciplinarity have so far analyzed these processes of knowledge construction through the lens of geographical proximity (see Lee et al., 2010, for exception). As such, the IUEM building itself constituted a boundary setting in the sense of Mattor et al. (2014) for the LEMAR laboratory, favoring the daily meeting of scientists from different disciplines and stimulating the emergence of the working hypothesis and the interdisciplinary studies that have been conducted in the 2000's to test it. Clearly, interactions did exist before IUEM, but uniting all the research groups under one roof, increased the opportunities for exchange. As we shall see, the same is presently happening concerning the inclusion of humanities researchers at IUEM today.

The Humanities Enter the Game

The interactions between natural sciences and the humanities around the proliferation of non-indigenous species in the Bay of Brest and eutrophication have become more apparent in the last decade. In the early 2000's, more interaction was stimulated by requests for information from the scallop fishing community facing the effects of the proliferation of *C. fornicata* (see section Construction of a Basis for Interdisciplinary Knowledge About the Bay of Brest). The extremely high abundances of *C. fornicata* were threatening the sustainability of a scallop restocking program started in the early 1980s, through direct (scallop shell scrapping) and indirect (competition for space) effects (Frésard and Boncoeur, 2006). The fishermen needed an economic evaluation for a containment project intended to make the restocking program consistent with the presence of the exotic species, which led to funding a Ph.D. project (Frésard, 2008, under the supervision of an economist, J. Boncoeur, AMURE laboratory "Centre de droit et d'économie de la mer"). Interactions were also encouraged by the French Ministry of the Environment which launched the national INVABIO program (INVAsions BIOlogiques, first call for proposals in February 2000) to fund more humanities-oriented research on non-indigenous species (Dalla Bernardina, 2010). In Brest, two INVABIO projects were funded (2001–2005) to explore the impacts of *C. fornicata* proliferation and its possible containment on the benthic ecosystem (INVABIO I, Coordinator: G. Thouzeau, LEMAR) and on the pelagic ecosystem (INVABIO II, Coordinator: A. Leynaert, LEMAR). Both projects included socio-economic and ethnological components.

These projects yielded important information published separately by the different scientific communities. In the Bay of Brest, the objectives of INVABIO I were to quantify: (1) the impact of small-scale *C. fornicata* removal by dredging on ecosystem functioning (Martin, 2005); (2) the potential changes in predator-prey interactions due to *C. fornicata* and starfish proliferations; and (3) the economic cost and socio-anthropological perception of the invasion (sustainable management). The INVABIO I project was about the restocking of the areas cleaned of slipper limpets with *P. maximus* juveniles (3-cm shell height). The overall cost of the 5-year project was estimated at 3.05 M Euros in the early 2000's. In the end, only the third objective of the INVABIO I project, which also benefited from INVABIO II funding, was fulfilled (Frésard and Boncoeur, 2006), as the local fishermen committee did not get the EU and French funding required for the dredging and restocking operations, for reasons that remain to be understood (cf section Construction of a Basis for Interdisciplinary Knowledge About the Bay of Brest). In the INVABIO II project, the impacts of further proliferation or containment of *C. fornicata* proliferation on phytoplankton dynamics was studied in mesocosm experiments (Fouillaron et al., 2007; Claquin et al., 2010). The costs and benefits analysis published by Frésard and Boncoeur (2006) demonstrated the major importance of indirect effects (competition for space) of the non-indigenous species on the scallop fishery and the importance of combining scallop restocking and local control of the invasion, which could reduce by half the cost of the latter. From an ethnological perspective, another study clearly demonstrated that problems created by non-indigenous species were poorly known by the public, which constitutes a strong impediment to putting in place sustainable management programs for the Bay (Chlous, 2014).

If the inclusion of economists in such programs was expected, the inclusion of an ethnologist was more original. As noted by Menozzi and Pellegrini (2012), the expectation of such sociological studies is related to the perception and representations of biological invasions by different categories of stakeholders as well as to the acceptability of different management options. The aim was then to produce knowledge on human-nature relationships and stimulate thinking about the different ways to manage such invasions (Dalla Bernardina, 2010). Unfortunately, several factors contributed to a clear lack of interactions between the ethnologist and the biologists, according to Chlous (2014), related to the fact that the ethnologist was associated only during the last stages of the proposal writing and that her scientific concerns were poorly taken into account. Indeed, there is a persistent criticism that humanities are being used as window dressing by natural scientists. At the same time, humanities scholars are sometimes reluctant to dive into projects driven by natural sciences. This is a common discussion topic in interdisciplinary projects, including how trust is built between two or more academic communities (Mooney et al., 2013). It is a problem of comprehension that often goes both ways and requires efforts from scholars to take the time to understand the other's objectives, disciplines, language, and way of conducting research (Mattor et al., 2014). There may be historical disparities between disciplines to contend with, such as differences in relative size (in terms of numbers of persons, instrumentation, and funding) and investigative style (especially in the treatment of qualitative information). Staying within disciplinary silos during training does not help with bridging these gaps (Hart et al., 2015). Finally, project durations of only 2–3 years long are too short for trust-building within groups and several boundary settings have been created recently at IUEM to stimulate such interactions.

More Recent Moves Toward Interdisciplinarity at IUEM

If proximity is crucial to overcoming barriers against interdisciplinarity (Reckers and Hansen, 2015), it is not enough, as other barriers extend well beyond a need for frequent interactions. If we are to tackle the complexity of social and ecological systems this requires interactions between very distinct epistemic communities, each of which use different ontologies and epistemologies (Hart et al., 2015, and references therein). They require that scholars take the time and the risk to understand the concepts and tools of other disciplines' cultures, and vocabularies; one also has to admit that developing a shared, if not common, language, or a joint conceptual framework, is not for everyone and strongly depends upon individual commitments or propensities (Mattor et al., 2014). It takes time and it is not rapidly rewarding in terms of scientific articles, which are at the core of a scientist's career progression.

This leads to a second series of difficulties associated with the way universities are organized into academic departments and training programs. Disciplinary divisions within universities are a strong impediment for their having a role in sustainability challenges (Hart et al., 2015). Based on their experience within the Inter-American Institute for global change research (IAI), Pittman et al. (2016) have highlighted the importance of stimulating interdisciplinarity through, not only new incentives using calls for joint proposals but also by: (i) providing space for experiential learning by researchers, (ii) facilitating networking and teamwork across disciplines, (iii) exposing researchers to new concepts and tools, (iv) maintaining persistent mentorship and support for cultivating cross-disciplinary thinking, (v) connecting research to tangible problems, and (vi) monitoring program calls, project selection and implementation. In relation to point (v), it is worth noting that 90% of the researchers involved in IAI's programs indicated the importance of having practical outcomes as a motivating factor for their participation in interdisciplinary research.

Within the IUEM, several interactions between disciplines were already occurring. For example geographers of the LETG-Brest (Littoral, Environnement, Télédétection, Géomatique) laboratory had worked with biologists from the LEMAR laboratory to study biodiversity and human activities, particularly dredging on maerl beds, and lawyers and economists of the AMURE laboratory worked with sedimentologists of the DO (Domaines Océaniques) laboratory to study risks associated with coastal erosion and submersion. For nearly 20 years, a citizen science program to monitor the quality of the water of 13 rivers in region Brittany on a weekly basis has been in existence (Abott et al., 2018) and a forum on citizen science was organized in 2014 to explore scientific, learning and ethical dimensions of such programs.

Nonetheless, if proximity was of major importance for the encounters of scientists working in the parts of the same ecological system, it appeared insufficient for facilitating deeper collaborations on broader topics, and particularly to working on topics in sustainability. Hence, the boundary settings within IUEM itself were moved. Members of the institute undertook several initiatives to identify shared research goals among humanities and natural marine sciences and new paths for conducting joint research and training. First, the *Zone Atelier Brest-Iroise* (ZABrI, part of the French LTER network) was created (in 2012) with the aim of developing conditions for the construction of interdisciplinary projects around the larger objective of understanding the functioning and trends of the Bay of Brest social-ecological system by encouraging stronger interactions between scientists and stakeholders within a sustainability perspective. Entirely new activities arose mixing art and science in the early 2010's, such as for example, the Belmont Forum funded ARTISTICC project which produced unique, hybrid public outreach projects from the mutual investments of artists and scientists. In addition, a trans-disciplinary training module "Science and Society" was introduced in 2012 in the marine sciences Master program (Hubert et al., 2015). A new summer school "Université d'été mer-éducation" was also created that same year, that trains fifty high school teachers in marine sciences and helps them create interdisciplinary courses for their classes.

Three years later, a new core research funding theme on social-ecological systems was added to the LabexMer program (a financial instrument dedicated exclusively to French marine sciences initiatives created in 2011). While, geographers had played a pivotal role in one of its thematic axes since the beginning, as has been seen elsewhere in other interdisciplinary programs (see review in Mooney et al., 2013), the new axis encourages the co-construction of projects involving natural and social and human sciences. For instance, researchers wishing to explore the societal implications of their research using socio-ecological frameworks, such as Ostrom (2009) or Collins et al. (2010).

Finally, a new research group was launched during 2014 within IUEM, "ApoliMer" (Political Anthropology of the Sea). This group associates the SSP with natural sciences studies of marine environments and seeks to integrate both perspectives (Mazé et al., 2015, 2017), primarily through studies concerning the decision-making processes and the sustainable governance of coastal social-ecological systems. These new interactions and perspectives suggested by ApoliMer have raised key questions at the science-policy interface presented in this article that are discussed in the following section.

KEY QUESTIONS AT THE SCIENCE-POLICY-COMMUNITY INTERFACES

In this last section, we put forward key questions about the situation 15 years ago (**Figure 5**) and the present-day situation (**Figure 6**) in the Bay of Brest which arose and arise at the interface between science and decision-making at both the community and political levels.

What Prevented a Containment Project 15 Years Ago?

By the mid-2000s, the fishing community imagined a containment project to protect the restocking program started by the spat hatchery from the excessive abundance of

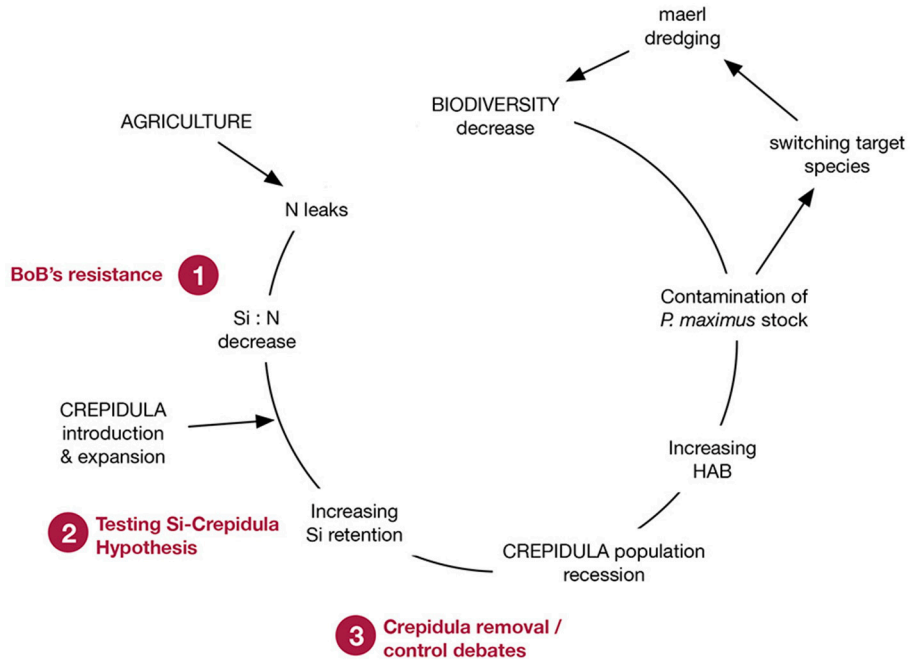

FIGURE 5 | Scientific questions that were raised between 1995 and 2005, concerning the long resistance of the ecosystem to the effects of increasing N delivery from land and changing nutrient ratios (1), the emergence and the testing of the Si/*Crepidula* hyporthesis (2) and the key questions raised at the science-policy-community interface concerning a possible control of the *Crepidula* proliferation (3).

C. fornicata. The scientific community was concerned that an eradication project would cause the collapse of the ecosystem due to the potential role of this species in the prevention of toxic phytoplankton blooms. Many questions were raised (3, in **Figure 5**), by both fishermen and scientists who met to discuss these issues, such as: what to do with the slipper limpets once removed from the seabed and at what cost? Which species would come back following dredging and eradication? What would be the impact on benthic nutrient fluxes and the functioning of the whole ecosystem? How much *C. fornicata* biomass could be removed from the ecosystem without affecting the benthic nutrient fluxes? Controls versus "*laissez-faire*" is always a major management question regarding non-indigenous species (Menozzi and Pellegrini, 2012) and at that time, the latter was chosen. As mentioned earlier, slipper limpet abundances declined monotonically in recent years, with few hypotheses to explain this decrease. But 10 years ago, when *C. fornicata* was thought to endanger the Great Scallop fishery, was this option of "*laissez-faire*" a real choice? Is it because scientists met with fishermen, explained the silicate pump/*C. fornicata* hypothesis? Is it because of the large uncertainties associated with the recolonization of the seabed, or with the impacts on nutrient fluxes and possible toxic phytoplankton blooms? Or is it only because of a lack of funding for removing the slipper limpets and replacing them by scallop juveniles? Answering these questions will require detailed examination by human and social scientists. It implies a reconstruction of the socio-history of the processes at that time and of the interactions between scientists and fishermen, ecosystem managers and decision makers. This socio-history would best be elaborated by crossing political sociology and the sociology of science, bringing another perspective to the new political sociology of science (Frickel and Moore, 2006).

The present situation in the Bay of Brest raises several questions to be explored within natural sciences and human and social sciences, as well as at the interface between these two cultures (Snow, 1959). Within the natural sciences, it will be important to verify that the earlier model (Laruelle et al., 2009) of a link between toxic phytoplankton blooms and a decline in *C. fornicata* abundances is true (4 in **Figure 6**), and to understand the causes of the *Crepidula* recession (4b in **Figure 6**). Answering the first question relates to the validation of the silicate pump/*C. fornicata* hypothesis, now that the C*repidula* numbers are declining; this would imply completing a new inventory of its spatial distribution and biomass, as well as repeating experiments similar to those conducted 15 years ago to test the validity of this hypothesis, in particular those on benthic fluxes and the re-evaluation of biogeochemical budgets. Addressing the second question (related to the recession of the invader) would imply exploring different hypotheses, such as the presence of a pathogen and its possible effects on the *C. fornicata* life cycle, the appearance of a predator for *C. fornicata* (namely starfish), and/or changes in oxygen concentrations at the sediment-water interface. But establishing these links should not overlook additional questions related to the social-ecological system (Liu et al., 2007), more specifically at the interface between science

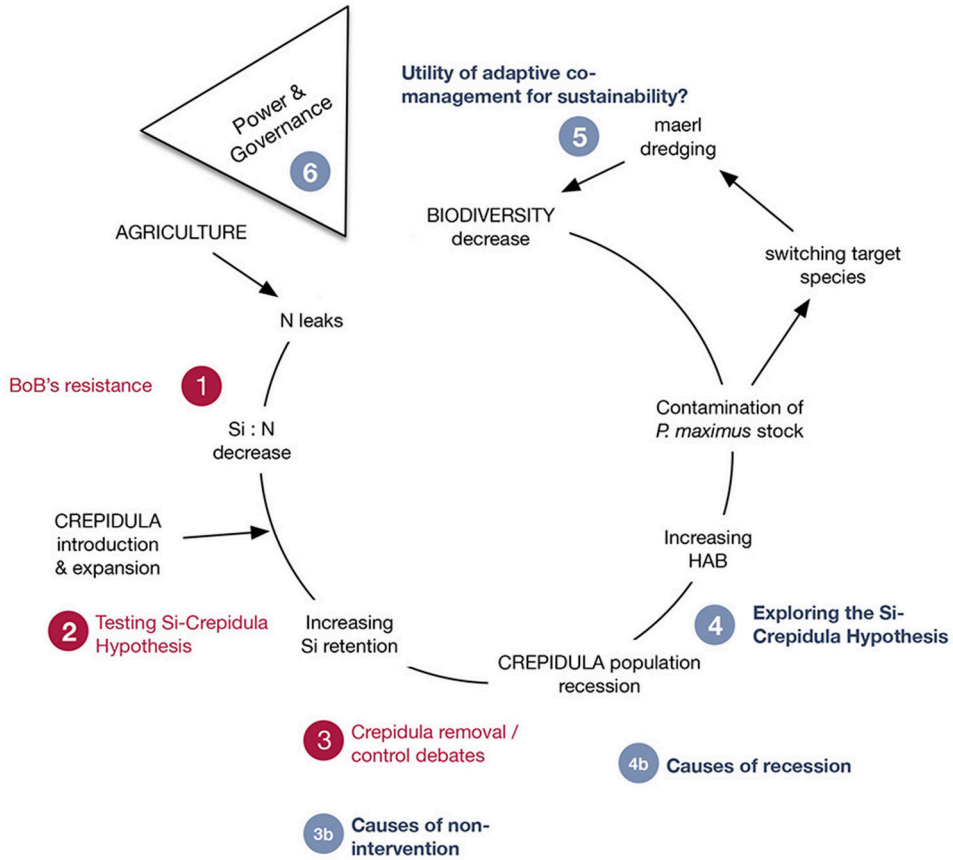

FIGURE 6 | Scientific questions raised today, for natural sciences concerning the causes of the recession of *Crepidula* (4 and 4b) and raised and addressed through an interdisciplinary approach involving the social sciences of politics, regarding the causes of the non-intervention 15 years ago concerning the possible control of *Crepidula* proliferation (3b), the fishing activities on maerl habitat and its impacts on biodiversity (5) and the relations between these fishing activities and agricultural activities on land, that question the governance of the land-ocean continuum (6).

and policy and between scientists and the fishing and farming communities. It is important to recall that the current situation with fishermen dredging on maerl beds arose because toxic phytoplankton blooms prevent harvesting the Great Scallop. These blooms may be linked to changing nutrient ratios modified by *C. fornicata* recession. In addition, the importance of Si in this particular system resulted from the earlier disruption of Si:N and Si:P ratios that originated with the excessive N inputs from intensive agriculture practices in the surrounding watersheds. This cascade of events (**Figure 4**) now yields a fascinating set of interdisciplinary questions at the science-policy interface.

Is Co-adaptive Management a Sufficient Condition for Sustainability?

Why does dredging on maerl beds continue today (question 5 in **Figure 6**), despite the location of these beds within a Natura 2000 area and the clear evidence of their destruction by this technique? How come the tight relationships between fishermen and scientists who have been working together for decades in this ecosystem, have not led to a more sustainable management of these maerl beds? Indeed, interactions between the scientific community and the fishing community have not been restricted to specific interventions in the past. The Great Scallop fishery in the Bay of Brest is relatively small (between 300 and 400 tons per year over the last 15 years) but is very important to the local heritage and economic markets. In the last 50 years, fishermen have had to adapt to several external constraints (Danto et al., in prep.): changes in water quality due to land-derived pollution, invasion of non-indigenous species, epidemics or abrupt climate variations, such as the winter 1962–63 which led to a sharp decline of the scallop standing stock (and a strong decline in landings: from 1,500 tons annually down to <100 tons before the Tinduff hatchery opened).

Since the early 1970's and in collaboration with the local scientific community, fishermen have diversified their activities and experimented developing the stocks or aquaculture of oyster, clam and salmon species. They co-constructed these programs with the scientific community, first with IFREMER (*Institut Français de l'Exploitation de la Mer*) then with benthic marine biologists at the *Université de Bretagne Occidentale*. These programs were funded by local and national authorities who strongly supported this community which was demonstrating

a strong capacity to adapt under difficult conditions. By the early 1980's, the "*Ecloserie du Tinduff,*" a spat hatchery, launched a restocking program for the Great scallop. At the time, this hatchery was quite unusual, as there was only one other hatchery in Okaido (Japan). It is beyond the scope of this paper to document the origins and changes in the practice of this activity. Our purpose here is to simply indicate that these experiments and the creation of this innovative structure which have saved the local Great scallop fishery up to now, have been possible only through the tight connection between the fishing and scientific communities. If these exchanges are a good example of what we would call today "adaptive co-management" (Kofinas, 2009), the present-day situation in the Bay of Brest clearly demonstrates that this is by no means a permanent guarantee of the successful management of biological resources.

It will be crucial to investigate the reasons for this dysfunctioning to move toward sustainability in this ecosystem. Again, key questions need to be investigated at the interface between science, policy and communities. How do the different social groups (professionals/corporations, scientists), with their diverse interests, take charge of this case (fisheries entrepreneurs versus biodiversity conservationists)? How have institutions seized the question? What are the different forms of collective mobilization, conflict and conflict resolution? Is there a consensus and who ultimately decides? The question of decision is so crucial that the most recent program devoted to the study of the interaction between dredging and habitat modification in Natura 2000 areas, which was launched in 2016 by the local fishing authorities with participation by natural scientists, is called DECIDER (to decide, in French). This program aims to reconcile the activities of dredging and preservation of the maerl beds, through the evaluation of the interactions between gear and habitat on the Natura 2000 sites.

What Form of Governance Between Land and Ocean?

Moving landward, more questions arise related to the importance of Si in the system and to excessive N inputs encouraged by intensive agricultural practices. For instance, it would be important to investigate the perception of the Si biogeochemical cycle by decision-makers and whether or not it is being taken into account at the same level (e.g., through systematical measurement) as the N and P cycles. Most long-term observations of water quality in the Brittany region do not include this parameter, despite its demonstrated importance in coastal environments. Is it because of poor knowledge transmission between science and management/decision makers, the so-called "knowledge gap" (Jasanoff, 1990)? Is it because managers know that they can control N and P inputs but not Si inputs? More generally, are the regulation services linked to nutrient recycling really taken into account by decision makers, as easily as provisioning services for example? These questions relate to the way complexity of ecosystems is accounted for at the science-policy interface and to the complexity of this interface itself. Indeed, the chain of events as described in **Figure 4** involves the Si biogeochemical cycle and an "invisible" invader. It is more subtle than the direct effect of excessive N inputs leading to visible and odorous green tides. This calls into question the treatment of complexity and the quality of the indicators that are used to evaluate the ecological and biogeochemical status of a given ecosystem. Have we developed the most appropriate set of indicators that can account for this complexity? This is where it is crucial that social scientists have the possibility to work in close interaction with natural scientists, to explore the way scientific knowledge is being produced and used - or not - in the decision-making process (Mazé et al., 2017).

These questions about complexity and the knowledge gap should not prevent action to be taken, as we also often know enough to do so. But other factors, beyond scientific evidence, are to be taken into account. Green tides have been a major public issue in Brittany for the last 50 years, leading to major conflicts at the land-ocean interface which are still unresolved. Here again, national, regional, and local authorities are working apparently side by side with professionals of agriculture and scientists, to promote changing agricultural practices on the watersheds and reduce the impact of this sector on water quality and ecosystem services. Under the aegis of the GIS CRESEB ("Groupement d'Intérêt Scientifique, Centre de Recherche et d'Expertise sur l'Eau en Bretagne") funded by the Brittany Region in the early 2010's, a permanent group of scientists, covering many disciplines from agronomy to marine biogeochemistry, from sociology to law and economics, is meeting regularly to discuss how to best accompany the projects of local territories in the region subject to litigation, to favor the transformation toward sustainability. Scientists involved in this group discuss their role in this transformation, being aware of the difficulty of such an exercise, thanks to earlier experiences with French national plans against green algae proliferation. In parallel to these efforts, important decisions are taken by public authorities that allow the persistence of the agro-industrial agriculture model, already denounced in several reports from NGO's and from the "Cour des comptes." Power issues here play a key role in this blockage between the state, the agro-industrial lobby and the impact on farmers, their practices, human health and ecosystems. What is the role of power relations in the conditions of possibility and impossibility of transformation to sustainability? What is the role of scientists in the process of reflection, accompanying this transformation? The argument about the lack of knowledge continues to be mobilized, thus promoting inaction, and what does it means in terms of instrumentalization? This is where political science could provide major insight into the so-called implementation gap, related to inertia of the institutional and political systems. Many factors have been put forward to explain it. They have been identified through the "path dependency" concept, ratchet effects and other self-reinforcing mechanisms. Within the framework of the new political sociology of science (Frickel and Moore, 2006), we need to address the use of scientific knowledge by decision makers, taking into account the diversity of interests and exploring the decision-making context and process, combining knowledge, and power, something which is too rarely done in environmental studies (Fabinyi et al., 2014) which is especially the case when dealing with transformation more than with adaptation (Olsson et al., 2014).

As tentatively shown in **Figure 6** (6), addressing these questions of power and governance of the land-ocean continuum may be one way to "close the loop" and re-link the communities of agriculture and fishing/aquaculture. For a long time, agriculture and fishing have been closely related in Brittany, often with a single person sharing his time between both activities. Today practices have changed, and nitrate leaks have become an element of division between the two communities. The cascade of events described earlier (section The Bay of Brest ecosystem since WWII and **Figure 4**) demonstrates the complexity of the ecosystem functioning. However, the way we ask the questions at the science-policy interface in this section (5 and 6 in **Figure 6**), from maerl beds to agricultural practices, suggests that we now address the complexity of the social-ecological system, taking into account these retro-actions from sea to land. This implies that scientists, the different stakeholders and decision-makers work together and that interdisciplinarity makes progress, especially between natural and human and social sciences.

PERSPECTIVES

Following the description of the environmental trends observed in the Bay of Brest over the past five decades, a series of questions has been raised at the science-policy-communities interfaces. The social sciences of politics, in close collaboration with marine environmental sciences, will now analyze the decision-making process concerning the management of the Bay of Brest and the adjacent Iroise Sea, benefiting from the new boundary settings described in section Construction of a Basis for Interdisciplinary Knowledge About the Bay of Brest. From the perspective of historical and political sociology, it will be necessary to reconstruct the socio-history of the management of the bay, paying particular attention to the interactions between scientists, naturalists, fishermen, farmers and managers. The interaction between fishermen and farmers seems indeed necessary for negotiations to progress toward the sustainable management of the Bay of Brest because of the inextricable link between eutrophication and the ecological status of the bay which impacts severely fishing communities. This is what is meant in **Figure 6**, by the circular aspect of the figure and the triangle aiming at closing the circle, representing these questions to be addressed at the science-policy interface, which imply that we explore the governance of the land-sea continuum. These questions will have to evolve based on a reflection on the history of science and technology, but even more so in the context of the new political sociology of science so that we can grasp the power games around the question of expertise (Bérard and Crespin, 2010).

Exploring sustainability challenges requires strong interdisciplinary approaches and we have used our study case to derive important insights, particularly on the importance of geographical proximity and the establishment of boundary settings to stimulate a better integration of social and human sciences in the study of LTER sites, turning them into LTSER sites. Here again, the importance of creating boundary settings in immersion within an environment of natural sciences, reflects the role of geographical proximity but, this time at the interface between humanities and natural sciences. The creation of ApoliMer at IUEM and the recent arrival of economists and jurists from the AMURE laboratory within a just-completed extension (opened in 2016) of the IUEM building, achieves now, nearly two decades after the opening of the first buildings, the original intentions of the University to construct facilities suitable for interdisciplinary approaches by bringing together in a single location, researchers concerned with the marine environment.

This observation raises key questions that, we believe, should be taken extremely seriously by those in charge of the politics of science, concerning both research and training. Trust is an essential component of these interactions among scientists from different disciplines, and between science and society, and it takes time to build. We have seen in section Construction of a Basis for Interdisciplinary Knowledge About the Bay of Brest that the interdisciplinary knowledge built, first between pelagic and benthic scientists, and now between biogeochemists, ecologists, and political scientists (all authors on this manuscript), was and is possible mostly thanks to the existence of permanent research staff remaining in place over many years, and to the construction of infrastructures and boundary settings that facilitate long-term interactions among different epistemic communities. It appears that these crucial needs for sustainability science and action diverge strongly from the on-going growth of the scientific field, still favoring positions on soft money, extreme mobility, the precarious place of young researchers, and enhanced competition. Even the scientific careers of permanent staff continue to be evaluated mostly on the impact factor criteria, neglecting the time it takes for these scientists involved in inter- and trans-disciplinary approaches to build trust and fundamental knowledge that needs to be co-constructed, amongst various disciplines, and at the interface between scientific and other forms of knowledge. Last but not least, this evolution toward sustainability raises many other key questions, especially about the training of the next generation of students. Depth *versus* breadth is an important debate in Master and Ph.D. programs. Do we encourage training of "hybrid" students, better able to address complex problems but probably less specialized in one particular field, or do we train very specialized students and find new ways to help them being able to interact with other researchers from very distant fields? When should interdisciplinarity be introduced in a student cursus? Does a student trained interdisciplinary have equal chances to find a position related to his experience, within or outside academia, as one trained in a specific field? Most probably, the emergence of the field of sustainability science offers a wonderful field for the sociology of science, be it concerning training, or the many questions that this field raises concerning our role of scientists on this path toward sustainability.

AUTHOR CONTRIBUTIONS

OR has written the manuscript, with strong inputs from MR, CM, and JC-G regarding the content and the structure of the manuscript. Being native American, JC-G did a lot of editing as well. Other authors are listed in alphabetic order, they have contributed a lot to the research reviewed in this manuscript and provided important comments and suggestions on the manuscript.

FUNDING

The authors wish to thank the French CNRS for its funding through the Zone Atelier Brest-Iroise (ZABrI), part of the French LTER network. This is a contribution to the ARTISTICC project (Adaptation Research a Transdisciplinary Community and Policy Centered Approach), funded by the Belmont Forum International Opportunity Fund (2014–2017) and the SPA (Savoir, Pouvoir, Avoir) project funded (2017–2019) by the French CNRS (Mission for interdisciplinarity).

REFERENCES

Abott, B. W., Moatar, F., Gauthier, O., Fovet, O., Antoine, V., and Ragueneau, O. (2018). Trends and seasonality of river nutrients in agricultural catchments: 18 years of weekly citizen science in France. *Sci. Total Environ*. 624, 845–858. doi: 10.1016/j.scitotenv.2017.12.176

Amice, G., Wensel, J., and Grall, J. (2007). *Synthèse des Connaissances sur le Maërl: Écologie, état des Lieux des Bancs Français et Européens, Cadre Réglementaire.* Rapport UBO-IUEM LEMAR UMR 6539, CREOCEAN (coord.).

Armitage, D. R., Plummer, R., Berkes, F., Arthur, R. I., Charles, A. T., Davidson-Hunt, I. J., et al. (2009). Adaptive co-management for social-ecological complexity. *Front. Ecol. Environ.* 7, 95–102. doi: 10.1890/070089

Belin, C., Chapelle, A., Delmas, D., Nezan, E., and Siano, R. (2013). *DYNAPSE: DYNAmiques des Efflorescences et de la Toxicité des Espèces Phytoplanctoniques Nuisibles du Genre PSEudo-Nitzschia en Région Loire-Bretagne. IFREMER Report 2013 - R.INT.ODE/DYNECO/PELAGOS/2013-01.* Available online at: http://archimer.ifremer.fr/doc/00189/30035/28521.pdf (Accessed August 14, 2015).

Bérard, Y., and Crespin, R. (2010). *Aux Frontières de l'expertise. Dialogues Entre Savoirs et Pouvoirs.* Rennes: Presses Universitaires de Rennes, coll., Res Publica, 277.

Beucher, C., Tréguer, P., Corvaisier, R., Hapette, A. M., and Elskens, M. (2004). Production and dissolution of biosilica and changing microphytoplankton dominance in the Bay of Brest (France). *Mar. Ecol. Prog. Ser.* 267, 57–69. doi: 10.3354/meps267057

Billen, G., and Garnier, J. (2007). River basin nutrient delivery to the coastal sea: assessing its potential to sustain new production of non-siliceous algae. *Mar. Chem.* 106, 148–160. doi: 10.1016/j.marchem.2006.12.017

Binder, C. R., Hinkel, J., Bots, P. W. G., and Pahl-Wostl, C. (2013). Comparison of frameworks for analyzing social-ecological systems. *Ecol. Soc.* 18:26. doi: 10.5751/ES-05551-180426

Blanchard, M. (2009). Recent expansion of the slipper limpet population (Crepidula fornicata) in the Bay of Mont Saint-Michel (Western Channel, France). *Aquat. Living Resour.* 22, 11–19. doi: 10.1051/alr/2009004

Bremer, S., and Glavovic, B. (2013). Mobilizing knowledge for coastal governance: re-framing the science–policy interface for integrated coastal management. *Coast. Manage.* 41, 39–56. doi: 10.1080/08920753.2012.749751

Brundtland, G. H. (1987). *Our Common Future, Report of the World Commission on Environment and Development*. Oxford: Oxford University Press.

Brzezinski, M. A. (1985). The Si:N ratio of marine diatoms: interspecific variability and the effect of some environmental variables. *J. Phycol.* 21, 347–357. doi: 10.1111/j.0022-3646.1985.00347.x

Butler, J. R., Young, J. C., McMyn, I. A. G., Leyshon, B., Graham, I. M., Walker, I., et al. (2015). Evaluating adaptive co-management as conservation conflict resolution: learning from seals and salmon. *J. Environ. Manage.* 160, 212–225. doi: 10.1016/j.jenvman.2015.06.019

Carlton, J. T., and Geller, J. B. (1993). Ecological roulette: the global transport of nonindigeneous marine organisms. *Science* 261, 78–82. doi: 10.1126/science.261.5117.78

Chapelle, A., Le Gac, M., Labry, C., Siano, R., Quere, J., Caradec, F., et al. (2015). The Bay of Brest (France), a new risky site for toxic Alexandrium minutum bloom and PSP shellfish contamination. *Harmful Algae News* 51, 4–5.

Chauvaud, L. (1998). *La coquille Saint-Jacques en rade de Brest: Un Modèle Biologique D'étude des Réponses de la faune Benthique aux Fluctuations de l'environnemen.* Thèse de doctorat de l'Université de Bretagne Occidentale, spécialité Océanologie Biologique, Brest.

Chauvaud, L., Jean, F., Ragueneau, O., and Thouzeau, G. (2000).. Long-term variation of the Bay of Brest ecosystem: benthic-pelagic coupling revisited. *Mar. Ecol. Prog. Ser.* 200, 35–48. doi: 10.3354/meps200035

Chauvaud, L., Lorrain, A., Dunbar, R. B., Paulet, Y.-M., Thouzeau, G., Jean, F., et al. (2005). The shell of the Great Scallop Pecten maximus as a high frequency archive of paleoenvironmental change. *Geochem. Geophys. Geosyst.* 6, 1–15. doi: 10.1029/2004GC000890

Chauvaud, L., Thouzeau, G., and Paulet, Y.-M. (1998). Effects of environmental factors on the daily growth rate of Pecten maximus juveniles in the Bay of Brest. *J. Exp. Mar. Biol. Ecol.* 227, 83–111. doi: 10.1016/S0022-0981(97)00263-3

Chlous, F. (2014). *L'invasion Biologique de la Crépidule: une Question Sociale? L'ethnologue dans la Tourmente*. Available online at: http://www.ethnographiques.org, 27.

Christie, P. (2011). Creating space for interdisciplinary marine and coastal research: five dilemmas and suggested resolutions. *Environ. Conserv.* 38, 172–186. doi: 10.1017/S0376892911000129

Claquin, P., Ni Longphuirt, S., Fouillaron, P., Huonnic, P., Ragueneau, O., Klein, C., et al. (2010). Effects of simulated benthic fluxes on phytoplankton dynamic and photosynthetic parameters in a mesocosm experiment (Bay of Brest, France). *Estuar. Coast. Shelf Sci.* 86, 93–101. doi: 10.1016/j.ecss.2009.10.017

Cloern, J. E., Abreu, P. C., Carstensen, J., Chauvaud, L., Elmgren, R., Grall, J., et al. (2015). Human activities and climate variability drive fast-paced change across the world's estuarine-coastal ecosystems. *Glob. Chang. Biol.* 22, 513–529. doi: 10.1111/gcb.13059

Collins, S. L., Carpenter, S. R., Swinton, S. M., Orenstein, D. E., Childers, D. L., Gragson, T. L., et al. (2010). An integrated conceptual framework for long-term social–ecological research. *Front. Ecol. Environ.* 9, 351–357. doi: 10.1890/100068

Conley, D. J. (1997). Riverine contribution of biogenic silica to the oceanic silica budget. *Limnol. Oceanogr.* 42, 774–777. doi: 10.4319/lo.1997.42.4.0774

Conley, D. J., Schelske, C. L., and Stoermer, E. F. (1993). Modification of the biogeochemical cycle of silica with eutrophication. *Mar. Ecol. Prog. Ser.* 101, 179–192. doi: 10.3354/meps101179

Coquereau, L., Jolivet, A., Hégaret, H., and Chauvaud, L. (2017). Short-term behavioural responses of the great scallop Pecten maximus exposed to the toxic algal Alexandrium minutum measured by accelerometry and passive acoustics. *PLoS ONE* 11:e0160935. doi: 10.1371/journal.pone.0160935

Daily, G. C. (1997). "Introduction: what are ecosystem services?," in *Nature ís Services: Societal Dependence on Natural Ecosystems*, ed G. C. Daily (Washington, DC: Island Press), 1–10.

Dalla Bernardina, S. (2010). "Les invasions biologiques sous le regard des sciences de l'homme," in *Les Invasions Biologiques Une Question de Natures et de Sociétés*, eds R. Barbault and M. Atramentowicz (Quae: Paris), 65–108.

Dame, R. F. (1993). *Bivalve Filter Feeders In Estuarine and Coastal Ecosystem Processes*. Heidelberg: Springer-Verlag.

Del Amo, Y., Le Pape, O., Tréguer, P., Quéguiner, B., Menesguen, A., and Aminot, A. (1997). Impacts of high-nitrate freshwater inputs on macrotidal

ecosystems. I. Seasonal evolution of nutrient limitation for the diatom-dominated phytoplankton of the Bay of Brest (France). *Mar. Ecol. Prog. Ser.* 161, 213–224. doi: 10.3354/meps161213

Dutertre, M., Grall, J., Ehrhold, A., and Hamon, D. (2015). Environmental factors affecting maerl bed structure in Brittany (France). *Eur. J. Phycol.* 50, 371–383. doi: 10.1080/09670262.2015.1063698

Fabinyi, M., Evans, L., and Foale, S. J. (2014). Social-ecological systems, social diversity, and power: insights from anthropology and political ecology. *Ecol. Soc.* 19:28. doi: 10.5751/ES-07029-190428

Fabioux, C., Sulistiyani, Y., Haberkorn, H., Hégaret, H., and Soudant, P. (2015). Exposure to toxic Alexandrium minutum activates the antioxidant and detoxifying systems of the oyster *Crassostrea gigas*. *Harmful Algae* 48, 55–62. doi: 10.1016/j.hal.2015.07.003

Fouillaron, P., Claquin, P., L'Helguen, S., Huonnic, P., Martin-Jézéquel, V., Masson, A., et al. (2007). Response of a phytoplankton community to increased nutrient inputs: a mesocosm experiment in the Bay of Brest (France). *J. Exp. Mar. Biol. Ecol.* 351, 188–198. doi: 10.1016/j.jembe.2007.06.009

Frésard, M. (2008). *Analyse Économique de Contrôle d'une Invasion Biologique. Modélisation Théorique et Application aux Pêcheries de Coquille Saint-Jacques Envahies par la Crépidule.* Thèse de 3ème cycle, Université de Bretagne Occidentale.

Frésard, M., and Boncoeur, J. (2006). Costs and benefits of stock enhancement and biological invasion control: the case of the Bay of Brest scallop fishery. *Aquat. Living Resour.* 19, 299–305. doi: 10.1051/alr:2006031

Frickel, S., and Moore, K. (2006). *The New Political Sociology of Science: Institutions, Networks, and Power*. Madison, WI: University of Wisconsin Press.

Grall, J., and Glémarec, M. (1997). Using biotic indices to estimate macrobenthic community perturbations in the Bay of Brest. *Estuar. Coast. Shelf Sci.* 44 (Suppl. A), 43–53. doi: 10.1016/S0272-7714(97)80006-6

Grall, J., Guillamont, B., and Bajjouk, T. (2009). *Fiche de Synthèse d'habitat "Maërl"*. Rapport du REBENT.

Grall, J., and Hall-Spencer, J. M. (2003). Problems facing maerl conservation in Brittany. *Aqua. Conserv.* 13, 55–64. doi: 10.1002/aqc.568

Guarini, J.-M., Chauvaud, L., Cloern, J. E., Clavier, J., and Coston-Guarini, J. (2011). Seasonal variations in ectotherm growth rates: Quantifying growth as an intermittent non steady state compensatory process. *J. Sea Res.* 65, 355–361. doi: 10.1016/j.seares.2011.02.001

Guérin, L. (2004). *La Crépidule en Rade de Brest: Un Modèle Biologique d'espèce Introduite Proliférante en Réponse Aux Fluctuations de L'environnement*. Thèse de doctorat de l'Université de Bretagne Occidentale, Brest.

Hall-Spencer, J. M., Grall, J., Moore, P. G., and Atkinson, R. J. A. (2003). Bivalve fishing and maerl-bed conservation in France and the UK—retrospect and prospect. *Aqua. Conser.* 13, 33–41. doi: 10.1002/aqc.566

Hart, D. D., Bell, K. P., Lindenfeld, L. A., Jain, S., Johnson, T. R., Ranco, D., et al. (2015). Strengthening the role of universities in addressing sustainability challenges: the mitchell center for sustainability solutions as an institutional experiment. *Ecol. Soc.* 20:4. doi: 10.5751/ES-07283-200204

Hily, C. (1984). *Variabilité de la Macrofaune Benthique dans Les Milieux Hyper-Trophiques de la Rade de Brest.* Thèse de doctorat, Université de Bretagne Occidentale.

Hily, C. (1989). La mégafaune benthique de la rade de Brest : pre-échantillonnage par vidéo sous-marine. *Cah. Biol. Mar.* 30, 433–454.

Holling, C. S. (2001). Understanding the complexity of economic, ecological, and social systems. *Ecosystems* 4, 390–405. doi: 10.1007/s10021-001-0101-5

Hubert, A., Ragueneau, O., Sansjofre, P., and Tréguier, A.-M. (2015). "Exploration de controverses socio-scientifiques en sciences de la mer et du littoral: une unité d'enseignement interdisciplinaire associant doctorants et étudiants de Master," in *Actes du VIII colloque Questions de Pédagogie dans l'Enseignement Supérieur* (Brest), 509–519.

Jasanoff, S. (1990). *The Fifth Branch: Science Advisers as Policymakers.* Cambridge, MA; London: Harvard University Press.

Jean, F., and Thouzeau, G. (1995). Estimate of state variables of a trophic web model in the Bay of Brest. *Crit. Rev. Acad. Sci.* 318, 145–154.

Kates, R. W., Clark, W. C., Corell, R., Hall, J. M., Jaeger, C. C., Lowe, I., et al. (2001). Environment and development, sustainability science. *Policy Forum Sci.* 292, 641–642. doi: 10.1126/science.1059386

Kates, R. W. (2011). What kind of science is sustainability science? *Proc. Natl. Acad. Sci. U.S.A.* 108, 19449–19450. doi: 10.1073/pnas.1116097108

Kautsky, N., and Evans, S. (1987). Role of biodeposition by Mytilus edulis in the circulation of matter and nutrients in a Baltic coastal ecosystem. *Mar. Ecol. Prog. Ser.* 38, 201–212. doi: 10.3354/meps038201

Kofinas, G. P. (2009). "Adaptive co-management in social-ecological governance," in *Principles of Ecosystem Stewardship, Resilience-Based Natural Resource Management in a Changing World,* eds F. S. III. Chapin, G. P. Kofinas, and C. Folke (New York, NY: Springer), 77–101.

Kueffer, C. E., Underwood, E., Hirsch Hadorn, G., Holderegger, R., Lehning, M., Edwards, P. et al. (2012). Enabling effective problem-oriented research for sustainable development. *Ecol. Soc.* 17:8. doi: 10.5751/ES-05045-170408

Kwa, C. (2006). The programming of interdisciplinary research through informal science-policy interactions. *Sci. Public Policy* 33, 457–467. doi: 10.3152/147154306781778786

Lang, D. J., Wiek, A., Bergmann, M., Stauffacher, M., Martens, P., Moll, P., et al. (2012). Transdisciplinary research in sustainability science: practice, principles and challenges. *Sustain. Sci.* 7(Suppl. 1), 25–43. doi: 10.1007/s11625-011-0149-x

Laruelle, G., V., Roubeix, A., Sferratore, B., Brodhern, D., Ciuffa, D., Garnier, C., et al. (2009). Modeling the global silica cycle: response to temperature rise and river damming. *Glob. Biogeochem. Cyc.* 23:4031. doi: 10.3354/meps07884

Lee, K., Brownstein, J. S., Mills, R. G., and Kohane, I. S. (2010). Does Collocation Inform the Impact of Collaboration? *PLoS ONE* 5:e14279. doi: 10.1371/journal.pone.0014279

Le Pape, O., Del Amo, Y., Menesguen, A., Aminot, A., Quequiner, B., and Tréguer, P. (1996). Resistance of a coastal ecosystem to increasing eutrophic conditions: the Bay of Brest (France), a semi-enclosed zone of Western Europe. *Continent. Shelf Res.* 16:1885. doi: 10.1016/0278-4343(95)00068-2

Le Pape, O., and Menesguen, A. (1997). Hydrodynamic prevention of eutrophication in the Bay of Brest (France), a modelling approach. *J. Mar. Syst.* 12, 171–186. doi: 10.1016/S0924-7963(96)00096-6

Liu, J., Dietz, T., Carpenter, S. R., Alberti, M., Folke, C., Moran, E., et al. (2007). Complexity of coupled human and natural systems. *Science* 317, 1513–1516. doi: 10.1126/science.1144004

Lorrain, A., Paulet, Y.-M., Chauvaud, L., Savoye, N., Nezan, E., and Guerin, L. (2000). Growth anomalies in Pecten maximus from coastal waters (Bay of Brest, France): relationship with diatom blooms. *J. Mar. Biological. Assoc.* 80, 667–673. doi: 10.1017/S0025315400002496

Martin, S. (2005). *Rôle D'une Espèce Exploitée, le Maerl et D'une Espèce Invasive, la Crépidule, sur les Flux à L'interface eau-Sédiment en Rade de Brest*. Thèse de doctorat, Université de Bretagne Occidentale.

Martin, S., Thouzeau, G., Chauvaud, L., Jean, F., Guérin, L., and Clavier, J. (2006). Respiration, calcification and excretion of the invasive limpet, *Crepidula fornicata* L.: implications for carbon carbonate and nitrogen fluxes. *Limnol. Oceanogr.* 51, 1996–2007. doi: 10.4319/lo.2006.51.5.1996

Martin, S., Thouzeau, G., Richard, M., Chauvaud, L., Jean, F., and Clavier, J. (2007). Benthic community respiration in areas impacted by the invasive mollusk, *Crepidula fornicata* L. *Mar. Ecol. Prog. Ser.* 347, 51–60. doi: 10.3354/meps07000

Matson, P., Clark, W. C., and Anderson, K. (2016). *Pursuing Sustainability: A Guide to the Science and Practice*. Princeton University Press.

Mattor, K., Betsill, M., Huayhuaca, C., Huber-Stearns, H., Jedd, T., Sternlieb, F., et al. (2014). Transdisciplinary research on environmental governance: a view from the inside. *Environ. Sci. Policy* 42, 90–100. doi: 10.1016/j.envsci.2014.06.002

Mazé, C., Dahou, T., Ragueneau, O., Danto, A., Mariat-Roy, E., Raimonet, M., et al. (2017). Knowledge and power in integrated coastal management: for a political anthropology of the sea combined with the marine environment sciences. *Compte Rendus Geosci.* 349, 359–368. doi: 10.1016/j.crte.2017.09.008

Mazé, C., Ragueneau, O., Weisbein, J., and Mariat-Roy, E. (2015). Pour une anthropologie politique de la mer. *Rev. Int. Ethnograph.* 5, 189–202.

Millennium Ecosystem Assessment (2005). *Ecosystems and Human Well-being: Synthesis*. Washington, DC: Island Press.

Menozzi, M.-J., and Pellegrini, P. (2012). La gestion des espèces exotiques envahissantes: de la recherche d'une solution technique à la construction d'un collectif. *Sci. Eaux Territ.* 1, 106–113.

Meybeck, M. (1982). Carbon, nitrogen and phosphorus transport by world rivers. *Am. J. Sci.* 282, 401–450. doi: 10.2475/ajs.282.4.401

Mollinga, P. (2010). Boundary work and the complexity of natural resources management. *Crop Sci.* 50(Suppl. 1), S1–S9. doi: 10.2135/cropsci2009.10.0570

Mooney, H. A., Duraiappah, A., and Larigauderie, A. (2013). Evolution of natural and social science interactions in global change research programs. *Proc. Natl. Acad. Sci. U.S.A.* 110, 3665–3672. doi: 10.1073/pnas.1107484110

Moulin, F. Y., Guizien, K., Thouzeau, G., Chapalain, G., Mülleners, K., and Bourg, C. (2007). Impact of an invasive species, Crepidula fornicata L., on the hydrodynamic and transport properties of the benthic boundary layer. *Aqua. Living Resour.* 20, 15–31. doi: 10.1051/alr:2007012

Nézan, E., Chomérat, N., Bilien, G., Boulben, S., Duval, A., and Ryckaert, M. (2010). Pseudo-nitzschia australis on French Atlantic coast - an unusual toxic bloom. *Harmful Algae News* 41, 1–2.

Norkko, A., Hewitt, J. E., Thrush, S. F., and Funnell, T. (2001). Benthic-pelagic coupling and suspension feeding bivalves: linking site-specific sediment flux and biodeposition to benthic community structure. *Limnol. Oceanogr.* 46, 2067–2072. doi: 10.4319/lo.2001.46.8.2067

Officer, C. B., and Ryther, J. H. (1980). The possible importance of silicon in marine eutrophication. *Mar. Ecol. Prog. Ser.* 3, 83–91. doi: 10.3354/meps003083

Olsson, P., Galaz, V., and Boonstra, W. J. (2014). Sustainability transformations: a resilience perspective. *Ecol. Soc.* 19:1. doi: 10.5751/ES-06799-190401

Ostrom, E. (2009). A general framework for analyzing social-ecological systems. *Science* 325, 419–422. doi: 10.1126/science.1172133

Pantalos, M. (2015). *Clam Dredging and Maerl Bed Health in the South Basin of the Bay of Brest.* Mémoire de stage de Master 2, Université de Bretagne Occidentale.

Pittman, J., Tiessen, H., and Montana, E. (2016). *The Evolution of Interdisciplinarity Over 20 Years pf Global Change Research by the IAI*. A report from the Inter-American Institute for global change research.

Plummer, R., Armitage, D. R., and de Loë, R. C. (2013). Adaptive comanagement and its relationship to environmental governance. *Ecol. Soc.* 18:21. doi: 10.5751/ES-05383-180121

Pondaven, P., Ragueneau, O., Tréguer, P., Hauvespre, A., Dezileau, L., and Reyss, J.-L. (2000). Resolving the opal paradox in the Southern Ocean. *Nature* 405, 168–172. doi: 10.1038/35012046

Quéguiner, B. (1982). *Variations Qualitatives et Quantitatives du Phytoplancton dans un Écosystème Eutrophe Fortement Soumis aux Effets des Marées : la Rade de Brest.* Brest: Thèse de 3ème cycle, Université de Bretagne Occidentale, 123.

Ragueneau, O., Chauvaud, L., Leynaert, A., Thouzeau, G., Paulet, Y.-M., Bonnet, S., et al. (2002). Direct evidence of a biologically active coastal silicate pump: ecological implications. *Limnol. Oceanogr.* 47, 1849–1854. doi: 10.4319/lo.2002.47.6.1849

Ragueneau, O., Chauvaud, L., Moriceau, B., Leynaert, A., Thouzeau, G., Donval, A., et al. (2005). Biodeposition by an invasive suspension feeder impacts the biogeochemical cycle of Si in a coastal ecosystem (Bay of Brest, France). *Biogeochemistry* 75, 19–41. doi 10.1007/s10533-004-5677-3.

Ragueneau, O., Conley, D. J., DeMaster, D. J., Durr, H., and Dittert, N. (2010). "Si transformations along the land-ocean continuum: implications for the global C cycle. Dans: Carbon and nutrient fluxes in continental margins," in *IGBP Series,* L. Atkinson, K.-K. Liu, R. Quinones, and L. Talaue-MacManus (Berlin; Heidelberg: Springer-Verlag), 515–527.

Ragueneau, O., Conley, D. J., Ni Longphuirt, S., Slomp, C., and et Leynaert, A. (2006a). "A review of the Si biogeochemical cycle in coastal waters, I: diatoms in coastal food webs and the coastal Si cycle. Dans: Land-Ocean nutrient fluxes: silica cycle," in *SCOPE Book,* eds V. Ittekkot, C. Humborg, and J. Garnier (Washington, DC: Island Press), 163–195.

Ragueneau, O., Conley, D. J., Ni Longphuirt, S., Slomp, C., and et Leynaert, A. (2006b). "A review of the Si biogeochemical cycle in coastal waters, II: anthropogenic perturbation of the Si cycle and responses of coastal ecosystems. Dans: Land-Ocean nutrient fluxes: silica cycle," in *SCOPE Book*, eds V. Ittekkot, C. Humborg, and J. Garnier (Washington, DC: Island Press), 197–213.

Ragueneau, O., De Blas Varela, E., Tréguer, P., Quéguiner, B., and Del Amo, Y. (1994). Phytoplankton dynamics in relation to the biogeochemical cycle of silicon in a coastal ecosystem of Western Europe. *Mar. Ecol. Prog. Ser.* 106, 157–172. doi: 10.3354/meps106157

Ragueneau, O., Tréguer, P., Leynaert, A., Anderson, R. F., Brzezinski, M. A., DeMaster, D. J., et al. (2000). A review of the Si cycle in the modern ocean: recent progress and missing gaps in the application of biogenic opal as a paleoproductivity proxy. *Glob. Planet. Change* 26, 317–365. doi: 10.1016/S0921-8181(00)00052-7

Ragueneau, O., Quéguiner, B., and Tréguer, P. (1996). Contrast in biological responses to tidally-induced vertical mixing for two macrotidal ecosystems of Western Europe. *Estuar. Coast. Shelf Sci.* 42, 645–665. doi: 10.1006/ecss.1996.0042

Reckers, J. V., and Hansen, T. (2015). Interdisciplinary research and geography: overcoming barriers through proximity. *Sci. Public Policy* 42, 242–254. doi: 10.1093/scipol/scu048

Redfield, A. C. (1958). The biological control of chemical factors in the environment. *Am. Sci.* 46, 205–222.

Roberts, E. C., Davidson, K., and Gilpin, L. C. (2003). Response of temperate microplankton communities to N:Si ratio perturbation. *J. Plankton Res.* 25, 1–11. doi: 10.1093/plankt/fbg109

Rosenberg, N. (2009). Some critical episodes in the progress of medical innovation: an Anglo-American perspective. *Res. Policy* 38, 234–242. doi: 10.1016/j.respol.2008.12.007

Rousseau, V., Leynaert, A., Daoud, N., and Lancelot, C. (2002). Diatom succession, silicification and silicic acid availability in Belgian coastal waters (Southern North Sea). *Mar. Ecol. Prog. Ser.* 236, 61–73. doi: 10.3354/meps236061

Schultz, L., Folke, C., Österblom, H., and Olsson, P. (2015). Adaptive governance, ecosystem management and natural capital. *Proc. Natl. Acad. Sci. U.S.A.* 112, 7369–7374. doi: 10.1073/pnas.1406493112

Smayda, T. J. (1990). "Novel and nuisance of phytoplankton blooms in the sea: evidence for a global epimedia" in *Toxic Marine Phytoplankton,* eds E. Graneli (New York, NY: Elsevier Science Publishing Co), 29–40.

Snow, C. P. (1959). *The Two Cultures and the Scientific Revolution*. Cambridge: Cambridge University Press.

Stiger-Pouvreau, V., and Thouzeau, G. (2015). Marine species introduced on the French Channel-Atlantic coasts: a review of main biological invasions and impacts. *Open J. Ecol.* 5, 227–257. doi: 10.4236/oje.2015.55019

Thouzeau, G., Chauvaud, L., Grall, J., and Guérin, L. (2000). Do biotic interactions control pre-recruitment and growth of *Pecten maximus* (L.) in the Bay of Brest? *Crit. Rev. Acad. Sci.* 323, 815–825.

Tréguer, P., Nelson, D. M., Van Bennekom, A. J., DeMaster, D. J., Leynaert, A., and Quéguiner, B. (1995). The silica balance in the world ocean: a reestimate. *Science* 268, 375–379. doi: 10.1126/science.268.5209.375

Turner, R. K. (2015). "Introduction," in *Coastal Zones Ecosystem Services. Studies in Ecological Economics,* Vol. 9, eds R. K. Turner and M. Schaafsma (Cham: Springer), 1–7.

Van der Wal, R., Truscott, A., Pearce, I. S. K., Cole, L., Harris, M. P., and Wanless, S. (2008). Multiple anthropogenic changes cause biodiversity loss through plant invasion. *Glob. Chang. Biol.* 14, 1428–1436. doi: 10.1111/j.1365-2486.2008.01576.x

Conflict of Interest Statement: The authors declare that the research was conducted in the absence of any commercial or financial relationships that could be construed as a potential conflict of interest.

Copyright © 2018 Ragueneau, Raimonet, Mazé, Coston-Guarini, Chauvaud, Danto, Grall, Jean, Paulet and Thouzeau. This is an open-access article distributed under the terms of the Creative Commons Attribution License (CC BY). The use, distribution or reproduction in other forums is permitted, provided the original author(s) and the copyright owner are credited and that the original publication in this journal is cited, in accordance with accepted academic practice. No use, distribution or reproduction is permitted which does not comply with these terms.

frontiers in Marine Science

REVIEW
published: 11 April 2018
doi: 10.3389/fmars.2018.00125

Understanding Diatom Cell Wall Silicification—Moving Forward

Mark Hildebrand, Sarah J. L. Lerch and Roshan P. Shrestha*

Marine Biology Research Division, Scripps Institution of Oceanography, University of California, San Diego, La Jolla, CA, United States

The silicified cell walls of diatoms have inspired the interest of researchers for several centuries, and our understanding of their properties and formation has developed in synch with the development of observational and analytical techniques. Over the past 20 years, approaches used to characterize the molecular components involved in cell wall silicification have evolved, and this has provided significant insights into fundamental aspects of silicification, and promises to continue to do so. Diatom cell wall formation is highly dynamic but, apart from microscopic investigations, most previous molecular characterizations have been on completely formed structures, and thus only provide information on a static end point in the process. However, recent studies that monitor when components are made, and how they are transported to the silica deposition vesicle (SDV), indicate that investigation into the true dynamics of the process is possible. Real-time imaging and genetic manipulation offer the promise of elucidating the spatio-temporal dynamics of, and interactions between, components, which will be essential to understand how structure formation is controlled and coordinated. This review is aimed at describing the approaches that have been used to characterize diatom silicification, integrating newer concepts based on results from diverse approaches, and raising questions that still need to be addressed, leveraging the diverse tools and techniques we now have.

Keywords: diatom, silicification, AFIM, silica, trafficking, cell wall synthesis, *T. pseudonana*

OPEN ACCESS

Edited by:
Stephen B. Baines, Stony Brook University, United States

Reviewed by:
Mark Brzezinski, University of California, Santa Barbara, United States
Assaf Gal, Weizmann Institute of Science, Israel

****Correspondence:***
Mark Hildebrand
mhildebrand@ucsd.edu

Specialty section:
This article was submitted to Marine Biogeochemistry, a section of the journal Frontiers in Marine Science

Received: *13 December 2017*
Accepted: *23 March 2018*
Published: *11 April 2018*

Citation:
Hildebrand M, Lerch SJL and Shrestha RP (2018) Understanding Diatom Cell Wall Silicification—Moving Forward. Front. Mar. Sci. 5:125. doi: 10.3389/fmars.2018.00125

INTRODUCTION

The ability of diatoms to make silica-based cell walls has been the subject of fascination for centuries. It started with a microscopic observation by an anonymous English country nobleman in 1703, who observed an object that looked like a chain of regular parallelograms and debated whether it was just crystals of salt, or a plant (Anonymous, 1702). The viewer decided that it was a plant because the parallelograms didn't separate upon agitation, nor did they vary in appearance when dried or subjected to warm water (in an attempt to dissolve the "salt"). Unknowingly, the viewer's confusion captured the essence of diatoms—mineral utilizing plants. It is not clear when it was determined that diatom cell walls are made of silica, but in 1939 a seminal reference characterized the material as silicic acid in a "subcolloidal" state (Rogall, 1939). Identification of the main chemical component of the cell wall spurred investigations into how it was made. These investigations have involved, and been propelled by, diverse approaches including, microscopy, chemistry, biochemistry, material characterization, molecular biology, 'omics, and transgenic approaches. The results from this work have given us a better understanding of cell wall formation processes, establishing fundamental knowledge which can be used to create models that contextualize current findings and clarify how the process works.

The process of building a mineral-based cell wall inside the cell, then exporting it outside, is a massive event that must involve large numbers of genes and their protein products. The act of building and exocytosing this large structural object in a short time period, synched with cell cycle progression, necessitates substantial physical movements within the cell as well as dedication of a significant proportion of the cell's biosynthetic capacities.

It is nearly two decades since the first characterizations of the biochemical processes and components involved in diatom silicification (Hildebrand et al., 1997; Kröger et al., 1999, 2000, 2002). More recent work has provided insights into how higher order assembly of silica structures might occur (Tesson and Hildebrand, 2010, 2013; Scheffel et al., 2011). Very recent reports describe the identification of novel components involved in higher order processes, the dynamics documented through real-time imaging, and the genetic manipulation of silica structure (Kotzsch et al., 2017; Tesson et al., 2017). The approaches established in these recent works provide practical avenues to not only identify the components involved in silica cell wall formation but to elucidate their interactions and spatio-temporal dynamics. This type of holistic understanding will be necessary to achieve a more complete understanding of cell wall synthesis.

The purpose of this review is to summarize previous work in detail and provide a framework for future work which can take advantage of recent discoveries and tools to explore the dynamic nature of diatom cell wall formation.

GENERAL CHEMICAL FEATURES OF SILICA POLYMERIZATION

Silicon dissolved in an aqueous solution at neutral pH is primarily in the form of silicic acid, $Si(OH)_4$ (Iler, 1979). The solubility of a silicic acid solution is limited to around 2 mM, above that concentration silica (SiO_2) begins to polymerize into polymers with a range of lengths, forming an amorphous solid (Iler, 1979; Kley et al., 2014). The surface of forming silica has a net negative charge, and the morphology of the silica that forms varies depending on the solution's ionic strength and pH. In solutions near neutral pH and with low ionic strength, silica polymerizes as a sol consisting of individual particles which are formed due to repulsion between negatively charged particle surfaces. At lower pH or with higher ionic strength, the negative charges are neutralized, leading to aggregation of smaller particles, and in some conditions formation of a gel network. A gel network is desirable for creating a physically robust structure, and is the morphology generally observed in diatom silica, although silica morphology can vary depending on cell wall features (Round et al., 1990; Hildebrand et al., 2006).

SILICIC ACID TRANSPORT AND INTRACELLULAR STABILIZATION

Although not the primary focus of this review, the processes of silicic acid transport and stabilization at high concentrations are important aspects of diatom silicification. As a small, uncharged molecule, silicic acid can freely diffuse across membranes. Kinetic data indicate that, under environmentally relevant concentrations, diffusion can be the major mode of uptake (Thamatrakoln and Hildebrand, 2008). Under relatively low silicic acid concentrations, the silicon transporters (SITs) actively facilitate uptake (Hildebrand et al., 1997; Thamatrakoln and Hildebrand, 2008). SITs have been localized to the plasma membrane but it is not clear what intracellular membranes they may be targeted to (Shrestha and Hildebrand, 2015). Silicic acid transport mechanisms within the cell are unknown. Given the diffusibility of silicic acid, a transporter protein may not be required. Several studies (reviewed in Martin-Jezequel et al., 2000) have documented intracellular concentrations of soluble silicic acid substantially greater than its 2 mM saturation limit. How such high concentrations are maintained is still a mystery, but a likely hypothesis is that undescribed organic compounds associate with intracellular silicic acid, preventing polymerization. This hypothesis explains features of silicic acid transport in terms of transport against a potential concentration gradient (the gradient may not actually exist if the chemical form of silicic acid—bound or unbound—differs on two sides of a membrane) as well as high intracellular silicic acid concentrations (Martin-Jezequel et al., 2000).

MICROSCOPIC EVALUATION OF VALVE STRUCTURE AND FORMATION IN *THALASSIOSIRA PSEUDONANA*

Thalassiosira pseudonana has developed as the most intensively studied diatom species in regard to silicification, a schematic of its major structural features is shown in **Figure 1**. Several microscopic approaches, including scanning electron microscopy (SEM), transmission electron microscopy (TEM), and atomic force microscopy (AFM), have sufficiently high resolution to evaluate details of silica polymerization and structure formation in diatoms. The ability to enrich for cells undergoing cell wall formation allows for larger numbers of relevant images to be captured, providing more information on ephemeral phenomena such as intermediate structural stages. A synchronized culturing method was developed for *T. pseudonana* which enriches for cells making valves (Hildebrand et al., 2007). In this procedure, cells are starved for silicic acid for 24 h, during which time the majority (80%) of the cells arrest in the G1 phase of the cell cycle. Upon silicic acid replenishment, the cell cycle resumes, and cells complete G1, during which time girdle bands are synthesized. Cells then move into S phase succeeded by G2+M where daughter cells are formed within the mother cell. G2+M is followed by valve formation, and ultimately cell separation. The timing of cell cycle events is well-conserved except for the length of G1, which can last 1–4 h after silicic acid replenishment (Hildebrand et al., 2007). Based on findings in yeast, the variability in G1 length could relate to whether enough carbon is available for the cell to complete mitosis (Hall et al., 1998). Despite the variability in the timing of G1, the period of valve synthesis can easily be determined by staining cells with the fluorescent dyes rhodamine 123 or

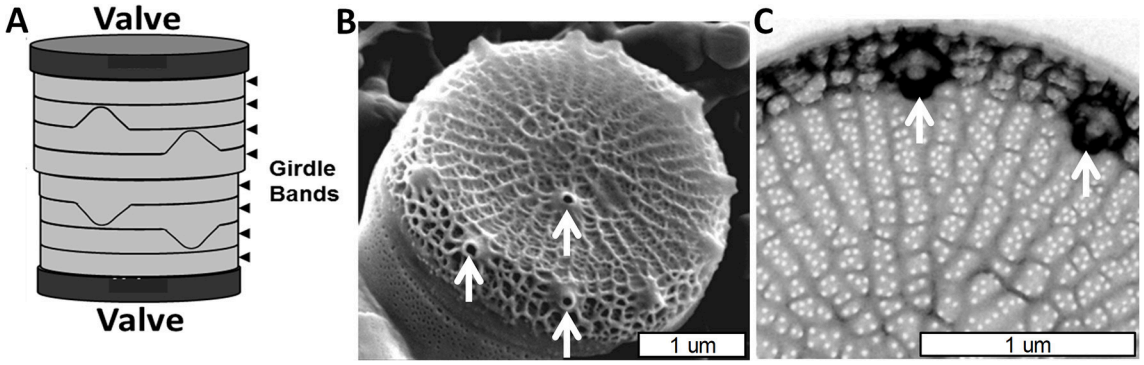

FIGURE 1 | Cell wall structure for *T. pseudonana*. **(A)** Schematic of the entire frustule, indicating valves and girdle bands. **(B)** Scanning electron micrograph (SEM) of the valve and associated first girdle band. **(C)** Transmission electron micrograph (TEM) of the valve, highlighting the rib and pore structure. White arrows denote a subset of the fultoportulae. From Hildebrand et al. (2006), reproduced with permission.

PDMPO (Li et al., 1989; Shimizu et al., 2001; Hildebrand et al., 2007), both of which incorporate into forming silica. Forming valves are visualized by a sharp demarcation of fluorescence at the cleavage area of the cell, and isolation of cells during this time enriches for those making valves. Culture synchronization is not perfect—in addition to less than 100% of all cells arresting in G1, subpopulations of cells can progress through the cell cycle at different rates. However, based on ongoing transcriptomic analysis (Hildebrand et al., in prep), the timing of distinct cell cycle related processes can be defined within 1 h windows.

The valves in *T. pseudonana* are circular, were measured (Hildebrand et al., 2006) at an average of 3.8 μm (±0.4) diameter, and consist of ribs radiating from an area called the pattern center (where valve formation is initiated) to the rim of the valve (**Figure 1B**). The valve surfaces are interspersed with numerous 18 nm (±3.1) diameter circular pores positioned between the ribs which cover ∼4% of the valve area (Hildebrand et al., 2006). The ribs are not strictly linear, but are consistently spaced (145 nm ± 13 between ribs) and branched to maintain this spacing when the distance between them increases beyond 162 nm (±16). There are also cross connections between the ribs (**Figure 1C**). The other major feature of the valve is the fultoportulae, which are larger cone shaped openings for secretion of chitin fibrils (Herth, 1979a,b; Round et al., 1990). Fultoportulae are always found on the rim of the valve, and generally a single fultoportula (but occasionally two or none) is found offset from the center of the valve (**Figures 1B,C**).

As in other diatom species, valve formation in *T. pseudonana* occurs in distinct steps. The first feature that resembles a valve component is called the base layer, which will form the proximal surface of the completed valve. The base layer is a footprint of the valve which includes the ribs and precursors to the fultoportulae, defining structure in the x and y plane (**Figures 2A,B**). The structure is very flexible at this stage (**Figure 2C** and Hildebrand et al., 2007). After base layer formation, the rim of the valve is built up and additional silicification occurs across the surface, eventually resulting in a robust rigid structure (**Figure 2D**). This process involves thickening the valve via expansion in the z-axis direction toward what will become the distal valve surface (**Figure 2E**).

The nanoscale morphology of the silica varies between different features and during different stages of the process. The ribs consist of an amalgam of nanoparticulate silica, whereas the area between the ribs is filled with silica characterized by a smooth branched morphology (**Figures 3A–C**). The nanopores on the surface appear to be formed by objects that obstruct silica polymerization, as they are initially irregular in shape, but become circular as the silica fills in around the proposed obstruction (**Figures 3B,C**). Such an interpretation is supported by AFM analysis of silica-associated organic material in other diatom species where material associated with pores projects above the base layer (Tesson and Hildebrand, 2013). In *T. pseudonana*, the distal surface ornamentation is composed of a third silica morphology which is deposited on top of the base layer ribs (**Figures 3D,E**).

In summary, there are two distinct major stages in *T. pseudonana* valve formation, 1) formation of the base layer which defines the valve shape in the x/y plane and major features of ribs, nanopores, and portulae, and 2) expansion in the z-axis direction by additional polymerization of silica to form a rigid structure. The silica morphology of the valve varies depending on the structural feature being made.

AN OVERVIEW OF THE ORGANIC MATERIALS ASSOCIATED WITH THE SDV

Silica structures in diatoms are formed within a membrane-bound compartment called the silica deposition vesicle (SDV) (Drum and Pankratz, 1964; Reimann et al., 1966; Schmid et al., 1981). The membrane surrounding the SDV is called the silicalemma. The SDV has not been isolated, which has complicated characterization of its components. Fortunately, both biochemical (Kröger et al., 1999, 2000, 2002; Wenzl et al., 2008; Scheffel et al., 2011; Kotzsch et al., 2017) and transcript response

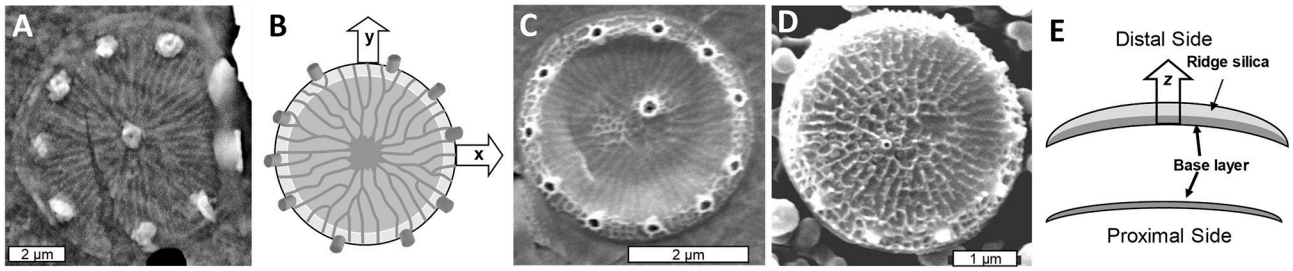

FIGURE 2 | Formation of the *T. pseudonana* valve. **(A)** SEM of the base layer. **(B)** Schematic of x/y axis expansion during base layer formation. **(C)** Intermediate stage of valve formation showing buildup of the rim, but lack of extensive silicification in the center. **(D)** Fully formed valve. **(E)** Cross section schematic of silica deposition in the distal z-axis direction with the lower image representing the initial base layer and the upper representing the fully silicified valve with the final rigid structure. From Hildebrand et al. (2006), reproduced with permission.

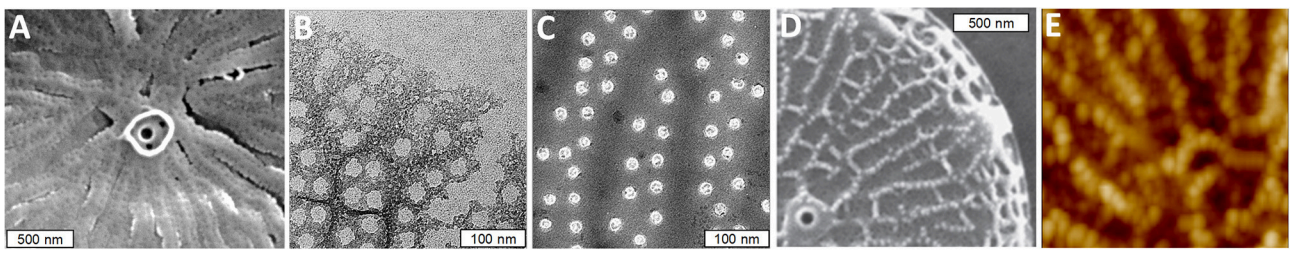

FIGURE 3 | Silica morphology during valve formation in *T. pseudonana*. **(A)** SEM of initially formed ribs and a precursor to the central fultoportula. **(B)** Network structure of initially deposited silica in the rib and pore area. **(C)** Mature pores, note circularity of the pores compared with **(B)**. **(D)** SEM of nanoparticles of silica on top of ribs on the distal valve surface. **(E)** Atomic force micrograph (AFM) of distal surface nanoparticles. From Hildebrand et al. (2006), reproduced with permission.

(Shrestha et al., 2012; Tesson et al., 2017) approaches have proven useful for the identification of components of the SDV.

To be described in more detail below, there are three general classes of proteins known to be associated with the SDV based on biochemical approaches used to purify them and sequence characteristics. A diagram depicting our current understanding of the relative arrangement of components associated with the SDV and the outcomes of various purification procedures is shown in **Figure 4**. Isolation and detergent cleaning of cell wall silica, followed by dissolution with ammonium fluoride (**Figure 4D**), isolated soluble silica-associated proteins and long chain polyamines (LCPAs) embedded within the silica (Kröger et al., 1999, 2000, 2002; Poulsen and Kröger, 2004; Wenzl et al., 2008). Isolation of insoluble material resulting from the same cleaning and dissolution procedure (**Figure 4D**) resulted in characterization of ammonium fluoride insoluble material (AFIM), or the insoluble organic matrix (Scheffel et al., 2011). Most recently, proteins associated with the silicalemma which are extracted by detergent treatment (**Figure 4B**) have been characterized (Kotzsch et al., 2017; Tesson et al., 2017). To date these are characterized by a single transmembrane domain that spans the silicalemma and have an intralumenal and cytoplasmic portion. Depending on their other associations, such as with the AFIM, such proteins may or may not be extracted solely by detergent (**Figure 4D**). Harsh acid treatment of diatom cell walls strips away all exposed organic material (Tesson and Hildebrand, 2013), but should leave silica-embedded material intact depending on its degree of exposure (**Figure 4C**).

In addition to protein-mediated structure formation, the SDV can also be passively molded (Mann, 1984); diatom silica structures have been observed molded around mitochondria (Pickett-Heaps et al., 1979), compression between daughter cells influences silica structure (van de Meene and Pickett-Heaps, 2002), and microtubules can leave indentations in valve structures (Tesson and Hildebrand, 2010). These observations indicate that the plasticity of the silicalemma can influence shape.

Long chain polyamines (LCPAs) are critical components of the silicification process, and appear to be abundant organic components of diatom silica (Kröger et al., 2000). The LCPAs are found embedded within the silica, and consist of repeating units of N-methyl-propylamine or propylamine attached to ornithine or putrescine which are methylated to different degrees. The number of repeat units varies between species. Incubation of purified LCPAs in a solution of silicic acid rapidly catalyzes the polymerization of silica (Kröger et al., 2000). Altering the ratios of different size classes of LCPAs impacts silica morphology, generally by changing nanoparticle dimensions.

The cytoskeleton plays a significant role in forming diatom silica structures, as evidenced by inhibitor studies and imaging (Chiappino and Volcani, 1977; Schmid, 1980; Blank and Sullivan, 1983; Pickett-Heaps et al., 1990; Pickett-Heaps, 1998a,b; van de Meene and Pickett-Heaps, 2002; Tesson and Hildebrand, 2010).

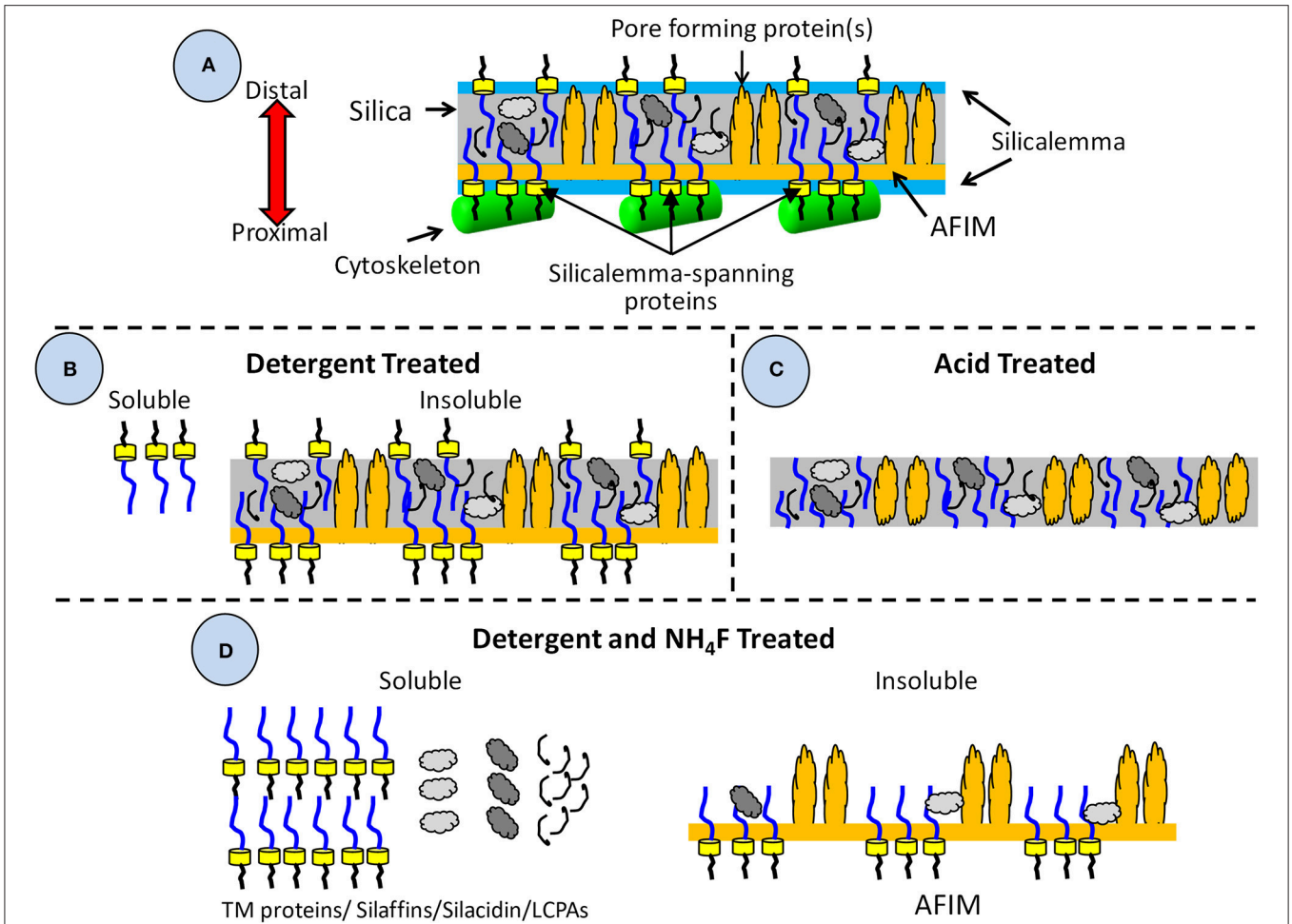

FIGURE 4 | Diagram of valve and associated components detailing their solubility in different detergents and isolation treatments. **(A)** All components associated with the valve during its formation including those embedded in the silica, or associated with the AFIM or silicalemma, including the cytoskeleton. **(B)** Components resulting from detergent extraction, which removes the cytoskeleton, silicalemma, and proteins associated with the silicalemma that are not embedded in the silica, leaving a soluble and insoluble fraction. **(C)** Components resulting from acid treatment, which removes all organic material external to the silica. It is assumed that embedded material is at least partially protected from acid degradation. **(D)** Components resulting from detergent extraction and dissolution of the silica by ammonium fluoride, resulting in a soluble fraction of silica-embedded and silicalemma components, and an insoluble fraction of the AFIM and any proteins that had become associated via crosslinking to it.

Spatial constraints and imaging support that the cytoskeleton is associated primarily, if not solely, with the proximal surface of the SDV, although protrusions extending through silica structures toward the distal side have been observed (Tesson and Hildebrand, 2010). Microtubules appear to be involved in providing a rigid framework for expansion of the SDV and positioning of components within valves. Additionally, microtubules define a major structure specific to pennate diatom species called the raphe (Pickett-Heaps et al., 1979, 1990). Actin defines the edges of active silica polymerization and both the overall and detailed structure of the silica. In centric diatoms, a ring of actin has been observed that defines the edge of the SDV, this ring expands as the SDV grows (van de Meene and Pickett-Heaps, 2002; Tesson and Hildebrand, 2010). In addition, there is excellent correspondence between the pattern of actin assembly over the valve and silica structure (Tesson and Hildebrand, 2010). These observations suggest that microtubules and actin are responsible for positioning components of the SDV that lead to meso- and micro-scale structural features. Although they are not a direct component of the SDV, they must interact with proteins of the SDV in order to translate their organizational patterns into a corresponding silica structure. A proposed mechanism for this will be discussed below.

THE ROLE OF CARBOHYDRATE POLYMERS IN SILICIFICATION

There is strong evidence for the involvement of carbohydrate polymers in silicification and structure formation, but their precise roles and contributions are not clear. For that reason, carbohydrate polymers are not included in the diagrams of

Figure 4. An additional complication is that different types of carbohydrate polymers are associated with cell wall components in different ways in different diatom species (Tesson and Hildebrand, 2013).

Mannose-6-phosphate was identified to be tightly associated with silica from *Stephanopyxis turris*, and because its amount increased upon silica dissolution, it was suggested to at least be partially embedded within the silica (Hedrich et al., 2013).

Evidence also indicates an association of chitin with diatom silica structures. Tesson and coworkers (Tesson et al., 2008) performed a solid state NMR analysis of SDS and H_2O_2 cleaned silica from *T. pseudonana* which showed the presence of several peaks corresponding to β (1→ 4) N-acetyl glucosamine of chitin. The authors attributed the peaks to contaminating chitin fibrils secreted from the cell, however, the signals were enriched as the material was further purified, which should not be the case with a contaminant. The data suggest an association between chitin and the silica. H_2O_2 treatment in aqueous solution does not necessarily degrade organic material, so it cannot be concluded whether the chitin was associated with the surface of the silica, or embedded within it.

Durkin et al. (2009) characterized chitin synthase genes from different diatom species, and identified them in species which do not secret chitin fibrils, suggesting another role for chitin. In *T. pseudonana* they detected chitin using FITC-conjugated wheat germ agglutinin and a chitin binding protein associated with the girdle bands. The staining indicated that chitin was accessible from the outer surface of the girdle bands. No chitin staining was observed in the valves. Previously, a class of highly abundant girdle band associated proteins with chitin binding domains were characterized in *T. pseudonana* (Davis et al., 2005), consistent with the observation of chitin associated with the girdle bands.

Brunner et al. (2009) used different centrifugation methods to distinguish between secreted chitin fibrils and chitin that might be otherwise associated with the cell. Cell walls were extracted with SDS and EDTA, with no other treatment. Material isolated by flow centrifugation had no visible chitin fibrils associated with it, yet NMR signals characteristic of chitin were seen. NaOH treatment removed NMR signals resulting from amino acid side chains, and enriched the chitin signals, indicating that chitin constituted 25–40% of the organic material associated with the silica. The authors showed images of organic material resulting from dissolution of the silica with HF, which mimicked the overall shape and size of the valves. At the time, the AFIM material had not yet been characterized, and given that the cleaning treatment did not include acid exposure (**Figure 4C**), the material imaged by Brunner et al., could have been the AFIM associated with *T. pseudonana* valves (Kotzsch et al., 2016). Considering that Durkin et al. (2009) only observed chitin associated with the girdle bands, it is not clear whether chitin is associated with the valves (the NMR signal could have been from girdle bands), and if so, whether it is a component of the organic material imaged by Brunner et al.

Tesson and Hildebrand characterized insoluble organic material associated with valves and girdle bands from a variety of diatom species, and included staining and carbohydrate quantitation approaches to characterize associated carbohydrate polymers (Tesson and Hildebrand, 2013). Two types of polymer were identified. One was a DAPI-stainable (polyanionic) material that was mannan-rich and found in all species. Staining only occurred after SDS treatment, suggesting that the material was masked in intact cells. The other was calcofluor-stainable and enriched in glucose, and thus was likely a β-1,3 glucan called callose previously identified in diatom cell walls (Waterkeyn and Bienfait, 1987). Although the DAPI-stained material was always immediately adjacent to the silica, the location and accessibility of the DAPI- and calcofluor-stained materials relative to cell wall components varied depending on the species, suggesting distinct roles (Tesson and Hildebrand, 2013). In two species that had calcofluor-stained material associated with forming valves, treatment with mycafungin (a specific beta 1–3 glucan synthesis inhibitor) dramatically altered silica structure morphology, indicating a strong influence on the structure formation process, but not on silica polymerization.

In summary, at least some form of carbohydrate polymer is involved in controlling the morphology of forming silica, but more work is needed to clarify the specific role(s) of carbohydrate polymers in diatom cell wall synthesis.

SOLUBLE PROTEINS ISOLATED BY DISSOLVING DETERGENT-CLEANED SILICA

The first proteins isolated from purified dissolved silica were the silaffins (Kröger et al., 1999). These were initially isolated from *Cylindrotheca fusiformis*, and consisted of peptides 15–22 amino acids in length with repeated sequence enriched in lysine and serine. The lysines were post translationally modified by methylation or addition of polyamine units, and the serines were phosphorylated (Kröger et al., 1999, 2002). Purified silaffins rapidly catalyzed polymerization of silica from a solution of silicic acid, and the morphology of the silica varied depending on the mixture of silaffins used (Kröger et al., 1999, 2002). Analysis of the gene encoding silaffin indicated a single polypeptide that was proteolytically processed into the shorter peptides, with proteolytic cleavage occurring after an RXL amino acid sequence (Kröger et al., 1999). A survey of silaffins in different diatom species revealed that most were larger polypeptides—in contrast to the smaller peptides in *C. fusiformis* (Kröger et al., 2000). A detailed characterization of silaffins in *T. pseudonana* (Poulsen and Kröger, 2004) provided key insights into properties of the larger silaffins. Three proteins were identified, TpSil 1/2 H, TpSil 1/2 L, and TpSil 3. TpSil 3 was a single polypeptide, and TpSil 1 and 2 were very similar proteins encoded by two different genes. TpSil 1/2 were synthesized as single proteins that were proteolytically cleaved into the H and L forms. The two forms had distinct influences over silica formation. In contrast to the *C. fusiformis* silaffins, none of the *T. pseudonana* silaffins had silica forming activity *in vitro* in the absence of LCPAs. In the presence of LCPAs, the H form of TpSil 1/2 initially promoted silica formation, then inhibited it as its concentration was increased, whereas the L form continued to promote silica formation as its concentration was increased. TpSil 3

also promoted silica formation at lower concentrations and inhibited it at higher. These results led to the distinction between "catalytic" silaffins that had a continuous stimulatory effect on silica formation, and "regulatory" silaffins that could both promote and inhibit silica formation depending on the protein concentration. The activities were attributed to differences in amino acid composition, and more specifically, posttranslational modification to amino acids. TpSil 1/2 H was enriched in hydroxyamino acids, which were likely glycosylated as evidenced by substantially higher carbohydrate content in TpSil 1/2 H relative to TpSil 1/2 L (Poulsen and Kröger, 2004). It had been demonstrated with a particular silaffin from *C. fusiformis*, natSil2, that carbohydrate and sulfate moieties inhibited polyamine-dependent silica formation, whereas protein-bound phosphate groups promoted it (Poulsen et al., 2003). TpSil 1/2 L lacked those particular inhibiting posttranslationally-added groups, and solely promoted silica formation due to the predominance of posttranslationally-added phosphate groups. TpSil 3 contained both types of side chain modifications, and displayed an intermediate ability to promote or repress silica formation.

Characterization of the various silaffins demonstrated that posttranslational modifications have a major influence on silica formation activity. Thus, although amino acid sequence comparisons are a valid way to assess the ability of proteins to control silica formation, it should be kept in mind that it is modification of the amino acids that are largely responsible.

Silica polymerization *in vitro* by LCPAs required the presence of polyanions in the form of phosphate or pyrophosphate (Kröger et al., 2000), which prompted a search for polyanionic organic material embedded within diatom silica that could serve a similar function. This resulted in the discovery of silacidin, a protein enriched in serine and the acidic amino acids aspartic and glutamic acid (Wenzl et al., 2008). In the presence of LCPAs and in the absence of phosphate, silacidin rapidly promoted silica formation *in vitro*, and was thus regarded as an excellent candidate for performing the anion role *in vivo*. Silacidin was encoded by a single open reading frame, but the protein was proteolytically cleaved after RXL sequences into smaller repeated peptides of 29–31 amino acids.

The described characterizations provided fundamental insights into the role of soluble silica-associated material. *In vitro* silica precipitation experiments have demonstrated a relationship between the size of the catalytic organic material and how ordered the resulting silica morphology was. The short silaffin peptides isolated from *C. fusiformis* silaffins precipitate silica spheres, with no higher order organization (Kröger et al., 1999). Similarly, LCPAs (Kröger et al., 2000), fully processed silacidins (Wenzl et al., 2008) and TpSil 1/2 L from *T. pseudonana* (Poulsen and Kröger, 2004) generate silica structures *in vitro* that lack higher order - they are agglomerations of randomly organized fused silica particles. Only in the presence of higher molecular weight silaffins do higher order structures form (Poulsen and Kröger, 2004). We propose that the smaller organic components are responsible for generating "filler" silica which can assume structure either through interaction with other peptides or by confinement within the SDV. Small molecular size would facilitate this by enabling freer diffusion and more degrees of freedom. Expansion of *T. pseudonana* valves in the z-axis direction could be an example of this filling process.

INSOLUBLE MATERIAL ASSOCIATED WITH DETERGENT-CLEANED SILICA

The silaffins lacked amino acid sequence conservation, and no clear homologs were found in genome searches, which prompted the examination of genes encoding proteins with similar amino acid composition, and not necessarily sequence, to the silaffins (Scheffel et al., 2011). A search was made of the *T. pseudonana* genome for proteins with an ER signal sequence (consistent with targeting to the SDV) and ≥18% serine and ≥10% lysine residues. Eighty-nine genes were identified, and a subset of six genes encoded proteins with conserved repetitive features, which were called cingulins. There were two types of cingulins, the "W" cingulins and the "Y" cingulins, which were named based on enrichment of their sequences for either tryptophan (W) or tyrosine (Y). GFP tagging of the cingulins indicated that they were exclusively associated with girdle bands (Scheffel et al., 2011). Subsequent characterization of insoluble material resulting from dissolution of cleaned silica revealed that the proteins were associated with "microrings" that precisely mimicked the girdle band dimensions and structure. The microring material was termed AFIM, or the insoluble organic matrix (**Figure 4**). It was proposed that the insolubility of the organic matrix was due to covalent cross-links between its protein components, which may include *O*-phosphoester bonds and *O*-glycosidic bonds (Kotzsch et al., 2016). Initial characterizations in *T. pseudonana* found the AFIM associated only with the girdle bands and not valves, although a valve associated AFIM was found in *Coscinodiscus wailesii* (Scheffel et al., 2011). Subsequent work identified a valve-like AFIM in *T. pseudonana* (Kotzsch et al., 2016). An extensive microscopic study of the insoluble organic matrix in a variety of diatom species (Tesson and Hildebrand, 2013) determined that the material was fibrous. Direct imaging showed that the material was associated exclusively with the proximal surface of the valves. The material could be DAPI-stained only after SDS treatment, which is consistent with it being obscured by the silicalemma, leading to the model for structural arrangement shown in **Figure 4**. The AFIM precisely mimicked valve features (**Figure 5**). Given its location and how it precisely mimics the proximal surface, it is reasonable to hypothesize that the AFIM constitutes an organized pattern for base layer formation. Imaging of the matrix in the location of pores identified projections of organic material (**Figures 5D,E**) around which silicification occurred. Comparison of AFM imaging of the AFIM with an SEM of the valve of *S. turris* shows that the pores in the valve are occluded by this material (**Figures 5E,F**). These observations support the hypotheses derived from observations of forming pores in **Figures 3B,C**. A consequence of this is that pores are not entirely open channels, but are at least lined, if not occluded, by organic material. The proteins that constitute these projections could impart a level of control over what passes

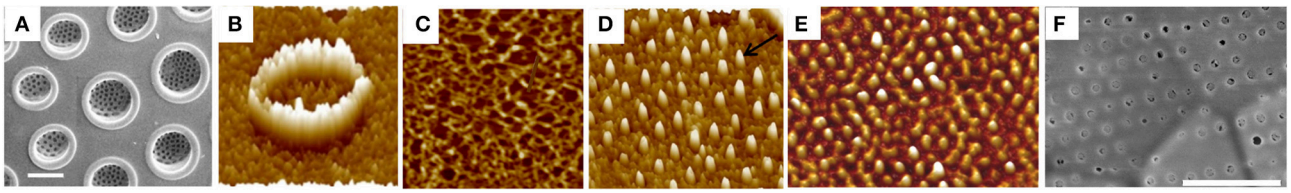

FIGURE 5 | Characterization of the AFIM, or insoluble organic matrix from *Coscinodiscus radiatus*. **(A)** SEM of Proximal valve surface, highlighting the large openings of the foramina. Scale bar = 5 μm. **(B)** AFM of region of foramina in the AFIM. **(C)** Fibrous structure of AFIM from proximal surface. **(D)** AFM of AFIM from a girdle band, showing projections that define pores. **(E)** AFM of AFIM from the valve of *Stephanopyxis turris*. **(F)** SEM of proximal valve surface of *S. turris*. Scale bar = 1 μm. Scan sizes are **(B)** = 1 μm, **(C)** = 1.2 μm, **(D)** = 2 μm, **(E)** = 3.6 μm. From Tesson and Hildebrand (2013), reproduced under the Creative Commons license.

through the pores. If so, this prompts a significant re-framing of how we think about transport processes of diatoms.

An elegant nuclear magnetic resonance (NMR) study substantiated the presence of an organic layer associated with the surface of silica in *S. turris* (Jantschke et al., 2015). Dynamic nuclear polarization solid state NMR on SDS/EDTA cleaned silica (which would not remove the AFIM—**Figure 4B**) identified an estimated 3 nm thick surface layer, which corresponded to direct measurements using AFM (Tesson and Hildebrand, 2013), enriched in protein and carbohydrate. Predominant amino acids were Asp, Gly, Ser, Glu, and Ala, as confirmed by both NMR and MS analyses. The bulk silica was enriched in LCPAs, and there was excellent agreement between the estimated thickness of the silica structure by NMR and the actual measured thickness. Several lines of evidence supported an abundance of β-strand protein secondary structure and random coils, which the authors proposed would help to establish compactness as well as intermolecular networking. These features correspond well with other studies mentioned previously related to the AFIM.

Biochemical and proteomic analysis of the AFIM from *T. pseudonana* identified seven proteins called "SiMats" which generally had amino acid sequence characteristics of known silicification proteins (Kotzsch et al., 2016). Most lysine residues in the identified AFIM proteins were post-translationally modified to contain short polyamine chains. SiMat1 was localized to the girdle band AFIM.

Two silaffins initially identified as being associated with the soluble fraction of cleaned dissolved silica, and one other protein later associated with the silicalemma, were also found associated with the insoluble fraction. A GFP fusion of TpSil3 was incorporated into the AFIM, although its abundance was lower than the cingulins (Scheffel et al., 2011). Mass spectrometry characterization of the *T. pseudonana* AFIM also identified a peptide from the C-terminal L form of TpSil 1/2 (Kotzsch et al., 2016). Although not noted in previous work, the extreme C-term of TpSil 1/2 has a transmembrane domain (Table S1) as predicted by TMHMM v.2.0 (Sonnhammer et al., 1998), so the L form could be associated with the silicalemma. Another explanation for the predominance of TpSil 1/2 and 3 in the soluble fraction, with a lesser amount in the insoluble fraction, could be incorporation of the silaffins in the latter (**Figure 4D**) by the proposed cross-linking phenomenon (Kotzsch et al., 2016). Described in more detail in the following section, a silicalemma-associated protein called Sin1 was initially isolated from the AFIM and named SiMat7 (Kotzsch et al., 2016).

SILICALEMMA-ASSOCIATED PROTEINS

As stated previously, the cytoskeleton has a substantial influence over silica structure, and in particular actin assembly patterns have been correlated with silica structures (Tesson and Hildebrand, 2010). Actin assembles outside of the SDV; therefore, its assembly pattern must be transmitted into the SDV lumen for it to influence silica patterning. Robinson and Sullivan (1987) proposed that silicalemma-spanning proteins could serve as intermediates that translate cytoskeletal assembly patterns into similar silica structures. Such proteins would be predicted to have a transmembrane domain, a cytoplasmic portion that could interact with the cytoskeleton (either directly or indirectly), and an intralumenal portion that would either have characteristics of silicification proteins, or domains that would facilitate interactions with such proteins or LCPAs (**Figure 6**). They also could have different characteristics depending on which region of membrane they are in. In the proximal silicalemma, they could interact with the AFIM. These interactions would not be possible from the distal membrane unless they extended completely across the SDV lumen (**Figure 6**), if the interactions do not occur one would surmise that this subset of silicalemma associated proteins might be extractable by detergent. Examination of genes upregulated during valve formation in synchronized cultures of *T. pseudonana* resulted in the identification of a multiple silicalemma-associated candidate proteins with predicted ER targeting, a single transmembrane segment, and sequence features characteristic of silica-associated proteins (Tesson et al., 2017). One protein, called SAP1 (Silicalemma Associated Protein), was used to identify two other proteins (SAP2 and 3) with similar characteristics in the *T. pseudonana* genome. These proteins constitute a gene family in diatoms, and are found mainly in other centric diatom species. They have a longer N-terminal portion which is enriched in serine, and which in SAP3 was associated with silica in the SDV lumen. The SAPs also have a shorter C-terminal portion which contains a conserved, but undefined, sequence domain found in the other SAPs. The SAPs have the structural organization predicted by Robinson and Sullivan, but the C-terminal portion does not match any known cytoskeleton-interacting sequence. It is possible that (1) the

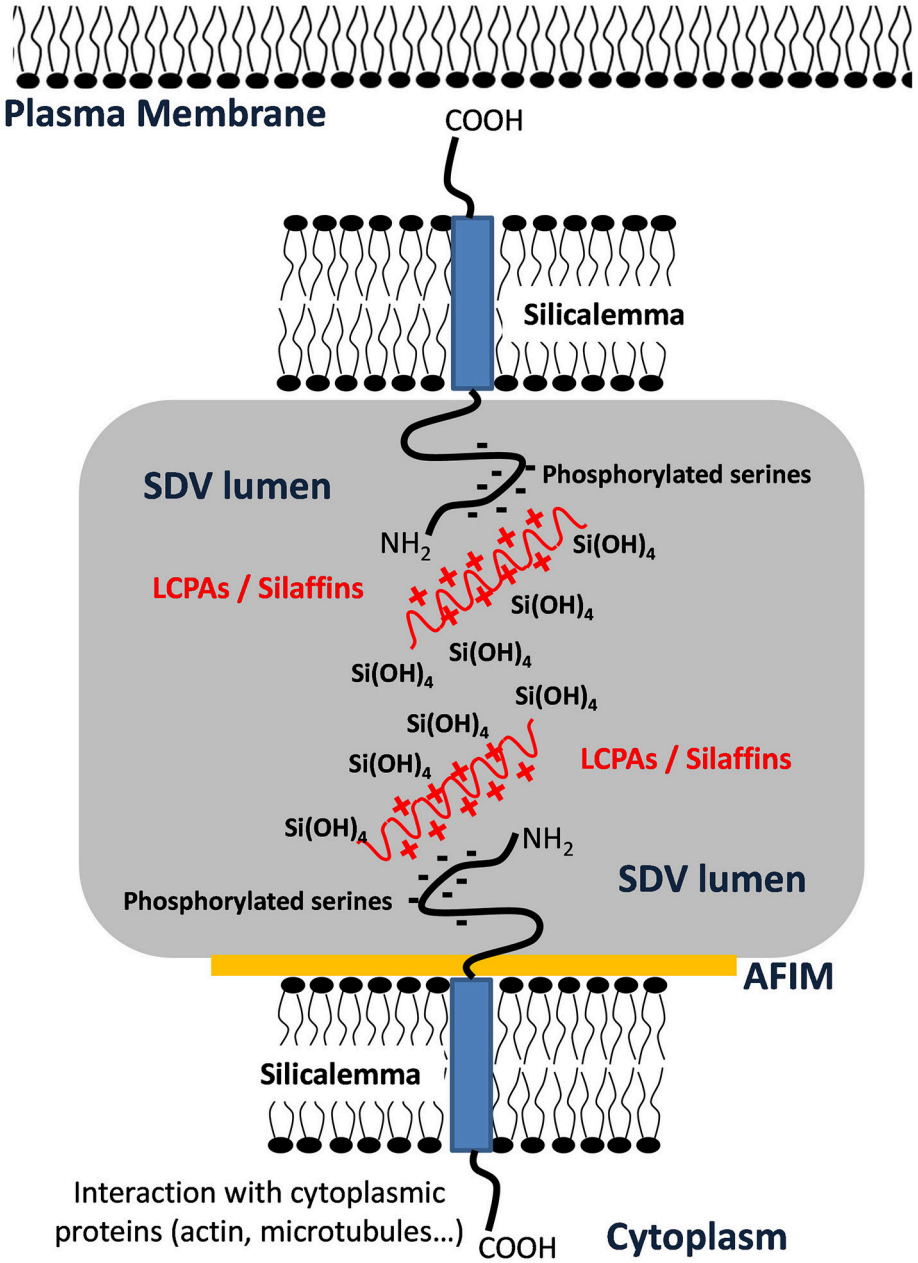

FIGURE 6 | Schematic representation of transmembrane protein organization into the SDV membrane showing putative interactions of phosphorylated serine with Long Chain Polyamines (LCPAs) or silaffins inside the SDV lumen and interaction with cytoplasmic proteins via the cytoplasmic domain. This figure was modified from Tesson et al. (2017) and is based on a model by Robinson and Sullivan (1987).

conserved sequence is a novel cytoskeleton-interacting sequence, (2) the SAPs interact indirectly with the cytoskeleton via other proteins, or (3) these particular proteins have no interaction with the cytoskeleton. SAP1 and SAP3, when tagged with GFP on their C-termini, were seen associated with forming silica structures in both the girdle bands and valves. In addition, SAP3 was associated with a relatively large intracellular vesicle, and an increase in GFP fluorescence over time during silicon starvation suggested that the protein accumulated there (Tesson et al., 2017). The C-terminal GFP tagged proteins were never observed in the completed cell wall, and evidence was presented that proteolytic cleavage to remove the C-terminus of SAP3 occurred. If the C-terminus was involved in interacting with other proteins, this cleavage could cease the interaction. One possibility in this scenario is that interactions with the cytoskeleton must be terminated in order for the valve to be exocytosed. Tagging of SAP3 in the N-terminal region with GFP indicated that this portion was embedded in the silica. Transcript knockdown of

SAP1 and 3 using antisense and RNAi approaches generated distinct phenotypic changes in silica structure. These were the first demonstrations of genetic manipulation of silica structure in a diatom. SAP3 knockdowns displayed a lack of decoration of the distal surface where silica particles are normally found on top of the ribs (**Figure 7**). SAP1 knockdowns displayed aberrations in proximal surface silicification separately or in addition to alterations in the location of their pattern forming centers (**Figure 7**), which is the characteristic location of valve formation initiation. It is known that the pattern forming center is positioned by microtubules (Pickett-Heaps et al., 1990), therefore, it is possible that SAP1 knockdown interferes with the interactions of SDV-associated proteins and microtubules. These results demonstrate that manipulation of a single gene can generate a consistent alteration in silica structure. This indicates that the role of specific proteins can be probed using genetic manipulation approaches.

A distinct silicalemma-associated protein, called Silicanin-1 (Sin1) has also been characterized (Kotzsch et al., 2017), which was the same protein characterized as the AFIM-associated SiMat7 (Kotzsch et al., 2016). Similar to the SAPs, Sin1 has a long intralumenal N-terminal region, a single transmembrane segment, and a short cytoplasmic sequence. The N-terminal region was shown to be embedded within the silica and the C-terminal region appeared to be proteolytically released. Sin1 was found associated with both girdle bands and valves. The dynamics of Sin1 localization over time were determined, showing that the protein was associated with the plasma membrane as well as an intracellular vesicle (similar in appearance to that found with SAP3). Sin1 was recruited to the SDV during silica formation, and then dispersed into the plasma membrane afterwards. Unique targeting signals must be involved to accomplish this. No direct function of the protein in valve formation was demonstrated, but it was shown that recombinantly-expressed protein assembled into clusters in a pH-dependent manner—at lower pH (similar to the SDV lumen), clusters formed, and at higher pH, they disaggregated. pH-dependent aggregation was also demonstrated for the cingulins (Kotzsch et al., 2016).

For Sin1, antibody accessibility experiments indicated that <20% of the protein was accessible in the silica relative to the AFIM (Kotzsch et al., 2016), meaning that most of the protein was embedded in the silica. As such, SDS extraction would not be expected to produce the highest yields, although it would isolate protein localized to other cellular locations such as the plasma membrane or an intracellular vesicle. A similar situation may exist for the SAPs; SAP3 was found embedded in the silica (Tesson et al., 2017) but also could be extracted with detergent only. In this case the most abundant source of the protein could have been from the intracellular vesicle.

One hypothesis regarding the role of silica- or silicalemma-associated proteins is that if they are exclusively localized to one particular macroscale structure (valve or girdle band) they could be involved in formation of the specific features of that structure, but if they are localized to different structures, they may be involved in more general silicification processes. Following this line of reasoning, because SAP3 was associated with both valves and girdle bands, both structures contain nanoparticulate silica on their distal surfaces (Hildebrand et al., 2006), and knockdown of SAP3 prevented formation of the distal valve nanoparticulate silica, perhaps SAP3 performs a general function of facilitating distal nanoparticulate silica formation. Similarly, although a specific function for Sin1 has not been defined, we would propose that it plays a similar role in valve and girdle band silicification. In contrast, the cingulins have only been identified associated with girdle bands, suggesting that they are involved in the meso- or micro-scale processes specifically associated with shaping the girdle bands.

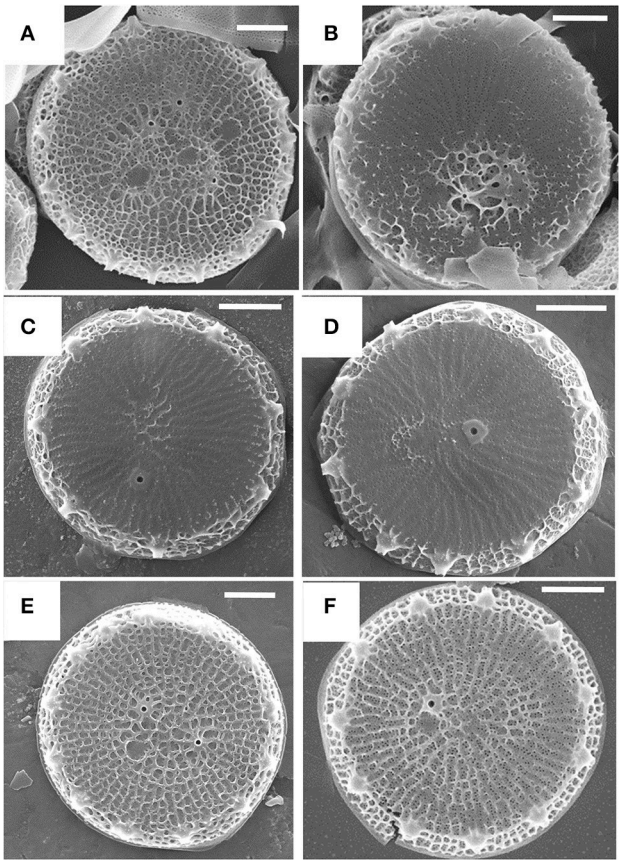

FIGURE 7 | Alterations in *T. pseudonana* valve structure resulting from antisense knockdowns of TpSAP1 **(A,B)** and TpSAP3 **(C,D)**. Wild-type controls are **(E,F)**. From Tesson et al. (2017), reproduced under the Creative Commons license.

TRANSCRIPT EXPRESSION PATTERNS

Because formation of diatom cell wall structures is intimately associated with the cell cycle, it may seem logical that the induction of transcripts for silicification proteins relate to the formation of particular structures at particular times in the cell cycle. TpSil3 served as the first marker for valve formation, because it was specifically upregulated during that period (Frigeri et al., 2006). However, analysis of transcript expression

patterns obtained from synchronized cultures of *T. pseudonana* (Shrestha et al., 2012) indicated that known and proposed genes encoding proteins involved in silicification have distinct expression patterns and maxima (Hildebrand and Lerch, 2015), which do not necessarily relate to the timing of formation of structures. A recent microarray analysis confirms this conclusion (Brembu et al., 2017). As detailed in the following, there appear to be four major types of responses, which cover all major stages of the cell cycle.

In **Figure 8**, we examine a whole genome microarray response (Shrestha et al., 2012) of three classes of genes encoding proteins peripherally involved in silicification, the silicon transporters (SITs), chitin synthases, and aminopropyltransferases (APTs) and a spermidine synthase that may be involved in polyamine synthesis.

Transcript behavior for SITs was previously documented (Shrestha and Hildebrand, 2015; Brembu et al., 2017)—SIT1 and 2 are upregulated during silicon starvation, then generally downregulated upon silicon replenishment until an increase in M phase, followed by downregulation thereafter (**Figure 8**). As suggested, because silicic acid can freely diffuse into the cell, the SITs do not have to substantially contribute to uptake, and appear to play more of a regulatory role over silicic acid metabolism (Shrestha and Hildebrand, 2015). Shrestha and Hildebrand proposed that SIT upregulation during M phase could be due to a need to populate the new daughter cell with SITs rather than a silicic acid requirement.

Various enzymatic steps are involved in polyamine and LCPA synthesis, and key enzymes to elongate the polyamines have fused aminopropyltransferase (APT) and S-adenosylmethionine decarboxylase (SDS) domains (Michael, 2011). Polyamines also contain spermidine and therefore require its synthesis (Michael, 2016). We plot the expression pattern for four APT/ SDS genes and one spermidine synthase in *T. pseudonana* in **Figure 8**. Four of the five genes are upregulated during valve formation. Two of the three APTs (Thaps3_267946 and 261161) had predicted ER targeting, which could be consistent with elongation of LCPAs in the steps prior to formation of the SDV or within the SDV itself. The spermidine synthase, Thaps3_17140, also had predicted ER targeting, and was upregulated during valve formation.

As discussed, chitin is closely associated with the cell wall and plays some role in its formation. Three chitin synthases were identified in the genome, and all three were at least somewhat upregulated during valve formation (**Figure 8**). Although this increase in transcripts occurs when chitin putatively involved in valve formation would be needed, it is also at a time when the fultoportulae should be made. The synthesizing machinery for chitin fibril extrusion is positioned under the fultoportulae, and is likely to be a permanent fixture once in place (Herth, 1979a,b). It is therefore unclear whether upregulation of the synthases during valve formation relates to making chitin for valve formation or positioning the chitin synthesizing machinery for daughter cells.

In **Figure 9**, we show the transcript response of genes encoding proteins known to be involved in silicification, which includes the silaffins, silacidin, cingulins, SiMat proteins, the SAPs, and Sin1. These encompass proteins embedded within the silica, in the AFIM, and associated with the SDV membrane. The

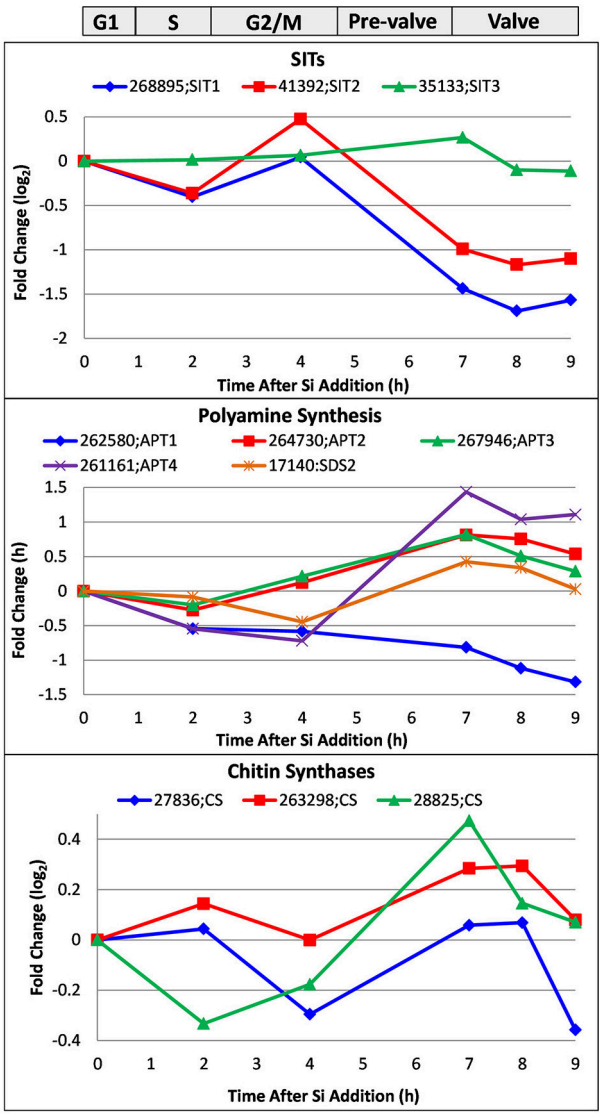

FIGURE 8 | Whole genome microarray analysis of transcript level changes of proteins peripherally involved in *T. pseudonana* silicification. Log base 2 fold changes relative to 0 h are plotted. Transcripts were measured in a synchronized culture where cell cycle progression began after silicic addition to a silicon-starved culture. Approximate timing of different cell cycle stages is shown at top. Data are from Shrestha et al. (2012).

responses fell into four categories. The valve formation response, which was modeled after the established Sil3 pattern (Frigeri et al., 2006), included Sil3, CinW1 and 2, SiMat3 and 5, and SAP1. The S or M phase response (**Figure 9**) displayed maximum upregulation between 2 and 4 h, and included the Y cingulins, Cin W3, SiMat1, 2, 4, and SiMat7/Sin1. The valve and S/M phase responses have been substantiated in a recent transcriptomic analysis (Brembu et al., 2017). In our analysis, four genes exhibited patterns of either little change related to cell cycle stage, or down regulation during the synchrony (**Figure 9**), including Sil1 and 4, silacidin, and SAP2. SAP3, which was examined in a distinct RNAseq time course synchrony (Tesson et al., 2017),

exhibited a distinct pattern from previously described (Shrestha et al., 2012; Brembu et al., 2017), with maximal upregulation during pre-valve formation, between mitosis and valve formation at 5 h (**Figure 9**).

AMINO ACID SEQUENCE FEATURES OF KNOWN SILICIFICATION PROTEINS

The amino acid composition of known proteins involved in silicification is shown in **Figure 10**. The most abundant amino acids (5% or higher) were Ser, Gly, Lys, Asp, Ala, Thr, Glu, and Pro. Since these proteins play different functional roles, we compared the amino acid composition (Table S2) between subsets of proteins, separating them into categories as the silaffins, AFIM associated proteins, and silicalemma-associated proteins (silacidin has a highly distinct amino acid composition and different properties than the silaffins and was therefore excluded). We acknowledge that individual proteins in a given category could also have different functional roles which would influence amino acid composition, hence we do not include any statistical comparison between categories. Differences between the categories were accentuated by comparing ratios of all three and plotting them on a $\log_2$ scale (**Figure 10**). The silaffins were enriched over the other two categories in Ala, Glu, and Met, and depleted in Asn, Cys, Gln, Trp, and Tyr. The silaffins were also depleted in Gly relative to the AFIM proteins. The AFIM proteins were enriched in amino acids depleted in the silaffins and depleted in those enriched in the silaffins. The silicalemma associated proteins were generally enriched in Ala, Arg, Asn, Gln, and His relative to the silaffins, and depleted in those same amino acids relative to the AFIM. Phe, Pro, Ser, Thr, and Val were similarly conserved across all categories. Comparing the averages of the ratios for all amino acids in each pairwise comparison indicates that the AFIM and silicalemma associated proteins had more similar amino acid composition than either compared with the silaffins. In context of the transcript data discussed below these trends may have implications for temporal regulation of different types of proteins based on amino acid based functions.

We examined whether specific amino acids or amino acid motifs were enriched in the known silicification proteins (Table S1). Cysteine was completely absent in 9 of the 20 proteins, but was enriched above the average found in all proteins (1.55%) in 7 of them, specifically in Sil1 H, CinY1, SiMat3-7, and SAP3 (Table S1). Even though Cys is not very highly enriched in Sin1/SiMat7, analysis indicates that 8 cysteines are conserved in a large protein family related to Sin1/SiMat7 in *T. pseudonana* and *Phaeodactylum tricornutum* (Brembu et al., 2017), indicating an important functional role. Cysteine is typically involved in disulfide bonding as a means of stabilizing protein tertiary structure. Tryptophan was not highly abundant among the proteins with the exception of the CinW's. SAP1 and 3 were somewhat enriched in Trp. It was proposed that Trp could facilitate aggregation of the CinW's under acidic conditions (Kotzsch et al., 2016). The "KXXK" motif (which includes KXK, KXXK, and KXXXK) has been proposed to promote silicification via posttranslational modification of the lysines and be involved

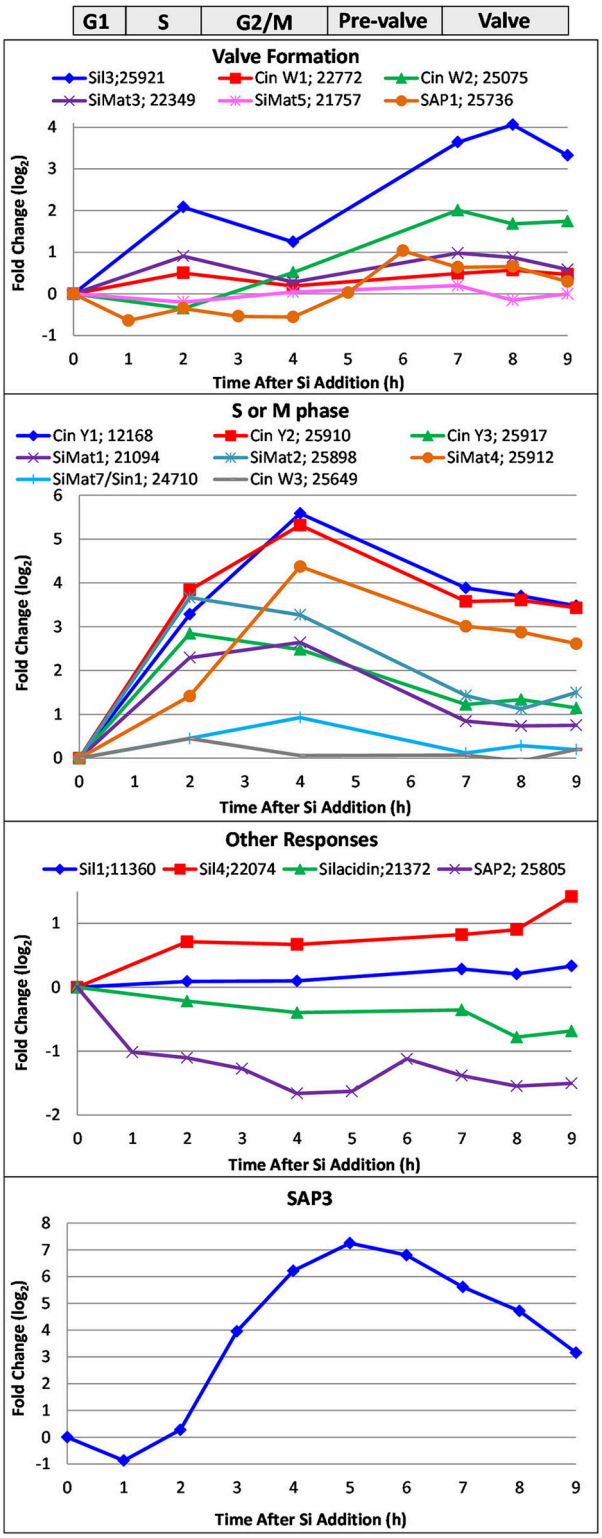

FIGURE 9 | Whole genome microarray analysis of transcript level changes of proteins known to be involved in silicification in *T. pseudonana*. Log base 2 fold changes relative to 0 h are plotted. Transcripts were measured in a synchronized culture where cell cycle progression began after silicic addition to a silicon-starved culture. Approximate timing of different cell cycle stages are shown at top. Data are from Shrestha et al. (2012).

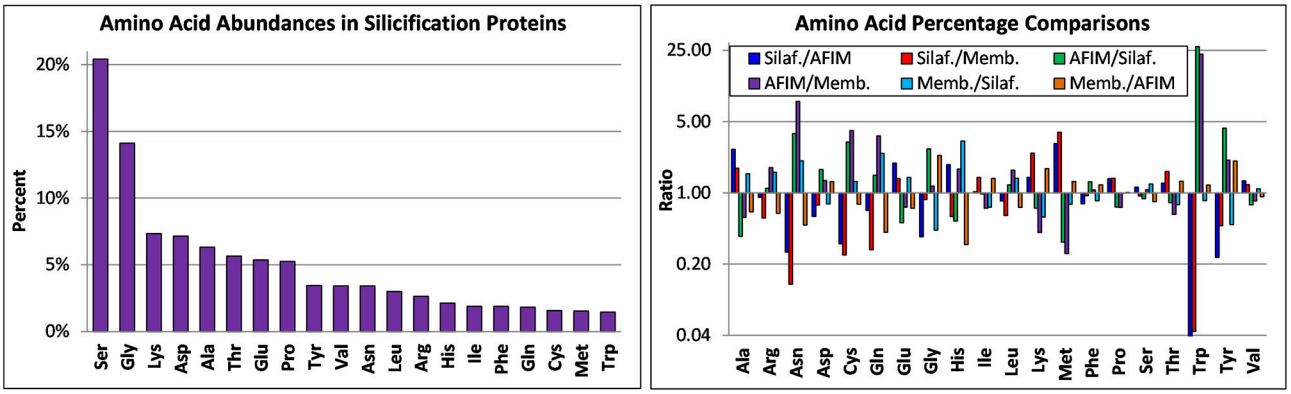

FIGURE 10 | Amino acid composition of silicification proteins based on analysis of their published sequences. Top, amino acid abundances of all proteins, bottom, ratio of amino acid abundances for different classes of proteins, including silaffins (Silaf), those associated with the AFIM (AFIM), and the SDV membrane or silicalemma (Memb).

in targeting proteins to the SDV (Poulsen et al., 2013). It is highly enriched in many of the proteins, up to 45% of the total amino acids in Sil1/2 L are KXXK (Table S1). Recent analyses have identified other KXXK motif containing silicification candidate proteins in *T. pseudonana* (Brembu et al., 2017). If X=Ser, then that side chain could be phosphorylated. If repeated every 4 amino acids in an alpha helical structure, the side chains would consistently orient toward one side, providing a spatial constraint. Analysis of the silaffins and cingulins indicates a prevalence of clusters of KXXKs, with the average spacing between lysines of 4.4 residues. In an alpha helix, that would be equivalent to 1.25 turns between lysines. If in a beta strand structure, which was shown to be enriched in silica associated proteins by NMR in *S. turris* (Jantschke et al., 2015), side chains repeated on average of 4.4 residues would tend to orient in the opposite directions. These data lend credence to the concept of specific orientation of the side chains in these motifs. The SAPs lack a KXXK motif entirely, and in Sin1 and silacidin it is depleted relative to its average prevalence in all proteins. PT or TP repeats were common in the known silicification proteins, and have been noted in other candidate silicification proteins implicated by transcript response (Brembu et al., 2017). In the context of the threonine being glycosylated, the glycosyl group would be found on the same face of the helix in a repeat, or in a beta strand structure, facing in the same orientation. It has been noted that repeated sequence patterns generates regular arrays of spatial and functional groups, useful for structural packing or for one to one interactions with target molecules (Katti et al., 2000). Glycosylated residues can stimulate silica formation at low concentration, and inhibit it at higher concentration (Poulsen and Kröger, 2004), thus proteins containing PT repeats could regulate the extent of silicification. Sil1/2 H has a high percentage of PT repeats, and it has been shown to regulate the extent of silicification (Poulsen and Kröger, 2004). The CinY's are enriched in PT repeats, also suggesting a regulatory role. Sil3 and 4 were specifically enriched in MS or SM motifs (Table S1), which were largely absent from the other proteins. It is unclear what their effect would be on silicification, although the serine could be phosphorylated.

All of the known silicification proteins have a signal peptide based on Signal P (Bendtsen et al., 2004) prediction, indicative of ER targeting, however six of them actually had predicted periplastid compartment (PPC) targeting because they have a predicted ER signal peptide along with a robust chloroplast targeting prediction (Emanuelsson et al., 1999) lacking the characteristic ASAFAP sequence (specifically lacking an aromatic residue at the F-position—Kilian and Kroth, 2005; Gruber et al., 2007) at the cleavage site between the two targeting sequences. GFP fusions of all of these proteins were experimentally localized to within the silica or silicalemma, therefore we interpret the PPC targeting as a prediction artifact. Interestingly, in an examination of SDV targeting signals, Poulsen et al. (2013) determined that particular sequences targeted TpSil3 to a sub-compartment in the ER, which looked very similar to authentic PPC localization. This suggests that silicification proteins with a PPC targeting motif could be targeted to the SDV by a distinct route than other SDV-associated proteins. Dynamic localization data indicates that Sin1 is targeted to the plasma membrane and then recruited to the SDV (Kotzsch et al., 2017).

The concept of identifying conserved domains in silicification protein amino acid sequences will be important moving forward since conserved domains should endow specific functional properties. This is especially important considering that the amino acid composition, and not sequence, appears to be relevant to function in many of the proteins. A conserved domain stands out from such background sequence. The conserved domain identified in the SAPs and its presence in a protein family conserved across diatom species (Tesson et al., 2017) indicates that it has some importance for the function of the proteins. A conserved set of eight cysteines is diagnostic of a Sin1/SiMat7 protein family in *T. pseudonana* and *P. tricornutum* (Brembu et al., 2017). The Marine Microbial Eukaryote Transcriptome Sequencing Project (MMETSP) dataset, which contains 650 assembled, functionally annotated marine microbial

transcriptomes (Keeling et al., 2014), is a good resource to perform cross-species comparisons of these and other candidate genes (Brembu et al., 2017). Sequences that are conserved across diverse species could either be involved in general aspects of silicification or not involved at all, whereas sequences conserved in a subset of species, for example the *Thalassiosirales*, could be involved in processes related to formation of specific structures in those species.

THE RELATIONSHIPS BETWEEN EXPRESSION PATTERNS, AMINO ACID COMPOSITION, AND TARGETING

Transcript expression patterns, when combined with observations of amino acid composition and targeting, give a more comprehensive picture of silicification protein regulation than any single line of evidence can provide. This data shows interesting trends relating the timing of transcript induction to encoded protein properties and has implications for the trafficking and regulation of silicification related proteins.

A subset of genes involved in silicification are upregulated during either S or M phase, or have expression patterns which do not respond to any canonical cell cycle events (**Figure 9**). SAP3 transcripts are also induced between M phase and valve formation. We are particularly intrigued by the expression pattern of SAP3 as its transcript peak coincides with the period when we propose that SDV assembly is occurring. This hypothesis is supported by dynamic localization of Sin1, where it is localized to the silicalemma prior to or concurrent with the initiation of silica polymerization (Kotzsch et al., 2017).

The responses described above do not relate to the formation of a particular silica structure. It should be noted that **Figure 9** shows changes in transcript levels, not absolute abundance, so lack of induction does not mean a protein is not being expressed. However, transcript induction at a particular time is consistent with an increase in the protein encoded by that transcript (with the caveat that the relation between transcript and protein abundance can vary). Upregulation of silicification related genes when cell wall structures are not being made suggests that encoded proteins are synthesized in advance of when they are needed for cell wall synthesis. The cingulins were localized to the girdle bands (Scheffel et al., 2011), yet transcripts for Cin W1 and 2 have a valve response, and the other cingulins have an S or M phase response (**Figure 9**). Sil3, SAP1 and 3, and Sin1 were localized to both valves and girdle bands (Scheffel et al., 2011; Kotzsch et al., 2017; Tesson et al., 2017), but have valve-formation, S or M phase, or pre-valve transcript responses. Sil1, the only protein that has been localized exclusively to the valves, had relatively little change in transcript abundance over the cell cycle. These observations are also consistent with intracellular accumulation of silicification proteins prior to their use. SAP3 and Sin1 were directly shown to accumulate in the cell (Kotzsch et al., 2017; Tesson et al., 2017). Intracellular accumulation of GFP-tagged protein was not documented for Sil1/2 and 4 (Poulsen et al., 2013), the cingulins (Scheffel et al., 2011) or SAP1 (Tesson et al., 2017), even though the transcript data suggests that accumulation could occur. These proteins either didn't accumulate prior to use, the GFP tag could have been rapidly removed and degraded, or GFP fluorescence could have been inhibited if the protein was present in an acidic environment (Poulsen et al., 2013).

One possible explanation for the accumulation of silicification proteins is that it would be challenging for the cell to make the large amount of all proteins required to create the cell wall in the short time period allotted. Stockpiling protein that could then be targeted *en mass* to the SDV would circumvent overloading the synthesis system. Such an approach could also impart a level of regulation over the process if particular proteins can co-exist in storage locations such that they don't catalyze silicification, but then can do so when combined with other separately stored proteins.

Following this concept, a potentially interesting observation stems from categorizing the amino acid composition of proteins according to transcript expression patterns, in which we compare the three expression categories (valve formation, S or M phase, and other) to the mean of all proteins irrespective of category (**Figure 11**). The "other" category proteins are enriched (at least 1.5-fold $\log_2$) in Arg and Glu, and depleted (at least 0.5-fold $\log_2$) in Cys, Gly, Trp, and Tyr relative to proteins in the other expression categories. The valve formation and S or M phase response proteins are similar to each other, with exceptions being that the valve formation response group is depleted for Thr and enriched in Trp. The general tendency is that amino acids that have interaction or aggregation properties are enriched or depleted. These include electrostatic (Arg, Glu), covalent (Cys), and hydrophobic (Trp, Tyr) interactions. The average pI of proteins in the different expression categories also differ, with the other category ($pI_{ave} = 9.13 \pm 2.1$, $n = 4$) being basic, and the valve ($pI_{ave} = 6.52 \pm 2.1$, $n = 6$) and S or M phase ($pI_{ave} = 6.29 \pm 1.9$, $n = 8$) categories being slightly acidic. Given the proposed models for electrostatic interactions and pH-dependent aggregation phenomenon demonstrated for silaffins and Sin1 (Kröger et al., 1999; Kotzsch et al., 2016, 2017), this data infers that expression stage-specific biases could relate to functional requirements related to protein-protein interactions at different stages in the process.

Direct observational data indicates that there are multiple means of targeting and trafficking proteins to the SDV. One way is direct targeting to the SDV, apparently through a sub compartment of the ER, as demonstrated in Sil3 (Poulsen et al., 2013). Amino acid substitution experiments (Poulsen et al., 2013) were consistent with posttranslational modification of lysines and serines being essential for silaffin targeting. The former can be modified by methyl groups and polyamine chains, and the latter by phosphate or carbohydrate moieties (Poulsen and Kröger, 2004). An analogy was made (Poulsen and Kröger, 2004) to the targeting of proteins from the trans Golgi network to the lysosome, which involves a post-translational modification to incorporate mannose 6-phosphate. This suggests in this case that modifications to the amino acids, and not the amino acid sequence, determine targeting. A second mode of targeting is through large intracellular vesicles, as seen with GFP fusions of SAP3 and Sin1 (Kotzsch et al., 2017; Tesson et al., 2017).

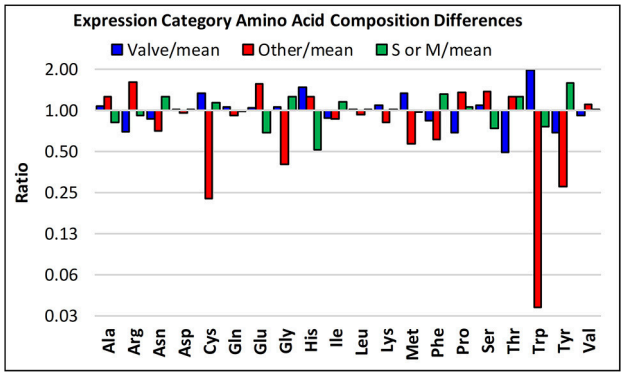

FIGURE 11 | Amino acid enrichments based on expression response category. The ratios of the abundances of particular amino acids are plotted, comparing three of the different transcript expression patterns defined in **Figure 9**, specifically, valve, S or M phase, and "other".

Initial data is consistent with these being the location of protein accumulation (Tesson et al., 2017). Presumably, these vesicles fuse with the SDV during valve formation. The third documented mode of targeting is recruitment from the plasma membrane, as occurs with Sin1. This protein is targeted to both the intracellular vesicle and plasma membrane, and is recruited to the SDV from the plasma membrane during valve formation, then returns to the plasma membrane afterwards (Kotzsch et al., 2017). Because the protein is also localized to both valves and girdle bands, there must be versatility built into the targeting and possibly a repurposing process beyond what is typical for secreted proteins. Although a role in silicification is likely for SDV associated Sin1, it is unclear what role the protein might play in the plasma membrane.

The reason(s) for these diverse targeting and trafficking processes is unclear, but we can return to hypotheses about the need to synthesize and store particular proteins in advance and/or to maintain particular combinations of proteins separately until assembly in the SDV. The system could provide a means of checks and balances, for example, unless requirements (e.g., adequate abundance) for a particular protein are met, then subsequent processes will not occur. This would be especially important in terms of valve formation, where ideally the cell would be able to assess whether it was capable of completing the valve before attempting to make it, as an incompletely formed valve could severely compromise cellular integrity. There is support for this hypothesis in relation to function and expression patterns of some known silicification genes. Silaffin 1/2 and silacidin lack cell cycle specific transcript responses, and silacidin and Sil1/2 L solely promote silica formation (Poulsen and Kröger, 2004; Wenzl et al., 2008). Under depleted silicon conditions, there is increased processing of Sil 1/2 from H to L form and also an increase in the amount of silacidin in the cell wall (Richthammer et al., 2011), consistent with silica formation capability being favored. In contrast, TpSil3 has regulatory activity with regards to silica formation (Poulsen and Kröger, 2004), and is expressed during valve formation. Because of the substantial differences in their timing of maximal expression, TpSil3 may also use a distinct targeting route compared with TpSil1/2 and silacidins. A simplistic view is that under silicon limiting conditions the cell prepares for silica formation by increasing the amount of silicification promoting proteins, but it is not until some level of regulation over silica formation can be imparted that structures such as the valve are made.

A HYPOTHESIS ABOUT THE TIMING OF EVENTS IN VALVE FORMATION

Based on the expression and targeting discussion, as well as other data in the literature, we propose a series of events that occur during valve formation in *T. pseudonana*. These events are delineated by hypothesized checkpoints, events which must be completed in full before cell wall formation can progress. An initial checkpoint is related to the availability of silicic acid. In *T. pseudonana*, the majority of cells arrest in the G1 phase of the cell cycle if silicic acid levels are insufficient (Brzezinski et al., 1990; Hildebrand et al., 2007). This prevents initiation of the division process. During valve formation, the cytoskeleton appears to be involved in positioning mesoscale structures via microtubules, and patterning the overall surface features by actin (Tesson and Hildebrand, 2010). For this to occur, an interaction between the cytoskeletal components and SDV must exist, and based on the model of Robinson and Sullivan (1987), this is facilitated through the silicalemma associated proteins. Thus, the assembly of the cytoskeleton and the SDV must be coordinated. Additionally, because the AFIM precisely mimics mesoscale silica structure, its constituent proteins must be assembled in the SDV with similar timing. We suggest that the silicalemma associated proteins either appear first, or concurrently with proteins of the AFIM. Either scenario would facilitate cytoskeletal-based positioning of components to organize them for base layer formation. It should be noted that the initial deposition appears to occur prior to when the SDV has reached its final position and dimensions, ion abrasion SEM (IASEM) of an extremely early stage of silica deposition showed a flexible structure with base layer features, which was positioned near one edge of the cell (Hildebrand et al., 2009). Because complete base layer intermediate structures are commonly observed by standard SEM (Hildebrand et al., 2006), we propose that their complete formation, likely mediated in part via actin controlled expansion of the SDV (Tesson and Hildebrand, 2010) and the AFIM (Tesson and Hildebrand, 2013) as previously described, serves as the second checkpoint in valve formation. This would ensure that z-axis expansion was triggered only after x/y axis expansion was complete, ensuring that z-axis structures covered the entirety of the valve.

An important question related to the process of z-axis expansion and the hypothesis that proteins of the SDV are accumulated as precursors, is what prevents silica polymerization at cellular locations other than the SDV, and what stimulates silica formation to occur? For the former, the lack of high enough silicic acid concentrations might be a factor, but because silicic acid freely diffuses across membranes (Thamatrakoln and Hildebrand, 2008), there would be a lack of control over its supply once it entered the cell. We suggest that a shift in pH within the

SDV is an important trigger for silicification, and that a lack of pH change in other compartments could prevent silica formation. Data supports the importance of low pH for silica formation; non-postranslationally modified *C. fusiformis* silaffins had a silica forming optima at pH 7, whereas the native silaffins were optimal at pH 5 (Kröger et al., 1999). Recombinant Sin1, cingulins CinY2 and CinW2 all exhibited silica polymerization and aggregation at low pH (Kotzsch et al., 2016, 2017). Lower pH is also a fundamental chemical characteristic of formation of silica network structures (Iler, 1979), such as those seen in diatoms. Lowering the pH in intracellular compartments typically occurs by proton pumping by the vacuolar H^+-ATPase or VHA (Finbow and Harrison, 1997), and we suggest VHA involvement in SDV acidification. This would provide an overall control over the process distinct from the involvement of silicification proteins and LCPAs. Some aspects of structure formation may not be pH dependent, for example, given the distinct stage of base layer formation, and its distinct silica structure compared with the bulk of the valve silica, it could be formed in the absence of a pH shift. Z-axis expansion in which the existing base layer valve structure is filled in could be an example of a pH dependent process.

AREAS FOR ATTENTION MOVING FORWARD

The continuing investigation into understanding how diatoms make their silica cell walls has involved a variety of techniques which were state-of-the-art when initially applied. These techniques have not only have improved our understanding of cell wall formation, but in combination, provide different perspectives on the process (Hildebrand and Lerch, 2015). Understanding the outcomes of various cell wall extraction procedures has affected our interpretations of the role of specific organic components in silicification. The logical approach of isolating organic material embedded within detergent-cleaned silica as essential components of the silicification process resulted in the seminal discoveries of the silaffins, LCPAs, and silacidins (Kröger et al., 1999, 2000, 2002; Poulsen and Kröger, 2004; Wenzl et al., 2008). Consistent with our hypotheses about soluble silicification proteins, silica formed by them exhibits nanoscale, but not highly organized meso- or micro-scale order. Later characterization of insoluble organic material resulting from the same isolation procedure identified material (the AFIM) that has a clear relation to higher order structural features (Scheffel et al., 2011; Tesson and Hildebrand, 2013). As discussed, although chitin appears to play an important role in structure formation, to date purification procedures have not enabled distinction between a possible structural arrangement of chitin and the AFIM. To completely remove organic material associated with the surface of the silica, acid treatment is required (**Figure 4C**)—detergent or peroxide treatment is insufficient. A model that addressed the relation between the cytoskeleton and silica structures formed within the SDV (Robinson and Sullivan, 1987), led to the investigation of silicalemma-associated proteins (currently the SAPs and Sin1), and the genetic manipulation demonstration that they are involved in structure formation (Tesson et al., 2017). It is not clear, however, whether these proteins interact with the cytoskeleton.

Microscopic approaches have provided fundamental insights and will continue to be important in understanding the spatial relationships of organic components and silica structures, these relationships are essential for understanding the function of the organic components. A current limitation in linking molecular entities with ultrastructure is the insufficient resolution of confocal or other optical sectioning microscopy to image fluorescent proteins. The first application of super-resolution fluorescence microscopy on TpSil3 (Gröger et al., 2016) suggests a direction to move toward. In this study, three different fluorescent proteins fused to TpSil3 displayed fluorescence of the protein embedded in silica, with resolution on the order of 25 nm. One issue is that the three proteins exhibited distinct localization patterns in the silica, with the exception of a lack of localization at the fultoportulae, thus it is unclear which protein provides the most accurate assessment of localization, or whether any do. Independent verification using another microscopy technique such as immunogold labeling could clarify that. An unanswered question is whether incorporation of a normally soluble protein (GFP) into silica within the acidic SDV will affect the assembly or localization properties of native silica associated proteins—this also indicates a need for independent localization verification. A combination of localization with genetic manipulation could be especially useful.

We are still in the process of identifying the complete set of proteins involved in silicification, and although significant progress has been made, considering the total number of proteins that must be required, there is more to be done. Both biochemical characterization and transcriptomic analyses have been useful approaches for identifying silicification proteins. Reference transcriptomic datasets may also be good sources for further identification, particularly if efforts are made to identify novel conserved motifs or domains. In this and a previous review (Hildebrand and Lerch, 2015), we identified distinct transcript expression patterns for silicification genes, which expand upon the initial use of only the valve expression pattern (Frigeri et al., 2006; Shrestha et al., 2012) these expression patterns may be useful in further candidate protein identification (Brembu et al., 2017).

In addition to identifying new proteins involved in cell wall formation there are also many unknowns in relatively well-studied areas of this process. Although it has been established that the cytoskeleton is largely responsible for shaping the SDV and positioning structures within it, the dynamics of cytoskeletal movements during structure formation has not been extensively investigated in *T. pseudonana*. Although not discussed in this review, the process of cell wall exocytosis and the required dynamics of the cytoskeleton and silicalemma associated proteins are also important processes. If SAP3 and Sin1 do associate with in some way with the cytoskeleton or other proteins, proteolytic cleavage of their C-termini could be related to the need to release the SDV after silica formation is complete, enabling exocytosis. The involvement of carbohydrate polymers in silicification is also not well-understood, though they are closely associated with diatom silica, and play a role in structure formation (Tesson et al.,

2008; Brunner et al., 2009; Durkin et al., 2009; Hedrich et al., 2013; Tesson and Hildebrand, 2013).

A major emphasis for future work should be better understanding the dynamic processes of cell wall formation. Dynamic imaging approaches have only recently applied to follow the course of events in silicification (Kotzsch et al., 2017). Given the previous discussions, understanding the trafficking processes and timing of key events should provide essential information to understand SDV assembly and associated regulation of its components. Synchronization is a useful approach, but is limited by the fact that even under synchronization individual cells differ in their precise stage of cell wall synthesis—thus details about precise timing are obscured. Imaging single cells progressing through the cell cycle should provide the necessary temporal resolution, thus high-resolution time course imaging on single cells, coupled with co-localization of proteins tagged with different fluorescent markers, is a particularly promising approach.

Given the power of genetically-based approaches to elucidate complex cellular phenomenon such as the cell cycle in yeast, application of genetic manipulation approaches should contribute substantially to clarifying the processes of silicification. Understanding the roles of an individual protein found in a complex assembly of other proteins can be facilitated by selectively removing or decreasing the amount of that protein by knockdown or knockout approaches. One consideration is that the effects of knockdown on structure could be so severe that daughter cells are inviable, and the change in silica structure could not be propagated, and hence, not visualized. In this case, conditional knockdowns could be useful. The most well-developed conditional promoter for diatoms is for nitrate reductase (Poulsen and Kroger, 2005; Poulsen et al., 2006), which is upregulated in the presence of nitrate, and downregulated in ammonium. However, experiments done in our lab (Lerch, unpublished data) indicate that *T. pseudonana* valve morphology can vary significantly depending on the nitrogen source in the growth medium, which puts a practical limitation on the use of the nitrate reductase promoter in silicification investigations. Identifying another inducible promoter would be a great help. If a suitable inducible promoter was developed, it could be coupled with a synchronized cultivation approach where the knockdown was induced and cells could be isolated after valve formation to evaluate its effect. In this scenario, lack of propagation of daughter cells would not be an issue. Genetic approaches could also improve our understanding of the biochemistry involved by enabling sequence specific alterations in proteins to probe their functions.

Despite an abundant fascination with diatom silica structures, and the growing number of applications which use them, improvement in our understanding of how the structures are made is needed. One reason for this is the lack of precedence for a phenomenon similar to diatom silicification in other biological systems. Each significant discovery in the diatom realm has been novel and required demonstration at a fundamental level. The proteins involved also have unique characteristics, which makes understanding their functions more challenging. Despite the challenges, multiple aspects of cell wall formation have been described through a combination of experimental approaches. We expect that the recent breakthroughs in identifying a new class of SDV associated proteins (Kotzsch et al., 2017; Tesson et al., 2017), the presence of transcriptomic datasets to probe for candidate silicification genes (Shrestha et al., 2012; Keeling et al., 2014; Brembu et al., 2017), dynamic and higher resolution imaging (Gröger et al., 2016; Kotzsch et al., 2017) and genetic manipulation approaches (Tesson et al., 2017) will complement the previously established characterization approaches to allow the field to move forward with a better understanding of the dynamic spatial and temporal protein interactions that are responsible for generating silica structure in a coordinated and controlled manner.

AUTHOR CONTRIBUTIONS

MH assembled an initial draft of the manuscript; MH, SL, and RS were involved in editing and completion.

ACKNOWLEDGMENTS

Diatom silicification research in the Hildebrand lab has been supported by Air Force Office of Scientific Research Multidisciplinary University Research Initiative Grants RF00965521 and FA9550-10-1-0555.

SUPPLEMENTARY MATERIAL

The Supplementary Material for this article can be found online at: https://www.frontiersin.org/articles/10.3389/fmars.2018.00125/full#supplementary-material

REFERENCES

Anonymous (1702). Two letters from a Gentleman in the Country, relating to Mr. Leeuwenhoek's Letter in Transaction, no. 283. *Philos. Trans. R. Soc. Lond. B* 23, 1494–1501.

Bendtsen, J. D., Nielsen, H., Heijne, G. V., and Brunak, S. (2004). Improved prediction of signal peptides: SignalP 3.0. *J. Mol. Biol.* 340, 783–795. doi: 10.1016/j.jmb.2004.05.028

Blank, G. S., and Sullivan, C. W. (1983). Diatom mineralization of silicic acid. IV. The effect of microtubule inhibitors on silicic acid metabolism in *Navicula saprophila*. *J. Phycol.* 19, 39–44

Brembu, T., Skogen Chauton, M., Winge, P., Bones, A. M., and Vadstein, O. (2017). Dynamic responses to silicon in *Thalassiosira pseudonana* – Identification, characterisation, and classification of signature genes and their corresponding protein motifs. *Sci. Rep.* 7:4865. doi: 10.1038/s41598-017-04921-0

Brunner, E., Richthammer, P., Ehrlich, H., Paasch, S., Simon, P., Ueberlein, S., et al. (2009). Chitin-based organic networks: an integral part of cell wall biosilica in

the diatom *Thalassiosira pseudonana*. *Angew. Chem. Int. Ed.* 48, 9724–9727. doi: 10.1002/anie.200905028

Brzezinski, M. A., Olson, R. J., and Chisholm, S. W. (1990). Silicon availability and cell-cycle progression in marine diatoms. *Mar. Ecol. Prog. Ser.* 67, 83–96. doi: 10.3354/meps067083

Chiappino, M. L., and Volcani, B. E. (1977). Studies on the biochemistry and fine structure of silica shell formation in diatoms. VIII. Sequential cell wall development in the pennate *Navicula*. *Protoplasma* 93, 205–221. doi: 10.1007/BF01275654

Davis, A. K., Hildebrand, M., and Palenik, B. (2005). A stress-induced protein associated with the girdle band region of the diatom *Thalassiosira pseudonana*. *J. Phycol.* 41, 577–589. doi: 10.1111/j.1529-8817.2005.00076.x

Drum, R. W., and Pankratz, S. H. (1964). Post mitotic fine structure of *Gomphonerna parvulum*. *J. Ultrastruct. Res.* 10, 217–223.

Durkin, C. A., Mock, T., and Armbrust, E. V. (2009). Chitin in diatoms and its association with the cell wall. *Euk. Cell* 8, 1038–1050. doi: 10.1128/EC.00079-09

Emanuelsson, O., Nielsen, H., and Von Heijne, G. (1999). ChloroP, a neural network-based method for predicting chloroplast transit peptides and their cleavage sites. *Protein Sci.* 8, 978–984. doi: 10.1110/ps.8.5.978

Finbow, M. E., and Harrison, M. A. (1997). The vacuolar H+-ATPase: a universal proton pump of eukaryotes. *Biochem. J.* 15, 697–712. doi: 10.1042/bj3240697

Frigeri, L. G., Radabaugh, T. R., Haynes, P. A., and Hildebrand, M. (2006). Identification of proteins from a cell wall fraction of the diatom *Thalassiosira pseudonana*: Insights into silica structure formation. *Mol. Cell. Proteomics* 5, 182–193. doi: 10.1074/mcp.M500174-MCP200

Gröger, P., Poulsen, N., Klemm, J., Kröger, N., and Schlierf, M. (2016). Establishing super-resolution imaging for proteins in diatom biosilica. *Sci. Rep.* 6:36824. doi: 10.1038/srep36824

Gruber, A., Vugrinec, S., Hempel, F., Gould, S. B., and Maier, U. G. (2007). Protein targeting into complex diatom plastids: functional characterisation of a specific targeting motif. *Plant Mol. Biol.* 64, 519–530. doi: 10.1007/s11103-007-9171-x

Hall, D. D., Markwardt, D. D., Parviz, F., and Heideman, W. (1998). Regulation of the Cln3-Cdc28 kinase by cAMP in *Saccharomyces cerevisiae*. *EMBO J.* 3, 4370–4378. doi: 10.1093/emboj/17.15.4370

Hedrich, R., Machill, S., and Brunner, E. (2013). Biomineralization in diatoms-phosphorylated saccharides are part of *Stephanopyxis turris* biosilica. *Carb. Res.* 365, 52–60. doi: 10.1016/j.carres.2012.11.001

Herth, W. (1979a). Site of beta-chitin fibril formation in centric diatoms. 1. Pores and fibril formation. *J. Ultrastruc. Res.* 68, 6–15.

Herth, W. (1979b). Site of beta-chitin fibril formation in centric diatoms. 2. Chitin-forming cytoplasmic structures. *J. Ultrastruc. Res.* 68, 16–27.

Hildebrand, M., Frigeri, L., and Davis, A. K. (2007). Synchronized growth of *Thalassiosira pseudonana* (Bacillariophyceae) provides novel insights into cell wall synthesis processes in relation to the cell cycle. *J. Phycol.* 43, 730–740. doi: 10.1111/j.1529-8817.2007.00361.x

Hildebrand, M., Kim, S., Shi, D., Scott, K., and Subramaniam, S. (2009). 3D imaging of diatoms with ion-abrasion scanning electron microscopy. *J. Struct. Biol.* 166, 316–328. doi: 10.1016/j.jsb.2009.02.014

Hildebrand, M., and Lerch, S. J. L. (2015). Diatom silica biomineralization: parallel development of approaches and understanding. *Semin. Cell Dev. Biol.* 46, 27–35. doi: 10.1016/j.semcdb.2015.06.007

Hildebrand, M., Volcani, B. E., Gassmann, W., and Schroeder, J. I. (1997). A gene family of silicon transporters. *Nature* 385, 688–689.

Hildebrand, M., York, E., Kelz, J. I., Davis, A. K., Frigeri, L. G., Allison, D. P., et al. (2006). Nano-scale control of silica morphology and three-dimensional structure during diatom cell wall formation. *J. Mater. Res.* 21, 2689–2698. doi: 10.1557/jmr.2006.0333

Iler, R. K. (1979). *The Chemistry of Silica: Solubility, Polymerization, Colloid and Surface Properties, and Biochemistry*. New York: Wiley-Interscience.

Jantschke, A., Koers, E., Mance, D., Weingarth, M., Brunner, E., and Baldus, M. (2015). Insight into the supramolecular architecture of intact diatom biosilica from DNP-supported solid-state NMR spectroscopy. *Angew. Chem. Int. Ed.* 54, 15069–15073. doi: 10.1002/anie.201507327

Katti, M. V., Sami-Subbu, R., Ranjekar, P. K., and Gupta, V. S. (2000). Amino acid repeat patterns in protein sequences: their diversity and structural-functional implications. *Prot. Sci.* 9, 1203–1209. doi: 10.1110/ps.9.6.1203

Keeling, P. J., Burki, F., Wilcox, H. M., Allam, B., Allen, E. E., Amaral-Zettler, L. A., et al. (2014). The marine microbial eukaryote transcriptome sequencing project (MMETSP): Illuminating the functional diversity of eukaryotic life in the oceans through transcriptome sequencing. *PLoS Biol.* 12:e1001889. doi: 10.1371/journal.pbio.1001889

Kilian, O., and Kroth, P. G. (2005). Identification and characterization of a new conserved motif within the presequence of proteins targeted into complex diatom plastids. *Plant J.* 41, 175–183. doi: 10.1111/j.1365-313X.2004.02294.x

Kley, M., Kempter, A., Boyko, V., and Huber, K. (2014). Mechanistic studies of silica polymerization from supersaturated aqueous solutions by means of time-resolved light scattering. *Langmuir* 30, 12664–12674. doi: 10.1021/la502730y

Kotzsch, A., Groeger, P., Pawolski, D., Bomans, P. H. H., Sommerdijk, N. A. J. M., Schlierf, M., et al. (2017). Silicanin-1 is a conserved diatom membrane protein involved in silica biomineralization. *BMC Biol.* 15:65. doi: 10.1186/s12915-017-0400-8

Kotzsch, A., Pawolski, D., Milentyev, A., Shevchenko, A., Scheffel, A., Poulsen, N., et al. (2016). Biochemical composition and assembly of biosilica-associated insoluble organic matrices from the diatom *Thalassiosira pseudonana*. *J. Biol. Chem.* 291, 4982–4997. doi: 10.1074/jbc.M115.706440

Kröger, N., Deutzmann, R., Bergsdorf, C., and Sumper, M. (2000). Species-specific polyamines from diatoms control silica morphology. *Proc. Natl. Acad. Sci. U.S.A.* 97, 14133–14138. doi: 10.1073/pnas.260496497

Kröger, N., Deutzmann, R., and Sumper, M. (1999). Polycationic peptides from diatom biosilica that direct silica nanosphere formation. *Science* 286, 1129–1132. doi: 10.1126/science.286.5442.1129

Kröger, N., Lorenz, S., Brunner, E., and Sumper, M. (2002). Self-assembly of highly phosphorylated silaffins and their function in biosilica morphogenesis. *Science* 298, 584–586. doi: 10.1126/science.1076221

Li, C.-W., Chu, S., and Lee, M. (1989). Characterizing the silicon deposition vesicle of diatoms. *Protoplasma* 151, 158–163.

Mann, D. G. (1984). "An ontogenetic approach to diatom systematics," in *Proceedings of the Seventh International Diatom Symposium,* ed D. G. Mann (Koenigstein: Koeltz), 113.

Martin-Jezequel, V., Hildebrand, M., and Brzezinski, M. A. (2000). Silicon metabolism in diatoms: Implications for growth. *J. Phycol.* 36, 821–840. doi: 10.1046/j.1529-8817.2000.00019.x

Michael, A. J. (2011). Molecular machines encoded by bacterially-derived multi-domain gene fusions that potentially synthesize, N-methylate and transfer long chain polyamines in diatoms *FEBS Lett.* 585, 2627–2634. doi: 10.1016/j.febslet.2011.07.038

Michael, A. J. (2016). Polyamines in Eukaryotes, bacteria and archea. *J. Biol. Chem.* 291, 14896–14903. doi: 10.1074/jbc.R116.734780

Pickett-Heaps, J. (1998a). Cell division and morphogenesis of the centric diatom *Chaetoceros decipiens* (Bacillariophyceae) I. Living cells. *J. Phycol.* 34, 989–994.

Pickett-Heaps, J. (1998b). Cell division and morphogenesis of the centric diatom *Chaetoceros decipiens* (Bacillariophyceae) II. Electron microscopy and a new paradigm for tip growth. *J. Phycol.* 34, 995–1004.

Pickett-Heaps, J. D., Tippit, D. H., and Andreozzi, J. A. (1979). Cell division in the pennate diatom Pinullaria, I. V. Valve morphogenesis. *Biol. Cell* 35, 199–206.

Pickett-Heaps, J., Schmid, A.-M. M., and Edgar, L. A. (1990). The cell biology of diatom valve formation. *Prog. Phycol. Res.* 7, 1–168.

Poulsen, N., Chesley, P. M., and Kroger, N. (2006). Molecular genetic manipulation of the diatom *Thalassiosira pseudonana* (Bacillariophyceae). *J. Phycol.* 42, 1059–1065. doi: 10.1111/j.1529-8817.2006.00269.x

Poulsen, N., and Kroger, N. (2005). A new molecular tool for transgenic diatoms - Control of mRNA and protein biosynthesis by an inducible promoter-terminator cassette. *FEBS J.* 272, 3413–3423. doi: 10.1111/j.1742-4658.2005.04760.x

Poulsen, N., and Kröger, N. (2004). Silica morphogenesis by alternative processing of silaffins in the diatom *Thalassiosira pseudonana*. *J. Biol. Chem.* 279, 42993–42999. doi: 10.1074/jbc.M407734200

Poulsen, N., Scheffel, A., Sheppard, V. C., Chesley, P. M., and Kröger, K. (2013). Pentalysine clusters mediate silica targeting of silaffins in *Thalassiosira pseudonana*. *J. Biol. Chem.* 288, 20100–20109. doi: 10.1074/jbc.M113.469379

Poulsen, N., Sumper, M., and Kroger, N. (2003). Biosilica formation in diatoms: characterization of native silaffin-2 and its role in silica morphogenesis. *Proc. Natl. Acad. Sci. U.S.A.* 100, 12075–12080. doi: 10.1073/pnas.2035131100

Reimann, B. E. F., Volcani, B. E., and Lewin, J. C. (1966). Studies on the biochemistry and fine structure of silica shell formation in diatoms. II. The structure of the cell wall of *Navicula pelliculosa* (Breb.) Hilse. *J. Phycol.* 2, 74–84.

Richthammer, P., Bçrmel, M., Brunner, E., and van Pee, K. H. (2011). Biomineralization in diatoms: the role of silacidins. *ChemBioChem* 12, 1362–1366. doi: 10.1002/cbic.201000775

Robinson, D. H., and Sullivan, C. W. (1987). How do diatoms make silicon biominerals? *TIBS* 12, 151–154.

Rogall, E. (1939). Uber den feinbau der kieselmembran der diatomeen. *Planta* 29, 279–281.

Round, F. E., Crawford, R. M., and Mann, D. G. (1990). *The Diatoms: Biology and Morphology of the Genera.* Cambridge: Cambridge University Press.

Scheffel, A., Poulsen, N., Shian, S., and Kröger, N. (2011). Nanopatterned protein microrings from a diatom that direct silica morphogenesis. *Proc. Natl. Acad. Sci. U.S.A.* 108, 3175–3180. doi: 10.1073/pnas.1012842108

Schmid, A. M., Borowitzka, M. A., and Volcani, B. E. (1981). "Morphogenesis and biochemistry of diatom cell walls," in *Cell Biology Monographs: Cytomorphogenesis in Plants, Vol. 8,* ed O. Kiermayer (Wien: Springer-Verlag), 63.

Schmid, A.-M. M. (1980). Valve morphogenesis in diatoms: a pattern-related filamentous system in pennates and the effect of APM, colchicine, and osmotic pressure. *Nova Hedwiga* 33, 811–847

Shimizu, K., Del Amo, Y., Brzezinski, M. A., Stucky, G. D., and Morse, D. E. (2001). A novel fluorescent silica tracer for biological silicification studies. *Chem. Biol.* 8, 1051–1060. doi: 10.1016/S1074-5521(01)00072-2

Shrestha, R. P., and Hildebrand, M. (2015). Evidence for a regulatory role of diatom silicon transporters in cellular silicon responses. *Euk. Cell* 14, 29–40. doi: 10.1128/EC.00209-14

Shrestha, R. P., Tesson, B., Norden-Krichmar, T., Federowicz, S., Hildebrand, M., and Allen, A. E. (2012). Whole transcriptome analysis of the silicon response of the diatom *Thalassiosira pseudonana. BMC Genomics* 13:499. doi: 10.1186/1471-2164-13-499

Sonnhammer, E. L. L., von Heijne, G., and Krogh, A. (1998). "A hidden Markov model for predicting transmembrane helices in protein sequences," in *Proc. Sixth Int. Conf. on Intelligent Systems for Molecular Biology,* eds J. Glasgow, T. Littlejohn, F. Major, R. Lathrop, D. Sankoff, and C. Sensen (Palo Alto, CA: AAAI Press), 175–182.

Tesson, B., and Hildebrand, M. (2010). Extensive and intimate association of the cytoskeleton with forming silica in diatoms: control over patterning on the meso- and micro-scale. *PLoS ONE* 5:e14300. doi: 10.1371/journal.pone.0014300

Tesson, B., and Hildebrand, M. (2013). Characterization and localization of insoluble organic matrices associated with diatom cell walls: insight into their roles during cell wall formation. *PLOS ONE* 8:e61675. doi: 10.1371/journal.pone.0061675

Tesson, B., Lerch, S. J. L., and Hildebrand, M. (2017). Characterization of a new protein family associated with the silica deposition vesicle membrane enables genetic manipulation of diatom silica. *Sci. Rep.* 7:13457. doi: 10.1038/s41598-017-13613-8

Tesson, B., Masse, S., Laurent, G., Maquet, J., and Livage, J. (2008). Contribution of multi-nuclear solid state NMR to the characterization of the *Thalassiosira pseudonana* diatom cell wall. *Anal. Bioanal. Chem.* 390, 1889–1898. doi: 10.1007/s00216-008-1908-0

Thamatrakoln, K., and Hildebrand, M. (2008). Silicon uptake in diatoms revisited: a model for saturable and nonsaturable uptake kinetics and the role of silicon transporters. *Plant Physiol.* 146, 1397–1407. doi: 10.1104/pp.107.107094

van de Meene, A. M. L., and Pickett-Heaps, J. D. (2002). Valve morphogenesis in the centric diatom *Proboscia alata* Sundstrom. *J. Phycol.* 38, 351–363. doi: 10.1046/j.1529-8817.2002.01124.x

Waterkeyn, L., and Bienfait, A. (1987). Localization and function of beta 1,3-glucans (callose and chrysolaminarin) in *Pinnularia* genus (Diatoms). *Cellule* 74, 199–226.

Wenzl, S., Hett, R., Richthammer, P., and Sumper, M. (2008). Silacidins: highly acidic phosphopeptides from diatom shells assist in silica precipitation *in vitro*. *Angew. Chem. Int. Ed. Engl.* 47, 1729–1732. doi: 10.1002/anie.200704994

Conflict of Interest Statement: The authors declare that the research was conducted in the absence of any commercial or financial relationships that could be construed as a potential conflict of interest.

Copyright © 2018 Hildebrand, Lerch and Shrestha. This is an open-access article distributed under the terms of the Creative Commons Attribution License (CC BY). The use, distribution or reproduction in other forums is permitted, provided the original author(s) and the copyright owner are credited and that the original publication in this journal is cited, in accordance with accepted academic practice. No use, distribution or reproduction is permitted which does not comply with these terms.

frontiers in Marine Science

REVIEW
published: 10 April 2018
doi: 10.3389/fmars.2018.00123

Optical Properties of Nanostructured Silica Structures From Marine Organisms

*Ali Mcheik[1,2,3], Sophie Cassaignon[2], Jacques Livage[2], Alain Gibaud[4], Serge Berthier[3,5] and Pascal J. Lopez[1]**

[1] Unité Biologie des Organismes et Ecosystèmes Aquatiques, Muséum National d'Histoire Naturelle, Centre National de la Recherche Scientifique (UMR-7208), Sorbonne Université, Institut de Recherche pour le Développement, Université de Caen Normandie, Université des Antilles, Paris, France, [2] Sorbonne Université, Centre National de la Recherche Scientifique (UMR-7574), Collège de France, Laboratoire de Chimie de la Matière Condensée de Paris, Paris, France, [3] Sorbonne Université, Centre National de la Recherche Scientifique (UMR-7588), Institut des Nanosciences de Paris, Paris, France, [4] Université du Maine, Centre National de la Recherche Scientifique (UMR-6283), Institut des Molécules et Matériaux du Mans, Le Mans, France, [5] Université Paris Diderot, Paris, France

Light is important for the growth, behavior, and development of both phototrophic and autotrophic organisms. A large diversity of organisms used silica-based materials as internal and external structures. Nano-scaled well-organized silica biomaterials are characterized by a low refractive index and an extremely low absorption coefficient in the visible range, which make them interesting for optical studies. Recent studies on silica materials from glass sponges and diatoms, have pointed out very interesting optical properties, such as light waveguiding, diffraction, focusing, and photoluminescence. Light guiding and focusing have been shown to be coupled properties found in spicule of glass sponge or shells of diatoms. Moreover, most of these interesting studies have used purified biomaterials and the properties have addressed in non-aquatic environments, first in order to enhance the index contrast in the structure and second to enhance the spectral distribution. Although there is many evidences that silica biomaterials can present interesting optical properties that might be used for industrial purposes, it is important to emphases that the results were obtained from a few numbers of species. Due to the key roles of light for a large number of marine organisms, the development of experiments with living organisms along with field studies are require to better improve our understanding of the physiological and structural roles played by silica structures.

Keywords: diatoms, sponges, photonics materials, light-silica interaction, biosilica

OPEN ACCESS

Edited by:
Brivaela Moriceau, UMR6539 Laboratoire des Sciences de L'environnement Marin (LEMAR), France

Reviewed by:
Christian Maibohm, Laboratório Ibérico Internacional de Nanotecnologia (INL), Portugal
Hermann Ehrlich, Freiberg University of Mining and Technology, Germany

***Correspondence:**
Pascal J. Lopez
pascal-jean.lopez@mnhn.fr

Specialty section:
This article was submitted to Marine Biogeochemistry, a section of the journal Frontiers in Marine Science

Received: *09 October 2017*
Accepted: *22 March 2018*
Published: *10 April 2018*

Citation:
Mcheik A, Cassaignon S, Livage J, Gibaud A, Berthier S and Lopez PJ (2018) Optical Properties of Nanostructured Silica Structures From Marine Organisms. Front. Mar. Sci. 5:123. doi: 10.3389/fmars.2018.00123

INTRODUCTION

Silica biominerals are the results of various internal or external biological processes that lead to the formation of composite materials with a large variety of composition, hierarchical structures, and probably functions. Silicon biomineralization capability is encountered in various organisms from bacteria to humans, including organisms that belong to the Archaeplastida as well as a large diversity of other photosynthetic and non-photosynthetic protists (i.e., unicellular organisms that are free-living or aggregated into simple colonies, such as eukaryotic algae, protozoans, or slime molds; Raven and Giordano, 2009; Ehrlich et al., 2010a).

The formation of these silica structures might however contribute to the protection of cell in such harsh environment. In terrestrial environments, a large number of land plants were known to mobilize significant quantities of silica in different tissues, where silica might serve as a structural scaffolding element, and can be involved in defense against herbivores and pathogens (Liu et al., 2017; Luyckx et al., 2017; Wang et al., 2017), or against various abiotic stresses (Cooke and Leishman, 2016). Silica minerals where also shown to contribute to optimize the light regime in the leaf (Pierantoni et al., 2017), and proposed to be involve in protecting the land plants against UV-radiation (Schaller et al., 2013).

In the marine environment, the silica frustule made by diatoms which can present extraordinary mechanical strength (Hamm et al., 2003; Aitken et al., 2016), contribute to their mechanical defense against grazers and it was shown that the silicification level can influence interactions between diatoms and grazers (Pondaven et al., 2007; Schultes et al., 2010; Liu et al., 2016), for example heterotrophic dinoflagellates preferentially feed on diatoms with low silica content (Zhang et al., 2017). The overall density of the silica wall also affects the overall sinking rate of diatoms, and help the cells in escaping from predators and parasites, avoiding high light intensity, or finding new resource areas (Raven and Waite, 2004). The silica spicules provide support and defense to marine sponges (Burns and Ilan, 2003; Rohde and Schupp, 2011), correspond to an import feature that can serve as anchoring structure to hold on the sea floor (Ehrlich et al., 2010b; Monn et al., 2015; Monn and Kesari, 2017). However, the exact roles and properties of such silica structures for light perception, UV protection or signal transduction has been rarely investigated *in vivo*. One of the reason is the difficulty to develop precise measurement with living cells also because of the interferences of the organic matter but also the large impacts of organelles like the chloroplast which can greatly interfere with light and fluorescence signal analyses. Nevertheless, understanding the physical properties of purified silica-based biomaterials which is important to novel develop industrial applications, might also give some insight to better understand their putative biological. The interactions between light and silica material is the focus of this review starting from some theoretical background to the recent advances in this field.

THEORETICAL BACKGROUND

Light Guidance and Reflection

In order to understand guiding light ability, fundamental physical principles on the injection of light into materials structure and propagation of electromagnetic waves must be recalled. Light propagation over long distances is based on the total reflection phenomenon. When a light ray falls on a diopter that is a plan surface separating two different media of different refractive index n_1 and n_2, a part of this beam is reflected and leaves again in the medium of incidence at an angle θ_R equal to that of incidence θ_i, while the remaining part continues its path in the second medium at an angle θ_r different from the angle of incidence, so called refracted beam. The famous law of Snell-Descartes connects these different angles:

$$\begin{cases} \theta_i = \theta_R \\ n_1 \sin(\theta_i) = n_2 \sin(\theta_r) \end{cases} \quad (1)$$

After the diopter, the refracted ray deviates from the normal one with an angle that depends on the two indexes values difference (**Figures 1A,B**). When the incidence angle exceeds a critical θ_c value (calculated by dividing n_2 by n_1), the refracted light is tangential to the surface: there is no longer refraction and the light is totally reflected (**Figure 1C**). For this exact angle, it is said the wave is evanescent and propagates by damping rapidly along the surface.

Now for an optical fiber which consists of a core presenting an n_H index slightly higher than n_c the cladding index, when a light wave penetrates into the core at an angle $> \theta_c$ it propagates from one end to the other without any loss (**Figure 1D**). If the incidence angle at the fiber inlet is too high, part of the beam is transmitted through the cladding at each reflection, and the wave is quickly damped (**Figure 1E**). As is often the case for fibers in the air or immersed, the index of the external environment is lower than that of the cladding, the light can penetrate and spread in the cladding (**Figure 1F**), so called "cladding modes." Optical fibers are characterized by their numerical aperture (N.A) that define light cone acceptance of the fiber, where the critical angle is related to the indexes of the core and the cladding by:

$$\text{N.A} = \sin\theta_c = \sqrt{n_H^2 - n_C^2} \quad (2)$$

If a ray of light penetrates the fiber by its cone, then it will be guided by internal total reflection, otherwise, it will not be guided.

Light in Photonic Structures

We shall also briefly recall the fundamental principles of photonics and show how it differs from wave optics. As the name suggests, photonics is the art of manipulating photons. We therefore use the corpuscular model of light, established by Einstein and Planck in the early twentieth century. In this model light is a flux of particles called photons characterized by their energy *E*, spin *S*, and wave vector *k*. The wave vector is related to the momentum that contains all information on the direction of propagation. Well-known relations relate these quantities to the different characteristics of the electromagnetic field in the wave model:

$$\begin{cases} E = h\nu \\ k = \frac{2\pi}{\lambda} \end{cases} \quad (3)$$

where ν is the frequency of the wave and λ its wavelength. The spin is connected to the circular polarization of the wave, but we will not use this quantity in these reminders.

In an interaction between light and matter, matter is characterized by its complex index

$$N = n - ik^m \quad (4)$$

where n is the refractive index of the material. The imaginary part k^m will be considered as negligible in our purpose. In

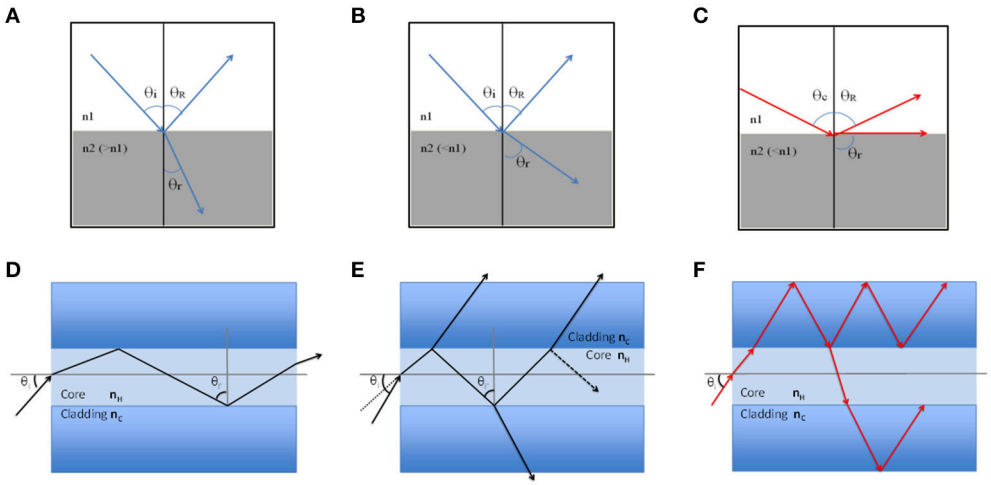

FIGURE 1 | Schematic representation of light reflection and guiding. **(A)** Schematic light refraction between two different media with $\theta_i < \theta_C$ and $n_2 > n_1$; **(B)** Light refraction with $\theta_i < \theta_C$ and $n_2 < n_1$; **(C)** Total light reflection with $\theta_i \geq \theta_C$ that indicates the evanescent field; **(D)** Light in-coupling at one fiber end with $\theta_i > \theta_C$. It propagates without losses all along the fiber; **(E)** Light in-coupling with $\theta_i < \theta_C$. Part of the wave penetrates the cladding and can escape in the outer medium; **(F)** Cladding modes, the wave penetrates and propagates in the cladding.

periodically structured materials also called "photonic crystals" (Johnson et al., 1999; Johnson and Joannopoulos, 2001) a proper way to deal with, is to consider the periodic material as a particle of a lattice constant "a" and a wave vector $|K_a| = 2\pi/a$. In the same way, a wave of spatial period λ can be represented as a particle (photon) of wave vector $|k| = 2\pi/\lambda$. The interaction between these two particles is then treated as an elastic shock satisfying the conservation principles of energy, momentum, and angular momentum. Quantum mechanics shows that momentum exchanges are quantified and occur with K multiples. An incident photon of wave vector k will emerge from the structure with a wave vector k′ such that:

$$k - k' = \pm nK_a \tag{5}$$

In linear optics, k and k' having the same modulus, this relation (5) allows an easy diffraction wave direction determination. Moreover, each time $|k|$ is a multiple of $|K_a|$ there is an exchange of momentum where light can no longer propagate in the structure and it is totally reflected. The consequence is the appearance of forbidden frequency bands whose width depends on the contrast of the index of the materials. This mechanical approach of the light-matter interaction allows the diffractive and interferential phenomenon explanation.

LIGHT PROPAGATION IN GLASS SPONGE MATERIALS

A huge variety of marine and freshwater sponges have been described, with an estimated diversity in the order of 9,000 species (Van Soest et al., 2012), and trace fossil record down to the lowest Cambrian (Chang et al., 2017). Among them the Demospongiae (> 7,000 species) and the Hexactinellida (∼ 600 species) can present silica spicules of different structure and morphology, ranging from a few microns (microscleres), to millimeters and up to several meters long (megascleres).

Spicule structure investigations reported that silica spheres are arranged in microscopic concentric rings bind together by organic matrix that elaborate laminated spicules. However, the number and the thickness of the layers depend not only on the diameter of the spicule, but also on the species considered, and on the age of the sponge. In *Euplectella* sp. spicules are assembled into bundles and form macroscopic cylindrical square-lattice consolidated by diagonal ridges (**Figures 2A,B**). In this species the alternation between the central and the surrounding silica materials was show to present light collecting effects and to allow strong mechanical rigidity and stability (Aizenberg et al., 2004, 2005). Ptychographic nano-tomography methods were used for deeper investigation of the internal structure of anchoring spicule from *Euplectella aspergillum* (Birkbak et al., 2016). This technic revealed that the central filament is composed of organic (protein volume fraction ∼70%) and highly mineralized part, which exhibits circular symmetry. But interestingly, the axial filament was shown to be slightly offset from the spicule's central axis (Birkbak et al., 2016). Recently, other analyses of the structure and composition of the spicules of *Suberites domuncula* and *Tethya aurantium* showed that axial filament of both species is a three-dimensional crystal lattice of six-fold symmetry, with silica nano-spheres embedded within the organic lattice. Their axial filament found to play a scaffolding role in the final morphology of the spicule due to its enhanced growth in [001] direction (Werner et al., 2017).

Studies on the needle-shaped structures called strongyloxea spicules (axisymmetric silica rods) of *Tethya aurantia* have shown that spicule's tapering structures enhanced the buckling resistance compared to the same cylindrical structure (Monn and Kesari, 2017). *Strongyloxea* spicules have a strong Young's modulus of 72 GPa, which might be explained by the gathering

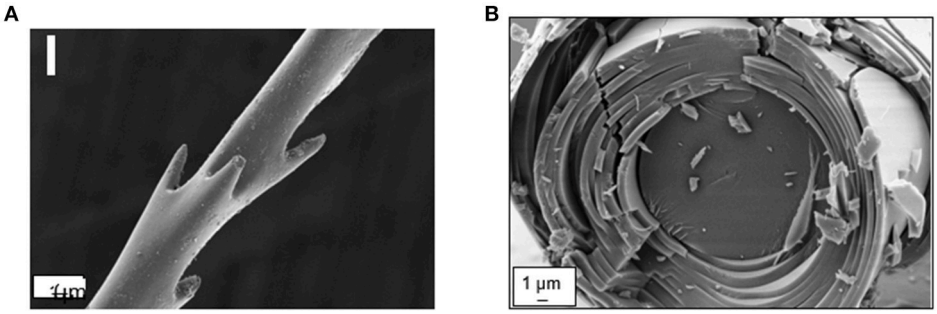

FIGURE 2 | (A) Cross-section Scanning Electron Microscopy image of *Euplectella aspergilium* spicule. **(B)** Zoomed SEM image on spicule's edge showing part of the core region and the concentric silica layers. The multilayer set (silica + organic) surrounding the core of the spicule, forms a homogeneous medium of an effective refractive index different from spicule core refractive index.

of spicules into bundles to increase mechanical properties. It was also proposed that structure-property connection is also related to buckling resistance, and spicule's tapering structures can be considered as an optimal form for this purpose (Monn et al., 2015; Monn and Kesari, 2017). Overall, spicules have been shown to present remarkable mechanical properties in different axes as buckling resistance and toughness enhancement.

Due to their resemblances to manmade fiber optics, spicules are interesting materials to investigate their optical properties, and to our knowledge the first investigations of optical properties of biosilica were performed with purified frustules (Gaino and Sara, 1994; Cattaneo-Vietti et al., 1996). Optical properties of *Hyalonema sieboldi* spicule have been studied by Nd:YAG laser pulses by second harmonic pulses method. It shows by laser irradiation that the fluorescence intensity of spicules increases in the long wavelength range and show a maximum at 770 nm. Saturation and large fluorescence lifetimes were also reported (Kul'chin et al., 2009). Recently, a study by femtosecond (fs)-pulsed laser method, demonstrated the optical properties of *Sericolophus hawaiicus* spicules. Such spicules were assumed to act as a natural supercontinuum generator that involves wavelengths between 650 and 900 nm and a maximum spectral propagation at $\lambda = 750$ nm. This optical property was assumed to be due to its bio-composite nature combining mineral biosilica and organic matrix, including chitin (Ehrlich et al., 2016).

Alternatively, fabrication of an artificial spicules by bio-mimicry have been reported along with their waveguiding ability (Polini et al., 2012). It's believed that spicules made by natural glass sponges or by biomimetic approaches have a great potential for applications in optics and might "replace" industrial fiber optics due to their advantages of low cost and low temperature fabrication (for reviews see Müller et al., 2006, 2009).

OPTICAL PROPERTIES OF DIATOMS THECAE

Diatoms are unicellular eukaryotic microalgae. They are represented in nature with a large variety of species and shapes, circular, pennate, cylindrical, and star shape. Since longtime, diatoms attracted the attention of scientists to address their important ecological roles (i.e., in carbon and silicon biogeochemical cycles Armbrust, 2009) and to describe their Si-biomineralization process (Hildebrand, 2008; Kroger, 2008; Ehrlich and Witkowski, 2015; Hildebrand and Lerch, 2015). Their fascinating silica shell architecture called frustule has evolved along millions of years to ensure the vitality of the cell by protecting it from predators and infections, ensuring metabolic exchange, maintaining the cellular integrity, and eventually interacting with incident light. Frustules present pillbox like shapes comprising two valves (epivalve and hypovalve) connected by porous silica rings named the girdle bands. Periodicity of the porous structure, symmetry, and the number of porous layers is species dependent.

Frustules: Interest for Optical Studies

Among the entire diatom studied, material scientists have focused on *Coscinodiscus* species, probably because of their relatively large cell size in the range of 100–200 µm width. *Coscinodiscus* present a highly structured frustule not only in two dimensions but also in 3-D (Sumper, 2002; Sar et al., 2008; Romann et al., 2015a,b; Aitken et al., 2016; Xing et al., 2017). The valve consists of three overlapping silica layers; the external side named cribrum, it includes smaller porous silica connections called cribellum and finally a third internal layer named foramen. The cribrum is connected to the foramen by silica walls named areola (**Figure 3**). The areola shows a honeycomb-like structure whereas foramen displays a hexagonal array of circular pores. More, foramen holes are aligned at the same time with the hexagonal pattern of areola and cribrum pores. It is also believed that the formation of these patterns is the result of a self-organized phase separation process (Sumper, 2002). There is no doubt that such porous biosilica nano-structured patterns have been found to be very interesting for optics and photonics investigations.

From an optical point of view two features are important to consider: the physical dimension of the periodic structure (number of porous silica layers, thickness, and holes diameters) and the refractive index contrast made by the complementarity of silica (refractive index $n \approx 1.45$) and air pores ($n = 1$) in the visible range. Indeed, most studies have been performed from

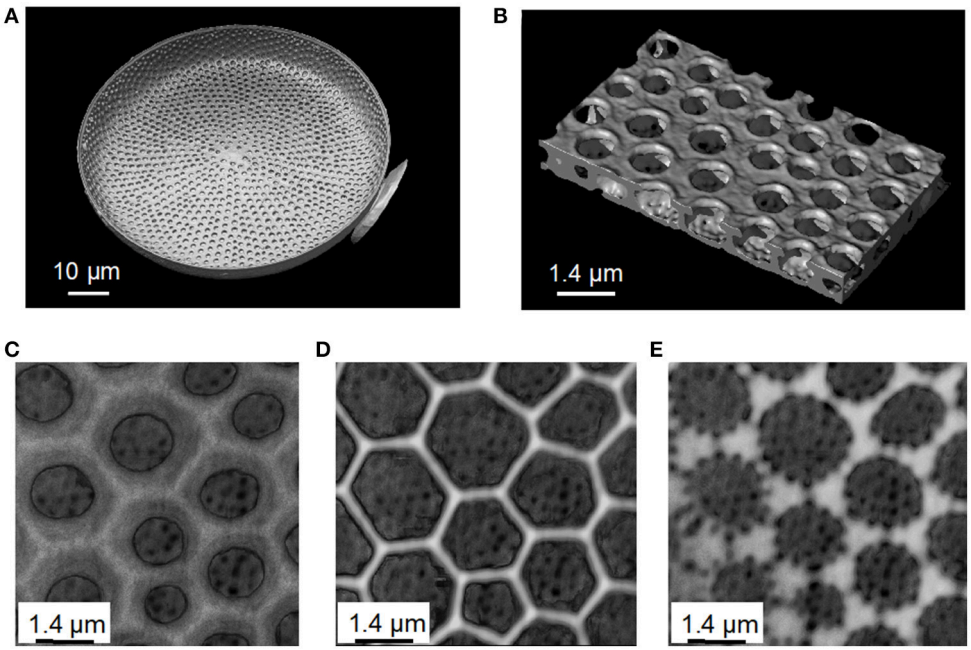

FIGURE 3 | Images of *Coscinodiscus sp*. diatom valve from X-Ray tomography data obtained at the European Synchrotron Radiation Facility (ESRF). **(A)** A complete valve view from the cellular face. On the right we see part of the needle used as a support to handle and rotate the valve face to the X-Ray beam. **(B)** 3D reconstruction image of the structure of the valve, where the up-side, foramen, is in the interior side of the cell. Foramen represents a periodic pores layer leading to a hexagonal network. **(C)** The areola layer connecting the Foramen (big holes inside the valve) to the cribrum. **(D)** The cribrum layer of the valve. **(E)** The cribellum layer.

purified materials and in air conditions, in order to ensure a relatively good refractive index contrast needed to enable and quantify some optical properties (i.e., light diffraction through silica/air patterns). The scale of holes, of specific layers should be in the order of light wavelengths, which then allow interaction with incoming wavelengths whether diffracting, scattering or guiding them. In addition, some diatom valves, such as the one from *Coscinodiscus*, present a periodic pattern of holes in one directional slab (alternation of slica/air holes) resembling to a slab waveguide photonic crystal. Periodicity and porosity in the structure enable light-frustule interaction and can be regarded as particle (photon)-particle (matter) interaction as described in the theoretical part before, so then incoming wavelengths can be diffracted, scattered, or guided.

Light Focusing and Concentration

The frustule of the diatom can be considered as a nano-structured biosilica shell that can act as a photonic crystal because of its hierarchical structure, which enable to envision several applications as for example micro-lenses, optical filters, and waveguides. **Table 1** summarizes most of recent studies reported in literature on the optical properties of diatoms frustules.

Light concentration and focusing ability of centric frustules was first studied for *Coscinodiscus wailesii* by illuminating a single valve by a red laser beam. It was demonstrated that the initial beam diameter of 100 µm was reduced about 12 times (∼ 10 µm diameter) at a distance around 104 µm from the valve position (De Stefano et al., 2007). This lens behavior was attributed to a coherent superposition of the transmitted unfocused wave fronts through the quasi-regular areolae of the valve. In 2010, it was further suggested that the light confinement could be attributed to the regular pore pattern and the superposition of diffracted wave fronts (De Tommasi et al., 2010). However, it was also shown for *C. wailesii* valve that the focusing distance from the reference's valve position (named z*) is wavelength dependent, where by illuminating with laser beam of 532, 557, 582, and 633 nm wavelengths result in the focused distances at 130, 115, 110, and 105 µm, respectively (De Tommasi et al., 2010). Furthermore, similar focusing behavior was shown for the centric single valve of *Arachnoidiscus* sp. where a 633 nm laser beam was confined at 163 µm from the valve (Ferrara et al., 2014).

These results suggest that light propagation through the valve doesn't only depend on the interaction with the silica itself but likely on the spatial distribution of the pores in the periodic structure, therefore centric valve can be considered as multifocal lens. Multifocal lens and waveguide ability by confocal hyper-spectral imaging was investigated for two centric diatoms *Cosinodiscus centralis* and *C. wailesii*, it was shown, at several wavelengths (485, 535, 625, and 675 nm), that multiple light cones were transmitted through the centric valve (Romann et al., 2015a,b). These authors also shown that light convergence depends on the valve orientation, where the intensity of transmitted light decreases strongly when the incident light illuminate the internal side of the valve (i.e., the foramen side), whereas the light intensity increases upon illumination of

TABLE 1 | Summary of studies on the optical properties of diatoms frustules.

Species	Method	Light source /Collected signal	Main results	References
Melosira variance	Microfiber spectroscopic method	Xenon/Transmitted	Absorption near 420 nm-efficient light harvesting antenna owing to their photonic crystalline characteristics	Yoneda et al., 2016
Coscinodiscus granii & concinnus	Spectroscopy	Halogen/Transmitted	Valves more transparent to visible spectrum than in UV	Ellegaard et al., 2016
C. wailesii & C. centralis	Confocal hyperspectral imaging	Tungsten-halogen/Spatial distribution	Light trapping depends on wavelength and the valve orientation, independently of the incident light angle	Romann et al., 2015a
Coscinodiscus centralis	Confocal micro-spectroscopy	Tungsten-halogen/Transmitted	Transmitted light enhanced at 636 and 663 nm. Focusing light depends on valve's orientation.	Romann et al., 2015b
Coscinodiscus sp.	Spectroscopy	Halogen/Transmitted & reflected	Light trapping by frustule's layer hence enhancement between 400 and 700 nm.	Chen et al., 2015
Coscinodiscus wailesii	Broadband supercontinuum laser	Supercontinum/Transmitted	Valve's filtering effects by position dependent optical diffraction.	Kieu et al., 2014
Arachnoidiscus sp.	Spectroscopy. Digital holography	Deuterium-Halogen & Laser/Transmitted	Green and red light more concentrated rather than bleu. Confinement of 633 nm wavelength occurs at 163 μm	Ferrara et al., 2014
Coscinodiscus wailesii	Spectroscopy	Tungsten/Transmitted	Lambda 532, 557, 582, and 633 nm are focalized at 130, 115, 110, and 105 μm, respectively. Focus distance depends strongly on the wavelength.	De Tommasi et al., 2010
Melosira variance	Spectroscopy	Xenon/Absorption	Absorption in bleu light wavelengths region at 200 μm from reference	Yamanaka et al., 2008
Coscinodiscus wailesii	Spectroscopy	Laser/Transmitted	The Laser beam of 100 μm diameter was focused to almost 10 um by the Cw valve at a distance near 104 μm	De Stefano et al., 2007
Coscinodiscus granii	Band diagram simulations (three dimensional calculations)		Valves and girdle bands can influence incoming light by coupling into waveguides with different photonic crystal modes. Red can only be coupled in the valve not in the girdle	Fuhrmann et al., 2004
Thalassiosira pseudonana	Spectrophotometer with an integrating sphere	Halogen/Absorption	Absorption in the range of 380–540 nm and 650–700 nm. Light limitation for cultures resulted in increased chlorophyll "a."	Stramski et al., 2002

external side (i.e., the cribrum side). Furthermore, tilting the incident light of 10° doesn't change the concentration behavior (Romann et al., 2015a,b). All of these reported strengthen the light focusing ability of valves from centric species.

A recent study by Chen et al. highlighted the light trapping effect of *Cosinodiscus* sp. species in photovoltaic application (Chen et al., 2015). For this purpose, *Coscinodiscus* sp. valves were deposited by floating assembly method on a 50 nm layer of low band-gap polymer PTB7:$PC_{71}BM$ photovoltaic active material. Absorption spectra of polymer coated diatoms sample showed a broadband enhancement (between 400 and 700 nm) estimated to be about 28% comparing to diatoms free sample. Moreover, in the same study, RCWA and FDTD simulation methods were applied to evaluate transmitted light behavior over the active layer. Results suggested that placing diatoms internal plate faced to the top of the PV active layer enhances the absorption efficiency by a factor of 1.41 from 380 to 800 nm. In addition, it was shown that this enhancement effect is the combination of the enhancement contribution by each separated layer in the valve's structure (Chen et al., 2015).

The light focusing, guiding, and trapping ability of frustules described above highlight the photonic crystal behavior of silica shells. T. Fuhrmann et al. were the first to perform band diagram simulations for valve and girdle bands of a centric species *Cosinodiscus granii* (Fuhrmann et al., 2004). Generated crystal photonics modes depend on the periodicity of the structure (lattice constant of each silica grid) the slab thickness and the incident wavelength. For *C. granii* valve and girdle bands influence incident light by coupling it into waveguides with distinct photonic crystal modes, for example red light was shown to be coupled in the valve but not in the girdle. It is also believed that to be able to exhibit a complete 2-D photonic crystal band-gaps, a refractive index contrast in the material of about 2 is needed (Knight, 2003). Kieu et al. reported the optical properties of a *C. wailesii* valve fixed on the top of an optical fiber by the external valve's side, by irradiating with coherent supercontinuum broadband laser (400–1,700 nm) a region of ∼20 μm (Kieu et al., 2014). Then they studied the diffracted and transmitted light through the valve as a function of the lattice constant in the periodic structure. When irradiated by

wavelengths at different angles, the hexagonal pattern generated colorful transmitted patterns. As a consequence, a white spotlight was observed on the screen without the valve in the setup, while changing the irradiated spot area on the valve changed its color. In addition, it was shown that the hexagonal colorful patterns resulted from the interaction with the periodic structure (Kieu et al., 2014).

All the above-mentioned studies were performed with frustules from centric diatoms, therefore with radial symmetry, so what about cylindrical frustules? Recently, the photonic crystalline characteristics of the cylindrical frustule of the diatom *Melosira variance* were reported (Yoneda et al., 2016). Clean frustules were studied with a microfiber spectroscopic method. The frustule was put on a micromanipulator and illuminated by a 10 μm sophisticated fiber optic end connected to a 300 W Xe lamp (300–1,100 nm) and transmitted light was collected and analyzed with a spectrometer. This method showed a fine space resolution due to the deployed micro-scale, which make it suitable to study the photonic crystallinity. When a frustule was irradiated through its internal side a transmittance valley was observed between 400 and 500 nm, while when it was irradiated perpendicular to the silica side wall, no particular valleys was observed. The authors concluded that transmitted spectra observed were related to the periodicity of the refractive index in the structure, and that the photonic crystalline characteristics assist light absorption but depending on the orientation (Yoneda et al., 2016).

Light Filtration

Frustules have also been investigated for their capability in protecting the cells against harmful wavelengths and excessive light intensities. In other word, acting as optical filters. It is known that diatoms use blue and red wavelengths for photosynthesis, so excess supply of blue light might generate active oxygen molecules that are dangerous for the living cell. It was proposed that the ordered porous silica shell might protect from dangerous UV and excessive wavelength intensities (Ellegaard et al., 2016).

Using *Melosira varians* frustules it was shown that the transmission of incident light was principally dependent in the wavelength, with enhanced transmission of red light and absorption in the blue range (Yamanaka et al., 2008). Such filtering behavior was also shown for circular valve from *Arachnoidiscus* sp. for which green and red wavelengths were shown to be more concentrated than blue light (Ferrara et al., 2014). In addition, in the case of UVB light it was shown that the light spot was very weak, and far away from the valve. These results were consistent with simulations (Ferrara et al., 2014).

Photoluminescence

A distinctive optical feature, photoluminescence (PL), was also observed with frustules. When porous biosilica was irradiated by UV wavelengths it emitted one or more PL peaks in the visible spectral region (Yoon and Goorsky, 1995; Cullis et al., 1997). Scientists investigated such features and their potential applications, for example in gas detection (**Table 2**). Photoluminescence responses of *Thalassiosira rotula* valves were examined when exposed to several gases and volatiles substances. Frustules irradiated by a He-Cd laser (325 nm) showed a multiband PL (between 450 and 690 nm) that was attributed to oxidized silicon nanocrystals (533 nm), porous silicon (609 nm), and hydrogenated amorphous silicon (661 nm). As a result, valves PL were quenched with electrophilic gases while they were enhanced for nucleophilic ones (De Stefano et al., 2005; Bismuto et al., 2008). Furthermore, PL of *T. rotula* frustules was quenched when exposed to $NO_{2(g)}$ flux, showing a high sensitivity in the order of sub-ppm level that it is strongly dependent on the structure, porosity, and gas nature (Bismuto et al., 2008). PL properties of the frustules from other centric and pennate species (*T. rotula*, *Cosinodiscus. Wailesii,* and *Cocconeis scutellum*) were also demonstrated, and high gas detection sensitivity was shown at room temperature (Setaro et al., 2007).

Photoluminescence was also investigated for chemically modified diatoms frustules. Townley et al. report a study on nickel sulfate modified *C. wailesii* frustules. When irradiated with a He-Cd laser (442 nm), intact frustules exhibit a broad PL peak (500–650 nm) while those growing with $NiSO_4$ quenched the PL (Townley et al., 2007). Photoluminescence of chemically modified frustules have been investigated, for medical purposes, by fixing antibodies on the silica shells. Antibodies doped frustules were irradiated by 325 nm laser's wavelength, which show a high sensitivity in the order of 1.2 nm.μm^{-1} and detection limit around 100 nmol.L^{-1} (De Stefano et al., 2009). Recently, frustules from the pennate diatom *Psammodictyon panduriforme* were investigated under 325 nm laser excitation. Frustules showed two emission peaks at 417 and 534 nm that were considered as radiative luminescence generated by oxygen-vacancy defects in the structure (Camargo et al., 2016). However, under pulse laser excitation, a single narrow emission peak was observed near 475 nm. This result was interpreted as the consequence of a putative quantum confinement effect due to the mesoporous silica and the quasi-regular pores in frustules structure (Camargo et al., 2016).

POTENTIAL APPLICATIONS OF BIOSILICA

Biosilica materials from marine organisms, and in particular diatom frustules have been proposed and used in several industrial applications from filtration, insulation, fine abrasion, mineral fillers, catalysts, pesticides, building materials, food additives, anti-caking agent, carriers, or coating (Harwood, 2010), and have been proposed to develop new bio-chemical sensors or nanotechnologies. Some of the present and future applications have to be based on the optical properties of the frustule (**Figure 4**).

The advances in the understanding of the biomineralization processes, have inspired the development of new materials. The identified biomineralization enzymes from sponges (i.e., silicateins) and diatoms, were used for applications in biomedicine such as prototyping and 3D bio-printing of customized structures for biomedical purposes (Lopez et al., 2005; Schröder et al., 2016). Several applications in vision such as bacterial sensors (by immobilization of the biosilica-encapsulated bacterial cells on a sensor chip); development of core-shell nanomaterials for nanomedicine applications and 3D

TABLE 2 | Photoluminescence studies on diatom frustules.

Species	Modified chemically	Main results	References
Psammodictyon panduriforme	No	PL emission peaks at 417 and 534 nm.	Camargo et al., 2016
Coscinodiscus concinnus	Yes	PL of frustules acts as synthetized quantum dots. PL of modified frustules shows high sensitivity toward antibodies.	De Stefano et al., 2009
Coscinodiscus wailesii (modified by nickel sulfate)	Yes	Intact diatoms exhibit a broad PL peak (500–650 nm). Growth with $NiSO_4$ quenches the PL.	Townley et al., 2007
T. rotula; C. wailesii and C. scutellum	No	Sensitivity depends on the used bio-silica (structure and porosity) and gases.	Setaro et al., 2007
Thalassiosira rotula	No	PL was quenched by NO_2 gas with high sensitivity in the order of the sub-ppm level.	Bismuto et al., 2008
Thalassiosira rotula	No	PL of diatoms was quenched with electrophiles and enhanced with nucleophilic gases.	De Stefano et al., 2005

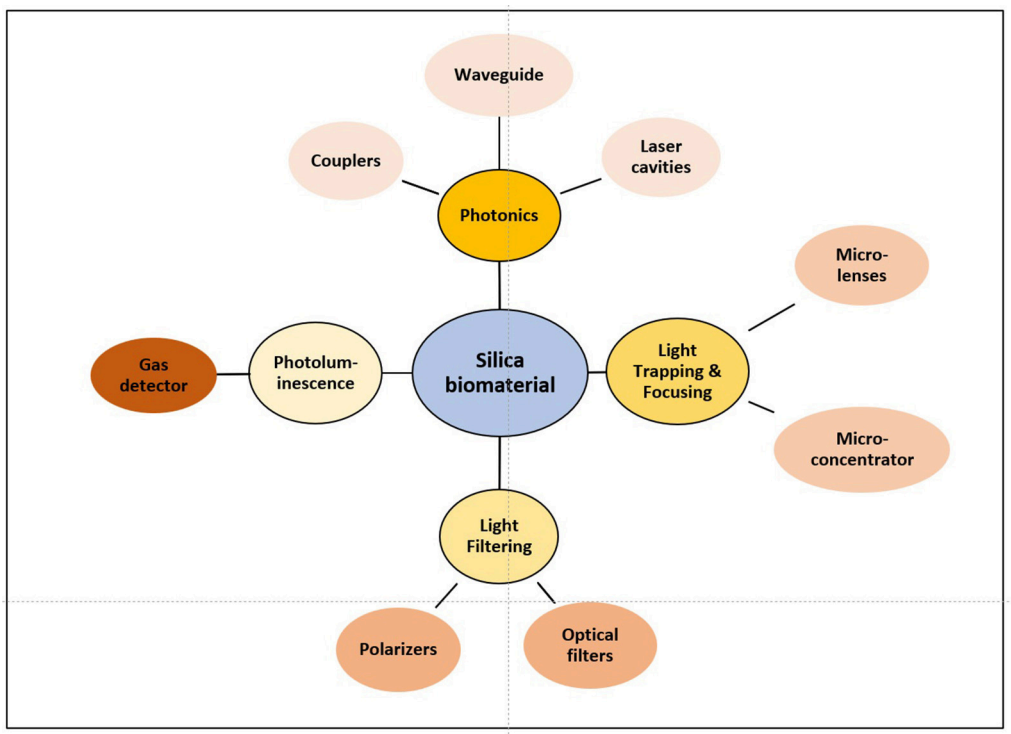

FIGURE 4 | Schematic representation of biosilica properties and their potential applications.

cell printing as promising materials for regenerative medicine. Modified biosilica from diatoms was also reported for biomedical applications as for example in drug delivery (Yang et al., 2011; Jo et al., 2016).

Frustules from diatoms have been investigated for their potential in biosensing, by exploiting their photoluminescence properties for gas detection. Frustules from *Aulacoseira* or *Thalassiosira* have been showed to be useful to detect trace of pure gas, as for example $NO_{(g)}$, $H_{2(g)}$, and $NO_{2(g)}$ (Bismuto et al., 2008; Leonardo et al., 2016). Since intact biosilica is still not efficient to distinguish substances in very complex mixtures, to increase sensitivity and specific substance identification, frustules were chemically modified on their silanol groups which could increase PL intensity and peak (Medarevic et al., 2016). Biosilica materials might have also great potential in the energy field. For example, in solar cells technologies, the ability of light trapping by diatoms valves could enhances light harvest (Chen et al., 2015), and for Dye Sensitized Solar Cells (DSSC) technology, TiO_2 modified frustules (Jeffryes et al., 2011). In these cited examples, the solar cells efficiency was increased by the mediation of natural silica. In lithium batteries, biosilica materials might also found application as anode material because of their Li

storage capability. Silicon nanostructures, obtained by reducing silica by magnesiothermic process, increase Li storage capacity in battery. For supercapacitors application, metal oxide modified biosilica seemed to enhance capacitance and cyclic stability (Sun et al., 2017). Natural silica is also under investigation for its potential as photoelectrodes for solar water electrolysis, production of hydrogen from water electrolysis, an important renewable source of energy. Biosilica is reduced to obtain porous silicon, a semiconductor necessary to enable water electrolysis reaction (Chandrasekaran et al., 2015).

Finally, biosilica was also explored for photonics applications due to their remarkable micro and nano-scalable 3D structures. The integration of luminescent dyes in the periodicity of the diatoms frustules is of high interest for scientists to elaborate new bio-hybrid luminescent materials that would be of great potential for application in photonics and laser technology. Organic dyes modified frustules had been reported in the literature. For example, the use of fluorescein-5-isothiocyanate and thiophene-benzothiadiazole-thiophene molecules, where shown to present interest in photonics and optoelectronics due to their important charge transport and high PL quantum yields in solid state (Vona et al., 2016). Furthermore, diatoms have been explored for their potential as nano-plasmonic sensors. *In-situ* growth of silver nanoparticles in frustule photonic crystal structures, show a label-free chemical and biological sensing based on surface enhanced Raman scattering, which can be of great interest for medical and food sensing applications (Kong et al., 2016).

CONCLUSION

We have focused here on light interaction in air condition mainly from purified biosilica materials, and have tried to emphases the importance of the structural organization of the sophisticated structured encountered in glass sponges and diatoms. Indeed, beside key roles in mechanical toughness and protection against predators, we question if is there any need for light modulation? This question arises because light-guiding process was demonstrated for biomaterials (i.e., glass-sponge spicules) extracted from marine organisms at depth where no light can reach. However, remarkable optical properties of sponge spicules were shown to compete manmade optical fibers in light guiding, and enable us to learn from nature and to envision soft processes to design new materials.

As mentioned above, most of the studies concerning the diatoms, have explored the optical properties of isolated frustules with hopefully almost no organic material remaining; even if the presence of trace contaminants has not been systematically analyzed. It remains that optical measurements have mostly failed to properly address the putative interaction of the incident light with the organic material. According to our knowledge such question remains open because on one side the presence of organic materials in the bio-silica, could eventually generate scattering effects, and therefore affect the propagation of light over long distances, but on the other side the low concentration of organic materials, might makes effects practically negligible. In addition, measurements have been generally performed in air and not in water. Valve orientation has also to be further considered as well as the complete structural organization. Indeed, in the environment the light hits the diatom cells from different directions.

Recent evidences suggested that the interaction between light and silica-based materials also applied in living organism (Ellegaard et al., 2016). Therefore, there is hope that in the future we might have more evidences on the role of the silica frustule to perform selective wavelength filtering, for example to collect specific photosynthetic wavelengths or to protect from dangerous once. Indeed, the putative roles of biomaterials in UV protections is a key question that should attract more and more attention for both marine (Xu et al., 2016) and terrestrial organisms (Schaller et al., 2013).

AUTHOR CONTRIBUTIONS

All authors listed have made a substantial, direct, and intellectual contribution to the work, and approved it for publication.

FUNDING

This work was supported by French state funds managed by the ANR within the Investissements d'Avenir Programme (ANR-11-IDEX-0004-02), and more specifically within the framework of the Cluster of Excellence MATISSE led by Sorbonne Université. Works in PL laboratory is also supported by the Labex DRIIHM, French programme Investissements d'Avenir (ANR-11-LABX-0010).

ACKNOWLEDGMENTS

The authors are grateful to Dr. Julie Villanova and the ESRF for beam time allocation. We also wish to thank Dr. Jean-Philippe Buffet, Dr. Alain Bulou, Landry Kamtcheu Ouanssi and Dr. Oxana Cherkas for their contribution to diatoms culture and some images acquisition.

REFERENCES

Aitken, Z. H., Luo, S., Reynolds, S. N., Thaulow, C., and Greer, J. R. (2016). Microstructure provides insights into evolutionary design and resilience of *Coscinodiscus* sp frustule. *Proc. Natl. Acad. Sci. U.S.A.* 113, 2017–2022. doi: 10.1073/pnas.1519790113

Aizenberg, J., Sundar, V. C., Yablon, A. D., Weaver, J. C., and Chen, G. (2004). Biological glass fibers: correlation between optical and structural properties. *Proc. Natl. Acad. Sci. U.S.A.* 101, 3358–3363. doi: 10.1073/pnas.0307843101

Aizenberg, J., Weaver, J. C., Thanawala, M. S., Sundar, V. C., Morse, D. E., and Fratzl, P. (2005). Skeleton of *Euplectella* sp.: structural hierarchy from the nanoscale to the macroscale. *Science* 309, 275–278. doi: 10.1126/science.1112255

Armbrust, E. V. (2009). The life of diatoms in the world's oceans. *Nature* 459, 185–192. doi: 10.1038/nature08057

Birkbak, M. E., Guizar-Sicairos, M., Holler, M., and Birkedal, H. (2016). Internal structure of sponge glass fiber revealed by ptychographic nanotomography. *J. Struct. Biol.* 194, 124–128. doi: 10.1016/j.jsb.2016.02.006

Bismuto, A., Setaro, A., Maddalena, P., De Stefano, L., and De Stefano, M. (2008). Marine diatoms as optical chemical sensors: a time-resolved study. *Sens. Actuat. B Chem.* 130, 396–399. doi: 10.1016/j.snb.2007.09.012

Burns, E., and Ilan, M. (2003). Comparison of anti-predatory defenses of Red Sea and Caribbean sponges. II. Physical defense. *Mar. Ecol. Prog. Ser.* 252, 115–123. doi: 10.3354/meps252115

Camargo, E., Jaime, P. C. J., Lin, C. F., Lin, M. S., Yu, T. Y., Wu, M. C., et al. (2016). Chemical and optical characterization of *Psammodictyon panduriforme* (Gregory) Mann comb. nov (Bacillariophyta) frustules. *Opt. Mat. Express* 6, 1436–1443. doi: 10.1364/OME.6.001436

Cattaneo-Vietti, R., Bavestrello, G., Cerrano, C., Sara, M., Benatti, U., Giovine, M., et al. (1996). Optical fibres in an Antarctic sponge. *Nature* 383, 397–398. doi: 10.1038/383397b0

Chandrasekaran, S., Nann, T., and Voelcker, N. H. (2015). Nanostructured silicon photoelectrodes for solar water electrolysis. *Nano Energy* 17, 308–322. doi: 10.1016/j.nanoen.2015.08.022

Chang, S., Feng, Q. L., Clausen, S., and Zhang, L. (2017). Sponge spicules from the lower Cambrian in the Yanjiahe formation, South China: the earliest biomineralizing sponge record. *Palaeogeogr. Palaeoclimatol. Palaeoecol.* 474, 36–44. doi: 10.1016/j.palaeo.2016.06.032

Chen, X. F., Wang, C., Baker, E., and Sun, C. (2015). Numerical and experimental investigation of light trapping effect of nanostructured diatom frustules. *Sci. Rep.* 5:11977. doi: 10.1038/srep11977

Cooke, J., and Leishman, M. R. (2016). Consistent alleviation of abiotic stress with silicon addition: a meta-analysis. *Funct. Ecol.* 30, 1340–1357. doi: 10.1111/1365-2435.12713

Cullis, A. G., Canham, L. T., and Calcott, P. D. J. (1997). The structural and luminescence properties of porous silicon. *J. Appl. Phys.* 82, 909–965. doi: 10.1063/1.366536

De Stefano, L., Rea, I., Rendina, I., De Stefano, M., and Moretti, L. (2007). Lensless light focusing with the centric marine diatom Coscinodiscus walesii. *Opt. Express* 15, 18082–18088. doi: 10.1364/OE.15.018082

De Stefano, L., Rendina, I., De Stefano, M., Bismuto, A., and Maddalena, P. (2005). Marine diatoms as optical chemical sensors. *Appl. Phys. Lett.* 87, 396–399. doi: 10.1063/1.2140087

De Stefano, L., Rotiroti, L., De Stefano, M., Lamberti, A., Lettieri, S., Setaro, A., et al. (2009). Marine diatoms as optical biosensors. *Biosens. Bioelectron.* 24, 1580–1584. doi: 10.1016/j.bios.2008.08.016

De Tommasi, E., Rea, I., Mocella, V., Moretti, L., De Stefano, M., Rendina, I., et al. (2010). Multi-wavelength study of light transmitted through a single marine centric diatom. *Opt. Express* 18, 12203–12212. doi: 10.1364/OE.18.012203

Ehrlich, H., Demadis, K. D., Pokrovsky, O. S., and Koutsoukos, P. G. (2010a). Modern views on desilicification: biosilica and abiotic silica dissolution in natural and artificial environments. *Chem. Rev.* 110, 4656–4689. doi: 10.1021/cr900334y

Ehrlich, H., Deutzmann, R., Brunner, E., Cappellini, E., Koon, H., Solazzo, C., et al. (2010b). Mineralization of the metre-long biosilica structures of glass sponges is templated on hydroxylated collagen. *Nat. Chem.* 2, 1084–1088. doi: 10.1038/nchem.899

Ehrlich, H., Maldonado, M., Parker, A. R., Kulchin, Y. N., Schilling, J., Kohler, B., et al. (2016). Supercontinuum generation in naturally occurring glass sponges spicules. *Adv. Opt. Mater.* 4, 1608–1613. doi: 10.1002/adom.201600454

Ehrlich, H., and Witkowski, A. (2015). "Biomineralization in diatoms: the organic templates," in *Evolution of Lightweight Structures: Analyses and Technical Applications, Vol 6*, ed C. Hamm (Dordrecht: Springer), 39–58.

Ellegaard, M., Lenau, T., Lundholm, N., Maibohm, C., Friis, S. M. M., Rottwitt, K., et al. (2016). The fascinating diatom frustule-can it play a role for attenuation of UV radiation? *J. Appl. Phycol.* 28, 3295–3306. doi: 10.1007/s10811-016-0893-5

Ferrara, M. A., Dardano, P., De Stefano, L., Rea, I., Coppola, G., Rendina, I., et al. (2014). Optical properties of diatom nanostructured biosilica in Arachnoidiscus sp: micro-optics from mother nature. *PLoS ONE* 9:e103750. doi: 10.1371/journal.pone.0103750

Fuhrmann, T., Landwehr, S., El Rharbi-Kucki, M., and Sumper, M. (2004). Diatoms as living photonic crystals. *Appl. Phys. B* 78, 257–260. doi: 10.1007/s00340-004-1419-4

Gaino, E., and Sara, M. (1994). Siliceous spicules of tethya-seychellensis (*Porifera*) support the growth of a green-alga - a possible light conducting system. *Mar. Ecol. Prog. Ser.* 108, 147–151. doi: 10.3354/meps108147

Hamm, C. E., Merkel, R., Springer, O., Jurkojc, P., Maier, C., Prechtel, K., et al. (2003). Architecture and material properties of diatom shells provide effective mechanical protection. *Nature* 421, 841–843. doi: 10.1038/nature01416

Harwood, D. M. (2010). "Diatomite," in *The Diatoms: Applications for the Environmentals and Earth Sciences, 2nd Edn.*, eds J. P. Smol and E. F. Stoermer (Cambridge: Cambridge University Press), 570–574.

Hildebrand, M. (2008). Diatoms, biomineralization processes, and genomics. *Chem. Rev.* 108, 4855–4874. doi: 10.1021/cr078253z

Hildebrand, M., and Lerch, S. J. (2015). Diatom silica biomineralization: parallel development of approaches and understanding. *Semin. Cell Dev. Biol.* 46, 27–35. doi: 10.1016/j.semcdb.2015.06.007

Jeffryes, C., Campbell, J., Li, H. Y., Jiao, J., and Rorrer, G. (2011). The potential of diatom nanobiotechnology for applications in solar cells, batteries, and electroluminescent devices. *Energy Environ. Sci.* 4, 3930–3941. doi: 10.1039/c0ee00306a

Jo, B. H., Kim, C. S., Jo, Y. K., Cheong, H., and Cha, H. J. (2016). Recent developments and applications of bioinspired silicification. *Korean J. Chem. Eng.* 33, 1125–1133. doi: 10.1007/s11814-016-0003-z

Johnson, S. G., Fan, S. H., Villeneuve, P. R., Joannopoulos, J. D., and Kolodziejski, L. A. (1999). Guided modes in photonic crystal slabs. *Phys. Rev. B* 60, 5751–5758. doi: 10.1103/PhysRevB.60.5751

Johnson, S. G., and Joannopoulos, J. D. (2001). Block-iterative frequency-domain methods for Maxwell's equations in a planewave basis. *Opt. Express* 8, 173–190. doi: 10.1364/OE.8.000173

Kieu, K., Li, C., Fang, Y., Cohoon, G., Herrera, O. D., Hildebrand, M., et al. (2014). Structure-based optical filtering by the silica microshell of the centric marine diatom *Coscinodiscus wailesii*. *Opt. Express* 22, 15992–15999. doi: 10.1364/OE.22.015992

Knight, J. C. (2003). Photonic crystal fibres. *Nature* 424, 847–851. doi: 10.1038/nature01940

Kong, X. M., Squire, K., Li, E. W., LeDuff, P., Rorrer, G. L., Tang, S. N., et al. (2016). Chemical and biological sensing using diatom photonic crystal biosilica with *in-situ* growth plasmonic nanoparticles. *IEEE Trans. Nanobiosci.* 15, 828–834. doi: 10.1109/TNB.2016.2636869

Kroger, N., and Poulsen, N. (2008). Diatoms–from cell wall biogenesis to nanotechnology. *Annu. Rev. Genet.* 42, 83–107. doi: 10.1146/annurev.genet.41.110306.130109

Kul'chin, Y. N., Voznesenski, S. S., Bukin, O. A., Bezverbnyi, A. V., Drozdov, A. L., Nagorny, I. G., et al. (2009). Spicules of glass sponges as a new type of self-organizing natural photonic crystal. *Optics Spectrosc.* 107, 442–447. doi: 10.1134/S0030400X09090227

Leonardo, S., Prieto-Simon, B., and Campas, M. (2016). Past, present and future of diatoms in biosensing. *Trends Anal. Chem.* 79, 276–285. doi: 10.1016/j.trac.2015.11.022

Liu, H., Chen, M., Zhu, F., and Harrison, P. J. (2016). Effect of diatom silica content on copepod grazing, growth and reproduction. *Front. Mar. Sci.* 3:89. doi: 10.3389/fmars.2016.00089

Liu, J., Zhu, J. W., Zhang, P. J., Han, L. W., Reynolds, O. L., Zeng, R. S., et al. (2017). Silicon supplementation alters the composition of herbivore induced plant volatiles and enhances attraction of parasitoids to infested rice plants. *Front. Plant Sci.* 8:1265. doi: 10.3389/fpls.2017.01265

Lopez, P. J., Desclés, J., Allen, A. E., and Bowler, C. (2005). Prospects in diatom research. *Curr. Opin. Biotechnol.* 16, 180–186. doi: 10.1016/j.copbio.2005.02.002

Luyckx, M., Hausman, J. F., Lutts, S., and Guerriero, G. (2017). Silicon and plants: current knowledge and technological perspectives. *Front. Plant Sci.* 8:411. doi: 10.3389/fpls.2017.00411

Medarevic, D. P., Losic, D., and Ibric, S. R. (2016). Diatoms - nature materials with great potential for bioapplications. *Hemijska Industrija* 70, 613–627. doi: 10.2298/HEMIND150708069M

Monn, M. A., and Kesari, H. (2017). A new structure-property connection in the skeletal elements of the marine sponge *Tethya aurantia* that guards against buckling instability. *Sci. Rep.* 7:39547. doi: 10.1038/srep39547

Monn, M. A., Weaver, J. C., Zhang, T. Y., Aizenberg, J., and Kesari, H. (2015). New functional insights into the internal architecture of the laminated anchor

spicules of *Euplectella aspergillum*. *Proc. Natl. Acad. Sci. U.S.A.* 112, 4976–4981. doi: 10.1073/pnas.1415502112

Müller, W. E. G., Wang, X. H., Cui, F. Z., Jochum, K. P., Tremel, W., Bill, J., et al. (2009). Sponge spicules as blueprints for the biofabrication of inorganic-organic composites and biomaterials. *Appl. Microbiol. Biotechnol.* 83, 397–413. doi: 10.1007/s00253-009-2014-8

Müller, W. E., Wendt, K., Geppert, C., Wiens, M., Reiber, A., and Schroder, H. C. (2006). Novel photoreception system in sponges? Unique transmission properties of the stalk spicules from the hexactinellid Hyalonemasieboldi. *Biosens. Bioelectron.* 21, 1149–1155. doi: 10.1016/j.bios.2005.04.017

Pierantoni, M., Tenne, R., Brumfeld, V., Kiss, V., Oron, D., Addadi, L., et al. (2017). Plants and light manipulation: the integrated mineral system in okra leaves. *Adv. Sci.* 4:1600416. doi: 10.1002/advs.201600416

Polini, A., Pagliara, S., Camposeo, A., Cingolani, R., Wang, X. H., Schroder, H. C., et al. (2012). Optical properties of *in-vitro* biomineralised silica. *Sci. Rep.* 2:607. doi: 10.1038/srep00607

Pondaven, P., Gallinari, M., Chollet, S., Bucciarelli, E., Sarthou, G., Schultes, S., et al. (2007). Grazing-induced changes in cell wall silicification in a marine diatom. *Protist* 158, 21–28. doi: 10.1016/j.protis.2006.09.002

Raven, J. A., and Giordano, M. (2009). Biomineralization by photosynthetic organisms: evidence of coevolution of the organisms and their environment? *Geobiology* 7, 140–154. doi: 10.1111/j.1472-4669.2008.00181.x

Raven, J. A., and Waite, A. M. (2004). The evolution of silicification in diatoms: inescapable sinking and sinking as escape? *New Phytol.* 162, 45–61. doi: 10.1111/j.1469-8137.2004.01022.x

Rohde, S., and Schupp, P. J. (2011). Allocation of chemical and structural defenses in the sponge Melophlus sarasinorum. *J. Exp. Mar. Biol. Ecol.* 399, 76–83. doi: 10.1016/j.jembe.2011.01.012

Romann, J., Valmalette, J. C., Chauton, M. S., Tranell, G., Einarsrud, M. A., and Vadstein, O. (2015a). Wavelength and orientation dependent capture of light by diatom frustule nanostructures. *Sci. Rep.* 5:17403. doi: 10.1038/srep17403

Romann, J., Valmalette, J. C., Røyset, A., and Einarsrud, M. A. (2015b). Optical properties of single diatom frustules revealed by confocal microspectroscopy. *Opt. Lett.* 40, 740–743. doi: 10.1364/OL.40.000740

Sar, E. A., Sunesen, I., and Hinz, F. (2008). Fine morphology of coscinodiscus jonesianus and coscinodiscus commutatus and their transfer to coscinodiscopsis gen. Nov. *Diatom Res.* 23, 401–421. doi: 10.1080/0269249X.2008.9705766

Schaller, J., Brackhage, C., Bäucker, E., and Dudel, E. G. (2013). UV-screening of grasses by plant silica layer? *J. Biosci.* 38, 413–416. doi: 10.1007/s12038-013-9303-1

Schröder, H. C., Grebenjuk, V. A., Wang, X. H., and Muller, W. E. G. (2016). Hierarchical architecture of sponge spicules: biocatalytic and structure-directing activity of silicatein proteins as model for bioinspired applications. *Bioinspir. Biomim.* 11:041002. doi: 10.1088/1748-3190/11/4/041002

Schultes, S., Lambert, C., Pondaven, P., Corvaisier, R., Jansen, S., and Ragueneau, O. (2010). Recycling and uptake of $Si(OH)_4$ when protozoan grazers feed on diatoms. *Protist* 161, 288–303. doi: 10.1016/j.protis.2009.10.006

Setaro, A., Lettieri, S., Maddalena, P., and De Stefano, L. (2007). Highly sensitive optochemical gas detection by luminescent marine diatoms. *Appl. Phys. Lett.* 91:051921. doi: 10.1063/1.2768027

Stramski, D., Sciandra, A., and Claustre, H. (2002). Effects of temperature, nitrogen, and light limitation on the optical properties of the marine diatom *Thalassiosira pseudonana*. *Limnol. Oceanogr.* 47, 392–403. doi: 10.4319/lo.2002.47.2.0392

Sumper, M. (2002). A phase separation model for the nanopatterning of diatom biosilica. *Science* 295, 2430–2433. doi: 10.1126/science.1070026

Sun, X. W., Zhang, Y. X., and Losic, D. (2017). Diatom silica, an emerging biomaterial for energy conversion and storage. *J. Mater. Chem. A* 5, 8847–8859. doi: 10.1039/C7TA02045G

Townley, H. E., Woon, K. L., Payne, F. P., White-Cooper, H., and Parker, A. R. (2007). Modification of the physical and optical properties of the frustule of the diatom *Coscinodiscus wailesii* by nickel sulfate. *Nanotechnology* 18:295101. doi: 10.1088/0957-4484/18/29/295101

Van Soest, R. W. M., Boury-Esnault, N., Vacelet, J., Dohrmann, M., Erpenbeck, D., De Voogd, N. J., et al. (2012). Global diversity of sponges (*Porifera*). *PLoS ONE* 7:e35105. doi: 10.1371/journal.pone.0035105

Vona, D., Lo Presti, M., Cicco, S. R., Palumbo, F., Ragni, R., and Farinola, G. M. (2016). Light emitting silica nanostructures by surface functionalization of diatom algae shells with a triethoxysilane-functionalized pi-conjugated fluorophore. *Mrs Adv.* 1, 3817–3823. doi: 10.1557/adv.2015.21

Wang, M., Gao, L. M., Dong, S. Y., Sun, Y. M., Shen, Q. R., and Guo, S. W. (2017). Role of silicon on plant-pathogen interactions. *Front. Plant Sci.* 8:701. doi: 10.3389/fpls.2017.00701

Werner, P., Blumtritt, H., and Natalio, F. (2017). Organic crystal lattices in the axial filament of silica spicules of *Demospongiae*. *J. Struct. Biol.* 198, 186–195. doi: 10.1016/j.jsb.2017.03.005

Xing, Y., Yu, L. H., Wang, X. L., Jia, J. Q., Liu, Y. Y., He, J. Y., et al. (2017). Characterization and analysis of Coscinodiscus genus frustule based on FIB-SEM. *Prog. Nat. Sci. Mater. Int.* 27, 391–395. doi: 10.1016/j.pnsc.2017.04.019

Xu, J. T., Bach, L. T., Schulz, K. G., Zhao, W. Y., Gao, K. S., and Riebesell, U. (2016). The role of coccoliths in protecting *Emiliania huxleyi* against stressful light and UV radiation. *Biogeosciences* 13, 4637–4643. doi: 10.5194/bg-13-4637-2016

Yamanaka, S., Yano, R., Usami, H., Hayashida, N., Ohguchi, M., Takeda, H., et al. (2008). Optical properties of diatom silica frustule with special reference to blue light. *J. Appl. Phys.* 103:074701. doi: 10.1063/1.2903342

Yang, W. R., Lopez, P. J., and Rosengarten, G. (2011). Diatoms: self assembled silica nanostructures, and templates for bio/chemical sensors and biomimetic membranes. *Analyst* 136, 42–53. doi: 10.1039/C0AN00602E

Yoneda, S., Ito, F., Yamanaka, S., and Usami, H. (2016). Optical properties of nanoporous silica frustules of a diatom determined using a 10 μm microfiber probe. *Jpn. J. Appl. Phys.* 55:072001. doi: 10.7567/JJAP.55.072001

Yoon, H., and Goorsky, M. S. (1995). "Systematic study of the structural and luminescence properties of P-type porous silicon," in *Materials Research Society Symposium - Proceedings*, Vol. 378, 893–898.

Zhang, S., Liu, H., Ke, Y., and Li, B. (2017). Effect of the silica content of diatoms on protozoan grazing. *Front. Mar. Sci.* 4:202. doi: 10.3389/fmars.2017.00202

Conflict of Interest Statement: The authors declare that the research was conducted in the absence of any commercial or financial relationships that could be construed as a potential conflict of interest.

Copyright © 2018 Mcheik, Cassaignon, Livage, Gibaud, Berthier and Lopez. This is an open-access article distributed under the terms of the Creative Commons Attribution License (CC BY). The use, distribution or reproduction in other forums is permitted, provided the original author(s) and the copyright owner are credited and that the original publication in this journal is cited, in accordance with accepted academic practice. No use, distribution or reproduction is permitted which does not comply with these terms.

frontiers in Marine Science

ORIGINAL RESEARCH
published: 28 March 2018
doi: 10.3389/fmars.2018.00102

Transparent Exopolymeric Particles (TEP) Selectively Increase Biogenic Silica Dissolution From Fossil Diatoms as Compared to Fresh Diatoms

Jordan Toullec and Brivaëla Moriceau*

Laboratoire des Sciences de l'Environnement Marin, UMR 6539 CNRS, Institut Universitaire Européen de la Mer (IUEM), Université de Bretagne Occidentale (UBO), Plouzané, France

Diatom production is mainly supported by the dissolution of biogenic silica ($bSiO_2$) within the first 200 m of the water column. The upper oceanic layer is enriched in dissolved and/or colloidal organic matter, such as exopolymeric polysaccharides (EPS) and transparent exopolymeric particles (TEP) excreted by phytoplankton in large amounts, especially at the end of a bloom. In this study we explored for the first time the direct influence of TEP-enriched diatom excretions on $bSiO_2$ dissolution. Twelve dissolution experiments on fresh and fossil diatom frustules were carried out on seawater containing different concentrations of TEP extracted from diatom cultures. Fresh diatom frustules were cleaned from the organic matter by low ash temperature, and fossil diatoms were made from diatomite powder. Results confirm that newly formed $bSiO_2$ dissolved at a faster rate than fossil diatoms due to a lower aluminum (Al) content. Diatom excretions have no effect on the dissolution of the newly formed $bSiO_2$ from *Chaetoceros muelleri.* Reversely, the diatomite specific dissolution rate constant and solubility of the $bSiO_2$ were positively correlated to TEP concentrations, suggesting that diatom excretion may provide an alternative source of dSi when limitations arise.

Keywords: exopolysaccharide, diatom excretion, diatomite, *Chaetoceros muelleri*, biogenic silica, $bSiO_2$ dissolution, TEP

OPEN ACCESS

Edited by:
Toshi Nagata,
The University of Tokyo, Japan

Reviewed by:
Marta Plavsic,
Rudjer Boskovic Institute, Croatia
Hiroshi Ogawa,
The University of Tokyo, Japan

****Correspondence:***
Jordan Toullec
brivaela.moriceau@univ-brest.fr

Specialty section:
This article was submitted to Marine Biogeochemistry, a section of the journal Frontiers in Marine Science

Received: *08 September 2017*
Accepted: *12 March 2018*
Published: *28 March 2018*

Citation:
Toullec J and Moriceau B (2018) Transparent Exopolymeric Particles (TEP) Selectively Increase Biogenic Silica Dissolution From Fossil Diatoms as Compared to Fresh Diatoms. Front. Mar. Sci. 5:102. doi: 10.3389/fmars.2018.00102

INTRODUCTION

The terrestrial lithosphere is composed of 27% (by weight) silicon. As a nutrient and required element of various marine organisms, silicon has an important part in biogeochemical processes. At a global scale, silica and carbon cycles are coupled by silicifying organisms via photosynthesis. In the marine realm, diatoms (Bacillariophyceae), unicellular phytoplankton with an absolute requirement for silicon to build their frustules composed of amorphous polymerised silica ($bSiO_2$), are key silicifying organisms that play an important role in the marine biogeochemical cycling of carbon. They are responsible for nearly 40% of the global primary production (Nelson et al., 1995; Rousseaux and Gregg, 2013). This contribution to the carbon cycle varies greatly according to the oceanic region and period of the year. For example, the contribution of diatoms to the global primary production varies between 25% in oligotrophic conditions (Brzezinski et al., 2011) to 75% in eutrophic ocean areas (Nelson et al., 1995). Diatoms are also a major component of the marine

biological carbon pump (Smetacek, 1999; Jin et al., 2006; Sanders et al., 2014) and are the base of some of the most successful food webs (Irigoien et al., 2002).

Approximately 50–60% of diatomaceous biogenic silica ($bSiO_2$) produced in the euphotic layer is remineralized within the first 100–200 m of the water column (Tréguer et al., 1995; Van Cappellen et al., 2002; Passow et al., 2003). This process of $bSiO_2$ dissolution provides diatoms with their main source of dissolved silicon, in the form of dissolved silica (dSi), which in turn, supports diatom growth for 50% of the global silicon budget established by Tréguer and De La Rocha (2013). Silica dissolution in the surface ocean of the northwest African upwelling regions was sufficient to supply all silicic acid taken up by phytoplankton (Nelson and Goering, 1977; Nelson et al., 1981). As such, biogenic silica dissolution is an important process that needs to be better understood and quantified, with particular emphasis on its variability in different environmental contexts. The dissolution of $bSiO_2$ depends on abiotic factors, such as specific surface area, temperature, salinity, pressure, pH, and aluminum concentration (Van Cappellen et al., 2002; Loucaides et al., 2012). Less studied, biotic factors also influence $bSiO_2$ dissolution. Diatom frustules are surrounded by an organic coating that needs to be removed by prokaryotes before dissolution of the frustule can begin (Bidle and Azam, 2001). In addition, biogenic silica dissolution depends on nutritive growth conditions of the diatoms (Boutorh et al., 2016). The process of silicification is known to be influenced by stressful conditions, such as nutrient limitation (Boyle, 1998; Takeda, 1998; Lasbleiz et al., 2014) and/or the presence of grazers (Pondaven et al., 2007).

Polysaccharides (EPS) are abundant in the surface waters of the global ocean and are typically found in the nutrient limited conditions at the end of a phytoplankton bloom (Passow, 2002a; Claquin et al., 2008). EPS are mainly secreted by diatoms and bacteria, though other types of phytoplankton can also contribute (Passow, 2002a). EPS are sticky and easily aggregate to form transparent exopolymeric particles (TEP), an essential trigger for mass flocculation during a phytoplankton bloom (Mari and Kiørboe, 1996; Passow, 2002b). Their size ranges from colloidal (1 kDa) to 100 μm, and they can reach abundances of 40,000 particles mL^{-1} or 11 mg X_{eq} L^{-1} (Mari and Burd, 1998; Passow, 2002b), contributing to ∼10–25% of the DOM pool in surface waters (Passow, 2002b; Thornton, 2014). In such conditions, when turbulence favors collisions, TEP promote aggregation with cells included in the TEP matrix. In diatom aggregates $bSiO_2$ dissolution is slower than in the surrounding seawater (Moriceau et al., 2007b). The decrease of $bSiO_2$ dissolution rates inside aggregates have, for the first time, been attributed to the longer viability of aggregated diatoms (Garvey et al., 2007) and to higher dSi concentrations in the pore water due to adsorption processes (Moriceau et al., 2007a, 2014). Another hypothesis is that the TEP matrix also protects the $bSiO_2$ against dissolution. EPS inhibits the dissolution of Al-enriched lithogenic silica ($lSiO_2$), such as feldspar, kaolinite, and quartz (Welch and Ullman, 1993, 1996; Ullman et al., 1996). Conversely, in some cases, bacterial byproducts such as organic acids promote $lSiO_2$ dissolution (Welch and Ullman, 1993, 1996; Vandevivere et al., 1994) which is much more resistant to dissolution than $bSiO_2$. If this is true, it can be of great importance for the dissolution occurring both in the surface layer and in sediments. Similar to what can be found in the surface layer, TEP are sometimes concentrated at the surface of sediments due to massive sedimentation of aggregates or from the direct activity of benthic organisms (Wotton, 2004). Despite their abundance in the surface waters and sediments, two important components of the water column for $bSiO_2$ dissolution processes, no study has measured the influence of TEP on the dissolution of diatomaceous $bSiO_2$. In this context, the goal of the present study is to understand the influence of TEP concentrations on the dissolution of freshly cleaned and fossil diatom $bSiO_2$.

MATERIALS AND METHODS

In order to understand how diatom excretion products influence $bSiO_2$ dissolution, we conducted two sets of dissolution experiments under batch conditions. Each set of conditions consisted of amorphous silica dissolution experiments in seawater containing different concentrations of TEP-enriched diatom excretion products. The dissolution of two different types of silica: Fossil diatoms and fresh diatoms, were evaluated. For the first set of experiments we used diatomite (fossil diatoms), for the second set of experiments we used dead diatoms *Chaetoceros muelleri* cleaned from their organic coating.

Samples Preparation

$bSiO_2$ from diatomite (fossil diatoms) exists as a commercial product, a fine powder that is a chalk-like, soft, friable, earthy, very-fine grained, and siliceous sedimentary rock, usually light in color. The measured Si:Al ratio (moles:moles) of the diatomite was 4.8. Fresh $bSiO_2$ from diatoms came from a culture of *C. muelleri* (strain CCAP 1010-3) provided by Ifremer's Argenton experimental station (Argenton, France). Fresh algae cultures were grown using a Conway culture medium (Salinity = 35.2 PSU), at 20°C with 100 μmol m^{-2} s^{-1} light on a 24:0 h light:dark cycle. The final cell concentration was 3.9×10^6 cells mL^{-1} after we isolated diatom byproducts and $bSiO_2$. Ten liters of this culture solution was centrifuged at 3,000 g for 10 min at 15°C (Thermo Scientific Heraeus® Multifuge® 3SR Plus). Following protocols commonly used for $bSiO_2$ dissolution experiments, the pellets were rinsed three times with milliQ water to remove salts and residual dSi, centrifuged, and then frozen at −20°C prior lyophilisation during 72 h. Fresh diatom $bSiO_2$ was cleaned from the external organic membrane by low ash combustion in a plasma oven (Gala intrumente® Plasma—ACE_5; Dixit and Van Cappellen, 2003; Loucaides et al., 2008). Despite the 10 L of highly concentrated diatom culture, we were only able to collect 254 μmol of $bSiO_2$.

TEP Gradient

In order to extract byproducts from diatoms, another 10 L of *C. muelleri* culture at the stationary phase was kept in the dark for several days at 20°C. Diatom by-products were isolated from the diatoms by filtration through a 1 μm polycarbonate filter (*C. muelleri*, single cell size range from 4 to 6 μm). The resulting seawater was strongly enriched in TEP (TEP > 0.4 μm: 4.1 ±

1 mg X_{eq} L^{-1}) and contained no diatoms. Five solutions were prepared from different mixtures of the TEP-enriched medium and natural seawater from the Bay of Brest, pre-filtered using a 0.22 μm polycarbonate filter (Salinity = 33.5 PSU, $[SiOH_4]$ = 8 μmol L^{-1}, $[NO_3]$ =18.35 μmol L^{-1}, $[NO_2]$ = 0.20 μmol L^{-1}, $[PO_4]$ = 0.45 μmol L^{-1}). We expected an increasing TEP concentration range from the mixing of the two mother solutions. TEP-enriched to seawater vol:vol ratios were 0 for D1, 0.25 for D2, 0.5 for D3, 0.75 for D4, and 1 for D5. The salinity change in our medium from D1 to D5 did not exceed 1.7 PSU.

Batch Preparation

Nine 500 mL polycarbonate batches were used in the diatomite experiment: D1, D2, D3, D4, and D5, with D1 and D5 in triplicate. Each batch contained 15 mg of diatomite. For the second set of experiments with freshly cleaned diatoms, due to the low amount of $bSiO_2$ collected from the 10 L of *C. muelleri* culture, only three polycarbonate batches of 125 mL were prepared using three dilutions: D1, D2, and D5. The initial $bSiO_2$ concentrations were ∼500 μM in all batches.

Dissolution Experiment

All batches were incubated in the dark, at 16°C, during 30 days on a shaking table for continuous agitation, allowing for a better homogenization of the particles in the batch. Batch cultures were kept ajar during the 30 days, in order to preserve gases exchanges, which have been proven to limit CO_2 surplus and pH changes (Suroy et al., 2014, 2015; Boutorh et al., 2016). The dSi concentrations were measured on a daily basis for 4 days, and every second day until the end of the experiment.

TEP Sampling and Measurement

The method of Passow and Alldredge (1995) was used for TEP measurements. Three to five replicates for each solution were sampled at the beginning of the experiment. Under low-pressure conditions, 15 ml was filtered onto 0.4 μm polycarbonate filters (according to Passow and Alldredge, 1995) and stained with 0.5 mL of a 0.02% aqueous solution of pre-filtered Alcian blue in 0.06% acetic acid (pH 2.5). Filters were kept at −20°C until analysis. Filters were soaked for 2 h in 6 mL of 80% H2SO4 under agitation. The absorption measured at 787 nm in a 1 cm cuvette was converted into grams of Gum Xanthan equivalent per liter (g Xeq L^{-1}) using a calibration curve done for our working solution of Alcian blue.

Dissolved and Particulate Biogenic Silica Measurements

Samples were filtered through 0.4 μm polycarbonates Millipore filters. Filtrates were preserved at 4°C in 15 mL polycarbonate falcon tubes prior to analysis for dSi. Millipore filters were dried during 24 h at 55°C inside Petri box, and then kept at room temperature before digestion and analysis for $bSiO_2$. Filters were digested in 8 mL of NaOH (0.2 M) during 4 h at 90°C under constant agitation. Digestion was stopped by cooling the solution and neutralized with 2 mL of chloride acid (1 M). All samples were then centrifuged at 3,000 g at 20°C during 5 min. Supernatants containing the dissolved silica (dSi), were analyzed by AutoAnalyzer.

Chemistry Analysis

Silicic Acid (dSi) was analyzed using the automated colorimetric method on a Technicon AutoAnalyzer according to the protocol established by Tréguer and Le Corre (1975) and optimized by Aminot and Kérouel (2007). Samples are guided by a pump in a continuous flux, through a circuit in which dissolved silica (dSi) reacts with ammonium molybdate, at low pH, to produce β-silicomolybdique acid. This acid is then reduced by methylamino-4-phenol sulfite and a sodium sulfite solution, resulting in a final product absorbing at 810 nm.

Kinetic Calculation

In the present study, $bSiO_2$ dissolution was monitored by following the dSi concentration with time (Equation 1) as described as:

$$dSi_{(t)} = dSi_{(e)}.\left(1 - e^{-Kt}\right) \quad (1)$$

The specific dissolution rate constant (K, d^{-1}) was determined using the slope at the origin of the plot of the $ln\left(\frac{dSi_{(e)} - (dSi_{(t)} - dSi_{(0)})}{dSi_{(e)}}\right)$ vs. time (Equation 2), which corresponds to exponential dissolution phases (Kamatani and Riley, 1979; Greenwood et al., 2001; Truesdale et al., 2005; Roubeix et al., 2008).

$$\frac{d\left[ln\left(\frac{dSi_{(e)} - (dSi_{(t)} - dSi_{(0)})}{dSi_{(e)}}\right)\right]}{dt} = -K \quad (2)$$

Where $dSi_{(t)}$ is dSi concentration (μmol L^{-1}) measured at time t (day), $dSi_{(0)}$ is initial dSi concentration (μmol L^{-1}), and $dSi_{(e)}$ is the dSi concentration reached at the plateau (μmol L^{-1}). For diatomite dissolution experiments, $dSi_{(e)}$ corresponds to the apparent solubility of the $bSiO_2$, because the 500 μM $bSiO_2$ initially added was never totally dissolved in the dissolution batch. For the $bSiO_2$ dissolution experiments using the freshly cleaned diatoms, $dSi_{(e)}$ is equal to the initial $bSiO_2$ concentration (μmol L^{-1}).

Statistical Analysis

Correlations between the kinetic parameters of $bSiO_2$ (specific dissolution rate constant and apparent solubility of the $bSiO_2$) and TEP concentrations are tested with non-parametric Spearman rank correlation, using R software with function: cor.test() method = "Spearman."

RESULTS

TEP concentrations (>0.4 μm) increased from D1 to D5, with values from 2.4 ± 0.2 to 4.7 ± 0.2 mg X_{eq} L^{-1} (**Table 1**).

The dissolution of $bSiO_2$ was clearly visible in the two sets of experiments from the progressive increase of the dSi concentrations with time (**Figures 1**, **2**). This increase was steeper for freshly cleaned diatoms than for fossil diatoms. In the fresh $bSiO_2$ dissolution experiments, a small plateau of dSi

TABLE 1 | Initial TEP concentrations for each experimental batch condition, calculated specific dissolution rate constant (K), and apparent solubility of the $bSiO_2$ for fossil diatoms cleaned diatoms.

Batches	TEP > 0.4 μm (mg X_{eq} L^{-1})	TEP > 0.2 μm (mg X_{eq} L^{-1})	$bSiO_2$	Specific dissolution rate constant (d^{-1})	Apparent solubity of $bSiO_2$ (μmol L^{-1})
D1	2.4 (±0.2)	5.7 (±0.8)	Cleaned diatoms	0.3	–
			Fossil diatoms	0.17 (±0.01)	62 (±6)
D2	2.7 (±0.2)	7.0	Cleaned diatoms	0.3	–
			Fossil diatoms	0.19	87
D3	3.7 (± 0.5)	7.3	Fossil diatoms	0.19	1,02
D4	4.7 (±0.2)	9.1	Fossil diatoms	0.29	127
D5	4.1 (±1.6)	7.7 (±0.5)	Cleaned diatoms	0.18	–
			Fossil diatoms	0.24 (±0.07)	163 (±18)

concentration was observed when all the $bSiO_2$ initially added to the batch was dissolved. In the dissolution batch containing fossil diatoms, the dSi concentrations stabilized after 120 h when they reached a plateau (**Figure 1**) equivalent to the apparent solubility of the $bSiO_2$. The apparent solubility of the $bSiO_2$ also increased from D1 to D5, with values from 62 μM in D1, 87 μM in D2, 102 μM in D3, 127 μM in D4, and 163 μM in D5 (**Table 1**, **Figure 1**).

Diatomite specific dissolution rate constants varied from 0.16 to 0.35 d^{-1} from D1 to D5 (**Table 1**). The specific dissolution rate constants of the freshly cleaned diatoms (*C. muelleri*) varied from 0.18 to 0.31 d^{-1} (**Table 1**). Our constants are close to the average specific dissolution rate constants of 0.15 ± 0.15 d^{-1} given for cleaned frustules by Roubeix et al. (2008). For diatomite dissolution, a significant correlation was revealed between specific dissolution rate constants and >0.4μm TEP concentrations (**Figure 3**; Spearman correlation = 0.7*, *p*-value = 0.022, $N = 9$ experiments). Similarly, a significant correlation was found between apparent solubility of the $bSiO_2$ and >0.4 μm TEP concentrations (**Figure 3**; Spearman correlation = 0.867**, *p*-value = 0.002, $N = 9$ experiments). By contrast, no correlation between specific dissolution rate constants and TEP concentrations was observed for the freshly cleaned diatoms (**Figure 3**).

DISCUSSION

Specific dissolution rate constant and apparent solubility of $bSiO_2$ were correlated with TEP concentration. We were able to create a concentration gradient of TEP in the dissolution batches from the different dilutions between the TEP-enriched medium and the natural filtered seawater. TEP concentrations in D1 that contained only 0.22 μm filtered natural seawater were negligible (2.4 ± 0.2 mg X_{eq} L^{-1}). TEP are sticky particles (Passow, 2002b; Mari et al., 2017) that aggregate easily in solution, especially under continuous agitation. The different solutions also contained <0.2 μm TEP. With this fraction, TEP concentrations were on average twice as high (**Table 1**). Our measurement suggests that in the filtered seawater, small TEP particles (lower than 0.2 μm) have aggregated into TEP particles with diameters larger than 0.4 μm. As most of the studies are measuring TEP >0.4 μm, we decided to refer only to these measurements when talking about TEP concentrations in the following discussion. Finally, we obtained TEP concentrations ranging from 2 to 6 mg X_{eq} L^{-1} that reflect what can be seen *in situ* according to Passow and Alldredge (1995), who gave natural values in a range of 0.02–11 mg X_{eq} L^{-1}.

Dissolved silica (dSi) concentrations increased with time following the pattern generally seen in similar dissolution experiments. We observed some variability in the dissolution pattern with dSi concentrations data higher or lower than expected from Equation (1). At such high TEP concentrations, as seen *in situ* with high concentrations of phytoplankton, the seawater viscosity is influenced, affecting the swimming behavior of the zooplankton (Seuront, 2006). High viscosity decreases the diffusion of the dSi (Eyring, 1936), which may explain the variability of dSi concentrations as compared to the normal pattern, despite the mixing of the batches.

The $bSiO_2$ from cleaned frustules dissolved on average five times faster than $bSiO_2$ still surrounded by an external membrane (0.03 vs. 0.15 d^{-1}, Roubeix et al., 2008). In our study, we measured similar dissolution rates for the cleaned $bSiO_2$ from fresh *C. muelleri* with an average specific dissolution rate constant of 0.22 d^{-1}. $bSiO_2$ dissolved at 0.3 d^{-1} in the two batches containing less TEP, while in the third dissolution experiment the rate constant was 0.18 d^{-1}. One experiment is not sufficient to clearly demonstrate a potential influence of diatom excretion on $bSiO_2$ dissolution. However, a similar trend was observed in the study by Roubeix et al. (2008), in which they suggested a possible "blockage effect," due to the physical coating of the $bSiO_2$ surface that may slow down access to the surface by water molecules.

At similar TEP concentrations, $bSiO_2$ from freshly cleaned frustules dissolved slightly faster than $bSiO_2$ from diatomite (0.3 vs. 0.18 d^{-1}, **Table 1**). During its stay in the sediment, "reverse weathering" processes such as Al-Si substitutions progressively decreased the reactivity of the $bSiO_2$ (Van Bennekom et al., 1991). A partial explanation for the difference in the dissolution rate constant measured between diatomite and fresh $bSiO_2$ could be a different Al content: The Si:Al ratio of the diatomite used in this study was 4.8 compared to the 20–40 commonly found for fresh diatoms (Ragueneau et al., 2005). In our study, most of the amorphous silica from the diatomite stayed in its particulate phase, with the apparent

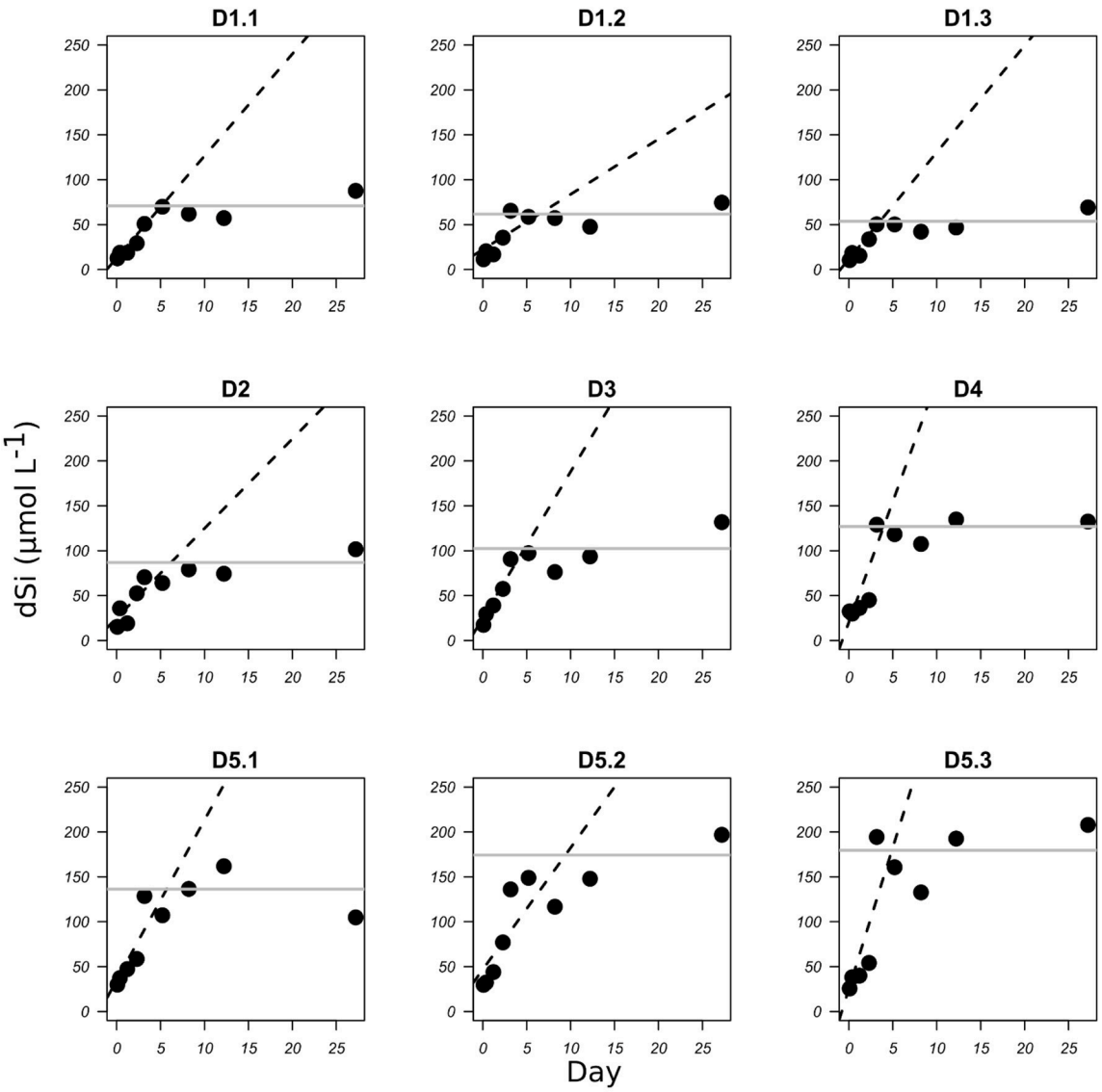

FIGURE 1 | $bSiO_2$ dissolution of diatomite expressed as the increase in dSi concentration (μmol L^{-1}) with time (days) for each TEP concentration D1 to D5 (see **Table 1** for corresponding TEP concentrations). Dashed lines represent the linear regression for the initial part of the graphs. Gray lines represent the mean apparent solubility of the $bSiO_2$.

solubility of the $bSiO_2$ going from 62 to 165 μmol L^{-1}. By comparison, the solubility measured by Loucaides et al. (2008) for diatomite was 1,150 μM at 25°C and a pH of 8. However, the diatomite used in his study contained a lot less Al, and Al incorporation inside diatom frustules can also change solubility (Van Bennekom et al., 1991). An important result of our study is the correlation between the apparent solubility of the $bSiO_2$ in the fossil diatoms batch and the TEP concentrations (Spearman correlation = 0.867**, *p*-value = 0.002). It has been suggested that dSi may adsorb on the TEP (Moriceau et al., 2014), which would explain the high dSi concentrations measured inside aggregates despite sometimes very low dSi concentrations in the surrounding seawater (Brzezinski et al., 1997). Our correlation between TEP concentrations and solubility of the $bSiO_2$ tends to strengthen this hypothesis.

In our experiment, the influence of diatom byproducts on $bSiO_2$ dissolution was monitored using the TEP concentrations because (1) diatoms generally produced EPS and TEP in larger quantities (Myklestad and Haug, 1972; Myklestad, 1974, 1995; Myklestad et al., 1989) and (2) previous experiments already showed an influence of polysaccharides on lithogenic SiO_2 dissolution (Welch and Vandevivere, 1994). The $bSiO_2$ specific dissolution rate constants of fossil diatoms were also correlated to TEP concentrations. As it was impossible to extract TEP from the rest of the diatom byproducts, and because the

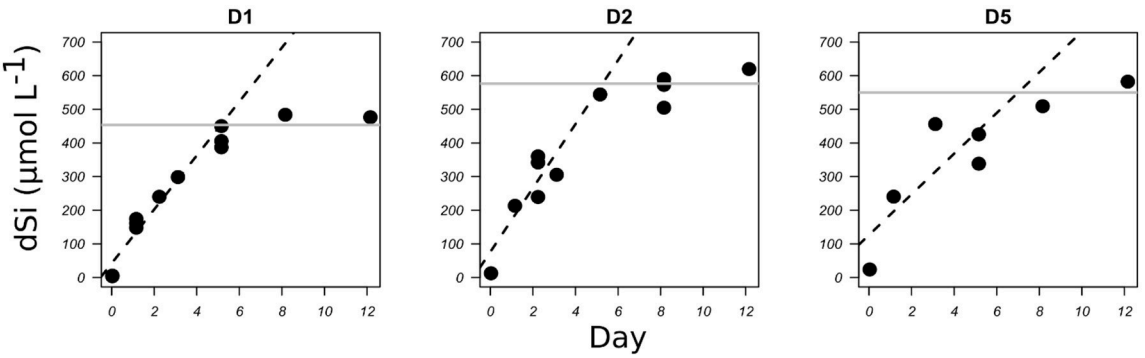

FIGURE 2 | $bSiO_2$ dissolution of freshly cleaned diatom frustules of *C. muelleri* expressed as the increase in dSi concentration (μmol L^{-1}) with time (days) for three TEP concentrations (see **Table 1**). Dashed lines represent the linear regression for the initial part of the graphs. Gray lines represent the dSi concentrations at the plateau, in these cases the initial $bSiO_2$ concentrations.

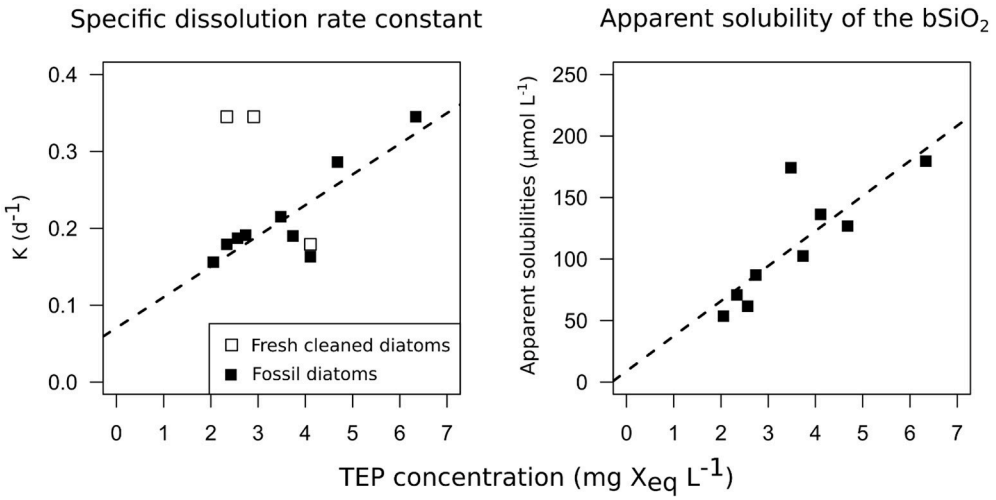

FIGURE 3 | Correlations between the dissolution kinetics measured during the 12 dissolution experiments and TEP concentrations. On the left panel, $bSiO_2$ specific dissolution rate constants (d^{-1}) are plotted vs. TEP concentrations (>0.4 μm TEP, mg X_{eq} mL^{-1}). On the right panel, $bSiO_2$ apparent solubility of the $bSiO_2$ (μmol L^{-1}) are plotted vs. TEP concentrations (mg X_{eq} mL^{-1}). Open squares represent *C. muelleri* and solid squares represent diatomite.

culture was not axenic, we must also have created a gradient of other molecules and bacteria concentration in the other dissolution batch. Analyses of diatom excretions at the end of a phytoplankton bloom or at the stationary phase in the culture showed considerable amounts of amino acids, proteoglycans, and extracellular polysaccharides containing residues of rhamnose, fucose, and galactose, with the carbohydrate contribution sometimes reaching 80–90% of the total extracellular release (Myklestad and Haug, 1972; Myklestad, 1974, 1995; Myklestad et al., 1989). Previous studies evidenced that fresh microbial EPS extracted from bacteria inhibit or promote the dissolution of $lSiO_2$ (Welch and Vandevivere, 1994; Ullman et al., 1996), and organic acids such as glucuronic acids favor $lSiO_2$ dissolution (Welch and Ullman, 1993, 1996; Vandevivere et al., 1994). However, the variation of the $bSiO_2$ specific dissolution rate constants with the concentration of diatom byproducts could also be due to compounds other than polysaccharides, or to bacteria. To our knowledge no study has directly measured the potential influence of other byproducts such as amino acids. Concerning bacteria, proteolytic activities have little effect on $bSiO_2$ dissolution, except for the removal of organic matter associated to the frustules occurring in the first days of the dissolution (Bidle and Azam, 2001). In our study we used frustules cleaned from their organic coating and indeed the dissolution of the $bSiO_2$ from freshly cleaned diatoms was not increased by the bacteria gradient possibly resulting from our protocol. Roubeix et al. (2008) also hypothesized that bacterial colonization increases $bSiO_2$ dissolution by creating a microenvironment with high ectoproteolytic activity at the diatom surface or by releasing organic compounds that can facilitate diatom $bSiO_2$ dissolution (Roubeix et al., 2008). Rather, in their experiment they observed (1) no influence of bacterial

activity and (2) a decrease of the dissolution rates when using cleaned frustules. Dissolution of the fossil $bSiO_2$ was influenced by the gradient of diatom excretion/associated bacteria but had no influence or, possibly, an opposite effect on the $bSiO_2$ dissolution of freshly cleaned frustules. If true, this would mean that diatoms or associated bacteria from the *C. muelleri* cultures are able to selectively increase the dissolution of $bSiO_2$ from fossil diatoms but not the $bSiO_2$ dissolution from the freshly cleaned diatoms.

More recently, other works from Akagi's team showed that by measuring rare earth elements on diatom frustules the dissolution of lithogenic silica in surface water could be an unexpected source of dSi for diatom growth (Akagi et al., 2011, 2014; Akagi, 2013a,b). Our experiment nicely complements their findings by adding a "how." Indeed, as it has been shown in a forest where mycorrhizal symbiosis with the roots of trees promotes the weathering of nutrients by releasing organic molecules (Griffiths et al., 1994), we can propose a similar hypothesis with diatoms. Bacteria associated to diatoms can selectively increase dissolution of silicate minerals (Vandevivere et al., 1994). Diatoms have acquired an ability to exudate specific organic molecules that can increase the dissolution of lithogenic silica and not their own biogenic silica. This strategy could be advantageous during silicate limitation episodes, whereby lithogenic silica becomes a source of silicon. This would be possible if diatoms produce organic ligands with a high affinity for Al. Removal of Al in preference to Si in Al enriched silica would increase lithogenic silica and fossil $bSiO_2$ dissolution without weakening their own frustule.

CONCLUSION

The main goal of this study was to understand the influence of TEP on biogenic silica dissolution. We used two different types of $bSiO_2$: fossil diatoms (diatomite) and cleaned frustules of cultured diatoms (*C. muelleri*). Our results evidenced a correlation between TEP concentrations and $bSiO_2$ dissolution rate constants and solubility of the $bSiO_2$ for fossil diatoms, however diatom excretions had no influence on $bSiO_2$ dissolution from freshly cleaned frustules, except for possible protection at the highest TEP concentration.

In the light of the results obtained here, diatom byproducts seem to favor Al-enriched silica dissolution, such as bacterial EPS do for feldspars and aluminosilicates (Welch and Ullman, 1993, 1996; Vandevivere et al., 1994) as compared to fresh $bSiO_2$. In case of limitations, TEP are produced in greater quantities by diatoms that may provide them with an unexpected source of nutrients through the increase of weathering. This would explain the Rare Earth concentrations sometimes measured on diatom frustules and confirm the theory that diatoms may directly uptake silica on lithogenic particles.

AUTHOR CONTRIBUTIONS

JT writing paper, laboratory experiment, sample analysis, data treatment; BM writing paper, support in lab experiment, supervisor.

ACKNOWLEDGMENTS

We would like to thank the Argenton Ifremer experiment station for providing us the algae. We thank Jill Naomi Sutton for her help in editing the English language manuscript, Lucie Blondel for the ICP-AES analysis of diatomite, and everyone else in LEMAR for assistance during the experiment. This work was partly supported by the ANR BIOPSIS project, grant ANR-16-CE01-0002-01 of the French Agence Nationale de la Recherche, and by the CHIBIDO team of the LEMAR.

REFERENCES

Akagi, T. (2013a). Rare earth element (REE)–silicic acid complexes in seawater to explain the incorporation of REEs in opal and the "leftover" REEs in surface water: new interpretation of dissolved REE distribution profiles. *Geochim. Cosmochim. Acta* 113, 174–192. doi: 10.1016/j.gca.2013.03.014

Akagi, T. (2013b). Revision of the dissolution kinetics of aggregated settling particles. *Mem. Fac. Sci. Kyushu Univ. Ser. Earth Planet Sci.* 33, 1–5. Available online at: http://hdl.handle.net/2324/1397628

Akagi, T., Fu, F., Hongo, Y., and Takahashi, K. (2011). Composition of rare earth elements in settling particles collected in the highly productive North Pacific Ocean and Bering Sea: implications for siliceous-matter dissolution kinetics and formation of two REE-enriched phases. *Geochim. Cosmochim. Acta* 75, 4857–4876. doi: 10.1016/j.gca.2011.06.001

Akagi, T., Yasuda, S., Asahara, Y., Emoto, M., and Takahashi, K. (2014). Diatoms spread a high epsilon Nd-signature in the North Pacific Ocean. *Geochem. J.* 48, 121–131. doi: 10.2343/geochemj.2.0292

Aminot, A., and Kérouel, R. (2007). *Dosage Automatique des Nutriments Dans les Eaux Marines: Méthodes en Flux Continu*, ed Quae (Plouzané: Ifremer).

Bidle, K. D., and Azam, F. (2001). Bacterial control of silicon regeneration from diatom detritus: significance of bacterial ectohydrolases and species identity. *Limnol. Oceanogr.* 46, 1606–1623. doi: 10.4319/lo.2001.46.7.1606

Boutorh, J., Moriceau, B., Gallinari, M., Ragueneau, O., and Bucciarelli, E. (2016). Effect of trace metal-limited growth on the postmortem dissolution of the marine diatom *Pseudo-nitzschia delicatissima*. *Glob. Biogeochem. Cycles* 30, 57–69. doi: 10.1002/2015GB005088

Boyle, E. (1998). Oceanography pumping iron makes thinner diatoms. *Nature* 393, 733–734. doi: 10.1038/31585

Brzezinski, M. A., Baines, S. B., Balch, W. M., Beucher, C. P., Chai, F., Dugdale, R. C., et al. (2011). Co-limitation of diatoms by iron and silicic acid in the equatorial Pacific. *Deep Sea Res. Part II Top. Stud. Oceanogr.* 58, 493–511. doi: 10.1016/j.dsr2.2010.08.005

Brzezinski, M. A., Phillips, D. R., Chavez, F. P., Friederich, G. E., and Dugdale, R. C. (1997). Silica production in the Monterey, California, upwelling system. *Limnol. Oceanogr.* 42, 1694–1705. doi: 10.4319/lo.1997.42.8.1694

Claquin, P., Probert, I., Lefebvre, S., and Veron, B. (2008). Effects of temperature on photosynthetic parameters and TEP production in eight species of marine microalgae. *Aquat. Microb. Ecol.* 51, 1–11. doi: 10.3354/ame01187

Dixit, S., and Van Cappellen, P. (2003). Predicting benthic fluxes of silicic acid from deep-sea sediments. *J. Geophys. Res. Oceans* 108:3334. doi: 10.1029/2002JC001309

Eyring, H. (1936). Viscosity, plasticity, and diffusion as examples of absolute reaction rates. *J. Chem. Phys.* 4, 283–291. doi: 10.1063/1.1749836

Garvey, M., Moriceau, B., and Passow, U. (2007). Applicability of the FDA assay to determine the viability of marine phytoplankton under different environmental conditions. *Mar. Ecol. Prog. Ser.* 352, 17–26. doi: 10.3354/meps07134

Greenwood, J. E., Truesdale, V. W., and Rendell, A. R. (2001). Biogenic silica dissolution in seawater—*in vitro* chemical kinetics. *Prog. Oceanogr.* 48, 1–23. doi: 10.1016/S0079-6611(00)00046-X

Griffiths, R. P., Baham, J. E., and Caldwell, B. A. (1994). Soil solution chemistry of ectomycorrhizal mats in forest soil. *Soil Biol. Biochem.* 26, 331–337. doi: 10.1016/0038-0717(94)90282-8

Irigoien, X., Harris, R. P., Verheye, H. M., Joly, P., Runge, J., Starr, M., et al. (2002). Copepod hatching success in marine ecosystems with high diatom concentrations. *Nature* 419, 387–389. doi: 10.1038/nature01055

Jin, X., Gruber, N., Dunne, J. P., Sarmiento, J. L., and Armstrong, R. A. (2006). Diagnosing the contribution of phytoplankton functional groups to the production and export of particulate organic carbon, CaCO2, and opal from global nutrient and alkalinity distributions: diagnosing phytoplankton functional groups. *Glob. Biogeochem. Cycles* 20:GB201. doi: 10.1029/2005GB002532

Kamatani, A., and Riley, J. P. (1979). Rate of dissolution of diatom silica walls in seawater. *Mar. Biol.* 55, 29–35. doi: 10.1007/BF00391714

Lasbleiz, M., Leblanc, K., Blain, S., Ras, J., Cornet-Barthaux, V., Hélias Nunige, S., et al. (2014). Pigments, elemental composition (C, N, P, and Si), and stoichiometry of particulate matter in the naturally iron fertilized region of Kerguelen in the Southern Ocean. *Biogeosciences* 11, 5931–5955. doi: 10.5194/bg-11-5931-2014

Loucaides, S., Cappellen, P. V., and Behrends, T. (2008). Dissolution of biogenic silica from land to ocean: role of salinity and pH. *Limnol. Oceanogr.* 53, 1614–1621. doi: 10.4319/lo.2008.53.4.1614

Loucaides, S., Van Cappellen, P., Roubeix, V., Moriceau, B., and Ragueneau, O. (2012). Controls on the recycling and preservation of biogenic silica from biomineralization to burial. *Silicon* 4, 7–22. doi: 10.1007/s12633-011-9092-9

Mari, X., and Burd, A. (1998). Seasonal size spectra of transparent exopolymeric particles (TEP) in a coastal sea and comparison with those predicted using coagulation theory. *Mar. Ecol. Prog. Ser.* 163, 63–76. doi: 10.3354/meps163063

Mari, X., and Kiørboe, T. (1996). Abundance, size distribution and bacterial colonization of transparent exopolymeric particles (TEP) during spring in the Kattegat. *J. Plankton Res.* 18, 969–986. doi: 10.1093/plankt/18.6.969

Mari, X., Passow, U., Migon, C., Burd, A. B., and Legendre, L. (2017). Transparent exopolymer particles: effects on carbon cycling in the ocean. *Prog. Oceanogr.* 151, 13–37. doi: 10.1016/j.pocean.2016.11.002

Moriceau, B., Gallinari, M., Soetaert, K., and Ragueneau, O. (2007b). Importance of particle formation to reconstructed water column biogenic silica fluxes. *Glob. Biogeochem. Cycles* 21:GB3012. doi: 10.1029/2006GB002814

Moriceau, B., Garvey, M., Ragueneau, O., and Passow, U. (2007a). Evidence for reduced biogenic silica dissolution rates in diatom aggregates. *Mar. Ecol. Prog. Ser.* 333, 129–142. doi: 10.3354/meps333129

Moriceau, B., Laruelle, G., Passow, U., Van Cappellen, P., and Ragueneau, O. (2014). Biogenic silica dissolution in diatom aggregates: insights from reactive transport modelling. *Mar. Ecol. Prog. Ser.* 517, 35–49. doi: 10.3354/meps11028

Myklestad, S. (1974). Production of carbohydrates by marine planktonic diatoms. I. Comparison of nine different species in culture. *J. Exp. Mar. Biol. Ecol.* 15, 261–274. doi: 10.1016/0022-0981(74)90049-5

Myklestad, S., and Haug, A. (1972). Production of carbohydrates by the marine diatom Chaetoceros affinis var. *willei* (Gran) Hustedt. I. Effect of the concentration of nutrients in the culture medium. *J. Exp. Mar. Biol. Ecol.* 9, 125–136. doi: 10.1016/0022-0981(72)90041-X

Myklestad, S., Holm-Hansen, O., Vårum, K. M., and Volcani, B. E. (1989). Rate of release of extracellular amino acids and carbohydrates from the marine diatom *Chaetoceros affinis*. *J. Plankton Res.* 11, 763–773. doi: 10.1093/plankt/11.4.763

Myklestad, S. M. (1995). Release of extracellular products by phytoplankton with special emphasis on polysaccharides. *Sci. Total Environ.* 165, 155–164. doi: 10.1016/0048-9697(95)04549-G

Nelson, D. M., and Goering, J. J. (1977). Near-surface silica dissolution in the upwelling region off northwest Africa. *Deep Sea Res.* 24, 65–73.

Nelson, D. M., Goering, J. J., and Boisseau, D. W. (1981). "Consumption and regeneration of silicic acid in three coastal upwelling systems," in *Coastal Upwelling*, ed F. A. Richards (Washington, DC: American Geophysical Union), 242–256.

Nelson, D. M., Tréguer, P., Brzezinski, M. A., Leynaert, A., and Quéguiner, B. (1995). Production and dissolution of biogenic silica in the ocean: revised global estimates, comparison with regional data and relationship to biogenic sedimentation. *Glob. Biogeochem. Cycles* 9, 359–372. doi: 10.1029/95GB01070

Passow, U. (2002a). Production of transparent exopolymer particles (TEP) by phyto- and bacterioplankton. *Mar. Ecol. Prog. Ser.* 236, 1–12. doi: 10.3354/meps236001

Passow, U. (2002b). Transparent exopolymer particles (TEP) in aquatic environments. *Prog. Oceanogr.* 55, 287–333. doi: 10.1016/S0079-6611(02)00138-6

Passow, U., and Alldredge, A. L. (1995). A dye-binding assay for the spectrophotometric measurement of transparent exopolymer particles (TEP). *Limnol. Oceanogr.* 40, 1326–1335. doi: 10.4319/lo.1995.40.7.1326

Passow, U., Engel, A., and Ploug, H. (2003). The role of aggregation for the dissolution of diatom frustules. *FEMS Microbiol. Ecol.* 46, 247–255. doi: 10.1016/S0168-6496(03)00199-5

Pondaven, P., Gallinari, M., Chollet, S., Bucciarelli, E., Sarthou, G., Schultes, S., et al. (2007). Grazing-induced changes in cell wall silicification in a marine diatom. *Protist* 158, 21–28. doi: 10.1016/j.protis.2006.09.002

Ragueneau, O., Savoye, N., Del Amo, Y., Cotten, J., Tardiveau, B., and Leynaert, A. (2005). A new method for the measurement of biogenic silica in suspended matter of coastal waters: using Si:Al ratios to correct for the mineral interference. *Cont. Shelf Res.* 25, 697–710. doi: 10.1016/j.csr.2004.09.017

Roubeix, V., Becquevort, S., and Lancelot, C. (2008). Influence of bacteria and salinity on diatom biogenic silica dissolution in estuarine systems. *Biogeochemistry* 88, 47–62. doi: 10.1007/s10533-008-9193-8

Rousseaux, C., and Gregg, W. (2013). Interannual variation in phytoplankton primary production at a global scale. *Remote Sens.* 6, 1–19. doi: 10.3390/rs6010001

Sanders, R., Henson, S. A., Koski, M., De La Rocha, C. L., Painter, S. C., Poulton, A. J., et al. (2014). The biological carbon pump in the North Atlantic. *Prog. Oceanogr.* 129, 200–218. doi: 10.1016/j.pocean.2014.05.005

Seuront, L. (2006). Effect of salinity on the swimming behaviour of the estuarine calanoid copepod *Eurytemora affinis*. *J. Plankton Res.* 28, 805–813. doi: 10.1093/plankt/fbl012

Smetacek, V. (1999). Diatoms and the ocean carbon cycle. *Protist* 150, 25–32. doi: 10.1016/S1434-4610(99)70006-4

Suroy, M., Moriceau, B., Boutorh, J., and Goutx, M. (2014). Fatty acids associated with the frustules of diatoms and their fate during degradation:a case study in *Thalassiosira weissflogii*. *Deep Sea Res. Part I Oceanogr. Res. Pap.* 86, 21–31. doi: 10.1016/j.dsr.2014.01.001

Suroy, M., Panagiotopoulos, C., Boutorh, J., Goutx, M., and Moriceau, B. (2015). Degradation of diatom carbohydrates: a case study with N- and Si-stressed *Thalassiosira weissflogii*. *J. Exp. Mar. Biol. Ecol.* 470, 1–11. doi: 10.1016/j.jembe.2015.04.018

Takeda, S. (1998). Influence of iron availability on nutrient consumption ratio of diatoms in oceanic waters. *Nature* 393, 774–777. doi: 10.1038/31674

Thornton, D. C. O. (2014). Dissolved organic matter (DOM) release by phytoplankton in the contemporary and future ocean. *Eur. J. Phycol.* 49, 20–46. doi: 10.1080/09670262.2013.875596

Tréguer, P., and Le Corre, P. (1975). *Manuel d'Analyse des sels Nutritifs dans l'eau de Mer (Utilisation de l'autoAnalyseur II), Université de Bretagne Occidentale, 2nd Edn.* Laboratoire d'Océanographie Chimique, Université de Bretagne Occidentale, Brest.

Tréguer, P. J., and De La Rocha, C. (2013). The world ocean silica cycle. *Annu. Rev. Mar. Sci.* 5, 477–501. doi: 10.1146/annurev-marine-121211-172346

Tréguer, P., Nelson, D. M., Van Bennekom, A. J., DeMaster, D. J., Leynaert, A., and Queguiner, B. (1995). The silica balance in the world ocean: a reestimate. *Science* 268, 375–379. doi: 10.1126/science.268.5209.375

Truesdale, V. W., Greenwood, J. E., and Rendell, A. (2005). The rate-equation for biogenic silica dissolution in seawater – new hypotheses. *Aquat. Geochem.* 11, 319–343. doi: 10.1007/s10498-004-7921-9

Ullman, W. J., Kirchman, D. L., Welch, S. A., and Vandevivere, P. (1996). Laboratory evidence for microbially mediated silicate mineral dissolution in nature. *Chem. Geol.* 132, 11–17. doi: 10.1016/S0009-2541(96)00036-8

Van Bennekom, A. J., Buma, A. G. J., and Nolting, R. F. (1991). Dissolved aluminium in the Weddell-Scotia Confluence and effect of Al on the dissolution kinetics of biogenic silica. *Mar. Chem.* 35, 423–434. doi: 10.1016/S0304-4203(09)90034-2

Van Cappellen, P., Dixit, S., and van Beusekom, J. (2002). Biogenic silica dissolution in the oceans: reconciling experimental and field-based dissolution rates. *Glob. Biogeochem. Cycles* 16, 23-1–23-10. doi: 10.1029/2001GB001431

Vandevivere, P., Welch, S. A., Ullman, W. J., and Kirchman, D. L. (1994). Enhanced dissolution of silicate minerals by bacteria at near-neutral pH. *Microb. Ecol.* 27, 241–251. doi: 10.1007/BF00182408

Welch, S. A., and Ullman, W. J. (1993). The effect of organic acids on plagioclase dissolution rates and stoichiometry. *Geochim. Cosmochim. Acta* 57, 2725–2736. doi: 10.1016/0016-7037(93)90386-B

Welch, S. A., and Ullman, W. J. (1996). Feldspar dissolution in acidic and organic solutions: compositional and pH dependence of dissolution rate. *Geochim. Cosmochim. Acta* 60, 2939–2948. doi: 10.1016/0016-7037(96)00134-2

Welch, S. A., and Vandevivere, P. (1994). Effect of microbial and other naturally occurring polymers on mineral dissolution. *Geomicrobiol. J.* 12, 227–238. doi: 10.1080/01490459409377991

Wotton, R. S. (2004). The ubiquity and many roles of exopymers in aquatic systems. *Sci. Mar.* 68, 13–21. doi: 10.3989/scimar.2004.68s113

Conflict of Interest Statement: The authors declare that the research was conducted in the absence of any commercial or financial relationships that could be construed as a potential conflict of interest.

The reviewer HO and handling Editor declared their shared affiliation.

Copyright © 2018 Toullec and Moriceau. This is an open-access article distributed under the terms of the Creative Commons Attribution License (CC BY). The use, distribution or reproduction in other forums is permitted, provided the original author(s) and the copyright owner are credited and that the original publication in this journal is cited, in accordance with accepted academic practice. No use, distribution or reproduction is permitted which does not comply with these terms.

frontiers in Marine Science

ORIGINAL RESEARCH
published: 22 March 2018
doi: 10.3389/fmars.2018.00082

Copepods Boost the Production but Reduce the Carbon Export Efficiency by Diatoms

Brivaëla Moriceau[1], Morten H. Iversen[2], Morgane Gallinari[1], Antti-Jussi O. Evertsen[3], Manon Le Goff[1], Beatriz Beker[1], Julia Boutorh[1], Rudolph Corvaisier[1], Nathalie Coffineau[1], Anne Donval[1], Sarah L. C. Giering[4], Marja Koski[5], Christophe Lambert[1], Richard S. Lampitt[4], Alain Le Mercier[1], Annick Masson[1], Herwig Stibor[6], Maria Stockenreiter[6] and Christina L. De La Rocha[1]*

[1] Laboratoire des Sciences de l'environnement Marin (LEMAR) UMR6539 CNRS/UBO/IFREMER/IRD, Université de Bretagne Occidentale, Institut Universitaire Européen de la Mer (IUEM), Technopole Brest-Iroise, Plouzané, France, [2] Alfred Wegener Institute for Polar and Marine Research, MARUM, University of Bremen, Bremen, Germany, [3] Department of Biology, Norwegian University of Science and Technology, Trondheim, Norway, [4] National Oceanography Centre Southampton, Natural Environment Research Council, University of Southampton, Southampton, United Kingdom, [5] Institute for Aquatic Resources (DTU Aqua), Technical University of Denmark, Charlottenlund, Denmark, [6] Biology II, Aquatic Ecology, Ludwig-Maximilians-Universität München, Planegg-Martinsried, Germany

OPEN ACCESS

Edited by:
Eric 'Pieter Achterberg, GEOMAR Helmholtz Centre for Ocean Research Kiel, Germany

Reviewed by:
Jan Taucher, GEOMAR Helmholtz Centre for Ocean Research Kiel, Germany
Javier Arístegui, University of Las Palmas de Gran Canaria, Spain

***Correspondence:**
Brivaëla Moriceau
moriceau@univ-brest.fr

Specialty section:
This article was submitted to Marine Biogeochemistry, a section of the journal Frontiers in Marine Science

Received: *08 August 2017*
Accepted: *26 February 2018*
Published: *22 March 2018*

Citation:
Moriceau B, Iversen MH, Gallinari M, Evertsen A-JO, Le Goff M, Beker B, Boutorh J, Corvaisier R, Coffineau N, Donval A, Giering SLC, Koski M, Lambert C, Lampitt RS, Le Mercier A, Masson A, Stibor H, Stockenreiter M and De La Rocha CL (2018) Copepods Boost the Production but Reduce the Carbon Export Efficiency by Diatoms. Front. Mar. Sci. 5:82. doi: 10.3389/fmars.2018.00082

The fraction of net primary production that is exported from the euphotic zone as sinking particulate organic carbon (POC) varies notably through time and from region to region. Phytoplankton containing biominerals, such as silicified diatoms have long been associated with high export fluxes. However, recent reviews point out that the magnitude of export is not controlled by diatoms alone, but determined by the whole plankton community structure. The combined effect of phytoplankton community composition and zooplankton abundance on export flux dynamics, were explored using a set of 12 large outdoor mesocosms. All mesocosms received a daily addition of minor amounts of nitrate and phosphate, while only 6 mesocosms received silicic acid (dSi). This resulted in a dominance of diatoms and dinoflagellate in the +Si mesocosms and a dominance of dinoflagellate in the −Si mesocosms. Simultaneously, half of the mesocosms had decreased mesozooplankton populations whereas the other half were supplemented with additional zooplankton. In all mesocosms, POC fluxes were positively correlated to Si/C ratios measured in the surface community and additions of dSi globally increased the export fluxes in all treatments highlighting the role of diatoms in C export. The presence of additional copepods resulted in higher standing stocks of POC, most probably through trophic cascades. However it only resulted in higher export fluxes for the −Si mesocosms. In the +Si with copepod addition (+Si +Cops) export was dominated by large diatoms with higher Si/C ratios in sinking material than in standing stocks. During non-bloom situations, the grazing activity of copepods decrease the export efficiency in diatom dominated systems by changing the structure of the phytoplankton community and/or preventing their aggregation. However, in flagellate-dominated system, the copepods increased phytoplankton growth, aggregation and fecal pellet production, with overall higher net export not always visible in term of export efficiency.

Keywords: biogenic silica, POC, marine snow, zooplankton, mesocosm, Bay of Hopavågen, plankton community, biological pump

INTRODUCTION

The export of particulate organic carbon (POC) from the surface ocean, in terms of the overall amount or as the fraction of local net primary production, varies seasonally as well as regionally (Lutz et al., 2002; Boyd and Trull, 2007; Honjo et al., 2008; Buesseler and Boyd, 2009; Lam et al., 2011; Henson et al., 2012; Siegel et al., 2016). Numerous factors intervene in this variability: turbulence, stratification, and mixed layer depth; phytoplankton community composition; the rates, timing, and extent of seasonality of primary production; meso- and microzooplankton abundance and feeding strategies; the aggregation of particulate organic matter (POM) into large, rapidly sinking particles of marine snow; and the occurrence of ballast particles like biogenic silica, calcium carbonate, and dust. The actions and interactions of these factors determine the ocean food web, which either recycles most of the organic matter in the surface ocean (resulting in only minor export to depth) or is "leaky" (exporting a large portion of the net primary production to depth). It is necessary to understand food web interactions in order to predict the biological pump's variability and its ability to sequester CO_2 in a future ocean with warmer temperatures, higher CO_2, more acidity, and differing nutrient inputs and ratios compared to the present ocean (Bopp, 2005; Passow and Carlson, 2012; Alvain et al., 2013; Bopp et al., 2013).

Relationships between food webs, ballast minerals and fluxes have been investigated in various physical regimes. On the smaller scale of such investigations are microcosm studies of sinking particles in rolling tanks (Shanks and Trent, 1980; Passow and De La Rocha, 2006) and flow through systems (Ploug et al., 2008; Long et al., 2015) that allow controlled examination of selected processes and interactions. At the other extreme are regional and global scale studies based on models, remote sensing, and observational data from time-series, cameras, autonomous platforms, and sediment traps (Klaas and Archer, 2002; Honjo et al., 2008; Klaas et al., 2008; Lee et al., 2009; Lam et al., 2011; Assmy et al., 2013; Quéguiner, 2013; Giering et al., 2014; Sanders et al., 2014; Guidi et al., 2016). However, whereas small scale laboratory investigations allow full control over environmental variables and mechanistic investigations, they often lack natural community composition. Field studies allow identification of larger scale patterns and correlations with environmental variables but no clear identification of causal relationships owing to complex confounding factors. Mesocosms offer a middle ground, where some of the control of small scale laboratory experiments is combined with parts of the complexity of environmental variables of field observations. Mesocosms enclose part of an *in situ* water column allowing manipulations of target parameters. Mesocosms are large enough to host a reasonably complex food web (e.g., including micro- and mesozooplankton) (Wassmann et al., 1996; Svensen et al., 2001; Sommer et al., 2004; Stibor et al., 2004; Olsen et al., 2006; Stange et al., 2017) while still allow controlled manipulations of parameters such as nutrients, ballast minerals, turbulence, and phytoplankton and zooplankton community composition.

A small number of mesocosm experiments have been used to study phytoplankton community interactions and POC export. Early work noted a strong link between the addition of silicic acid (in addition to nitrate and phosphate) and POC export fluxes (Wassmann et al., 1996). It was hypothesized that the addition of silicic acid promoted the growth of diatoms, which increased export of POC (Engel et al., 2002; Kemp et al., 2006; Kemp and Villareal, 2013; Rynearson et al., 2013; Lasbleiz et al., 2014). However, later studies showed that artificial mixing of upper water layers also initiated aggregate formation even in the absence of diatoms, suggesting that diatoms (and indirectly silicic acid) were not the sole trigger of high POC fluxes (Svensen et al., 2001, 2002). Several factors could results in high POC export, including phytoplankton aggregation of both diatom and non-diatom phytoplankton and zooplankton grazing, suggesting that the whole plankton community structure - more than just presence of diatoms–is important to determine export fluxes (Gehlen et al., 2006; Guidi et al., 2016).

Generally carbon export follows the seasonality of primary production but is even more dependent on the fraction of slow-sinking versus fast-sinking aggregates, with higher export for fast sinking aggregates (Moriceau et al., 2007; Henson et al., 2015). However, the influence of seasonality and plankton community composition on global export efficiency (proportion of primary production that is transported below the mixed layer depth) is still poorly understood. Except for recent studies on the impact of acidification or elevated CO_2 concentrations (Paul et al., 2015; Bach et al., 2016; Spilling et al., 2016; Gazeau et al., 2017) most mesocosms studies have focused on the processes that lead to export during phytoplankton bloom conditions, even though non-blooming periods can potentially be important for global export fluxes, and can be periods of efficient export of carbon and $bSiO_2$ (Fujii and Chai, 2005; Morris et al., 2007; Lam et al., 2011). Efficient export during non-bloom conditions has been linked to zooplankton abundance, which can repackage small particles into dense, fast-sinking particles (Lalande et al., 2016).

We designed a mesocosm study to investigate the link between plankton composition and export flux during non-blooming conditions. We explicitly tested the impact of zooplankton abundance on export fluxes for two different phytoplankton populations.

MATERIALS AND METHODS

Study Area

The experiment was conducted in 2012, between August 2 and 24 in the Bay of Hopavågen (63° 36′ N, 9° 33′ E), a tidally-driven, semi-enclosed marine lagoon on the west coast of Norway, 20 km west of the outlet of the Trondheimsfjord (**Figure 1**). This semi-enclosed marine lagoon has a maximum depth of 32 m, a volume of roughly 6.7×10^6 m^3, and exchanges roughly 14% of its water daily with the ocean through a narrow inlet (van Marion, 1996).

Nutrient concentrations in the lagoon at the time of the experiment were extremely low ($< 1\,\mu$M for silicic acid, $<0.3\,\mu$M for ammonium, and $<0.1\,\mu$M for nitrate, nitrite, and phosphate). Concentrations of chlorophyll a (Chl) in the upper 10 m of the lagoon at the time of the experiment ranged from 0.5 to 2.4 mg m^{-3}, corresponding well to the typical average summer

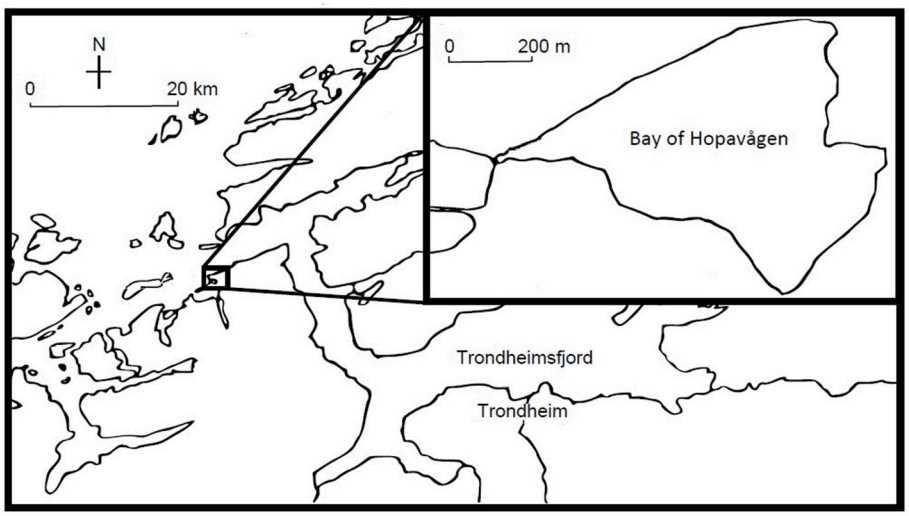

FIGURE 1 | The Bay of Hopavågen.

concentrations for this lagoon (between 1–3 mg m^{-3}, Olsen et al., 2006).

Mesozooplankton commonly found in the Bay of Hopavågen include the ctenophore *Bolinopsis* sp., calanoid copepods (such as *Temora* sp., *Centropages* sp., and *Pseudocalanus* sp.) at an average summer concentration of 20 ind L^{-1}, the cyclopoid copepod *Oithona* sp., and the appendicularian *Okipleura* sp. (van Marion, 1996; Stibor et al., 2004; Vadstein et al., 2004). The phytoplankton community in the lagoon consists of diatoms (e.g., *Rhizosolenia* sp., *Skeletonema* sp., *Thalassiosira* sp., *Nitzschia* sp., and *Pseudonitzschia* sp.), autotrophic picoplankton, dinoflagellates (e.g., *Gymnodinium* sp., *Prorocentrum* sp.), and nanoflagellates (Sommer et al., 2005).

Mesocosms

Each mesocosm consisted of a 10 m deep polyethylene tube, with a diameter of approximately 1 m, a volume of roughly 9 m^3, and a sealed, conical bottom. The twelve mesocosms were filled on August 2 by lowering the entire mesocosm bag to a depth of 10 m and then raising the top gently back up to the surface. The filled mesocosms were secured to a raft that was anchored in the deepest part of the Bay of Hopavågen.

The light conditions in each mesocosm were similar, with light intensities of 15–20% of surface light at 1 m depth (generally around 100 μmol m^{-2} s^{-1}) and ∼1% at ∼6 m depth (**Figure 2**). These conditions were similar to the light intensities observed in the Bay of Hopavågen (around the mesocosms) during the experiment (∼40% ∼300 μmol m^{-2} s^{-1} at 1 m and 8% at 6 m).

To avoid disturbances of formed aggregates within the mesocosms and to avoid interfering with sinking fluxes, the mesocosms were not mixed during the experiment. However, some small-scale mixing and turbulence might have occurred within the mesocosms due to waves and tidal currents within the Bay of Hopavågen during the study. According to the Chl profiles, the upper 2 m of the mesocosm bags were well-mixed (**Figure 2**). Turbulence was not measured during the experiment, but previous work in similar types of mesocosms suggested that the energy dissipation rates in the mesocosms would have been on the order of 10^{-9}–10^{-8} m^2 s^{-3}, corresponding to a wind velocity of 3–6 m s^{-1} (Svensen et al., 2001).

In the Bay of Hopavågen, nutrients are resupplied daily by the natural water inflow (Sommer et al., 2004). We mimicked the natural nutrient input by manually adding nutrient to the enclosed mesocosms, using nitrogen concentrations that compensated for the loss of N caused by sedimentation and Redfield ratios for phosphorus and silicon additions as described in previous studies (Sommer et al., 2005; Olsen et al., 2006). Such nutrients additions maintained the low natural phytoplankton concentrations yet avoided accumulation of unrealistically high concentrations of phytoplankton biomass (Børsheim et al., 2005).

Twelve mesocosms were set up in total, allowing the investigation of four different treatments in triplicate. The treatments were (1) silicate addition and decreased copepod abundance (+Si −Cops), (2) silicate addition and increased copepod abundance (+Si +Cops), (3) no silicate addition and decreased copepod abundance (−Si −Cops), (4) no silicate addition and increased copepod abundance (−Si +Cops). Nutrients were added via an 8-m long tube. The tube was lowered slowly to a depth of 8 m in each mesocosm and then fully filled with a nutrient solution calculated to add the required concentration of nutrients to each mesocosm. The tube was then slowly lifted out to minimize disturbances of the water in the mesocosms. Through the process of displacement, this allowed the nutrients to distribute evenly throughout the water column of the mesocosms (Olsen et al., 2007). Nutrients uptake are lower in the dark (Dortch and Maske, 1982; Litchman et al., 2004) and samplings were done in the morning. Nutrients were added in the evening to avoid contamination of the morning sampling, and began the day after the bags were filled (on the evening of August 3) and 4.5 days before the first day of sampling. Previous

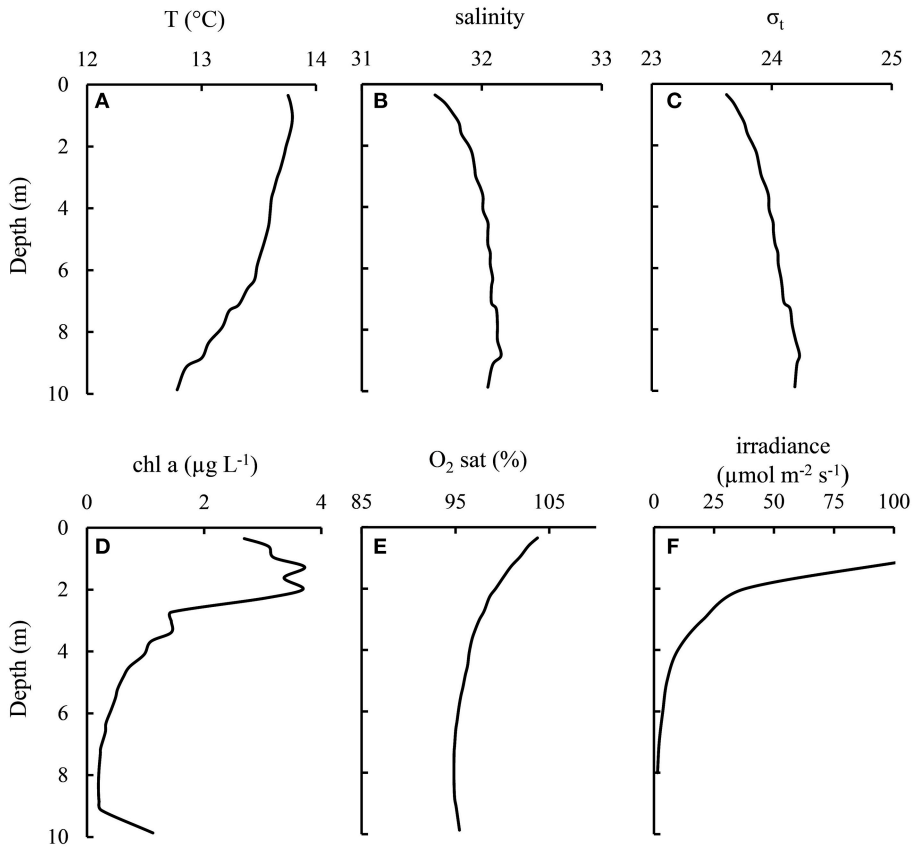

FIGURE 2 | Typical physical conditions within the mesocosms as exemplified by bag 3 (+Si −Cops) on August 23–24 (experiment Days 16–17).

study evidenced that such a time lag allows the phytoplankton communities to differentiate depending on nutrient additions (Gismervik et al., 2002; Sommer et al., 2004; Larsen et al., 2015).

Following Stibor et al. (2004), mesozooplankton concentrations were reduced in the −Cops treatments by repeated vertical hauls with a 150-µm plankton net (Sommer et al., 2004; Stibor et al., 2004). We refer to these mesocosm as '+Si −Cops' and '−Si −Cops', respectively. In the evening of August 7 (5 days after the filling of the bags and 1 day before the first sampling day), we increased the copepod abundance in the +Cops treatments by adding copepods (4 copepods per liter), mainly *Centropages* sp. and *Oithona* sp., collected from the lagoon using a 150-µm plankton net.

Sample Collection and Analysis

Day 1 of the sampling was on the morning of August 8, 5.5 days after filling the bag and 4.5 days after the first nutrient addition. The sampling period lasted 17 days in total. On Days 1, 3, 6, 10, 13 and 16 of the sampling period, depth-integrated samples of the upper 4.5 m of the mesocosms were collected between 7:00 and 8:00 in the morning. Sampling was done by repeated and slow deployments of a 1 m long integrated water sampler. We collected a total of 12-20 L from each mesocosm (0.1–0.2% of initial water volume), depending on the sampling strategy of the day. Water samples were placed in opaque 20 L LDPE carboys (Nalgene), which were subsampled for total and fractionated particulate organic carbon (POC) and nitrogen (PON), biogenic silica ($bSiO_2$), pigments, nutrients, phytoplankton cell counts, and microscopic taxonomy of phytoplankton.

Sinking particles were collected with sediment traps from 8 m depth three times during the course of the experiment, from Day 3 to Day 8, from Day 9 to Day 12, and from Day 14 to Day 17. This was done with cylindrical sediment traps with an aspect ratio (height to width) of 6 in mesocosms in two of each treatment triplicate. In the four remaining mesocosms (one of each treatment triplicate), we deployed gel traps (McDonnell and Buesseler, 2010) at 8 m to collect and preserve the size and structure of the sinking particles. The gel traps were only deployed for 2 days in order to avoid individual particles landing on top of each other in the gel. Gel traps were deployed on Day 3, 8, and 14.

Phytoplankton community compositions were determined for one of each treatment triplicates (four mesosocosms in total) four times during the sampling period. Water samples were preserved with Lugol's iodine (1% final concentration) and taxonomically identified to species level using an inverted microscope (Utermöhl, 1958).

Samples for particulate organic carbon (POC) and for particulate organic nitrogen (PON) were filtered onto precombusted (450°C, 5 h) 25-mm GF/F filters (0.7-μm nominal pore size, Whatman). Every second sampling day, POC/PON samples were size fractionated before filtration using different screens. Size fractions were 0.7–2.7, 2.7–20, 20–44, 44–100, and >100 μm. Filters were rinsed with MilliQ water to remove salts and dried overnight at 60°C. Inorganic carbon was removed from the filters by fuming with HCl before analysis with a Flash 1112 Series elemental CN analyzer (ThermoQuest).

Samples for Chl a were filtered onto GF/F filters (0.7-μm nominal pore size, Whatman) and immediately frozen in liquid nitrogen. The filters were stored at −80°C until analysis by HPLC (Shimadzu LC-10A HPLC system with LC Solution software; Shimadzu). The HPLC system was calibrated with pigment standards (DHI Water and Environment).

Samples for biogenic silica ($bSiO_2$) were filtered onto 0.4-μm polycarbonate filters (Millipore), dried overnight at 60°C and stored at room temperature until digestion and analysis. $bSiO_2$ in the samples was dissolved in 0.2 M NaOH at 100°C for 60 min (Ragueneau et al., 2005) and neutralized with 1 M HCl for silicic acid analysis by colorimetry. Particulate $bSiO_2$ concentrations were corrected for lithogenic contribution following a second digestion of the particulate matter to yield the Si:Al ratio of the lithogenic silica (Ragueneau et al., 2005). Aluminum was determined via inductively coupled plasma optical emissions spectroscopy (ICP-OES).

Samples for nitrate, nitrite, silicic acid, phosphate and ammonium were filtered through 0.4-μm polycarbonate filters (Millipore) and analyzed using a Bran+Luebbe AAIII auto-analyzer. Concentrations of ammonium in water samples were measured manually on a spectrophotometer (Shimatzu UV 1700) following Koroleff (1969).

Statistical Analysis

To test and differentiate the effect of time from the effect of the different treatments: +Si vs. −Si and +Cops vs. −Cops, a two-way or three-way analysis of variance (ANOVA) with a multiple comparison procedure (Holm-Sidak method) were applied to our data set (Sigmaplot 12, Systat Software, Inc.,) except for sediment traps data for which only two replicates were done. The overall significance level was chosen as $p < 0.05$.

RESULTS

Nutrient Concentrations and Uptake

At the beginning of the sampling period, phosphate concentrations were lower in the +Si mesocosms than in the −Si mesocosms (0.02 ± 0.02 μM vs. 0.06 ± 0.03 μM). Phosphate concentrations in the mesocosms increased during the first 10 days of the experiment. After Day 10, however, concentrations of phosphate decreased in all but the +Si +Cops mesocosms (**Figure 3A**). The total net phosphate uptake during the sampling period (**Figure 4A**, **Table 1**) in the −Si −Cops mesocosms (0.11 ± 0.02 μM) was lower than in the other three treatments (+Si −Cops: 0.17 ± 0.04 μM; +Si +Cops: 0.16 ± 0.04 μM; −Si +Cops: 0.18 ± 0.01 μM).

Concentrations of silicic acid (dSi) in the −Si treatments remained close to zero throughout the experiment (**Figure 3B**), suggesting no measureable net dSi uptake in these mesocosms. In the +Si mesocosms, there was no dSi uptake between Days 6 and 10, with net dSi uptake between Day 1 and 6 and between Day 10 and 16 (**Figure 4C**). The total net dSi utilization in the mesocosms during the sampling period was 1.4 ± 1.0 μM (+Si −Cops), 2.5 ± 0.9 μM (+Si +Cops), 0.0 ± 0.1 μM (−Si −Cops), and −0.1 ± 0.1 μM (−Si +Cops) (**Table 1**).

Continuously increasing cumulative net utilization of DIN in the +Si mesocosms resulted in lower concentrations compared to −Si mesocosms (**Figures 3F**, **4E**, **Table 1**). In addition to the daily external input of nitrate of 0.22 μM, we observed DIN production likely caused by ammonium regeneration within the mesocosms. This was evident from the mid-experiment peak in ammonium concentrations in all mesocosms (**Figure 3E**). Following Day 10, however, ammonium concentrations decreased, except in +Si +Cops, were the decrease started at Day 13, suggesting that uptake exceeded regeneration in all mesocosms in the final days of the experiment. During the same period, nitrate, nitrite and overall DIN concentrations declined (**Figures 3C,D**), suggesting increased rates of DIN uptake rather than a decrease in the rates of ammonium regeneration (n.b. over the 17 day duration of the experiment, we would not expect to see notable amounts of nitrate being regenerated).

In the +Si mesocosms, net removal rates of DIN were, on average, 2–3 times faster than net removal rates of dSi (**Table 1**). Since dSi removal rates were undetectable in the −Si mesocosms, we could not calculate a net uptake ratio of DIN to dSi for these mesocosms. DIN to phosphate uptake ratios remained reasonably close to Redfield values of 16:1 in most of the mesocosms (**Table 1**).

Standing Stocks and Phytoplankton Composition

Integrated standing stocks of POC (upper 4.5 m) decreased during the first days of the experiments and stabilized after Day 3 for +Cops mesocosms and after Day 6 for −Cops mesocosms (**Figure 5A**). The mean POC concentrations over the experimental period were 18.5 ± 6.4 μmol POC L^{-1} in the +Si −Cops, 24.7 ± 7.7 μmol POC L^{-1} for the +Si +Cops, 14.4 ± 4.9 μmol POC L^{-1} for the −Si −Cops and 21.0 ± 4.1 μmol POC L^{-1} for the −Si +Cops treatments, with values ranging from 10 to 37 μmol POC L^{-1}. Average POC concentrations were similar to those measured in the lagoon at the end of the experiment (19.5 μmol POC L^{-1}; **Figure 5A**) and to those obtain at similar nutrient additions in Børsheim et al. (2005). Standing stocks of POC in the upper 4.5 m of the mesocosms differed more between treatments than between the replicates for each individual treatments or for each replicate over time (two way ANOVA $\alpha = 0.01$; $p < 0.001$). POC standing stocks were higher in +Si mesocosms than in the other treatments at the beginning of the sampling period. Differences in POC standing stocks decreased over time. POC standing stocks were similar for +Cops and −Cops treatments until Day 3, but started to differ

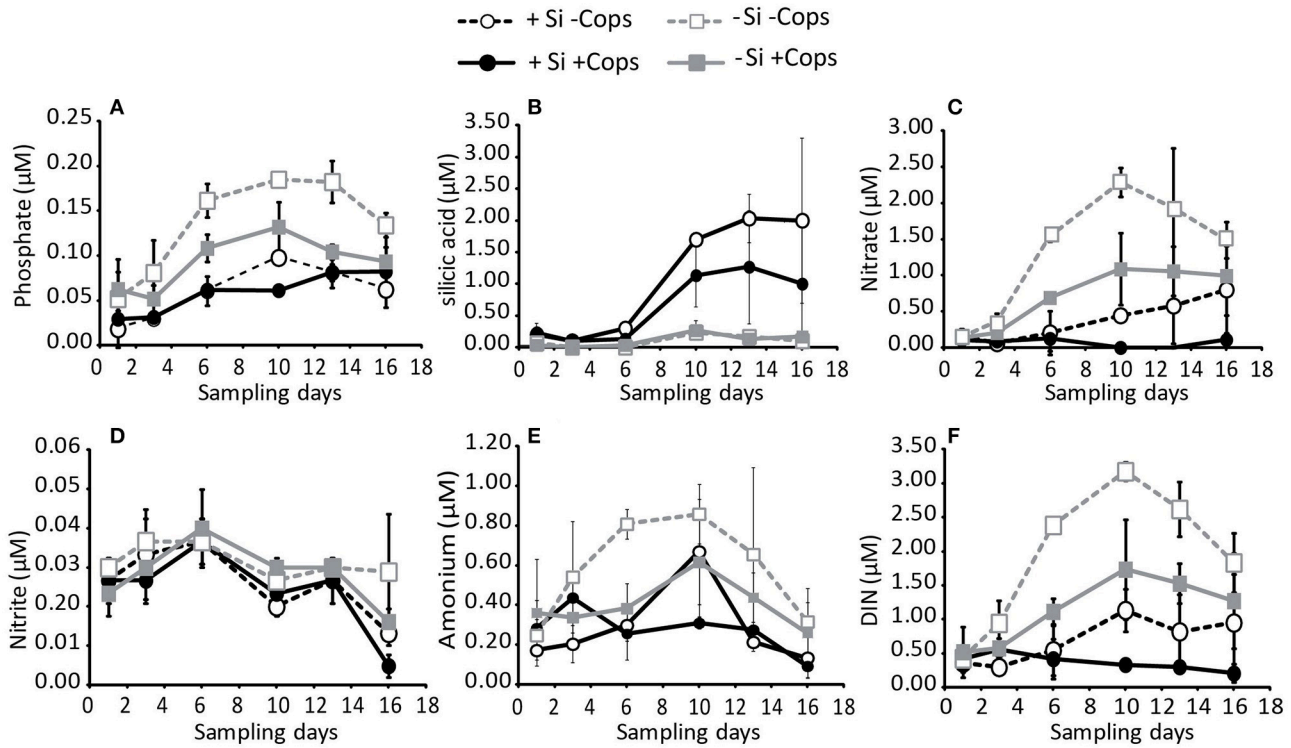

FIGURE 3 | Concentrations in the upper 4.5 m of the nutrients **(A)** phosphate, **(B)** silicate, **(C)** nitrate, **(D)** nitrite, **(E)** ammonium, and **(F)** total DIN. Data points and error bars represent averages and standard deviations for the three mesocosms of each treatment.

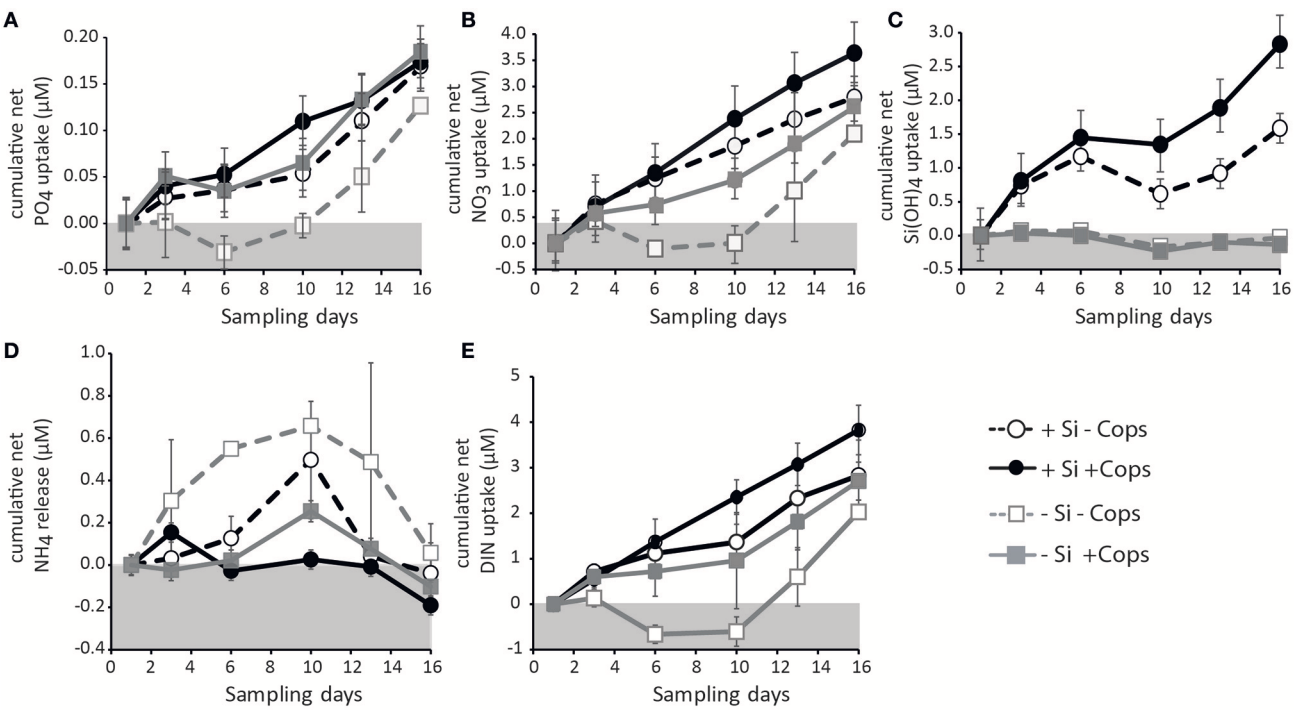

FIGURE 4 | Cumulative net uptake in the different mesocosm treatments of **(A)** phosphate, **(B)** nitrate, **(C)** silicate, and **(E)** total DIN. **(D)** show the cumulative net regeneration of ammonium. Data points and error bars represent averages and standard deviations for the three mesocosms of each treatment.

TABLE 1 | Total net nutrient removal during the experiment, ratios between removal, and average number of species during the duration of the experiment.

Mesocosms	Total net removal			Ratios of total net removal		Average number of species		
	PO4	DIN	Si(OH)4	DIN/Si	DIN/P	total	Diatoms	Dinoflagellates
+Si −Cops	0,17	2,8	1,4	2,0	16,6	13	4	8
+Si +Cops	0,16	3,8	2,5	1,5	23,9	19	4	12
−Si −Cops	0,11	2,0	0	-	18,5	11	2	8
−Si +Cops	0,18	2,7	−0,1	-	15,1	16	2	12

after Day 6, with more POC present in the +Cops mesocosms. Over the whole sampling period, POC concentrations were significantly higher in the six mesocosms that had received a supplement of copepods compared to those where copepods had been removed (Three way ANOVA; $p<0.001$). We also observed significantly higher POC concentrations in +Si −Cops compared to −Si −Cops and in +Si +Cops compared to −Si +Cops (Three way ANOVA; $p = 0.006$).

On the last sampling day (Day 16), the +Si +Cops mesocosms reached an average standing stock of POC of 25.3 ± 0.9 μmol POC L^{-1} and the −Si +Cops mesocosms an average of 23.6 ± 2.4 μmol POC L^{-1} compared to 17.6 ± 2.6 μmol POC L^{-1} and 15.6 ± 0.7 μmol POC L^{-1} in the +Si +Cops and −Si −Cops mesocosms, respectively.

Concentrations of total PON were also relatively stable during the experiment with significant differences between +Cops and −Cops mesocosms. However, unlike POC standing stocks, differences between +Si +Cops and −Si +Cops or +Si −Cops and −Si −Cops treatments were not significant (**Figure 5B**). C to N ratios (C/N) of the organic matter in the upper 4.5 m of the +Si mesocosms decreased from 6.7 ± 0.8 mol mol^{-1} on Day 1 to 4.4 ± 0.5 mol mol^{-1} on Day 6 and remained close to that for the rest of the experiment. The C/N of the −Si mesocosms averaged 4.4 ± 0.3 mol mol^{-1} during the experiment. The C/N ratios of the standing stocks were very similar between treatments with an average for the entire experiment of 4.7 ± 0.8 mol mol^{-1} (**Figure 5C**).

Concentrations of Chl a ranged from 0.5 to a maximum of 4.7 μg L^{-1} (**Figure 5D**). Chl a concentrations were generally within the range for non-bloom conditions, in accordance with the nutrient addition (Børsheim et al., 2005). Standing stocks of Chl a decreased rapidly in the +Si mesocosms, from 3.0 ± 0.5 and 4.2 ± 0.4 μg/L on Day 1 for the +Cops and −Cops respectively, to 0.6 ± 0.2 and 0.7 ± 0.2 μg/L on Day 6. After Day 6, Chl a increased until the end of the experiment to reach 2.3 ± 0.4 μg/L in +Si +Cops and 1.1 ± 0.6 μg/L in the +Si −Cops. Except for the first day of the sampling period, Chl a concentrations were higher in the +Cops mesocosms (three way ANOVA; $p < 0.001$; **Figure 5D**). The −Si −Cops mesocosms also experienced a decrease from Day 1 to Day 6 (1.9 ± 0.2 μg/L to 0.5 ± 0.1 μg/L), before increasing to 0.9 ± 0.4 μg/L at the end. The −Si +Cops mesocosms Chl a concentrations was less variable. Chl a concentrations slightly decreased from 2.2 μg/L on Day 1 to 1.4 ± 0.4 μg/L at the end. The final average concentrations of Chl a in the −Si +Cops mesocosms were lower than those in the +Si +Cops (1.4 ± 0.4 μg L^{-1} vs. 2.3 ± 0.4 μg/L, respectively, on Day 16), but they were still ∼30% greater than the average final concentrations in the +Si −Cops and −Si −Cops (1.1 ± 0.6 and 0.9 ± 0.4 μg L^{-1}, respectively).

Integrated concentrations of $bSiO_2$ in the upper 4.5 m of the −Si mesocosms, decreased to 0 and 0.1 μmol/L for −Cops and +Cops at Day 6 respectively. At the beginning of the sampling period, $bSiO_2$ concentrations were 0.8 ± 0.1 μmol/L and 0.7 ± 0.1 μmol/L for the −Cops and +Cops respectively. In the +Si mesocosms, $bSiO_2$ concentrations generally increased from Day 1 to Day 3 and then declined until Day 10 before increasing again until the end of the experiment (**Figure 5E**). At the end of the experiment, the $bSiO_2$ integrated concentrations in the upper 4.5 m of the +Si +Cops mesocosms, averaged 1.6 ± 0.6 μmol L^{-1}, which was roughly 3-fold higher than that measured in the +Si −Cops mesocosms (0.5 ± 0.6 μmol L^{-1}). The molar Si to POC ratios (Si/C) of standing stocks mirrored the changes in $bSiO_2$ concentrations rather than reflecting overall patterns in the POC standing stocks (**Figure 5F**). Outside the mesocosms, Si/C ratios were around 0.015, which is similar to the lowest ratios reported for North Atlantic Waters (Ragueneau et al., 2002). The +Si mesocosms had Si/C ratios of 0.04–0.10, similar to global ocean average (0.04–0.25, Ragueneau et al., 2002). The Si/N ratios in the nutrient stocks of +Si treatments were higher than 1, the average Si/N utilization in the +Si mesocosms was around 1 with fluctuations from 0.6 and 2.1.

POC standing stocks and Chl a concentrations were both high at the beginning of the experiments especially in the +Si mesocosms. Chl a estimated from CTD measurements 2 days before the beginning of the sampling period gave an average value of 2 mg/L. The daily uptake rate estimated from the total nutrient additions were also lower than the first uptake calculated during the experiment (0.2 vs. 0.3 μM/days for nitrate, 0.004 μM/days vs. 0.02 μM/days for phosphate and 0.3 vs. 0.3 μM/days for silicate), suggesting that no phytoplankton bloom had developed before the sampling period. Throughout the entire experiment, and in all treatments, 30–50% of the total biomass was in the 2.7–20 μm size fractions, while the other four size-fractions (0.7–2.7 μm, 20–44 μm, 44–100 μm, and > 100 μm) each had between 10 and 20% of the total biomass.

Taxonomic analysis confirmed that differing nutrient additions induced changes in phytoplankton population, with diatoms and flagellates dominating the +Si treatments, and flagellates alone dominating the −Si treatments (**Figure 6**). We identified up to 43 phytoplankton species in the +Si +Cops mesocosms with an average of 19 over the entire sampling period (**Table 1**). By contrast, a maximum of 23 species were

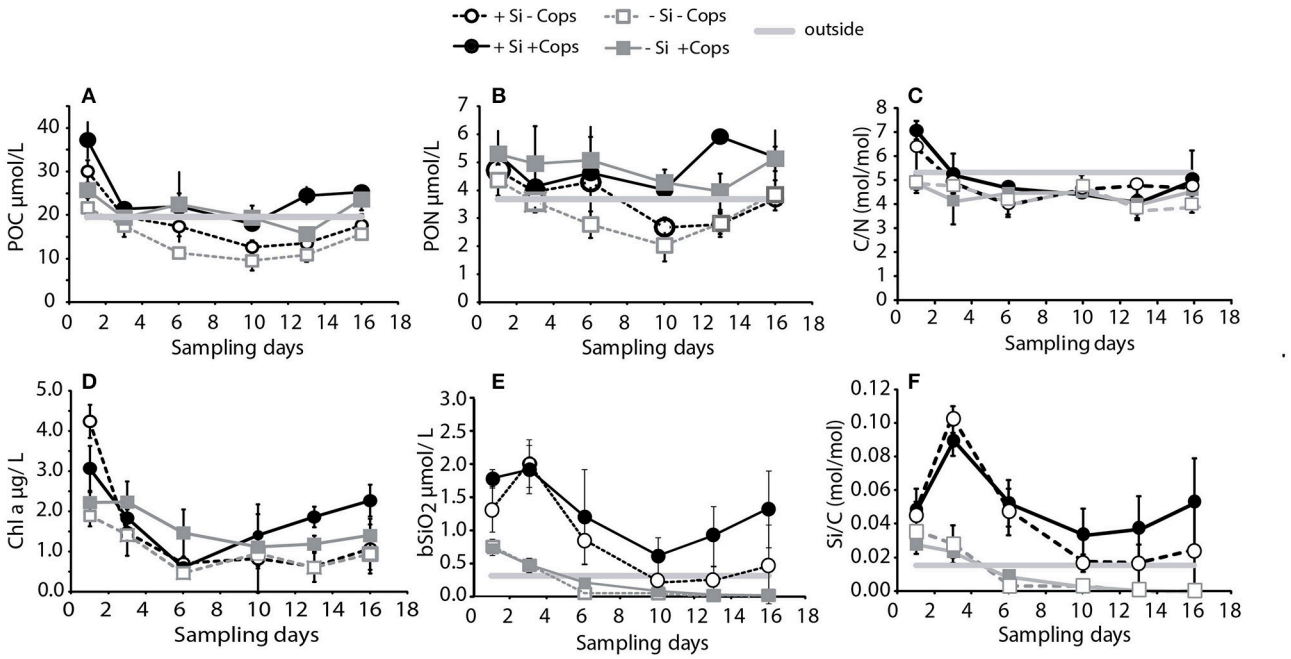

FIGURE 5 | Composition of standing stocks of biomass in the upper 4.5 m of the four treatments: **(A)** POC, **(B)** PON, **(C)** C/N, **(D)** chlorophyll a, **(E)** bSiO2, and **(F)** Si/C. Data points and error bars represent averages and standard deviations for the three mesocosms of each treatment. Gray lines represent concentrations in the Bay outside mesocosms as measured at the end of the experiment (Day 16).

found in the +Si −Cops, with an average of 13. For the −Si mesocosms, the maximum number of species in +Cops and −Cops treatments was 24 and 17, respectively, with an average total amount of species of 16 and 11 for −Si +Cops and −Si −Cops treatments, respectively. In the +Si +Cops treatments, diatom concentrations decreased from Day 3 to Day 10, after which their abundance increased (**Figure 6**). At Day 13, diatoms concentrations were much lower in the +Si mesocosms. This result was not mirrored by standing stock measurement of $bSiO_2$ concentrations or by total cell concentrations according to cytometry. This sudden change of diatom concentrations may therefore potentially be due to analytical problems with phytoplankton enumeration at this sampling day.

In the +Si treatments, 97% of the diatom populations were constituted by small species (cell volume $< 2500\ \mu m^3$) until Day 6. *Skeletonema marinoii* (diameter ∼10 µm) dominate all treatments until Day 3 and disappeared from −Si mesocosms thereafter. From Day 13 the diatom population of the +Si −Cops treatments switched from small *S. marinoii* to medium sized-diatoms, with *Cylindrotheca closterium* (50 to 125 µm length) forming most of the population in +Si −Cops while *Leptocylindrus danicus* constituted more than 90% of the +Si +Cops diatom population. The +Si treatments also developed a large population of dinoflagellates, with the *Gymnodinium* sp. dominating the dinoflagellates population, except for the +Si −Cops after Day 6 when *Scripsiella* contribute for more than 50% to the dinoflagellates population.

Dinoflagellates dominated the −Si treatments from Day 3 until the end of the experiments, with *Gymnodinium* sp. and *Scrippsiella* (*trochoida* and *sweenea*) making up 60 to 95% of the total dinoflagellates community in terms of cell abundance. *Gymnodinium* sp. dominate the community before Day 6 and *Scrippsiella* after.

Sinking Fluxes

Gel traps showed that sinking particles mostly consisted of fecal pellets and large aggregates such as marine snow. During the first trap deployment the +Si −Cops mesocosms particle fluxes were characterized by a higher contribution of marine snow and fewer fecal pellets than the +Si +Cops treatments. The flux composition between these two treatments became more similar toward the end of the study. At the end of the study, particle fluxes in the +Si treatments where characterized by more marine snow aggregates than the −Si that had a much higher contribution by fecal pellets (**Figure 7**). Sinking fluxes of POC, PON, and $bSiO_2$ decreased over time (**Figure 7**), not mirroring standing stocks in the upper 4.5 m of the mesocosms (**Figure 5**). The total POC exported during the experiment was 1.47 ± 0.30 g of C m^{-2} in the +Si −Cops, 1.05 ± 0.28 g of C m^{-2} in the +Si +Cops, 0.78 ± 0.10 g of C m^{-2} in the −Si −Cops and 0.86 ± 0.24 g of C m^{-2} in the −Si +Cops (**Figure 8**). The C/N ratio of the material sinking into sediment traps was higher than the C/N ratios found in the suspended particles with more variability between traps than between treatments (C/N in standing stocks $= 4.5 \pm 0.6$; C/N in sinking particles $= 7.6 \pm 2.0$). The difference between C/N in sediment traps and standing stocks was very pronounced in the −Si −Cops at the end of the experiment, when flux C/N ratios value reached an average of 10.6 ± 5.

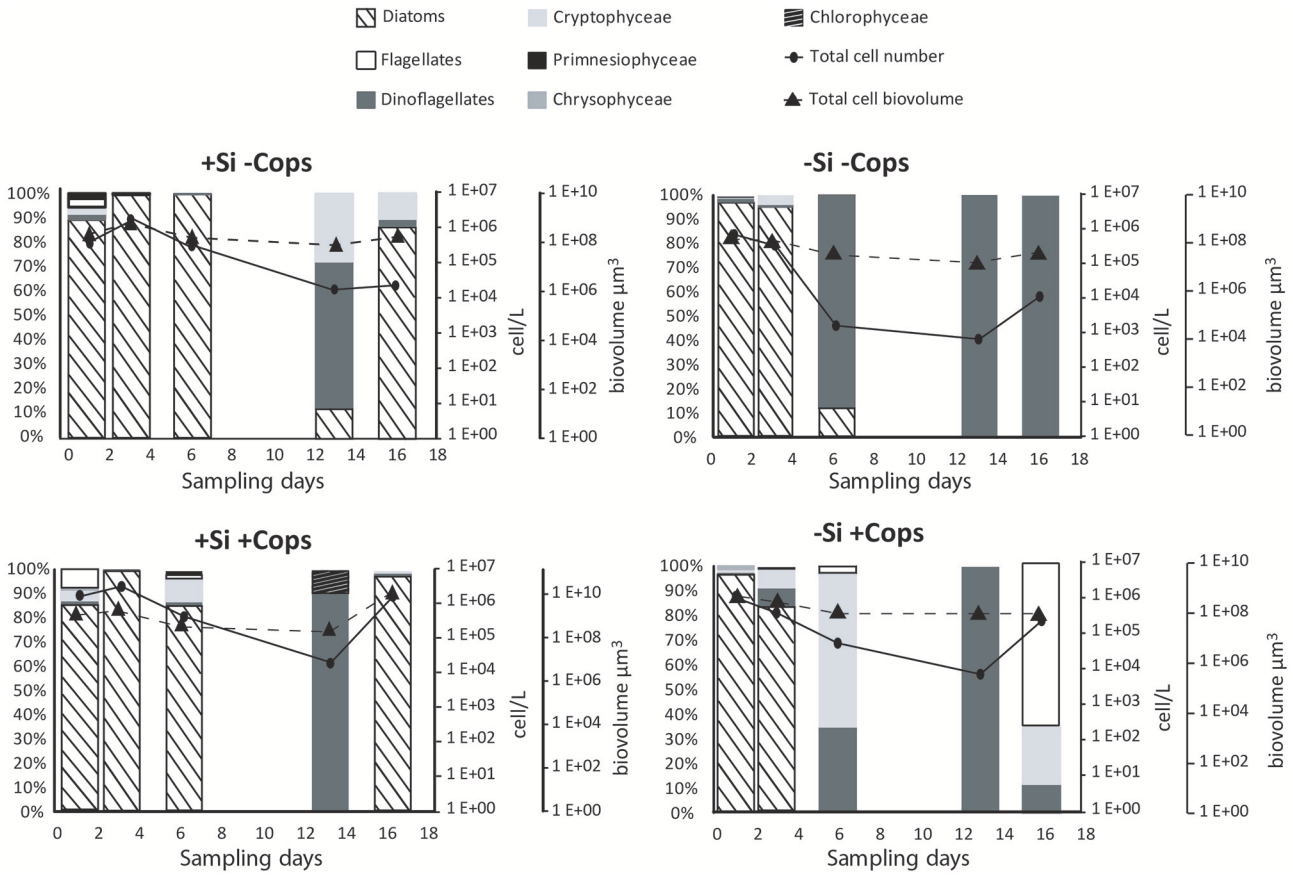

FIGURE 6 | Phytoplankton community structure in the different mesocosm treatments, in percentage, total cell numbers and biovolume.

The ratios of $bSiO_2$ to POC of sinking particles (Si/C) were twice those measured in suspended particles (**Figure 8**). This difference increased with elevated copepod abudances. Despite the lack of measurable $bSiO_2$ in the suspended particles after day 6, Si/C ratios for the sinking material were still 0.02 in the −Si mesocosms and some diatoms were observed in the sediment traps. The POC fluxes were positively correlated to the Si/C ratios of the standing stocks (**Figure 9**). Only the sinking material of the traps set up at day 8 and 16 were analyzed for the phytoplankton taxonomy. Small diatoms formed 96 to 100% of the diatom fluxes collected in all traps except at the end of the experiment. In the +Si −Cops the medium sized (<125 µm) *Cylindrotheca closterium* formed 60% of the diatom cell numbers found in the sediment traps. The contribution of *Proboscia alata* increased in the +Si +Cops to achieve half of the sinking at the end.

DISCUSSION

Diatoms with their ballasted frustule (Armstrong et al., 2002; François et al., 2002) have long been recognized to be efficient for downward transport of matter (Smetacek, 1985; Nelson et al., 1995; Sarmiento et al., 2004). Recent studies are challenging this belief highlighting rather potential links between export and the structure of the whole plankton community (Henson et al., 2012; Lima et al., 2014; Guidi et al., 2016). Additionally a combination of poorly understood processes, such as gravitational settling as aggregates or fecal pellets, physical transport of particulate and dissolved organic matter, or zooplankton disaggregation or migration may also contribute substantially to downward transport of matter (Sanders et al., 2014; Turner, 2015; Siegel et al., 2016).

Impact of Phytoplankton Community Structure

Daily addition of small amount of dSi triggered the growth of diatoms in the +Si mesocosms and globally increased POC fluxes (**Figure 8**), with however, 50 to 100-fold less carbon exported per unit dSi in our non-blooming situation compared to similar bloom simulating experiment (Wassmann et al., 1996). All treatments showed strong positive correlations between the POC fluxes and the Si to POC ratios of suspended material in the upper 5 m of the mesocoms (**Figure 9**) suggesting that the magnitude of POC export was first driven by the presence of diatoms. This is supported by the high POC flux in the +Si −Cops at Day 6 (**Figure 7**) and by the high export efficiency in the +Si −Cops mesocosms, in terms

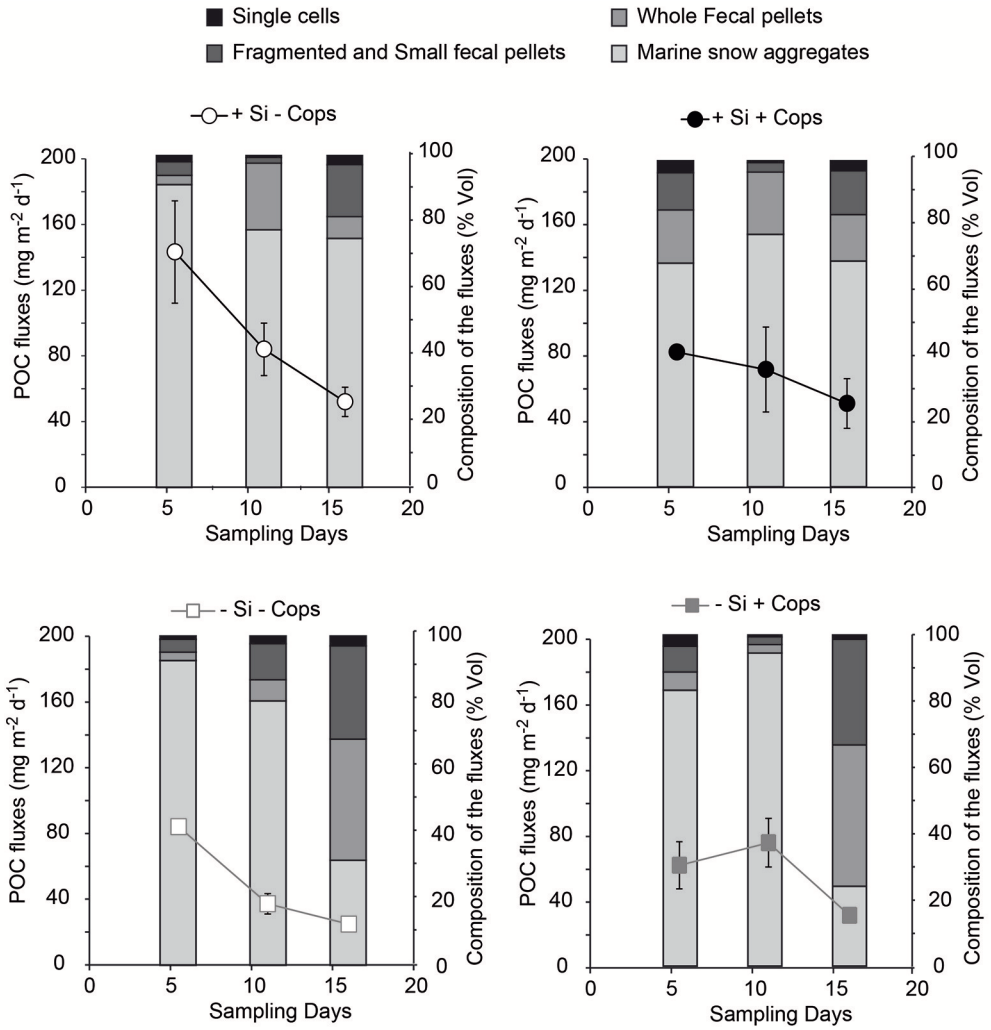

FIGURE 7 | Composition of the particle fluxes in the four treatments, measured from images of gel traps and POC fluxes in sediment traps.

of the amount of POC produced reaching the sediment traps (**Figure 10**). Globally, POC flux intensities follow the aggregate contribution to the flux, with downward trend when the aggregate contribution to fluxes decrease (**Figure 7**). On the +Si mesocosms the aggregate contribution was slightly lower than the average aggregate contributions in the flux of the −Si mesocosms at Day 6 and 11, when *Gymnodinium* sp. dominate the phytoplankton population. However, when aggregate contribution to the flux is similarly high such as seen at Day 6 for +Si −Cops and −Si −Cops, the flux is almost twice as high in the diatom dominated treatment compared to −Si treatments. Aggregation capacity is not restricted to diatom species (Cataletto et al., 1996), but diatom aggregates transport more carbon than non-ballasted aggregates due to higher density and sinking rates (Long et al., 2015). However, even for non-diatom species, decreased aggregation involved lower fluxes as seen at the end of the experiment in −Si mesocosms in association to the growth of *Scrippsiela* sp..

Aggregate contribution to the fluxes stay around 82% in the +Si −Cops, where the aggregating species *Skeletonema marinoii,* and *Pseudonitzschia sp* and *Cylindroteca closterium* prevailed (Cataletto et al., 1996). In the +Si +Cops the aggregating *S. marinoii* constituted most of the diatom population at the beginning of the sampling period. The non-aggregating *Leptocylindrus danicus* (Cataletto et al., 1996) that dominate diatom population at the end were not visible in the sediment traps where the aggregates still formed 70% of the particles collected. Instead the large non-aggregating *Proboscia alata* and the small aggregating *S. marinoii* were majoritary in the sediment traps confirming that size may be also an important factor, together with ballast and aggregation capacity for an efficient carbon export.

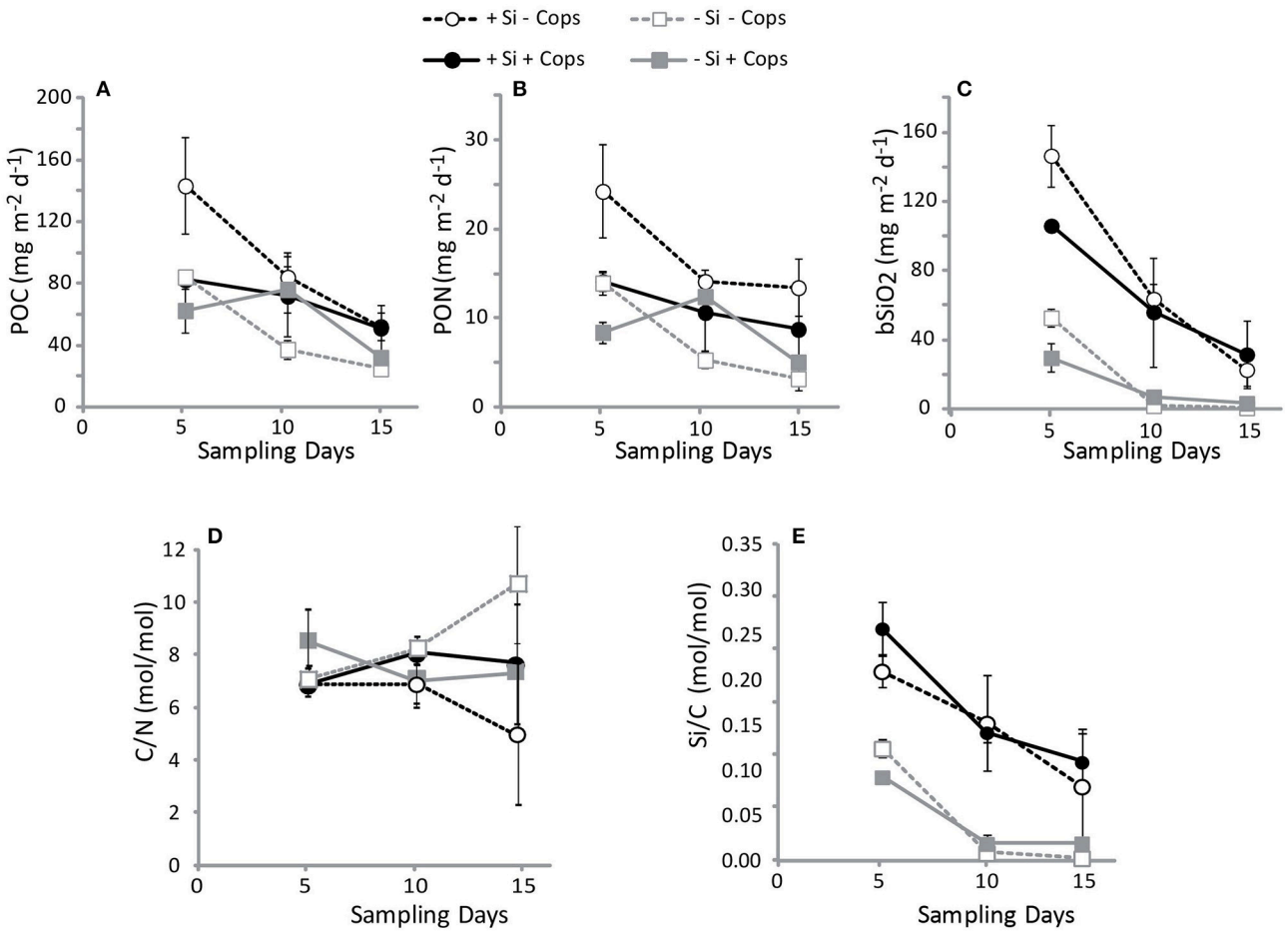

FIGURE 8 | Flux of material into the sediment traps and its elemental composition averaged for each mesocosm treatment. **(A)** POC, **(B)** PON, **(C)** $bSiO_2$, **(D)** the C/N of the sinking flux, and **(E)** the Si/C of the sinking flux.

The Importance of Zooplankton Abundance to POC Flux

The global role of zooplankton for POC export is difficult to quantify since zooplankton indirectly influence export by changing the structure of the phytoplankton community, from small to larger species as seen in the previous paragraph and in other study (Quéguiner, 2013). Moreover, zooplankton activity may both (1) increase POC fluxes by converting slow-sinking single cells into fast-sinking fecal pellets and (2) reduce the flux by fragmenting large aggregates into small particle with slow sinking velocities and high degradation in the surface ocean (Iversen and Poulsen, 2007; Giering et al., 2014; Sanders et al., 2014). In our mesocosm study, higher copepod concentrations resulted in higher standing stock of phytoplankton (**Figure 4**) and in higher phytoplankton diversity (**Table 1**). The flagellate diversity appeared to be mainly driven by the copepod presence. Diatom diversity was more influenced by the silicic acid addition but the dominant species change depending on the copepod abundances (**Table 1**). Higher phosphate and nitrate uptake in the +Cops treatments compared to the −Cops treatments (**Figure 4**), suggest that the phytoplankton community benefitted from the presence of mesozooplankton. Such a counter-intuitive influence of meso-zooplankton addition on phytoplankton growth has already been observed in other studies (Sommer et al., 2001, 2004, 2005). The silicate uptake also increased with copepods addition (**Figure 4**). This could be explained by the change of diatoms community toward more silicified species (Assmy et al., 2013; Quéguiner, 2013), or by the increase of diatom silicification in the presence of grazers (Pondaven et al., 2007). Grazers feeding activity may also increase the remineralization of the dead diatom frustules (Schultes et al., 2010). Such an effect would benefit diatom growth but couldn't be seen in our study because we only measured the net uptake. Moreover, the trophic connections are much more complex than only copepods and prey. Additionally, trophic cascades can explain the increased phytoplankton biomass in the +Cops mesocosms (Gismervik et al., 2002; Sommer et al., 2004; Stibor et al., 2004). Copepods may partially feed on microzooplankton. The grazing pressure of micro-zooplankton on phytoplankton would then be reduced as observed in previous mesocosm experiments (Gismervik

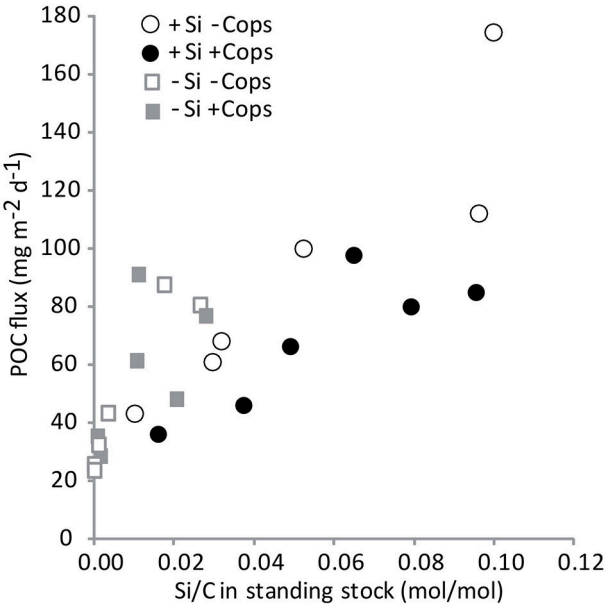

FIGURE 9 | POC fluxes versus Si/C ratios in the standing stocks in the upper 4.5 m.

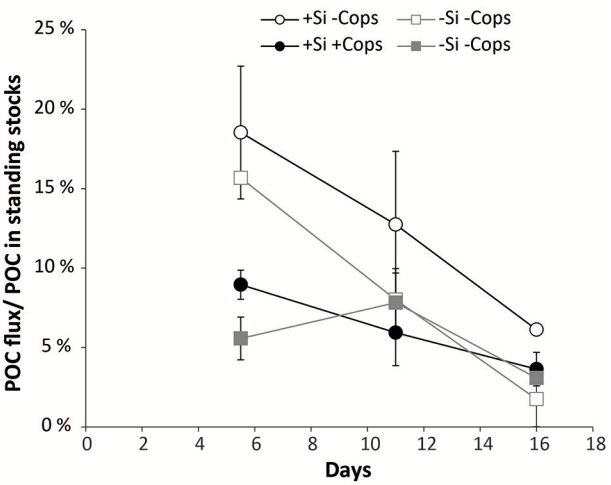

FIGURE 10 | Export efficiency: proportion of the POC produced in the surface layer, collected in the sediment traps versus time for the four treatments +Si −Cops, +Si +Cops, −Si −Cops and −Si −Cops.

et al., 2002; Stibor et al., 2004). In this case, an increase of the copepods abundance mean a decrease of the grazing pressure on phytoplankton, and an increase of the phytoplankton net growth.

In terms of export fluxes, we observed that elevated copepod concentrations decreased the POC flux in the +Si while the opposite was observed for −Si treatments (**Figure 8**). The highest difference can be seen for +Si at Day 6 where copepods strongly impact the flux composition decreasing aggregate contribution to the flux (from 92 to 68% for −Cops and +Cops, respectively, **Figure 7**). This could have resulted from two mechanisms, a mechanic breakage of the aggregates (Alldredge et al., 1990; Dilling and Alldredge, 2000) or by changing diatom community because diatoms are not equal in terms of aggregation capacity (Cataletto et al., 1996). However until Day 6 the aggregating species *Skeletonema marinoii* dominate the two treatments suggesting at this time that physical breakage of aggregates by zooplankton feeding and swimming activities must have prevailed. But copepods activities also influenced the diatom community: in the +Si +Cops, the biovolume of the diatom population increased toward the end (**Figure 6**) with larger species progressively dominating the diatom community (from *S. marinoii* to *L. danicus*). We also observed an impact of copepod activity on the species composition of the sinking material. Similarly to observations done in the Kerguelen area, preferential feeding by copepods resulted in an increased proportion of heavily silicified diatoms in the sinking flux (Quéguiner, 2013) even when they are not so well represented in the surface water populations. Diatom composition of the export fluxes in +Si −Cops reflected that of the suspended diatom community, but most of the material recovered in the +Si +Cops traps were constituted by the large and heavily silicified *Proboscia alata* and aggregates of *S. marinoii*.

Reversely in the −Si mesocosms, higher copepod concentrations were associated with increased POC fluxes, with a stronger contribution of aggregates at Day 11 and of intact fecal pellets toward the end of the mesocosm study (**Figure 7**). While the intensity of the POC fluxes generally follow the aggregate contribution to the flux, the slight decrease of the flux intensity at the end in the −Si +Cops mesocosm traps confirm that fecal pellets production can compensate for the disaggregation process in a non-diatom situation.

Overall, our data suggests that zooplankton decreased the efficiency of the system to export POC in diatom dominated ecosystem (**Figure 10**). For dinoflagellates dominated systems, the net export is increasing due to the positive effect of copepod activity on phytoplankton growth. However, except at Day 6, the efficiency of the system in terms of how much of POC production was exported was not affected by copepod abundance (**Figure 10**). Instead of copepods simply ingesting and repackaging phytoplankton into fecal pellets in proportions similar to the community composition in the mixed layer, copepods actively shape the phytoplankton community structure in the surface layer and in the export fluxes by selective grazing which determines which phytoplankton species are being retained in the upper ocean, and which ones are being exported.

CONCLUSIONS

In our large scale experimental non-bloom conditions, POC fluxes were positively correlated to Si/C in all mesocosms, highlighting the global importance of diatoms for POC export. The addition of dSi increased POC fluxes, confirming the results by Wassmann et al. (1996). Lightly silicified diatoms, which dominated water column in most mesocosms during our study, drive the export through aggregation when copepods concentration is decreased. With elevated copepod

concentrations, net phytoplankton growth globally increased, probably due to trophic cascade effect. Grazing pressure also structure the phytoplankton community, with a shift from small to medium or large diatoms in the water column and in the export fluxes. Simultaneously aggregates are mechanically broken by copepod activity which is not compensated by the increase density of the diatoms escaping the grazing. These two opposite effects in diatom dominated ecosystem resulted in a net decrease of the export efficiency. Reversely by favoring phytoplankton growth and formation of fast sinking fecal pellets, copepods increase the net export by non-diatom species, but do not clearly change the export efficiency.

AUTHOR CONTRIBUTIONS

BM and CD contributed to the conception of the experiment, to find the fundings, to the acquisition, analysis, and interpretation of data and wrote the manuscript. MI and MG contributed to the conception of the experiment, to the acquisition, analysis, and interpretation of data and writting of the manuscript. ML, RL, HS, MS, and A-JE, contributed to the conception of the experiment, to the acquisition and analysis of data and revised the manuscript. BB, JB, RC, NC, AD, SG, MK, CL, AL, and AM contributed to the acquisition and analysis of data and revised the manuscript.

ACKNOWLEDGMENTS

Immeasurable thanks are owed to everyone whose technical support and advice made this experiment possible: A. Neyts, HS, RC, AL, E. Achterberg, O. Vadstein, Y. Olsen, and M. St. John. This research was supported by the European Community's 7th Framework Programme's Integrating Activity HYDRALAB IV (No. 261520) and Integrating Project EURO-BASIN (No. 264933). Thank you to the two reviewers that greatly help to improve this manuscript.

REFERENCES

Alldredge, A. L., Granata, T. C., Gotschalk, C. C., and Dickey, T. D. (1990). The physical strength of marine snow and its implications for particle disaggregation in the ocean. *Limnol. Oceanogr.* 35, 1415–1428. doi: 10.4319/lo.1990.35.7.1415

Alvain, S., Le Quéré, C., Bopp, L., Racault, M.-F., Beaugrand, G., Dessailly, D., et al. (2013). Rapid climatic driven shifts of diatoms at high latitudes. *Remote Sens. Environ.* 132, 195–201. doi: 10.1016/j.rse.2013.01.014

Armstrong, R. A., Lee, C., Hedges, J. I., Honjo, S., and Wakeham, S. G. (2002). A new, mechanistic model for organic carbon fluxes in the ocean based on the quantitative association of POC with ballast minerals. *Deep Sea Res. II* 49, 219–236. doi: 10.1016/S0967-0645(01)00101-1

Assmy, P., Smetacek, V., Montresor, M., Klaas, C., Henjes, J., Strass, V. H., et al. (2013). Thick-shelled, grazer-protected diatoms decouple ocean carbon and silicon cycles in the iron-limited Antarctic Circumpolar Current. *Proc. Natl. Acad. Sci. U.S.A.* 110, 20633–20638. doi: 10.1073/pnas.1309345110

Bach, L. T., Taucher, J., Boxhammer, T., Ludwig, A., The Kristineberg, KOSMOS Consortium., Achterberg, E. P., et al. (2016). Influence of ocean acidification on a natural winter-to-summer plankton succession: first insights from a long-term mesocosm study draw attention to periods of low nutrient concentrations. *PLoS ONE* 11:e0159068. doi: 10.1371/journal.pone.0159068

Bopp, L. (2005). Response of diatoms distribution to global warming and potential implications: a global model study. *Geophys. Res. Lett.* 32:L19606. doi: 10.1029/2005GL023653

Bopp, L., Resplandy, L., Orr, J. C., Doney, S. C., Dunne, J. P., Gehlen, M., et al. (2013). Multiple stressors of ocean ecosystems in the 21st century: projections with CMIP5 models. *Biogeosciences* 10, 6225–6245. doi: 10.5194/bg-10-6225-2013

Børsheim, K. Y., Vadstein, O., Myklestad, S. M., Reinertsen, H., Kirkvold, S., and Olsen, Y. (2005). Photosynthetic algal production, accumulation and release of phytoplankton storage carbohydrates and bacterial production in a gradient in daily nutrient supply. *J. Plankton Res.* 27, 743–755. doi: 10.1093/plankt/fbi047

Boyd, P. W., and Trull, T. W. (2007). Understanding the export of biogenic particles in oceanic waters: Is there consensus? *Prog. Oceanogr.* 72, 276–312. doi: 10.1016/j.pocean.2006.10.007

Buesseler, K. O., and Boyd, P. W. (2009). Shedding light on processes that control particle export and flux attenuation in the twilight zone of the open ocean. *Limnol. Oceanogr.* 54, 1210–1232. doi: 10.4319/lo.2009.54.4.1210

Cataletto, B., Feoli, E., Umani, S. F., Monti, M., and Pecchiar, I. (1996). Analyses of the relationship between mucous aggregates and phytoplankton communities in the Gulf of Trieste (Northern Adriatic Sea) by multivariate techniques. *Mar. Ecol.* 17, 291–307. doi: 10.1111/j.1439-0485.1996.tb00509.x

Dilling, L., and Alldredge, A. L. (2000). Fragmentation of marine snow by swimming macrozooplankton: A new process impacting carbon cycling in the sea. *Deep Sea Res. Part Oceanogr. Res. Pap.* 47, 1227–1245. doi: 10.1016/S0967-0637(99)00105-3

Dortch, Q., and Maske, H. (1982). Dark uptake of nitrate and nitrate reductase activity of a red-tide population off peru. *Mar. Ecol. Prog. Ser.* 9, 299-303. doi: 10.3354/meps009299

Engel, A., Goldthwait, S., Passow, U., and Alldredge, A. L. (2002). Temporal decoupling of carbon and nitrogen dynamics in a mesocosm diatom bloom. *Limnol. Oceanogr.* 47, 753–761. doi: 10.4319/lo.2002.47.3.0753

François, R., Honjo, S., Krishfield, R., and Manganini, S. (2002). Factors controlling the flux of organic carbon to the bathypelagic zone of the ocean. *Glob. Biogeochem. Cycles* 16, 34-1–34-20. doi: 10.1029/2001GB001722

Fujii, M., and Chai, F. (2005). Effects of biogenic silica dissolution on silicon cycling and export production. *Geophys. Res. Lett.* 32:L05617. doi: 10.1029/2004GL022054

Gazeau, F., Sallon, A., Pitta, P., Tsiola, A., Maugendre, L., Giani, M., et al. (2017). Limited impact of ocean acidification on phytoplankton community structure and carbon export in an oligotrophic environment: results from two short-term mesocosm studies in the Mediterranean Sea. *Estuar. Coast. Shelf Sci.* 186, 72–88. doi: 10.1016/j.ecss.2016.11.016

Gehlen, M., Bopp, L., Emprin, N., Aumont, O., Heinze, C., and Ragueneau, O. (2006). Reconciling surface ocean productivity, export fluxes and sediment composition in a global biogeochemical ocean model. *Biogeosci. Discuss.* 3, 803–836. doi: 10.5194/bgd-3-803-2006

Giering, S. L., Sanders, R., Lampitt, R. S., Anderson, T. R., Tamburini, C., Boutrif, M., et al. (2014). Reconciliation of the carbon budget in the ocean/'s twilight zone. *Nature* 507, 480–483. doi: 10.1038/nature13123

Gismervik, I., Olsen, Y., and Vadstein, O. (2002). "Micro-and mesozooplankton response to enhanced nutrient input—a mesocosm study," in *Sustainable Increase of Marine Harvesting: Fundamental Mechanisms and New Concepts* (Dordrecht: Springer), 75–87.

Guidi, L., Chaffron, S., Bittner, L., Eveillard, D., Larhlimi, A., Roux, S., et al. (2016). Plankton networks driving carbon export in the oligotrophic ocean. *Nature* 532, 465–470. doi: 10.1038/nature16942

Henson, S. A., Sanders, R., and Madsen, E. (2012). Global patterns in efficiency of particulate organic carbon export and transfer to the deep ocean. *Glob. Biogeochem. Cycles* 26:GB1028. doi: 10.1029/2011GB004099

Henson, S. A., Yool, A., and Sanders, R. (2015). Variability in efficiency of particulate organic carbon export: a model study. *Glob. Biogeochem. Cycles* 29, 33–45. doi: 10.1002/2014GB004965

Honjo, S., Manganini, S. J., Krishfield, R. A., and Francois, R. (2008). Particulate organic carbon fluxes to the ocean interior and factors controlling the biological

pump: a synthesis of global sediment trap programs since 1983. *Prog. Oceanogr.* 76, 217–285. doi: 10.1016/j.pocean.2007.11.003

Iversen, M., and Poulsen, L. K. (2007). Coprohexy, coprophagy, and coprochaly in the copepods Calanus helgolandicus, Pseudocalanus elongatus, and Oithona similis. *Mar. Ecol. Prog. Ser.* 350, 79–89. doi: 10.3354/meps07095

Kemp, A. E. S., Pearce, R. B., Grigorov, I., Rance, J., Lange, C. B., Quilty, P., et al. (2006). The production of giant marine diatoms and their export at oceanic frontal zones: implications for Si and C flux in stratified oceans. *Glob. Biogeochem. Cycles* 20:GB4S04. doi: 10.1029/2006GB002698

Kemp, A. E. S., and Villareal, T. A. (2013). High diatom production and export in stratified waters – A potential negative feedback to global warming. *Prog. Oceanogr.* 119, 4–23. doi: 10.1016/j.pocean.2013.06.004

Klaas, C., and Archer, D. E. (2002). Association of sinking organic matter with various types of mineral ballast in the deep sea: implications for the rain ratio. *Glob. Biogeochem. Cycles* 16, 63-1–63-14. doi: 10.1029/2001GB001765

Klaas, C., Verity, P. G., and Schultes, S. (2008). Determination of copepod grazing on natural plankton communities: correcting for trophic cascade effects. *Mar. Ecol. Prog. Ser.* 357, 195–206. doi: 10.3354/meps07262

Koroleff, F. (1969). Direct determination of ammonia in natural waters as indophenol blue. *ICES CM* 100:9.

Lalande, C., Moriceau, B., Leynaert, A., and Morata, N. (2016). Spatial and temporal variability in export fluxes of biogenic matter in Kongsfjorden. *Polar Biol.* 39, 1725–1738. doi: 10.1007/s00300-016-1903-4

Lam, P. J., Doney, S. C., and Bishop, J. K. B. (2011). The dynamic ocean biological pump: Insights from a global compilation of particulate organic carbon, $CaCO_3$, and opal concentration profiles from the mesopelagic: the dynamic ocean biological pump. *Glob. Biogeochem. Cycles* 25:GB3009. doi: 10.1029/2010GB003868

Larsen, A., Egge, J. K., Nejstgaard, J. C., Di Capua, I., Thyrhaug, R., Bratbak, G., et al. (2015). Contrasting response to nutrient manipulation in Arctic mesocosms are reproduced by a minimum microbial food web model. *Limnol. Oceanogr.* 60, 360–374. doi: 10.1002/lno.10025

Lasbleiz, M., Leblanc, K., Blain, S., Ras, J., Cornet-Barthaux, V., Hélias Nunige, S., et al. (2014). Pigments, elemental composition (C, N, P, and Si), and stoichiometry of particulate matter in the naturally iron fertilized region of Kerguelen in the Southern Ocean. *Biogeosciences* 11, 5931–5955. doi: 10.5194/bg-11-5931-2014

Lee, C., Peterson, M. L., Wakeham, S. G., Armstrong, R. A., Cochran, J. K., Miquel, J. C., et al. (2009). Particulate organic matter and ballast fluxes measured using time-series and settling velocity sediment traps in the northwestern Mediterranean Sea. *Deep Sea Res. Part II Top. Stud. Oceanogr.* 56, 1420–1436. doi: 10.1016/j.dsr2.2008.11.029

Lima, I. D., Lam, P. J., and Doney, S. C. (2014). Dynamics of particulate organic carbon flux in a global ocean model. *Biogeosciences* 11, 1177–1198. doi: 10.5194/bg-11-1177-2014

Litchman, E., Klausmeier, C. A., and Bossard, P. (2004). Phytoplankton nutrient competition under dynamic light regimes. *Limnol. Oceanogr.* 49, 1457–1462. doi: 10.4319/lo.2004.49.4_part_2.1457

Long, M., Moriceau, B., Gallinari, M., Lambert, C., Huvet, A., Raffray, J., et al. (2015). Interactions between microplastics and phytoplankton aggregates : impact on their respective fates. *Mar. Chem.* 175, 39-46. doi: 10.1016/j.marchem.2015.04.003

Lutz, M., Dunbar, R., and Caldeira, K. (2002). Regional variability in the vertical flux of particulate organic carbon in the ocean interior: regional variability in vertical poc flux. *Glob. Biogeochem. Cycles* 16, 11-1–11-18. doi: 10.1029/2000GB001383

McDonnell, A. M., and Buesseler, K. O. (2010). Variability in the average sinking velocity of marine particles. *Limnol. Oceanogr.* 55, 2085–2096. doi: 10.4319/lo.2010.55.5.2085

Moriceau, B., Gallinari, M., Soetaert, K., and Ragueneau, O. (2007). Importance of particle formation to reconstructed water column biogenic silica fluxes. *Glob. Biogeochem. Cycles* 21:GB3012. doi: 10.1029/2006GB002814

Morris, P. J., Sanders, R., Turnewitsch, R., and Thomalla, S. (2007). 234Th-derived particulate organic carbon export from an island-induced phytoplankton bloom in the Southern Ocean. *Crozet Nat. Iron Bloom Export Exp.* 54, 2208–2232. doi: 10.1016/j.dsr2.2007.06.002

Nelson, D. M., Tréguer, P., Brzezinski, M. A., Leynaert, A., and Quéguiner, B. (1995). Production and dissolution of biogenic silica in the ocean: revised global estimates, comparison with regional data and relationship to biogenic sedimentation. *Glob. Biogeochem. Cycles* 9, 359–372. doi: 10.1029/95GB01070

Olsen, Y., Agustí, S., Andersen, T., Duarte, C. M., Gasol, J. M., Gismervik, I., et al. (2006). A comparative study of responses in plankton food web structure and function in contrasting European coastal waters exposed to experimental nutrient addition. *Limnol. Oceanogr.* 51, 488–503. doi: 10.4319/lo.2006.51.1_part_2.0488

Olsen, Y., Andersen, T., Gismervik, I., and Vadstein, O. (2007). Protozoan and metazoan zooplankton-mediated carbon flows in nutrient-enriched coastal planktonic communities. *Mar. Ecol. Prog. Ser.* 331, 67–83. doi: 10.3354/meps331067

Passow, U., and Carlson, C. A. (2012). The biological pump in a high CO2 world. *Mar. Ecol. Prog. Ser.* 470, 249–271. doi: 10.3354/meps09985

Passow, U., and De La Rocha, C. L. (2006). Accumulation of mineral ballast on organic aggregates. *Glob. Biogeochem. Cycles* 20:GB1013. doi: 10.1029/2005GB002579

Paul, A. J., Bach, L. T., Schulz, K.-G., Boxhammer, T., Czerny, J., Achterberg, E. P., et al. (2015). Effect of elevated CO_2 on organic matter pools and fluxes in a summer Baltic Sea plankton community. *Biogeosciences* 12, 6181–6203. doi: 10.5194/bg-12-6181-2015

Ploug, H., Iversen, H. M., and Fischer, G. (2008). Ballast, sinking velocity, and apparent diffusivity within marine snow and zooplankton fecal pellets: Implications for substrate turnover by attached bacteria. *Limnol. Oceanogr.* 53, 1878–1886. doi: 10.4319/lo.2008.53.5.1878

Pondaven, P., Gallinari, M., Chollet, S., Bucciarelli, E., Sarthou, G., Schultes, S., et al. (2007). Grazing-induced changes in cell wall silicification in a marine diatom. *Protist* 158, 21–28. doi: 10.1016/j.protis.2006.09.002

Quéguiner, B. (2013). Iron fertilization and the structure of planktonic communities in high nutrient regions of the Southern Ocean. *Deep Sea Res. Part II Top. Stud. Oceanogr.* 90, 43–54. doi: 10.1016/j.dsr2.2012.07.024

Ragueneau, O., Dittert, N., Pondaven, P., Tréguer, P., and Corrin, L. (2002). Si/C decoupling in the world ocean: is the Southern Ocean different? *Deep Sea Res. II* 49, 3127–3154. doi: 10.1016/S0967-0645(02)00075-9

Ragueneau, O., Savoye, N., Del Amo, Y., Cotten, J., Tardiveau, B., and Leynaert, A. (2005). A new method for the measurement of biogenic silica in suspended matter of coastal matter: using Si:Al ratios to correct for the mineral interference. *Cont. Shelf Res.* 25, 697–710. doi: 10.1016/j.csr.2004.09.017

Rynearson, T. A., Richardson, K., Lampitt, R. S., Sieracki, M. E., Poulton, A. J., Lyngsgaard, M. M., et al. (2013). Major contribution of diatom resting spores to vertical flux in the sub-polar North Atlantic. *Deep Sea Res. Part Oceanogr. Res. Pap.* 82, 60–71. doi: 10.1016/j.dsr.2013.07.013

Sanders, R., Henson, S. A., Koski, M., Christina, L., Painter, S. C., Poulton, A. J., et al. (2014). The biological carbon pump in the North Atlantic. *Prog. Oceanogr.* 129, 200–218. doi: 10.1016/j.pocean.2014.05.005

Sarmiento, J. L., Dunne, J., and Armstrong, R. A. (2004). Do We now understand the ocean's biological pump? *US JGOFS Newsl.* 12, 1–5.

Schultes, S., Lambert, C., Pondaven, P., Corvaisier, R., Jansen, S., and Ragueneau, O. (2010). Recycling and Uptake of Si (OH) 4 when Protozoan Grazers Feed on Diatoms. *Protist* 161, 288–303. doi: 10.1016/j.protis.2009.10.006

Shanks, A. L., and Trent, J. D. (1980). Marine snow: sinking rates and potential role in marine flux. *Deep Sea Res. I* 27, 137–144. doi: 10.1016/0198-0149(80)90092-8

Siegel, D. A., Buesseler, K. O., Behrenfeld, M. J., Benitez-Nelson, C. R., Boss, E., Brzezinski, M. A., et al. (2016). Prediction of the export and fate of global ocean net primary production: the EXPORTS science plan. *Front. Mar. Sci.* 3:22. doi: 10.3389/fmars.2016.00022

Smetacek, V. (1985). Role of sinking in diatom life history cycles: ecological, evolutionary and geological significance. *Mar. Biol.* 84, 239–251. doi: 10.1007/BF00392493

Sommer, F., Saage, A., Santer, B., Hansen, T., and Sommer, U. (2005). Linking foraging strategies of marine calanoid copepods to patterns of nitrogen stable isotope signatures in a mesocosm study. *Mar. Ecol. Prog. Ser.* 286, 99–106. doi: 10.3354/meps286099

Sommer, U., Hansen, T., Stibor, H., and Vadstein, O. (2004). Persistence of phytoplankton responses to different Si: N ratios under mesozooplankton grazing pressure: a mesocosm study with Northeast Atlantic plankton. *Mar. Ecol. Prog. Ser.* 278, 67–75. doi: 10.3354/meps278067

Sommer, U., Sommer, F., Santer, B., Jamieson, C., Boersma, M., Becker, C., et al. (2001). Complementary impact of copepods and cladocerans on phytoplankton. *Ecol. Lett.* 4, 545–550. doi: 10.1046/j.1461-0248.2001.00263.x

Spilling, K., Schulz, K. G., Paul, A. J., Boxhammer, T., Achterberg, E. P., Hornick, T., et al. (2016). Effects of ocean acidification on pelagic carbon fluxes in a mesocosm experiment. *Biogeosciences* 13, 6081–6093. doi: 10.5194/bg-13-6081-2016

Stange, P., Bach, L. T., Le Moigne, F. A., Taucher, J., Boxhammer, T., and Riebesell, U. (2017). Quantifying the time lag between organic matter production and export in the surface ocean: implications for estimates of export efficiency. *Geophys. Res. Lett.* 44, 268–276. doi: 10.1002/2016GL070875

Stibor, H., Vadstein, O., Lippert, B., Roederer, W., and Olsen, Y. (2004). Calanoid copepods and nutrient enrichment determine population dynamics of the appendicularian Oikopleura dioica: a mesocosm experiment. *Mar. Ecol. Prog. Ser.* 270, 209–215. doi: 10.3354/meps270209

Svensen, C., Egge, J. K., and Stiansen, J. E. (2001). Can silicate and turbulence regulate the vertical flux of biogenic matter? a mesocosm study. *Mar. Ecol. Prog. Ser.* 217, 67–80. doi: 10.3354/meps217067

Svensen, C., Nejstgaard, J. C., Egge, J. K., and Wassmann, P. (2002). Pulsing versus constant supply of nutrients (N, P and Si): effect on phytoplankton, mesozooplankton and vertical flux of biogenic matter. *Sci. Mar.* 66, 189–203. doi: 10.3989/scimar.2002.66n3189

Turner, J. T. (2015). Zooplankton fecal pellets, marine snow, phytodetritus and the ocean's biological pump. *Prog. Oceanogr.* 130, 205–248. doi: 10.1016/j.pocean.2014.08.005

Utermöhl, H. (1958). Zur Vervollkommnung der quantitativen Phytoplanktonmethodik. Mitteilungen Int. *Vereiningung F,r Theor. Angew. Limnol.* 9, 1–38.

Vadstein, O., Stibor, H., Lippert, B., Løseth, K., Roederer, W., Sundt-Hansen, L., et al. (2004). Moderate increase in the biomass of omnivorous copepods may ease grazing control of planktonic algae. *Mar. Ecol. Prog. Ser.* 270, 199–207. doi: 10.3354/meps270199

van Marion, P., (1996). *Ecological studies in Hopavågen, A Landlocked Bay at Agdenes.* Sør-Trøndelag: NTNU Vitenskapsmuseet.

Wassmann, P., Egge, J. K., Reigstad, M., and Aksnes, D. L. (1996). Influence of dissolved silicate on vertical flux of particulate biogenic matter. *Mar. Pollut. Bull.* 33, 10–21. doi: 10.1016/S0025-326X(97)00130-6

Conflict of Interest Statement: The authors declare that the research was conducted in the absence of any commercial or financial relationships that could be construed as a potential conflict of interest.

The reviewer JT and handling Editor declared their shared affiliation.

Copyright © 2018 Moriceau, Iversen, Gallinari, Evertsen, Le Goff, Beker, Boutorh, Corvaisier, Coffineau, Donval, Giering, Koski, Lambert, Lampitt, Le Mercier, Masson, Stibor, Stockenreiter and De La Rocha. This is an open-access article distributed under the terms of the Creative Commons Attribution License (CC BY). The use, distribution or reproduction in other forums is permitted, provided the original author(s) and the copyright owner are credited and that the original publication in this journal is cited, in accordance with accepted academic practice. No use, distribution or reproduction is permitted which does not comply with these terms.

frontiers in Marine Science

REVIEW
published: 06 February 2018
doi: 10.3389/fmars.2018.00022

Competition between Silicifiers and Non-silicifiers in the Past and Present Ocean and Its Evolutionary Impacts

Katharine R. Hendry[1†], Alan O. Marron[2†], Flora Vincent[3†], Daniel J. Conley[4,5], Marion Gehlen[6], Federico M. Ibarbalz[3], Bernard Quéguiner[7] and Chris Bowler[3]*

[1] Department of Earth Sciences, Bristol University, Bristol, United Kingdom, [2] Department of Applied Mathematics and Theoretical Physics, Centre for Mathematical Sciences, University of Cambridge, Cambridge, United Kingdom, [3] Institut de Biologie de l'Ecole Normale Supérieure, Ecole Normale Supérieure, Centre National de la Recherche Scientifique, Institut National de la Santé et de la Recherche Médicale, PSL Research University, Paris, France, [4] Department of Geology, Lund University, Lund, Sweden, [5] Stellenbosch Institute for Advanced Study, Stellenbosch, South Africa, [6] Institut Pierre-Simon-Laplace, Laboratoire des Sciences du Climat et de l'Environnement, Gif-sur-Yvette, France, [7] Aix Marseille Univ, Université de Toulon, Centre National de la Recherche Scientifique/INSU, IRD, MIO, UM 110, Marseille, France

OPEN ACCESS

Edited by:
Eric 'Pieter Achterberg, GEOMAR Helmholtz Centre for Ocean Research Kiel (HZ), Germany

Reviewed by:
Nils Kröger, Technische Universität Dresden, Germany
Pascal Jean Lopez, Centre National de la Recherche Scientifique (CNRS), France
Mark Hildebrand, University of California, San Diego, United States

***Correspondence:**
Chris Bowler
cbowler@biologie.ens.fr

† These authors are joint first authors and have contributed equally to this work.

Specialty section:
This article was submitted to Marine Biogeochemistry, a section of the journal Frontiers in Marine Science

Received: *22 September 2017*
Accepted: *17 January 2018*
Published: *06 February 2018*

Citation:
Hendry KR, Marron AO, Vincent F, Conley DJ, Gehlen M, Ibarbalz FM, Quéguiner B and Bowler C (2018) Competition between Silicifiers and Non-silicifiers in the Past and Present Ocean and Its Evolutionary Impacts. Front. Mar. Sci. 5:22. doi: 10.3389/fmars.2018.00022

Competition is a central part of the evolutionary process, and silicification is no exception: between biomineralized and non-biomineralized organisms, between siliceous and non-siliceous biomineralizing organisms, and between different silicifying groups. Here we discuss evolutionary competition at various scales, and how this has affected biogeochemical cycles of silicon, carbon, and other nutrients. Across geological time we examine how fossils, sediments, and isotopic geochemistry can provide evidence for the emergence and expansion of silica biomineralization in the ocean, and competition between silicifying organisms for silicic acid. Metagenomic data from marine environments can be used to illustrate evolutionary competition between groups of silicifying and non-silicifying marine organisms. Modern ecosystems also provide examples of arms races between silicifiers as predators and prey, and how silicification can be used to provide a competitive advantage for obtaining resources. Through studying the molecular biology of silicifying and non-silicifying species we can relate how they have responded to the competitive interactions that are observed, and how solutions have evolved through convergent evolutionary dynamics.

Keywords: diatoms, silicifiers, radiolarians, silicic acid transporters, silicification

INTRODUCTION

Biomineralization refers to the precipitation of minerals by living organisms (Simkiss and Wilbur, 1989). It may occur as a by-product of the normal metabolism of the organism under indirect genetic control—related to the cellular processes that create the conditions for incidental biomineral formation—and with no pre-concentration of specific mineral ions. Alternatively, the composition of the biominerals formed can be entirely dependent on the environmental conditions, for example, the formation of iron oxide by brown algae (Lee and Kugrens, 1989). By contrast, biologically controlled biomineralization requires direct genetic control, generates characteristically patterned structures, and involves selective uptake and pre-concentration of mineral ions.

In nature, we observe a wide array of biominerals (see **Figure 1**), ranging from iron oxide to strontium sulfate (Raven and Knoll, 2010), with calcareous biominerals being particularly notable (Knoll, 2003; Knoll and Kotrc, 2015). However, the most taxonomically widespread biomineral is silica ($SiO_2 \cdot nH_2O$), being present in all eukaryotic supergroups (Marron et al., 2016b). Notwithstanding, the degree of silicification can vary even between closely related taxa, from being found in composite structures with other biominerals (e.g., limpet teeth; Sone et al., 2007), to forming minor structures (e.g., ciliate granules; Foissner et al., 2009) or being a major structural constituent of the organism (Preisig, 1994). The most extreme degree of silicification is evident in the diatoms, where almost all species have an obligate requirement for silicon to complete cell wall formation and cell division (Darley and Volcani, 1969; Martin-Jézéquel et al., 2000). Biogeochemically and ecologically, diatoms are believed to be the most important silicifiers in modern marine ecosystems, with radiolarians (polycystine and phaeodarian rhizarians), silicoflagellates (dictyochophyte and chrysophyte stramenopiles), and sponges with prominent roles as well. In contrast, the major silicifiers in terrestrial ecosystems are the land plants (embryophytes), with other silicifying groups (e.g., testate amoebae) having a minor role.

Broadly, biomineralized structures are believed to have evolved and diversified where the energetic cost of biomineral production is less than the expense of producing an equivalent organic structure (Mann, 2001; Raven and Waite, 2004; Finkel and Kotrc, 2010). Raven (1983) calculated that the energetic costs of silicic acid uptake and silica structure formation is substantially more efficient than forming the same volume of an organic structure (∼20x more for lignin and 10x for polysaccharides like cellulose). Based on the structural model of biogenic silica of Hecky et al. (1973), Lobel et al. (1996) identified by biochemical modeling a low-energy reaction pathway for nucleation and growth of silica. The combination of organic and inorganic components within biomineralized structures often results in enhanced properties compared to exclusively organic or inorganic materials. With respect to biogenic silica, this can result in the production of much stronger structures, such as siliceous diatom frustules having the highest strength per unit density of any known biological material (Hamm et al., 2003; Aitken et al., 2016), or sponge spicules being many times more flexible than an equivalent structure made of pure silica (Ehrlich et al., 2008; Shimizu et al., 2015). As a result, biogenic silica structures are utilized for support (Weaver et al., 2007), feeding (Nesbit and Roer, 2016), predation defense (Pondaven et al., 2007; Friedrichs et al., 2013; Hartley et al., 2016) and environmental protection as a component of cyst walls (Preisig, 1994). Biogenic silica also has useful optical properties for light transmission and modulation in organisms as diverse as plants (Schaller et al., 2013), diatoms (Fuhrmann et al., 2004; Yamanaka et al., 2008; Romann et al., 2015), sponges (Sundar et al., 2003), and molluscs (Dougherty et al., 2014). There is also evidence that silicification is used as a detoxification response in snails (Desouky et al., 2002) and plants (Neumann and zur Nieden, 2001), sequestering harmful substances such as aluminum and zinc within the biogenic silica to ensure the correct functioning of cellular metabolism. Diatom biosilica has even been suggested to play a role as a pH buffer for the enzymatic activity of carbonic anhydrase, aiding the acquisition of inorganic carbon for photosynthesis (Milligan and Morel, 2002).

The myriad of functions and benefits of biomineralization raises an important question: why do some organisms biomineralize while others do not? Furthermore, why is there such a diversity of biominerals besides silicon, when silicon is so abundant, comprising 28% of the Earth's crust? The answer to these questions lies in the evolutionary interplay between biomineralization and geochemistry, and in the competitive interactions that have arisen from these dynamics. Fundamentally whether an organism produces silica or not involves evolutionary trade-offs and competition between silicifiers themselves, and with non-silicifying organisms (both those which utilize other biominerals, and non-mineralizing groups). Mathematical models and controlled experiments of resource competition in phytoplankton have demonstrated the rise to dominance of different algal species based on nutrient backgrounds in defined media. These have been part of fundamental studies in ecology (Tilman, 1977; Sommer, 1994). However, the vast diversity of organisms that thrive in a complex array of biotic and abiotic interactions in oceanic ecosystems are a challenge to such minimal models and experimental designs, whose parameterization and possible combinations, respectively, limit the interpretations that can be built on them. Here we broadly extend our attention into other types of data from which competition can be inferred: the geological record, the distribution of species in modern marine ecosystems, and phenomena at the cellular and molecular levels (summarized in **Table 1**).

EVOLUTIONARY COMPETITION ACROSS GEOLOGICAL TIME

Competition between organisms is usually driven by a limited supply of a commonly used resource. For organisms that are biomineralizers of silica, orthosilicic acid—which we will refer to as silicic acid throughout, to distinguish from cellular silicon—is one such important limiting resource (Tilman et al., 1982). Silicic acid is released by the dissolution of biogenic silica and silicate minerals by biological and chemical weathering processes, and by hydrothermal activity, up to a solubility limit of 1.2–2.2 mM in water depending on the ambient physicochemical properties (Gunnarsson and Arnórsson, 2000). The drawdown of oceanic silicic acid through geological time has been attributed to biological utilization (Siever, 1991) and may have resulted in skeletal changes in marine silicifiers (Maldonado et al., 1999; Racki and Cordey, 2000; Lazarus et al., 2009; Finkel and Kotrc, 2010; Finkel et al., 2010; van Tol et al., 2012). To what extent these changes are a result of competition between silicifiers is still matter of debate.

The evolution of organisms that transport silicon into their cells has a long history (Marron et al., 2016b), likely going back to the evolution of cyanobacteria in the Archean (Dvorák et al., 2014). As silicic acid is a small molecule, and is mostly

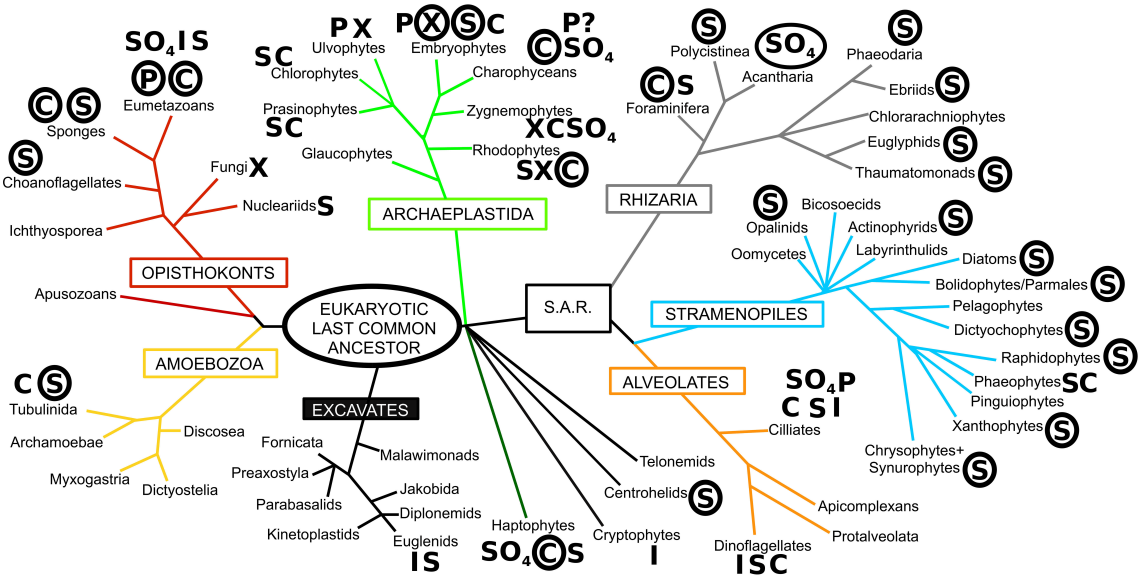

FIGURE 1 | The diversity of biomineralization across the eukaryotes. The phylogeny is based on that of Adl et al. (2012) with major eukaryotic supergroups named in boxes. Letters next to taxon names denote the presence of biomineralization, with circled letters indicating prominent and widespread use of that biomineral. S, silica; C, calcium carbonate; P, calcium phosphate; I, iron (magnetite/goethite); X, calcium oxalate; SO_4, sulfates (calcium/barium/strontium), ? denotes uncertainty in report. Based on Ensikat et al. (2016), Gal et al. (2012), Knoll (2003), Knoll and Kotrc (2015), Marron et al. (2016b), Raven and Knoll (2010), Weich et al. (1989), and references therein.

present in an undissociated form ($Si(OH)_4$) under seawater pH conditions (Del Amo and Brzezinski, 1999), it is possible for silicic acid to diffuse across the cell membrane (Raven, 1983; Thamatrakoln and Hildebrand, 2008). In the high silicic acid Precambrian ocean, diffusion from the surrounding Si-saturated seawater could result in silica precipitating freely within the cytoplasm, interfering with cellular processes and disabling the functioning of the cell. Consequently, silicon transporters are proposed to have arisen initially to prevent intracellular toxicity by removing it from the cytoplasm (Marron et al., 2016b). Recently, cyanobacteria microfossils that contain nanocrystals of greenalite with the approximate composition of $Si_2O_5(OH)_4Fe^{2+}$ (Lepot et al., 2017) have been found in the 1.88 Ga Gunflint Iron Formation, suggesting Fe biomineralization, which may also have protected oxygenic photosynthesisers against Fe^{2+} toxicity during the Paleoproterozoic.

It is inferred from the proliferation of biomineralized fossils in the geological record at the end of the Proterozoic and into the early Paleozoic that the ocean witnessed large reductions in silicic acid (Conley et al., 2017). The appearance of biomineralization (Kouchinsky et al., 2011; Knoll and Kotrc, 2015) likely led to evolutionary "arms races" with organisms using biomineralized structures to reduce predation rates, resulting in competition for an important shared resource (Smith and Szathmáry, 1995). This arms race produced a proliferation of non-silicic acid users and some highly efficient silicic acid users, the latter outcompeting inefficient users leading to their extinction.

There is widespread evidence in the geological record for such a decline in silicic acid and coincidental macroevolutionary changes in silicifying groups. For example, changes in chert precipitation occurred due to the increased abundance of radiolarians in the lower to early Middle Ordovician, which may have reduced the abundance of sponges overall and forced the relocation of remaining sponge species from shallow to deep-water environments as surface waters became depleted in silicic acid (Kidder and Tomescu, 2016). In addition to the geological record, the timing of independent losses of silicon transporters (Marron et al., 2016b) further support the hypothesis that significant declines in silicic acid concentrations during the Paleozoic (Conley et al., 2017) led to evolutionary changes in the biochemical pathways of silicification and efficiency of silicon uptake.

However, it was the evolution of diatoms with their superior ability to utilize Si, due to their unique complement of Silicon Transporter (SIT) genes (Hildebrand et al., 1997, 1998), that led to the reduction of oceanic silicic acid concentrations to the low levels observed in the global ocean today (Tréguer and De La Rocha, 2013). Diatoms, with their obligate requirement for Si to complete their cell cycle, are strong competitors for silicic acid. This, combined with diatom features not related to Si (e.g., nutrient acquisition and storage, light harvesting, bloom formation), must have produced new competitive interactions that were previously unseen in the Paleozoic oceans (Knoll and Follows, 2016). Recent studies have robustly demonstrated the presence of very low oceanic silicic acid concentrations since at least 60 Ma, most likely as a result of the drawdown of silicic acid by diatom biomineralization (Fontorbe et al., 2016, 2017), which is tens of millions of years before the time period envisioned by Siever (1991) and others. Conley et al. (2017) have hypothesized that if such a global decrease in oceanic silicic acid concentrations

TABLE 1 | Examples of competitive interactions involving the use of silica, as seen from geology, ecology, and cellular/molecular biology.

Level	Competitors	Description	Reference
Geological times	Radiolarians and sponges	Reduction of abundance and relocation of sponges in the early Middle Ordovican	Kidder and Tomescu, 2016
	Rise of diatoms: Diatoms and other silicifiers	Reduction of oceanic silicic acid in the Cenozoic (or even Mesozoic) era	Sims et al., 2006; Fontorbe et al., 2016, 2017
	Diatoms and sponges	Post-Mesozoic decline of certain sponge spicule morphologies	Maldonado et al., 1999
	Diatoms and radiolarians; Diatoms and silicoflagellates	Silicificaton and shell-thickness/spine morphology, decline of radiolarians in the low latitudes throughout the Cenozoic (reason still debated)	Lazarus et al., 2009; van Tol et al., 2012; Cermeño et al., 2015
Ecology in modern oceans	Diatoms and polycystines	Main users of silica	de Vargas et al., 2015
	Within silicifiers	Resistance against predators	Lebour, 1922; Marshall and Orr, 1955; Campbell et al., 2009; van Tol et al., 2012
	Silicifiers and others	Segregative pattern	Lima-Mendez et al., 2015
Cellular and molecular biology	Diatoms	Different morphologies that affect sinking, predation, light capture, viral resistance and nutrient uptake	Hamm et al., 2003; Fuhrmann et al., 2004; Raven and Waite, 2004; Losic et al., 2006; Sims et al., 2006; Pondaven et al., 2007; Yamanaka et al., 2008; Finkel and Kotrc, 2010; Nakov et al., 2014; Romann et al., 2015
	Diatoms and other silicifiers	Independent inventions of SITs in other silicifiers; SIT diversification in diatoms	Thamatrakoln et al., 2006; Durkin et al., 2016; Marron et al., 2016b
		Secondary loss of biosilicification in other silicifiers	Maldonado, 2009; Kozhemyako et al., 2010; Lahr et al., 2013, 2015; Zlatogursky, 2016
		Facultative biosilicification	Sandgren et al., 1996; Kessenich et al., 2014; Yamada et al., 2014; Leadbeater, 2015; Morueta-Holme et al., 2016

occurred, it must predate the Cenozoic and perhaps began with the appearance of silicifying diatoms in the Mesozoic (Sims et al., 2006).

Both the geological record and molecular phylogenetics concur that, whilst the majority of the main morphological groups of diatoms had arisen by the end of the Cretaceous (Kotrc and Knoll, 2015), there was a rapid expansion and diversification of diatoms in the Cenozoic (Siever, 1991; **Figure 2**). The most recent compilations have shown two short-lived major abundance peaks near the Eocene–Oligocene boundary and in the late Oligocene, with a shift in diatom abundance in sediments during the middle Miocene to globally higher values which have largely persisted to the modern day (Lazarus et al., 2014; Renaudie, 2016). There remains a lively debate in the scientific literature surrounding the drivers of the diatom expansion, mostly relating to shifts in the supply of silicic acid to the ocean due to changes in climate and weathering regimes. A correlation between a recent diatom diversity compilation and paleoclimate archives (oxygen and carbon isotopes from carbonates) indicates that there could be a direct link between temperature and diatom evolution throughout the Neogene (Lazarus et al., 2014). Climatically induced changes in oceanic circulation and mixing due to the opening of marine gateways may have altered nutrient availability in the euphotic zone and driven macroevolutionary shifts in the size of marine pelagic diatoms through the Cenozoic (Finkel et al., 2005). For example, geochemical archives point toward an increase in silicic acid supply to the surface Southern Ocean at the Eocene-Oligocene boundary, likely due to the opening of the Drake Passage and Tasman Seaway and the formation of a "proto circum-Antarctic current," and coinciding with the large peak in diatom diversification (Egan et al., 2013). The rapid rise of diatoms in the Cenozoic has also been attributed to the impact of orogeny on weathering (Misra and Froelich, 2012) with periods of enhanced continental weathering fluxes and increased silicic acid input to the oceans (Cermeño et al., 2015). Correlation between diatom abundance peaks and shifts in seawater strontium and osmium isotopic composition also hint at a strong control by silicate weathering on diatom deposition (Finkel et al., 2005). However, it is a major challenge to tease apart the impacts of oceanic circulation and weathering on diatom diversification and abundance due to the inherent coincidence in timing of the major orogenic episodes and shifts in oceanic circulation throughout the Cenozoic (Benoiston et al., 2017).

The expansion of diatoms, with their strong affinity for silicic acid, is likely to have led to competition with other silificiers, especially in intermediate and shallow depths where silicic acid is present only in low—and potentially limiting—concentrations. Here the fossil record provides an archive for examining possible signs of competition in the geological past. The post-Mesozoic decline of certain sponge spicule morphologies, indicative of high silicic acid conditions in specimens from shallower waters, has been interpreted as showing competitive exclusion of sponges by diatoms (Maldonado et al., 1999). However, the exact timing of the decline in these spicules from shallower waters relative to diatom-driven changes in silicic acid is not well-constrained. If oceanic silicic acid declined earlier than the

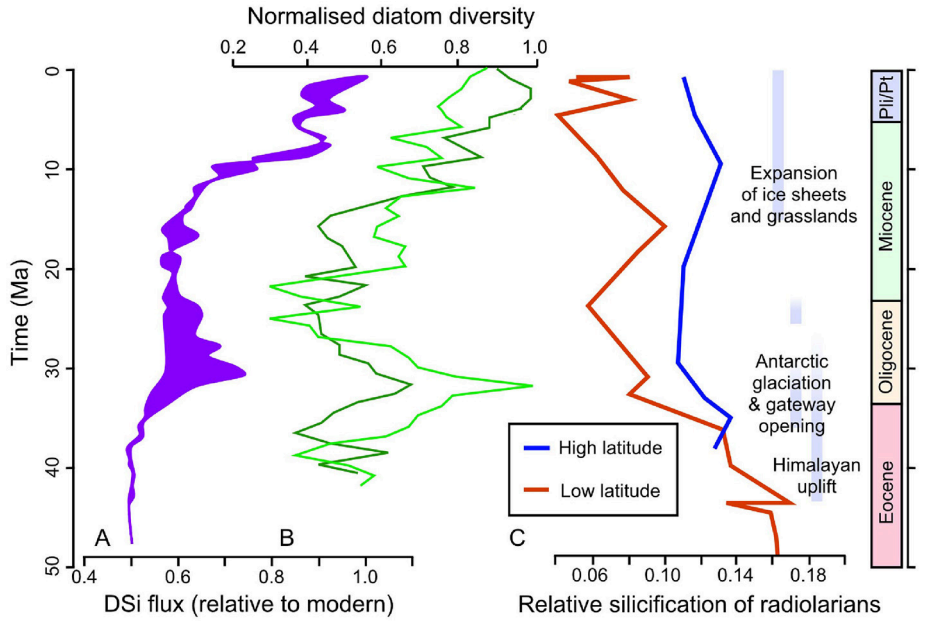

FIGURE 2 | Cenozoic records of silicifying organisms and environmental drivers. **(A)** An approximate range of silicic acid fluxes relative to modern fluxes, encompassing global flux estimates modeled using the Cenozoic lithium isotope record of Misra and Froelich (2012) and Southern Ocean fluxes modeled using marine clay mineralogy. Note that a number of key assumptions are made to model these fluxes: the fluxes were modeled assuming a change in the ratio of suspended clays to silicic acid through time in order to account for a potential increase in incongruent silicate weathering, and a two-fold increase in silicic acid content of rivers over the last 50 My. **(B)** Diatom diversity curves calculated using the unweighted lists subsampling method of Cermeño et al. (2015) (lime green line) and the consensus diversity curve of Lazarus et al. (2014) (dark green line line). **(C)** Calculated silicification of radiolarians through the Cenozoic, from Lazarus et al. (2009).

Cretaceous-Paleogene boundary (Conley et al., 2017), then the exclusion of sponges from shallower waters either occurred due to competition at an earlier stage, or was driven by an alternative factor.

Changes in the size of radiolarians in the fossil record also provide evidence of macroevolution likely driven by competition. The silicification and shell-thickness of radiolarians in the low latitudes decline throughout the Cenozoic, whilst the higher latitude specimens remain invariant (Lazarus et al., 2009). This latitudinal pattern of change suggests that radiolarians increasingly struggled to obtain sufficient silicic acid in the lower latitude, oligotrophic waters, which were increasingly depleted of silicic acid due to a combination of diatom drawdown and shifts in oceanic circulation. However, despite the coincidence in timing, the decline in low-latitude radiolarian size does not necessarily point to competition as a driver of macroevolution. Mathematical models of competition between radiolarians and diatoms have been used to investigate this problem further. These experiments show that the reduction in radiolarian shell size is not sufficient to explain diatom diversification changes, which were more likely driven by an increase in resources and were linked inherently to their geographical distribution (Cermeño et al., 2015; **Figure 2**). However, these models are limited by the availability of reliable data on silicic acid inputs and fossil abundance records.

A combination of competitive interactions for silicic acid with other silicifiers and the effect of predator-prey arms races may govern macroevolutionary trends in silicoflagellate morphology (van Tol et al., 2012). Across the Cenozoic, silicoflagellate skeletons show two diverging trends: spineless species become smaller, whereas spiny species display decreased levels of silicification but increased numbers and length of spines. It has been interpreted that grazing pressure necessitated a siliceous skeleton for protection, as other phytoplankton (e.g., coccolithophores) also possessed biomineralized defenses. However, competition from diatoms reduced silicic acid availability and therefore increased the cost of producing such a skeleton. In response silicoflagellates may have evolved either to maintain the degree of silicification but became smaller overall, or to utilize spines as a method of retaining a large size and defensive structure but at a lower silicon requirement. These evolutionary trade-offs saw the extinction of large, spineless silicoflagellates as ecosystems changed through geological time to feature both high grazing pressure and low silicon availability.

One additional route for examining competition as a driver of silicifier macroevolution is the timing and extent of biochemical changes in silicon uptake pathways. The evolution of biochemical pathways for silicification have been investigated by resolving the different gene families that express, for example, silicon transporters in different silicifiers (Marron et al., 2016b). The affinity for silicic acid and the uptake efficiency of the different transporter families could then be assessed to determine the potential for competitive interaction between different silicifying groups, between and within major taxonomic groupings. Isotope

geochemistry could also be used as an additional tool for investigating this problem. Silicon transport into and within the cell is likely the basis for the fractionation of stable Si isotopes. All silicifiers investigated to date fractionate Si isotopes relative to the seawater in which they grow, but sponges have a more variable and potentially greater isotopic fractionation than either diatoms or radiolarians (de la Rocha et al., 1997; Hendry and Robinson, 2012; Hendry et al., 2014; Abelmann et al., 2015). Such isotopic fractionation may be related to the biochemical pathways involved in Si metabolism, and may reflect the organism's affinity for silicic acid and efficiency of uptake and utilization. As such, Si isotopes may be a useful tool for examining the evolution of silicification.

EVOLUTIONARY COMPETITION IN MODERN ECOSYSTEMS

There are numerous examples of silicified structures being used by organisms to gain a competitive advantage in contemporary ecosystems. The siliceous lorica of choanoflagellates show a range of morphologies (Leadbeater et al., 2009), differing in size and density of siliceous components. This has been connected to niche partitioning, from large open structures that are required to maintain a planktonic lifestyle through the water column, to densely packed lorica of biofilm-inhabiting species (Leadbeater, 2015). The diatom *Phaeodactylum tricornutum* also displays evidence for optimizing its degree of silicification for deeper and colder waters (Zhao et al., 2014). Some wetland plants, notably rice, employ silica as a supplement to cellulose or lignin for structural strengthening, which allows taller growth and aids in competition for light (Cooke and Leishman, 2011).

The optical properties of silica can also be employed to aid in the absorption of light by photosynthetic organisms. Diatom frustules have been proposed to modulate solar wavelengths and direction for optimum absorption of light for photosynthesis (Yamanaka et al., 2008; Romann et al., 2015), while amorphous silica (in combination with microsporine-like amino acids) can help protect against harmful ultraviolet radiation (Ingalls et al., 2010). These adaptations can establish competitive interactions with other photosynthetic organisms that use different biominerals (e.g., calcium carbonate in coccolithophores Taylor et al., 2017, calcium oxalate in plants He et al., 2014), or organic components (e.g., flavonoids, Schaller et al., 2013) for similar photoprotective purposes.

Analysis of the distribution of silicifiers in the contemporary ocean at large spatial scale can bring additional insights about the evolution of competition between different groups. During the course of the *Tara* Oceans expedition (Karsenti et al., 2011; Bork et al., 2015), a worldwide characterization of pelagic plankton ecosystems was performed using DNA metabarcoding and microscopy correlated with key environmental parameters in a way that would, beyond acquisition of data, create a well-structured dataset to address broad ecological and evolutionary questions. Using a non-destructive *in situ* imaging system to visualize organisms directly in the water column (Underwater Vision Profiler, UVP), Biard et al. (2016) focused on the abundance of giant Rhizaria in a variety of pelagic ecosystems in the upper 500 meters of the water column. Rhizaria is a supergroup of unicellular eukaryotes composed of three subphyla: Radiolaria, Cercozoa, and Foraminifera, some of which are silicified (Moreira et al., 2007; **Figure 1**). Radiolaria are divided into two major lineages: the siliceous skeleton producing Polycystinea (including the two orders Nassellaria and Spumellaria) and non-silicified Spasmaria (including Acantharia and Taxopodida; Krabberød et al., 2011). Phaeodaria, an asymbiotic rhizarian taxon with widespread biosilicification and extensively silicified lineages, was initially classified in Radiolaria and is now placed among the Cercozoa as revealed by molecular phylogeny (Polet et al., 2004). Phaeodaria was the most important contributor to rhizarian biomass at all latitudes in the 100–500 m depth layer, displaying an even distribution worldwide. On the contrary, photosymbiotic non-silicified Collodaria dominated the top 100 m of the water column at low latitudes, showing that these orders of Rhizaria display different ecological preferences and vertical stratification.

Additionally, the use of the 18S ribosomal DNA molecular marker to chart microbial diversity by metabarcoding (Taberlet et al., 2012) enabled a high-resolution taxonomic description of planktonic communities across several depths and various size fractions with reasonable accuracy (de Vargas et al., 2015), and was found to be a good proxy for cell number, at least within the diatoms (Malviya et al., 2016). Analysis of the *Tara* Oceans metabarcoding data revealed that diatom diversity was high in the open ocean, contrary to what was generally considered, and also confirmed diatom prevalence in regions of high productivity and at high latitudes. Ocean circulation choke points such as Cape Agulhas and the Drake Passage were found to be important in constraining diatom distribution and diversity (Malviya et al., 2016).

Beyond individual studies of major silicifying groups, comparative analysis can be performed using the *Tara* Oceans data set (de Vargas et al., 2015). Functional annotation of the silicifying organisms (based on Marron et al., 2016b), followed by mapping of their distribution across the global ocean, reveals major patterns (**Figure 3**). The silicifier community is largely size-delineated: the smallest size fraction (0.8–5 micron) contains a large diversity of silicifying organisms in nearly constant proportions. Dictyochophyceae, Polycystinea, and Chrysophyceae are the major taxonomic groups present in this size fraction, together with Bacillariophyta (diatoms) at some locations. Although less abundant, the constant presence of Centrohelida and Choanoflagellates suggests that ecological niche enables the coexistence of several taxonomic groups.

A larger size fraction of micro-plankton (20–180 microns) displays a very different trend. Diversity within the silicifier community drops, and is composed essentially of only Bacillariophyta and Polycystinea, so much so that both taxonomic groups represent over 99% percent of the micro-planktonic silicifier community across the vast majority of the global ocean. Diatoms and polycystines occur in highly variable proportions, where diatoms dominate the cold high-latitude regions. Co-existence between both groups is rare, whereby the presence of one of the organisms appears to exclude the

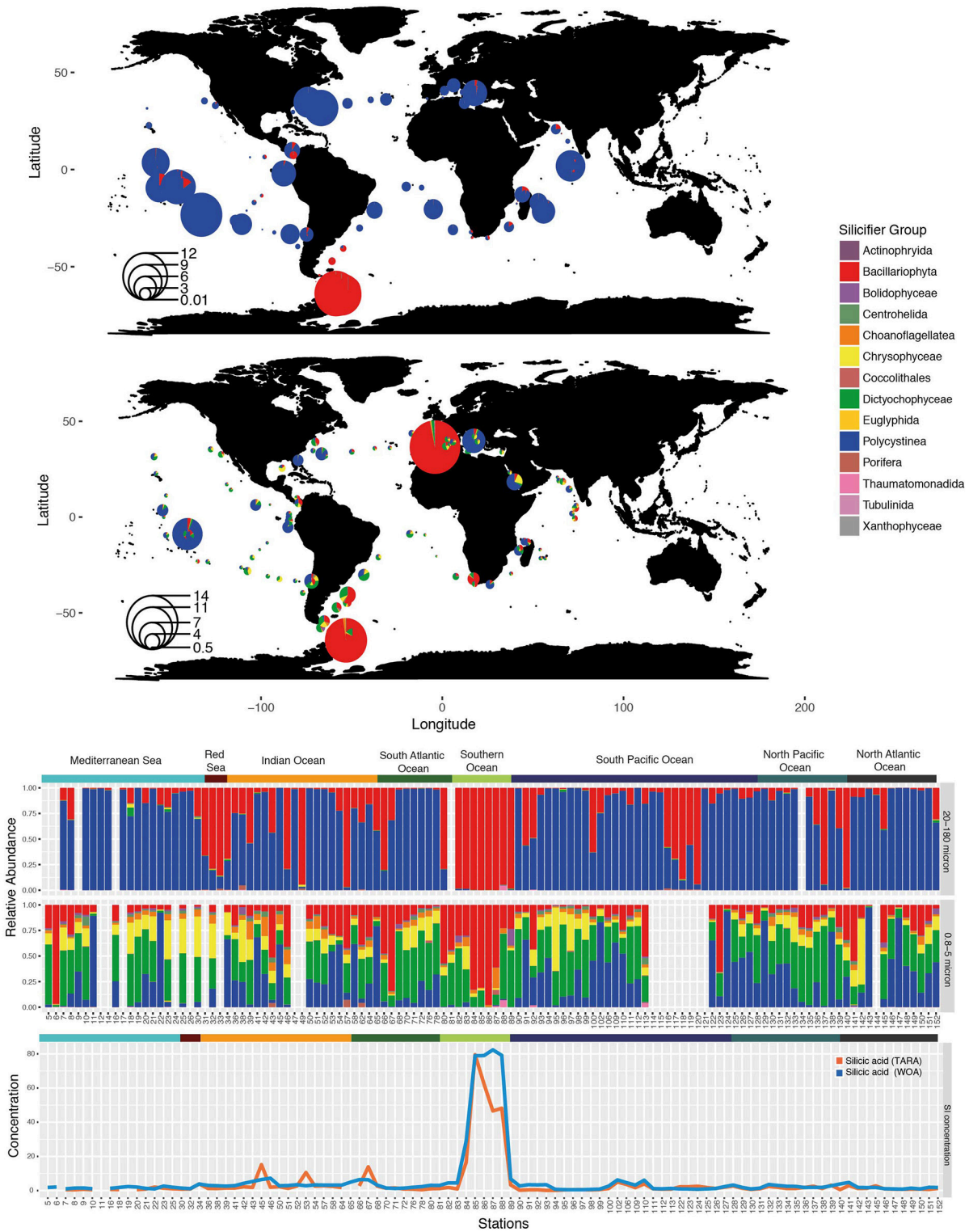

FIGURE 3 | Distribution of silicifiers in the sunlit ocean based on metabarcoding abundance data from the *Tara* Oceans expedition. **(Top)** Silicifiers in surface waters of the 20–180 micron size fraction—divide radius by 20 for log transformed relative abundance. **(Middle)** Silicifiers in surface waters of the 0.8–5 micron size fraction—divide radius by 30 for log transformed relative abundance. The size of the bubble corresponds to the importance of silicifiers with respect to the whole planktonic community. **(Bottom)** Composition of the silicifiers' community in surface waters at each sampling station and *in situ* silicic acid concentrations (in μM) obtained either from discrete *Tara* Oceans samples or from the World Ocean Atlas (woa13). Ocean provinces are indicated.

other, which may also reflect special adaptations to nutritional environments as opposed as eutrophic, oligotrophic, or HNLC areas.

Diatom expansion 65 Ma ago has been attributed to their superior competitive ability for silicic acid uptake relative to radiolarians, the latter experiencing a reduction in weight of their tests (Harper and Knoll, 1975). It is therefore expected that at high silicic acid concentrations, Radiolaria, with their inferior silicic acid uptake ability should have a better chance to thrive alongside diatoms. Yet, in the modern ocean, regions with high silicic acid concentrations (Southern Ocean, *Tara* stations TARA_084 to TARA_089) are still strongly dominated by large populations of diatoms (Platt et al., 2009) in which they can represent over three quarters of the whole planktonic community (**Figure 3**), according to the metabarcoding survey. This hints to the possibility that biotic or abiotic factors other than silicic uptake are responsible for diatom dominance.

The relative abundance of the silica biomineralizing groups with respect to other micro-plankton in the *Tara* Oceans data (**Figure 4**) is largely dependent on nutrient availability (silicic acid, nitrate, phosphate), in particular in the Southern Ocean, the Indian Ocean and around the Marquesas Islands in the Pacific Ocean. However, silicic acid concentrations do not appear to be concomitant in specific stations in the Mediterranean Sea or in the North Atlantic Ocean where nutrient concentrations are low and yet silicifiers are highly abundant, perhaps reflecting a time lag between silicic acid availability and diatom uptake and bloom. Moreover, focused studies in the Mediterranean ecosystems do not report diatom dominance, with the exception of the spring bloom in the North West Mediterranean and Adriatic Sea. Most of the Mediterranean Sea is oligotrophic with diatoms restricted to more or less discrete deep layers at the boundary with the Levantine Intermediate Water (the saltiest water mass that forms in the eastern Mediterranean Sea), suggesting a strong bottom-up control by nutrients, including silicic acid (Leblanc et al., 2003; Crombet et al., 2011). Additionally, the North Atlantic planktonic community changes in the course of the productive season, and silicic acid can also limit diatom uptake and growth (Leblanc et al., 2005).

Because some diatoms thrive in modestly nutrient-rich regions, other factors must therefore explain their success (Green et al., 2008). The continual reshaping of communities by mortality, allelopathy, symbiosis, and other processes show that community interactions exert strong selective pressure on marine microbes (Strom, 2008). This reflects the "Eltonian shortfall," introduced by Hortal et al. (2015) in a review on current major flaws in biodiversity research and refers to our lack of knowledge about "biotic interactions." It is likely that studying these top down pressures on biomineralizing organisms will complement our understanding of their evolution.

A prominent role of biomineralization in modern ecosystems is in defensive and feeding interactions between predators (feeding structures such as teeth) and prey (defensive structures such as spines, shells and tests). In embryophytes, silicification has a wide-ranging defensive role (He et al., 2014; Ensikat et al., 2016; Hartley et al., 2016), from abrasive phytoliths to complex structures such as trichomes, and even by inducing anti-herbivore and anti-pathogen metabolic responses (Ye et al., 2013). These defenses lead to multiple competitive interactions, with differential effects on different types of insect feeding (Massey et al., 2006), between insect and mammalian herbivores, or between large and small mammalian herbivores (Hartley et al., 2016). There are also complex competitive interactions between plants regarding their silicified defenses, which depend on various biotic (plant species, herbivore population cycles) and abiotic factors (soil conditions, climate; Garbuzov et al., 2011; Hartley et al., 2016). This can lead to herbivore-plant specialization and alter plant community and ecosystem structure.

Metazoan herbivores such as copepods (crustaceans) presumably exercise strong pressure on diatoms, silicoflagellates, and polycystines by feeding on them (Lebour, 1922; Marshall and Orr, 1955; Campbell et al., 2009; van Tol et al., 2012). Several feeding experiments have investigated the coevolution between

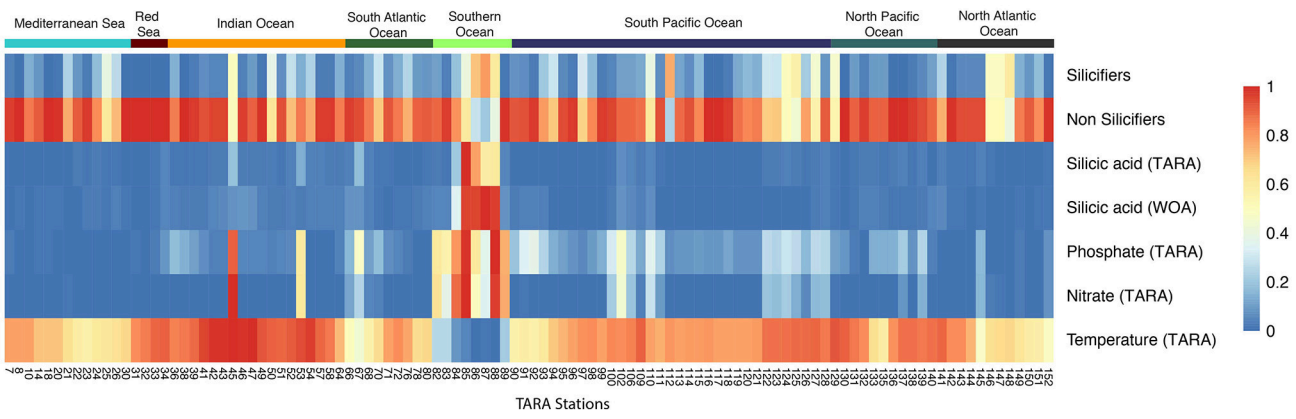

FIGURE 4 | Heatmap of the relative abundance between silicifiers and non-silicifiers and major environmental parameters across *Tara* Oceans stations. The relative abundance of silicifiers outcompetes that of non-silicifiers in specific locations but not always concomitant with high nutrient availability. Colored rectangles on top of the heatmap correspond to ocean provinces.

copepods and diatoms. Some adaptations are mechanical: copepods modify their feeding tools by increased silicification of the mouthparts (Itoh, 1970; Miller et al., 1980, 1990; Michels et al., 2012) in response to which diatoms adjust their protective frustules, leading to an arms race that fuels evolutionary processes (Hamm and Smetacek, 2007). Some diatoms that dominate blooms experience less grazing mortality than do co-occurring species (Assmy et al., 2007; Strom et al., 2007): it was shown that in the presence of preconditioned media that contained herbivores, diatoms develop grazing-resistant morphologies such as increased cell wall silicification (Pondaven et al., 2007; Ratti et al., 2013; Zhang et al., 2017). Silicification of diatom genera also depends on their ecological niche, wherein diatoms that thrive at depth under low light and in the nutrient gradient display low growth rates, and thus must be silicified to protect against grazing (Quéguiner, 2013). The silica cell wall therefore provides not only a "constitutive mechanical protection" for the cell but also a plastic trait that responds to grazing pressure promoting the diversification of ecological niches for a single taxonomic group. Differential biosilicification within a specific group may also have major effects on global nutrient recycling such as the decoupling of silicon and carbon cycles through complex biotic interactions influencing sedimentation pathways in the iron-limited Southern Ocean (e.g., Assmy et al., 2013; Quéguiner, 2013).

Experimental evidence suggests that biotic interactions not only shape the arms race between species, but also affect species range (Bateman et al., 2012; Araujo and Rozenfeld, 2014), inducing non-random co-distribution of species at large spatial scales of hundreds of kilometers for macro-organisms (Gotelli et al., 2010), both at regional and continental scales. Therefore, understanding the degree to which occurrences of species are constrained by the distributions of other species at broad scales of resolution and extent likely links back toward ecological and evolutionary mechanisms shaping the success of functional groups. This can be investigated through the use of co-occurrence networks (Gravel et al., 2011). Empirical studies have historically focused on competition (Gause, 1934; Hardin, 1960), revealing that in its extreme form competition leads to co-exclusion of the interacting species (MacArthur, 1972). As part of the recent *Tara* Oceans expedition, determinants of community structure in global ocean plankton communities were assessed using microbial association networks to create the *Tara* Oceans Interactome (Lima-Mendez et al., 2015). Pairwise links between species were computed based on how frequently they were found to co-occur in similar samples (positive correlations) or, on the contrary, if the presence of one organism negatively correlated with the presence of another (negative correlations). At a global scale (**Figure 5**), major taxonomic groups have shown higher positive correlations than negative ones, except diatoms and polycystines (Morueta-Holme et al., 2016). Instead diatoms and polycystines showed an unusually high proportion of negative correlations, which was statistically significant within silicifiers as a whole. This defines diatoms and polycystines as segregators. Conversely, plankton functional traits approaches show that silicifiers display a segregative pattern compared to other major interacting organisms in the plankton, in particular toward meso- and proto-zooplankton as well as parasites (**Figure 5**). It is therefore the interplay between abiotic and biotic factors that shape the distribution of biomineralizing organisms in the modern ocean, in which competition for silicic acid coupled with differential grazing pressures seem to be important drivers of the spatio-temporal structure of silicifier communities across the ocean. The data in **Figures 4**, **5** indicate that temperature is a particularly important abiotic factor.

CELLULAR AND MOLECULAR ASPECTS OF EVOLUTIONARY COMPETITION

Evidence for evolutionary competition can also be found in the molecular biology of biomineralization. The gain, loss and convergence of the molecular mechanisms responsible for nutrient uptake and biomineral patterning illustrates how silicifying and non-silicifying organisms compete for common resources and produce similar solutions to solve these evolutionary problems.

Competition between diatom species has driven their diversification into various ecological niches (Sims et al., 2006; Nakov et al., 2014). This is mirrored in the diversification of diatom morphologies, from the macrostructural level of frustule shapes, spines and chains right down to the different micro- and nanopatterns of the frustule (Gordon et al., 2009; Finkel and Kotrc, 2010). Isolation of macromolecules found in diatom frustules, and *in vitro* studies of their silica polymerization activity, has led to the development of a model whereby micropatterns are produced by interactions between several components. Silica polymerizes on a structural scaffold composed of glycoproteins and other organic macromolecules, the ammonium fluoride insoluble matrix (Brunner et al., 2009; Tesson and Hildebrand, 2013; Kotzsch et al., 2016). The morphology and mesoscale patterning of the forming diatom silica is also controlled by interactions with the cytoskeleton as the silicon deposition vesicle (SDV) expands, and by components of the membrane surrounding the SDV (the silicalemma; Tesson and Hildebrand, 2010a,b; Tesson et al., 2017). The polymerization rate in these *in vitro* experiments, and therefore the nanoscale patterning (including formation of plates and pores), has been shown to be influenced by proteins including silaffins (Kröger et al., 2002), silacidins (Wenzl et al., 2008), and long-chain polyamines (LCPAs; Kröger et al., 2000; Sumper and Kröger, 2004). Some unique frustule structures are marked out by them containing specific biosilica-related proteins, such as cingulins that form the girdle bands linking the two valves of the frustule (Scheffel et al., 2011). The number, size and shape of girdle bands vary between diatom species, and this may be connected to variations in cingulin repertoires. Furthermore, it is not only the content and protein sequence of these molecules that has been demonstrated through *in vitro* experiments to control their silica polymerization and patterning activity, but also their ratios and post-translational processing like cleavage, glycosylation, phosphorylation, or the addition of quaternary ammonium groups (Kröger et al., 2002; Poulsen and Kröger, 2004; Lopez et al., 2005; Sumper et al., 2007; Wenzl et al., 2008).

A

Taxonomic group	Total number of edges	Number of positive edges	Number of negative edges	ratio +/-
Syndiniales	20576	16573	4003	4.14
Arthropoda	18743	11958	6785	1.76
Dinophyceae	14565	9892	4673	2.12
Polycystina	5931	2365	3566	0.66
MAST	5759	4405	1354	3.25
Prymnesiophyceae	4790	4188	602	6.96
Bacillariophyta	4369	2120	2249	0.94
Acantharea	4272	3475	797	4.36
Cyanobacteria	2947	2186	761	2.87
Oceanospirillales	2674	1712	962	1.78
Rickettsiales	2340	1939	401	4.84
Spirotrichea	2216	1543	673	2.29
Chaetognatha	2159	1637	522	3.14
Apicomplexa	2152	1496	656	2.28

B

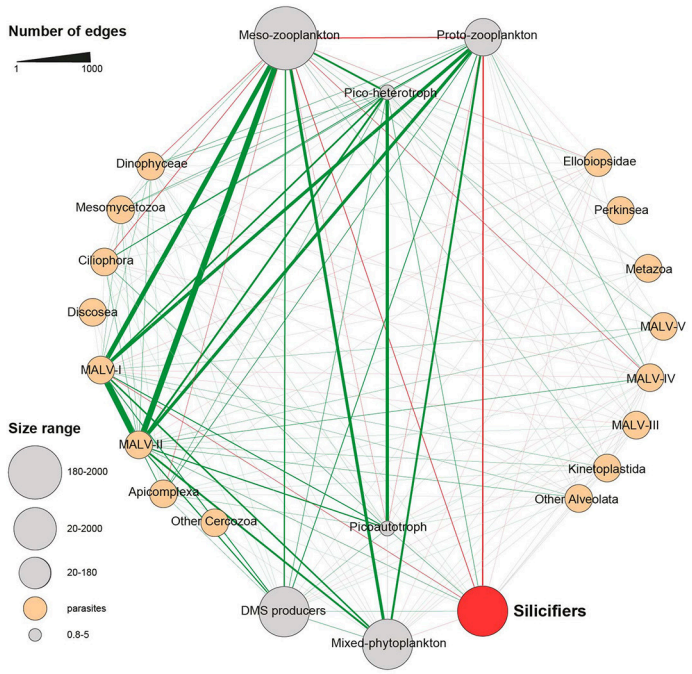

FIGURE 5 | Silicifiers in the *Tara* Oceans global ocean co-occurrence network. **(A)** Proportion of positive and negative correlations for the major taxonomic groups. Silicifiers are highlighted in red. **(B)** Plankton functional types (PFTs) subnetwork. PFTs encapsulate individual barcodes based on their trophic strategy and role in global biogeochemical cycles. Edges width reflects the number of correlations between the corresponding metanodes. Over-represented links (multiple-test corrected $P < 0.05$) are colored in green if they represent co-presences and in red if they represent exclusions; gray means non-overrepresented combinations. When both co-presences and exclusions were significant, the edge is shown as co-presence. Silicifiers emcompass Bacillariophyta and Polycystina. Figure adapted from Lima-Mendez et al. (2015) and reproduced with permission from AAAS.

Diatom morphology can control features such as sinking rates (Smayda, 1970; Raven and Waite, 2004; Nakov et al., 2014), predation (Hamm et al., 2003; Pondaven et al., 2007), light perception (Fuhrmann et al., 2004; Yamanaka et al., 2008; Romann et al., 2015), viral resistance (Losic et al., 2006), and nutrient uptake (Finkel and Kotrc, 2010). Given that it has been demonstrated that the content of the polymerization-influencing components differs between species (Kröger et al., 2000; Sumper and Lehmann, 2006; Bowler et al., 2008), it is conceivable that evolutionary modifications of the silica patterning mechanisms can help individuals to out-compete other diatoms in certain ecological niches. This would eventually lead to the emergence

of new species with characteristic morphologies of the siliceous frustule. In this way, the study of diatom silica formation and patterning mechanisms, combined with a phylogenetic framework, can reveal the evolutionary interactions between competition and frustule silicification.

In addition to diatoms, many other siliceous groups feature species-specific morphologies and micropatterning, with only limited variation depending on environmental conditions. Examples include loricate choanoflagellates (Leadbeater et al., 2009), thaumatomonads (Scoble and Cavalier-Smith, 2014), chrysophytes (van Tol et al., 2012), and ascidians (Monniot et al., 1992). Repeatedly we can observe the evolution of similar morphologies in distantly related taxa, such as micropores in the siliceous components of choanoflagellates (Leadbeater, 2015), chrysophytes (Sandgren et al., 1996), diatoms (Finkel and Kotrc, 2010), and haptophytes (Yoshida et al., 2006); spines and spicules in radiolarians (Kunitomo et al., 2006), dictyochophytes (Preisig, 1994), centrohelids (Zlatogursky, 2016), and sponges (Weaver et al., 2007); or tablets and scales in haptophytes (Yoshida et al., 2006), rhizarians (Nomura and Ishida, 2016), synurophytes (Sandgren et al., 1996), amoebozoans (Lahr et al., 2013), and brachiopods (Williams et al., 2001). Though the genes governing the production of these silica patterns are not fully understood, many parallels with the molecular biology of diatom silicification are emerging, such as a role for glycoproteins in choanoflagellates (Gong et al., 2010) and synurophytes (Ludwig et al., 1996), cytoskeleton-mediated shaping of the growing silica structure in multiple taxa (Leadbeater, 2015; Nomura and Ishida, 2016) and the presence of post-translationally modified LCPAs in haptophyte (Durak et al., 2016) and sponge (Matsunaga et al., 2007) silica. These polymerization mechanisms have apparently evolved independently from those in diatoms, suggesting repeated recruitment of similar molecules for silica formation and patterning, and therefore a similar role for silicification-related evolutionary competition and speciation as diatoms.

A critical step in silica biomineralization (Martin-Jézéquel et al., 2000), and therefore a major aspect of evolutionary competition between silicifiers, is the uptake and concentration of silicic acid from the external environment. The nature of this competition has changed over geological time in conjunction with changes in the biogeochemical cycling of silicon (Racki and Cordey, 2000; Maliva et al., 2005; Finkel and Kotrc, 2010; Knoll and Kotrc, 2015; Conley et al., 2017). In turn, this is reflected in the evolutionary molecular biology of silicon transport mechanisms.

The first proteins capable of transporting silicon across a plasma membrane to be identified were the SIT (Silicon Transporter) family (Hildebrand et al., 1997). The SIT protein (see **Figure 6A**) has a characteristic 10-transmembrane domain structure, with two conserved GXQ motifs arranged in a roughly symmetrical pattern at the cytoplasmic sides of transmembrane helices 2 and 3, and the extracellular sides of transmembrane helices 7 and 8 (Thamatrakoln et al., 2006). These motifs are proposed to be involved in forming an aqueous vestibule to allow an alternating access mechanism for silicon transport (in conjunction with Na^+) across the membrane (Knight et al., 2016). This four-GXQ domain characteristic of the *SIT* gene family is highly distinctive, being found only in the 10-transmembrane domain *SITs* and in the closely related, 5-transmembrane domain *SIT-Ls* (Silicon Transporter-Like; Durak et al., 2016). *SIT-Ls* resemble "halved-*SITs*" (see **Figure 6B**), and are believed to be the ancestral genes that underwent duplication to give rise to *SITs* (Durak et al., 2016; Marron et al., 2016b). This situation is analogous to the gene duplication and fusion events that are believed to have produced pseudo-symmetrical transporter proteins (Keller et al., 2014), exemplified best in the SWEET and semi-SWEET glucose transporters of eukaryotes and bacteria (Feng and Frommer, 2015; Tao et al., 2015).

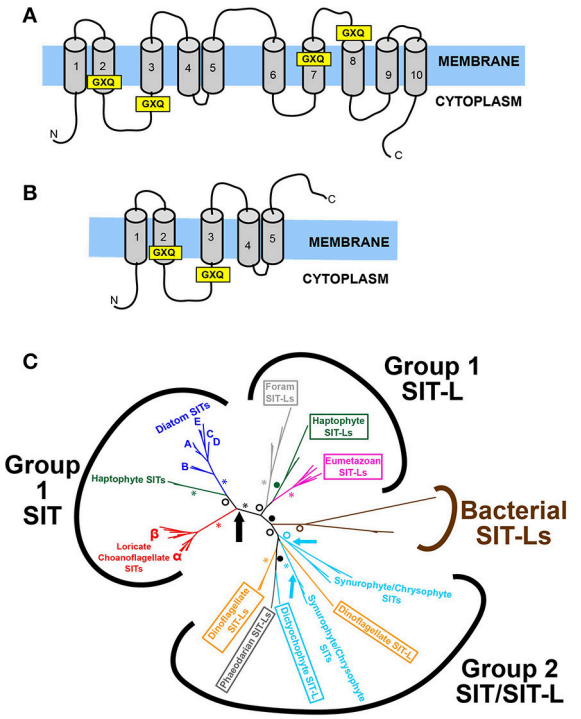

FIGURE 6 | The structure and evolution of SITs and SIT-Ls. **(A)** Structure of the SIT (Silicon Transporter) protein, demonstrating the characteristic 10 transmembrane domains (TMD) and four GXQ motifs, located at the cytoplasmic side of TMD 2 and 3, and at the extracellular side of TMD 7 and 8. **(B)** Structure of the SIT-L (Silicon Transporter Like) protein, with 5 TMDs and two GXQ motifs. The SIT structure resembles a "double" SIT-L, with the C-terminal half having been inverted relative to the N-terminal half and fused together. This suggests that SITs evolved by duplication, inversion and fusion of SIT-L subunits. **(C)** Unrooted radial tree based on a maximum likelihood phylogenetic analysis of *SITs* and *SIT-Ls*. The eukaryotic genes form two main subgroups distinct from the bacterial *SIT-Ls*, and largely follow the species phylogeny except for the paraphyletic stramenopile, rhizarian, and dinoflagellate sequences in Group 2. The diatom and loricate choanoflagellate *SIT* sub-groups are also shown. Arrows indicate inferred duplication-inversion-fusion events that gave rise to 10 TMD *SITs*. Brown, Bacteria; Dark Green, Haptophyte; Gray, Rhizarian (Light Gray, Foraminiferan); Bright Red, Choanoflagellate; Magenta, Metazoan; Orange, Dinoflagellate; Dark Blue, Diatoms; Light Blue, Other Stramenopiles; Black, multi-taxon. SIT-L sequences are in boxes. Statistical support values for selected nodes are indicated by asterisks (100% support), closed circles (90–99% support) or open circles (>70% support). Figures adapted from Marron et al. (2016b).

Members of the Silicon Transporter gene family have been identified across a broad taxonomic range, in all eukaryotic supergroups save for archaeplastids, excavates and amoebozoans (with the caveat that no sequence data are currently available from silicifying excavates or amoebozoans) and are also found in some bacterial species. *SITs* are present in many highly-silicified species, most obviously siliceous stramenopiles (diatoms, chrysophyte/synurophytes, and dictyochophytes) but also siliceous choanoflagellates and haptophytes. In contrast *SIT-L* genes are often found in primarily calcareous groups (foraminifera, metazoans, calcareous haptophytes), although *SIT-Ls* were identified in silicifying groups such as phaeodarians and dinoflagellates. What is notable is that though some species contain multiple *SITs* or *SIT-Ls*, taxa expressing both *SIT* and *SIT-L* genes are rare: of the species examined only the haptophyte *Scyphosphaera apsteinii* possessed both, with the apparently non-silicifying dictyochophyte genus *Florenciella* having some evidence for both *SIT* and *SIT-L* genes (Marron et al., 2016b). This points to there being some sort of functional difference between SIT and SIT-L transporters, possibly with *SITs* being superior in some way, or with *SIT-L* genes being connected to calcification (Durak et al., 2016). It is notable that the geological record of heavily silicifying SIT-L-containing species show a decline in silicification and diversity (Lazarus et al., 2009; van Tol et al., 2012) coincident with the rise of the diatoms from the Mesozoic, again hinting at a "functional superiority" of SITs in competition for silicic acid uptake, though the nature of this advantage remains unresolved. Furthermore, siliceous sponges, which apparently lack either *SITs* or *SIT-Ls* (Marron et al., 2016b), show a similar decline in their degree of silicification and ecological dominance over this time (Maldonado et al., 1999). Again, this is suggestive of SIT-based mechanisms providing some type of competitive advantage over other uptake systems as silicic acid levels fell over geological time and competition for silicon increased.

When the *SIT/SIT-L* phylogeny is compared to species phylogenies, an interesting picture emerges (see **Figure 6C**). Three main eukaryotic clades are resolved: a monophyletic *SIT-only* clade containing diatom, choanoflagellate, and haptophyte genes; a monophyletic *SIT-L* only clade containing foraminferan, metazoan, and haptophyte genes; and a polyphyletic clade featuring both *SIT* and *SIT-L* genes from radiolarians, dinoflagellates and various non-diatom stramenopiles (Marron et al., 2016b). In this analysis, the stramenopile *SITs* branch in two distinct groups with high statistical support, with diatoms being separate from chrysophytes/synurophytes, and dictyochophytes. This distinction also emerges when the phylogeny is analyzed with an alignment of *SIT-L*, *SIT* N-terminal and *SIT* C-terminal sequences (i.e., artificially splitting the *SITs* into two, roughly equal 5-transmembrane sequences each containing two GXQ motifs). In this case the diatom N- and C-termini branch with the relevant N-and C-termini of the choanoflagellate and haptophyte *SITs*. The 5-transmembrane sequences of other stramenopile *SITs* however branch paraphyletically, again together with radiolarian and dinoflagellate *SIT-Ls*. These phylogenies provide a strong molecular signal for the stramenopile *SITs* having evolved via multiple, independent duplications. In this scenario, the diatom *SITs* arose from a single gene duplication and fusion event that also gave rise to the haptophyte and loricate choanoflagellate *SITs*, and must have occurred early in eukaryotic evolution, before these groups diverged deep in the Precambrian (Parfrey et al., 2011). The phylogenetic signal supports the scenario that the other stramenopile *SITs* arose from at least two other duplication-fusion events within the ochrophyte stramenopile clade itself, but after diatoms diverged, potentially as recently as the Mesozoic (Brown and Sorhannus, 2010; Derelle et al., 2016). It is hypothesized that this is a remarkable case of convergent molecular evolution, and that the independent invention of *SITs* from *SIT-Ls* was in response to competition for silicic acid from the rise of the diatoms after the Jurassic period (Marron et al., 2016b). As diatoms came to dominate the global silicon cycle, other heavily silicifying groups required more complex or more efficient uptake mechanisms and transporters to compete. What also emerges from these molecular analyses is that the last common ancestor of all ochrophytes must have possessed an *SIT-L* gene, and that diatoms have lost these *SIT-Ls*, again hinting at a superiority of *SITs* over *SIT-L*-based uptake systems in the competition for silicon.

Diatom domination of marine phytoplankton can be attributed to several ecological advantages (Armbrust et al., 2004), but of particular relevance to silicification is that they possess multiple modes of silicic acid uptake (Martin-Jézéquel et al., 2000; Thamatrakoln and Hildebrand, 2008). At lower silicic acid levels ($\leq$30 μM), the majority of uptake is by SIT-mediated active transport, while at higher concentrations silicic acid enters the cell by diffusion (Thamatrakoln and Hildebrand, 2008; Shrestha and Hildebrand, 2015). The concentration gradient is created by binding of silicic acid to intracellular binding components in the cytoplasm, the character of which remains unknown (Thamatrakoln and Hildebrand, 2008; Spinde et al., 2011). This means that at higher silicic acid levels, diatoms can internally control uptake depending on the rate of silica polymerization in the SDV. The cytoplasmic binding compounds also allow diatoms to maintain a soluble intracellular silicon pool, with spare capacity permitting "surge uptake" of silicic acid following short-term silicon starvation (Thamatrakoln and Hildebrand, 2008). This is highly advantageous, allowing diatoms to take advantage of transient silicon sources in patchy environments like ocean gyres. The different modes of diatom silicic acid uptake are in contrast to other silicifiers such as sponges, which appear to only employ active transport and display maximum uptake efficiency at much higher silicic acid concentrations (Maldonado et al., 2011).

At ecologically-relevant silicon concentrations experienced by diatoms in modern oceans, active SIT-mediated uptake dominates. Diatom species generally possess multiple *SIT* genes (Hildebrand et al., 1998). These paralogs display differences in expression levels, the timing of their expression in the cell cycle, protein abundances and their sub-cellular localization (Thamatrakoln and Hildebrand, 2007; Sapriel et al., 2009; Shrestha et al., 2012; Shrestha and Hildebrand, 2015). These differences are believed to allow neofunctionalization of each SIT, evolving roles as silicon sensors, silicon transporters, targeting of different SIT proteins to specific cellular locations (Shrestha and

Hildebrand, 2015), specialization for the uptake of certain silicon species (Sapriel et al., 2009) or for differential characteristics of substrate affinity versus transport capacity. This allows for maximal uptake at various silicic acid concentrations in the external environment (Thamatrakoln et al., 2006; Thamatrakoln and Hildebrand, 2007, 2008). This suite of *SITs* is hypothesized to allow adaptation to varying conditions and allows the diatom cell to sense silicon availability, ensuring that it can meet the silicon requirements of frustule synthesis and so complete cell division.

This highlights the central role that silicon and silicification play in diatom biology (Martin-Jézéquel et al., 2000). Indeed, silicic acid limitation influences wider diatom cellular biology and results in transcriptional changes of genes related to multiple metabolic pathways (Mock et al., 2008; Shrestha et al., 2012), just as is seen for other essential nutrients like iron or nitrate. It is therefore unsurprising that diatoms have evolved such complex systems to accumulate and compete for silicic acid. This even extends to chemosensory responses of the motile raphid pennate diatom *Seminavis robusta* toward sources of silicic acid, and remarkably *away* from sources of germanium (Bondoc et al., 2016), since germanium exposure disrupts biosilicification and is therefore toxic to siliceous organisms (Marron et al., 2016a).

Phylogenetic evidence (see **Figure 6C**) demonstrates that *SIT* diversification occurred within the diatom lineage itself (Marron et al., 2016b). More detailed phylogenetic analyses of diatom *SITs* can be divided into five main clades (A–E), though the deep branching order between these clades is poorly resolved due to low statistical support (Durkin et al., 2016). The paraphyletic Clade B was found to be the most basal, and Clade B-type *SITs* are found throughout the various diatom groups. The other clades, however, have limited taxonomic distributions, for example Clade A only being present in pennate diatoms, and Clade E being unique to the Thalassiosirales. Therefore, diatom *SITs* underwent multiple independent duplications and diversifications within different lineages, with the more recently evolving diatom lineages (e.g., raphid pennates) having more complex *SIT* repertoires. This complexity is reflected in transcriptional analyses of diatoms under nutrient starvation, and in natural diatom assemblages. The expression levels and ratios of the various *SIT* clades differ according to silicic acid levels, with the more derived *SIT* types being more prominent over the basal Clade B *SITs* in low silicic acid environments compared to waters with higher silicic acid levels. This is hypothesized to allow diatom species to co-occur by employing different approaches to utilize limited silicic acid, and to out-compete other silicifying groups (Durkin et al., 2016). It also suggests a certain "directionality" of diatom *SIT* evolution, with new *SIT* clades evolving in new lineages to adapt to the drawdown of ocean silicic acid concentrations that occurred as the diatoms themselves diversified and came to dominate the oceans (Sims et al., 2006; Finkel and Kotrc, 2010).

Silicon Transporter diversification has also occurred in other taxa (see **Figure 6C**), with some stramenopiles expressing multiple *SITs*, and evidence for independent duplications of *SIT-Ls* in both foraminifera (*Ammonia* sp.) and Phaeodarian radiolarians (Marron et al., 2016b). The most prevalent case of this is in the siliceous loricate choanoflagellates, which display evidence for a *SIT* gene duplication event early in their evolution (Leadbeater, 2015). All loricate choanoflagellates examined were found to possess two *SIT* gene types, termed *SITα* and *SITβ* (Marron et al., 2016b). Transcriptional analysis of these *SIT* types under varying silicic acid concentrations demonstrated that the *SITα* genes were highly expressed, and their expression levels responded to silicic acid availability, while the *SITβ* genes were always expressed at a low level, irrespective of the environmental silicic acid concentration. This closely resembles the situation in diatoms (see above), where some *SIT* genes are highly expressed and silicon-responsive, while other types have low expression unresponsive to silicon, suggesting that *SITα* and *SITβ* have evolved different roles, possibly as specialized transporters or silicon sensors (Thamatrakoln and Hildebrand, 2007; Shrestha and Hildebrand, 2015). The similar diversification and sub-functionalization of SITs in parallel in both choanoflagellates and diatoms is proposed to be an example of convergent evolution in response to increased competition for silicic acid. This mirrors the hypothesis for the convergent evolution of 10-transmembrane domain *SITs* in the stramenopiles (see above). It is likely that future research will identify other cases of transporter diversification due to increased competition for silicic acid, potentially in the multiple rhizarian *SIT-Ls*, horsetail silicon transporters or the proposed silicon-related *Lsi2*-like gene family found in the siliceous sponges (Grégoire et al., 2012; Marron et al., 2016b; Vivancos et al., 2016).

The phylogenetic distribution of silicon-related active transporters reveals evidence for multiple and widespread losses of *SIT*, *SIT-L,* and *Lsi2*-like genes throughout the eukaryotes (Marron et al., 2016b). There is strong evidence for the loss of *SIT-Ls* across most bilaterian lineages, of losses of *SITs* and *SIT-Ls* across the coccolithophorid haptophytes and for losses of *SITs* and SIT-Ls multiple times throughout the stramenopiles. Indeed, barring rampant eukaryote-to-eukaryote horizontal gene transfer events (Ku et al., 2015), it is likely that SITs and/or SIT-Ls were present in the last common ancestor of all eukaryotes, and that multiple independent gene loss events only occurred after the main eukaryotic lineages and supergroups had diverged. Similarly, the distribution of *Lsi2*-like genes across the eukaryotes strongly supports that they were present in the eukaryotic last common ancestor (Marron et al., 2016b), but that they were independently lost in multiple lineages, for example deuterostome eumetazoans, fungi or apicomplexans.

It has been hypothesized that these active silicon transporters were originally required as part of a detoxification mechanism for life in the high-silicon Precambrian ocean (Marron et al., 2016b). Geological evidence for abiotic silica precipitation in sediments from the Neoproterozoic demonstrates that at the time that the eukaryote supergroups were originating and diversifying (Parfrey et al., 2011) oceanic silicic acid concentrations were high enough to allow autopolymerization into silica (Iler, 1979; Maliva et al., 1989, 2005; Siever, 1992; Grenne and Slack, 2003). Uncontrolled formation of silica free in the cytoplasm, potentially mediated by localized pH environments or accelerated by polyamines, would cause massive disruption to cellular metabolism. Unprotected by a membrane the freely polymerizing silica could occlude and adsorb proteins, nucleic acids, and other macromolecules

within its structure or on its surface (e.g., Betancor and Luckarift, 2008; Vandeventer et al., 2013). Therefore organisms must have required a system for silicon homeostasis, to bind or sequester silicic acid within the cytoplasm and then remove it from the cell. This is reflected in the bidirectional transportation capacity of SITs, where they could be employed to transport silicon out of the cell against a concentration gradient (Thamatrakoln and Hildebrand, 2008; Knight et al., 2016). In ancient oceans there would have been a strong selective pressure to maintain a molecular machinery for silicon detoxification, as has also been suggested for the employment of mucins as anti-calcification mechanisms in early animals (Marin et al., 1996; Wood et al., 2017).

Major geochemical and biological upheavals around the Precambrian/Cambrian boundary changed the competitive interactions and evolutionary pressures acting on these detoxification and homeostasis mechanisms. Most notable was the appearance and diversification of biomineralized hard parts (Knoll, 2003; Knoll and Kotrc, 2015), believed to have originated by modification and co-opting of the detoxification mechanisms (Wood et al., 2017). The innovation of biomineralized structures for feeding, movement and protection established an evolutionary arms race (Knoll, 2003; Cohen, 2005). This gave rise to biomineralization becoming more significant, with organisms producing larger and more prominent calcified or silicified structures. The biosilicified structures would have acted as silicon sinks, with the burial of biogenic silica skeletons sequestering silicon in the sediments. The outcome of this was that by the early Phanerozoic oceanic silicic acid concentrations were substantially reduced from Neoproterozoic levels (Maliva et al., 1989; Racki and Cordey, 2000), below the threshold for autopolymerization and removing the threat of harmful silica precipitation free in the cytoplasm. This would have removed the selective pressure to possess silicon detoxification mechanisms, and organisms could gain a competitive advantage by not diverting resources to such an unnecessary metabolic pathway, hence resulting in gene losses. The exception were those organisms which had re-deployed the silicon homeostasis machinery to produce siliceous structures. In these cases, silicon became a scarce resource, requiring the evolution of more sophisticated transport systems in the acquiring of silicic acid uptake to meet the metabolic requirements of biosilicification. This reflects the evolutionary biology of other elements, where they are initially toxic, before becoming metabolically useful and finally ending up as limiting nutrients and the subject of evolutionary competition (Rickaby, 2015).

In some cases, the solution to the problem of this scarcity was to secondarily lose biosilicification and the associated molecular mechanisms. An excellent example of this occurs within the haptophytes. Some species, such as *Prymnesium neolepis* (Yoshida et al., 2006) and *S. apsteinii* (Drescher et al., 2012) produce wholly- or partially siliceous scales, while some calcareous species such as *Calcidiscus leptoporus* possess SIT-Ls and have a metabolic requirement for silicon to complete normal production of their calcified scales (Durak et al., 2016). Other species however, have lost SIT-Ls (and SITs), and show no effect of germanium toxicity disrupting biomineralization. One such species is *Emiliania huxleyi*, a calcifying haptophyte known to produce blooms of major ecological importance, and which is believed to have evolved relatively recently in the Cenozoic (Liu et al., 2010; Taylor et al., 2017). What is notable is that *E. huxleyi* blooms often occur following diatom blooms, raising the possibility that while diatoms enjoy a competitive advantage in silicon-replete waters, non-silicifying species like *E. huxleyi* have evolved to out-compete and succeed siliceous phytoplankton in silicon-deplete waters where they can continue to grow and produce biomineralized structures (Durak et al., 2016). In this way, the abandonment of any metabolic requirement for silicon opens new ecological niches and provides opportunities to gain new competitive advantages.

Molecular phylogenetics has revealed many other cases where non-silicifying species have evolved from heavily silicified ancestors. This is evident in land plants, with basal groups tending to be highly siliceous (e.g., liverworts) while some derived taxa (e.g., conifers) have low silicon contents and lack phytoliths (Hodson et al., 2005). Although there is some debate as to the evolutionary relationships between the main sponge groups (Sperling et al., 2010), the widespread distribution of non-siliceous species in otherwise siliceous sponge clades, and the similarity of the organic components of siliceous and collagenous skeletons, means that silicification was lost and/or re-evolved multiple times in the sponges (Ehrlich et al., 2007a,b; Maldonado, 2009; Kozhemyako et al., 2010). Similar evidence for independent losses and reinventions of biosilicification can be found in the centrohelids, a taxonomically enigmatic group of protists (Zlatogursky, 2016). Based on current phylogenetic data, centrohelids have evolved silicified structures ranging from scales to spines, but in some species these have been modified into organic-only scales and spines, or even been reduced so that the cell is covered only by a mucous sheath. Parallel evolution is also observed in the Arcellid testate amoebae, with convergent gains and losses of biosiliceous or organic tests (Lahr et al., 2013, 2015), or even the ability to form a test by agglutination of exogenous siliceous particles such as quartz grains, a strategy also developed by some coastal tintinnids.

A possible analog of the scenarios that saw these losses of biosilicification is the situation where silicification is facultative in some organisms (as opposed to the obligate silicification found in groups such as diatoms). This can occur under conditions of extreme silicon limitation, as in the tectiform choanoflagellates or synurophytes which produce naked, but otherwise healthy, cells if starved of silicon (Sandgren et al., 1996; Leadbeater, 2015). It may also be connected to stages in the life cycle, for example in juvenile brachiopods (Williams et al., 2001), or resembling in the haploid/diploid distinction between calcified and uncalcified stages of the *E. huxleyi* life cycle (Taylor et al., 2017) as has recently been suggested to occur in loricate choanoflagellates (Thomsen and Østergaard, 2017). The capacity for facultative silicification could be a combination of the two, as in the diatom *P. tricornutum*, unique amongst the diatoms in its ability to survive without a siliceous frustule. A combination of life cycle stage (Kessenich et al., 2014) and silicon availability (Yamada et al., 2014) has been put forward for explaining the evolution

of the naked bolidophytes and siliceous parmales. As these are the sister lineages to diatoms the molecular mechanisms regulating their biosilicification are crucial to understanding how the complex silicon-related metabolism of diatoms evolved.

We therefore observe how evolutionary competition and the associated trade-offs are central to the presence of silicification: biomineralized silica structures are only maintained when they confer a competitive advantage. Silicification would be lost when the total metabolic cost of biosilicification exceeds the benefit, for example due to the energetic cost of silicic acid acquisition or silica polymerization, restrictions on mobility due to the presence of a skeleton or the additional weight per unit volume of silica versus organic structures. Alternatively, it could be metabolically cheaper (either in cost of formation or of lifestyle trade-offs) to build a functionally equivalent structure from another biomineral (such as calcium phosphate or calcium carbonate shells), from organic components (e.g., chitin, cellulose, or collagen) or even to utilize the silica structures of other organisms (Lahr et al., 2015). Under this hypothesis these structures would provide similar competitive advantages, such as protection, while allowing survival in new (often silicon-depleted) niches. This could potentially lead to the loss of the molecular mechanisms for silicon transport and silica polymerization, producing a developmental legacy that restricts the potential for future evolutionary innovations, and reinforces the competitive interactions between silicifiers and non-silicifiers.

FUTURE DIRECTIONS

Recent years have witnessed several new discoveries that have expanded and improved our understanding of silica biomineralization. Fossil sampling and isotopic analyses of new sediment records have modified our view of the geological history of silicon biogeochemistry (Fontorbe et al., 2016). The massive increase in large-scale sequencing data has greatly aided research into the molecular biology of silica biomineralization, both through whole-genome sequencing within groups like diatoms and plants, and via transcriptome sequencing of new and previously poorly researched siliceous taxa (Keeling et al., 2014; Beisser et al., 2017; Caron et al., 2017; Tirichine et al., 2017). Many new genes associated with biosilicification have been identified (Kotzsch et al., 2016), including the recognition that active silicon transporter gene families are much more ancient and widely distributed amongst the eukaryotes than previously thought (Marron et al., 2016b). This has been complemented by the discovery of new silicifying species (Ichinomiya et al., 2011), most notably silicon accumulation in some strains of the hugely ecologically important cyanobacteria *Synechococcus* (Baines et al., 2012). Combined with metagenomic surveys and geochemical monitoring (Mutsuo et al., 2015; Sunagawa et al., 2015) it will be possible to gain a much deeper knowledge of the role of different marine groups in silicon biogeochemistry and how competitive interactions govern their ecology, distribution and response to changing climatic conditions (Mock et al., 2016).

These advances have contributed to hypotheses for a greater role of silicon in biology, for example in protein folding (Eglin et al., 2006). We are also beginning to recognize a link between phosphate transporters and silicic acid uptake in groups as disparate as cyanobacteria and mammals (Brzezinski et al., 2017; Ratcliffe et al., 2017) that may be underpinned by a more general system for metalloid metabolism (Bienert et al., 2007). This could contribute to satisfying metabolic requirements for silicon in taxa like phaeophyte brown algae, which are known to biosilicify (Mizuta and Yasui, 2012; Tarakhovskaya et al., 2012) but with no currently identified silicon transporter genes (Marron et al., 2016b). These observations blur the boundary between silicifying and non-silicifying species, illustrated by the requirement for silicon in processes such as haptophyte calcium carbonate formation (Durak et al., 2016), amorphous calcium carbonate formation in plant cystoliths (Gal et al., 2012) and in the early developmental stages of the vertebrate calcium phosphate skeleton (Carlisle, 1981); or given the uptake of silicic acid (Fuhrman et al., 1978) and presence of silicon transporters in apparently non-mineralizing species (e.g., *Florenciella*; Marron et al., 2016b). This has implications for understanding the evolution and competitive interactions between silicifiers and non-silicifiers in the living world.

AUTHOR CONTRIBUTIONS

All authors listed have made a substantial, direct, and intellectual contribution to the work, and approved it for publication.

ACKNOWLEDGMENTS

KH was funded by the European Research Council (Starter Grant ICY-LAB-678371) and a Royal Society University Research Fellowship.

AM was funded by the European Research Council (Advanced Investigator grant no. 247333) and a Wellcome Trust Senior Investigator Award to Raymond E. Goldstein (University of Cambridge, UK).

CB acknowledges funding from the ERC Advanced Award "Diatomite," the LouisD Foundation, the Gordon and Betty Moore Foundation, and the French Government "Investissements d'Avenir" programmes MEMO LIFE (ANR-10-LABX-54), PSL* Research University (ANR-1253 11-IDEX-0001-02), and OCEANOMICS (ANR-11-BTBR-0008). CB also thanks the Radcliffe Institute of Advanced Study at Harvard University for a Scholars Fellowship during the 2016-2017 academic year. This article is contribution number 70 of the *Tara* Oceans project.

BQ acknowledges funding by OSU Pytheas, EUROMARINE consortium, and Labex OT-Med (no. ANR-11-LABEX-0061) from the "Investissements d'Avenir" program of the French National Research Agency through the A*MIDEX project (no. ANR-11-IDEX-0001-02), as sponsors of the SILICAMICS workshop where initiation of this paper took place.

REFERENCES

Abelmann, A., Gersonde, R., Knorr, G., Zhang, X., Chapligin, B., Maier, E., et al. (2015). The seasonal sea-ice zone in the glacial Southern Ocean as a carbon sink. *Nat. Commun.* 6, 8136. doi: 10.1038/ncomms9136

Adl, S. M., Simpson, A. G. B., Lane, C. E., Lukeš, J., Bass, D., Bowser, S. S., et al. (2012). The revised classification of eukaryotes. *J. Eukaryot. Microbiol.* 59, 429–493. doi: 10.1111/j.1550-7408.2012.00644.x

Aitken, Z. H., Luo, S., Reynolds, S. N., Thaulow, C., and Greer, J. R. (2016). Microstructure provides insights into evolutionary design and resilience of *Coscinodiscus* sp. frustule. *Proc. Natl. Acad. Sci. U.S.A.* 113, 2017–2022. doi: 10.1073/pnas.1519790113

Araujo, M. B., and Rozenfeld, A. (2014). The geographic scaling of biotic interactions. *Ecography* 37, 406–415. doi: 10.1111/j.1600-0587.2013.00643.x

Armbrust, E. V., Berges, J. A., Bowler, C., Green, B. R., Martinez, D., Putnam, N. H., et al. (2004). The genome of the diatom *Thalassiosira pseudonana*: ecology, evolution, and metabolism. *Science* 306, 79–86. doi: 10.1126/science.1101156

Assmy, P., Henjes, J., Klaas, C., and Smetacek, V. (2007). Mechanisms determining species dominance in a phytoplankton bloom induced by the iron fertilization experiment EisenEx in the Southern Ocean. *Deep Sea Res. Part I Oceanogr. Res. Pap* 54, 340–362. doi: 10.1016/j.dsr.2006.12.005

Assmy, P., Smetacek, V., Montresor, M., Klaas, C., Henjes, J., et al. (2013). Thick-shelled, grazer-protected diatoms decouple ocean carbon and silicon cycles in the iron-limited Antarctic Circumpolar Current. *Proc. Natl. Acad. Sci. U.S.A.* 110, 20633–20638 doi: 10.1073/pnas.1309345110

Baines, S. B., Twining, B. S., Brzezinski, M. A., Krause, J. W., Vogt, S., Assael, D., et al. (2012). Significant silicon accumulation by marine picocyanobacteria. *Nat. Geosci.* 5, 886–891. doi: 10.1038/ngeo1641

Bateman, B. L., Vanderwal, J., Williams, S. E., and Johnson, C. N. (2012). Biotic interactions influence the projected distribution of a specialist mammal under climate change. *Divers. Distrib.* 18, 861–872. doi: 10.1111/j.1472-4642.2012.00922.x

Beisser, D., Graupner, N., Bock, C., Wodniok, S., Grossmann, L., Vos, M., et al. (2017). Comprehensive transcriptome analysis provides new insights into nutritional strategies and phylogenetic relationships of chrysophytes. *PeerJ* 5:e2832. doi: 10.7717/peerj.2832

Benoiston, A.-S., Ibarbalz, F. M., Bittner, L., Guidi, L., Jahn, O., Dutkiewicz, S., et al. (2017). The evolution of diatoms and their biogeochemical functions. *Proc. R. Soc. B Biol. Sci.* 372:20160397. doi: 10.1098/rstb.2016.0397

Betancor, L., and Luckarift, H. R. (2008). Bioinspired enzyme encapsulation for biocatalysis. *Trends Biotechnol.* 26, 566–572. doi: 10.1016/j.tibtech.2008.06.009

Biard, T., Stemmann, L., Picheral, M., Mayot, N., Vandromme, P., Hauss, H., et al. (2016). *In situ* imaging reveals the biomass of giant protists in the global ocean. *Nature* 532, 504–507. doi: 10.1038/nature17652

Bienert, G. P., Schüssler, M. D., and Jahn, T. P. (2007). Metalloids: essential, beneficial or toxic? Major intrinsic proteins sort it out. *Trends Biochem. Sci.* 33, 20–26. doi: 10.1016/j.tibs.2007.10.004

Bondoc, K. G. V., Heuschele, J., Gillard, J., Vyverman, W., and Pohnert, G. (2016). Selective silicate-directed motility in diatoms. *Nat. Commun.* 7:10540. doi: 10.1038/ncomms10540

Bork, P., Bowler, C., de Vargas, C., Gorsky, G., Karsenti, E., and Wincker, P. (2015). *Tara* Oceans studies plankton at planetary scale. *Science* 348, 873–873. doi: 10.1126/science.aac5605

Bowler, C., Allen, A. E., Badger, J. H., Grimwood, J., Jabbari, K., Kuo, A., et al. (2008). The *Phaeodactylum* genome reveals the evolutionary history of diatom genomes. *Nature* 456, 239–244. doi: 10.1038/nature07410

Brown, J. W., and Sorhannus, U. (2010). A molecular genetic timescale for the diversification of autotrophic stramenopiles (Ochrophyta): substantive underestimation of putative fossil ages. *PLoS ONE* 5:e12759. doi: 10.1371/journal.pone.0012759

Brunner, E., Richthammer, P., Ehrlich, H., Paasch, S., Simon, P., Ueberlein, S., et al. (2009). Chitin in biosilica chitin-based organic networks: an integral part of cell wall biosilica in the diatom *Thalassiosira pseudonana*. *Angew. Chem.* 48, 9724–9727. doi: 10.1002/anie.200905028

Brzezinski, M. A., Krause, J. W., Baines, S. B., Collier, J. L., Ohnemus, D. C., and Twining, B. S. (2017). Patterns and regulation of silicon accumulation in *Synechococcus* spp. *J. Phycol.* 53, 764–761. doi: 10.1111/jpy.12545

Campbell, R. G., Sherrb, E. N., Ashjian, C. J., Plourde, S., Sherrb, B. F., Hille, V., et al. (2009). Mesozooplanktonprey preference and grazing impact in the Western Arctic Ocean. *Deep Sea Res. Part II Top. Stud. Oceanogr.* 56, 1274–1289. doi: 10.1016/j.dsr2.2008.10.027

Carlisle, E. M. (1981). "Silicon in bone formation," in *Silicon and Siliceous Structures in Biological Systems*, eds T. L. Simpson and B. Volcani (New York, NY: Springer-Verlag), 69–94.

Caron, D. A., Alexander, H., Allen, A. E., Archibald, J. M., Armbrust, E. V., Bachy, C., et al. (2017). Probing the evolution, ecology and physiology of marine protists using transcriptomics. *Nat. Rev. Microbiol.* 15, 6–20. doi: 10.1038/nrmicro.2016.160

Cermeño, P., Falkowski, P. G., Romero, O. E., Schaller, M. F., and Vallina, S. M. (2015). Continental erosion and the Cenozoic rise of marine diatoms. *Proc. Natl. Acad. Sci. U.S.A.* 112, 4239–4244. doi: 10.1073/pnas.1412883112

Cohen, B. L. (2005). Not armour, but biomechanics, ecological opportunity and increased fecundity as keys to the origin and expansion of the mineralized benthic metazoan fauna. *Biol. J. Linn. Soc.* 85, 483–490. doi: 10.1111/j.1095-8312.2005.00507.x

Conley, D. J., Frings, P. J., Fontorbe, G., Clymans, W., Stadmark, J., Hendry, K. R., et al. (2017). Biosilicification drives a decline of dissolved Si in the oceans through geologic time. *Front. Mar. Sci.* 4:397. doi: 10.3389/fmars.2017.00397

Cooke, J., and Leishman, M. R. (2011). Is plant ecology more siliceous than we realise? *Trends Plant Sci.* 16, 61–68. doi: 10.1016/j.tplants.2010.10.003

Crombet, Y., Leblanc, K., Quéguiner, B., Moutin, T., Rimmelin, P., Ras, J., et al. (2011). Deep silicon maxima in the stratified oligotrophic Mediterranean Sea. *Biogeosciences* 8, 459–475. doi: 10.5194/bg-8-459-2011

Darley, W. M., and Volcani, B. E. (1969). Role of silicon in diatom metabolism: a silicon requirement for deoxyribonucleic acid synthesis in the diatom silicon requirement for DNA synthesis in the diatom *Cylindrotheca fusiformis* Reimann and Lewin. *Exp. Cell Res.* 58, 334–342. doi: 10.1016/0014-4827(69)90514-X

de la Rocha, C., Brzezinski, M. A., and DeNiro, M. J. (1997). Fractionation of silicon isotopes by marine diatoms during biogenic silica formation, *Geochim. Cosmochim. Acta* 61, 5051–5056. doi: 10.1016/S0016-7037(97)00300-1

de Vargas, C., Audic, S., Henry, N., Decelle, J., Mahé, F., Logares, R., et al. (2015). Eukaryotic plankton diversity in the sunlit ocean. *Science* 348:1261605. doi: 10.1126/science.1261605

Del Amo, Y., and Brzezinski, M. A. (1999). The chemical form of dissolved Si taken up by marine diatoms. *J. Phycol.* 35, 1162–1170. doi: 10.1046/j.1529-8817.1999.3561162.x

Derelle, R., López-García, P., Timpano, H., and Moreira, D. (2016). A phylogenomic framework to study the diversity and evolution of stramenopiles (=heterokonts). *Mol. Biol. Evol.* 33, 2890–2898. doi: 10.1093/molbev/msw168

Desouky, M., Jugdaohsingh, R., McCrohan, C. R., White, K. N., and Powell, J. J. (2002). Aluminum-dependent regulation of intracellular silicon in the aquatic invertebrate *Lymnaea stagnalis*. *Proc. Natl. Acad. Sci. U.S.A.* 99, 3394–3399. doi: 10.1073/pnas.062478699

Dougherty, L. F., Johnsen, S., Caldwell, R. L., and Marshall, N. J. (2014). A dynamic broadband reflector built from microscopic silica spheres in the "disco" clam *Ctenoides ales*. *J. R. Soc. Interface* 11:20140407. doi: 10.1098/rsif.2014.0407

Drescher, B., Dillaman, R. M., and Taylor, A. R. (2012). Coccolithogenesis in *Scyphosphaera apsteinii* (Prymnesiophyceae). *J. Phycol.* 48, 1343–1361. doi: 10.1111/j.1529-8817.2012.01227.x

Durak, G. M., Taylor, A. R., Walker, C. E., Probert, I., de Vargas, C., Audic, S., et al. (2016). A role for diatom-like silicon transporters in calcifying coccolithophores. *Nat. Commun.* 7:10543. doi: 10.1038/ncomms10543

Durkin, C. A., Koester, J. A., Bender, S. J., and Armbrust, E. V. (2016). The evolution of silicon transporters in diatoms. *J. Phycol.* 52, 716–734. doi: 10.1111/jpy.12441

Dvorák, P., Casamatta, D. A., Poulíčkov,á, A., Hašler, P., Ondrej, V., and Sanges, R. (2014). *Synechococcus*: 3 billion years of global dominance. *Mol. Ecol.* 23, 5538–5551, doi: 10.1111/mec.12948

Egan, K., Rickaby, R. E. M., Hendry, K. R., and Halliday, A. N. (2013). Opening the gateways for diatoms primes Earth for Antarctic glaciation. *Earth Planet. Sci. Lett.* 375, 34–43. doi: 10.1016/j.epsl.2013.04.030

Eglin, D., Shafran, K. L., Livage, J., Coradin, T., and Perry, C. C. (2006). Comparative study of the influence of several silica precursors on collagen

self-assembly and of collagen on Si speciation and condensation. *J. Mater. Chem.* 16, 4220–4230. doi: 10.1039/B606270A

Ehrlich, H., Heinemann, S., Heinemann, C., Simon, P., Tabachnick, K. R., Bazhenov, V. V., et al. (2008). Nanostructural organization of naturally occurring composites - Part I: silica-collagen-based biocomposites. *J. Nanomater.* 2008:623838. doi: 10.1155/2008/623838

Ehrlich, H., Krautter, M., Hanke, T., Simon, P., Knieb, C., Heinemann, S., et al. (2007a). First evidence of the presence of chitin in skeletons of marine sponges - Part II: glass sponges (Hexactinellida: Porifera). *Biophys. J.* 308, 473–483. doi: 10.1002/jez.b.21174

Ehrlich, H., Maldonado, M., Spindler, K., Eckert, C., Hanke, T., and Born, R. (2007b). First evidence of chitin as a component of the skeletal fibers of marine sponges. Part, I. Verongidae (Demospongia : Porifera). *J. Exp. Zool. B. Mol. Dev. Evol.* 308B, 347–356. doi: 10.1002/jez.b.21156

Ensikat, H.-J., Geisler, T., and Weigend, M. (2016). A first report of hydroxylated apatite as structural biomineral in Loasaceae-plants' teeth against herbivores. *Sci. Rep.* 6:26073. doi: 10.1038/srep26073

Feng, L., and Frommer, W. B. (2015). Structure and function of SemiSWEET and SWEET sugar transporters. *Trends Biochem. Sci.* 40, 480–486. doi: 10.1016/j.tibs.2015.05.005

Finkel, Z. V., and Kotrc, B. (2010). Silica use through time: macroevolutionary change in the morphology of the diatom fustule. *Geomicrobiol. J.* 27, 596–608. doi: 10.1080/01490451003702941

Finkel, Z. V., Katz, M. E., Wright, J. D., Schofieid, O. M., and Falkowski, P. G. (2005). Climatically driven macroevolutionary patterns in the size of marine diatoms over the Cenozoic. *Proc. Natl. Acad. Sci. U.S.A.* 102, 8927–8932. doi: 10.1073/pnas.0409907102

Finkel, Z. V., Matheson, K. A., Regan, K. S., and Irwin, A. J. (2010). Genotypic and phenotypic variation in diatom silicification under paleo-oceanographic conditions. *Geobiology* 8, 433–445. doi: 10.1111/j.1472-4669.2010.00250.x

Foissner, W., Weissenbacher, B., Krautgartner, W.-D., and Lütz-Meindl, U. (2009). A cover of glass: first report of biomineralized silicon in a ciliate, *Maryna umbrellata* (Ciliophora: Colpodea). *J. Eukaryot. Microbiol.* 56, 519–530. doi: 10.1111/j.1550-7408.2009.00431.x

Fontorbe, G., Frings, P. J., De La Rocha, C. L., Hendry, K. R., and Conley, D. J. (2016). A silicon depleted North Atlantic since the Palaeogene: evidence from sponge and radiolarian silicon isotopes. *Earth Planet. Sci. Lett.* 453, 67–77. doi: 10.1016/j.epsl.2016.08.006

Fontorbe, G., Frings, P. J., De La Rocha, C. L., Hendry, K. R., and Conley, D. J. (2017). Enrichment of dissolved silica in the deep Equatorial Pacific during the Eocene-Oligocene. *Paleoceanography*, 32, 848–863. doi: 10.1002/2017PA003090

Friedrichs, L., Hörnig, M., Schulze, L., Bertram, A., Jansen, S., and Hamm, C. (2013). Size and biomechanic properties of diatom frustules influence food uptake by copepods. *Mar. Ecol. Prog. Ser.* 481, 41–51. doi: 10.3354/meps10227

Fuhrman, J., Chisholm, S., and Guillard, R. (1978). Marine alga *Platymonas* sp. accumulates silicon without apparent requirement. *Nature* 272, 244–246. doi: 10.1038/272244a0

Fuhrmann, T., Landwehr, S., El Rharbl-Kucki, M., and Sumper, M. (2004). Diatoms as living photonic crystals. *Appl. Phys. B Lasers Opt.* 78, 257–260. doi: 10.1007/s00340-004-1419-4

Gal, A., Hirsch, A., Siegel, S., Li, C., Aichmayer, B., Politi, Y., et al. (2012). Plant cystoliths : a complex functional biocomposite of four distinct silica and amorphous calcium carbonate phases. *Chem. A Eur. J.* 18, 10262–10270. doi: 10.1002/chem.201201111

Garbuzov, M., Reidinger, S., and Hartley, S. E. (2011). Interactive effects of plant-available soil silicon and herbivory on competition between two grass species. *Ann. Bot.* 108, 1355–1363. doi: 10.1093/aob/mcr230

Gause, G. F. (1934). Experimental analysis of Vito Volterra's mathematical theory of the struggle for existence. *Science* 79, 16–17.

Gong, N., Wiens, M., Schröder, H. C., Mugnaioli, E., Kolb, U., and Müller, W. E. G. (2010). Biosilicification of loricate choanoflagellate: organic composition of the nanotubular siliceous costal strips of *Stephanoeca diplocostata*. *J. Exp. Biol.* 213, 3575–3585. doi: 10.1242/jeb.048496

Gordon, R., Losic, D., Tiffany, M. A., Nagy, S. S., and Sterrenburg, F. A. (2009). The Glass Menagerie: diatoms for novel applications in nanotechnology. *Trends Biotechnol.* 27, 116–127. doi: 10.1016/j.tibtech.2008.11.003

Gotelli, N. J., Graves, G. R., and Rahbek, C. (2010). Macroecological signals of species interactions in the Danish avifauna. *Proc. Natl. Acad. Sci. U.S.A.* 107, 5030–5035. doi: 10.1073/pnas.0914089107

Gravel, D., Massol, F., Canard, E., Mouillot, D., and Mouquet, N. (2011). Trophictheory of island biogeography. *Ecol. Lett.* 14, 1010–1016. doi: 10.1111/j.1461-0248.2011.01667.x

Green, J. L., Bohannan, B. J. M., and Whitaker, R. J. (2008). Microbial biogeography: from taxonomy to traits. *Science* 320, 1039–1043. doi: 10.1126/science.1153475

Grégoire, C., Rémus-Borel, W., Vivancos, J., Labbé, C., Belzile, F., and Bélanger, R. R. (2012). Discovery of a multigene family of aquaporin silicon transporters in the primitive plant *Equisetum arvense*. *Plant J.* 72, 320–330. doi: 10.1111/j.1365-313X.2012.05082.x

Grenne, T., and Slack, J. F. (2003). Paleozoic and Mesozoic silica-rich seawater: evidence from hematitic chert (jasper) deposits. *Geology* 31, 319–322. doi: 10.1130/0091-7613(2003)031<0319:PAMSRS>2.0.CO;2

Gunnarsson, I., and Arnórsson, S. (2000). Amorphous silica solubility and the thermodynamic properties of H_4SiO_4 in the range of 0° to 350°C at P_{sat}. *Geochim. Cosmochim. Acta* 64, 2295–2307. doi: 10.1016/S0016-7037(99)00426-3

Hamm, C. E., Merkel, R., Springer, O., and Jurkojc, P. (2003). Architecture and material properties of diatom shells provide effective mechanical protection. *Nature* 421, 841–843. doi: 10.1038/nature01416

Hamm, C., and Smetacek, V. (2007). "Armor: why, when, and how," in *Evolution of Primary Producers in the Sea*, eds P. Falkowski and A. H. Knoll (Amsterdam: Elsevier), 311–332.

Hardin, G. (1960). The competitive exclusion principle. *Science* 131, 1292–1297. doi: 10.1126/science.131.3409.1292

Harper, H. E., and Knoll, A. H. (1975). Silica, diatoms, and cenozoic radiolarian evolution. *Geology* 3, 175–177. doi: 10.1130/0091-7613(1975)3<175:SDACRE>2.0.CO;2

Hartley, S. E., DeGabriel, J. L., and Cooke, J. (2016). The ecology of herbivore-induced silicon defences in grasses. *Funct. Ecol.* 30, 1311–1322. doi: 10.1111/1365-2435.12706

He, H., Veneklaas, E. J., Kuo, J., and Lambers, H. (2014). Physiological and ecological significance of biomineralization in plants. *Trends Plant Sci.* 19, 166–174. doi: 10.1016/j.tplants.2013.11.002

Hecky, R. E., Mopper, K., Kilham, P., and Degens, E. T. (1973). The amino acids and sugar composition of diatom cell-walls. *Mar. Biol.* 19, 323–331. doi: 10.1007/BF00348902

Hendry, K. R., and Robinson, L. F. (2012). The relationship between silicon isotope fractionation in sponges and silicic acid concentration: modern and core-top studies of biogenic opal. *Geochim. Cosmochim. Acta* 81, 1–12. doi: 10.1016/j.gca.2011.12.010

Hendry, K. R., Robinson, L. F., McManus, J. F., and Hays, J. D. (2014). Silicon isotopes indicate enhanced carbon export efficiency in the North Atlantic during deglaciation. *Nat. Commun.* 5, 3107. doi: 10.1038/ncomms4107

Hildebrand, M., Dahlin, K., and Volcani, B. E. (1998). Characterization of a silicon transporter gene family in *Cylindrotheca fusiformis*: sequences, expression analysis, and identification of homologs in other diatoms. *Mol. Gen. Genet.* 260, 480–486. doi: 10.1007/s004380050920

Hildebrand, M., Volcani, B. E., Gassman, W., and Schroeder, J. (1997). A gene family of silicon transporters. *Nature* 385, 688–689. doi: 10.1038/385688b0

Hodson, M. J., White, P. J., Mead, A., and Broadley, M. R. (2005). Phylogenetic variation in the silicon composition of plants. *Ann. Bot.* 96, 1027–1046. doi: 10.1093/aob/mci255

Hortal, J., de Bello, F., Diniz-Filho, J. A. F., Lewinsohn, T. M., Lobo, J. M., and Ladle, R. J. (2015). Seven shortfalls that beset large-scale knowledge of biodiversity. *Annu. Rev. Ecol. Evol. Syst.* 46, 523–549. doi: 10.1146/annurev-ecolsys-112414-054400

Ichinomiya, M., Yoshikawa, S., Kamiya, M., Ohki, K., Takaichi, S., and Kuwata, A. (2011). Isolation and characterization of parmales (Heterokonta/Heterokontophyta/Stramenopiles) from the Oyashio Region, Western North Pacific. *J. Phycol.* 47, 144–151. doi: 10.1111/j.1529-8817.2010.00926.x

Iler, R. K. (1979). *The Chemistry of Silica*. New York, NY: Wiley.

Ingalls, A. E., Whitehead, K., and Bridoux, M. C. (2010). Tinted windows: the presence of the UV absorbing compounds called mycosporine-like amino acids

embedded in the frustules of marine diatoms. *Geochim. Cosmochim. Acta* 74, 104–115. doi: 10.1016/j.gca.2009.09.012

Itoh, K. (1970). A consideration on feeding habits of planktonic copepods in relation to the structure of their oral parts. *Bull. Plankton Soc. Japan* 17: 1–10.

Karsenti, E., Acinas, S. G., Bork, P., Bowler, C., De Vargas, C., Raes, J., et al. (2011). A holistic approach to marine eco-systems biology. *PLoS Biol.* 9:e1001177. doi: 10.1371/journal.pbio.1001177

Keeling, P. J., Burki, F., Wilcox, H. M., Allam, B., Allen, E. E., Amaral-Zettler, L. A., et al. (2014). The marine microbial eukaryote transcriptome sequencing project (MMETSP): illuminating the functional diversity of eukaryotic life in the oceans through transcriptome sequencing. *PLoS Biol.* 12:e1001889. doi: 10.1371/journal.pbio.1001889

Keller, R., Ziegler, C., and Schneider, D. (2014). When two turn into one: evolution of membrane transporters from half modules. *Biol. Chem.* 395, 1379–1388. doi: 10.1515/hsz-2014-0224

Kessenich, C. R., Ruck, E. C., Schurko, A. M., Wickett, N. J., and Alverson, A. J. (2014). Transcriptomic insights into the life history of bolidophytes, the sister lineage to diatoms. *J. Phycol.* 50, 977–983. doi: 10.1111/jpy.12222

Kidder, D. L., and Tomescu, I. (2016). Biogenic chert and the Ordovician silica cycle. *Palaeogeogr. Palaeoclimatol. Palaeoecol.* 458, 29–38. doi: 10.1016/j.palaeo.2015.10.013

Knight, M. J., Senior, L., Nancolas, B., Ratcliffe, S., and Curnow, P. (2016). Direct evidence of the molecular basis for biological silicon transport. *Nat. Commun.* 7:11926. doi: 10.1038/ncomms11926

Knoll, A. H. (2003). "Biomineralization and evolutionary history," in *Reviews in Mineralogy and Geochemistry: Biomineralization*, eds P. M. Dove, J. J. Deyoreo, and S. Weiner (Washington, DC: Mineralogical Society of America), 329–356.

Knoll, A. H., and Follows, M. J. (2016). A bottom-up perspective on ecosystem change in Mesozoic oceans. *Proc. R. Soc. B* 283:20161755. doi: 10.1098/rspb.2016.1755

Knoll, A. H., and Kotrc, B. (2015). "Protistan skeletons: a geologic history of evolution and constraint," in *Evolution of Lightweight Structures*, ed C. Hamm (Dordrecht: Springer), 1–16.

Kotrc, B., and Knoll, A. H. (2015). A morphospace of planktonic marine diatoms. I. Two views of disparity through time. *Paleobiology* 41, 45–67. doi: 10.1017/pab.2014.4

Kotzsch, A., Pawolski, D., Milentyev, A., Shevchenko, A., Scheffel, A., Poulsen, N., et al. (2016). Biochemical composition and assembly of biosilica-associated insoluble organic matrices from the diatom *Thalassiosira pseudonana*. *J. Biol. Chem.* 291, 4982–4997. doi: 10.1074/jbc.M115.706440

Kouchinsky, A., Bengtson, S., Runnegar, B., Skovsted, C., Steiner, M., and Vendrasco, M. (2011). Chronology of early Cambrian biomineralization. *Geol. Mag.* 149, 221–251. doi: 10.1017/S0016756811000720

Kozhemyako, V. B., Veremeichik, G. N., Shkryl, Y. N., Kovalchuk, S. N., Krasokhin, V. B., Rasskazov, V. A., et al. (2010). Silicatein genes in spicule-forming and nonspicule-forming Pacific demosponges. *Mar. Biotechnol.* 12, 403–409. doi: 10.1007/s10126-009-9225-y

Krabberød, A. K., Bråte, J., Dolven, J. K., Ose, R. F., Klaveness, D., Kristensen, T., et al. (2011). Radiolaria divided into Polycystina and Spasmaria in combined 18S and 28S rDNA phylogeny. *PLoS ONE* 6:e23526. doi: 10.1371/journal.pone.0023526

Kröger, N., Deutzmann, R., Bergsdorf, C., and Sumper, M. (2000). Species-specific polyamines from diatoms control silica morphology. *Proc. Natl. Acad. Sci. U.S.A* 97, 14133–14138. doi: 10.1073/pnas.260496497

Kröger, N., Lorenz, S., Brunner, E., and Sumper, M. (2002). Self-assembly of highly phosphorylated silaffins and their function in biosilica morphogenesis. *Science* 298, 584–586. doi: 10.1126/science.1076221

Ku, C., Nelson-sathi, S., Roettger, M., Sousa, F. L., Lockhart, P. J., Bryant, D., et al. (2015). Endosymbiotic origin and differential loss of eukaryotic genes. *Nature* 524, 427–437. doi: 10.1038/nature14963

Kunitomo, Y., Sarashina, I., Iijima, M., Endo, K., and Sashida, K. (2006). Molecular phylogeny of acantharian and polycystine radiolarians based on ribosomal DNA sequences, and some comparisons with data from the fossil record. *Eur. J. Protistol.* 42, 143–153. doi: 10.1016/j.ejop.2006.04.001

Lahr, D. J. G., Bosak, T., Lara, E., and Mitchell, E. A. D. (2015). The Phanerozoic diversification of silica-cycling testate amoebae and its possible links to changes in terrestrial ecosystems. *PeerJ* 3:e1234. doi: 10.7717/peerj.1234

Lahr, D. J. G., Grant, J. R., and Katz, L. A. (2013). Multigene phylogenetic reconstruction of the tubulinea (Amoebozoa) corroborates four of the six major lineages, while additionally revealing that shell composition does not predict phylogeny in the arcellinida. *Protist* 164, 323–339. doi: 10.1016/j.protis.2013.02.003

Lazarus, D. B., Kotrc, B., Wulf, G., and Schmidt, D. N. (2009). Radiolarians decreased silicification as an evolutionary response to reduced Cenozoic ocean silica availability. *Proc. Natl. Acad. Sci. U.S.A.* 106, 9333–9338. doi: 10.1073/pnas.0812979106

Lazarus, D., Barron, J., Renaudie, J., Diver, P., and Türke, A. (2014). Cenozoic planktonic marine diatom diversity and correlation to climate change. *PLoS ONE* 9:e84857. doi: 10.1371/journal.pone.0084857

Leadbeater, B. S. C. (2015). *The Choanoflagellates: Evolution, Biology and Ecology*. Cambridge: Cambridge University Press.

Leadbeater, B. S. C., Yu, Q., Kent, J., and Stekel, D. J. (2009). Three-dimensional images of choanoflagellate loricae. *Proc. R. Soc. B Biol. Sci.* 276, 3–11. doi: 10.1098/rspb.2008.0844

Leblanc, K., Leynaert, A., Fernandez, I. C., Rimmelin, P., Moutin, T., Raimbault, P., et al. (2005). A seasonal study of diatom dynamics in the North Atlantic during the POMME experiment (2001): evidence for Si limitation of the spring bloom. *J. Geophys. Res.* 110:C07S14. doi: 10.1029/2004JC002621

Leblanc, K., Quéguiner, B., Garcia, N., Rimmelin, P., and Raimbault, P. (2003). Silicon cycle in the NW Mediterranean Sea: seasonal study of a coastal oligotrophic site. *Oceanol. Acta* 26, 339–355. doi: 10.1016/S0399-1784(03)00035-5

Lebour, M. V. (1922). The food of plankton organisms. *J. Mar. Biol. Assoc. U. K.* 12, 644–677. doi: 10.1017/S0025315400009681

Lee, R. E., and Kugrens, P. (1989). Biomineralization of the stalks of *Anthophysa vegetans*. *J. Phycol.* 25, 591–596. doi: 10.1111/j.1529-8817.1989.tb00265.x

Lepot, K., Addad, A., Knoll, A. H., Wang, J., Troadec, D., Béché, A., et al. (2017). Iron minerals within specific microfossil morphospecies of the 1.88 Ga Gunflint Formation. *Nat. Commun.* 8:14890. doi: 10.1038/ncomms14890

Lima-Mendez, G., Faust, K., Henry, N., Decelle, J., Colin, S., Carcillo, F., et al. (2015). Determinants of community structure in the global plankton interactome. *Science* 348:1262073 doi: 10.1126/science.1262073

Liu, H., Aris-Brosou, S., Probert, I., and De Vargas, C. (2010). A time line of the environmental genetics of the haptophytes. *Mol. Biol. Evol.* 27, 161–176. doi: 10.1093/molbev/msp222

Lobel, K. D., West, J. K., and Hench, L. L. (1996). Computational model for protein-mediated biomineralization of the diatom frustule. *Mar. Biol.* 126, 353–360. doi: 10.1007/BF00354617

Lopez, P. J., Desclés, J., Allen, A. E., and Bowler, C. (2005). Prospects in diatom research. *Curr. Opin. Biotechnol.* 16, 180–186. doi: 10.1016/j.copbio.2005.02.002

Losic, D., Rosengarten, G., Mitchell, J. G., and Voelcker, N. H. (2006). Pore architecture of diatom frustules: potential nanostructured membranes for molecular and particle separations. *J. Nanosci. Nanotechnol.* 6, 982–989. doi: 10.1166/jnn.2006.174

Ludwig, M., Lind, J., Miller, E., and Wetherbee, R. (1996). High molecular mass glycoproteins associated with the siliceous scales and bristles of *Mallomonas splendens* (Synurophyceae) may be involved in cell surface development and maintenance. *Planta* 199, 219–228. doi: 10.1007/BF00196562

MacArthur, R. H. (1972). *Geographical Ecology: Patterns in the Distribution of Species*. Princeton, NJ: Princeton University Press.

Maldonado, M. (2009). Embryonic development of verongid demosponges supports the independent acquisition of spongin skeletons as an alternative to the siliceous skeleton of sponges. *Biol. J. Linn. Soc.* 97, 427–447. doi: 10.1111/j.1095-8312.2009.01202.x

Maldonado, M., Carmona, M. C., and Cruzado, A. (1999). Decline in Mesozoic reef-building in sponges explained by silicon limitation. *Nature* 401, 785–788. doi: 10.1038/44560

Maldonado, M., Navarro, L., Grasa, A., Gonzalez, A., and Vaquerizo, I. (2011). Silicon uptake by sponges: a twist to understanding nutrient cycling on continental margins. *Sci. Rep.* 1:30. doi: 10.1038/srep00030

Maliva, R. G., Knoll, A. H., and Siever, R. (1989). Secular change in chert distribution: a reflection of evolving biological participation in the silica cycle. *Palaois* 4, 513–532. doi: 10.2307/3514743

Maliva, R. G., Knoll, A. H., and Simonson, B. M. (2005). Secular change in the Precambrian silica cycle: insights from chert petrology. *Geol. Soc. Am. Bull.* 117, 835–845. doi: 10.1130/B25555.1

Malviya, S., Scalco, E., Audic, S., Vincent, F., Veluchamy, A., Poulain, J., et al. (2016). Insights into global diatom distribution and diversity in the world's ocean. *Proc. Natl. Acad. Sci.* 113, E1516–E1525. doi: 10.1073/pnas.1509523113

Mann, S. (2001). *Biomineralization. Principles and Concepts in Bioinorganic Materials Chemistry*. Oxford: Oxford University Press.

Marin, F., Smith, M., Isa, Y., Muyzer, G., and Westbroek, P. (1996). Skeletal matrices, muci, and the origin of invertebrate calcification. *Proc. Natl. Acad. Sci. U.S.A.* 93, 1554–1559. doi: 10.1073/pnas.93.4.1554

Marron, A. O., Chappell, H., Ratcliffe, S., and Goldstein, R. E. (2016a). A model for the effects of germanium on silica biomineralization in choanoflagellates. *J. R. Soc. Interface* 13:20160485. doi: 10.1098/rsif.2016.0485

Marron, A. O., Ratcliffe, S., Wheeler, G. L., Goldstein, R. E., King, N., Not, F., et al. (2016b). The evolution of silicon transport in eukaryotes. *Mol. Biol. Evol.* 33, 3226–3248. doi: 10.1093/molbev/msw209

Marshall, S. M., and Orr, A. P. (1955). *The Biology of a Marine Copepod, Calanus finmarchicus (Gunnerus)*. London: Oliver and Boyd.

Martin-Jézéquel, V., Hildebrand, M., and Brzezinski, M. A. (2000). Silicon metabolism in diatoms: implications for growth. *J. Phycol.* 36, 821–840. doi: 10.1046/j.1529-8817.2000.00019.x

Massey, F. P., Ennos, A. R., and Hartley, S. U. E. E. (2006). Silica in grasses as a defence against insect herbivores: contrasting effects on folivores and a phloem feeder. *J. Anim. Ecol.* 75, 595–603. doi: 10.1111/j.1365-2656.2006.01082.x

Matsunaga, S., Sakai, R., Jimbo, M., and Kamiya, H. (2007). Long-chain polyamines (LCPAs) from marine sponge: possible implication in spicule formation. *Chembiochem* 8, 1729–1735. doi: 10.1002/cbic.200700305

Michels, J., Vogt, J., and Gorb, S. N. (2012). Tools for crushing diatoms–opal teeth in copepods feature a rubber-like bearing composed of resilin. *Sci. Rep.* 2: 465. doi: 10.1038/srep00465

Miller, C. B., Nelson, D. M., Guillard, R. R. L., and Woodward, B. L. (1980). Effects of media with low silicic acid concentrations on tooth formation in *Acartia tonsa* (Copepoda, Calanoida). *Biol. Bull.* 159, 349–363. doi: 10.2307/1541099

Miller, C. B., Nelson, D. M., Weiss, C., and Soeldner, A. H. (1990). Morphogenesis of opal teeth in calanoid copepods. *Mar. Biol.* 106, 91–101. doi: 10.1007/BF02114678

Milligan, A. J., and Morel, F. M. M. (2002). A proton buffering role for silica in diatoms. *Science* 297, 1848–1850. doi: 10.1126/science.1074958

Misra, S., and Froelich, P. N. (2012). Lithium isotope history of Cenozoic seawater: changes in silicate weathering and reverse weathering. *Science* 335, 818–823. doi: 10.1126/science.1214697

Mizuta, H., and Yasui, H. (2012). Protective function of silicon deposition in *Saccharina japonica* sporophytes (Phaeophyceae). *J. Appl. Phycol.* 24, 1177–1182. doi: 10.1007/s10811-011-9750-8

Mock, T., Daines, S. J., Geider, R., Collins, S., Metodiev, M., Millar, A. J., et al. (2016). Bridging the gap between omics and earth system science to better understand how environmental change impacts marine microbes. *Glob. Chang. Biol.* 22, 61–75. doi: 10.1111/gcb.12983

Mock, T., Samanta, M. P., Iverson, V., Berthiaume, C., Robison, M., Holtermann, K., et al. (2008). Whole-genome expression profiling of the marine diatom *Thalassiosira pseudonana* identifies genes involved in silicon bioprocesses. *Proc. Natl. Acad. Sci. U.S.A.* 105, 1579–1584. doi: 10.1073/pnas.0707946105

Monniot, F. O., Martojai, R., and Monniot, C. (1992). Silica distribution in ascidian ovaries, a tool for systematics. *Systematics* 20, 541–552. doi: 10.1016/0305-1978(92)90008-2

Moreira, D., von der Heyden, S., Bass, D., López-García, P., Chao, E., and Cavalier-Smith, T. (2007). Global eukaryote phylogeny: combined small- and large-subunit ribosomal DNA trees support monophyly of Rhizaria, Retaria and Excavata. *Mol. Phylogenet. Evol.* 44, 255–266. doi: 10.1016/j.ympev.2006.11.001

Morueta-Holme, N., Blonder, B., Sandel, B., McGill, B. J., Peet, R. K., Ott, J. E., et al. (2016). A network approach for inferring species associations from co-occurrence data. *Ecography* 39, 1139–1150. doi: 10.1111/ecog.01892

Mutsuo, I., Lopes dos Santos, A., Gourvil, P., Yoshikawa, S., Kamiya, M., Ohki, K., et al. (2015). Diversity and oceanic distribution of Parmales and Bolidophyceae, a picoplankton group closely related to diatoms. *ISMEJ* 10, 2419–2434. doi: 10.1038/ismej.2016.38

Nakov, T., Ashworth, M., and Theriot, E. C. (2014). Comparative analysis of the interaction between habitat and growth form in diatoms. *ISME J.* 9, 246–255. doi: 10.1038/ismej.2014.108

Nesbit, K. T., and Roer, R. D. (2016). Silicification of the medial tooth in the blue crab *Callinectes sapidus*. *J. Morphol.* 277, 1648–1660. doi: 10.1002/jmor.20614

Neumann, D., and zur Nieden, U. (2001). Silicon and heavy metal tolerance of higher plants. *Phytochemistry* 56, 685–692. doi: 10.1016/S0031-9422(00)00472-6

Nomura, M., and Ishida, K. (2016). Fine-structural observations on siliceous scale production and shell assembly in the testate amoeba *Paulinella chromatophora*. *Protist* 167, 303–318. doi: 10.1016/j.protis.2016.05.002

Parfrey, L. W., Lahr, D. J. G., Knoll, A. H., and Katz, L. A. (2011). Estimating the timing of early eukaryotic diversification with multigene molecular clocks. *Proc. Natl. Acad. Sci. U.S.A.* 108, 13624–13629. doi: 10.1073/pnas.1110633108

Platt, T., White, G. N. III., Zhai, L., Sathyendranath, S., and Roy, S. (2009). The phenology of phytoplankton blooms: ecosystem indicators from remote sensing. *Ecol. Modell.* 220, 3057–3069. doi: 10.1016/j.ecolmodel.2008.11.022

Polet, S., Berney, C., Fahrni, J., and Pawlowski, J. (2004). Small-subunit ribosomal RNA gene sequences of Phaeodarea challenge the monophyly of Haeckel's Radiolaria. *Protist* 155, 53–63. doi: 10.1078/1434461000164

Pondaven, P., Gallinari, M., Chollet, S., Bucciarelli, E., Sarthou, G., Schultes, S., et al. (2007). Grazing-induced changes in cell wall silicification in a marine diatom. *Protist* 158, 21–28. doi: 10.1016/j.protis.2006.09.002

Poulsen, N., and Kröger, N. (2004). Silica morphogenesis by alternative processing of silaffins in the diatom *Thalassiosira pseudonana*. *J. Biol. Chem.* 279, 42993–42999. doi: 10.1074/jbc.M407734200

Preisig, H. R. (1994). Siliceous structures and silicification in flagellated protists. *Protoplasma* 181, 29–42. doi: 10.1007/BF01666387

Quéguiner, B. (2013). Iron fertilization and the structure of planktonic communities in high nutrient regions of the Southern Ocean. *Deep Sea Res. Part II Top. Stud. Oceanogr.* 90, 43–54. doi: 10.1016/j.dsr2.2012.07.024

Racki, G., and Cordey, F. (2000). Radiolarian palaeoecology and radiolarites: is the present the key to the past? *Earth Sci. Rev.* 52, 83–120. doi: 10.1016/S0012-8252(00)00024-6

Ratcliffe, S., Jugdaohsingh, R., Vivancos, J., Marron, A., Deshmukh, R., Ma, J. F., et al. (2017). Identification of a mammalian silicon transporter. *Am. J. Physiol. Cell Physiol.* 312, C550–C561. doi: 10.1152/ajpcell.00219.2015

Ratti, S., Knoll, A. H., and Giordano, M. (2013). Grazers and phytoplankton growth in the oceans: an experimental and evolutionary perspective. *PLoS ONE* 8:e77349. doi: 10.1371/journal.pone.0077349

Raven, J. A. (1983). The transport and function of silicon in plants. *Biol. Rev.* 58, 179–207. doi: 10.1111/j.1469-185X.1983.tb00385.x

Raven, J. A., and Knoll, A. H. (2010). Non-skeletal biomineralization by eukaryotes: matters of moment and gravity. *Geomicrobiol. J.* 27, 572–584. doi: 10.1080/01490451003702990

Raven, J. A., and Waite, A. M. (2004). The evolution of silicification in diatoms: inescapable sinking and sinking as escape? *New Phytol.* 162, 45–61. doi: 10.1111/j.1469-8137.2004.01022.x

Renaudie, J. (2016). Quantifying the Cenozoic marine diatom deposition history: links to the C and Si cycles. *Biogeosciences* 13, 6003–6014. doi: 10.5194/bg-13-6003-2016

Rickaby, R. E. M. (2015). Goldilocks and the three inorganic equilibria: how Earth's chemistry and life coevolve to be nearly in tune. *Philos. Trans. R. Soc. A* 373:20140188. doi: 10.1098/rsta.2014.0188

Romann, J., Valmalette, J.-C., Chauton, M. S., Tranell, G., Einarsrud, M.-A., and Vadstein, O. (2015). Wavelength and orientation dependent capture of light by diatom frustule nanostructures. *Sci. Rep.* 5:17403. doi: 10.1038/srep17403

Sandgren, C. D., Hall, S. A., and Barlow, S. B. (1996). Siliceous scale production in chrysophyte and synurophyte algae.1. Effects of silica-limited growth on cell silica content, scale morphology, and the construction of the scale layer of *Synura petersenii*. *J. Phycol.* 32, 675–692. doi: 10.1111/j.0022-3646.1996.00675.x

Sapriel, G., Quinet, M., Heijde, M., Jourdren, L., Tanty, V., and Luo, G. (2009). Genome-wide transcriptome analyses of silicon metabolism in *Phaeodactylum tricornutum* reveal the multilevel regulation of silicic acid transporters. *PLoS ONE* 4:e7458. doi: 10.1371/journal.pone.0007458

Schaller, J., Brackhage, C., Bäucker, E., and Dudel, E. G. (2013). UV-screening of grasses by plant silica layer? *J. Biosci.* 38, 413–416. doi: 10.1007/s12038-013-9303-1

Scheffel, A., Poulsen, N., Shian, S., and Kröger, N. (2011). Nanopatterned protein microrings from a diatom that direct silica morphogenesis. *Proc. Natl. Acad. Sci. U.S.A.* 108, 3175–3180. doi: 10.1073/pnas.1012842108

Scoble, J. M., and Cavalier-Smith, T. (2014). Scale evolution, sequence phylogeny, and taxonomy of thaumatomonad Cercozoa: 11 new species and new genera *Scutellomonas, Cowlomonas, Thaumatospina and Ovaloplaca*. *Eur. J. Protistol.* 50, 270–313. doi: 10.1016/j.ejop.2013.12.005

Shimizu, K., Amano, T., Bari, M. R., Weaver, J. C., Arima, J., and Mori, N. (2015). Glassin, a histidine-rich protein from the siliceous skeletal system of the marine sponge *Euplectella*, directs silica polycondensation. *Proc. Natl. Acad. Sci. U.S.A.* 112, 11449–11454. doi: 10.1073/pnas.1506968112

Shrestha, R. P., and Hildebrand, M. (2015). Evidence for a regulatory role of diatom silicon transporters in cellular silicon responses. *Eukaryot. Cell* 14, 29–40. doi: 10.1128/EC.00209-14

Shrestha, R. P., Tesson, B., Norden-Krichmar, T., Federowicz, S., Hildebrand, M., and Allen, A. E. (2012). Whole transcriptome analysis of the silicon response of the diatom *Thalassiosira pseudonana*. *BMC Genomics* 13:499. doi: 10.1186/1471-2164-13-499

Siever, R. (1991). "Silica in the oceans: biological-geochemical interplay," in *Scientists on Gaia*, eds S. Schneider and P. Boston (Cambridge, MA: MIT Press), 287–295.

Siever, R. (1992). The silica cycle in the Precambrian. *Geochim. Cosmochim. Acta* 56, 3265–3272. doi: 10.1016/0016-7037(92)90303-Z

Simkiss, K., and Wilbur, K. M. (1989). *Biomineralization. Cell Biology and Mineral Deposition.* San Diego CA: Academic Press Inc.

Sims, P. A., Mann, D. G., and Medlin, L. K. (2006). Evolution of the diatoms: insights from fossil, biological and molecular data. *Phycologia* 45, 361–402. doi: 10.2216/05-22.1

Smayda, T. J. (1970). The suspension and sinking of phytoplankton in the sea. *Oceanogr. Mar. Biol. Annu. Rev.* 8, 353–414.

Smith, J. M., and Szathmáry, E. (1995). *The Major Transitions in Evolution*. Oxford: Oxford University Press.

Sommer, U. (1994). The impact of light intensity and daylength on silicate and nitrate competition among marine phytoplankton. *Limnol. Oceanogr.* 39, 1680–1688. doi: 10.4319/lo.1994.39.7.1680

Sone, E. D., Weiner, S., and Addadi, L. (2007). Biomineralization of limpet teeth: a cryo-TEM study of the organic matrix and the onset of mineral deposition. *J. Struct. Biol.* 158, 428–444. doi: 10.1016/j.jsb.2007.01.001

Sperling, E. A., Robinson, J. M., Pisani, D., and Peterson, K. J. (2010). Where's the glass? Biomarkers, molecular clocks, and microRNAs suggest a 200-Myr missing Precambrian fossil record of siliceous sponge spicules. *Geobiology* 8, 24–36. doi: 10.1111/j.1472-4669.2009.00225.x

Spinde, K., Pachis, K., Antonakaki, I., Paasch, S., Brunner, E., and Demadis, K. D. (2011). Influence of polyamines and related macromolecules on silicic acid polycondensation: relevance to "Soluble Silicon Pools"? *Chem. Mater.* 23, 4676–4687. doi: 10.1021/cm201988g

Strom, S. L. (2008). Microbial ecology of ocean biogeochemistry: a community perspective. *Science* 320, 1043–1045. doi: 10.1126/science.1153527

Strom, S. L., Macri, E. L., and Olson, B. (2007). Microzooplankton grazing in the coastal Gulf of Alaska: variations in top-down control of phytoplankton. *Limnol. Oceanogr.* 52, 1480–1494. doi: 10.4319/lo.2007.52.4.1480

Sumper, M., and Kröger, N. (2004). Silica formation in diatoms: the function of long-chain polyamines and silaffins. *J. Mater. Chem.* 14, 2059–2065. doi: 10.1039/B401028K

Sumper, M., and Lehmann, G. (2006). Silica pattern formation in diatoms: species- specific polyamine biosynthesis. *ChemBioChem* 7, 1419–1427. doi: 10.1002/cbic.200600184

Sumper, M., Hett, R., Lehmann, G., and Wenzl, S. (2007). A code for lysine modifications of a silica biomineralizing silaffin protein. *Angew. Chem.* 46, 8405–8408. doi: 10.1002/anie.200702413

Sunagawa, S., Coelho, L. P., Chaffron, S., Kultima, J. R., Labadie, K., Salazar, G., et al. (2015). Structure and function of the global ocean microbiome. *Science* 348, 1–10. doi: 10.1126/science.1261359

Sundar, V. C., Yablon, A. D., Grazul, J. L., Ilan, M., and Aizenberg, J. (2003). Fibre-optical features of a glass sponge. *Nature* 424, 899–900. doi: 10.1038/424899a

Taberlet, P., Coissac, E., Pompanon, F., Brochmann, C., and Willerslev, E. (2012). Towards next-generation biodiversity assessment using DNA metabarcoding. *Mol. Ecol.* 21, 2045–2050. doi: 10.1111/j.1365-294X.2012.05470.x

Tao, Y., Cheung, L. S., Li, S., Eom, J.-S., Chen, L.-Q., Xu, Y., et al. (2015). Structure of a eukaryotic SWEET transporter in a homotrimeric complex. *Nature* 527, 259–263. doi: 10.1038/nature15391

Tarakhovskaya, E. R., Kang, E.-J., Kim, K.-Y., and Garbary, D. J. (2012). Effect of GeO_2 on embryo development and photosynthesis in *Fucus vesiculosus* (Phaeophyceae). *Algae* 27, 125–134. doi: 10.4490/algae.2012.27.2.125

Taylor, A. R., Brownlee, C., and Wheeler, G. (2017). Coccolithophore cell biology : chalking up progress. *Ann. Rev. Mar. Sci.* 9, 283–310. doi: 10.1146/annurev-marine-122414-034032

Tesson, B., and Hildebrand, M. (2010a). Dynamics of silica cell wall morphogenesis in the diatom *Cyclotella cryptica*: substructure formation and the role of microfilaments. *J. Struct. Biol.* 169, 62–74. doi: 10.1016/j.jsb.2009.08.013

Tesson, B., and Hildebrand, M. (2010b). Extensive and intimate association of the cytoskeleton with forming silica in diatoms: control over patterning on the meso- and micro-scale. *PLoS ONE* 5:e14300. doi: 10.1371/journal.pone.0014300

Tesson, B., and Hildebrand, M. (2013). Characterization and localization of insoluble organic matrices associated with diatom cell walls: insight into their roles during cell wall formation. *PLoS ONE* 8:e61675. doi: 10.1371/journal.pone.0061675

Tesson, B., Lerch, S. J. L., and Hildebrand, M. (2017). Characterization of a new protein family associated with the silica deposition vesicle membrane enables genetic manipulation of diatom silica. *Sci. Rep.* 7, 13457. doi: 10.1038/s41598-017-13613-8

Thamatrakoln, K., Alverson, A. J., and Hildebrand, M. (2006). Comparative sequence analysis of diatom silicon transporters: toward a mechanistic model of silicon transport. *J. Phycol.* 42, 822–834. doi: 10.1111/j.1529-8817.2006.00233.x

Thamatrakoln, K., and Hildebrand, M. (2007). Analysis of *Thalassiosira pseudonana* silicon transporters indicates distinct regulatory levels and transport activity through the cell cycle. *Eukaryot. Cell* 6, 271–279. doi: 10.1128/EC.00235-06

Thamatrakoln, K., and Hildebrand, M. (2008). Silicon uptake in diatoms revisited: a model for saturable and nonsaturable uptake kinetics and the role of silicon transporters. *Plant Physiol.* 146, 1397–1407. doi: 10.1104/pp.107.107094

Thomsen, H. A., and Østergaard, J. B. (2017). Circumstantial evidence of life history events in loricate choanoflagellates. *Eur. J. Protistol.* 58, 26–34. doi: 10.1016/j.ejop.2016.12.004

Tilman, D. (1977). Resource competition between plankton algae: an experimental and theoretical approach. *Ecology* 58, 338–348. doi: 10.2307/1935608

Tilman, D., Kilham, S. S., and Kilham, P. (1982). Phytoplankton community ecology: the role of limiting nutrients. *Annu. Rev. Ecol. Syst.* 13, 349–372. doi: 10.1146/annurev.es.13.110182.002025

Tirichine, L., Rastogi, A., and Bowler, C. (2017). Recent progress in diatom genomics and epigenomics. *Curr. Opin. Plant Biol.* 36, 46–55. doi: 10.1016/j.pbi.2017.02.001

Tréguer, P. J., and De La Rocha, C. L. (2013). The world ocean silica cycle. *Annu. Rev. Mar. Sci.* 5, 477–501. doi: 10.1146/annurev-marine-121211-172346

van Tol, H. M., Irwin, A. J., and Finkel, Z. V. (2012). Macroevolutionary trends in silicoflagellate skeletal morphology: the costs and benefits of silicification. *Paleobiology* 38, 391–402. doi: 10.1666/11022.1

Vandeventer, P. E., Mejia, J., Nadim, A., Johal, M. S., and Niemz, A. (2013). DNA adsorption to and elution from silica surfaces: influence of amino acid buffers. *J. Phys. Chem. B* 117, 10742–10749. doi: 10.1021/jp405753m

Vivancos, J., Deshmukh, R., Grégoire, C., Rémus-Borel, W., Belzile, F., and Bélanger, R. R. (2016). Identification and characterization of silicon efflux transporters in horsetail (*Equisetum arvense*). *J. Plant Physiol.* 200, 82–89. doi: 10.1016/j.jplph.2016.06.011

Weaver, J. C., Aizenberg, J., Fantner, G. E., Kisailus, D., Woesz, A., Allen, P., et al. (2007). Hierarchical assembly of the siliceous skeletal lattice of the hexactinellid sponge *Euplectella aspergillum*. *J. Struct. Biol.* 158, 93–106. doi: 10.1016/j.jsb.2006.10.027

Weich, R. G., Lundberg, P., Vogel, H. J., and Jensén, P. (1989). Phosphorus-31 NMR studies of cell wall-associated calcium-phosphates in *Ulva lactuca*. *Plant Physiol.* 90, 230–236. doi: 10.1104/pp.90.1.230

Wenzl, S., Hett, R., Richthammer, P., and Sumper, M. (2008). Silacidins : highly acidic phosphopeptides from diatom shells assist in silica precipitation *in vitro*. *Angew. Chem.* 47, 1729–1732. doi: 10.1002/anie.200704994

Williams, A., Lüter, C., and Cusack, M. (2001). The nature of siliceous mosaics forming the first shell of the brachiopod *Discinisca*. *J. Struct. Biol.* 134, 25–34. doi: 10.1006/jsbi.2001.4366

Wood, R., Ivantsov, A. Y., and Zhuravlev, A. Y. (2017). First macrobiota biomineralization was environmentally triggered. *Proc. R. Soc. B Biol. Sci.* 284, 20170059. doi: 10.1098/rspb.2017.0059

Yamada, K., Yoshikawa, S., Ichinomiya, M., Kuwata, A., Kamiya, M., and Ohki, K. (2014). Effects of silicon-limitation on growth and morphology of *Triparma laevis* NIES-2565 (Parmales, Heterokontophyta). *PLoS ONE* 9:e103289. doi: 10.1371/journal.pone.0103289

Yamanaka, S., Yano, R., Usami, H., Hayashida, N., Ohguchi, M., Takeda, H., et al. (2008). Optical properties of diatom silica frustule with special reference to blue light. *J. Appl. Phys.* 103, 74701. doi: 10.1063/1.2903342

Ye, M., Song, Y., Long, J., Wang, R., Baerson, S. R., Pan, Z., et al. (2013). Priming of jasmonate-mediated antiherbivore defense responses in rice by silicon. *Proc. Natl. Acad. Sci. U.S.A.* 110, E3631–E3639. doi: 10.1073/pnas.1305848110

Yoshida, M., Noël, M. H., Nakayama, T., Naganuma, T., and Inouye, I. (2006). A haptophyte bearing siliceous scales: ultrastructure and phylogenetic position of *Hyalolithus neolepis* gen. et sp. nov. (Prymnesiophyceae, Haptophyta). *Protist* 157, 213–234. doi: 10.1016/j.protis.2006.02.004

Zhang, S., Liu, H., Ke, Y., and Li, B. (2017). Effect of the silica content of diatoms on protozoan grazing. *Front. Mar. Sci.* 4:202. doi: 10.3389/fmars.2017.00202

Zhao, P., Gu, W., Wu, S., Huang, A., He, L., Xie, X., et al. (2014). Silicon enhances the growth of *Phaeodactylum tricornutum* Bohlin under green light and low temperature. *Sci. Rep.* 4:3958. doi: 10.1038/srep03958

Zlatogursky, V. V. (2016). There and back again: parallel evolution of cell coverings in centrohelid heliozoans. *Protist* 167, 51–66. doi: 10.1016/j.protis.2015.12.002

Conflict of Interest Statement: The authors declare that the research was conducted in the absence of any commercial or financial relationships that could be construed as a potential conflict of interest.

Copyright © 2018 Hendry, Marron, Vincent, Conley, Gehlen, Ibarbalz, Quéguiner and Bowler. This is an open-access article distributed under the terms of the Creative Commons Attribution License (CC BY). The use, distribution or reproduction in other forums is permitted, provided the original author(s) and the copyright owner are credited and that the original publication in this journal is cited, in accordance with accepted academic practice. No use, distribution or reproduction is permitted which does not comply with these terms.

frontiers in Earth Science

REVIEW
published: 30 January 2018
doi: 10.3389/feart.2017.00112

A Review of the Stable Isotope Bio-geochemistry of the Global Silicon Cycle and Its Associated Trace Elements

Jill N. Sutton [1], Luc André [2], Damien Cardinal [3], Daniel J. Conley [4,5], Gregory F. de Souza [6], Jonathan Dean [7,8], Justin Dodd [9], Claudia Ehlert [10], Michael J. Ellwood [11], Patrick J. Frings [12,13], Patricia Grasse [14], Katharine Hendry [15], Melanie J. Leng [8,16], Panagiotis Michalopoulos [17], Virginia N. Panizzo [16,18] and George E. A. Swann [16,18]*

[1] Université de Brest - UMR 6539 CNRS/UBO/IRD/Ifremer, LEMAR - IUEM, Plouzané, France, [2] Earth Sciences Department, Royal Museum for Central Africa, Tervuren, Belgium, [3] LOCEAN Laboratory, Sorbonne Universités (UPMC, Univ Paris 06), Centre National de la Recherche Scientifique, IRD, MNHN, Paris, France, [4] Department of Geology, Lund University, Lund, Sweden, [5] Stellenbosch Institute for Advanced Study, Stellenbosch, South Africa, [6] Institute of Geochemistry and Petrology, ETH Zurich, Zurich, Switzerland, [7] School of Environmental Sciences, University of Hull, Hull, United Kingdom, [8] NERC Isotope Geosciences Facilities, British Geological Survey, Nottingham, United Kingdom, [9] Geology and Environmental Geosciences, Northern Illinois University, DeKalb, IL, United States, [10] Max Planck Research Group for Marine Isotope Geochemistry, Institute for Chemistry and Biology of the Marine Environment, University of Oldenburg, Oldenburg, Germany, [11] Research School of Earth and Ocean Sciences, Australian National University, Canberra, ACT, Australia, [12] Earth Surface Geochemistry, Helmholtz Centre Potsdam GFZ German Research Centre for Geosciences, Potsdam, Germany, [13] Department of Geoscience, Swedish Museum of Natural History, Stockholm, Sweden, [14] Ocean Circulation and Climate Dynamics, GEOMAR Helmholtz Centre for Ocean Research Kiel, Kiel, Germany, [15] School of Earth Sciences, University of Bristol, Bristol, United Kingdom, [16] Centre for Environmental Geochemistry, University of Nottingham, Nottingham, United Kingdom, [17] Hellenic Centre for Marine Research, Institute of Oceanography, Anavyssos, Greece, [18] School of Geography, University of Nottingham, Nottingham, United Kingdom

OPEN ACCESS

Edited by:
Brivaela Moriceau, Centre National de la Recherche Scientifique (CNRS), France

Reviewed by:
Peter Croot, National University of Ireland Galway, Ireland
Anne-Julie Cavagna, Vrije Universiteit Brussel, Belgium

***Correspondence:**
Jill N. Sutton
jill.sutton@univ-brest.fr

Specialty section:
This article was submitted to Marine Biogeochemistry, a section of the journal Frontiers in Earth Science

Received: *29 May 2017*
Accepted: *21 December 2017*
Published: *30 January 2018*

Citation:
Sutton JN, André L, Cardinal D, Conley DJ, de Souza GF, Dean J, Dodd J, Ehlert C, Ellwood MJ, Frings PJ, Grasse P, Hendry K, Leng MJ, Michalopoulos P, Panizzo VN and Swann GEA (2018) A Review of the Stable Isotope Bio-geochemistry of the Global Silicon Cycle and Its Associated Trace Elements. Front. Earth Sci. 5:112. doi: 10.3389/feart.2017.00112

Silicon (Si) is the second most abundant element in the Earth's crust and is an important nutrient in the ocean. The global Si cycle plays a critical role in regulating primary productivity and carbon cycling on the continents and in the oceans. Development of the analytical tools used to study the sources, sinks, and fluxes of the global Si cycle (e.g., elemental and stable isotope ratio data for Ge, Si, Zn, etc.) have recently led to major advances in our understanding of the mechanisms and processes that constrain the cycling of Si in the modern environment and in the past. Here, we provide background on the geochemical tools that are available for studying the Si cycle and highlight our current understanding of the marine, freshwater and terrestrial systems. We place emphasis on the geochemistry (e.g., Al/Si, Ge/Si, Zn/Si, $\delta^{13}C$, $\delta^{15}N$, $\delta^{18}O$, $\delta^{30}Si$) of dissolved and biogenic Si, present case studies, such as the Silicic Acid Leakage Hypothesis, and discuss challenges associated with the development of these environmental proxies for the global Si cycle. We also discuss how each system within the global Si cycle might change over time (i.e., sources, sinks, and processes) and the potential technical and conceptual limitations that need to be considered for future studies.

Keywords: C – N – O - Si isotopes, biogenic silica, element/Si ratios, biogeochemical cycles, silicon

INTRODUCTION

The global silicon (Si) cycle is of great interest due to the role that silicate weathering has played in maintaining climatic stability on geological time scales (Siever, 1991; Frings et al., 2016; Conley et al., 2017) and because Si is an important nutrient for many organisms in marine and freshwater ecosystems. It occurs as silicate minerals in association with all rock types (igneous, metamorphic, sedimentary). Weathering, biological and geochemical transformations, transport and interactions with other elements (in particular nutrients and carbon) form the basis of the global biogeochemical Si cycle (Frings et al., 2016). The global Si cycle has evolved through geologic time with overall declines in oceanic dissolved Si due to the uptake and deposition by organisms (Siever, 1991; Conley et al., 2017). While the modern Si biogeochemical cycle is influenced by anthropogenic forcing (Laruelle et al., 2009), the processes of weathering and burial as biogenic silica ($bSiO_2$) are the dominant processes in the biogeochemical Si cycle.

The paper aims to review the use of Si stable isotopes and associated trace elements in order to address the following questions:

(1) What is the bio-geochemistry of biogenic silica?
(2) What is the current state of knowledge regarding the influence of biogenic silica on the global Si cycle?
(3) What is the influence of early to late sediment diagenesis on biogenic silica, and thus its utility as an environmental proxy for palaeoceanographic interpretation?

Although modeling is not being covered in the review, its importance cannot be underscored as it has been increasingly used to understand the mechanisms controlling Si isotope fractionation (e.g., Qin et al., 2016) and the development of the Si isotope composition as a tracer of biogeochemical silicon cycle in modern and past natural systems (e.g., Gao et al., 2016).

Silicon Reservoirs

The chemical weathering of silicate minerals and the eventual cycling of weathered products (clays, dissolved Si) provide the starting point of Si bio-geochemistry and its interaction with other elemental cycles such as carbon. Silicate weathering represents an important sink of atmospheric CO_2 over geological time scales (Berner et al., 1983; Wollast and Mackenzie, 1989; Brady and Carroll, 1994) and depends on temperature and precipitation. Thus, the rate at which weathering occurs will be enhanced through changes in global temperature (White and Blum, 1995).

Silicon rarely occurs as the pure element in nature and appears most often in combination with oxygen to form solid silicate minerals or amorphous compounds (including biogenic Si), or in aqueous solutions it occurs as orthosilicic acid ($Si(OH)_4$) (Iler, 1979). Silicon exists in major pools in dissolved and solid forms in all reservoirs: extra-terrestrial, continental (e.g., soil, vegetation, hydrothermal), freshwater (e.g., rivers, lakes, groundwater, organisms, sediment), atmospheric (e.g., aerosols), and oceanic (e.g., water column, organisms, sediment and pore-waters, oceanic crust, hydrothermal), (**Figure 1**). The dominant transformation processes are weathering of silicate rocks and the formation of secondary minerals and release of dissolved Si, uptake of dissolved Si by organisms for the biomineralization of biogenic Si, and the remineralization of Si. Coastal regions are of special importance here because they support a large fraction of the global primary production and control the transfer of dissolved and particulate nutrients from land to the open ocean (Conley et al., 1993; Rabouille et al., 2001).

Biomineralization, the Structure of Biogenic Silica, and Its Relevance to the Global Si Cycle

Many organisms use dissolved Si, including diatoms, silicoflagellates, radiolarians, sponges, and higher plants, to produce solid $bSiO_2$ structures. Biogenic silica, also called biogenic opal, is the second most abundant mineral type formed by organisms after calcium carbonate (Brümmer, 2003). Biogenic silica is amorphous and its density, hardness, solubility, viscosity and composition may vary considerably (Perry et al., 2003). The silica structures are based upon a random network of SiO_4 tetrahedral units connected through covalently linked Si-O-Si bonds of variable bond angle and bond lengths (Mann and Perry, 1986). All silicifying organisms utilize $Si(OH)_4$; however, each silicifying organism has a unique biomineralizing pathway.

Details on the process of silicification can be found in the literature for diatoms (Hildebrand et al., 1997; Martin-Jezequel et al., 2000; Claquin et al., 2002; Hildebrand, 2008; Thamatrakoln and Hildebrand, 2008; Brunner et al., 2009; Thamatrakoln and Kustka, 2009), sponges (Wilkinson and Garrone, 1980; Reincke and Barthel, 1997; Cha et al., 1999; Maldonado et al., 1999, 2005; Brümmer, 2003; Uriz et al., 2003; Muller et al., 2007; Schröder et al., 2007), and higher plants (Takahashi et al., 1990; Ma et al., 2001, 2006).

Globally, diatoms (unicellular autotrophic algae) dominate the $bSiO_2$ production with an estimate of 240 ± 40 Tmol yr^{-1} (Tréguer and De La Rocha, 2013) (**Figure 1**). The degree of $bSiO_2$ production (i.e., silicification) of diatom frustules can vary significantly, even within the same species, and is primarily a function of ambient dissolved Si (DSi) concentration and cellular growth rate, whereby the $bSiO_2$ content of a cell decreases during DSi limitation and/or accelerated growth (Martin-Jezequel et al., 2000; Claquin et al., 2002; Baines et al., 2010).

Until recently, the relevance of marine siliceous sponges on the Si cycle has been largely ignored and their role is currently being re-visited with a biogenic Si production estimated at 3.6 ± 3.7 Tmol yr^{-1} (Maldonado et al., 2005; Tréguer and De La Rocha, 2013) (**Figure 1**).

Higher plants produce roughly 84 (60–180) Tmol yr^{-1} of biogenic Si (phytoliths) (**Figure 1**), which is within a similar order of magnitude as diatom production (Conley, 2002). All plants that grow on soil contain Si in their tissues, whereby Si uptake and concentrations vary greatly among species depending on the different capacities for Si uptake by the roots (Takahashi et al., 1990; Ma et al., 2001). Active Si uptake has been suggested for Si-accumulating plants that are characterized by high Si concentrations (>1% dry weight in the leaves) and a molar Si:Ca

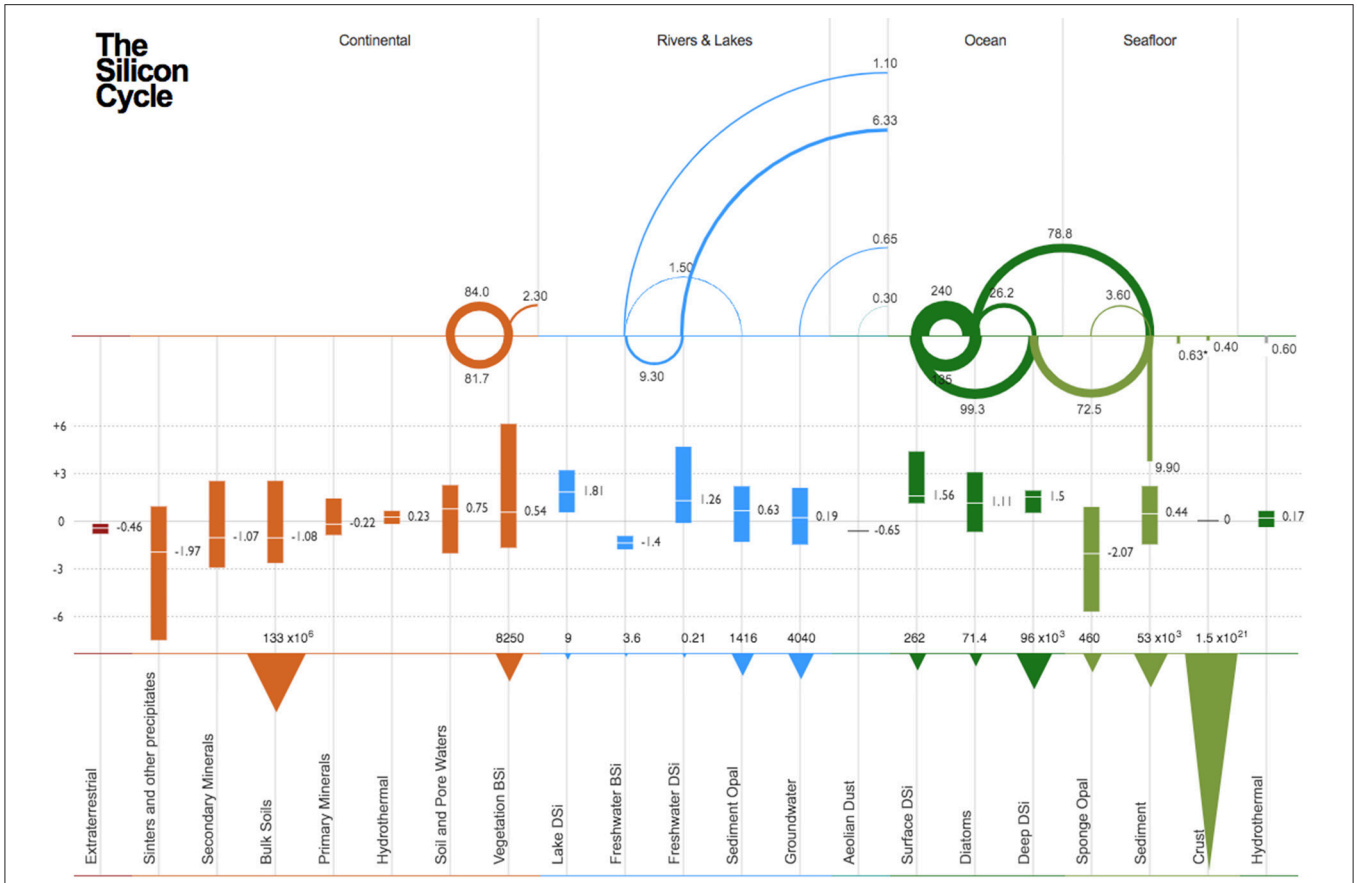

FIGURE 1 | Schematic of the modern day global Si cycle grouped by reservoir and their associated δ^{30}Si values (in ‰). The figure is divided into three parts. The upper part indicating the magnitude of the fluxes (in 10^{12}mol yr^{-1}; Tmol yr^{-1}) between each reservoir, the middle part showing their associated δ^{30}Si values, and the lower part showing reservoir size. The fluxes are numerically and figuratively represented, moving in a clockwise manner (e.g., In the Ocean compartment, there is a flux of 240 Tmol yr^{-1} from Surface DSi to Diatoms, after the Diatoms dissolve, there is 135 Tmol yr^{-1} flux back from the Diatoms to the Surface DSi in the upper water column). In the case where the flux points downwards (e.g., 9.90 Tmol yr^{-1} within the sediment reservoir), the flux is effectively removed from the system. * Value assumed to underestimate flux (see section Diagenetic Silica Precipitation and Reverse Weathering). Estimates for the Si fluxes were obtained from the following sources: Carey and Fulweiler (2012), Frings et al. (2016), Laruelle et al. (2009), Tréguer and De La Rocha (2013). Estimates for the range of δ^{30}Si values were obtained from the following sources: Ehlert et al. (2016); Figure 2 from Frings et al. (2016) and references therein; Varela et al. (2016) and Panizzo et al. (2017). All data used to prepare this figure are available in Table S1.

ratio >1, whereas non-accumulating plants have a passive or discriminating Si uptake system (Takahashi et al., 1990; Ma et al., 2001). After uptake, DSi is rapidly transported through the plant to the different tissues within the transpiration stream. Due to transpirational water loss, DSi is gradually concentrated, and phytoliths are formed by precipitation in plant cells when the concentration increases above 2 mM. Thus, phytoliths vary in size and shape depending on the cell type, plant organ and plant species they are deposited in Madella et al. (2005).

Global Si Cycle Over Time

The global oceanic Si cycle has evolved through geologic time primarily due to the uptake of dissolved Si and subsequent biomineralization by organisms, especially sponges, radiolarians and diatoms (Siever, 1991). Substantial advances have occurred in our understanding of the evolution of the geological Si cycle through the use of the fossil record, silica isotope geochemistry and the phylogenomics of biosilicification (Conley et al., 2017; Hendry et al., 2018). The first biological impacts on the Si cycle are hypothesized to have occurred with the evolution of cyanobacteria in the Archean with further decreases in the mid-Proterozoic with evolution of eukaryotes capable of Si biomineralization. Decreases in oceanic DSi occurred prior to the start of the Phanerozoic with the evolution of widespread, large-scale skeletal bio-silicification. Due to the increased usage of dissolved Si by radiolarians in the lower to early Middle Ordovician, the loci of sponges shifted from shallow to deep-water basinal environments (Kidder and Tomescu, 2016). Finally, it is the appearance and subsequent proliferation of diatoms, with their superior ability to utilize low concentrations of DSi, that decreased DSi to the low levels observed in the global oceans today (Tréguer and De La Rocha, 2013). The impact of orogeny, e.g., the uplift of the Himalayas with periods of enhanced continental weathering fluxes in the Cenozoic (Misra and Froelich, 2012) could have increased DSi input to the oceans (Cermeño et al., 2015), although there is no evidence of

large-scale changes in DSi concentrations in the geologic record (Fontorbe et al., 2016, 2017).

In the recent years, there have been a considerable number of studies on palaeo-environments of the Archean (4 – 2.5 Ga) and Proterozoic (2.5 – 0.5 Ga). Most use Si - O isotopes, elemental ratios (Ge/Si, REEs) or other isotopic systems (Fe, S…) associated to silica in Banded Iron Formations (e.g., André et al., 2006; Heck et al., 2011; Delvigne et al., 2012), cherts (e.g., Robert and Chaussidon, 2006; Chakrabarti et al., 2012) or paleosols (e.g., Delvigne et al., 2016). These studies all use the knowledge gained from modern, experimental and/or less ancient palaeo-records to interpret geochemical records, in order to reconstruct, for instance, the ocean temperature and oxygen levels, input of hydrothermal, and intensity of weathering. However, it is still challenging to provide a clear picture of these ancient environments because the studies have divergent results. A multi-proxy approach is therefore required. This is particularly needed to assess the level of preservation of the samples in order to take into account diagenesis while interpreting the geochemical signals into reconstruction of paleo-environments (Marin-Carbonne et al., 2014).

Modern day anthropogenic factors have a strong influence on the global Si cycle, for example through increases in CO_2, temperature and changes in hydrological regimes and erosion, variations in agriculture and land use, eutrophication and changes in nutrient stoichiometry in coastal regions, and river damming (e.g., Rickert et al., 2002; Struyf et al., 2004, 2010; Laruelle et al., 2009; Clymans et al., 2011; Carey and Fulweiler, 2012). Anthropogenic perturbations of the global biogeochemical Si cycle are due to the gradual aggradation or depletion of the amorphous SiO_2 pool held in continental soils (Barão et al., 2015; Vandevenne et al., 2015) and aquatic sediments (Frings et al., 2014b) in response to these changing environmental forcings (Struyf and Conley, 2012) and river damming (Conley et al., 1993). Our emerging understanding is that DSi inputs from the continents have potentially altered the magnitude and $\delta^{30}Si$ composition of DSi supplied to the open ocean mostly because of changes occurring on the continent as well as changes of the silica sink on continental margins (Bernard et al., 2010; Frings et al., 2016). This includes short time scales such as anthropogenic impacts (not only on Si, but also on other nutrients e.g., N, P, Fe) and possibly to an extent large enough to impact whole-ocean isotopic signatures on the timescale of Quaternary glacial cycles. Thus, the sensitivity of biogeochemical Si cycling to anthropogenic pressure, especially in coastal regions, will likely be highlighted in the future (Laruelle et al., 2009; Bernard et al., 2010) and the continental Si cycle should not be neglected when interpreting pre-Quaternary long-term $\delta^{30}Si_{bSiO2}$ records from marine sediment records (Egan et al., 2013; Fontorbe et al., 2016).

STABLE SILICON ISOTOPE RATIOS TO STUDY THE GLOBAL SI CYCLE

Silicon has three naturally occurring stable isotope with the following mean abundances: ^{28}Si: 92.23%, ^{29}Si: 4.67%, and ^{30}Si: 3.10%. The Si isotope composition is expressed in delta notation ($\delta^{n}Si$) and can be calculated according to the following formula:

$$\delta^{n}Si_{x}(‰) = ([(^{n}Si/^{28}Si)_{x-}(^{n}Si/^{28}Si)_{standard})] / [(^{n}Si/^{28}Si)_{standard}]) \times 1000 \quad (1)$$

where n can represent ^{29}Si or ^{30}Si, x refers to either $bSiO_2$ or DSi and standard is the atomic ratio of the heavy and light Si isotopes of the quartz standard (NBS28).

Several processes have been shown to fractionate Si isotopes, which explain why this tool can be used to trace the Si biogeochemical cycle. The extent of isotopic fractionation is defined by the isotopic fractionation factor (α) that can be expressed by Hoefs (2009):

-for kinetic isotopic exchange (irreversible reaction)

$$\alpha = k_{28Si}/k_{30Si}$$

Where k refers to the rate constants for the reaction of light and heavy isotopes.

-for equilibrium

$$\alpha = (^{30}Si : ^{28}Si)_{A}/(^{30}Si : ^{28}Si)_{B}$$

Where A and B are two chemical substances, typically the substrate (A) and the product (B) of the reaction.

For practical and analytical reasons, Si isotope ratios and Si isotope fractionation are reported in delta notation with the permil (‰) scale. A useful way to think about Si isotope values is as fractionation of Si isotopes, or the difference between the $\delta^{30}Si$ values of DSi and $bSiO_2$ as described by ε in Equation (2) and calculated (Criss, 1999) as:

$$\varepsilon \cong 1000 \bullet (\alpha_{bSiO2-DSi} - 1) \quad (2)$$

where $\alpha_{bSiO2-DSi}$ is the isotopic fractionation factor between the product ($bSiO_2$) and the substrate (DSi). Note the lack of redox speciation and organic complexation for silicon limits fractionation effects to predominately inorganic kinetic exchange factors, contrary to many other elements (Wiederhold, 2015).

The following is a description of the systems, processes and transformations that control the global silica cycle, and the known constraints on the $\delta^{30}Si$ (see **Figure 1**).

Weathering

Weathering is a major process that fractionates Si isotopes in the critical zone. When primary minerals ($-0.90 < \delta^{30}Si < +1.40‰$, **Figure 1**) are weathered, light Si isotopes are preferentially incorporated into secondary minerals ($-2.95 < \delta^{30}Si < +2.5‰$) releasing a DSi pool that generally has an enriched isotope composition ($-1 < \delta^{30}Si < +2‰$) (cf. reviews of Opfergelt and Delmelle, 2012; Frings et al., 2016), **Figure 1**, Supplementary Table 1 and references therein). Adsorption of silicic acid onto Fe oxy-hydroxides (Delstanche et al., 2009) and Al hydroxides (Oelze et al., 2014) has also been demonstrated to preferentially immobilize the lighter Si isotopes. As discussed in section Rivers, all these processes are particularly complex on seasonal to geological timescales (Ziegler et al., 2005) and explain most of the higher $\delta^{30}Si_{DSi}$ of continental waters.

Vegetation

Significant fractionation has been observed during the uptake of Si by plant roots (Opfergelt et al., 2006a,b; Ding et al., 2008a,b; Sun et al., 2008) and exogenous material on the surface of vegetation (Engström et al., 2008), although the transporters behind both forms of uptake remain largely unknown. The δ^{30}Si composition of these plants (**Figure 1**), and in particular of phytoliths is in the first instance regulated by the physical environment around the plant including the soluble Si concentration of the medium (Opfergelt et al., 2006b), the weathering of the soil substrate (Opfergelt et al., 2008) and soil organic matter (Ding et al., 2008a). Beyond this, there is clear evidence that significant isotopic fractionation can occur between plants with increased fractionation in heavy Si accumulators (Ding et al., 2005, 2008a,b; Opfergelt et al., 2006a,b). Rayleigh fractionation during the transportation of Si within plants also causes heavier isotopes to be concentrated within the xylem whilst lighter isotopes are preferentially deposited in phytoliths lower down the plant (Ding et al., 2005, 2008a,b; Opfergelt et al., 2006a,b; Hodson et al., 2008). Phytoliths have higher dissolution rates than other silicate materials (e.g., tephra, clay, feldspars, quartz), and provide a major source of DSi in some soil/terrestrial environments (Derry et al., 2005; Struyf et al., 2009; Cornelis et al., 2010; Opfergelt et al., 2010).

Freshwater

Rivers

Over the past two decades, several studies of δ^{30}Si in DSi in freshwaters have been published, but we are still only beginning to understand the controls and variability of δ^{30}Si in freshwaters. Since the first data of DSi in freshwaters by De La Rocha (De La Rocha et al., 2000), δ^{30}Si has been analyzed from a number of rivers (and lakes) across the world including the Congo River and tributaries (Cardinal et al., 2010; Hughes et al., 2011), the Tana River (Hughes et al., 2012), the Yellow and Yangtze Rivers (Ding et al., 2004, 2011), the Kalix River in Sweden (Engström et al., 2010), Swiss alpine rivers (Georg et al., 2006), and most recently from the Nile River (Cockerton et al., 2013), the Amazon river and tributaries (Hughes et al., 2013), areas of central Siberia (Pokrovsky et al., 2013; Panizzo et al., 2017) and the Ganges (Fontorbe et al., 2013; Frings et al., 2015). The range in δ^{30}Si from freshwaters, thus far analyzed, now stands at −0.17 to +4.66‰ (**Figure 1**).

In big-picture terms, (almost) every measurement ever made of river water DSi has been heavier than the parent material. When river water DSi concentrations are normalized to a conservative element (typically Na, which is common in silicate rocks), then it becomes clear that Si is removed from solution, either into secondary clay minerals or some form of $bSiO_2$, and that this removal is associated with a discrimination against the heavier isotopes of Si. This is consistent with our understanding derived from the microscale (e.g., Steinhoefel et al., 2011; Schuessler and von Blanckenburg, 2014) to the soil-column scale (e.g., Opfergelt et al., 2012; Pogge von Strandmann et al., 2012). These all show that the new secondary mineral phases have less of the heavier isotopes relative to river waters. The same discrimination is also well established for plants (Ding et al., 2005, 2008a; Opfergelt et al., 2006a,b), freshwater diatoms (Alleman et al., 2005; Panizzo et al., 2016) and sponges, which preferentially utilize ^{28}Si over ^{30}Si (and ^{29}Si), thus leading to an increase in δ^{30}Si in the host water.

Broadly, δ^{30}Si values in river waters reflect the weathering regime, which is ultimately a mass-balance constraint. We can conceptualize two end-member weathering regimes: "kinetically limited" and "supply limited" (almost equivalent to the geomorphological terms "transport limited" and "weathering limited"; see e.g., Stallard and Edmond, 1983). Kinetic limitation refers to a situation where the weathering flux (solute, DSi) is operating at maximum capacity for the conditions; increasing the factors that control the weathering rate (essentially temperature or water supply) will increase the rate of DSi export, because there is an excess of fresh material to be weathered. This could be e.g., the high Himalaya, the Andes, or (sub) glacial catchments (Georg et al., 2007; Fontorbe et al., 2013; Opfergelt et al., 2013) where physical erosion greatly outpaces chemical weathering. At very high erosion rates (low weathering intensity or congruency) river δ^{30}Si is low: there is no time, and no thermodynamic driving force, for clays to form, soils to develop or biology to have a meaningful influence on the δ^{30}Si measured in a stream.

The other end-member (supply limited) is where essentially all material leaves the catchment as a dissolved flux; the rate of solute generation is limited by how quickly material is supplied. Increasing the factors that control the weathering rate (temperature or water supply) will not increase Si export, because there is nothing left to be weathered. In this case the conversion of parent material (bedrock) to river solute is (near-) complete, then there can be no observable fractionation: the river takes on the composition of the bedrock, regardless of how much $bSiO_2$ cycling is taking place in the catchment (and assuming steady-state, and no loss of $bSiO_2$). This is the case in e.g., the lowland, blackwater tributaries of the Amazon (Hughes et al., 2013) and the Congo (Cardinal et al., 2010), where the interpretation is that the swampy, organic-matter-rich environments are conducive to the dissolution of previously formed clays.

Along a gradient of weathering intensity (0 to 1, where 0 is all material exported by physical erosion, and 1 where all denudation occurs as dissolved fluxes), the offset between source material (bedrock) and river δ^{30}Si should be zero at both ends and peak somewhere in the middle (Bouchez et al., 2013). The same is true for Li isotopes (Henchiri et al., 2016); in general, the isotopic separation along a weathering regime gradient is much clearer for Li (δ^{7}Li) than δ^{30}Si (see e.g., Dellinger et al., 2015; Frings et al., 2016). Superimposed on the above is the role of vegetation (see section Vegetation).

All the work published on the major catchment/riverine systems (e.g., Cockerton et al., 2013) highlight the complexity of lake/drainage basin systems, and clearly illustrate that both Si concentrations and δ^{30}Si are closely controlled by a mixture of weathering/erosion processes [regulated by the wider climate system (De La Rocha et al., 2000; Opfergelt and Delmelle, 2012)], aquatic productivity and catchment soil, vegetation. Studies of the Congo Basin, for example, have shown that $\delta^{30}Si_{DSi}$ is mainly regulated by the intensity of silicate weathering/secondary mineral formation across the drainage

basin with spatial variations further driven by the type of weathering regime and the extent to which clays are dissolved by organic matter (Cardinal et al., 2010). These abiotic processes are then superimposed by seasonal biological processes, in particular by diatom biomineralization in the dry season, which exports significant amounts of Si out of the water column (Hughes et al., 2011). Other examples also account for the downstream increase in Nile River δ^{30}Si to the progressive uptake of DSi by diatoms and other Si-accumulating organisms (Cockerton et al., 2013). Indeed, Cockerton et al. (2013) showed significant seasonal variations in δ^{30}Si from freshwaters, with higher δ^{30}Si in the dry season (+1.54 to +4.66‰) than the wet season (+0.48 to +3.45‰) due to reduced mobilization of dissolved Si from the catchment relative to its aquatic demand. These examples demonstrate the superimposed (often seasonal) control that freshwater $bSiO_2$ plays in regulating δ^{30}Si signatures, where abiotic processes (chemical weathering and secondary mineral formation) otherwise dominate.

Additional examples also show the potential importance of vegetation in altering the Si concentration and/or δ^{30}Si and regulating the flux of Si both into/out of river waters (Alleman et al., 2005; Ding et al., 2011; Hughes et al., 2011; Cockerton et al., 2013; Pokrovsky et al., 2013). For example, along the Yangtze River uptake of DSi by grasses in wetlands and rice in paddy fields drives a progressive increase in $\delta^{30}Si_{DSi}$ due to better phytolith preservation in areas of high phytolith production and/or low phytolith dissolution (Ding et al., 2004). In contrast the net impact of vegetation on $\delta^{30}Si_{DSi}$ seems to be minimal in the Okavango Delta, Congo and Amazon Basin due to the rapid dissolution/recycling of phytoliths (Cardinal et al., 2010; Hughes et al., 2013; Frings et al., 2014b).

Work on smaller aquatic systems has also shown significant temporal variations in $\delta^{30}Si_{DSi}$. In a boreal river in North Sweden seasonal changes in $\delta^{30}Si_{DSi}$ of 0.8‰ were attributed to: (1) the release of plant derived $bSiO_2$/phytoliths (low δ^{30}Si) during snow melt; (2) changing inputs from headwaters; and (3) diatom biomineralization (Engström et al., 2010). Similarly, seasonal changes in $\delta^{30}Si_{DSi}$ of up to 0.6‰ were observed in a series of rivers in Switzerland (Georg et al., 2006), whilst variations in a series of Icelandic rivers have been linked to differential erosion rates and secondary minerals formation (Opfergelt et al., 2013).

Other studies have shown a significant anthropogenic impact on $\delta^{30}Si_{DSi}$, often in response to land use changes and dam construction (Sun et al., 2011; Hughes et al., 2012; Delvaux et al., 2013). As a case study, along the River Nile, intensive water management through the irrigation/retention of waters behind dams exerts a significant control on $\delta^{30}Si_{DSi}$ (Cockerton et al., 2013). In the Tana River (Kenya), downstream increases (decreases) in $\delta^{30}Si_{DSi}$ (DSi) are attributed to both greater water retention time and the higher diatom DSi utilization in dams and reservoirs (Hughes et al., 2012), which leads to heavier (+0.54‰) downstream DSi compositions and a 41% decrease in concentrations. Similarly, outside of diatom growth season periods, the $\delta^{30}Si_{DSi}$ signature of Scheldt River (Belgium) tributaries (a human disturbed watershed) are negatively correlated to the percentage of forest cover ($r^2 = 0.95$, p-value < 0.01) and positively correlated to the percentage of arable land cover ($r^2 = 0.70$, p-value < 0.08) in the basin, suggesting that land use is a major control here on $\delta^{30}Si_{DSi}$ signatures (Delvaux et al., 2013). All of these examples document how temporal (namely seasonal) and spatial changes in riverine $\delta^{30}Si_{DSi}$ in both small and large drainage basins, can have great impact upon the delivery of DSi and $\delta^{30}Si_{DSi}$ to the oceans over time (Frings et al., 2016).

Challenges in Interpreting River Geochemistry

As outlined above, the cycling of DSi in river water is not a straightforward process. In general, we have a good conceptual understanding of the qualitative nature of the processes and the associated fractionations, but quantifying the fractionation at each step in the processes is often challenging. This is not a problem that is unique to Si isotope systematics (see Eiler et al., 2014).

The key steps in the generation of river water DSi include: (1) dissolution of the primary mineral, (2) incorporation of some fraction of this as a secondary phase, (3) bio-cycling and soil-column processes. Each of these steps is associated with multiple fractionations: We are beginning to understand that the (overall) Si isotope fractionation associated with any given process is extremely variable. Note that an analogy can be made with the ongoing work on biological Si fractionation (Sutton et al., 2013; Hendry et al., 2015). This range in observable isotope fractionation occurs because each phase transformation is typically several steps, each with their own fractionation. For example, the weathering of a primary silicate mineral to a secondary clay (e.g., plagioclase to kaolinite) will potentially involve breaking of bonds in mineral surface, diffusion across a leached layer and/or thin mineral-fluid boundary layer, de-solvation/coordination into and from solution, transfer to the precipitation site, and the forming of new bonds in the new mineral. Each step can involve isotope fractionation, plus various mass-balance constraints that regulate how much this fractionation can be expressed. They also involve fractionations of two fundamentally different manners: kinetic and equilibrium, which arise from Newtonian dynamics and bond-strength effects, respectively. Importantly, these fractionation events tend to cause opposing fractionation of the Si isotopes and complicate the interpretations of the resulting δ^{30}Si values.

Laboratory experiments confirm that the combined fractionations associated with important processes (Si adsorption or precipitation) are both rate and temperature dependent (Geilert et al., 2014; Oelze et al., 2014, 2015; Roerdink et al., 2015), conclusions that are corroborated by well-designed field experiments (Geilert et al., 2015). In general, it is clear that there is no such thing as a single fractionation factor for a given process. This makes it hard to quantitatively interpret e.g., river DSi at a large scale, especially without a robust independent estimate of "f_{Si}," the fraction of Si remaining in solution. Catchment mass-balance models (e.g., Bouchez et al., 2013)) can help, but require that river sediment is collected and measured simultaneously and assume catchment steady-state. Predicting the magnitude, and even direction, of changes in the δ^{30}Si values of river water during glacial-interglacial transitions is confounded by multiple parameters that are only qualitatively

understood. It is not clear, for example, if these transitions would result in a congruent weathering regime.

Lakes

Lacustrine systems represent a key component of the continental Si cycle, although only a handful of results have been published to date (**Figure 1**). Whilst riverine inputs cause initial lake profiles to be primarily a function of upstream catchment processes (weathering of rock and productivity inputs), subsequent in-lake DSi biomineralization can significantly modify DSi/$\delta^{30}Si_{DSi}$ before waters continue through the outflow and eventually into the marine system (Alleman et al., 2005; Opfergelt et al., 2011). As with the oceans, siliceous productivity in lakes is primarily a function of light and nutrient availability. Accordingly, spatial/temporal patterns of DSi/$\delta^{30}Si_{DSi}$ can often be linked to factors including mixing/stratification regimes, which regulate the supply of nutrient rich deep waters to the photic zone and the retention of organisms in surface waters (Alleman et al., 2005).

The net efficiency of the biological pump in transferring Si from the water column into the sediment record is often higher in lakes than marine systems, due to lower dissolution rates that are in turn influenced by faster rates of sinking and sediment accumulation. However, in instances where dissolution is significant, for example in response to elevated pH or salinity, the impacts are clearly observed with elevated DSi concentrations and lower $\delta^{30}Si$ (Opfergelt et al., 2011). Importantly, the contemporary studies carried out to date all highlight the potential for $\delta^{30}Si$ to be used to study temporal changes in Si cycling, for example through the use of sediment cores. Whilst several organisms (diatoms, radiolaria, sponges) have been explored for this purpose in marine environments, work on freshwater systems has so far focused on diatoms with few data for other organisms (e.g., sponges Hughes et al., 2011). Calibrations have replicated marine studies in demonstrating a fractionation factor of *ca.* −1.1‰ that is independent of temperature and species (Alleman et al., 2005). Furthermore, contemporary data of $\delta^{30}Si_{diatom}$ from open sediment traps placed down the Lake Baikal water profile found a near constant $\delta^{30}Si_{diatom}$ composition, suggesting the full preservation of the signal through the water column (Panizzo et al., 2016). More importantly, their comparison with $\delta^{30}Si_{diatom}$ in surface sediments, where high diatom valve dissolution occurs, argued for the absence of a Si isotope fractionation associated with diatom dissolution (Panizzo et al., 2016).

Challenges in Interpreting Lake Geochemistry and Palaeolimnological Records

As outlined above, there have been a handful of studies to date that have examined the application of $\delta^{30}Si_{DSi}$ in limnological settings (Alleman et al., 2005; Opfergelt et al., 2011; Panizzo et al., 2016, 2017). Lakes, in addition to the soil-vegetation system, play an important role in buffering continental DSi export to the oceans. Previous assumptions were that this buffering capacity of the continental Si cycle was in steady-state; however, this has now been challenged (Frings et al., 2014a). Frings et al. (2014a) highlight the effectiveness of lacustrine environments in retaining DSi in sediments via the $bSiO_2$ pump, which on a global scale can translate to a net export of between 21 and 27% of river DSi export. This equates to an estimation of 1.53 Tmol yr^{-1} (Frings et al., 2014a) (**Figure 1**). These data highlight the challenges in underpinning global estimates of lake biogeochemical cycling (particularly for large lakes and reservoirs) to better constrain the evolution of the global biogeochemical cycling of Si.

Marine

Silicon plays an important role in the marine realm as a vital macronutrient for silicifying organisms such as diatoms, radiolarians, siliceous sponges and silicoflagellates. Due to their short lifetimes and the dynamic, boom-bust nature of their populations, diatoms are dominantly responsible for the cycling of Si *within* the ocean, due to the large fluxes associated with their uptake and export of Si (**Figure 1**), although other siliceous organisms may contribute to sedimentary standing stocks of Si in some regions (Maldonado et al., 2011). Diatoms are thought to be responsible for up to ∼40% of oceanic primary productivity (Nelson et al., 1995), and are especially efficient at exporting carbon from the surface ocean (Buesseler, 1998), giving them an important role in the oceanic biological pump of carbon. The marine cycles of Si and C are thus linked, albeit not in any simple manner, due to the differential cycling of Si; the release of Si from diatom frustules is slower relative to the remineralization of C from diatom cells (Bidle and Azam, 1999; Ragueneau et al., 2000; Bidle et al., 2002; Smetacek et al., 2012). The largest Si fluxes within the global ocean are the result of diatom uptake in and export from the surface ocean (Tréguer and De La Rocha, 2013) (**Figure 1**), most of which takes place in the upwelling regions of the high-latitude open ocean (Honjo et al., 2008) as well as in coastal upwelling regions. Diatoms preferentially take up the lighter isotopes of Si during silicification (De La Rocha et al., 1997; Milligan, 2004; Sutton et al., 2013), resulting in a higher $\delta^{30}Si_{DSi}$ signature in surface ocean DSi (**Figure 1**). Seawater $\delta^{30}Si_{DSi}$ variations are thus primarily created by the fractionation by diatom uptake in the euphotic zone of the ocean, where these photosynthesizers grow. This surface fractionation, combined with the oceanic circulation, is the major control on the global oceanic distribution of $\delta^{30}Si_{DSi}$, which has highlighted some key features of the nature of marine Si cycling in recent years. However, other processes such as hydrothermal activity, and early sedimentary diagenesis are poorly quantified, and thus their impact on the interpretation of Si isotope and trace element signals in sedimentary $bSiO_2$ remains unknown

Global Water Column Distribution

Since active fractionation of $\delta^{30}Si$ by diatoms occurs within the euphotic zone of the ocean, the most extreme $\delta^{30}Si_{DSi}$ values are found within the uppermost 100 m of the water column, with values reaching above +3‰ both in highly nutrient-depleted oligotrophic gyres (with DSi concentrations <1 μM; Reynolds et al., 2006; Grasse et al., 2013) as well as in the slightly more Si-rich high-latitude upwelling regions (with DSi concentrations of 2–13 μM; Varela et al., 2004; Fripiat et al., 2011; de Souza et al., 2012a). These values are amongst the most highly fractionated $\delta^{30}Si$ values reported in the literature (Reynolds, 2011), and at any given location within the ocean, the surface ocean

represents the highest $\delta^{30}Si_{DSi}$ value found in the water column (e.g., Cardinal et al., 2005; Cavagna et al., 2011; Ehlert et al., 2012). Below the maximum in the surface ocean, depth profiles of $\delta^{30}Si_{DSi}$ typically show a monotonic decrease with depth, mirroring the increase in DSi concentration. The steepness of this isotopic gradient varies with oceanographic setting, with sharp $\delta^{30}Si_{DSi}$ decreases observed in upwelling regions where DSi concentrations increase quickly with depth (e.g., Cardinal et al., 2005; Ehlert et al., 2012). Elsewhere in the open ocean, where the silicicline is depressed and DSi concentrations increase only slowly through the uppermost 1,000 m of the water column, $\delta^{30}Si_{DSi}$ values remain elevated to intermediate depths, and can reach up to +1.8‰ at depths of ∼800 m (de Souza et al., 2012a). These elevated values, which result from fractionation of $\delta^{30}Si$ within the euphotic zone, provide robust evidence that the $bSiO_2$-poor nature of the upper ocean is due to the spreading of DSi-depleted water masses that derive from the Southern Ocean, as initially suggested by Sarmiento et al. (2004). These water masses, Sub-Antarctic Mode Water (SAMW) and Antarctic Intermediate Water (AAIW), form from high-latitude surface water masses from which DSi has been stripped by the uptake of heavily silicified Southern Ocean diatoms. This DSi depletion is associated with an isotope fractionation, imparting SAMW and AAIW a high $\delta^{30}Si_{DSi}$ signature (de Souza et al., 2012a), a process that has been dubbed "Southern Ocean isotope distillation" by Brzezinski and Jones (Brzezinski and Jones, 2015). The high $\delta^{30}Si_{DSi}$ signature of SAMW and AAIW is exported to the upper ocean at a near-global scale (De La Rocha et al., 1998; de Souza et al., 2012a,b; Brzezinski and Jones, 2015; Singh et al., 2015). The upper-ocean $\delta^{30}Si_{DSi}$ distribution thus reflects the importance of Southern Ocean water-mass subduction in resupplying DSi, together with other major nutrients, to the nutrient-poor low-latitude upper ocean. The major exception to this strong Southern Ocean influence is the DSi-rich upper ocean of the North Pacific Ocean (Reynolds et al., 2006), which obtains its DSi inventory via upwelling in the subarctic Pacific and also influences the upper-ocean $\delta^{30}Si_{DSi}$ distribution of the equatorial Pacific (Beucher et al., 2008, 2011; de Souza et al., 2012a).

By far the most coherent large-scale $\delta^{30}Si_{DSi}$ variability in the global ocean is observed in the deep and abyssal ocean, below about 2,000 m. Here, DSi concentrations vary by a factor of ∼20, from a little over 10 μM in the DSi-poor waters formed in the North Atlantic Ocean, to over 180 μM in the old, DSi-rich waters of the North Pacific Ocean (Garcia et al., 2014). The strongest DSi gradient is observed within the deep waters of the Atlantic Ocean, where DSi-poor North Atlantic Deep Water (NADW) overlies DSi-rich abyssal waters of Southern Ocean origin (Antarctic Bottom Water, AABW). This DSi gradient is associated with a coherent $\delta^{30}Si_{DSi}$ gradient between isotopically light AABW (+1.2‰) and isotopically heavy NADW with values up to +1.8‰ (de Souza et al., 2012b; Brzezinski and Jones, 2015). It has been argued that the elevated $\delta^{30}Si_{DSi}$ value of NADW is the result of the cross-equatorial transport of a heavy $\delta^{30}Si_{DSi}$ signature by SAMW and AAIW, which flow northward in the Atlantic Ocean to close the upper limb of the meridional overturning circulation (Ehlert et al., 2012; de Souza et al., 2015), illustrating the degree to which Southern Ocean Si utilization and the associated "distillation" of isotopes affects the $\delta^{30}Si_{DSi}$ distribution at the global scale even in the deep ocean. Indeed, this Southern Ocean influence would appear to extend as far north as the Arctic Ocean: recent work has shown that Arctic deep waters Ocean bear the most elevated $\delta^{30}Si_{DSi}$ values in the global ocean, with values averaging +1.9‰ (Varela et al., 2016). Since the Arctic Ocean receives most of its inflow from intermediate waters of the northern Atlantic Ocean, which are influenced by AAIW, the low-DSi, high-$\delta^{30}Si_{DSi}$ end-member characteristics of the deep Arctic Ocean may ultimately derive from Southern Ocean isotope "distillation," although the role of more local processes such as Si cycling within the Arctic Ocean as well as Si input from riverine discharge need to be investigated in more detail.

Apart from the Atlantic and Arctic Oceans, the deep water $\delta^{30}Si_{DSi}$ distribution shows markedly little variability, with Indian and Pacific Ocean deep waters exhibiting $\delta^{30}Si_{DSi}$ values of around +1.2‰ to +1.3‰ (Beucher et al., 2008, 2011; de Souza et al., 2012a; Grasse et al., 2013; Singh et al., 2015), i.e., essentially invariant considering the degree of analytical consistency between laboratories (Reynolds et al., 2007; Grasse et al., 2017). Although there are some hints of heterogeneity in the North Pacific, e.g., in the Cascadia Basin proximal to the North American continent (Beucher et al., 2008), when compared to the ∼0.5‰ meridional gradient observed in the Atlantic Ocean, $\delta^{30}Si_{DSi}$ variability in the Indian and Pacific Oceans is neither particularly significant nor systematic. A possible explanation for this homogeneity comes from a modeling study of the controls on the deep ocean $\delta^{30}Si_{DSi}$ distribution (de Souza et al., 2014), which found that deep water $\delta^{30}Si_{DSi}$ values outside the Atlantic and Arctic Oceans are very strongly governed by the export of isotopically light DSi-rich abyssal water from the Southern Ocean.

Hydrothermal Vents

There are two types of hydrothermal vents that influence the marine Si cycle: (A) on-ridge hot (near critical point) black smoker fluids and, (B) warm (>45°C) and cool (<20°C) Ridge Flank Hydrothermal Fluids (RFHF). They are inherently similar in terms of the Si transfer to the ocean because (a) reactions at high and low temperature leach Si from the oceanic crust, resulting in high (17 ± 3 mmol/kg for hot) and moderate ($\sim 0.5 \pm 0.2$ mmol/kg for warm and cool) DSi hydrothermal fluids and (b) cooling of the hot fluids or warming of the cool and warm fluids removes DSi through precipitation of smectite-like clays before their venting from the seabed (Wheat and McManus, 2005). At a global scale, high temperature hydrothermal DSi fluxes can be constrained at a maximal of 0.14 ± 0.02 Tmol yr^{-1} using a Si input of 17 ± 3 mmol/kg (the average concentration in hydrothermal vents at an exit temperature of 300°C) with a water flux at 8×10^{12} kg yr^{-1} (Coogan and Dosso, 2012). However, the influence of hydrothermal inputs on the global marine Si cycle remain uncertain due to the paucity of $\delta^{30}Si$ data available. To date, the only published data are two data points (−0.4‰ and −0.2‰) for hydrothermal vents on the East Pacific Rise (De La Rocha et al., 2000).

Sedimentary Processes

Upon deposition on the seabed, recycling of SiO_2 during early diagenesis in marine sediments involves: (a) initial dissolution of $bSiO_2$ and/or detrital siliceous phases and consequent DSi build-up in marine pore waters (b) flux of dissolved Si out of the sediments and (c) $bSiO_2$ reconstitution and/or precipitation of SiO_2-rich diagenetic solid phases. The three recycling processes take place simultaneously and ultimately control DSi fluxes and diagenetic SiO_2 deposition and storage in marine sediments (Dixit et al., 2001; Aller, 2014) (**Figure 1**). When early diagenetic siliceous precipitates are rich in seawater-derived cations (e.g., K, Mg) the precipitation process is called "reverse weathering" and the cation-rich precipitates "reverse weathering products" (Mackenzie and Garrels, 1966; Michalopoulos and Aller, 1995).

Pore water and biogenic silica preservation

The $\delta^{30}Si$ of pore waters from marine sediments is an indicator of diagenetic turnover of Si and its impact on the preservation of environmental signals in $bSiO_2$ (Ehlert et al., 2016). In fine-grained terrigenous sediments of the Amazon delta these authigenic Al-Si phases form at a rate as high as 280 μmol Si cm^{-2} yr^{-1} (Michalopoulos and Aller, 2004). In shelf sediments the rate is thought to be substantially lower at around 56 μmol Si cm^{-2} yr^{-1}, which, however, means that approximately 24% of the total dissolving $bSiO_2$ re-precipitates in the upper few centimeters of the sediment (Ehlert et al., 2016). Several experimental studies have shown that such Si precipitation is associated with strong enrichment of light Si isotopes up to −4.5‰ in the product although they were not focused on sediment—pore water diagenesis (e.g., Geilert et al., 2014; Oelze et al., 2014, 2015; Roerdink et al., 2015).

To date, there have been only a few studies that investigated the effect of diagenesis on preservation of the primary environmental signal in $bSiO_2$ and they found potentially differing results. Demarest et al. (2009) reported a preferential release of light Si isotopes during partial dissolution of $bSiO_2$ in batch reactors, whereas leaching experiments with sediments showed no fractionation (Wetzel et al., 2014; Tatzel et al., 2015). In young hemi-pelagic sediments, the early diagenetic formation of new Al-Si phases is focused in the topmost layer of the sediment column (ca. 0–10 cm sediment depth). Ehlert et al. (2016) found pore waters from the Peruvian shelf with high $\delta^{30}Si$ (average 1.46 ± 0.22‰) with the highest values occurring close to the sediment–water interface. These values were enriched compared to $bSiO_2$ in the cores (average 0.85 ± 0.28‰) and overlying bottom water (<1.5‰), which is consistent with the formation of authigenic Al-Si phases from the dissolving $bSiO_2$. The fractionation factor between the precipitates and the pore waters was estimated at −2.0‰. However, the isotope composition of the $bSiO_2$ seemed to remain constant within the reactive surface layer where most of the dissolution and precipitation occurred, which makes isotopic fractionation during dissolution unlikely. From leaching experiments on older Pleistocene and Pliocene sediments, Tatzel et al. (2015) report that the formation of authigenic Al-Si phases should be 2‰ lighter than the pore waters they formed from, in agreement with previous experimental results (Delstanche et al., 2009; Geilert et al., 2014; Oelze et al., 2014, 2015). However, the authors observed an increase of the Si isotope composition of the preserved SiO_2 during phase transformation from opal-A to opal-CT. The reason for this was an isotope exchange between SiO_2 and pore water, and the Si isotope increase was higher with an increase in the amount of detrital material in the sediment.

Diagenetic silica precipitation and reverse weathering

It has been proposed that reverse weathering reactions in marine sediments are significant oceanic sinks for K, Mg, and alkalinity (Mackenzie and Garrels, 1966; Rude and Aller, 1994; Michalopoulos and Aller, 1995, 2004; Sun et al., 2016). The precipitation process can also involve the uptake of minor elements (Li, Ge, F) into new authigenic siliceous phases, which can act as primary sinks and thus balance the oceanic mass and isotopic budget. The incorporation of redox-sensitive elements (e.g., Fe) depends on the availability and early diagenetic cycling of the relevant element in dissolved form.

Currently, the flux of reverse weathering on the global Si cycle is estimated at −0.63 ± 0.6 Tmol yr^{-1} (Frings et al., 2016) or 1.5 ± 0.5 (Tréguer and De La Rocha, 2013) (**Figure 1**, Table S1), however, it is assumed that this flux is under-estimated. It has been proposed that reactive $bSiO_2$ that has undergone reconstitution/dissolution/re-precipitation transformations remains partially unaccounted for (Michalopoulos and Aller, 2004; Presti and Michalopoulos, 2008) using the traditional operational leach method of DeMaster (1981). However, measurements of cosmogenic ^{32}Si incorporated in reactive SiO_2 products indicate that even the modified alkaline leach methods used to date in high sediment accumulation rates underestimate the amount of reconstituted $bSiO_2$ and authigenic silicates stored in deltaic sediments (Rahman et al., 2016). Thus the conservative estimates for the net storage of altered $bSiO_2$ and authigenic silicates in deltaic sediments range from 2–3x in the Mississippi (Presti and Michalopoulos, 2008) to 5–10x in the Amazon (Michalopoulos and Aller, 2004). Based on ^{32}Si, actual storage in the Amazon delta may be 2–3x greater (i.e., 3–4.5 Tmol yr^{-1}) than the best recent conservative estimates (Rahman et al., 2016).

In general, the impact of dissolution, diagenesis and reverse weathering on the stable isotope analysis of $bSiO_2$ are poorly understood. Whilst it is possible to assess the degree of recrystallization of $bSiO_2$ through geological time (De La Rocha, 2003), there are some early stage dissolution and diagenetic processes that can occur in the water column and shallow sediments that may be more challenging to detect. However, studies seem to indicate that with high $bSiO_2$ concentrations in the sediments, the original $\delta^{30}Si$ of the $bSiO_2$ is more likely to be preserved because exchange with pore water and the formation of authigenic Al-Si phases is limited.

Additional Challenges in Interpreting Marine Data

In addition to environmental alteration (see sections Pore Water and Biogenic Silica Preservation and Diagenetic Silica Precipitation and Reverse Weathering) and any analytical challenges associated with the separation and cleaning (see section Multi-proxy Geochemical Approaches in Palaeoceanography) of $bSiO_2$ from sediment cores, ensuring the effective removal of any contaminant phases (Morley et al., 2004;

Egan et al., 2012), there are a number of different biological and ecological assumptions that are required for the interpretation of both Si and oxygen isotopes ($\delta^{18}O$) in diatom $bSiO_2$.

Firstly, many downcore studies assume a constant $\delta^{30}Si$ fractionation factor of $-1.1 \pm 0.4‰$, which was based on the initial culture studies carried out by De La Rocha et al. (1997). However, more recent studies show that this fractionation factor may be more variable, and potentially species-specific, based on both field studies (e.g., Varela et al., 2004; Beucher et al., 2007; Ehlert et al., 2012; Fripiat et al., 2012) and culture experiments (Sutton et al., 2013).

Secondly, the mathematical models of DSi utilization also assume a starting value of $\delta^{30}Si_{DSi}$ for the upwelling water, which supplies the essential nutrients to diatoms in the surface layer. To a certain extent, this can be estimated using simple box models (e.g., Beucher et al., 2007), and/or deep-water archives [see section Palaeoceanographic (and Palaeolimnological) Applications below Horn et al., 2011; Egan et al., 2013]. There is a potential that changes in water mass circulation, or end-member composition, could impact the distribution of silicon isotope ratios in the oceans (Hendry and Robinson, 2012) (see section Global Water Column Distribution). Furthermore, changes in inputs and—potentially—biological productivity and diatom $bSiO_2$ burial could change the whole ocean Si isotope budget over periods of time longer than the residence time of Si in the ocean, 10–15 thousand years (Frings et al., 2016; Hawkings et al., 2017).

PALAEOCEANOGRAPHIC (AND PALAEOLIMNOLOGICAL) APPLICATIONS

The stable isotopic composition of biogenic $bSiO_2$, together with the concentration and stable isotope composition of trace elements within the $bSiO_2$, provide a useful source of palaeoceanographic data. The remains of silicifiers, isolated from marine sediments, are effective archives of marine Si cycling at different depths within the water column, yielding key information about DSi supply and utilization by marine algae. Si cycling by algae is important to quantify if we are to understand the processes that are critical to the cycling of carbon in the Earth's climate system, such as changes in organic carbon production and export, oceanic circulation and chemical weathering (Frings et al., 2016). Biogenic SiO_2 has the potential to provide records of marine Si cycling throughout the Cenozoic in the case of diatoms, and further back into the Meso- and Palaeozoic in the case of radiolarians and sponges, as it is well-preserved and widespread in sediments, and can be readily assessed for diagenesis through XRD analysis (e.g., De La Rocha, 2003). In addition, $bSiO_2$ archives are useful in climatically important locations where the more traditional, carbonate-based palaeoceanographic archives (principally foraminifera) are poorly preserved, such as the Quaternary Southern Ocean.

In the following sections, we will provide a summary of the $bSiO_2$-based palaeoceanographic tools available, including trace element geochemistry (section Trace Element Geochemistry of Diatoms and Sponges) and major element stable isotope methods (section Major Element Stable Isotope Ratios in Diatoms, Sponges and Radiolarians). These sections emphasize the value of multi-archive and –proxy approaches to better constrain changes in silicon (bio)geochemistry and examples of such applications are provided within the context of palaeoceanography in section Multi-proxy Geochemical Approaches in Palaeoceanography (e.g., Silicic Acid Leakage Hypothesis). Although we will focus on the more widely studied silicifying organisms (diatoms, sponges and radiolarians), there is a wealth of other silicifying organisms in the oceans that are yet to be explored for their potential as oceanographic archives.

Trace Element Geochemistry of Diatoms and Sponges

Biogenic silica incorporates low quantities of trace elements into the structure. Although often in parts per million—or less—the concentrations of these elements (often normalized to Si) can reveal information about the environmental conditions during growth. Many of these elements show strong correlations with DSi in seawater and exhibit "refractory nutrient-like" profiles.

Aluminum

Aluminum is one of the most abundant, but highly variable, trace elements in $bSiO_2$ ranging from 0.0001 to 0.1 g/g (e.g., Hendry et al., 2011). Although Al uptake occurs by adsorption and is present in associated clay phases (van Bennekom and van der Gaast, 1976; Moran and Moore, 1988), Al is also incorporated into living diatom $bSiO_2$ that is still protected by an organic matrix (Gehlen et al., 2002). X-ray absorption spectra at the Al-K edge show that Al occurs in 4-fold co-ordination, with tetrahedra inserted inside the $bSiO_2$ framework, although samples of diatom $bSiO_2$ taken from natural marine waters show both 4- and 6-fold co-ordination, possibly as a result of clay contamination (Gehlen et al., 2002). Whilst there appear to be some climatic signals in Al/Si in diatom $bSiO_2$ (e.g., Hendry et al., 2011), Al/Si appears to be highly susceptible to rapid alteration during early sedimentation processes, most likely sourced from clay material (Ren et al., 2013) increasing an order of magnitude or more between water column or sediment trap samples and sediment core tops in both laboratory and field studies (Koning et al., 2002, 2007; Loucaides et al., 2010; Hendry et al., 2011). In addition to Al concentration analysis, diatom $bSiO_2$ ^{26}Al and ^{10}Be have also been explored as archives of marine cosmogenic nuclide concentrations (Lal et al., 2006). Less is known about the Al content of other silicifiers, although limited data indicate that the Al/Si of fresh sponge $bSiO_2$ is lower than that of diatoms (<0.0002 g/g; Hendry and Andersen, 2013).

Germanium

In the ocean, dissolved inorganic germanium (Ge) cycles in a manner similar to that of DSi, with Ge uptake and regeneration from diatom frustules being the main control on its oceanic distribution (Froelich and Andreae, 1981; Froelich et al., 1989; Mortlock and Froelich, 1996; Sutton et al., 2010). Although Ge mimics Si, differences in their geochemical behavior can occur reflecting differences in the oceanic inputs and losses and subtle differences in the biogeochemical cycling of these two elements within the ocean. Because of differences in molecular weight and subtle differences in chemistries, the uptake, incorporation

and regeneration of Ge from diatom $bSiO_2$ is also non-ideal. These differences are especially apparent at low DSi and Ge concentrations where there is apparent discrimination of Ge during Si uptake via $bSiO_2$ formation (Sutton et al., 2010), which lead to significant non-zero Ge intercept and slightly non-linear behavior of the global Ge-Si relationship ($[Ge] = 0.76 \pm 0.00[Si] + 0.08 \pm 0.17$, $r^2 = 1.00$, $n = 248$, Ge in pmol L^{-1} and Si in μmol L^{-1}). The fractionation of Ge during uptake with Si is readily apparent in deep sea sponges which have a lower affinity for Si uptake (Froelich and Barthel, 1997; Reincke and Barthel, 1997; Maher et al., 2006).

The two main sources of Ge and Si to the ocean are mineral weathering and hydrothermal fluids (Mortlock and Froelich, 1987; Mortlock et al., 1993; Kurtz et al., 2002). Weathering produces low Ge:Si ratios (Ge/Si) input ratios as reflected in the Ge/Si for rivers (0.3–1.2 μmol/mol), while hydrothermal fluids have higher Ge/Si input ratios (8–14 μmol/mol) (Mortlock and Froelich, 1987; Mortlock et al., 1993; Kurtz et al., 2002). The two main sinks for Ge removal from the ocean are through incorporation into $bSiO_2$ and Ge lost via in non-opal phases (Murnane et al., 1989; Hammond et al., 2000, 2004; King et al., 2000; McManus et al., 2003). Currently, there is debate about the magnitude and loss via the 'missing Ge sink' (Hammond et al., 2000, 2004; King et al., 2000; McManus et al., 2003; Baronas et al., 2016; Rouxel and Luais, 2017). Recently Baronas et al. (2016) have suggested that Ge loss from the ocean appears to be dependent on pore-water oxidation–reduction reactions and the formation authigenic aluminosilicate (see section Sedimentary Processes) minerals within marine sediments. Note, a recent study looking at the links between Ge isotopes and silicon in Hawaiian hydrothermal vents has shown the potential of this new isotopic system to trace the fate of hydrothermal elements released into the ocean (Escoube et al., 2015).

While inorganic Ge can be lost from solution through incorporation into biogenic silica and association with authigenic mineral formation, there is a large unreactive organic Ge pool within the dissolved phase; monomethyl- and dimethyl-germanium. The formation of these two species is relatively unknown, but it is speculated to be continentally derived and lost under anoxic conditions (Lewis et al., 1985, 1988, 1989). The residence time for these methylated forms of Ge are on the order of 100,000+ years, which is considerably longer than that of inorganic Ge.

In addition, inorganic Ge can form stable complexes with organic molecules (e.g., humic acids) containing di- and polyfunctional carboxylic acids, polyalcohols and ortho-diphenols functional groups. Complexation of Ge by humic acids in freshwater regimes needs to be considered with interpreting variations in the Ge/Si ratio for the global ocean through time with respect to terrestrial inputs (Pokrovski and Schott, 1998). The organic Ge complexation has also been suggested to explain the low Ge/Si ratio in phytoliths due to different pathways of Ge relative to Si in the plant: Ge is not discriminated against at the root–soil solution interface but it is organically trapped in roots, in contrast to Si (Delvigne et al., 2009).

The Ge/Si imprinted into diatom frustules has proven useful for palaeo-reconstructions but it gives no information regarding the sizes of the Si and Ge oceanic pools. The overall Ge/Si for the diatom $bSiO_2$ from the Southern Ocean is relatively constant and appears to reflect seawater Ge/Si (Shemesh et al., 1988; Froelich et al., 1989); however, the late Pleistocene diatom Ge/Si record shows clear, systematic variations between interglacial (Ge/Si = 0.70–0.78 μmol/mol) and glacial periods (Ge/Si = 0.45–0.60 μmol/mol) (Froelich et al., 1989; Mortlock et al., 1991; Bareille et al., 1998) suggesting that size of either the Si or the Ge pool has varied (Murnane et al., 1989; Froelich et al., 1992; Hammond et al., 2000, 2004; King et al., 2000; McManus et al., 2003). To date, little progress has been made to follow up on this earlier work and our understanding on what drives the large variations has little advanced since the work of King et al. (2000), Hammond et al. (2004), and McManus et al. (2003) (see Rouxel and Luais, 2017 for more detail).

Zinc

Zinc is incorporated into diatom $bSiO_2$ in approximately 1–20 ppm levels. Culture studies show that the Zn/Si content of diatom $bSiO_2$ relate to the concentration of free Zn^{2+} ions in the ambient seawater (Ellwood and Hunter, 1999). However, more recent observations of Zn speciation in the Southern Ocean question this link, because the variability in free Zn^{2+} ion concentrations are not captured by diatom $bSiO_2$ Zn/Si (Baars and Croot, 2011). Field studies support a link between diatom $bSiO_2$ Zn/Si and productivity and diatom $bSiO_2$ burial rates, although the mechanism behind this relationship is less clear and could relate to nutrient uptake vs. supply, growth rate or salinity (Hendry and Rickaby, 2008; Andersen et al., 2011). The Zn/Si ratio of diatom $bSiO_2$ from sediment cores, which appears to be less susceptible to initial alteration of the $bSiO_2$ as compared to Al/Si (Hendry and Rickaby, 2008), has been used in a small number of studies as a proxy for changes in Zn supply to surface waters in the open ocean and coastal Southern Ocean regions (Ellwood and Hunter, 2000; Hendry and Rickaby, 2008). Recent studies indicate that a large proportion of Zn uptake by diatoms is into the organic material in the cell rather than the $bSiO_2$, challenging its use as a palaeoceanographic proxy (Twining et al., 2003). Thorough cleaning protocols are required to ensure only the Zn incorporated into the silica structure is analyzed (Hendry and Rickaby, 2008; Andersen et al., 2011).

Zinc isotopes (denoted by $\delta^{66}Zn$) in diatom $bSiO_2$ ranges from 0.7 to 1.5‰ and appears to relate to changes in seawater $\delta^{66}Zn$ composition because of biological drawdown of isotopically light Zn by phytoplankton. If this is the case, then $\delta^{66}Zn$ in diatom $bSiO_2$ from sediment cores has the potential to be used as an archive of Zn biogeochemical cycling in the past (Andersen et al., 2011). However, Zn isotopic fractionation during incorporation into diatoms appears to be determined by whether the diatom is utilizing a high or low-affinity Zn transport mechanism, in addition to ambient free Zn^{2+} concentrations, and is also heavily influenced by surface adsorption and organic matter incorporation (John et al., 2007; Zhao et al., 2014).

One study has shown that Zn/Si in sponges relates to the flux of particulate organic carbon (POC) to sediments (Ellwood et al., 2004), leading to its potential use as an export production proxy (Ellwood et al., 2005). Sponge $\delta^{66}Zn$ systematics appear

to differ between major groups of silicifying sponges: $\delta^{66}Zn$ reflects seawater zinc isotopic values in Hexactinellids, whereas Demosponge $\delta^{66}Zn$, most likely reflects a combination of internal isotopic fractionation and fractionation of isotopes in dietary organic matter (Hendry and Andersen, 2013).

Major Element Stable Isotope Ratios in Diatoms, Sponges and Radiolarians

Given that $bSiO_2$ is high-purity SiO_2, the most straightforward targets for geochemical analysis are stable Si and oxygen isotope ratios (denoted by $\delta^{30}Si$ and $\delta^{18}O$, respectively). However, other major elements, including C and N that are encased within the $bSiO_2$, have also been analyzed. Here, we review recent developments in the use of major isotope systems in $bSiO_2$ produced by diatoms, sponges and radiolarians as palaeoceanographic proxies.

Carbon

Increasingly, studies of carbon isotopes are turning to the analysis of specific organisms rather than bulk organic matter so that changes in the carbon cycle can be better investigated without the complication of a mixed source. For example, $\delta^{13}C$ analysis can be undertaken on the cellular (occluded) organic matter in diatoms, which is well protected from degradation by the frustule. During photosynthesis, organic carbon matter is formed from both HCO_3^- and $CO_{2(aq)}$ and incorporated into diatoms (Tortell and Morel, 2002). The main control on $\delta^{13}C_{diatom}$ is the balance between supply and demand for Dissolved Inorganic Carbon (DIC), driven by variations in biological productivity or carbon cellular concentrations. Organisms, including diatoms, preferentially use ^{12}C over ^{13}C, so as photosynthetic demand for DIC rises, increasing amounts of ^{12}C are removed from the DIC pool, leading to progressively higher $\delta^{13}C_{diatom}$ (Laws et al., 1995). Other factors that could influence $\delta^{13}C_{diatom}$ include changes in the $\delta^{13}C_{DIC}$ of inputs to the water column, particularly in the lacustrine environment where the sources of the carbon supplied will be more variable (Barker et al., 2013), dissolution of diatoms, which releases carbon into the ambient water, and changes in $CO_{2(aq)}$ concentration (Laws et al., 1995; Rau et al., 1996, 1997). Therefore, if factors such as inter-species vital effects can be controlled for (Des Combes et al., 2008), or if samples of a single species are analyzed (Swann and Snelling, 2015), then changes in $\delta^{13}C_{diatom}$ can be used to reconstruct environmental changes. In marine sediments, this is usually primary productivity (e.g., Shemesh et al., 1995; Panizzo et al., 2014; Swann and Snelling, 2015) and/or changes in CO_2 (Heureux and Rickaby, 2015; Stoll et al., 2017). In the case of lake sediments, $\delta^{13}C_{diatom}$ is used to reconstruct changes in the balance between the source and amount of carbon supply and the productivity within the lake ecosystem (e.g., Barker et al., 2013).

Nitrogen

The measurement of variations in diatom-bound stable isotopes of nitrogen (expressed as $\delta^{15}N$) is a powerful tool to reconstruct past nitrogen (N) utilization from palaeo-archives (e.g., Sigman et al., 1999; Robinson et al., 2004). To date, ~10 studies have used diatom-bound $\delta^{15}N$ obtained from sediment cores to reconstruct palaeo N cycling, with a strong focus on the Southern Ocean (e.g., Crosta and Shemesh, 2002; Robinson et al., 2004, 2005; Robinson and Sigman, 2008; Horn et al., 2011). Shemesh et al. (1993) was the first to develop a method that used the organic matter contained within the hydrated SiO_2 matrix of the diatom, making it possible to measure diatom-bound N stable isotopes (^{15}N and ^{14}N). However, during the last decade the chemical preparation has systematically improved (e.g., Sigman et al., 1999; Robinson et al., 2004). During nitrate uptake, diatoms preferentially incorporate the lighter isotope (^{14}N) into the organic matter (e.g., Altabet et al., 1991; Montoya and McCarthy, 1995), which affects the isotope composition of both the diatom and the residual nitrate. An enzymatic pathway catalyzes this process, where nitrate is reduced to nitrite by nitrate reductase (e.g., Needoba et al., 2003), which can lead to high fractionation factors of up to 14.0‰ in cultured polar diatoms (Horn et al., 2011). Generally, the fractionation of diatom-bound $\delta^{15}N$ shows a broad range (1–14‰), with high $\delta^{15}N$ variations among diatom species (1.9–11.2‰) with weak relationship between $\delta^{15}N$ and cellular size and/or surface area (Horn et al., 2011). Unlike bulk sedimentary $\delta^{15}N$, which is routinely measured to reconstruct N cycling (N utilization and N-loss process), preparation of diatom-bound $\delta^{15}N$ is more time consuming and cost intensive (Robinson et al., 2012), but does not appear to be isotopically altered by early bacterial diagenesis (e.g., Freudenthal et al., 2001).

Oxygen

The oxygen isotope ($\delta^{18}O$) values of calcareous marine microfossils, notably foraminifera, have been used extensively to constrain changes in ocean dynamics (such as global ice volume) over the past 70 Ma of Earth history (e.g., Zachos, 2001; Lisiecki and Raymo, 2005). Antarctic ice volume has likely played a significant role in Cenozoic deep water formation, oceanic circulation, and global-scale climate variations; however, poor preservation of calcareous fossils in high-latitude marine sediments has limited attempts to expand the geographical resolution of the benthic marine carbonate oxygen isotope record (Sarmiento and Toggweiler, 1984; Elderfield and Rickaby, 2000; Lisiecki and Raymo, 2005; Raymo et al., 2006). Unlike carbonate minerals, $bSiO_2$ is generally well preserved in high-latitude marine sediments; therefore, the $\delta^{18}O$ values of diatom $bSiO_2$ from these regions have the potential to vastly expand our understanding of coupled ice-ocean dynamics (e.g., DeMaster, 2003; Swann and Leng, 2009).

Little is known about spicule $\delta^{18}O$ systematics, although there appear to be complex biological vital effects in freshwater sponges (Matteuzzo et al., 2013). A study of a marine carnivorous sponge $\delta^{18}O$ showed large fractionation effects and highly heterogeneous isotopic behavior within one individual (Hendry et al., 2015). One downcore study indicates that there are systematic offsets between spicule and diatom $bSiO_2$ $\delta^{18}O$ (Snelling et al., 2014).

Silicon

Many (at least 25) glacial-interglacial records, from marine sediment cores, of $\delta^{30}Si$ of silicifying organisms (i.e., diatoms, sponges, radiolarians) display a similar trend:

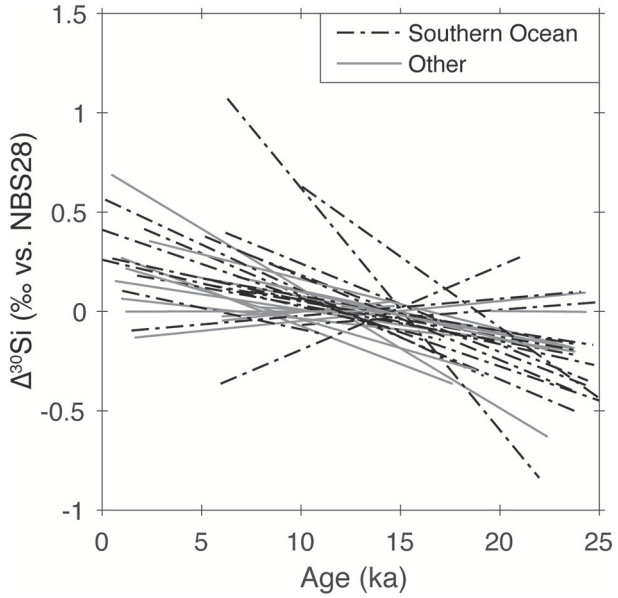

FIGURE 2 | Least-squares regression lines fit though sedimentary $\delta^{30}Si_{bSiO2}$ records from 25 ka to present, standardized to mean $\delta^{30}Si$ of the record: almost all records show an increase from the glacial to the Holocene, with an average trend of ca. 0.045‰ ka-1, suggestive of a common mechanism. Data are from Beucher et al. (2007), Brzezinski et al. (2002), De La Rocha et al. (1998), Doering et al. (2016), Ehlert et al. (2013), Ellwood et al. (2010), Hendry et al. (2010), Hendry et al. (2014), Hendry et al. (2012), Horn et al. (2011), Kim et al. (2017), Maier et al. (2013), Panizzo et al. (2014), Pichevin et al. (2012), Pichevin et al. (2009), Sutton (2011), and Xiong et al. (2015).

lower glacial $\delta^{30}Si$, higher interglacial $\delta^{30}Si$ (see **Figure 2**). While this general pattern has been noted before, most of the records have been interpreted in isolation in terms of nutrient palaeo-utilization (or Si concentrations, for spicule records), and conclusions are related to local-regional nutrient supply (ocean circulation). Trace metal ratios (see section Trace Element Geochemistry of Diatoms and Sponges) may provide an additional constraint but interpretation is difficult since the marine budgets of both the elements (i.e., the trace element, together with the Si cycle) are poorly constrained.

Diatoms

Silicon isotope ratios in diatom $bSiO_2$ have been used widely as a proxy for marine DSi utilization in surface waters due to the preferential fractionation of the lighter isotope of Si during diatom silicification (see section Marine for more detail). The proxy works on the premise that as diatoms grow in a "parcel" of seawater and progressively use up the available DSi, both the remaining DSi and the $bSiO_2$ produced at any instant become progressively isotopically heavier (see section Marine for detail). The fractionation can be modeled, assuming either closed or open distillation of Si isotopes, allowing the back-calculation of past utilization from downcore diatom $\delta^{30}Si$ archives (De La Rocha et al., 1997, 1998; Varela et al., 2004). The calculation assumes a known and constant fractionation factor, denoted by epsilon (see section Stable Silicon Isotope Ratios to Study the Global Si Cycle).

Similar to marine work (Varela et al., 2004; Closset et al., 2015), lake sediment traps have shown the $\delta^{30}Si$ signature of diatoms ($\delta^{30}Si_{diatom}$) to be resilient to dissolution and preserved through the water column into the sediment record (Panizzo et al., 2016). Accordingly, $\delta^{30}Si_{diatom}$ from lacustrine sediment cores can be used to reconstruct past changes in biogeochemical cycling at the catchment/drainage basin scale. Whilst only a limited number of palaeolimnological studies have been undertaken, all demonstrate the potential for $\delta^{30}Si_{diatom}$ to constrain long-term changes in the Si cycling in relation to catchment processes and/or physical limnological. For example, a record from Arctic Siberia covering the last 31 ka demonstrates that rates of DSi utilization are governed by catchment weathering and ice-cover duration together and mixing in the water column (Swann et al., 2010). Elsewhere, records from East Africa demonstrate the importance of monsoonal rainfall and their associated impact on vegetation in regulating the Si cycle. In the upper White Nile basin results reveal that higher monsoonal rainfall and associated increases in forest cover and chemical weathering increased the flux of DSi from land to rivers during the late-glacial/mid-Holocene, conditions that reversed after 5.5 ka with the emergence of dryer conditions and open vegetation/crops (Cockerton et al., 2015). Further east in Kenya measurements of $\delta^{30}Si_{diatom}$ in a lake demonstrate that high levels of glacial diatom productivity were supported by increased fluxes of Si from the sparse catchment (Street-Perrott et al., 2008). Subsequent reductions in aquatic productivity then coincide with the development of grasslands and other Holocene vegetation, in response to increase monsoonal rainfall, which reduced Si transportation to the lake (Street-Perrott et al., 2008).

The potential of $\delta^{30}Si$ is particularly evident in regions where climate change and anthropogenic lake catchment alteration (e.g., nutrient loading) are prompting limnological responses (e.g., increased duration of lake stratification and warmer surface water temperatures), which impact within lake biogeochemical cycling (Panizzo et al., 2017). For example, the approach has been demonstrated as a means to identify biogeochemical responses to climate change (Street-Perrott et al., 2008; Swann et al., 2010) and its value over more recent timescales is also stressed here as a means to address current pressures. Comprehensive contemporary limnological monitoring is also emphasized (Opfergelt et al., 2011) to enable quantitative estimations of seasonal DSi and $bSiO_2$ cycling (via open or closed system modeling), by providing key constraints on deep-surface water $\delta^{30}Si_{DSi}$ exchange, Si residency times and Si uptake (Panizzo et al., 2016, 2017). These data also serve to validate conventional palaeolimnological approaches, which can be applied to constrain continental $bSiO_2$ export from lake and reservoirs, particularly under a projected future of enhanced anthropogenic and climatic pressures on these systems.

Siliceous sponges

Unlike diatoms, there is evidence that siliceous sponges have a variable fractionation of Si isotopes with respect to seawater. A compilation of modern sponge spicules, and core top

spicules, reveals that there is a statistically significant non-linear relationship between sponge $\delta^{30}Si$, or the difference between seawater and spicule $\delta^{30}Si$ (denoted by $\Delta^{30}Si$), and ambient DSi concentrations during sponge growth (Hendry et al., 2010; Wille et al., 2010; Hendry and Robinson, 2012). This empirical calibration means that there is a great potential for spicule $\delta^{30}Si$ in sediment cores to be used as a proxy for bottom water DSi concentrations in the past, providing key information about the supply of waters that feed diatom productivity (Hendry et al., 2010; Hendry and Robinson, 2012). The relationship is robust between laboratories (Hendry et al., 2011), and whilst the mechanism behind this relationship remains unclear, the observations are consistent with a strong growth-rate dependence on DSi uptake in sponges (Wille et al., 2010; Hendry and Robinson, 2012). The relationship between DSi and sponge $\delta^{30}Si$ appears to hold for different filter-feeding sponges from different taxonomic groupings and ocean basins, growing in significantly different temperature, salinity and pH conditions (Hendry and Robinson, 2012). Furthermore, spicules from core top sediments also fall on the same calibration line, indicating minimal impact of early diagenetic processes (Hendry and Robinson, 2012). However, unusual biomineralization processes and potentially the internalization and isolation of the aquiferous system in highly-derived carnivorous sponges result in $\delta^{30}Si$ values that deviate significantly from the global compilation (Hendry et al., 2015). Further investigation into different biomineralization pathways—and their impacts on isotopic fractionation—would be beneficial. Studies of isotopic fractionation by sponges grown in culture will add a great deal to our understanding of spicule geochemistry and biomineralization mechanisms.

Radiolaria

There have been fewer studies into the stable isotope composition of radiolarians compared to diatoms and sponges, and their use as palaeoceanographic archives is very much in its infancy. Radiolarian Si and oxygen isotope fractionation factors are challenging to constrain from culture studies because they are difficult to grow under laboratory conditions and field studies are limited by knowledge regarding the migration, strong biogeographic distributions and relatively sparse numbers (Suzuki and Aita, 2011). However, there have been a small number of studies that have attempted to constrain a fractionation factor for Si isotopes in radiolarians, which have estimated a similar fractionation range as for modern diatoms (ca. −0.5 to −2.1‰; Hendry et al., 2014; Abelmann et al., 2015). As such, there is potential for radiolarian $\delta^{30}Si$ to be used, in combination with modeling efforts, to constrain mid-depth to surface DSi systematics. In short, more sediment records of $\delta^{30}Si$ in sponges and radiolarians are needed to estimate nutrient concentrations and distribution with reorganizations in ocean circulation.

Multi-proxy Geochemical Approaches in Palaeoceanography

The Southern Ocean plays a key role in climate variability, via heat transport and atmospheric greenhouse gas changes, over glacial-interglacial timescales through both physical and biogeochemical mechanisms. One such mechanism to explain at least part of the atmospheric CO_2 changes observed in ice core records is the Silicic Acid Leakage Hypothesis SALH (Brzezinski et al., 2002; Matsumoto et al., 2002). The SALH proposes that enhanced dust deposition in the Southern Ocean during glacial periods causes physiological changes in diatoms, such that they take up less DSi relative to other nutrients (i.e., N, P), resulting in the export of DSi enriched waters via AAIW (Ellwood et al., 2010; Rousseau et al., 2016). Supply of relatively DSi-rich Mode Waters at lower latitude would enhance the growth of diatoms over carbonate producers, altering ocean alkalinity leading to a reduction in atmospheric CO_2 (Matsumoto and Sarmiento, 2008).

Geochemical archives locked up in $bSiO_2$ can be used to test the SALH. A recent example, used both oxygen and Si isotopes in diatoms and radiolarians, from glacial-aged sediments from the Southern Ocean, to provide reconstructions of seasonal nutrient cycling. Data show strong variability in the mixed layer depth in the seasonal sea-ice zone, which allowed for sufficient nutrient exchange between surface and deeper waters, thereby fueling carbon drawdown in an otherwise highly stratified glacial Southern Ocean (Abelmann et al., 2015). Diatom $\delta^{30}Si$ and organic-bound $\delta^{15}N$ archives from the Southern Ocean have also been coupled with a spicule $\delta^{30}Si$ record of bottom water DSi concentrations to investigate DSi utilization across the last glacial termination. By modeling the diatom Si-uptake, assuming the spicules reflect the supply of DSi, these archives demonstrate periods of intense upwelling and a greater utilization of the DSi supply in response to changes in iron availability during the deglaciation period (Horn et al., 2011).

In addition to using the relative $bSiO_2$ accumulation rates between the Southern Ocean and lower latitudes as a test for Si export (e.g., Bradtmiller et al., 2009; Meckler et al., 2013), it is possible to use combined geochemical proxy records to test the SALH (Rousseau et al., 2016). Biogenic SiO_2 archives point toward abrupt shifts in productivity and DSi utilization at glacial terminations, rather than changes on glacial-interglacial timescales (e.g., using coupled spicule, hand-picked radiolarian and diatoms from archives in the Sargasso Sea; Hendry and Brzezinski, 2014). Such observations, and other geochemical records, have led to the formulation of a new Silicic Acid Ventilation Hypothesis, which posits that sluggish glacial Southern Ocean overturning primed southern sourced Mode Waters to cause major changes in nutrient distribution during periods of abrupt climate change in low latitude regions influenced by intense ventilation (Hendry and Brzezinski, 2014; Hendry et al., 2016).

Challenges for Palaeo-Record Interpretation

Cleaning of $bSiO_2$

The cleaning of $bSiO_2$ remains an important challenge in $\delta^{30}Si_{bSiO2}$, $\delta^{18}O_{bSiO2}$, $\delta^{13}C_{diatom}$, and $\delta^{15}N_{diatom}$ reconstructions. Contamination, via the presence of residual tephras or clays can compromise the precision of reconstructions, with the

introduction of significant isotopic offsets (Morley et al., 2005; Lamb et al., 2007; Brewer et al., 2008). This is often more pronounced for diatoms (and radiolarians; Abelmann et al., 2015) due to the ability for contaminant valve adherence and occlusion, over sponge spicules that can be picked. Clay $\delta^{30}Si$ compositions are estimated between −2.95‰ and +2.5 (Douthitt, 1982; Georg et al., 2009; Opfergelt and Delmelle, 2012), which can significantly lower reported $\delta^{30}Si_{diatom}$ values [published values range between −0.07 and +3.05‰; (De La Rocha et al., 2000; Cardinal et al., 2007; Sun et al., 2013; Panizzo et al., 2014, 2016)] and outside of analytical uncertainty, while high sample presence of different phases of $bSiO_2$ can have a similar effect (e.g., $\delta^{30}Si_{sponge}$ signatures vary between −5.72 and +0.87‰ Douthitt, 1982; De La Rocha, 2003; Wille et al., 2010; Hendry and Robinson, 2012). As a result, purity is routinely demonstrated visually (via scanning electron microscopy) and via quantitative assessments of sample geochemistry (e.g., Al_2O_3) (Brewer et al., 2008; Chapligin et al., 2012). These serve, in the first instance, to demonstrate the efficiency of cleaning (SiO_2:Al_2O_3 >1) and robustness of reconstructions. When not possible, these data permit contamination mass-balance calculations and a compositional offset correction of reported data (Brewer et al., 2008; Mackay et al., 2011, 2013; Wilson et al., 2014). There have been a number of methodological advancements following the earliest published $bSiO_2$ cleaning protocols (Labeyrie and Juillet, 1982; Shemesh et al., 1988, 1995; Morley et al., 2004), which demonstrate that in order to address the challenges in $bSiO_2$ cleaning, methods should be tailored depending on the characteristics of individual samples and frequent visual inspection should be carried out throughout.

Constant Silicon Isotope Fractionation Factor

Application of the $\delta^{30}Si$ proxy for DSi utilization, assumes a constant fractionation factor (see section Stable Silicon Isotope Ratios to Study the Global Si Cycle). This has been challenged with evidence of species-dependent $\delta^{30}Si$ fractionation variability between DSi and $bSiO_2$ phases (Sutton et al., 2013). The work of Sutton et al. (2013) suggests that interpretation of marine sediment-based reconstructions, should include an evaluation of species composition for more accurate interpretations of $\delta^{30}Si$ downcore variability. While these data shed light on potential species effects, each diatom strain in the Sutton et al. (2013) study was grown under its specific optimal environmental conditions in order to minimize the influence of external environmental factors (e.g., irradiance and/or temperature). The influence of environment on $\delta^{30}Si$ composition in diatoms has yet to be shown under laboratory controlled conditions. Data from *in-situ*/natural settings, have not documented a species effect (e.g., Cardinal et al., 2007; Fripiat et al., 2012; Closset et al., 2015) although if anything this clearly demonstrates the need to better understand the variability of $\delta^{30}Si$ in diatoms.

Similarly, it is essential to take any different ecological preferences of the diatoms present in the sediment core into consideration. There may be significant differences in when and where particular dominant species are growing, or if there is a pronounced preservation bias toward more heavily silicified species. For example, late season diatoms may bloom in already modified surface waters and large, deep-dwelling diatoms may opportunistically utilize DSi supplies that are hundreds of meters deep that has a different $\delta^{30}Si_{DSi}$ compared to near surface waters (Hendry and Brzezinski, 2014; Xiong et al., 2015). Another example is in Sea-Ice Zone of the Southern Ocean, where diatoms living within the sea-ice bear heavier $\delta^{30}Si$ than diatoms in the surrounding waters due to a closed system where silicic acid can be limited (Fripiat et al., 2007; Panizzo et al., 2014).

Application of $\delta^{18}O$ as a Palaeoceanographic Proxy

Despite an extensive effort by many researchers over the past five decades (e.g., Mopper and Garlick, 1971; Labeyrie, 1979; Labeyrie and Juillet, 1982; Chung-Ho and Hsueh-Wen, 1985; Leclerc and Labeyrie, 1987; Matheney and Knauth, 1989; Shemesh et al., 1992; Swann and Leng, 2009; Pike et al., 2013; Crespin et al., 2014; Abelmann et al., 2015), uncertainty associated with the $bSiO_2$-water oxygen isotope fractionation has limited the application of $bSiO_2$ $\delta^{18}O$ values as a palaeoceanographic proxy. The disparate $bSiO_2$-water fractionation factors have been attributed to two primary causes: (1) methodological biased and/or incomplete removal of hydroxyl oxygen, and (2) potential alteration of $\delta^{18}O$ values during $bSiO_2$ formation/diagenetic alteration of $\delta^{18}O$ values on geologic timescales. The analytical bias has been addressed thorough an inter-laboratory comparison that showed no significant difference in $\delta^{18}O$ values across a range of dehydration and analytical techniques (Chapligin et al., 2011); therefore, the only remaining source of uncertainty is in the $bSiO_2$-water fractionation relationship recorded by the diatom $bSiO_2$.

Diatoms from laboratory cultures and marine sediment traps seem to have a reproducible $bSiO_2$-water fractionation relationship (Matheney and Knauth, 1989; Brandriss et al., 1998; Schmidt et al., 2001; Dodd et al., 2017) that is different from the $bSiO_2$-water fractionation relationship recorded by sedimentary diatoms and quartz-water equilibrium (e.g., Leclerc and Labeyrie, 1987; Matheney and Knauth, 1989; Schmidt et al., 2001). Even within sedimentary marine diatom $bSiO_2$ archives, there does not appear to be a single $bSiO_2$-water fractionation relationship. Leclerc and Labeyrie (1987) published a $bSiO_2$-water fractionation for marine diatoms from core-top sediments and surface waters ($\delta^{18}O_{water}$ and T); however, within their dataset, $\delta^{18}O$ values of diatom $bSiO_2$ from high-latitude cores overestimated surface water temperatures by several °C. Shemesh et al. (1992) proposed the high-latitude diatoms represented a fundamentally different $bSiO_2$-water fractionation factor; however, a recent re-examination of $bSiO_2$-water fractionation factors over the entire range of formation temperatures (0–850°C) suggest that marine diatoms may record the same $bSiO_2$-water fractionation relationship has high-temperature opal/quartz (Sharp et al., 2016).

A uniform $bSiO_2$-water fractionation factor implies that living diatoms most likely precipitate $bSiO_2$ out of isotopic equilibrium (e.g., Brandriss et al., 1998; Dodd et al., 2017); however, sedimentary (aka mature) diatom $bSiO_2$ most likely approaches quartz-water equilibrium (Sharp et al., 2016). It is,

therefore, likely that the $\delta^{18}O$ values of diatom $bSiO_2$ record a combination of diagenetic (e.g., sedimentary pore water) conditions. Further work is needed to establish the timing, degree, and mechanism of diagenetic changes to diatom $\delta^{18}O$ values; however, experimental studies suggest a combination of dehydroxylation and precipitation of abiogenic SiO_2 (e.g., Dodd et al., 2017).

CONCLUSIONS AND PERSPECTIVES

The bio-geochemical analyses used to study the global biogeochemical cycling of Si (e.g., stable isotopes and associated trace elements), are emerging as useful tools to examine the influence that silicifying organisms have on the different reservoirs of Si (e.g., atmospheric, terrestrial, freshwater, and marine). Over the past 20 years, the ongoing development of specific low temperature bio-geochemical tools (e.g., $\delta^{30}Si$ in silicifying organisms) has provided useful information for the reconstruction of past Si cycling and hints at the influence that environmental change can have on the global Si cycle. In addition, these tools provide knowledge on the role that silicifying organisms have on other major biogeochemical cycles (e.g., N and C). As outlined in this review, the main requirements for the future development of the bio-geochemical tools used to evaluate the global Si cycle are to:

1. Continue to produce high quality data (e.g., sample preparation, chemical procedure, mass spectrometric analysis, data analysis, the development of robust models, and the need for more data-model comparisons).
2. Use multiple bio-geochemical tools simultaneously, i.e., a single isotope system is not perfect and should be coupled with other bio-geochemical proxies (e.g., Ge/Si) and parameters (e.g., salinity, temperature).
3. Better understand what controls the fractionation factors of the various bio-geochemical tools used to study the role of siliceous organisms (e.g., sponges, diatoms, radiolaria, picophytoplankton) and globally important processes (e.g., reverse weathering, dissolution) on the global fluxes of Si.
4. Provide information on complex (though key) systems, e.g., estuaries and coastal environments, continental seas (e.g., the Arctic Ocean), sediment diagenesis (anoxic vs. bio-active), hydrothermal activity, soil systems, and particle–water interactions.

The global Si cycle starts with the chemical weathering of silicate minerals, is transformed and re-distributed into lakes, rivers, terrestrial and freshwater organisms, soils, aerosols, seawater marine organisms, and sediment, and eventually becomes a mineral once again. During these various transformations, Si interacts with numerous other major (e.g., C, N) and minor (e.g., Al, Ge, Zn) elements and, in turn, influences their biogeochemical cycles. Investigation of the movement, transformation, and fractionation of the stable isotopes and associated elements involved in the bio-geochemical cycling of Si provides knowledge not only to help constrain the distribution and behavior of the global Si fluxes and their potential variability over time, but also provides knowledge on the mechanisms of Si biomineralization. This information is essential for understanding the short- and long-term variation in the range of these data, which are used to evaluate the utility of these bio-geochemical tools for palaeoceanographic interpretation.

AUTHOR CONTRIBUTIONS

JS and KH conceived of the project. JS drafted the manuscript with substantial contributions to the work by all authors. The manuscript was edited and approved by all authors.

FUNDING

The work by JS was supported by the "Laboratoire d'Excellence" LabexMER (ANR-10-LABX-19) and co-funded by a grant from the French government under the program "Investissements d'Avenir," and by a grant from the Regional Council of Brittany (SAD programme). DJC was partially supported by the Knut and Alice Wallenberg Foundation (KAW Wallenberg Scholar) and the Swedish Research Council. This review article has benefited from funding by the European Union Seventh Framework Programme under grant agreement n°294146 (project MuSiCC, Marie Curie CIG to DC). GdS is supported by a Marie Skłodowska-Curie Research Fellowship under EU Horizon2020 (GA #708407). JuD was supported by the American Chemical Society Petroleum Research Fund (Grant # 53798-DNI2). CE acknowledges financial support by the Institute for Chemistry and Biology of the Marine Environment (Oldenburg, Germany) and the Max Planck Institute for Marine Microbiology (Bremen, Germany). KH is funded by The Royal Society (UF120084) and the European Research Council (ERC-2015-StG - 678371_ICY-LAB). PG acknowledges funding by the Collaborative Research Centre 754 "Climate-Biogeochemistry interactions in the Tropical Ocean" (www.sfb754.de), supported by the Deutsche Forschungsgemeinschaft (DFG).

ACKNOWLEDGMENTS

We thank the organizers of Silicamics and the Silica Group (UMR 6539 CNRS/UBO/IRD/Ifremer, LEMAR - IUEM - 29280 - Plouzané, France) for providing the initiative to write this review. We also thank J. Martinez, of GraphicProtype, for his conceptual and illustrative help with the main figure (**Figure 1**).

SUPPLEMENTARY MATERIAL

The Supplementary Material for this article can be found online at: https://www.frontiersin.org/articles/10.3389/feart.2017.00112/full#supplementary-material

REFERENCES

Abelmann, A., Gersonde, R., Knorr, G., Zhang, X., Chapligin, B., Maier, E., et al. (2015). The seasonal sea-ice zone in the glacial Southern Ocean as a carbon sink. *Nat. Commun.* 6:8136. doi: 10.1038/ncomms9136

Alleman, L. Y., Cardinal, D., Cocquyt, C., Plisnier, P.-D. P.-D., Descy, J.-P. J.-P., Kimirei, I., et al. (2005). Silicon isotope fractionation in Lake Tanganyka and its main tributaries. *J. Great Lakes Res.* 31, 509–519. doi: 10.1016/S0380-1330(05)70280-X

Aller, R. C. (2014). "Sedimentary diagenesis, depositional environments, and benthic fluxes," in *Treatise on Geochemistry, Second Edition*, Vol. 8, eds H. D. Holland and K. K. Turekian (Oxford: Elsevier), 293–334.

Altabet, M. A., Deuser, W. G., Honjo, S., and Stienen, C. (1991). Seasonal and depth-related changes in the source of sinking particles in the North Atlantic. *Nature* 354, 136–139. doi: 10.1038/354136a0

Andersen, M. B., Vance, D., Archer, C., Anderson, R. F., Ellwood, M. J., and Allen, C. S. (2011). The Zn abundance and isotopic composition of diatom frustules, a proxy for Zn availability in ocean surface seawater. *Earth Planet. Sci. Lett.* 301, 137–145. doi: 10.1016/j.epsl.2010.10.032

André, L., Cardinal, D., Alleman, L. Y., and Moorbath, S. (2006). Silicon isotopes in ∼ 3. 8 Ga West Greenland rocks as clues to the Eoarchaean supracrustal Si cycle. *Earth Planet. Sci. Lett.* 245, 162–173. doi: 10.1016/j.epsl.2006.02.046

Baars, O., and Croot, P. L. (2011). The speciation of dissolved zinc in the Atlantic sector of the Southern Ocean. *Deep Sea Res. II Top. Stud. Oceanogr.* 58, 2720–2732. doi: 10.1016/j.dsr2.2011.02.003

Baines, S. B., Twining, B. S., Brzezinski, M. A., Nelson, D. M., and Fisher, N. S. (2010). Causes and biogeochemical implications of regional differences in silicification of marine diatoms. *Glob. Biogeochem. Cyc.* 24:GB4031.

Barão, L., Vandevenne, F., Clymans, W., Frings, P., Ragueneau, O., Meire, P., et al. (2015). Alkaline-extractable silicon from land to ocean: a challenge for biogenic silicon determination. *Limnol. Oceanogr. Methods* 13, 329–344. doi: 10.1002/lom3.10028

Bareille, G., Labracherie, M., Mortlock, R. A., Maier-Reimer, E., and Froelich, P. N. (1998). A test of (Ge/Si)(opal) as a paleorecorder of (Ge/Si)(seawater). *Geology* 26, 179–182.

Barker, P. A., Hurrell, E. R., Leng, M. J., Plessen, B., Wolff, C., Conley, D. J., et al. (2013). Carbon cycling within an East African lake revealed by the carbon isotope composition of diatom silica: A 25-ka record from Lake Challa, Mt. Kilimanjaro. *Quat. Sci. Rev.* 66, 55–63. doi: 10.1016/j.quascirev.2012.07.016

Baronas, J. J., Hammond, D. E., Berelson, W. M., McManus, J., and Severmann, S. (2016). Germanium–silicon fractionation in a river-influenced continental margin: The Northern Gulf of Mexico. *Geochim. Cosmochim. Acta* 178, 124–142. doi: 10.1016/j.gca.2016.01.028

Bernard, C. Y., Laruelle, G. G., Slomp, C. P., and Heinze, C. (2010). Impact of changes in river fluxes of silica on the global marine silicon cycle: a model comparison. *Biogeosciences* 7, 441–453. doi: 10.5194/bg-7-441-2010

Berner, R. A., Lasaga, A. C., and Garrels, R. M. (1983). The carbonate-silicate geochemical cycle and its effect on atmospheric carbon dioxide over the past 100 million years. *Am. J. Sci.* 283, 641–683. doi: 10.2475/ajs.283.7.641

Beucher, C. P., Brzezinski, M. A., and Crosta, X. (2007). Silicic acid dynamics in the glacial sub-Antarctic: Implications for the silicic acid leakage hypothesis. *Global Biogeochem. Cycles* 21:GB3015. doi: 10.1029/2006GB002746

Beucher, C. P., Brzezinski, M. A., and Jones, J. L. (2008). Sources and biological fractionation of Silicon isotopes in the Eastern Equatorial Pacific. *Geochim. Cosmochim. Acta* 72, 3063–3073. doi: 10.1016/j.gca.2008.04.021

Beucher, C. P., Brzezinski, M. A., and Jones, J. L. (2011). Mechanisms controlling silicon isotope distribution in the Eastern Equatorial Pacific. *Geochim. Cosmochim. Acta* 75, 4286–4294. doi: 10.1016/j.gca.2011.05.024

Bidle, K. D., and Azam, F. (1999). Accelerated dissolution of diatom silica by marine bacterial assemblages. *Nature* 397, 508–512. doi: 10.1038/17351

Bidle, K. D., Manganelli, M., and Azam, F. (2002). Regulation of oceanic silicon and carbon preservation by temperature control on bacteria. *Science* 298, 1980–1984. doi: 10.1126/science.1076076

Bouchez, J., Von Blanckenburg, F., and Schuessler, J. A. (2013). Modeling novel stable isotope ratios in the weathering zone. *Am. J. Sci.* 313, 267–308. doi: 10.2475/04.2013.01

Bradtmiller, L. I., Anderson, R. F., Fleisher, M. Q., and Burckle, L. H. (2009). Comparing glacial and Holocene opal fluxes in the Pacific sector of the Southern Ocean. *Paleoceanography* 24, 1–20. doi: 10.1029/2008PA001693

Brady, P. V., and Carroll, S. A. (1994). Direct effects of CO2 and temperature on silicate weathering: Possible implications for climate control. *Geochim. Cosmochim. Acta* 58, 1853–1856. doi: 10.1016/0016-7037(94)90543-6

Brandriss, M. E., O'Neil, J. R., Edlund, M. B., and Stoermer, E. F. (1998). Oxygen isotope fractionation between diatomaceous silica and water. *Geochim. Cosmochim. Acta* 62, 1119–1125.

Brewer, T. S., Leng, M. J., Mackay, A. W., Lamb, A. L., Tyler, J. J., and Marsh, N. G. (2008). Unravelling contamination during MIS-10 to 12: Implications for atmospheric CO2. *Clim. Past* 4, 333–344. doi: 10.5194/cp-4-333-2008

Brümmer, F. (2003). "Living inside a glass box – silica in diatoms," in *Progress in Molecular and Subcellular Biology*, ed W. E. G. Müller (Berlin; Heidelberg: Springer-Verlag), 3–9.

Brunner, E., Gröger, C., Lutz, K., Richthammer, P., Spinde, K., and Sumper, M. (2009). Analytical studies of silica biomineralization: towards an understanding of silica processing by diatoms. *Appl. Microbiol. Biotechnol.* 84, 607–616. doi: 10.1007/s00253-009-2140-3

Brzezinski, M. A., and Jones, J. L. (2015). Coupling of the distribution of silicon isotopes to the meridional overturning circulation of the North Atlantic Ocean. *Deep Sea Res. II Top. Stud. Oceanogr.* 116, 79–88. doi: 10.1016/j.dsr2.2014.11.015

Brzezinski, M. A., Pride, C. J., Franck, V. M., Sigman, D. M., Sarmiento, J. L., Matsumoto, K., et al. (2002). A switch from Si(OH)(4) to NO3- depletion in the glacial Southern Ocean. *Geophys. Res. Lett.* 29, 1–4. doi: 10.1029/2001GL014349

Buesseler, K. O. (1998). The decoupling of production and partinulate export in the surface ocean. *Global Biogeochem. Cycles* 12, 297–310. doi: 10.1029/97GB03366

Cardinal, D., Alleman, L. Y., Dehairs, F., Savoye, N., Trull, T. W., and Andre, L. (2005). Relevance of silicon isotopes to Si-nutrient utilization and Si-source assessment in Antarctic waters. *Global Biogeochem. Cycles* 19:GB2007. doi: 10.1029/2004GB002364

Cardinal, D., Gaillardet, J., Hughes, H. J., Opfergelt, S., and André, L. (2010). Contrasting silicon isotope signatures in rivers from the Congo Basin and the specific behaviour of organic-rich waters. *Geophys. Res. Lett.* 37:L12403. doi: 10.1029/2010GL043413

Cardinal, D., Savoye, N., Trull, T. W., Dehairs, F., Kopczynska, E. E., Fripiat, F., et al. (2007). Silicon isotopes in spring Southern Ocean diatoms: Large zonal changes despite homogeneity among size fractions. *Mar. Chem.* 106, 46–62. doi: 10.1016/j.marchem.2006.04.006

Carey, J. C., and Fulweiler, R. W. (2012). The terrestrial silica pump. *PLoS ONE* 7:e52932. doi: 10.1371/journal.pone.0052932

Cavagna, A.-J., Fripiat, F., Dehairs, F., Wolf-Gladrow, D., Cisewski, B., Savoye, N., et al. (2011). Silicon uptake and supply during a Southern Ocean iron fertilization experiment (EIFEX) tracked by Si isotopes. *Limnol. Oceanogr.* 56, 147–160. doi: 10.4319/lo.2011.56.1.0147

Cermeño, P., Falkowski, P. G., Romero, O. E., Schaller, M. F., and Vallina, S. M. (2015). Continental erosion and the Cenozoic rise of marine diatoms. *Proc. Natl. Acad. Sci. U.S.A.* 112, 4239–4244. doi: 10.1073/pnas.1412883112

Cha, J. N. N., Shimizu, K., Zhou, Y., Christiansen, S. C. C., Chmelka, B. F. F., Stucky, G. D. D., et al. (1999). Silicatein filaments and subunits from a marine sponge direct the polymerization of silica and silicones *in vitro*. *Proc. Natl. Acad. Sci. U.S.A.* 96, 361–365, doi: 10.1073/pnas.96.2.361

Chakrabarti, R., Knoll, A. H., Jacobsen, S. B., and Fischer, W. W. (2012). Si isotope variability in Proterozoic cherts. *Geochimica et Cosmochimica Acta* 91, 187–201. doi: 10.1016/j.gca.2012.05.025

Chapligin, B., Leng, M. J., Webb, E., Alexandre, A., Dodd, J. P., Ijiri, A., et al. (2011). Inter-laboratory comparison of oxygen isotope compositions from biogenic silica. *Geochim. Cosmochim. Acta* 75, 7242–7256. doi: 10.1016/j.gca.2011.08.011

Chapligin, B., Meyer, H., Swann, G. E. A., Meyer-Jacob, C., and Hubberten, H. W. (2012). A 250 ka oxygen isotope record from diatoms at Lake El'gygytgyn, far east Russian Arctic. *Clim. Past* 8, 1621–1636. doi: 10.5194/cp-8-1621-2012

Chung-Ho, W., and Hsueh-Wen, Y. (1985). Oxygen isotopic compositions of DSDP Site 480 diatoms: Implications and applications. *Geochim. Cosmochim. Acta* 49, 1469–1478. doi: 10.1016/0016-7037(85)90296-0

Claquin, P., Martin-Jezequel, V., Kromkamp, J. C., Veldhuis, M. J. W., and Kraay, G. W. (2002). Uncoupling of silicon compared with carbon and nitrogen metabolisms and the role of the cell cycle in continuous cultures of *Thalassiosira*

Pseudonana (Bacillariophyceae) under light, nitrogen, and phosphorus control. *J. Phycol.* 38, 922–930. doi: 10.1046/j.1529-8817.2002.t01-1-01220.x

Closset, I., Cardinal, D., Bray, S. G., Thil, F., Djouraev, I., Rigual-Hernández, A. S., et al. (2015). Seasonal variations, origin, and fate of settling diatoms in the Southern Ocean tracked by silicon isotope records in deep sediment traps. *Glob. Biogeochem. Cycles* 29, 1495–1510f. doi: 10.1002/2015GB005180

Clymans, W., Struyf, E., Govers, G., Vandevenne, F., and Conley, D. J. (2011). Anthropogenic impact on amorphous silica pools in temperate soils. *Biogeosciences* 8, 2281–2293. doi: 10.5194/bg-8-2281-2011

Cockerton, H. E., Street-Perrott, F. A., Barker, P. A., Leng, M. J., Sloane, H. J., and Ficken, K. J. (2015). Orbital forcing of glacial/interglacial variations in chemical weathering and silicon cycling within the upper White Nile basin, East Africa: stable-isotope and biomarker evidence from Lakes Victoria and Edward. *Quat. Sci. Rev.* 130, 57–71. doi: 10.1016/j.quascirev.2015.07.028

Cockerton, H. E., Street-Perrott, F. A., Leng, M. J., Barker, P. A., Horstwood, M. S. A., and Pashley, V. (2013). Stable-isotope (H, O, and Si) evidence for seasonal variations in hydrology and Si cycling from modern waters in the Nile Basin: Implications for interpreting the quaternary record. *Quat. Sci. Rev.* 66, 4–21. doi: 10.1016/j.quascirev.2012.12.005

Conley, D. J. (2002). Terrestrial ecosystems and the global biogeochemical silica cycle. *Global Biogeochem. Cycles* 16, 1–8. doi: 10.1029/2002GB001894

Conley, D. J., Frings, P. J., Fontorbe, G., Clymans, W., Stadmark, J., Hendry, K. R., et al. (2017). Biosilicification drives a decline of dissolved Si in the oceans through geologic time. *Front. Mar. Sci.* 4:397. doi: 10.3389/fmars.2017.00397

Conley, D. J., Schelske, C. L., and Stoermer, E. F. (1993). Modification of the biogeochemical cycle of silica with eutrophication. *Mar. Ecol. Prog. Ser.* 101, 179–192. doi: 10.3354/meps101179

Coogan, L. A., and Dosso, S. (2012). An internally consistent, probabilistic, determination of ridge-axis hydrothermal fluxes from basalt-hosted systems. *Earth Planet. Sci. Lett.* 323–324, 92–101. doi: 10.1016/j.epsl.2012.01.017

Cornelis, J. T., Delvaux, B., Cardinal, D., André, L., Ranger, J., and Opfergelt, S. (2010). Tracing mechanisms controlling the release of dissolved silicon in forest soil solutions using Si isotopes and Ge/Si ratios. *Geochim. Cosmochim. Acta* 74, 3913–3924. doi: 10.1016/j.gca.2010.04.056

Crespin, J., Yam, R., Crosta, X., Mass,é, G., Schmidt, S., Campagne, P., et al. (2014). Holocene glacial discharge fluctuations and recent instability in East Antarctica. *Earth Planet. Sci. Lett.* 394, 38–47. doi: 10.1016/j.epsl.2014.03.009

Criss, R. E. (1999). *Principles of Stable Isotope Distribution*. New York, NY: rd University Press.

Crosta, X., and Shemesh, A. (2002). Reconciling down core anticorrelation of diatom carbon and nitrogen isotopic ratios from the Southern Ocean. *Paleoceanography* 17, 10-1–10-8. doi: 10.1029/2000PA000565

De La Rocha, C. L. (2003). Silicon isotope fractionation by marine sponges and the reconstruction of the silicon isotope composition of ancient deep water. *Geology* 31, 423–426. doi: 10.1130/0091-7613(2003)031<0423:SIFBMS>2.0.CO;2

De La Rocha, C. L., Brzezinski, M. A., and DeNiro, M. J. (1997). Fractionation of silicon isotopes by marine diatoms during biogenic silica formation. *Geochim. Cosmochim. Acta* 61, 5051–5056. doi: 10.1016/S0016-7037(97)00300-1

De La Rocha, C. L., Brzezinski, M. A., and DeNiro, M. J. (2000). A first look at the distribution of the stable isotopes of silicon in natural waters. *Geochim. Cosmochim. Acta* 64, 2467–2477. doi: 10.1016/S0016-7037(00)00373-2

De La Rocha, C. L., Brzezinski, M. A., DeNiro, M. J., and Shemesh, A. (1998). Silicon-isotope composition of diatoms as an indicator of past oceanic change. *Nature* 395, 680–683. doi: 10.1038/27174

de Souza, G. F., Reynolds, B. C., Johnson, G. C., Bullister, J. L., and Bourdon, B. (2012a). Silicon stable isotope distribution traces Southern Ocean export of Si to the eastern South Pacific thermocline. *Biogeosciences* 9, 4199–4213. doi: 10.5194/bg-9-4199-2012

de Souza, G. F., Reynolds, B. C., Rickli, J., Frank, M., Saito, M. A., Gerringa, L. J. A., et al. (2012b). Southern Ocean control of silicon stable isotope distribution in the deep Atlantic Ocean. *Global Biogeochem. Cycles* 26, 1–13. doi: 10.1029/2011GB004141

de Souza, G. F., Slater, R. D., Dunne, J. P., and Sarmiento, J. L. (2014). Deconvolving the controls on the deep ocean's silicon stable isotope distribution. *Earth Planet. Sci. Lett.* 398, 66–76. doi: 10.1016/j.epsl.2014.04.040

de Souza, G. F., Slater, R. D., Hain, M. P., Brzezinski, M. A., and Sarmiento, J. L. (2015). Distal and proximal controls on the silicon stable isotope signature of North Atlantic Deep Water. *Earth Planet. Sci. Lett.* 432, 342–353. doi: 10.1016/j.epsl.2015.10.025

Dellinger, M., Gaillardet, J., Bouchez, J., Calmels, D., Louvat, P., Dosseto, A., et al. (2015). Riverine Li isotope fractionation in the Amazon River basin controlled by the weathering regimes. *Geochim. Cosmochim. Acta* 164, 71–93. doi: 10.1016/j.gca.2015.04.042

Delstanche, S., Opfergelt, S., Cardinal, D., Elsass, F., André, L., and Delvaux, B. (2009). Silicon isotopic fractionation during adsorption of aqueous monosilicic acid onto iron oxide. *Geochim. Cosmochim. Acta* 73, 923–934. doi: 10.1016/j.gca.2008.11.014

Delvaux, C., Cardinal, D., Carbonnel, V., Chou, L., Hughes, H. J., and André, L. (2013). Controls on riverine δ^{30}Si signatures in a temperate watershed under high anthropogenic pressure (Scheldt - Belgium). *J. Mar. Syst.* 128, 40–51. doi: 10.1016/j.jmarsys.2013.01.004

Delvigne, C., Cardinal, D., Hofmann, A., and André, L. (2012). Stratigraphic changes of Ge/Si, REE+Y and silicon isotopes as insights into the deposition of a Mesoarchaean banded iron formation. *Earth Planet. Sci. Lett.* 355–356, 109–118. doi: 10.1016/j.epsl.2012.07.035

Delvigne, C., Opfergelt, S., Cardinal, D., Delvaux, B., and André, L. (2009). Distinct silicon and germanium pathways in the soil-plant system: evidence from banana and horsetail. *J. Geophys. Res.* 114, 1–11. doi: 10.1029/2008JG000899

Delvigne, C., Opfergelt, S., Cardinal, D., Hofmann, A., and André, L. (2016). Desilication in Archean weathering processes traced by silicon isotopes and Ge/Si ratios. *Chem. Geol.* 420, 139–147. doi: 10.1016/j.chemgeo.2015.11.007

Demarest, M. S., Brzezinski, M. A., and Beucher, C. P. (2009). Fractionation of silicon isotopes during biogenic silica dissolution. *Geochim. Cosmochim. Acta* 73, 5572–5583. doi: 10.1016/j.gca.2009.06.019

DeMaster, D. J. (1981). The supply and accumulation of silica in the marine-environment. *Geochim. Cosmochim. Acta* 45, 1715–1732. doi: 10.1016/0016-7037(81)90006-5

DeMaster, D. J. (2003). "The diagenesis of biogenic silica: chemical transformations occurring in the water column, seabed and crust," in *Treatise on Geochemistry*, Vol. 7, eds H. D. Holland and K. K. Turekian (Oxford: Elsevier), 87–98. doi: 10.1016/B0-08-043751-6/07095-X

Derry, L. A., Kurtz, A. C., Ziegler, K., and Chadwick, O. A. (2005). Biological control of terrestrial silica cycling and export fluxes to watersheds. *Nature* 433, 728–731. doi: 10.1038/nature03299

Des Combes, H. J., Esper, O., De La Rocha, C. L., Abelmann, A., Gersonde, R., Yam, R., et al. (2008). Diatom δ13C, δ15N, and C/N since the last glacial maximum in the Southern Ocean: potential impact of species composition. *Paleoceanography* 23, 1–12. doi: 10.1029/2008PA001589

Ding, T. P., Gao, J. F., Tian, S. H., Wang, H. B., and Li, M. (2011). Silicon isotopic composition of dissolved silicon and suspended particulate matter in the Yellow River, China, with implications for the global silicon cycle. *Geochim. Cosmochim. Acta* 75, 6672–6689. doi: 10.1016/j.gca.2011.07.040

Ding, T. P., Ma, G. R., Shui, M. X., Wan, D. F., and Li, R. H. (2005). Silicon isotope study on rice plants from the Zhejiang province, China. *Chem. Geol.* 218, 41–50. doi: 10.1016/j.chemgeo.2005.01.018

Ding, T. P., Tian, S. H., Sun, L., Wu, L. H., Zhou, J. X., and Chen, Z. Y. (2008a). Silicon isotope fractionation between rice plants and nutrient solution and its significance to the study of the silicon cycle. *Geochim. Cosmochim. Acta* 72, 5600–5615. doi: 10.1016/j.gca.2008.09.006

Ding, T. P., Zhou, J. X., Wan, D. F., Chen, Z. Y., Wang, C. Y., and Zhang, F. (2008b). Silicon isotope fractionation in bamboo and its significance to the biogeochemical cycle of silicon. *Geochim. Cosmochim. Acta* 72, 1381–1395. doi: 10.1016/j.gca.2008.01.008

Ding, T., Wan, D., Wang, C., and Zhang, F. (2004). Silicon isotope compositions of dissolved silicon and suspended matter in the Yangtze River, China. *Geochim. Cosmochim. Acta* 68, 205–216. doi: 10.1016/S0016-7037(03)00264-3

Dixit, S., Van Cappellen, P., and Van Bennekom, A. J. (2001). Processes controlling solubility of biogenic silica and pore water build-up of silicic acid in marine sediments. *Mar. Chem.* 73, 333–352. doi: 10.1016/S0304-4203(00)00118-3

Dodd, J. P., Wiedenheft, W., and Schwartz, J. M. (2017). Dehydroxylation and diagenetic variations in diatom oxygen isotope values. *Geochim. Cosmochim. Acta* 199, 185–195. doi: 10.1016/j.gca.2016.11.034

Doering, K., Ehlert, C., Grasse, P., Crosta, X., Fleury, S., Frank, M., et al. (2016). Differences between mono-generic and mixed diatom silicon isotope

compositions trace present and past nutrient utilisation off Peru. *Geochim. Cosmochim. Acta* 177, 30–47. doi: 10.1016/j.gca.2015.12.029

Douthitt, C. B. (1982). The geochemistry of the stable isotopes of silicon. *Geochim. Cosmochim. Acta* 46, 1449–1458. doi: 10.1016/0016-7037(82)90278-2

Egan, K. E., Rickaby, R. E. M., Hendry, K. R., and Halliday, A. N. (2013). Opening the gateways for diatoms primes Earth for Antarctic glaciation. *Earth Planet. Sci. Lett.* 375, 34–43. doi: 10.1016/j.epsl.2013.04.030

Egan, K. E., Rickaby, R. E. M., Leng, M. J., Hendry, K. R., Hermoso, M., Sloane, H. J., et al. (2012). Diatom silicon isotopes as a proxy for silicic acid utilisation: a Southern Ocean core top calibration. *Geochim. Cosmochim. Acta* 96, 174–192. doi: 10.1016/j.gca.2012.08.002

Ehlert, C., Doering, K., Wallmann, K., Scholz, F., Sommer, S., Grasse, P., et al. (2016). Stable silicon isotope signatures of marine pore waters – Biogenic opal dissolution versus authigenic clay mineral formation. *Geochim. Cosmochim. Acta* 191, 102–117. doi: 10.1016/j.gca.2016.07.022

Ehlert, C., Grasse, P., Mollier-vogel, E., Bo, T., Franz, J., Souza, G. F., et al. Frank, M. (2012). Factors controlling the silicon isotope distribution in waters and surface sediments of the Peruvian coastal upwelling. *Geochim. Cosmochim. Acta* 99, 128–145. doi: 10.1016/j.gca.2012.09.038

Ehlert, C., Grasse, P., and Frank, M. (2013). Changes in silicate utilisation and upwelling intensity off Peru since the Last Glacial Maximum–insights from silicon and neodymium isotopes. *Quat. Sci. Rev.* 72, 18–35. doi: 10.1016/j.quascirev.2013.04.013

Eiler, J. M., Bergquist, B., Bourg, I., Cartigny, P., Farquhar, J., Gagnon, A., et al. (2014). Frontiers of stable isotope geoscience. *Chem. Geol.* 372, 119–143. doi: 10.1016/j.chemgeo.2014.02.006

Elderfield, H., and Rickaby, R. (2000). Oceanic Cd/P ratio and nutrient utilization in the glacial Southern Ocean. *Nature* 405, 305–310. doi: 10.1038/35012507

Ellwood, M. J., and Hunter, K. A. (1999). Determination of the Zn/Si ratio in diatom opal: a method for the separation, cleaning and dissolution of diatoms. *Mar. Chem.* 66, 149–160. doi: 10.1016/S0304-4203(99)00037-7

Ellwood, M. J., and Hunter, K. A. (2000). The incorporation of zinc and iron into the frustule of the marine diatom *Thalassiosira pseudonana*. *Limnol. Oceanogr.* 45, 1517–1524. doi: 10.4319/lo.2000.45.7.1517

Ellwood, M. J., Kelly, M., Neil, H., and Nodder, S. D. (2005). Reconstruction of paleo-particulate organic carbon fluxes for the Campbell Plateau region of southern New Zealand using the zinc content of sponge spicules. *Paleoceanography* 20:PA3010. doi: 10.1029/2004PA001095

Ellwood, M. J., Kelly, M., Nodder, S. D., and Carter, L. (2004). Zinc/silicon ratios of sponges: a proxy for carbon export to the seafloor. *Geophys. Res. Lett.* 31:L12308. doi: 10.1029/2004GL019648

Ellwood, M. J., Wille, M., and Maher, W. (2010). Glacial silicic acid concentrations in the Southern Ocean. *Science* 330, 1088–1091. doi: 10.1126/science.1194614

Engström, E., Rodushkin, I., Ingri, J., Baxter, D. C., Ecke, F., Österlund, H., et al. (2010). Temporal isotopic variations of dissolved silicon in a pristine boreal river. *Chem. Geol.* 271, 142–152. doi: 10.1016/j.chemgeo.2010.01.005

Engström, E., Rodushkin, I., Öhlander, B., Ingri, J., and Baxter, D. C. (2008). Silicon isotopic composition of boreal forest vegetation in Northern Sweden. *Chem. Geol.* 257, 250–259. doi: 10.1016/j.chemgeo.2008.10.004

Escoube, R., Rouxel, O. J., Edwards, K., Glazer, B., and Donard, O. F. (2015). Coupled Ge/Si and Ge isotope ratios as geochemical tracers of seafloor hydrothermal systems: case studies at Loihi Seamount and East Pacific Rise 9 50′ N. *Geochimica et Cosmochimica Acta* 167, 93–112. doi: 10.1016/j.gca.2015.06.025

Fontorbe, G., De La Rocha, C. L., Chapman, H. J., and Bickle, M. J. (2013). The silicon isotopic composition of the Ganges and its tributaries. *Earth Planet. Sci. Lett.* 381, 21–30. doi: 10.1016/j.epsl.2013.08.026

Fontorbe, G., Frings, P. J., De La Rocha, C. L., Hendry, K. R., and Conley, D. J. (2016). A silicon depleted North Atlantic since the Palaeogene: Evidence from sponge and radiolarian silicon isotopes. *Earth Planet. Sci. Lett.* 453, 67–77. doi: 10.1016/j.epsl.2016.08.006

Fontorbe, G., Frings, P. J., De La Rocha, C. L., Hendry, K. R., and Conley, D. J. (2017). Enrichment of dissolved silica in the deep Equatorial Pacific during the Eocene-Oligocene. *Paleoceanography* 32, 848–863. doi: 10.1002/2017PA003090

Freudenthal, T., Wagner, T., Wenzhöfer, F., Zabel, M., and Wefer, G. (2001). Early diagenesis of organic matter from sediments of the eastern subtropical Atlantic: evidence from stable nitrogen and carbon isotopes. *Geochim. Cosmochim. Acta* 65, 1795–1808. doi: 10.1016/S0016-7037(01)00554-3

Frings, P. J., Clymans, W., Fontorbe, G., De La Rocha, C. L., and Conley, D. J. (2016). The continental Si cycle and its impact on the ocean Si isotope budget. *Chem. Geol.* 425, 12–36. doi: 10.1016/j.chemgeo.2016.01.020

Frings, P. J., Clymans, W., Fontorbe, G., Gray, W., Chakrapani, G., Conley, D. J., et al. (2015). Silicate weathering in the Ganges alluvial plain. *Earth Planet. Sci. Lett.* 427, 136–148. doi: 10.1016/j.epsl.2015.06.049

Frings, P. J., Clymans, W., Jeppesen, E., Lauridsen, T. L., Struyf, E., and Conley, D. J. (2014a). Lack of steady-state in the global biogeochemical Si cycle: Emerging evidence from lake Si sequestration. *Biogeochemistry* 117, 255–277. doi: 10.1007/s10533-013-9944-z

Frings, P. J., De La Rocha, C., Struyf, E., van Pelt, D., Schoelynck, J., Hudson, M. M., et al. (2014b). Tracing silicon cycling in the Okavango Delta, a sub-tropical flood-pulse wetland using silicon isotopes. *Geochim. Cosmochim. Acta* 142, 132–148. doi: 10.1016/j.gca.2014.07.007

Fripiat, F., Cardinal, D., Tison, J. L., Worby, A., and Andre, L. (2007). Diatom-induced silicon isotopic fractionation in Antarctic sea ice. *J. Geophys. Res.* 112:G02001. doi: 10.1029/2006JG000244

Fripiat, F., Cavagna, A.-J., Dehairs, F., Speich, S., André, L., and Cardinal, D. (2011). Silicon pool dynamics and biogenic silica export in the Southern Ocean inferred from Si-isotopes. *Ocean Sci.* 7, 533–547. doi: 10.5194/os-7-533-2011

Fripiat, F., Cavagna, A. J., Dehairs, F., De Brauwere, A., André, L., and Cardinal, D. (2012). Processes controlling the Si-isotopic composition in the Southern Ocean and application for paleoceanography. *Biogeosciences* 9, 2443–2457. doi: 10.5194/bg-9-2443-2012

Froelich, H., and Barthel, D. (1997). Silica uptake of the marine sponge Halichondria panicea in Kiel Bight. *Mar. Biol.* 128, 115–125. doi: 10.1007/s002270050075

Froelich, P. N., and Andreae, M. O. (1981). The marine geochemistry of Germanium: Ekasilicon. *Science* 213, 205–207. doi: 10.1126/science.213.4504.205

Froelich, P. N., Blanc, V., Mortlock, R. A., Chillrud, S. N., Dunstant, W., Udomkit, A., et al. (1992). River fluxes of dissolved silica to the ocean were higher during the glacials: Ge/Si in diatoms, rivers and oceans. *Palaeoceanography* 7, 739–768. doi: 10.1029/92PA02090

Froelich, P. N., Mortlock, R. A., and Shemesh, A. (1989). Inorganic germanium and silica in the Indian ocean: biological fractionation during (Ge/Si)opal formation. *Global Biogeochem. Cycles* 3, 79–88. doi: 10.1029/GB003i001p00079

Gao, S., Wolf-Gladrow, D. A., and Volker, C. (2016). Simulating the modern δ^{30}Si distribution in the oceans. *Glob. Biogeochem. Cycles* 30, 120–133. doi: 10.1002/2015GB005189

Garcia, H. E., Locarnini, R. A., Boyer, T. P., Antonov, J. I., Baranova, O. K., Zweng, M. M., et al. (2014). "World Ocean Atlas 2013, Volume 4: dissolved inorganic nutrients (phosphate, nitrate, silicate)," in *NOAA Atlas NESDIS*, ed S. Levitus (Silver Spring, MD: NOAA-NESDIS), 25.

Gehlen, M., Beck, L., Calas, G., Flank, A. M., Van Bennekom, A. J., and Van Beusekom, J. E. E. (2002). Unraveling the atomic structure of biogenic silica: evidence of the structural association of Al and Si in diatom frustules. *Geochim. Cosmochim. Acta* 66, 1601–1609. doi: 10.1016/S0016-7037(01)00877-8

Geilert, S., Vroon, P. Z., Keller, N. S., Gudbrandsson, S., Stefánsson, A., and van Bergen, M. J. (2015). Silicon isotope fractionation during silica precipitation from hot-spring waters: evidence from the Geysir geothermal field, Iceland. *Geochim. Cosmochim. Acta* 164, 403–427. doi: 10.1016/j.gca.2015.05.043

Geilert, S., Vroon, P. Z., Roerdink, D. L., Van Cappellen, P., and van Bergen, M. J. (2014). Silicon isotope fractionation during abiotic silica precipitation at low temperatures: Inferences from flow-through experiments. *Geochim. Cosmochim. Acta* 142, 95–114. doi: 10.1016/j.gca.2014.07.003

Georg, R. B., Reynolds, B. C., Frank, M., and Halliday, A. N. (2006). Mechanisms controlling the silicon isotopic compositions of river waters. *Earth Planet. Sci. Lett.* 249, 290–306. doi: 10.1016/j.epsl.2006.07.006

Georg, R. B., Reynolds, B. C., West, A. J., Burton, K. W., and Halliday, A. N. (2007). Silicon isotope variations accompanying basalt weathering in Iceland. *Earth Planet. Sci. Lett.* 261, 476–490. doi: 10.1016/j.epsl.2007.07.004

Georg, R. B., Zhu, C., Reynolds, B. C., and Halliday, A. N. (2009). Stable silicon isotopes of groundwater, feldspars, and clay coatings in the Navajo Sandstone aquifer, Black Mesa, Arizona, USA. *Geochim. Cosmochim. Acta* 73, 2229–2241. doi: 10.1016/j.gca.2009.02.005

Grasse, P., Brzezinski, M., Cardinal, D., de Souza, G. F., Andersson, P., Closset, I., et al. (2017). GEOTRACES inter-calibration of the stable silicon isotope

composition of dissolved silicic acid in seawater. *J. Anal. At. Spectrom.* 32, 562–578. doi: 10.1039/C6JA00302H

Grasse, P., Ehlert, C., and Frank, M. (2013). The influence of water mass mixing on the dissolved Si isotope composition in the Eastern Equatorial Pacific. *Earth Planet. Sci. Lett.* 380, 60–71. doi: 10.1016/j.epsl.2013.07.033

Hammond, D. E., McManus, J., and Berelson, W. M. (2004). Oceanic germanium/silicon ratios: Evaluation of the potential overprint of temperature on weathering signals. *Paleoceanography* 19:PA2016. doi: 10.1029/2003PA000940

Hammond, D. E., McManus, J., Berelson, W. M., Meredith, C., Klinkhammer, G. P., and Coale, K. H. (2000). Diagenetic fractionation of Ge and Si in reducing sediments: the missing Ge sink and a possible mechanism to cause glacial/interglacial variations in oceanic Ge/Si. *Geochim. Cosmochim. Acta* 64, 2453–2465. doi: 10.1016/S0016-7037(00)00362-8

Hawkings, J. R., Wadham, J. L., Benning, L. G., Hendry, K. R., Tranter, M., Tedstone, A., et al. (2017). Ice sheets as a missing source of silica to the polar oceans. *Nat. Commun.* 8:14198. doi: 10.1038/ncomms14198

Heck, P. R., Huberty, J. M., Kita, N. T., Ushikubo, T., Kozdon, R., and Valley, J. W. (2011). SIMS analyses of silicon and oxygen isotope ratios for quartz from Archean and Paleoproterozoic banded iron formations. *Geochim. Cosmochim. Acta* 75, 5879–5891. doi: 10.1016/j.gca.2011.07.023

Henchiri, S., Gaillardet, J., Dellinger, M., Bouchez, J., and Spencer, R. G. M. (2016). Riverine dissolved lithium isotopic signatures in low-relief central Africa and their link to weathering regimes. *Geophys. Res. Lett.* 43, 4391–4399. doi: 10.1002/2016GL067711

Hendry, K. R., and Andersen, M. B. (2013). The zinc isotopic composition of siliceous marine sponges: investigating nature's sediment traps. *Chem. Geol.* 354, 33–41. doi: 10.1016/j.chemgeo.2013.06.025

Hendry, K. R., and Brzezinski, M. A. (2014). Using silicon isotopes to understand the role of the Southern Ocean in modern and ancient biogeochemistry and climate. *Quat. Sci. Rev.* 89, 13–26. doi: 10.1016/j.quascirev.2014.01.019

Hendry, K. R., Georg, R. B., Rickaby, R. E. M., Robinson, L. F., and Halliday, A. N. (2010). Deep ocean nutrients during the Last Glacial Maximum deduced from sponge silicon isotopic compositions. *Earth Planet. Sci. Lett.* 292, 290–300. doi: 10.1016/j.epsl.2010.02.005

Hendry, K. R., Gong, X., Knorr, G., Pike, J., and Hall, I. R. (2016). Deglacial diatom production in the tropical North Atlantic driven by enhanced silicic acid supply. *Earth Planet. Sci. Lett.* 438, 122–129. doi: 10.1016/j.epsl.2016.01.016

Hendry, K. R., Leng, M. J., Robinson, L. F., Sloane, H. J., Blusztjan, J., Rickaby, R. E. M., et al. (2011). Silicon isotopes in Antarctic sponges: an interlaboratory comparison. *Antarct. Sci.* 23, 34–42. doi: 10.1017/S0954102010000593

Hendry, K. R., Marron, A. O., Vincent, F., Conley, D. J., Gehlen, M., Ibarbalz, F. M., et al. (2018). Competition between silicifiers and non-silicifiers in the past and present ocean and its evolutionary impacts. *Front. Mar. Sci.* doi: 10.3389/fmars.2018.00022

Hendry, K. R., and Rickaby, R. E. M. (2008). Opal (Zn/Si) ratios as a nearshore geochemical proxy in coastal Antarctica. *Paleoceanography* 23, 1–12. doi: 10.1029/2007PA001576

Hendry, K. R., and Robinson, L. F. (2012). The relationship between silicon isotope fractionation in sponges and silicic acid concentration: Modern and core-top studies of biogenic opal. *Geochim. Cosmochim. Acta* 81, 1–12. doi: 10.1016/j.gca.2011.12.010

Hendry, K. R., Robinson, L. F., Meredith, M. P., Mulitza, S., Chiessi, C. M., and Arz, H. (2012). Abrupt changes in high-latitude nutrient supply to the Atlantic during the last glacial cycle. *Geology* 40, 123–126. doi: 10.1130/G32779.1

Hendry, K. R., Robinson, L. F., McManus, J. F., and Hays, J. D. (2014). Silicon isotopes indicate enhanced carbon export efficiency in the North Atlantic during deglaciation. *Nat. Commun.* 5:3107. doi: 10.1038/ncomms4107

Hendry, K. R., Swann, G. E. A., Leng, M. J., Sloane, H. J., Goodwin, C., Berman, J., et al. (2015). Technical Note: Silica stable isotopes and silicification in a carnivorous sponge Asbestopluma sp. *Biogeosciences* 12, 3489–3498. doi: 10.5194/bg-12-3489-2015

Heureux, A. M. C., and Rickaby, R. E. M. (2015). Refining our estimate of atmospheric CO2 across the eocene-Oligocene climatic transition. *Earth Planet. Sci. Lett.* 409, 329–338. doi: 10.1016/j.epsl.2014.10.036

Hildebrand, M. (2008). Diatoms, biomineralization processes, and genomics.*Chem. Rev.* 108, 4855–4874, doi: 10.1021/cr078253z

Hildebrand, M., Volcani, B. E., Gassmann, W., and Schroeder, J. I. (1997). A gene family of silicon transporters. *ature* 385, 688–689,

Hodson, M. J., Parker, A. G., Leng, M. J., and Sloane, H. J. (2008). Silicon, oxygen and carbon isotope composition of wheat (*Triticum aestivum* L.) phytoliths: implications for palaeoecology and archaeology. *J. Quat. Sci.* 23, 331–339. doi: 10.1002/jqs.1176

Hoefs, J. (2009). *Stable Isotope Geochemistry*. Berlin; Heidelberg: Springer.

Honjo, S., Manganini, S. J., Krishfield, R. A., and Francois, R. (2008). Particulate organic carbon fluxes to the ocean interior and factors controlling the biological pump: a synthesis of global sediment trap programs since 1983. *Prog. Oceanogr.* 76, 217–285. doi: 10.1016/j.pocean.2007.11.003

Horn, M. G., Beucher, C. P., Robinson, R. S., and Brzezinski, M. A. (2011). Southern ocean nitrogen and silicon dynamics during the last deglaciation. *Earth Planet. Sci. Lett.* 310, 334–339. doi: 10.1016/j.epsl.2011.08.016

Hughes, H. J., Bouillon, S., André, L., and Cardinal, D. (2012). The effects of weathering variability and anthropogenic pressures upon silicon cycling in an intertropical watershed (Tana River, Kenya). *Chem. Geol.* 308–309, 18–25. doi: 10.1016/j.chemgeo.2012.03.016

Hughes, H. J., Sondag, F., Cocquyt, C., Laraque, A., Pandi, A., André, L., et al. (2011). Effect of seasonal biogenic silica variations on dissolved silicon fluxes and isotopic signatures in the Congo River. *Limnol. Oceanogr.* 56, 551–561. doi: 10.4319/lo.2011.56.2.0551

Hughes, H. J., Sondag, F., Santos, R. V., André, L., and Cardinal, D. (2013). The riverine silicon isotope composition of the Amazon Basin. *Geochim. Cosmochim. Acta* 121, 637–651. doi: 10.1016/j.gca.2013.07.040

Iler, R. K. (1979). *The Chemistry of Silica: Solubility, Polymerization, Colloid and Surface Properties, and Biochemistry*. New York, NY: Wiley.

John, S. G., Geis, R. W., Saito, M. A., and Boyle, E. A. (2007). Zinc isotope fractionation during high-affinity and low-affinity zinc transport by the marine diatom Thalassiosira oceanica. *Limnol. Oceanogr.* 52, 2710–2714. doi: 10.4319/lo.2007.52.6.2710

Kidder, D. L., and Tomescu, I. (2016). Biogenic chert and the Ordovician silica cycle. *Palaeogeogr. Palaeoclimatol. Palaeoecol.* 458, 29–38. doi: 10.1016/j.palaeo.2015.10.013

Kim, S., Khim, B.-K., Ikehara, K., Itaki, T., Shibahara, A., and Yamamoto, M. (2017). Millennial-scale changes of surface and bottom water conditions in the northwestern Pacific during the last deglaciation. *Glob. Planet. Change* 154, 33–43. doi: 10.1016/j.gloplacha.2017.04.009

King, S. L., Froelich, P. N., and Jahnke, R. A. (2000). Early diagenesis of germanium in sediments of the Antarctic South Atlantic: in search of the missing Ge sink. *Geochim. Cosmochim. Acta* 64, 1375–1390. doi: 10.1016/S0016-7037(99)00406-8

Koning, E., Epping, E., and Van Raaphorst, W. (2002). Determining biogenic silica in marine samples by tracking silicate and aluminium concentrations in alkaline leaching solutions. *Aquat. Geochem.* 8, 37–67. doi: 10.1023/A:1020318610178

Koning, E., Gehlen, M., Flank, A. M., Calas, G., and Epping, E. (2007). Rapid post-mortem incorporation of aluminum in diatom frustules: evidence from chemical and structural analyses. *Mar. Chem.* 106, 208–222. doi: 10.1016/j.marchem.2006.06.009

Kurtz, A. C., Derry, L. A., and Chadwick, O. A. (2002). Germanium-silicon fractionation in the weathering environment. *Geochim. Cosmochim. Acta* 66, 1525–1537. doi: 10.1016/S0016-7037(01)00869-9

Labeyrie, L., and Juillet, A. (1982). Oxygen isotopic exchangeability of diatom valve silica; interpretation and consequences for paleoclimatic studies. *Geochim. Cosmochim. Acta* 46, 967–975. doi: 10.1016/0016-7037(82)90052-7

Labeyrie, L. D. (1979). *La composition isotopique de l'oxygène de la silica des valves de diatomées. Mise au point d'une nouvelle méthode de paléoclimatologie quantitative.* Thesis, Université de Paris.

Lal, D., Charles, C., Vacher, L., Goswami, J. N., Jull, A. J. T., McHargue, L., et al. (2006). Paleo-ocean chemistry records in marine opal: implications for fluxes of trace elements, cosmogenic nuclides (10Be and 26Al), and biological productivity. *Geochim. Cosmochim. Acta* 70, 3275–3289. doi: 10.1016/j.gca.2006.04.004

Lamb, A. L., Brewer, T. S., Leng, M. J., Sloane, H. J., and Lamb, H. F. (2007). A geochemical method for removing the effect of tephra on lake diatom oxygen isotope records. *J. Paleolimnol.* 37, 499–516. doi: 10.1007/s10933-006-9034-5

Laruelle, G. G., Roubeix, V., Sferratore, A., Brodherr, B., Ciuffa, D., Conley, D. J., et al. (2009). Anthropogenic perturbations of the silicon cycle at the global scale: Key role of the land-ocean transition. *Global Biogeochem. Cycles* 23, 1–17. doi: 10.1029/2008GB003267

Laws, E. A. Popp, B. N., Bidigare, J. R. R., Kennicutt, M. C., and Macko, S. (1995). Dependence of phytoplankton carbon isotopic composition on growth rate and [CO2]aq: theoretical considerations and experimental results. *Geochim. Cosmochim. Acta* 59, 1131–1138. doi: 10.1016/0016-7037(95)00030-4

Leclerc, A. J., and Labeyrie, L. (1987). Temperature dependence of the oxygen isotopic fractionation between diatom silica and water. *Earth Planet. Sci. Lett.* 84, 69–74. doi: 10.1016/0012-821X(87)90177-4

Lewis, B. L., Froelich, P. N., and Andreae, M. O. (1985). Methylgermanium in natural waters. *Nature* 313, 303–305. doi: 10.1038/313303a0

Lewis, B. L., Andreae, M. O., Froelich, P. N., and Mortlock, R. A. (1988). A review of the biogeochemistry of germanium in natural waters. *Science Total Environ.* 73, 107–120. doi: 10.1016/0048-9697(88)90191-X

Lewis, B. L., Andreae, M. O., and Froelich, P. N. (1989). Sources and sinks of methylgermanium in natural waters. *Mar. Chem.* 27, 179–200. doi: 10.1016/0304-4203(89)90047-9

Loucaides, S., Michalopoulos, P., Presti, M., Koning, E., Behrends, T., and Van Cappellen, P. (2010). Seawater-mediated interactions between diatomaceous silica and terrigenous sediments: results from long-term incubation experiments. *Chem. Geol.* 270, 68–79. doi: 10.1016/j.chemgeo.2009.11.006

Lisiecki, L. E., and Raymo, M. E. (2005). A Pliocene-Pleistocene stack of 57 globally distributed benthic δ 18 O records. *Paleoceanography* 20:PA1003. doi: 10.1029/2004PA001071

Ma, J. F., Miyake, Y., and Takahashi, E. (2001). "Silicon as a beneficial element for crop plants," in *Silicon in Agriculture*, eds L. E. Datnoff, G. H. Snyder, and G. H. Korndorfer (Amsterdam: Elsevier), 17–39.

Ma, J. F., Tamai, K., Yamaji, N., Mitani, N., Konishi, S., Katsuhara, M., et al. (2006). A silicon transporter in rice. *Nature* 440, 688–691. doi: 10.1038/nature04590

Mackay, A. W., Swann, G. E. A., Brewer, T. S., Leng, M. J., Morley, D. W., Piotrowska, N., et al. (2011). A reassessment of late glacial - Holocene diatom oxygen isotope record from Lake Baikal using a geochemical mass-balance approach. *J. Quat. Sci.* 26, 627–634. doi: 10.1002/jqs.1484

Mackay, A. W., Swann, G. E. A., Fagel, N., Fietz, S., Leng, M. J., Morley, D., et al. (2013). Hydrological instability during the Last Interglacial in central Asia: a new diatom oxygen isotope record from Lake Baikal. *Quat. Sci. Rev.* 66, 45–54. doi: 10.1016/j.quascirev.2012.09.025

Mackenzie, F., and Garrels, R. (1966). Chemical mass balance between rivers and oceans.pdf. *Am. J. Sci.* 264, 19. doi: 10.2475/ajs.264.7.507

Madella, M., Aldexandre, A., and Ball, T. (2005). international code for phytolith nomenclature 1.0. *Ann. Bot.* 96, 253–260. doi: 10.1093/aob/mci172

Maher, W. A., Ellwood, M. J., Kelly, M., and De Deckker, P. (2006). Germanium incorporation into sponge spicules: development of a proxy for reconstructing inorganic germanium and silicon concentrations in seawater. *Geochim. Cosmochim. Acta* 70, A384–A384. doi: 10.1016/j.gca.2006.06.777

Maldonado, M., Carmona, M. C., Uriz, M. J., and Cruzado, A. (1999). Decline in Mesozoic reef-building sponges explained by silicon limitation. *Nature* 401, 785–788. doi: 10.1038/44560

Maier, E., Chapligin, B., Abelmann, A., Gersonde, R., Esper, O., Ren, J., et al. (2013). Combined oxygen and silicon isotope analysis of diatom silica from a deglacial subarctic Pacific record. *J. Quat. Sci.* 28:571 doi: 10.1002/jqs.2649

Maldonado, M., Carmona, C., Velasquez, Z., Puig, A., Cruzado, A., Lopez, A., et al. (2005). Siliceous sponges as a silicon sink: an overlooked aspect of benthopelagic coupling in the marine silicon cycle. *Limnol. Oceanogr.* 50, 799–809. doi: 10.4319/lo.2005.50.3.0799

Maldonado, M., Navarro, L., Grasa, A., Gonzalez, A., and Vaquerizo, I. (2011). Silicon uptake by sponges: a twist to understanding nutrient cycling on continental margins. *Sci. Rep.* 1, 30. doi: 10.1038/srep00030

Mann, S., and Perry, C. C. (1986). "Structural aspects of biogenic silica," in *Silicon Biochemistry, CIBA Foundation Symposium 121*, eds D. Evered and M. O'Connor (New York, NY: Wiley), 40–58.

Marin-Carbonne, J., Robert, F., and Chaussidon, M. (2014). The silicon and oxygen isotope compositions of Precambrian cherts: a record of oceanic paleo-temperatures? *Precambrian Res.* 247, 223–234. doi: 10.1016/j.precamres.2014.03.016

Martin-Jezequel, V., Hildebrand, M., and Brzezinski, M. A. (2000). Silicon metabolism in diatoms: implications for growth. *J. Phycol.* 36, 821–840. doi: 10.1046/j.1529-8817.2000.00019.x

Matheney, R. K., and Knauth, L. P. (1989). Oxygen-isotope fractionation between marine biogenic silica and seawater. *Geochim. Cosmochim. Acta* 53, 3207–3214. doi: 10.1016/0016-7037(89)90101-4

Matsumoto, K., and Sarmiento, J. L. (2008). A corollary to the silicic acid leakage hypothesis. *Paleoceanography* 23:PA2203. doi: 10.1029/2007PA001515

Matsumoto, K., Sarmiento, J. L., and Brzezinski, M. A. (2002). Silicic acid leakage from the Southern Ocean: a possible explanation for glacial atmospheric pCO(2). *Global Biogeochem. Cycles* 16, 1–23. doi: 10.1029/2001GB001442

Matteuzzo, M. C., Alexandre, A., Varajão, A. F. D. C., Volkmer-Ribeiro, C., Almeida, A. C. S., Varajão, C. A. C., et al. (2013). Assessing the relationship between the $\delta^{18}O$ signatures of siliceous sponge spicules and water in a∼tropical lacustrine environment (Minas Gerais, Brazil). *Biogeosci. Discuss.* 10, 12887–12918. doi: 10.5194/bgd-10-12887-2013

McManus, J., Hammond, D. E., Cummins, K., Klinkhammer, G. P., and Berelson, W. M. (2003). Diagenetic Ge-Si fractionation in continental margin environments: further evidence for a nonopal Ge sink. *Geochim. Cosmochim. Acta* 67, 4545–4557. doi: 10.1016/S0016-7037(03)00385-5

Meckler, A. N., Sigman, D. M., Gibson, K. A., François, R., Martínez-García, A., Jaccard, S. L., et al. (2013). Deglacial pulses of deep-ocean silicate into the subtropical North Atlantic Ocean. *Nature* 495, 495–498. doi: 10.1038/nature12006

Michalopoulos, P., and Aller, R. C. (1995). Rapid clay mineral formation in amazon delta sediments: reverse weathering and oceanic elemental cycles. *Science* 270, 614–617. doi: 10.1126/science.270.5236.614

Michalopoulos, P., and Aller, R. C. (2004). Early diagenesis of biogenic silica in the Amazon delta: alteration, authigenic clay formation, and storage. *Geochim. Cosmochim. Acta* 68, 1061–1085. doi: 10.1016/j.gca.2003.07.018

Milligan, A. J. (2004). Dynamics of silicon metabolism and silicon isotopic discrimination in a marine diatom as a function of pCO2. *Limnol. Oceanogr.* 49, 322–329. doi: 10.4319/lo.2004.49.2.0322

Misra, S., and Froelich, P. N. (2012). Lithium isotope history of Cenozoic seawater: changes in silicate weathering and reverse weathering. *Science* 335, 818–823. doi: 10.1126/science.1214697

Montoya, J. P., and McCarthy, J. J. (1995). Isotopic fractionation during nitrate uptake by phytoplankton grown in continuous culture. *J. Plankton Res.* 17, 439–464. doi: 10.1093/plankt/17.3.439

Mopper, K., and Garlick, G. . (1971). Oxygen isotope fractionation between biogenic silica and ocean water. *Geochim. Cosmochim. Acta* 35, 1185–1187. doi: 10.1016/0016-7037(71)90032-9

Moran, S. B., and Moore, R. M. (1988). Evidence from mesocosm studies for biological removal of dissolved aluminium from sea water. *Nature* 335, 706–708. doi: 10.1038/335706a0

Morley, D. W., Leng, M. J., Mackay, A. W., and Sloane, H. J. (2005). Late glacial and Holocene environmental change in the Lake Baikal region documented by oxygen isotopes from diatom silica. *Glob. Planet. Change* 46, 221–233. doi: 10.1016/j.gloplacha.2004.09.018

Morley, D. W., Leng, M. J., Mackay, A. W., Sloane, H. J., Rioual, P., and Battarbee, R. W. (2004). Cleaning of lake sediment samples for diatom oxygen isotope analysis. *J. Paleolimnol.* 31, 391–401. doi: 10.1023/B:JOPL.0000021854.70714.6b

Mortlock, R. A., Charles, C. D., Froelich, P. N., Zibello, M. A., Saltzman, J., Hays, J. D., et al. (1991). Evidence for lower productivity in the Antarctic Ocean during the last glaciation. *Nature* 351, 220–223. doi: 10.1038/351220a0

Mortlock, R. A., and Froelich, P. N. (1987). Continental weathering of germanium - Ge/Si in the global river discharge. *Geochim. Cosmochim. Acta* 51, 2075–2082. doi: 10.1016/0016-7037(87)90257-2

Mortlock, R. A., and Froelich, P. N. (1996). Determination of germanium by isotope dilution hydride generation inductively coupled plasma mass spectrometry. *Anal. Chim. Acta* 332, 277–284. doi: 10.1016/0003-2670(96)00230-9

Mortlock, R. A., Froelich, P. N., Feely, R. A., Massoth, G. J., Butterfield, D. A., and Lupton, J. E. (1993). Silica and germanium in pacific-ocean

hydrothermal vents and plumes. *Earth Planet. Sci. Lett.* 119, 365–378. doi: 10.1016/0012-821X(93)90144-X

Muller, W. E. G., Li, J. H., Schroder, H. C., Qiao, L., and Wang, X. H. (2007). The unique skeleton of siliceous sponges (Porifera; Hexactinellida and Demospongiae) that evolved first from the Urmetazoa during the Proterozoic: a review. *Biogeosciences* 4, 219–232. doi: 10.5194/bg-4-219-2007

Murnane, R. ., Leslie, B., Hammond, D. ., and Stallard, R. (1989). Germanium geochemistry in the Southern California Borderlands. *Geochim. Cosmochim. Acta* 53, 2873–2882. doi: 10.1016/0016-7037(89)90164-6

Needoba, J., Waser, N., Harrison, P., and Calvert, S. (2003). Nitrogen isotope fractionation in 12 species of marine phytoplankton during growth on nitrate. *Mar. Ecol. Prog. Ser.* 255, 81–91. doi: 10.3354/meps255081

Nelson, D. M., Treguer, P., Brzezinski, M. A., Leynaert, A., and Queguiner, B. (1995). Production and dissolution of biogenic silica in the ocean - revised global estimates, comparison with regional data and relationship to biogenic sedimentation. *Global Biogeochem. Cycles* 9, 359–372. doi: 10.1029/95GB01070

Oelze, M., von Blanckenburg, F., Bouchez, J., Hoellen, D., and Dietzel, M. (2015). The effect of Al on Si isotope fractionation investigated by silica precipitation experiments. *Chem. Geol.* 397, 94–105. doi: 10.1016/j.chemgeo.2015.01.002

Oelze, M., von Blanckenburg, F., Hoellen, D., Dietzel, M., and Bouchez, J. (2014). Si stable isotope fractionation during adsorption and the competition between kinetic and equilibrium isotope fractionation: Implications for weathering systems. *Chem. Geol.* 380, 161–171. doi: 10.1016/j.chemgeo.2014.04.027

Opfergelt, S., Burton, K. W., Pogge von Strandmann, P. A. E., Gislason, S. R., and Halliday, A. N. (2013). Riverine silicon isotope variations in glaciated basaltic terrains: Implications for the Si delivery to the ocean over glacial-interglacial intervals. *Earth Planet. Sci. Lett.* 369–370, 211–219. doi: 10.1016/j.epsl.2013.03.025

Opfergelt, S., Cardinal, D., André, L., Delvigne, C., Bremond, L., and Delvaux, B. (2010). Variations of δ30Si and Ge/Si with weathering and biogenic input in tropical basaltic ash soils under monoculture. *Geochim. Cosmochim. Acta* 74, 225–240. doi: 10.1016/j.gca.2009.09.025

Opfergelt, S., Cardinal, D., Henriet, C., Andre, L., and Delvaux, B. (2006a). Silicon isotope fractionation between plant parts in banana: *in situ* vs. *in vitro*. *J. Geochemical Explor.* 88, 224–227. doi: 10.1016/j.gexplo.2005.08.044

Opfergelt, S., Cardinal, D., Henriet, C., Draye, X., Andre, L., and Delvaux, B. (2006b). Silicon isotopic fractionation by banana (*Musa* spp.) grown in a continuous nutrient flow device. *Plant Soil* 285, 333–345. doi: 10.1007/s11104-006-9019-1

Opfergelt, S., and Delmelle, P. (2012). Silicon isotopes and continental weathering processes: assessing controls on Si transfer to the ocean. *Comptes Rendus Geosci.* 344, 723–738. doi: 10.1016/j.crte.2012.09.006

Opfergelt, S., Delvaux, B., André, L., and Cardinal, D. (2008). Plant silicon isotopic signature might reflect soil weathering degree. *Biogeochemistry* 91, 163–175. doi: 10.1007/s10533-008-9278-4

Opfergelt, S., Eiriksdottir, E. S. S., Burton, K. W. W., Einarsson, A., Siebert, C., Gislason, S. R. R., et al. (2011). Quantifying the impact of freshwater diatom productivity on silicon isotopes and silicon fluxes: Lake Myvatn, Iceland. *Earth Planet. Sci. Lett.* 305, 73–82. doi: 10.1016/j.epsl.2011.02.043

Opfergelt, S., Georg, R. B., Delvaux, B., Cabidoche, Y. M., Burton, K. W., and Halliday, A. N. (2012). Silicon isotopes and the tracing of desilication in volcanic soil weathering sequences, Guadeloupe. *Chem. Geol.* 326–327, 113–122. doi: 10.1016/j.chemgeo.2012.07.032

Panizzo, V., Crespin, J., Crosta, X., Shemesh, A., Massé, G., Yam, R., et al. (2014). Sea ice diatom contributions to Holocene nutrient utilization in East Antarctica. *Paleoceanography* 29, 328–343. doi: 10.1002/2014PA002609

Panizzo, V. N., Swann, G. E. A., Mackay, A. W., Vologina, E., Alleman, L., André, L., et al. (2017). Constraining modern-day silicon cycling in Lake Baikal. *Global Biogeochem. Cycles* 31, 556–574. doi: 10.1002/2016GB005518

Panizzo, V. N., Swann, G. E. A., Mackay, A. W., Vologina, E., Sturm, M., Pashley, V., et al. (2016). Insights into the transfer of silicon isotopes into the sediment record. *Biogeosciences* 13, 147–157. doi: 10.5194/bg-13-147-2016

Perry, C. C., Belton, D., and Shafran, K. (2003). "Studies of biosilicas; structural aspects, chemicalprinciples,model studies and the future," in *Silicon Biomineralization: Biology—Biochemistry—Molecular Biology—Biotechnology*, ed W. E. G. Müller (Berlin; Heidelberg: Springer), 269–299.

Pichevin, L., Ganeshram, R. S., Reynolds, B. C., Prahl, F., Pedersen, T. F., Thunell, R., et al. (2012). Silicic acid biogeochemistry in the Gulf of California: insights from sedimentary Si isotopes. *Paleoceanography* 27:PA2201. doi: 10.1029/2011PA002237

Pichevin, L., Reynolds, B., Ganeshram, R., Cacho, I., Pena, L., Keefe, K., et al. (2009). Enhanced carbon pump inferred from relaxation of nutrient limitation in the glacial ocean. *Nature* 459, 1114–1117. doi: 10.1038/nature08101

Pike, J., Swann, G. E. A., Leng, M. J., and Snelling, A. M. (2013). Glacial discharge along the west Antarctic Peninsula during the Holocene. *Nat. Geosci.* 6, 199–202. doi: 10.1038/ngeo1703

Pogge von Strandmann, P. A. E., Opfergelt, S., Lai, Y. J., Sigfússon, B., Gislason, S. R., and Burton, K. W. (2012). Lithium, magnesium and silicon isotope behaviour accompanying weathering in a basaltic soil and pore water profile in Iceland. *Earth Planet. Sci. Lett.* 339–340, 11–23. doi: 10.1016/j.epsl.2012.05.035

Pokrovski, G. S., and Schott, J. (1998). Experimental study of the complexation of silicon and germanium with aqueous organic species: implications for germanium and silicon transport and Ge/Si ratio in natural waters. *Geochim. Cosmochim. Acta* 62, 3413–3428. doi: 10.1016/S0016-7037(98)00249-X

Pokrovsky, O. S., Reynolds, B. C., Prokushkin, A. S., Schott, J., and Viers, J. (2013). Silicon isotope variations in Central Siberian rivers during basalt weathering in permafrost-dominated larch forests. *Chem. Geol.* 355, 103–116. doi: 10.1016/j.chemgeo.2013.07.016

Presti, M., and Michalopoulos, P. (2008). Estimating the contribution of the authigenic mineral component to the long-term reactive silica accumulation on the western shelf of the Mississippi River Delta. *Cont. Shelf Res.* 28, 823–838. doi: 10.1016/j.csr.2007.12.015

Qin, T., Wu, F., Wu, Z., and Huang, F. (2016). First-principles calculations of equilibrium fractionation of O and Si isotopes in quartz, albite, anorthite, and zircon. *Contrib. Mineral. Petrol.* 171:91. doi: 10.1007/s00410-016-1303-3

Rabouille, C., Mackenzie, F. T., and Ver, L. M. (2001). Influence of the human perturbation on carbon, nitrogen, and oxygen biogeochemical cycles in the global coastal ocean. *Geochim. Cosmochim. Acta* 65, 3615–3641. doi: 10.1016/S0016-7037(01)00760-8

Ragueneau, O., Tréguer, P., Leynaert, A., Anderson, R., Brzezinski, M., DeMaster, D., et al. (2000). A review of the Si cycle in the modern ocean: recent progress and missing gaps in the application of biogenic opal as a paleoproductivity proxy. *Glob. Planet. Change* 26, 317–365. doi: 10.1016/S0921-8181(00)00052-7

Rahman, S., Aller, R. C., and Cochran, J. K. (2016). Cosmogenic 32 Si as a tracer of biogenic silica burial and diagenesis: major deltaic sinks in the silica cycle. *Geophys. Res. Lett.* 43, 7124–7132. doi: 10.1002/2016GL069929

Rau, G. H., Riebesell, U., and Wolf-Gladrow, D. (1996). A model of photosynthetic 13C fractionation by marine phytoplankton based on diffusive molecular CO2 uptake. *Mar. Ecol. Prog. Ser.* 133, 275–285. doi: 10.3354/meps133275

Rau, G. H., Riebesell, U., and Wolf-Gladrow, D. (1997). CO 2aq -dependent photosynthetic 13 C fractionation in the ocean: a model versus measurements. *Global Biogeochem. Cycles* 11, 267–278. doi: 10.1029/97GB00328

Raymo, M. E., Lisiecki, L. E., Nisancioglu, K. H., Hemispheres, S., and Instead, O. (2006). Plio-Pleistocene ice volume, Antarctic climate, and the Global. *Science* 313, 492–496. doi: 10.1126/science.1123296

Reincke, T., and Barthel, D. (1997). Silica uptake kinetics of *Halichondria panicea* in kiel bight. *Mar. Biol.* 129, 591–593. doi: 10.1007/s002270050200

Ren, H., Brunelle, B. G., Sigman, D. M., and Robinson, R. S. (2013). Diagenetic aluminum uptake into diatom frustules and the preservation of diatom-bound organic nitrogen. *Mar. Chem.* 155, 92–101. doi: 10.1016/j.marchem.2013.05.016

Reynolds, B. C. (2011). "Silicon isotopes as tracers of terrestrial processes," in *Handbook of Environmental Isotope Geochemistry*, ed M. Baskaran (Berlin: Springer-Verlag), 87–104. doi: 10.1007/978-3-642-10637-8_6

Reynolds, B. C., Aggarwal, J., André, L., Baxter, D., Beucher, C., Brzezinski, M. A., et al. (2007). An inter-laboratory comparison of Si isotope reference materials. *J. Anal. At. Spectrom.* 22, 561–568. doi: 10.1039/B616755A

Reynolds, B. C., Frank, M., and Halliday, A. N. (2006). Silicon isotope fractionation during nutrient utilization in the North Pacific. *Earth Planet. Sci. Lett.* 244, 431–443. doi: 10.1016/j.epsl.2006.02.002

Rickert, D., Schlüter, M., and Wallmann, K. (2002). Dissolution kinetics of biogenic silica from the water column to the sediments. *Geochim. Cosmochim. Acta* 66, 439–455. doi: 10.1016/S0016-7037(01)00757-8

Robert, F., and Chaussidon, M. (2006). A palaeotemperature curve for the Precambrian oceans based on silicon isotopes in cherts. *Nature* 443, 969–972. doi: 10.1038/nature05239

Robinson, R. S., Brunelle, B. G., and Sigman, D. M. (2004). Revisiting nutrient utilization in the glacial Antarctic: evidence from a new method for diatom-bound N isotopic analysis. *Paleoceanography* 19:PA3001. doi: 10.1029/2003PA000996

Robinson, R. S., Kienast, M., Luiza Albuquerque, A., Altabet, M., Contreras, S., De Pol Holz, R., et al. (2012). A review of nitrogen isotopic alteration in marine sediments. *Paleoceanography* 27:PA4203 doi: 10.1029/2012PA002321

Robinson, R. S., and Sigman, D. M. (2008). Nitrogen isotopic evidence for a poleward decrease in surface nitrate within the ice age Antarctic. *Quat. Sci. Rev.* 27, 1076–1090. doi: 10.1016/j.quascirev.2008.02.005

Robinson, R. S., Sigman, D. M., DiFiore, P. J., Rohde, M. M., Mashiotta, T. A., and Lea, D. W. (2005). Diatom-bound 15N/14N: new support for enhanced nutrient consumption in the ice age subantarctic. *Paleoceanography* 20, 1–14. doi: 10.1029/2004PA001114

Roerdink, D. L., van den Boorn, S. H. J. M., Geilert, S., Vroon, P. Z., and van Bergen, M. J. (2015). Experimental constraints on kinetic and equilibrium silicon isotope fractionation during the formation of non-biogenic chert deposits. *Chem. Geol.* 402, 40–51. doi: 10.1016/j.chemgeo.2015.02.038

Rousseau, J., Ellwood, M. J., Bostock, H., and Neil, H. (2016). Estimates of late quaternary mode and intermediate water silicic acid concentration in the Pacific Southern Ocean. *Earth Planet. Sci. Lett.* 439, 101–108. doi: 10.1016/j.epsl.2016.01.023

Rouxel, O. J., and Luais, B. (2017). Germanium isotope geochemistry. *Rev. Mineral. Geochem.* 82, 601–656. doi: 10.2138/rmg.2017.82.14

Rude, P. D., and Aller, R. C. (1994). Fluorine uptake by Amazon continental shelf sediment and its impact on the global fluorine cycle. *Cont. Shelf Res.* 14, 883–907. doi: 10.1016/0278-4343(94)90078-7

Sarmiento, J. L., Gruber, N., Brzezinski, M. A., and Dunne, J. P. (2004). High-latitude controls of thermocline nutrients and low latitude biological productivity. *Nature* 427, 56–60. doi: 10.1038/nature02127

Sarmiento, J. L., and Toggweiler, J. R. (1984). A new model for the role of the oceans in determining atmospheric PCO2. *Nature* 308, 621–624. doi: 10.1038/308621a0

Schmidt, M., Botz, R., Rickert, D., Bohrmann, G., Hall, S. R., and Mann, S. (2001). Oxygen isotopes of marine diatoms and relations to opal-A maturation. *Geochim. Cosmochim. Acta* 65, 201–211. doi: 10.1016/S0016-7037(00)00534-2

Schröder, H. C., Natalio, F., Shukoor, I., Tremel, W., Schloßmacher, U., Wang, X., et al.(2007). Apposition of silica lamellae during growth of spicules in the demosponge *Suberites domuncula*: biological/biochemical studies and chemical/biomimetical confirmation. *J. Struct. Biol.* 159, 325–334. doi: 10.1016/j.jsb.2007.01.007

Schuessler, J. A., and von Blanckenburg, F. (2014). Testing the limits of micro-scale analyses of Si stable isotopes by femtosecond laser ablation multicollector inductively coupled plasma mass spectrometry with application to rock weathering. *Spectrochim. Acta Part B At. Spectrosc.* 98, 1–18. doi: 10.1016/j.sab.2014.05.002

Sharp, Z. D., Gibbons, J. A., Maltsev, O., Atudorei, V., Pack, A., Sengupta, S., et al. (2016). A calibration of the triple oxygen isotope fractionation in the SiO2–H2O system and applications to natural samples. *Geochim. Cosmochim. Acta* 186, 105–119. doi: 10.1016/j.gca.2016.04.047

Shemesh, A., Burckle, L. H., and Hays, J. D. (1995). Late Pleistocene oxygen isotope records of biogenic silica from the Atlantic sector of the Southern Ocean. *Paleoceanography* 10, 179–196. doi: 10.1029/94PA03060

Shemesh, A., Charles, C. D., and Fairbanks, R. G. (1992). Oxygen isotopes in biogenic silica: global changes in ocean temperature and isotopic composition. *Science* 256, 1434–1436. doi: 10.1126/science.256.5062.1434

Shemesh, A., Macko, S. A., Charles, C. D., and Rau, G. H. (1993). Isotopic evidence for reduced productivity in the glacial Southern Ocean. *Science* 262, 407–410. doi: 10.1126/science.262.5132.407

Shemesh, A., Mortlock, R. A., Smith, R. J., and Froelich, P. N. (1988). Determination of Ge/Si in marine siliceous microfossils - separation, cleaning and dissolution of diatoms and radiolaria. *Mar. Chem.* 25, 305–323. doi: 10.1016/0304-4203(88)90113-2

Siever, R. (1991). The silica cycle in the Precambrian. *Geochim. Cosmochim. Acta* 56, 3265–3272. doi: 10.1016/0016-7037(92)90303-Z

Sigman, D. M., Altabet, M. A., Francois, R., McCorkle, D. C., and Gaillard, J.-F. (1999). The isotopic composition of diatom-bound nitrogen in Southern Ocean sediments. *Paleoceanography* 14, 118–134. doi: 10.1029/1998PA900018

Singh, S. P., Singh, S. K., Bhushan, R., and Rai, V. K. (2015). Dissolved silicon and its isotopes in the water column of the Bay of Bengal: internal cycling versus lateral transport. *Geochim. Cosmochim. Acta* 151, 172–191. doi: 10.1016/j.gca.2014.12.019

Smetacek, V., Klaas, C., Strass, V. H., Assmy, P., Montresor, M., Cisewski, B., et al. (2012). Deep carbon export from a Southern Ocean iron-fertilized diatom bloom. *Nature* 487, 313–319. doi: 10.1038/nature11229

Snelling, A. M., Swann, G. E. A., Pike, J., and Leng, M. J. (2014). Pliocene diatom and sponge spicule oxygen isotope ratios from the Bering Sea: isotopic offsets and future directions. *Clim. Past* 10, 1837–1842. doi: 10.5194/cp-10-1837-2014

Stallard, R. F., and Edmond, J. M. (1983). Geochemistry of the Amazon: 2. The influence of geology and weathering environment on the dissolved load. *J. Geophys. Res. Ocean.* 88, 9671–9688. doi: 10.1029/JC088iC14p09671

Steinhoefel, G., Breuer, J., von Blanckenburg, F., Horn, I., Kaczorek, D., and Sommer, M. (2011). Micrometer silicon isotope diagnostics of soils by UV femtosecond laser ablation. *Chem. Geol.* 286, 280–289. doi: 10.1016/j.chemgeo.2011.05.013

Stoll, H. M., Mendez-Vicente, A., Abrevaya, L., Anderson, R. F., Rigual-Hernández, A. S., and Gonzalez-Lemos, S. (2017). Growth rate and size effect on carbon isotopic fractionation in diatom-bound organic matter in recent Southern Ocean sediments. *Earth Planet. Sci. Lett.* 457, 87–99. doi: 10.1016/j.epsl.2016.09.028

Street-Perrott, F. A., Barker, P. A., Leng, M. J., Sloane, H. J., Wooller, M. J., Ficken, K. J., et al. (2008). Towards an understanding of late quaternary variations in the continental biogeochemical cycle of silicon: multi-isotope and sediment-flux data for Lake Rutundu, Mt Kenya, East Africa, since 38 ka BP. *J. Quat. Sci.* 23, 375–387. doi: 10.1002/jqs.1187

Struyf, E., and Conley, D. J. (2012). Emerging understanding of the ecosystem silica filter. *Biogeochemistry* 107, 9–18. doi: 10.1007/s10533-011-9590-2

Struyf, E., Smis, A., Van Damme, S., Garnier, J., Govers, G., Van Wesemael, B., et al. (2010). Historical land use change has lowered terrestrial silica mobilization. *Nat. Commun.* 1:129. doi: 10.1038/ncomms1128

Struyf, E., Smis, A., Van Damme, S., Meire, P., and Conley, D. J. (2009). The global biogeochemical silicon cycle. *Silicon* 1, 207–213. doi: 10.1007/s12633-010-9035-x

Struyf, E., Van Damme, S., and Meire, P. (2004). Possible effects of climate change on estuarine nutrient fluxes: a case study in the highly nutrified Schelde estuary (Belgium, The Netherlands). *Estuar. Coast. Shelf Sci.* 60, 649–661. doi: 10.1016/j.ecss.2004.03.004

Sun, L., Wu, L. H., Ding, T. P., and Tian, S. H. (2008). Silicon isotope fractionation in rice plants, an experimental study on rice growth under hydroponic conditions. *Plant Soil* 304, 291–300. doi: 10.1007/s11104-008-9552-1

Sun, X., Andersson, P., Humborg, C., Gustafsson, B., Conley, D. J., Crill, P., et al. (2011). Climate dependent diatom production is preserved in biogenic Si isotope signatures. *Biogeosciences* 8, 3491–3499. doi: 10.5194/bg-8-3491-2011

Sun, X., Andersson, P. S., Humborg, C., Pastuszak, M., and Mörth, C. M. (2013). Silicon isotope enrichment in diatoms during nutrient-limited blooms in a eutrophied river system. *J. Geochemical Explor.* 132, 173–180. doi: 10.1016/j.gexplo.2013.06.014

Sun, X., Higgins, J., and Turchyn, A. V. (2016). Diffusive cation fluxes in deep-sea sediments and insight into the global geochemical cycles of calcium, magnesium, sodium and potassium. *Mar. Geol.* 373, 64–77. doi: 10.1016/j.margeo.2015.12.011

Sutton, J. (2011). *Germanium/Silicon and Silicon Isotope Fractionation by Marine Diatoms and Sponges and Utility as Tracers of Silicic Acid Utilization*. Thesis, Australian National University.

Sutton, J., Ellwood, M. J., Maher, W. A., and Croot, P. L. (2010). Oceanic distribution of inorganic germanium relative to silicon: Germanium discrimination by diatoms. *Global Biogeochem. Cycles* 24:GB2017. doi: 10.1029/2009GB003689

Sutton, J. N., Varela, D. E., Brzezinski, M. A., and Beucher, C. P. (2013). Species-dependent silicon isotope fractionation by marine diatoms. *Geochim. Cosmochim. Acta* 104, 300–309. doi: 10.1016/j.gca.2012.10.057

Suzuki, N., and Aita, Y. (2011). Radiolaria: achievements and unresolved issues: taxonomy and cytology. *Plankt. Benthos Res.* 6, 69–91. doi: 10.3800/pbr.6.69

Swann, G. E. A., and Leng, M. J. (2009). A review of diatom δ18O in palaeoceanography. *Quat. Sci. Rev.* 28, 384–398. doi: 10.1016/j.quascirev.2008.11.002

Swann, G. E. A., Leng, M. J., Juschus, O., Melles, M., Brigham-Grette, J., and Sloane, H. J. (2010). A combined oxygen and silicon diatom isotope record of late quaternary change in Lake El'gygytgyn, North East Siberia. *Quat. Sci. Rev.* 29, 774–786. doi: 10.1016/j.quascirev.2009.11.024

Swann, G. E. A., and Snelling, A. M. (2015). Photic zone changes in the north-west Pacific Ocean from MIS 4-5e. *Clim. Past* 11, 15–25. doi: 10.5194/cp-11-15-2015

Takahashi, E., Ma, J. F., and Miyake, Y. (1990). The possibility of silicon as an essential element for higher plants. *Comments Agric. Food Chem* 2, 99–122.

Tatzel, M., von Blanckenburg, F., Oelze, M., Schuessler, J. A., and Bohrmann, G. (2015). The silicon isotope record of early silica diagenesis. *Earth Planet. Sci. Lett.* 428, 293–303. doi: 10.1016/j.epsl.2015.07.018

Thamatrakoln, K., and Hildebrand, M. (2008). Silicon uptake in diatoms revisited: a model for saturable and nonsaturable uptake kinetics and the role of silicon transporters. *Plant Physiol.* 146, 1397–1407. doi: 10.1104/pp.107.107094

Thamatrakoln, K., and Kustka, A. B. (2009). When to say when: can excessive drinking explain silicon uptake in diatoms? *BioEssays* 31, 322–327. doi: 10.1002/bies.200800185

Tortell, P. D., and Morel, F. M. M. (2002). Sources of inorganic carbon for phytoplankton in the eastern Subtropical and Equatorial Pacific Ocean. *Limnol. Oceanogr.* 47, 1012–1022. doi: 10.4319/lo.2002.47.4.1012

Tréguer, P. J., and De La Rocha, C. L. (2013). The world ocean silica cycle. *Ann. Rev. Mar. Sci.* 5, 477–501. doi: 10.1146/annurev-marine-121211-172346

Twining, B. S., Baines, S. B., Fisher, N. S., Maser, J., Vogt, S., Jacobsen, C., et al. (2003). Quantifying trace elements in individual aquatic protist cells with a synchrotron X-ray fluorescence microprobe. *Anal. Chem.* 75, 3806–3816. doi: 10.1021/ac034227z

Uriz, M. J., Turon, X., Becerro, M. A., and Agell, G. (2003): Siliceous spicules and skeleton frameworks in sponges: origin, diversity, ultrastructural patterns, and biological functions. *Microsc. Res. Tech.* 62, 279–299. doi: 10.1002/jemt.10395

van Bennekom, A. J., and van der Gaast, S. J. (1976). Possible clay structures in frustules of living diatoms. *Geochim. Cosmochim. Acta* 40, 1149–1150. doi: 10.1016/0016-7037(76)90150-2

Vandevenne, F. I., Delvaux, C., Hughes, H. J., André, L., Ronchi, B., Clymans, W., et al. (2015). Landscape cultivation alters δ30Si signature in terrestrial ecosystems. *Sci. Rep.* 5:7732. doi: 10.1038/srep07732

Varela, D. E., Brzezinski, M. A., Beucher, C. P., Jones, J. L., Giesbrecht, K. E., Lansard, B., et al. (2016). Heavy silicon isotopic composition of silicic acid and biogenic silica in Arctic waters over the Beaufort shelf and the Canada Basin. *Global Biogeochem. Cycles* 30, 804–824. doi: 10.1002/2015GB005277

Varela, D. E., Pride, C. J., and Brzezinski, M. A. (2004). Biological fractionation of silicon isotopes in Southern Ocean surface waters. *Global Biogeochem. Cycles* 18, 1–8. doi: 10.1029/2003GB002140

Wetzel, F., de Souza, G. F., and Reynolds, B. C. (2014). What controls silicon isotope fractionation during dissolution of diatom opal? *Geochim. Cosmochim. Acta* 131, 128–137. doi: 10.1016/j.gca.2014.01.028

Wheat, C. G., and McManus, J. (2005). The potential role of ridge-flank hydrothermal systems on oceanic germanium and silicon balances. *Geochim. Cosmochim. Acta* 69, 2021–2029. doi: 10.1016/j.gca.2004.05.046

White, A. F., and Blum, A. E. (1995). Effects of climate on chemical weathering in watersheds. *Geochim. Cosmochim. Acta* 59, 1729–1747. doi: 10.1016/0016-7037(95)00078-E

Wiederhold, J. G. (2015). Metal stable isotope signatures as tracers in environmental geochemistry. *Environ. Sci. Technol.* 49, 2606–2624. doi: 10.1021/es504683e

Wille, M., Sutton, J., Ellwood, M. J., Sambridge, M., Maher, W., Eggins, S., et al. (2010). Silicon isotopic fractionation in marine sponges: a new model for understanding silicon isotopic variations in sponges. *Earth Planet. Sci. Lett.* 292, 281–289. doi: 10.1016/j.epsl.2010.01.036

Wilkinson, C. R., and Garrone, R. (1980). Ultrastructure of siliceous spicules and microsclerocytes in the marine sponge *Neofibularia irata* N. SP. *J. Morphol.* 166, 51–63. doi: 10.1002/jmor.1051660105

Wilson, K. E., Leng, M. J., and Mackay, A. W. (2014). The use of multivariate statistics to resolve multiple contamination signals in the oxygen isotope analysis of biogenic silica. *J. Quat. Sci.* 29, 641–649. doi: 10.1002/jqs.2729

Wollast, R., and Mackenzie, F. T. (1989). "Global Biogeochemical Cycles and Climate," in *Climate and Geo-Sciences: A Challenge for Science and Society in the 21st Century*, eds A. Berger, S. Schneider, and J. C. Duplessy (Dordrecht: Springer), 453–473.

Xiong, Z., Li, T., Algeo, T., Doering, K., Frank, M., Brzezinski, M. A., et al. (2015). The silicon isotope composition of *Ethmodiscus rex* laminated diatom mats from the tropical West Pacific: implications for silicate cycling during the last glacial maximum. *Paleoceanography* 30, 803–823. doi: 10.1002/2015PA002793

Zachos, J. (2001). Trends, rhythms, and aberrations in global climate 65 Ma to Present. *Science* 292, 686–693. doi: 10.1126/science.1059412

Zhao, Y., Vance, D., Abouchami, W., and De Baar, H. J. W. (2014). Biogeochemical cycling of zinc and its isotopes in the Southern Ocean. *Geochim. Cosmochim. Acta* 125, 653–672. doi: 10.1016/j.gca.2013.07.045

Ziegler, K., Chadwick, O. A., Brzezinski, M. A., and Kelly, E. F. (2005). Natural variations of δ30Si ratios during progressive basalt weathering, Hawaiian Islands. *Geochim. Cosmochim. Acta* 69, 4597–4610. doi: 10.1016/j.gca.2005.05.008

Conflict of Interest Statement: The authors declare that the research was conducted in the absence of any commercial or financial relationships that could be construed as a potential conflict of interest.

The handling editor declared a shared affiliation, though no other collaboration, with one of the authors, JS.

Copyright © 2018 Sutton, André, Cardinal, Conley, de Souza, Dean, Dodd, Ehlert, Ellwood, Frings, Grasse, Hendry, Leng, Michalopoulos, Panizzo and Swann. This is an open-access article distributed under the terms of the Creative Commons Attribution License (CC BY). The use, distribution or reproduction in other forums is permitted, provided the original author(s) and the copyright owner are credited and that the original publication in this journal is cited, in accordance with accepted academic practice. No use, distribution or reproduction is permitted which does not comply with these terms.

frontiers in Marine Science

REVIEW
published: 11 December 2017
doi: 10.3389/fmars.2017.00397

Biosilicification Drives a Decline of Dissolved Si in the Oceans through Geologic Time

Daniel J. Conley[1, 2], Patrick J. Frings[1, 3†], Guillaume Fontorbe[1], Wim Clymans[1, 4], Johanna Stadmark[1], Katharine R. Hendry[5], Alan O. Marron[6] and Christina L. De La Rocha[1]*

[1] Department of Geology, Lund University, Lund, Sweden, [2] Stellenbosch Institute for Advanced Study, Stellenbosch, South Africa, [3] Department of Geoscience, Swedish Museum of Natural History, Stockholm, Sweden, [4] Earthwatch Institute, Oxford, United Kingdom, [5] School of Earth Sciences, University of Bristol, Bristol, United Kingdom, [6] Department of Applied Mathematics and Theoretical Physics, Centre for Mathematical Sciences, University of Cambridge, Cambridge, United Kingdom

OPEN ACCESS

Edited by:
Stephen B. Baines, Stony Brook University, United States

Reviewed by:
X. Antón Álvarez-Salgado, Consejo Superior de Investigaciones Científicas (CSIC), Spain
Dirk De Beer, Max Planck Society (MPG), Germany

***Correspondence:**
Daniel J. Conley
daniel.conley@geol.lu.se

†Present Address:
Patrick J. Frings, Earth Surface Geochemistry, Helmholtz Centre Potsdam, GFZ German Research Centre for Geosciences, Potsdam, Germany

Specialty section:
This article was submitted to Marine Biogeochemistry, a section of the journal Frontiers in Marine Science

Received: *14 April 2017*
Accepted: *24 November 2017*
Published: *11 December 2017*

Citation:
Conley DJ, Frings PJ, Fontorbe G, Clymans W, Stadmark J, Hendry KR, Marron AO and De La Rocha CL (2017) Biosilicification Drives a Decline of Dissolved Si in the Oceans through Geologic Time. Front. Mar. Sci. 4:397. doi: 10.3389/fmars.2017.00397

Biosilicification has driven variation in the global Si cycle over geologic time. The evolution of different eukaryotic lineages that convert dissolved Si (DSi) into mineralized structures (higher plants, siliceous sponges, radiolarians, and diatoms) has driven a secular decrease in DSi in the global ocean leading to the low DSi concentrations seen today. Recent studies, however, have questioned the timing previously proposed for the DSi decreases and the concentration changes through deep time, which would have major implications for the cycling of carbon and other key nutrients in the ocean. Here, we combine relevant genomic data with geological data and present new hypotheses regarding the impact of the evolution of biosilicifying organisms on the DSi inventory of the oceans throughout deep time. Although there is no fossil evidence for true silica biomineralization until the late Precambrian, the timing of the evolution of silica transporter genes suggests that bacterial silicon-related metabolism has been present in the oceans since the Archean with eukaryotic silicon metabolism already occurring in the Neoproterozoic. We hypothesize that biological processes have influenced oceanic DSi concentrations since the beginning of oxygenic photosynthesis.

Keywords: silicates, diatoms, sponges, cyanobacteria, biogeochemical cycles

INTRODUCTION

Seminal work published a quarter of a century ago sketched a framework for the evolution of the oceanic Si cycle through Earth's history based on the geological record available at that time (**Figure 1A**). The narrative given by Maliva et al. (1989) and Siever (1991) suggested that, in the absence of silica biomineralizers, defined here as organisms that intentionally take dissolved Si (DSi) up across their cell membrane and control its precipitation as particulate silica to form a structure that is then used in a specific manner, the Precambrian Si cycle was dominated by inorganic reactions and diagenetic silicification. These processes resulted in the widespread deposition of cherts and ultimately controlled concentrations of DSi in the oceans. A biological takeover of oceanic DSi occurred with the evolution of silica biomineralizing eukaryotes during the Phanerozic and the subsequent deposition of DSi as biogenic Si (BSi). This simple framework divides the ocean Si cycle into periods of relative stasis separated by stepwise drops in ocean DSi

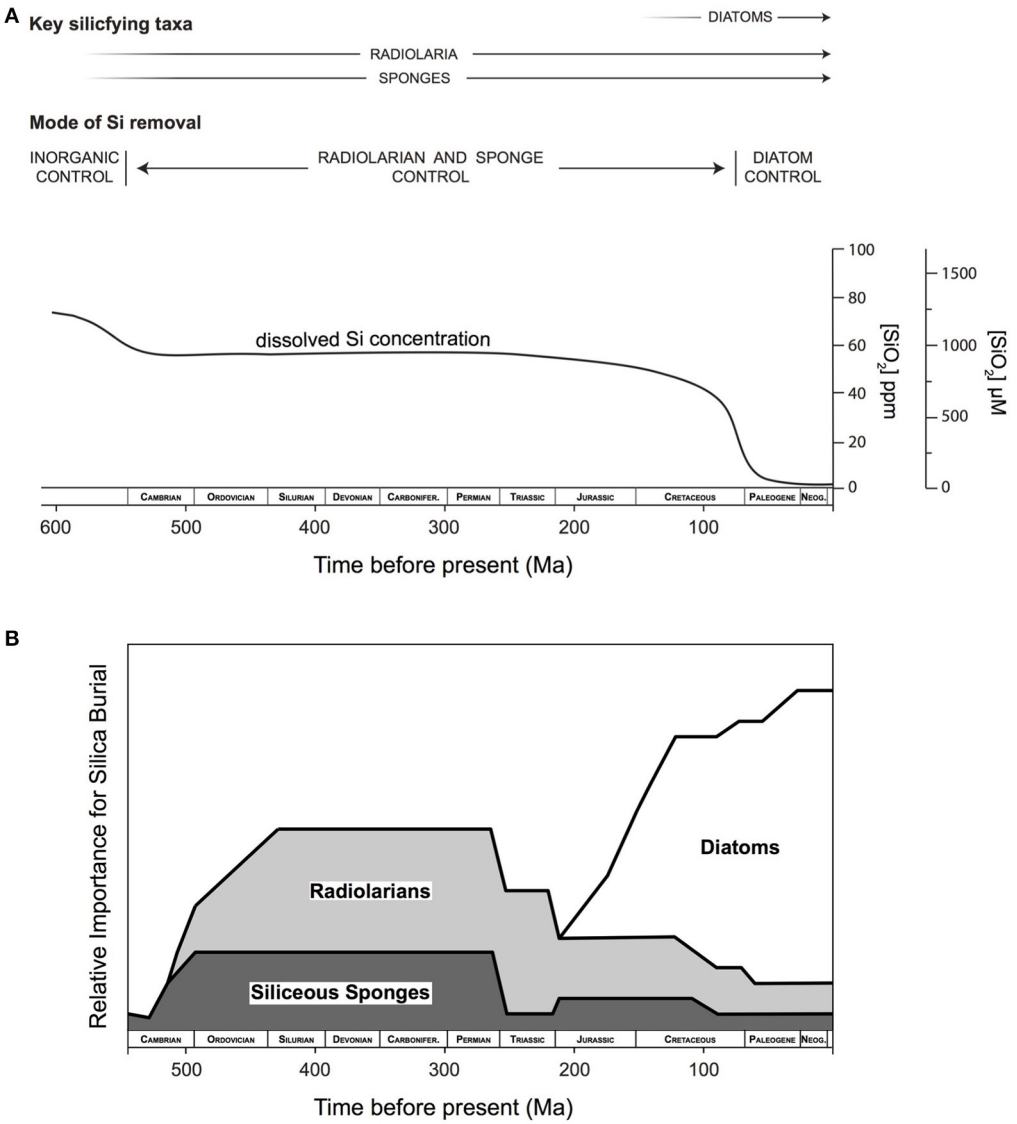

FIGURE 1 | The evolution of the oceanic Si cycle in the geologic record from the latest Precambrian to the present envisioned by Siever (1991). **(A)** In the absence of biosilicifiers dissolved Si (DSi) concentrations were determined by inorganic reactions with respect to amorphous silica solubility and/or with other Si-bearing phases. With the appearance of sponges and radiolarians in the early Phanerozoic biomineralization caused drawdown of DSi concentrations. However, DSi was rapidly reduced with the evolution and diversification of diatoms during the Cenozoic time period. From Schneider and Boston (1991) by permission of The MIT Press. **(B)** Qualitative interpretation of the relative role of the importance of radiolarians, sponges and diatoms present in the fossil record though geologic time (Redrawn from Kidder and Erwin, 2001). Reproduced with permission ©2001, The University of Chicago Press.

concentrations related to the appearance of various Si biomineralizing organisms starting with sponges and radiolarians in the early Phanerozic, followed by the radiation of diatoms in the Cenozoic (**Figure 1B**). In the decades since its publication, this paradigm has guided thinking on the Si cycle and on the evolution and distribution of Si biomineralizing organisms.

Part of the reason for the longevity of this simple view is that many features of the global Si cycle through geologic time remain poorly characterized and understood. For example, we do not have a good understanding of changes in the inputs of DSi to the ocean from continental weathering, although the flux of DSi solubilized from continental rocks has inevitably varied appreciably over Earth history in response to changing climatic or tectonic boundary conditions. One example of this is orogeny, which plays a critical role in controlling weathering intensity and secondary mineral formation, thereby influencing both the total DSi flux and its isotopic composition (Frings et al., 2015, 2016; Pogge von Strandmann and Hendersen, 2015). Thus while it is tempting to interpret changes in the quality or

quantity of siliceous marine sediments in the geologic record in terms of the prevailing DSi concentrations in the ocean, or evolutionary breakthroughs in biomineralization, there may also be a climatic or tectonic component to the signal, independent of biological cycling. Altogether, we lack a comprehensive understanding of the evolution of the Si cycle through geologic time.

At the same time, our understanding of the biological components of the Si cycle has grown enormously since the classic work of Siever, Maliva and co-workers. We appreciate the ability of organisms to pump DSi across membranes (Hildebrand, 2000) and how sequestration of Si by biomineralizing organisms influences the availability of DSi in aquatic ecosystems. We also have a great appreciation of the ecological roles of Si biomineralizers and their participation in other biogeochemical cycles (Van Cappellen, 2003). Study of Si cycling through ecologically important biomineralizing organisms in both aquatic (Knoll, 2003) and terrestrial environments (Trembath-Reichert et al., 2015) has identified and quantified many rates, reservoirs, and processes whose development, expansion, and variation over space and time has added complexity to not just the Si cycle but to ecosystems and the biogeochemical cycles intertwined with the Si cycle.

This is not just relevant to the Phanerozoic, when Si biomineralization irrefutably exists. Although earlier fossil evidence for silicifying organisms is scarce, and often controversial (Porter and Knoll, 2000; Sperling et al., 2010; Antcliffe et al., 2014; Chang et al., 2017), study of the evolutionary history of Si transporters used in biosilicification indicates a remarkably early appearance of transmembrane Si transport in eukaryotes. This challenges the hypothesis that the Precambrian oceans were controlled only by inorganic reactions. Instead, we suggest that oceanic DSi concentrations have both influenced and been influenced by the appearance and diversification of the Silicon Transporter (SIT) gene family roughly 2 billion years before the Phanerozoic (Marron et al., 2016).

In our analysis here, based on advances from fields ranging from biogeochemistry (Baines et al., 2012; Frings et al., 2016) to geogenomics (Baker et al., 2014; Marron et al., 2016), we assess our state of knowledge of the global Si cycle emphasizing the substantial advances that have emerged in the past quarter of a century. We will explore the possible levels of DSi in the oceans over geologic time based on evidence from the geologic record as well as concerning the evolution of the SIT gene family. Our aim with this assessment of the potential for biosilicification over geologic time is to help establish a basis for future research directions.

BIOGEOCHEMISTRY OF SILICA IN THE OCEANS

Two reasons for studying the Si cycle are commonly put forward. First, the process of the chemical weathering of silicate minerals is a primary drawdown mechanism of atmospheric CO_2 and is a key process in the geological C cycle (Walker et al., 1981). Therefore, understanding the global Si cycle can provide insight to the functioning of the weathering thermostat (Pogge von Strandmann et al., 2017). Second, DSi is a required nutrient for many organisms, both aquatic (Bowler et al., in review) and terrestrial (Conley and Carey, 2015). The availability of DSi in aquatic ecosystems controls the amount of diatom primary productivity, which today account for 40% of ocean primary productivity (Tréguer and De La Rocha, 2013).

Key aspects of the modern oceanic Si cycle have been explored to quantify the processes, sources, reservoirs, and sinks in the Si cycle (Tréguer and De La Rocha, 2013; Frings et al., 2016). The primary Si source is low-temperature chemical weathering of silicates in the continental crust (West et al., 2005; Misra and Froelich, 2012; Pogge von Strandmann and Hendersen, 2015), a process mediated in no small part by biological activity (Moulton and Berner, 1988). Other Si sources include high or low temperature alteration of ocean crust (McKenzie et al., 2016), and the dissolution of glacial (Hawkings et al., 2017), riverine, or aeolian particulates containing Si (Frings et al., 2014). The sources enter the ocean from rivers, meltwaters, groundwaters, as hydrothermal fluids and from the atmosphere (Tréguer and De La Rocha, 2013). The sinks include biosilicification and burial (Knoll, 2003) and the authigenesis of clay minerals (Mackenzie et al., 1967; Rahman et al., 2016).

Simple box models have been commonly used to provide insight into the long-term marine Si cycle (De La Rocha and Bickle, 2005; Yool and Tyrrell, 2005; Frings et al., 2016). For periods of time longer than the oceanic turnover time of DSi (ca. 10,000 years), global biosiliceous production is regulated by both the sources and the sinks of Si to the oceans. One of the key regulatory mechanisms is the dependence of particulate amorphous Si dissolution rates on ambient DSi concentrations, e.g.,

$$R = k \cdot (1 - DSi_{obs}/DSi_{sat}) \quad (1)$$

where R is the rate of dissolution and k is a rate constant, both in units of inverse time. k depends on a variety of factors including the specific surface area of the particle, its aluminum content, and ambient pressure, pH and temperature (Van Cappellen et al., 2002). DSi_{sat} is the apparent solubility and DSi_{obs} is the ambient DSi concentration. When DSi concentrations are high, such as hypothesized for the Phanerozoic (Siever, 1992) the rate of dissolution of particulate amorphous Si is slow and the preservation efficiency is thus enhanced. This is also due to the build-up of DSi in pore waters that enhances the preservation and ultimate burial of BSi. Conversely, when the oceans are depleted of DSi the larger difference between saturation and ambient concentration drives the dissolution of particulate amorphous Si.

Several other important factors influence the preservation of BSi in different geological settings. First, bacteria-mediated degradation of the organic matrix covering biomineralized cells enhances rates of BSi dissolution (Bidle and Azam, 1999), an effect which is greater in warmer waters both due to higher bacterial activity and by the more rapid dissolution of the BSi thus exposed (Bidle et al., 2002). Secondly, during periods when hypoxia and anoxia are prevalent there are fewer benthic organisms to enhance dissolution rates by consuming organic material and disturbing the sediments. The lack of benthic organisms and especially of bioturbation leads to greater

preservation of organic matter (Jessen et al., 2017) and BSi. Finally, the dissolution rates of sponge spicules (Bertolino et al., 2017), which are large, smooth and have low surface area (Uriz, 2006), are conspicuously slower (and sponge spicules are thus more easily preserved) than diatoms or radiolarians, which are riddled with pores, and can be amoured with spines.

CHANGING SI BIOGEOCHEMISTRY IN THE PRECAMBRIAN OCEANS

Siever (1992) postulated that for the early period in the geologic history of the Earth, the oceanic Si cycle must be thought of as one primarily controlled by abiotic, inorganic reactions. The diagenetic production of chert in marine environments was widespread during the Precambrian (Maliva et al., 1989, 2005; Siever, 1992; Konhauser et al., 2007) and Siever (1992) suggested that DSi in the Precambrian ocean was close to saturation with respect to amorphous Si, which would imply DSi concentrations in the range of 1,250–2,200 μM (Gunnarsson and Arnórsson, 2000). However, recent work has highlighted the role of different Si-bearing phases in controlling oceanic DSi concentrations (e.g., Fischer and Knoll, 2009; Zheng et al., 2016). Essentially, the problem lies in determining which Si phase(s) that may have occurred in the ancient ocean were governing the activity of DSi. This is a complex function of mineral thermodynamics, precipitation kinetics and ocean chemistry.

During much of the Archean, and more sporadically in the Proterozoic, thinly bedded or laminated sedimentary rocks containing on average 30% of iron and 40% or more of Si (Klein, 2005) were formed in marine basins in stratified water columns. These banded iron formations (BIFs) were mostly deposited prior to the initial rise of atmospheric oxygen at ∼2.45 Ga (Kump, 2008) when the ocean was anoxic and rich in dissolved iron. Dissolved ferrous iron, supplied from mid-ocean ridges and hydrothermal vents, was oxidized by various processes to ferric iron and deposited in association with Si in BIFs.

A number of mechanisms have been proposed to account for the massive deposition of Fe- and Si-rich sediments throughout much of the Precambrian and most of them do not involve biology (see Fischer and Knoll, 2009). However, oxidation of iron by organisms, such as cyanobacteria, in the water column may have played a key role in the formation of some of the BIFs (Rasmussen et al., 2015). Once formed, this biologically oxidized iron would have efficiently scavenged DSi from the water around it (Yee et al., 2003) and settled to the seabed. Indeed, recent studies have highlighted the importance of amorphous Fe–Si gels in the Precambrian Si cycle (Fischer and Knoll, 2009; Zheng et al., 2016). When ferrous iron is oxidized by anoxygenic photosynthesis (e.g., Chi Fru et al., 2013) or by photo-oxidation (e.g., Braterman et al., 1983) DSi readily adsorbs to the ferric hydroxide surface leading to the formation of particles, e.g., amorphous Fe(III)–Si gels, that sink to the sediments from the surface ocean along with organic matter (Fischer and Knoll, 2009).

If DSi concentrations in Precambrian seawater were determined only by the solubility of amorphous Si, as well as by sorption to minerals, oceanic DSi concentrations would have ranged between 1,000 and 2,000 μM (Siever, 1992; Maliva et al., 2005; Konhauser et al., 2007). By contrast, Si solubility for Fe(III)–Si gels varies between 500 and 1,500 μM at 20°C as a function of the Fe/Si ratio of the gel (Zheng et al., 2016), significantly lower than that of pure amorphous Si (1,860 μM) in water (Gunnarsson and Arnórsson, 2000). Thus Precambrian seawater DSi concentrations in surface waters were likely considerably lower than previous estimates.

Because the solubility of Fe(III)–Si gel varies with the Fe/Si ratio in the water column, any temporal changes in aqueous Fe contents in the Precambrian oceans, as might occur due to changes in hydrothermal inputs or concentrations of oxygen, may have also had an important impact on DSi concentrations in Precambrian seawater as well as other elements, notably other trace metals, such as P, As, Fe, Zn, and Cu (Rickaby, 2015; Chi Fru et al., 2016).

Changing Fe and Si balances in the Archean and Proterozoic oceans, reflecting changes in Si solubility driven by aqueous Fe(II) levels, may help explain the secular trend in Si isotope records (δ^{30}Si) in cherts and BIFs deposited during the Precambrian (**Figure 2**) (Reddy et al., 2016). Though the data are noisy, Precambrian cherts record δ^{30}Si of ∼0‰ in the Archean, rising to ∼2‰ in the Mesoproterozoic—with some isolated individual values of >4‰—before declining to Archean values in the late Neoproterozoic/early Phanerozoic. This long-term pattern has been noted before (e.g., Robert and Chaussidon, 2006; Chakrabarti et al., 2012; Chakrabarti, 2015) but remains enigmatic. Given that the BIF and chert δ^{30}Si record is one of the few windows to Precambrian Si cycling, understanding its drivers should be a priority. Robert and Chaussidon (2006) interpret the data as variable fractions of ocean Si removed by hydrothermal silificication, while Chakrabarti et al. (2012) favor a combination of different processes acting in concert.

The constraint of mass-balance in the Si cycle is a useful place to start—even for an ocean saturated with respect to Si, the residence time of Si would be ca. 200,000 years, assuming that the inputs were not drastically different to present. This means the weighted mean of the isotopic composition of the outputs must match the inputs over timescales longer than this. The Archean data (**Figure 2B**) thus have a straightforward interpretation: BIFs have low δ^{30}Si, perhaps accentuated by the relatively large and negative fractionation between DSi and Fe-Si gels (Δ^{30}Si = −3.2 to −2.3‰ at 23°C, depending on the Fe species present; Zheng et al., 2016). This would act to push the residual seawater toward higher δ^{30}Si, so the peritidal, early diagenetic Si deposits that eventually became cherts also have higher δ^{30}Si, and the two outputs together bracket ca. −1.5 to +1‰, a range which includes reasonable values for the weighted average of the inputs. Yet the situation in the Meso- and Neoproterozoic is not so straightforward; chert δ^{30}Si is higher, yet BIF deposition (providing the necessary complementary low δ^{30}Si sink) largely ceases after the Great Oxidation Event (GOE) at 2.45 Ga (Fischer and Knoll, 2009). This requires the presence of another, low δ^{30}Si Si sink in the later Proterozoic. Could such a sink be related to cyanobacteria shuttling Si to the deep ocean?

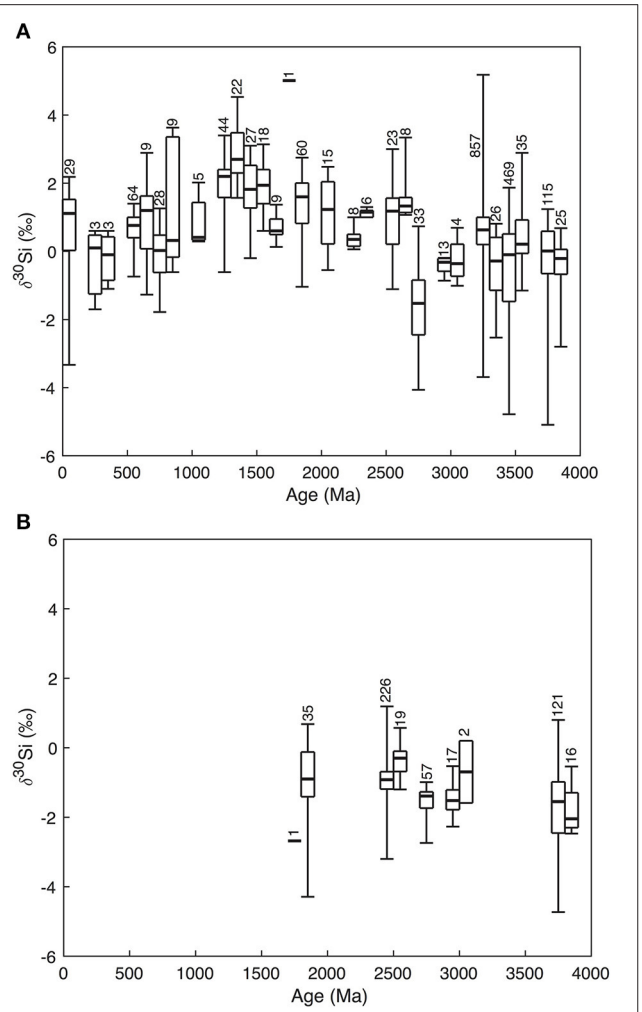

FIGURE 2 | Variations of δ^{30}Si in cherts **(A)** and BIFs **(B)** with geological age. The data are clustered into 100 My bins. Numbers represent the amount of individual datapoints used in the whisker boxes. Data from André et al. (2006), Robert and Chaussidon (2006), van den Boorn et al. (2007, 2010), Steinhoefel et al. (2009, 2010), Abraham et al. (2011), Heck et al. (2011), Chakrabarti et al. (2012), Delvigne (2012), Marin-Carbonne et al. (2014), Hu et al. (2013), Ramseyer et al. (2013), Geilert et al. (2014), Li et al. (2014), Brengman (2015), Stefurak et al. (2015), Delvigne et al. (2012), Wen et al. (2016), and Ding et al. (2017).

Recently, Ding et al. (2017) reported δ^{30}Si data for cherts from early and middle Proterozoic carbonate rocks and proposed that there was a drastic decrease in oceanic DSi concentrations and an increase in δ^{30}Si due to biological activity and the formation of stromatolites. The microbial role in hot spring silicification of stromatolites is well established and plays an important templating role for Si deposition (Konhauser et al., 2004), although they have been shown to contribute only marginally to the magnitude of silicification.

Another intriguing wrinkle to the Precambrian Si cycle has to do with cyanobacteria. Synchrotron XRF microscopy of natural and cultured individual cells of the modern marine photosynthetic picocyanobacteria *Synechococcus*, suggests that they accumulate Si at Si:P levels approaching that of diatoms (Baines et al., 2012). Further, decomposition of *Synechococcus* has been shown to produce extracellular polymeric substances (EPS) that themselves drive the production of minuscule "microblebs" of silica that, by adding dense ballast to aggregates, may enhance the export of picoplankton-derived material from the euphotic zone (Tang et al., 2014). These findings were initially controversial, especially as they have potentially significant importance to both carbon and Si cycling.

During the past few decades significant efforts have been made to infer the age of major evolutionary events along the tree of life using fossil-calibrated molecular clock-based methods (Eme et al., 2014). Molecular clocks use the mutation rate of biomolecules to deduce the time in prehistory when two or more life forms diverged. The main problems with molecular clocks include differences in fossil-based calibration points, differences in molecular clock rate models, differences in amino acid substitution rates among various parts of the dataset and uncertainty in the phylogenetic tree, thus limiting the precision that can be achieved in estimates of ancient molecular timescales (dos Reis et al., 2015). Cyanobacteria are at least 2.3–3 Ga old from molecular clock studies (Dvorák et al., 2014; Sanchez-Baracaldo, 2015), whereas fossil evidence (stromatolites, microfossils, carbon isotopes, biomarkers, signs of oxygen) from Greenland, Australia and elsewhere have raised the possibility of cyanobacteria older than 3 Gy, although these claims are disputed (Schirrmeister et al., 2016).

The major lineage of planktonic marine *Synechococcus* evolved approximately 650–600 Ma, based on molecular clock analyses (Sanchez-Baracaldo, 2015; Sanchez-Baracaldoa et al., 2017), with alternative clock analyses based on large genomic datasets suggesting an origin ∼1.5 Ga (Dvorák et al., 2014). Today this cyanobacterial group accounts for 25% of oceanic net primary production (Flombaum et al., 2013). Marron et al. (2016) has observed SIT-like (SIT-L) genes in two strains of *Synechococcus*. These Si transporters probably arose initially to prevent intracellular Si toxicity in the high DSi Precambrian oceans (Marron et al., 2016), meaning that they were used to transport Si out of the cell, or to sites where Si could be safely accumulated and sequestered. This would have been critical for survival, for in the absence of such a Si homeostasis mechanisms DSi could diffuse into cells from the surrounding DSi saturated seawater and reach concentrations where it would precipitate freely within the cytoplasm, interfering with cellular processes and disabling the functioning of the cell (Marron et al., 2016). Si transporting proteins can also have the ability to move other metalloids such as Ge (Durak et al., 2016) and As (Ma et al., 2008) across the cell membrane. Therefore Precambrian organisms, long before the advent of silica biomineralization, may have possessed and utilized Si transporting proteins as a detoxification mechanism particularly necessary in the high DSi environments at this time.

The reduced requirement for Si homeostasis in the modern low DSi oceans is postulated to be the reason for the widespread absence of SIT-Ls in most bacteria. However, some *Synechococcus* still possess SIT-Ls and accumulate Si suggests an important role

for Si within these cells (Baines et al., 2012; Ohnemus et al., 2016). Indeed, the water column inventory of Si in *Synechococcus* can exceed that of diatoms in some cases, although in today's DSi depleted oceans it is believed that most of the nanoparticles produced by *Synechococcus* are recycled within surface waters (Baines et al., 2012). However, BSi-like material deposited on fast settling particles containing extracellular polymeric substances associated with decomposing picophytoplankton (**Figure 3**) has been shown to be a relevant source of sinking particulate amorphous Si and could account for as much as 43% of the C export production at the Bermuda Time Series station (Tang et al., 2014).

These discoveries regarding *Synechococcus* support the idea that Fe–Si nanoparticles were important in the genesis of the banded iron formations (Rasmussen et al., 2015). Stefurak et al. (2014) presented evidence that many Archean cherts were deposited predominately as primary Si grains that precipitated within oceanic waters. However, the irregular size and shape of the Si granules in cherts show that aggregates are compacted and typically Si cemented (Stefurak et al., 2014). Our hypothesis is that nanoparticles produced by *Synechococcus*-like bacteria, along with those inorganically formed Fe-Si nanoparticles, were deposited and accumulated in Precambrian sediments and formed the origin of the Si grains in Archean cherts (Stefurak et al., 2014).

What follows from this hypothesis is that some form of biologically-mediated silica production by prokaryotes, if not *bona fide* intracellularly controlled and intentional Si biomineralization, likely occurred in the Precambrian ocean and participated in the removal of DSi from the water column. Calculation of pools and fluxes of Si nanoparticles produced by *Synechococcus* need to be made to assess the potential contribution to the oceanic Si cycle first for modern assemblages and then through geologic time.

Geogenomic studies have identified that gene families of active Si transporters (the SIT/SIT-L and Lsi2-like transporters) are present in multiple eukaryotic supergroups (Marron et al., 2016). Furthermore, phylogenetic analyses of these genes suggest that they have an origin in the Precambrian, possibly in the last common ancestor of all eukaryotes, an organism which is estimated to have lived approximately 1.7 Ga (Parfrey et al., 2011). Certainly there is good evidence from the available sequence data that Si transporters were present at the origin of major eukaryotic groups such as metazoans, haptophytes and ochrophyte stramenopiles, which have all been placed as occurring in the Precambrian (Neoproterozoic) by molecular clock analyses (Brown and Sorhannus, 2010; Parfrey et al., 2011).

The phylogenetic distribution of SITs, SIT-Ls, and Lsi2-like genes identified from modern eukaryotes indicates that widespread, independent losses of some or all of these transporters occurred independently in multiple lineages (Marron et al., 2016). This is exemplified by the distribution of Si transporters in the metazoans and their sister group, the choanoflagellates (Marron et al., 2013). SIT-Ls were identified from all three of the main bilaterian groups: lophotrochozoans (polychaete annelid worms), ecdysozoans (copepods) and deuterostomes (tunicates). The branching relationships of these metazoan SIT-Ls reflects the evolutionary relationships between the bilaterian groups, supporting the hypothesis that SIT-Ls were present in their last common ancestor, with gene loss events explaining their patchy distribution (Dunn et al., 2008).

Lsi2-like transporter genes, on the other hand, are found in siliceous choanoflagellates, siliceous sponges and silicifying lophotrochozoans (brachiopods, limpets and polychaete annelid worms). Once again, the gene tree mirrors the phylogenetic relationships, with the Lsi2-like sequences from siliceous choanoflagellates having sister-group relationships to the metazoan genes, and within that siliceous sponges and lophotrochozoans each forming two distinct clades (Marron et al., 2016). This points toward the last common ancestor of choanoflagellates and metazoans possessing an Lsi2-like gene, but with it being lost in the non-siliceous choanoflagellates, non-siliceous sponges and in many bilaterian lineages.

This restricts the timing of the origin of these Si transporters to *at least* before the evolution of the metazoans, i.e., before the earliest animal fossils appear in the Ediacaran. Similarly, we can restrict the widespread loss of SIT-L and Lsi2-like genes in the metazoans until after the divergence of the three main bilaterian clades, an event dated by molecular clock analyses as occurring 688–615 Ma (dos Reis et al., 2015; Cunningham et al., 2017). There exists the potential for metazoans, in addition to other eukaryotes, to have biological interactions with DSi at this time and to have played a role in the Precambrian Si cycle.

The question as to the extent of this interaction remains open. Fossil remains of biomineralization are limited until the late Neoproterozoic (e.g., the Ediacaran calcifying animals *Cloudinia* and *Namacalathus*, Cunningham et al., 2017). Furthermore, confirmed fossil evidence of Precambrian Si biomineralization by eukaryotes is scant: microfossils proposed to represent siliceous testate amoebae date to ∼740 Ma (Porter and Knoll, 2000), while fossil siliceous sponge spicules in the Precambrian remain controversial (Antcliffe et al., 2014; Chang et al., 2017). It is possible that biosilicification did occur in the Ediacaran oceans, and that there exists a long missing record of (for example) siliceous sponge spicules from that time that has been long lost to the ravages of geologic time (Sperling et al., 2010). Alternatively, it could be that eukaryotic biosilicification evolved convergently in different groups in the late Neoproterozoic, with several different sponge groups, but importantly also various protistan eukaryote taxa, independently utilizing DSi to construct skeletal elements and other structures. This hypothesis has some support from molecular biology, with some components of the biosilicification machinery (e.g., Si transporters for DSi uptake) having an ancient origin but other components (e.g., using polyamines for Si precipitation, use of collagen or chitin as scaffold molecules) apparently being independently recruited in different eukaryotic groups (Marron et al., 2016 and references therein).

These two theories notwithstanding, the massive proliferation of biomineralization and BSi in the fossil record at the end of the Proterozoic and into the early Palaeozoic saw large reductions in DSi, as evidenced by changes in the loci of chert precipitation in the sedimentary record (see below). The implication is that

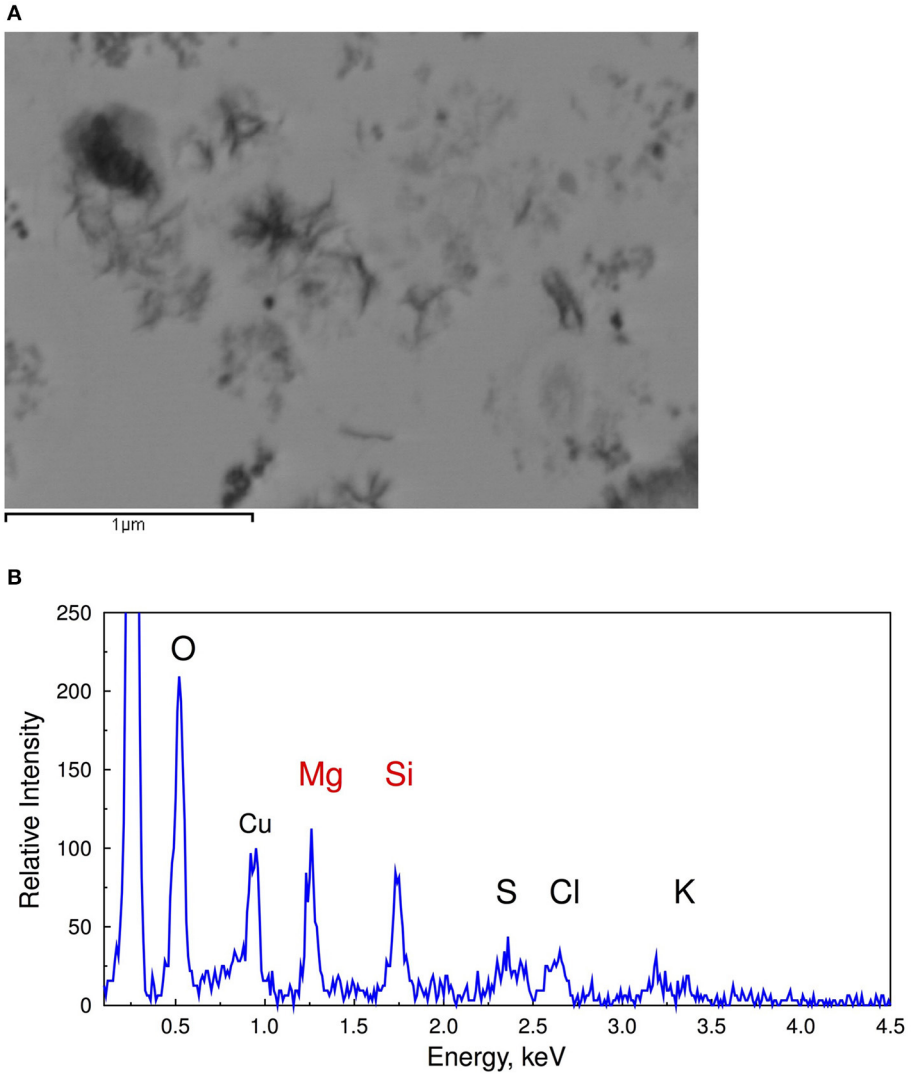

FIGURE 3 | Scanning transmission electron microscope images **(A)** and EDS spectra of decomposing *Synechococcus* cells **(B)** collected during dark incubation of cells after 15 days showing the association of silica with extracellular polymeric substance during the degradation of cyanobacterial cells (From Tang et al., 2014). Reprinted by permission from Macmillan Publishers Ltd: Tang et al. (2014). Copyright © 2014.

this removed the selective pressure for possessing a system for Si homeostasis and detoxification, causing the widespread, independent losses of Si transporters (SITs, SIT-Ls, and Lsi2-like transporters) across multiple different eukaryotic lineages (Marron et al., 2016). Only organisms that developed a metabolic requirement for DSi, for example for use as a biomineral, retained these transporters as a mechanism for DSi uptake from the external environment. In this way, DSi concentrations in the ocean came under more direct biological influence into the Phanerozoic.

In summary, the evidence presented suggests that biological interaction with Si, and possibly some forms of biosilicification, was present in the Precambrian oceans. If this could have permitted the shuttling of Si from the surface oceans then levels of DSi in parts of the surface oceans could have been as low as 500 µM (Zheng et al., 2016) during periods when BIFs were deposited (Fischer and Knoll, 2009), although it is likely the deep water DSi was close to saturated conditions. Bottom water DSi saturation would also increase the preservation potential in sediments of particulate Si formed by either gels or by nanoparticles by *Synechococcus*. However, when the widespread deposition of BIFs more or less ended with the appearance of an ocean containing oxygen then the Fe-Si gel deposition mechanism likely disappeared as well. Finally, the transition from bacterial to eukaryotic marine primary productivity in the Neoproterozoic was one of the most profound ecological revolutions in the Earth's history (Brocks et al., 2017), creating food webs and reorganizing the distribution of carbon and nutrients in the water column, increasing energy flow to higher trophic levels (Knoll, 2017).

BIOSILICIFICATION IN THE PALEOZOIC OCEANS

The consensus is that throughout the Phanerozoic, Si deposition has largely been mediated by biology (Siever, 1992). Ocean geochemistry underwent major upheavals around the Precambrian/Cambrian boundary (Brennan et al., 2004; Cui et al., 2016) and into the Palaeozoic. A concomitant biotic upheaval at this time was the appearance of biomineralized hard parts of materials like calcium carbonate, calcium phosphate, and silica. The resulting evolutionary arms race led to a proliferation of skeletonized organisms, including siliceous radiolarians and sponges (Cohen, 2005; Knoll and Kotrc, 2015). The resolution of the conflict (Smith and Szathmáry, 1995) produced a proliferation of non-DSi users and some highly efficient DSi users leading to the extinction of inefficient DSi users. The initiation of a sedimentary flux of BSi with subsequent preservation in sediments would have continued the decrease in oceanic DSi concentrations, as evidenced by the lack of Phanerozoic abiotic cherts outside of unusual environments like hydrothermal waters (Maliva et al., 2005). Siever (1991) estimated that DSi concentrations at the start of the Phanerozoic were on the order of 1,000 μM, which is already depleted relative to amorphous Si solubility.

Racki and Cordey (2000) used concepts from punctuated equilibrium and proposed that all major reorganizations of marine biosilicfiers lead to stepdown decreases in DSi levels through geologic time. They proposed that the first major changes in oceanic DSi concentrations occurred much earlier in the Phanerozoic than postulated by Siever (1991) beginning at the Permian-Triassic boundary. Thereafter, a series of major reorganizations in biota that biosilicify occurred that induced rapid decreases in DSi especially with the evolution of diatoms (Racki and Cordey, 2000).

Establishing the extent and timing of the changes in the silica cycle due to evolutionary and paleo-ecology shifts in silica secreting biota is, however, a task that needs more work. In a systematic review of the literature Schubert et al. (1997) determined that a large bias exists in the early literature because poorly preserved specimens have been neglected as taxonomists required well-preserved material to do their work, skewing microfossil-based attempts at reconstructing the Si cycle. Kidder and Erwin (2001) made qualitative estimates of the relative importance of Si burial through the Phanerozoic and assumed that plankton would be more effective than benthic sponges at removing DSi from the ocean. They hypothesized that once radiolarians arrived on the scene, their relative contribution to BSi production quickly dwarfed that of siliceous sponges. They further hypothesized that diatoms have dominated the ocean Si cycle since the late Jurassic (**Figure 1B**). But in truth, the extent to which these putative changes in sponge and radiolarian abundance/distribution changed oceanic DSi concentrations (Schubert et al., 1997; Racki and Cordey, 2000; Kidder and Erwin, 2001), and the extent to which they were themselves influenced by reduced DSi availability are not really known.

One of the lines of evidence supporting a decline in the ocean DSi inventory in the early Phanerozoic is a change in the sedimentary facies associated with sponges in the geological record. Kidder and Tomescu (2016) derived a mid-Ordovician retreat in sponges from lagoonal depositional environments toward deeper shelf settings. The interpretation is of a radiolarian driven DSi depletion of the surface ocean. The link between sponge distributions and DSi stems from the implicit assumption that siliceous sponges are unable to thrive at low DSi (e.g., Maldonado et al., 1999; Ritterbush et al., 2015), although siliceous sponge reefs in the modern oceans are still forming in some areas despite the relatively low DSi concentrations (10–40 μM) (Uriz, 2006; Chu and Leys, 2010; Maldonado et al., 2015). The modern day global distribution of sponges suggests that sponges are adapted to a great range of DSi conditions and the presence of sponges in the stratigraphic record must be treated cautiously (Alvarez et al., 2017).

Si biomineralization has been an important process for land plants over the course of their >400 My evolutionary history (Trembath-Reichert et al., 2015). On land the uptake of DSi and deposition by many vascular plants provides ecological, physiological, or structural benefits (Epstein, 1999), creating an active terrestrial Si cycle (Conley, 2002). The origin of terrestrial plants and the spread of rooted vascular plants to upland areas during the Devonian Period most likely had an important effect on many Earth processes (Lenton et al., 2012; though see Edwards et al., 2015). The activities of plants should increase the efficiency of continental weathering (Berner, 1997) through stimulated dissolution of bedrock (Schwartzman and Volk, 1989), thus enhancing the removal of atmospheric CO_2 (Berner, 1990) until a new steady state is reached in weathering. A wide range of geochemical carbon models assume weathering rates to be proportional to CO_2 fertilization of plant productivity, which acts as a key component of the silicate-weathering feedback (Pagani et al., 2009; Beerling et al., 2012). Similarly, plant functional trait evolution has been linked to stepwise changes in the long-term carbon cycle (e.g., Banwart et al., 2009).

The archaeplastid supergroup, to which land plants belong, is notable amongst eukaryotic supergroups for the lack of SIT or SIT-L transporters (Marron et al., 2016), despite widespread sequence data and the presence of several silicified taxa (such as horsetails, grasses, and the red alga *Porphyra purpurea*). Instead, Si uptake by land plants is performed by a combination of passive transmembrane channels and active Si effluxers (Ma and Yamaji, 2015). The active transporter is termed Lsi2 (*low-silicon 2*) (Ma et al., 2007). Lsi2-type genes are apparently ubiquitous in land plants, even in lineages which are not extensively silicified or which apparently lack Si-permeable transmembrane channels (Hodson et al., 2005; Trembath-Reichert et al., 2015; Marron et al., 2016). Importantly, Lsi2-type genes are found in the transcriptomes of both basal land plants and in the related charophyte green algae (see **Table 1**), while such sequences were not detected in more distantly related chlorophyte green algae (Marron et al., 2016). This strongly suggests that active Si transport is an ancient feature, and that Lsi2-type transporters predate the recruitment of NIPII-class transmembrane proteins

TABLE 1 | Examples of Lsi2-type active Si transporters from across the Charophycae.

Group	Sub-group	Species	Sequence ID	References
Charophyte algae	Klebsormidales	*Klebsormidium flaccidum*	kfl00337_0090	Hori and co-authors, 2014
	Zygnematales	*Spirogyra pratensis*	GBSM01008107.1 comp6609_c0_seq2	Van de Poel et al., 2016
Embryophytes (land plants)	Liverworts	*Marchantia polymorpha*	Mapoly0153s0006.1	Sequence retrieved from http://marchantia.info
	Mosses	*Physcomitrella patens*	XP_001772790	EMBL/Genbank database
	Lycopods	*Selaginella moellendorffii*	XP_002984369.1	EMBL/Genbank database
	Ferns	*Acrostichum aureum*	GEEI01039090	EMBL/Genbank database
	Horsetails	*Equisetum giganteum*	cds.Locus_1866_Transcript_1_2_m.4165	Vanneste et al., 2015
	"Gymnosperms"	*Pinus monticola*	GBQX01048264.1	EMBL/Genbank database
	Angiosperms (monocots)	*Oryza sativa*	ADH94038.1	EMBL/Genbank database
	Angiosperms (dicots)	*Cucumis sativus*	APT69295	EMBL/Genbank database

This demonstrates that Lsi2-like genes are present across all major living land plant groups is further evidence for an important role of Si in embryophytes biology, irrespective of the degree of silicification (Hodson et al., 2005). The fact that the Lsi2 gene family is also present in members of the charophyte green algae, a sister lineage of the embryophytes, and in basal land plant groups (liverworts and mosses) means that the earliest land plants also possessed such transporters.

as passive Si channels (Trembath-Reichert et al., 2015). While Si may play a wider role in land plant metabolism (e.g., Markovich et al., 2017), the primary function of active Si transport is presumably to enhance DSi uptake rates into the transpiration stream and toward sites of BSi precipitation. It is therefore reasonable to assume that even the earliest terrestrial plants could have played a role in the global Si cycle.

The feedbacks through enhanced weathering would also alter the flux of DSi from the continents and thus potentially alter oceanic DSi availability (Conley and Carey, 2015). A key issue to resolve is the extent to which global average river inputs of DSi could have changed due to plant-stimulated weathering (Moulton and Berner, 1988) for a given atmospheric concentration of pCO_2. Although the enhancement of silicate weathering by plants is expected to transiently increase the supply of DSi to the oceans, available data do not show an increase in numbers of chert deposits with the rise of plants (Kidder and Erwin, 2001). What has not been previously considered in the effect of plants on weathering, is the evolution of plants that accumulate phytolith BSi (Hodson et al., 2005), also allowing for more BSi accumulation on the continents (Struyf and Conley, 2012). However, phytolith BSi accumulated in soils on land is not an infinite sink, with the modern inventory comprising ca. 8.25×10^{15} mol Si (Laruelle et al., 2009), and is dwarfed by the magnitude of DSi inventory in the oceans, with the total modern day ocean Si inventory estimated to be 112×10^{15} mol (Gouretski and Koltermann, 2004), and was presumably an even smaller fraction than in the Paleozoic-Mesozoic ocean. Quirk et al. (2015) have challenged the suggestion that early land plants significantly enhanced total weathering arguing that the rise of rooted vascular plants and mycorrhizal fungi caused an increase in the production of pedogenic clays retaining Si on the continents, and thus lessening the impact of DSi transport to the global oceans.

Although Kidder and Erwin (2001) argued that there were large-scale changes in radiolarian and sponge abundances during the Paleozoic (**Figure 1B**), Siever (1991) suggested that the geologic record does not support the occurrence of widespread siliceous sediments and thus did not affect DSi in the global oceans (**Figure 1A**). More importantly, Maliva et al. (1989) argue that nodular chert formation predominated in the Paleozoic and was the result of DSi diffusion into sediments from the essentially infinite reservoir in the overlying water because there was insufficient biogenic precipitation. Kidder and Tomescu (2016) suggested that the evolution of the oceanic Si cycle through the early Paleozoic was a dynamic progression of biogeochemical adjustments driven by biological and earth system changes, which changed DSi availability driving the distribution of sponges and radiolarians in the ocean. Based on first principles (Equation 1), early biosilicification by radiolarians and sponges during the Paleozoic and subsequent deposition and burial of BSi should have resulted in global deceases in oceanic DSi availability because of the greater preservation efficiency at high oceanic DSi. Essentially, a small increase in biosiliceous productivity would be expected to have a disproportionate effect on the total DSi inventory. Declines in DSi would occur until the sinks were balanced by the sources (De La Rocha and Bickle, 2005). Our hypothesis is that DSi concentrations were reduced even further from saturating conditions at the start of the Phanerozoic, but biosilicification of sponges and radiolarians reduced DSi concentrations to an even lower level than previously appreciated.

TRANSITION TO AN OCEAN DOMINATED BY BIOSILICIFICATION

The narrative outlined by Siever (1991) envisages a transition, starting around the mid-Cretaceous and ending by the late Paleogene (**Figure 1A**), from a DSi-replete (ca. 1,000 μM) surface ocean, to DSi-depleted conditions broadly similar to the modern day (Maliva et al., 1989; Siever, 1991). This is period of Earth history with the most available data, thanks in large part to the efforts of the ocean drilling community over the past decades. Several lines of evidence are available to guide interpretation of late Mesozoic-Cenozoic Si cycling. The

Mesozoic saw huge changes in marine ecosystems compared to Palaeozoic seas (Knoll and Follows, 2016), including the appearance and radiation of many new phytoplankton groups such as dinoflagellates, diatoms, coccolithophorid haptophytes, and chrysophytes (Knoll, 2003; Katz et al., 2004; Sims et al., 2006). Diatoms, in particular, flourished during the Cenozoic, which has been interpreted to have caused a drawdown of DSi (Racki and Cordey, 2000). Fossil evidence also demonstrates the decline of siliceous sponge reefs in the late Mesozoic (Kidder and Tomescu, 2016). Muttoni and Kent (2007) clearly demonstrate an increase in chert intervals in DSDP and ODP sites during the early Eocene primarily from radiolarian deposition, although modeling and mass-balance principles clearly show that inputs and outputs are generally tightly coupled such that enhanced BSi burial likely reflects changes in DSi inputs (Yool and Tyrrell, 2005). Silicoflagellates (dictyochophyte), diatoms, and radiolarian microfossils (Lazarus et al., 2009; Finkel and Kotrc, 2010; van Tol et al., 2012), all show a trend towards more lightly silicified structures and more efficient DSi use through this phase.

The Cenozoic rise in diatom diversity has long been related to a concurrent decline in radiolarian test silicification (Harper and Knoll, 1975). Gradually decreasing Cenozoic radiolarian test weight suggests that competition for DSi resulted in coevolution between radiolaria and marine diatoms. More sophisticated attempts to answer the question include Lazarus et al. (2009). However, they determined that trends in shell size and silicification are statistically insignificant and are not correlated with each other. They concluded that there is no universal driver changing cell size in Cenozoic marine plankton. Conventionally, diatom diversification describes a steep, monotonic rise (Rabosky and Sorhannus, 2009), a view also questioned due to sampling bias (Lazarus et al., 2014). In low latitudes, increasing Cenozoic export of DSi to deep waters by diatoms and decreasing nutrient upwelling from increased water column stratification have created modern DSi-poor surface waters. Here, radiolarian silicification decreases significantly. The radiolarian decline in silicification could result from either macroevolutionary processes operating above the species level (punctuated equilibria) or anagenetic changes within lineages (Kotrc and Knoll, 2015). This change in the degree of silicification is less apparent at higher latitudes, most likely reflecting an ample supply of DSi via upwelling.

The minimum and maximum sizes of the diatom frustule have expanded in concert with increasing species diversity, although the mean area of the diatom frustule has been highly correlated with oceanic temperature gradients consistent with the hypothesis that climatically induced changes in oceanic mixing have altered nutrient availability in the euphotic zone and driven macroevolutionary shifts in the size of marine pelagic diatoms through the Cenozoic (Finkel et al., 2005). Fossil evidence of diatom biosilicification is present in the geologic record from ca. 190 Ma (Sims et al., 2006), yet molecular clock analyses indicate that diatoms originated closer to the Permian–Triassic boundary 250 Ma (Medlin et al., 1996; Graham and Wilcox, 2000; Sims et al., 2006), and that the diatom stem lineage may have even earlier origins in the mid-Paleozoic (Brown and Sorhannus, 2010).

Various hypotheses have been made as to why the diversification and increase in the global biomass of marine diatoms occurred only during the last 40 My of Earth's history and why diatoms were not successful earlier. Raven and Waite (2004) hypothesize that silicification could have evolved later in the evolutionary history of diatoms and would be an explanation for the lack of diatoms in the fossil record, although this does not agree with the evidence for an ancient evolution of SITs in this lineage (Marron et al., 2016). It may be the case that the ancestral diatoms have been partially silicified with plates rather than complete frustules, similar to the modern Parmales, the sister lineage of diatoms (Yamada et al., 2014). In this scenario the earliest diatoms may simply have gone unrecognized in the fossil record. The rapid rise of diatoms in the Cenozoic has also been attributed to the impact of orogeny on weathering (Misra and Froelich, 2012) with periods of enhanced continental weathering fluxes and increased DSi input to the oceans (Cermeño et al., 2015).

The rapid drawdown of DSi during the Cenozoic by diatoms attests to their competitive ability to efficiently remove DSi to low levels in the water column. Diatoms show a high degree of SIT diversification with an efficient suite of specialized transporters and uptake regimes allowing them to dominate DSi utilization amongst marine silicifiers (Thamatrakoln and Hildebrand, 2008; Durkin et al., 2016; Marron et al., 2016). Diatoms have an obligate requirement for Si to complete their life cycle and so cannot avoid competing for Si (Hildebrand, 2000). This combined with the other advantages unrelated to Si (e.g., nutrient acquisition and storage, light harvesting, bloom formation), must have produced trophic interactions that did not occur in Palaeozoic oceans, making the appearance of diatoms a game changer. Therefore, we hypothesize that diatoms had an impact on oceanic DSi concentrations much earlier in the geological record than previously thought.

Recently, Fontorbe et al. (2016) used δ^{30}Si from sponge spicules and radiolarian tests to derive the first long term empirical reconstruction of ocean DSi concentrations in the North Atlantic during the Paleocene and Eocene. Using a calibrated relationship between spicule δ^{30}Si and sponge Si isotope fractionation (Wille et al., 2010; Hendry and Robinson, 2012), they show that from 60 to 30 Ma DSi concentrations in the North Atlantic were consistently low, meaning that the transition to a low DSi ocean had to have begun prior to the Early Cenozoic (**Figure 4A**). Subsequent cores from the Pacific Ocean, showed (**Figure 4B**) that deep water DSi concentrations were also lower prior to 37 Ma (Fontorbe et al., 2017). The shift in radiolarian δ^{30}Si was interpreted as a consequence of changes in the δ^{30}Si of DSi sourced to the region through changing ocean circulation. The decrease in sponge δ^{30}Si is interpreted as a transition from low DSi concentrations to higher DSi concentrations, most likely related to the shift toward a solely Southern Ocean source of deep-water in the Pacific during the Paleogene consistent with results from ocean circulation tracers including neodymium isotopes and carbon isotopes (Fontorbe et al., 2017). Diatom and spicule δ^{30}Si records from the Southern Ocean are consistent with the establishment of a near modern system, with a proto-Antarctic Circumpolar Current (ACC), a full deep water pathway

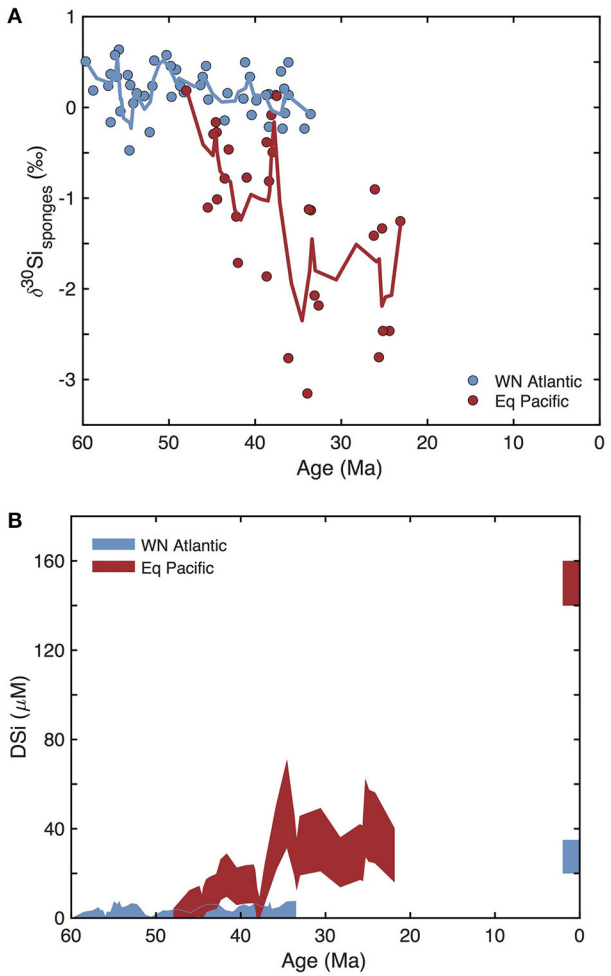

FIGURE 4 | (A) The range of δ^{30}Si of sponges from deep-sea drilling cores (Fontorbe et al., 2016, 2017). **(B)** The range of DSi concentrations in the Western North Atlantic (blue) and in the Equatorial Pacific (red) reconstructed from the δ^{30}Si of sponges and radiolarians from deep-sea drilling cores (Fontorbe et al., 2016, 2017). The blue and red bars for present time represent the modern DSi concentration in the bottom waters of both ocean basins.

through the Tasman Sea and Drake Passage, and associated high-latitude upwelling at the Eocene-Oligocene boundary (Egan et al., 2013). The emerging tools of Si stable isotope tracers (De La Rocha, 2002; Sutton et al., in review) have demonstrated that very low oceanic DSi concentrations may have occurred tens of millions of years before the time period envisioned by Siever (1991) and others for the drawdown of DSi by diatom biosilicification. We hypothesize that if such a global decrease in oceanic DSi concentrations occurred, it must predate 60 Ma and perhaps begin with the appearance of diatoms.

Although diatoms originated in the early Mesozoic (Medlin et al., 1996; Graham and Wilcox, 2000; Sims et al., 2006), peak diversification occurred in the Cenozoic (Rabosky and Sorhannus, 2009). Several rapid evolutionary turnovers in the diatom species composition have been observed at the Paleocene-Eocene boundary, and at the Eocene-Oligocene boundary. Here, we posit that rather than driving the drawdown in surface DSi concentration, the diversification of diatom species observed during the Cenozoic may have instead resulted from several external factors. Firstly, this diversification might have resulted from a change in the global distribution of DSi. The basinal distribution of DSi is dominated by ocean circulation (de Souza et al., 2014) with the AAC playing a key role in the dynamic of ocean circulation and nutrient distribution, most likely since the Eocene-Oligocene boundary around 34 Ma. The upwelling associated with the strong ACC would have promoted the growth of high-latitude diatom populations, which enhanced DSi uptake. Secondly, diatom diversification could have resulted from a change in the DSi delivery from land to ocean via increased transport of weathering products. Based on Li isotopes, Misra and Froelich (2012) argued for increasing weathering rates over the Cenozoic. Recently, this increase in the fluxes of weathering products has been invoked to explain the diatom diversification over the Cenozoic (Cermeño et al., 2015), again, drawing down DSi concentrations to the low levels that we suggest were experienced since the Mesozoic.

OCEANIC DSI DURING THE QUATERNARY

The modern ocean distribution of DSi is primarily controlled by the general ocean circulation and dissolution of BSi formed in the upper water column (de Souza et al., 2014). The general pattern consists of surface waters with low DSi concentrations due to the efficient uptake by diatoms (and to a lesser degree radiolarians, silicoflagellates and other silicifying organisms). Concentrations increase with depth via progressive dissolution of diatom frustules and radiolarian tests precipitated in the upper water column during their sinking (Tréguer and De La Rocha, 2013; Frings et al., 2016). An inter-basinal gradient also exists, related to the overturning circulation. Today, deepwaters formed in the North Atlantic from surface waters are DSi depleted due to the efficient uptake of DSi by diatoms. These newly formed bottom waters get progressively enriched in DSi as they are transported southward toward lower latitudes, ultimately ventilating in the Southern Ocean or the North Pacific. This general circulation pattern results in a bottom water basinal DSi concentration gradient with North Atlantic waters having the lowest levels of DSi (typically 20–30 μM) and the North Pacific waters being the most concentrated (up to 200 μM). In the Southern Ocean, the DSi increases polewards and with depth, as a result of remineralization, the mixing of water masses and the sloping isopycnal gradient resulting from the strong ACC (Pollard et al., 2002). Low utilization of DSi relative to other nutrients by diatoms in the iron-limited waters near the Polar Front, together with strong winter convection, results in the export of waters with high DSi:N (or P) ratios in the Antarctic Intermediate Waters (AAIW) into the Atlantic and the Pacific (Sarmiento et al., 2004).

Global changes in the total supply of DSi to the ocean have likely occurred throughout the Quaternary. Changes in weathering processes, as a result of the waxing and waning of ice-sheets during glacial cycles, and climatically-driven changes

in biological production could shift oceanic DSi over timescales equivalent to the residence time of Si in the ocean (∼10–15 ky; Georg et al., 2009; Frings et al., 2016). More regional changes in DSi distribution could be triggered on millennial to centennial timescales through changes in the configuration of oceanic circulation cells, wind-driven upwelling systems (Hendry et al., 2016), and biological changes in the regions of deep-water formation (Brzezinski et al., 2002; Bradtmiller et al., 2009; Meckler et al., 2013; Hendry and Brzezinski, 2014).

An implicit assumption in the global Si mass-balance remains that there exists a steady-state. At the moment, however, it is more likely that the global Si cycle, at least in the short term, is out of balance in response to changing inputs during the Anthropocene. Human activities such as deforestation, eutrophication, agriculture, and damming have altered weathering rates, amounts of terrestrial BSi production, and the amount of amorphous Si retained and/or released from soils and freshwater systems (Struyf et al., 2010). Our recent work demonstrates the gradual aggradation or depletion of the amorphous Si pool held in continental soils (Barão et al., 2015) and aquatic sediments (Frings et al., 2014) in response to changing environmental forcings (Struyf and Conley, 2012). Our emerging understanding is that DSi inputs from the continents (Frings et al., 2016) have potentially altered the magnitude and isotopic composition to an extent great enough to impact whole-ocean isotopic signatures on the timescale of Quaternary glacial cycles (Bernard et al., 2010). This suggests that the continental Si cycle should be seen as a potential contributory factor to any variability observed in oceanic DSi (Conley, 2002; Street-Perrott and Barker, 2008; Carey and Fulweiler, 2012).

SYNTHESIS: RECONSTRUCTION OF OCEANIC DSI CONCENTRATIONS IN DEEP TIME

The assumptions regarding the evolution of the biogeochemical cycle of Si in the oceans need to be reexamined. The two critical assumptions made by Maliva et al. (1989) regarding secular changes in the distribution of cherts was (1) that biological participation in the Si cycle began in the Phanerozoic with the advent of widespread eukaryotic skeletal biosilicification and (2) that based on the modern oceans, sponges and radiolarians in the past contributed to a lesser degree than diatoms in modifying oceanic DSi concentrations. The discovery by Baines et al. (2012) that the cyanobacterium *Synechococcus* was capable of accumulating significant quantities of Si and that bacterial-type SIT-L sequences were present in the prokaryotic size fraction of the *Tara Oceans* environmental metagenomic sequencing datasets (Sunagawa et al., 2015; Marron et al., 2016) disproves the first hypothesis, although the actual quantitative contribution of biosilicification by prokaryotes to the global Si cycle in the present and the past is currently unknown. Secondly, the role of radiolarians and sponges in modifying oceanic DSi concentrations has been questioned (Kidder and Tomescu, 2016) with shifts in the global distribution of radiolarians and sponges preserved in sediments related to changes in oceanic DSi concentrations. Finally, Fontorbe et al. (2017) suggest that the superior competitive ability of diatoms for DSi relative to other siliceous plankton such as radiolarians, likely rapidly reduced DSi concentrations early in their evolution as they increased in abundance to the low levels of DSi observed in the oceans today (Tréguer and De La Rocha, 2013). These changes occurred due to the innovation of more sophisticated and versatile DSi uptake mechanisms especially by diatoms (Thamatrakoln and Hildebrand, 2008; Durkin et al., 2016; Marron et al., 2016).

We present a third narrative regarding the evolution of the oceanic Si cycle (**Figure 5**). Significant biological and geological events occurred throughout geologic time that affected the global oceanic Si cycle (**Figure 6**). Our narrative suggests that Archean organisms possessed and utilized Di transporting proteins and decreases in DSi occurred already in the Precambrian reflecting first the evolution of cyanobacteria ca. 3,000 Ma (Dvorák et al., 2014) lowering DSi concentrations from saturation and contributing to the deposition of BSi. The deposition of BIFs (Fischer and Knoll, 2009) drove DSi in the surface oceans to 500–1,000 μM (Zheng et al., 2016) through the formation of Fe-Si gels. After the great oxidation event (Kump, 2008) DSi concentrations rapidly increased as the formation of BIFs were reduced and DSi concentrations were again controlled primarily by biological Si homeostasis mechanisms and cyanobacteria Si accumulation. We place DSi in the surface oceans below saturation because of biosilicification, although the deposition by prokaryotes was probably not sufficient to reduce whole-ocean DSi and is supported by chert deposition (Maliva et al., 1989, 2005). DSi was likely reduced in the Late Proterozoic with the evolution of significant eukaryotic biosilicification across multiple taxa (Knoll, 2017), including early siliceous sponges. This biomineralization revolution would have further reduced DSi sufficiently below saturation to account for the widespread, independent losses of silicon transporters postulated in Marron et al. (2016). The next significant DSi drop occurred in the lower to early Middle Ordovician with increased usage by sponges and radiolarians (Kidder and Tomescu, 2016). Finally, it is the appearance and subsequent proliferation of biosilicifying phytoplankton, most importantly the diatoms with their superior ability to reduce DSi concentrations to the low levels observed in the global oceans today (Tréguer and De La Rocha, 2013).

In today's oceans, DSi concentrations are largely biologically controlled, namely that BSi production through the uptake of DSi by fairly high affinity silica transporters and the biological templates guiding deposition mean that high rates of BSi production can be sustained at lower environmental concentrations of DSi. This allows for the same amount of material to be exported at lower DSi concentrations than is possible by abiotic control only or by a previously existing set of silica biomineralizers.

The response in changes in DSi is faster at high DSi concentrations due to a proclivity of preservation over dissolution of BSi (Equation 1; Van Cappellen et al., 2002). In addition, macroevolution can occur over relative short periods of geological time as a result of competitive exclusion. For example, Kidder and Tomescu (2016) suggest that the shifts between the loci of sponges from shallow to basinal

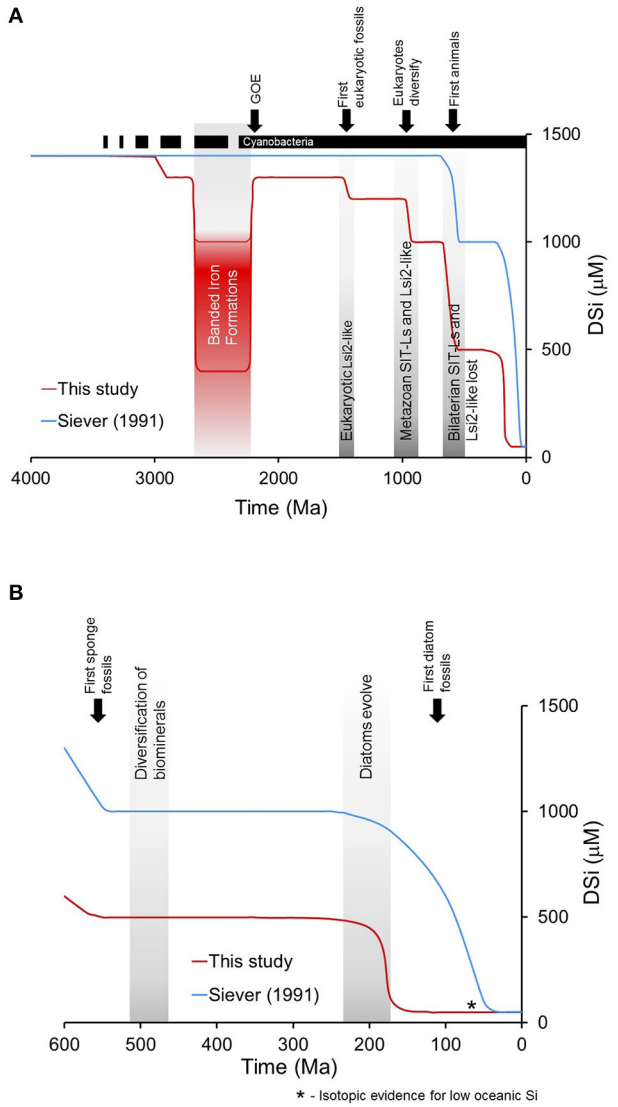

FIGURE 5 | The evolution of the oceanic Si cycle through geologic time envisioned by Siever (1991) (blue line) together with our narrative for reductions in DSi primarily through biosilicification (red line). **(A)** From the early Precambrian to the present with the major biological and geological events. The dotted line for cyanobacteria reflects the uncertainty in the timing of its evolution in the geological record. **(B)** DSi from the latest Precambrian to the present.

environments may have taken approximately 2–14 My in the late Lower to early Middle Ordovician as a result of DSi uptake by radiolarians. Futhermore, Ritterbush et al. (2015) has estimated that oceanic DSi changes could occur in timescales of 100–500 ky with an increase in DSi flux at the Jurassic-Triassic boundary as a consequence of the increased weathering of Central Atlantic Magmatic Province basalts. Models utilizing the sediment record are needed to constrain the rapidity of the response of sediment BSi burial to changes in the temporal distribution of DSi inputs to the oceans (Yool and Tyrrell, 2005; Lenton and Daines, 2017).

CHALLENGES TO EXISTING KNOWLEDGE

An Imperfect Geological Record

The lack of fossils to verify or falsify our hypothesis can simply be an artifact of a sparse geological record. There remains great potential for new discoveries with increased sampling and more focused investigations for the fossil remains of more diverse silicifying groups. However, a record of the rapid declines in DSi that occurred must be buried in ocean sediments most of which have been subducted and recycled by the movement of the continents. Whether or not the Siever (1991) narrative or the one presented here are possible, the question remains: where are the massive deposits of BSi that must have occurred with rapid drawdowns in ocean DSi concentrations? In addition, are these deposits resolvable by bulk measurements or isotopically, and can they be attributable to transient decreases in the ocean inventory of Si on the basis of mass-balance calculations?

Formation of Chert Deposits

High BSi sediments from the deposition of sponges, radiolarians and/or diatoms, which are precursors to chert formation, still occur today e.g., in places where productivity is high such as upwelling areas. The interpretation that DSi saturation occurred in bottom waters above chert nodule formation has been questioned (Ritterbush et al., 2015) with Moore's (2008) alternative explanation for chert formation as mobilization of amorphous hydrothermal deposits in deeper sediments, which removes chert nodules as indicators of DSi concentration through time. This brings into question an important tenant by Maliva et al. (1989) regarding chert deposition reflecting DSi concentration in the water column.

Does Sponge Abundance Reflect DSi?

Maldonado et al. (1999) suggested declines in reef building sponges occurred at the Cretaceous-Tertiary boundary because of DSi limitation as diatoms evolved. However, highly siliceous sponge reefs are still forming in selected areas of the modern oceans despite the relatively low DSi concentrations (Uriz, 2006; Chu and Leys, 2010; Maldonado et al., 2015). There are certainly other factors, such as food availability and ocean temperature (Kahn et al., 2012) that control the abundance and biosilicification of sponges (Alvarez et al., 2017).

Biosilicification Is Not the Only Factor

The first order interpretation is that DSi controls the morphology and biosilicification of organisms (Leadbeater and Jones, 1984; Finkel et al., 2010; Yamada et al., 2014). Yet, additional evolutionary selective pressures on the morphology of the siliceous diatom frustule have been identified, including changes in growth-limiting nutrients other than Si (Marchetti and Cassar, 2009), CO_2 (Milligan and Morel, 2002), and predation (Pondaven et al., 2007) have shaped the morphology of the frustule over geologic time (Finkel and Kotrc, 2010). In addition, Si transporter (SITs, SIT-Ls and Lsi2-like) genes are found in many eukaryotes that are not major biosilicifiers today (Marron et al., 2016), yet in some organisms (e.g., calcareous haptophytes) Si is required in trace amounts (Durak et al., 2016). Are there other factors that are contributing to changes in oceanic DSi in deep time?

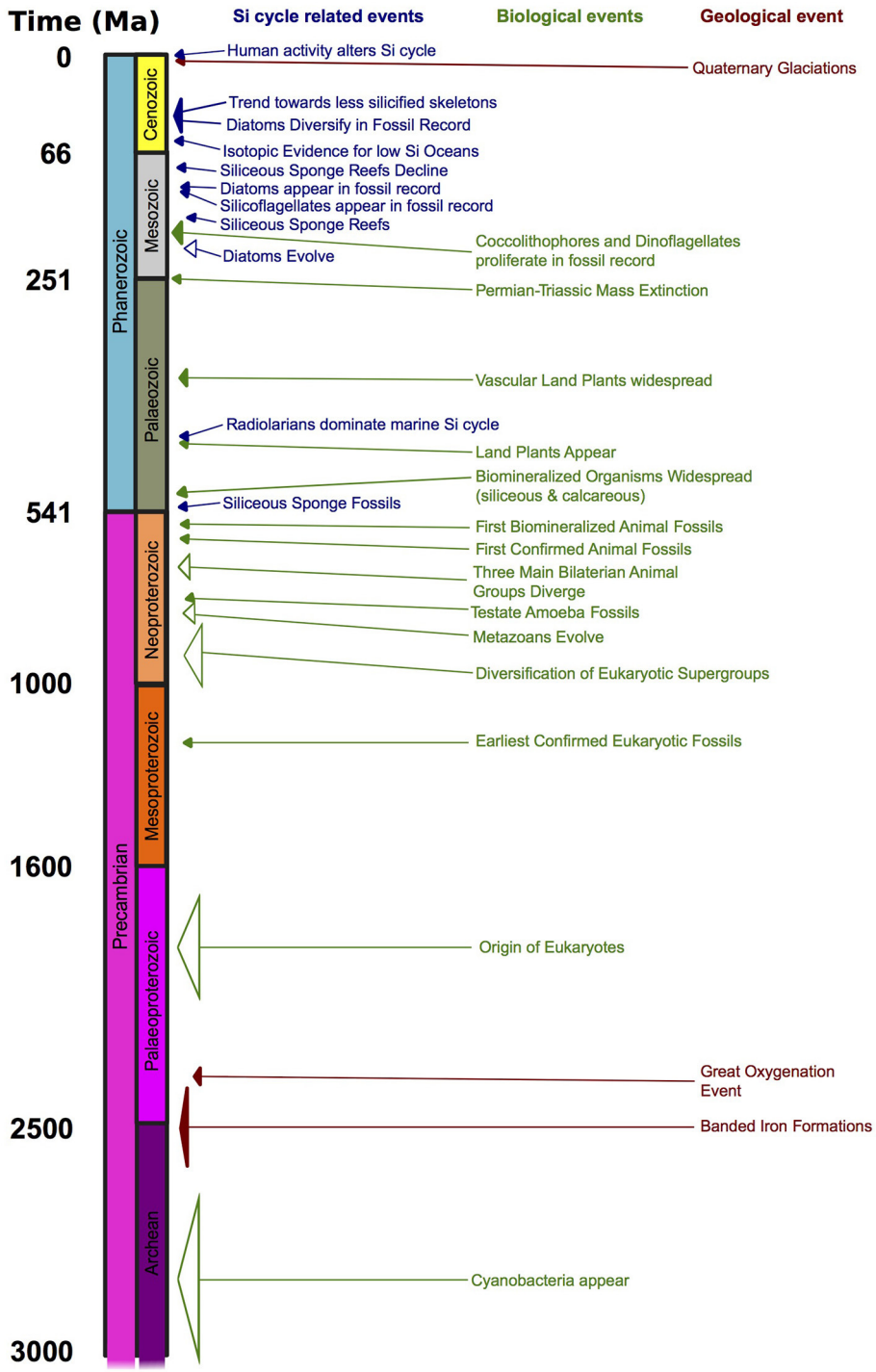

FIGURE 6 | Significant biological and geological events throughout geologic time that affect the global oceanic Si cycle. Events are color coded for the different types of events (blue for Si-related, green for biological, dark red for geological). The size of the open arrows denote uncertainty in the determination of the molecular clock dates.

Temporal Sensitivity of Marine DSi Concentration

All narratives describe changes in DSi as a linear process from high to low DSi concentrations with the evolution of specialized mechanisms for DSi uptake and biosilicification. A change in DSi fluxes to the ocean, can be caused for example by either changes in hydrothermal fluxes or by changes in continental weathering. Further investigations must be done to unravel the

amplitude and duration of such events that impact global DSi concentrations. In addition, there can be short-term changes in DSi fluxes (Frings et al., 2016) as well as fluctuations in the short-term production of biosilicifying organisms due to changes in the sources of DSi. For example, Ritterbush et al. (2015) argue that the Early Jurassic siliceous sponge takeover was likely permitted by an increased DSi flux as a consequence of weathering of the Central Atlantic Magmatic Province (CAMP) basalts. Does the volcanism associated with the formation of large igneous provinces (Kidder and Worsley, 2010) allow for changes in oceanic DSi concentrations or are inputs continuously balanced by burial?

CONCLUSION

Combining evidence from many different fields, e.g., biogeochemistry (Tréguer and De La Rocha, 2013), the study of the geological record (Maliva et al., 2005; Fischer and Knoll, 2009; Kidder and Tomescu, 2016), and the emerging field of geogenomics (Baker et al., 2014; Marron et al., 2016), we have identified changes in seawater DSi geochemistry by biosilicification (**Figure 5**). The first biological impacts on the Si cycle were likely due to the evolution of silicon homeostasis or detoxification mechanisms in the Proterozoic. We hypothesize that further decreases in DSi occurred prior to the start of the Phanerozoic with the evolution of widespread, large-scale skeletal biosilicification. DSi concentrations continued to be reduced by biomineralization and burial of BSi through deep time. Finally, we further hypothesize that the evolution of diatoms leads to a low DSi ocean already by the middle Mesozoic.

Our analysis suggests that the oceans have probably experienced lower DSi concentrations than previously appreciated (Siever, 1991). Our results challenge the Maliva et al. (1989, 2005) and the Siever (1991, 1992) framework and these results are contrary to what is currently believed. In addition, our analysis necessitates a revision of the singular role of DSi in driving the evolution of biosilicifying organisms in both marine and terrestrial systems, and the controls on global Si geochemistry.

It should be noted that the formation of Si-rich precipitates would also impact cycling of other elements especially in the Precambrian oceans, including iron, trace metals and phosphorus (e.g., Konhauser et al., 2007; Jones et al., 2015). In addition, the rise to ecological prominence of the diatoms is a relevant landmark in the history of the Earth system with a probable increase in the strength and efficiency of the biological pump and its impact on C (Renaudie, 2016). Therefore, the study of secular changes in the Si cycle bears on our general understanding of geochemical cycles in marine systems.

AUTHOR CONTRIBUTIONS

The manuscript was envisioned by DC. All authors participated in the discussion, writing and editing of the manuscript.

ACKNOWLEDGMENTS

This work was funded by a grant from the Knut and Alice Wallenberg Foundation and from the Swedish Research Council to DC. KH was funded by Royal Society grant #UF120084. AM was funded by a Wellcome Trust Senior Investigator Award to Raymond E. Goldstein, DAMTP, University of Cambridge. All appropriate permissions have been obtained from the copyright holders of any work that has been reproduced in the manuscript. We gratefully thank Daniel Brooks, Jack Middelburg, and Patricia Sánchez-Baracaldo for helpful comments and two reviewers.

REFERENCES

Abraham, K., Hofmann, A., Foley, S. F., Cardinal, D., Harris, C., Barth, M. G., et al. (2011). Coupled silicon–oxygen isotope fractionation traces Archaean silicification. *Earth Planet. Sci. Lett.* 301, 222–230. doi: 10.1016/j.epsl.2010.11.002

Alvarez, B., Frings, P. J., Clymans, W., Fontorbe, G., and Conley, D. J. (2017). Assessing the potential of sponges (Porifera) as indicators of ocean dissolved Si concentrations. *Front. Mar. Sci.* 4:373. doi: 10.3389/fmars.2017.00373

André, L., Cardinal, D., Alleman, L. Y., and Moorbath, S. (2006). Silicon isotopes in ∼3.8 Ga West Greenland rocks as clues to the Eoarchaean supracrustal Si cycle. *Earth Planet. Sci. Lett.* 245, 162–173. doi: 10.1016/j.epsl.2006.02.046

Antcliffe, J. B., Callow, R. H. T., and Brasier, M. D. (2014). Giving the early fossil record of sponges a squeeze. *Biol. Rev.* 89, 972–1004. doi: 10.1111/brv.12090

Baines, S. B., Twining, B. S., Brzezinski, M. A., Krause, J. W., Vogt, S., Assael, D., et al. (2012). Significant silicon accumulation by marine pico-cyanobacteria. *Nat. Geosci.* 5, 886–891. doi: 10.1038/ngeo1641

Baker, P. A., Fritz, S. C., Dick, C. W., Eckert, A. J., Horton, B. K., Manzoni, S., et al. (2014). The emerging field of *geogenomics*: constraining geological problems with genetic data. *Earth Sci. Rev.* 135, 38–47. doi: 10.1016/j.earscirev.2014.04.001

Banwart, S. A., Berg, A., and Beerling, D. J. (2009). Process-based modeling of silicate mineral weathering responses to increasing atmospheric CO_2 and climate change. *Glob. Biogeochem. Cycles* 23:GB4013. doi: 10.1029/2008GB003243

Barão, L., Vandevenne, F., Clymans, W., Frings, P., Ragueneau, O., Meire, P., et al. (2015). Alkaline-extractable silicon from land to ocean: a challenge for biogenic silicon determination. *Limnol. Oceanogr. Methods* 13, 329–344. doi: 10.1002/lom3.10028

Beerling, D. J., Taylor, L. L., Bradshaw, C. D. C., Lunt, D. J., Valdes, P. J., Banwart, S. A., et al. (2012). Ecosystem CO_2 starvation and terrestrial silicate weathering: mechanisms and global-scale quantification during the late Miocene. *J. Ecol.* 100, 31–41. doi: 10.1111/j.1365-2745.2011.01905.x

Bernard, C. Y., Laruelle, G. G., Slomp, C. P., and Heinze, C. (2010). Impact of changes in river fluxes of silica on the global marine silicon cycle: a model comparison. *Biogeosciences* 7, 441–453. doi: 10.5194/bg-7-441-2010

Berner, R. A. (1990). Atmospheric carbon dioxide levels over Phanerozoic time. *Science* 249, 1382–1386. doi: 10.1126/science.249.4975.1382

Berner, R. A. (1997). The rise of plants and their effect on weathering and atmospheric CO_2. *Science* 276, 544–546. doi: 10.1126/science.276.53 12.544

Bertolino, M., Cattaneo-Vietti, R., Pansini, M., Santini, C., and Giorgio Bavestrello, G. (2017). Siliceous sponge spicule dissolution: in field experimental evidences from temperate and tropical waters. *Estuar. Coast. Shelf Sci.* 184, 46–53. doi: 10.1016/j.ecss.2016.10.044

Bidle, K. D., and Azam, F. (1999). Accelerated dissolution of diatom silica by marine bacterial assemblages. *Nature* 397, 508–512. doi: 10.1038/17351

Bidle, K. D., Manganelli, M., and Azam, F. (2002). Regulation of oceanic silicon and carbon preservation by temperature control on bacteria. *Science* 298, 1980–1984. doi: 10.1126/science.1076076

Bradtmiller, L. I., Anderson, R. F., Fleisher, M. Q., and Burckle, L. H. (2009). Comparing glacial and Holocene opal fluxes in the Pacific sector of the Southern Ocean. *Paleoceanography* 24:PA2214. doi: 10.1029/2008PA001693

Braterman, P. S., Cairns-Smith, A. G., and Sloper, R. W. (1983). Photo-oxidation of hydrate Fe^{+3} - Significance for banded iron formation. *Nature* 303, 163–164. doi: 10.1038/303163a0

Brengman, L. A. (2015). *Distinguishing Primary Versus Secondary Geochemical and Silicon Isotope Characteristics of Precambrian Chert and Iron Formation.* Ph.D. Thesis, University of Tennessee.

Brennan, S. T., Lowenstein, T. K., and Horita, J. (2004). Seawater chemistry and the advent of biocalcification. *Geology* 32, 473–476. doi: 10.1130/G20251.1

Brocks, J. J., Jarrett, A. J. M., Sirantoine, E., Hallmann, C., Hoshino, Y., and Liyanage, T. (2017). The rise of algae in Cryogenian oceans and the emergence of animals. *Nature* 548, 578–581. doi: 10.1038/nature23457

Brown, J. W., and Sorhannus, U. (2010). A molecular genetic timescale for the diversification of autotrophic Stramenopiles (Ochrophyta): substantive underestimation of putative fossil ages. *PLoS ONE* 5:e12759. doi: 10.1371/journal.pone.0012759

Brzezinski, M. A., Sigman, D. M., Sarmiento, J. L., Matsumoto, K., Gruber, N., Rau, G. H., et al. (2002). A switch from $Si(OH)_4$ to NO_3^- depletion in the glacial Southern Ocean. *Geophys. Res. Lett.* 29:1564. doi: 10.1029/2001GL014349

Carey, J. C., and Fulweiler, R. W. (2012). The terrestrial silica pump. *PLoS ONE* 7:e52932. doi: 10.1371/journal.pone.0052932

Cermeño, P., Falkowski, P. G., Romero, O. E., Schaller, M. F., and Vallina, S. M. (2015). Continental erosion and the Cenozoic rise of marine diatoms. *Proc. Natl. Acad. Sci. U.S.A.* 112, 4239–4244. doi: 10.1073/pnas.1412883112

Chakrabarti, R. (2015). Silicon isotopes: from cosmos to benthos. *Curr. Sci.* 108, 246–254.

Chakrabarti, R., Knoll, A. H., Jacobsen, S. B., and Fischer, W. W. (2012). Si isotope variability in Proterozoic cherts. *Geochim. Cosmochim. Acta* 91, 187–201. doi: 10.1016/j.gca.2012.05.025

Chang, S., Feng, Q., Clausen, S., and Zhang, L. (2017). Sponge spicules from the lower Cambrian in the Yanjiahe Formation, South China: the earliest biomineralizing sponge record. *Palaeogeogr. Palaeoclimatol. Palaeoecol.* 474, 36–44. doi: 10.1016/j.palaeo.2016.06.032

Chi Fru, E., Hemmingsson, C., Mikaela Holm, M., Chiu, B., and Iñiguez, E. (2016). Arsenic-induced phosphate limitation under experimental Early Proterozoic oceanic conditions. *Earth Planet. Sci. Lett.* 434, 52–63. doi: 10.1016/j.epsl.2015.11.009

Chi Fru, E., Ivarsson, M., Kilias, S. P., Bengtson, S., Belivanova, V., Marone, F., et al. (2013). Fossilized iron bacteria reveal a pathway to the biological origin of banded iron formation. *Nat. Commun.* 4:2050. doi: 10.1038/ncomms3050

Chu, J. W. F., and Leys, S. P. (2010). High resolution mapping of community structure in three glass sponge reefs (Porifera, Hexactinellida). *Mar. Ecol. Prog. Ser.* 417, 97–113. doi: 10.3354/meps08794

Cohen, B. L. (2005). Not armour, but biomechanics, ecological opportunity and increased fecundity as keys to the origin and expansion of the mineralized benthic metazoan fauna. *Biol. J. Linn. Soc.* 85, 483–490. doi: 10.1111/j.1095-8312.2005.00507.x

Conley, D. J. (2002). Terrestrial ecosystems and the global biogeochemical silica cycle. *Glob. Biogechem. Cycles* 16:1121. doi: 10.1029/2002GB001894

Conley, D. J., and Carey, J. C. (2015). Silica cycling over geologic time. *Nat. Geosci.* 8, 431–432. doi: 10.1038/ngeo2454

Cui, H., Kaufman, A. J., Xiao, S., Peek, S., Cao, H., Min, X., et al. (2016). Environmental context for the terminal Ediacaran biomineralization of animals. *Geobiology* 14, 344–363. doi: 10.1111/gbi.12178

Cunningham, J. A., Liu, A. G., Bengtson, S., and Donoghue, P. C. J. (2017). The origin of animals: can molecular clocks and the fossil record be reconciled? *Bioessays* 39:1600120. doi: 10.1002/bies.201600120

De La Rocha, C. L. (2002). Measurement of silicon stable isotope natural abundances via multicollector inductively coupled plasma mass spectrometry (MC-ICP-MS). *Geochem. Geophys. Geosyst.* 3, 1–8. doi: 10.1029/2002GC000310

De La Rocha, C. L., and Bickle, M. J. (2005). Sensitivity of silicon isotopes to whole-ocean changes in the silica cycle. *Mar. Geol.* 217, 267–282. doi: 10.1016/j.margeo.2004.11.016

Delvigne, C. (2012). *The Archaean Silicon Cycle Insights from Silicon Isotopes and Ge/Si Ratios in Banded Iron Formations, Palaeosols and Shales*. Ph.D. Thesis. Universite Libre de Bruxelles, 181.

Delvigne, C., Cardinal, D., Hofmann, A., and André, L. (2012). Stratigraphic changes of Ge/Si, REE+ Y and silicon isotopes as insights into the deposition of a Mesoarchaean banded iron formation. *Earth Planet. Sci. Lett.* 355, 109–118. doi: 10.1016/j.epsl.2012.07.035

de Souza, G. F., Slater, R. D., Dunne, J. P., and Sarmiento, J. L. (2014). Deconvolving the controls on the deep ocean's silicon stable isotope distribution. *Earth Planet. Sci. Lett.* 398, 66–76. doi: 10.1016/j.epsl.2014.04.040

Ding, T. P., Gao, J. F., Tian, S. H., Fan, C. F., Zhao, Y., Wan, D. F., et al. (2017). The δ^{30}Si peak value discovered in middle Proterozoic chert and its implication for environmental variations in the ancient ocean. *Sci. Rep.* 7:44000. doi: 10.1038/srep44000

dos Reis, M., Thawornwattana, Y., Angelis, K., Telford, M. J., Donoghue, P. C. J., and Yang, Z. (2015). Uncertainty in the timing of origin of animals and the limits of precision in molecular timescales. *Curr. Biol.* 25, 2939–2950. doi: 10.1016/j.cub.2015.09.066

Dunn, C. W., Hejnol, A., Matus, D. Q., Pang, K., Browne, W. E., Smith, S. A., et al. (2008). Broad phylogenomic sampling improves resolution of the animal tree of life. *Nature* 452, 745–749. doi: 10.1038/nature06614

Durak, G. M., Taylor, A. R., Walker, C. E., Probert, I., Vargas, C., Audic, S., et al. (2016). A role for diatom-like silicon transporters in calcifying coccolithophores. *Nat. Commun.* 7:10543. doi: 10.1038/ncomms10543

Durkin, C., Koester, J. A., Bender, S. J., and Armbrust, E. V. (2016). The evolution of silicon transporters in diatoms. *J. Phycol.* 52, 716–731. doi: 10.1111/jpy.12441

Dvorák, P., Casamatta, D. A., Poulíčková, A., Hašler, P., Ondrej, V., and Sanges, R. (2014). *Synechococcus*: 3 billion years of global dominance. *Mol. Ecol.* 23, 5538–5551. doi: 10.1111/mec.12948

Edwards, D., Cherns, L., and Raven, J. A. (2015). Could land-based early photosynthesizing ecosystems have bioengineered the planet in mid-Palaeozoic times? *Palaeontology* 58, 803–837. doi: 10.1111/pala.12187

Egan, K., Rickaby, R. E. M., Hendry, K. R., and Halliday, A. N. (2013). Opening the gateways for diatoms primes Earth for Antarctic glaciation. *Earth Planet. Sci. Lett.* 375, 34–43. doi: 10.1016/j.epsl.2013.04.030

Eme, L., Sharpe, S. C., Brown, M. W., and Roger, A. J. (2014). On the age of eukaryotes: evaluating evidence from fossils and molecular clocks. *Cold Spring Harb. Perspecti. Biol.* 6:a016139. doi: 10.1101/cshperspect.a016139

Epstein, E. (1999). Silicon. *Annu. Rev. Plant Physiol. Plant Mol. Biol.* 50, 641–664. doi: 10.1146/annurev.arplant.50.1.641

Finkel, Z. V., Katz, M., Wright, J., Schofieid, O., and Falkowski, P. G. (2005). Climatically driven macroevolutionary patterns in the size of marine diatoms over the Cenozoic. *Proc. Natl. Acad. Sci. U.S.A.* 102, 8927–8932. doi: 10.1073/pnas.0409907102

Finkel, Z. V., and Kotrc, B. (2010). Silica use through time: macroevolutionary change in the morphology of the diatom fustule. *Geomicrobiol. J.* 27, 596–608. doi: 10.1080/01490451003702941

Finkel, Z. V., Matheson, K. A., Regan, K. S., and Irwin, A. J. (2010). Genotypic and phenotypic variation in diatom silicification under paleo-oceanographic conditions. *Geobiology* 8, 433–445. doi: 10.1111/j.1472-4669.2010.00250.x

Fischer, W. W., and Knoll, A. H. (2009). An iron shuttle for deepwater silica in Late Archean and early Paleoproterozoic iron formation. *GSA Bull.* 121, 222–235. doi: 10.1130/B26328.1

Flombaum, P., Gallegos, J. L., Gordillo, R. A., Rincóna, J., Zabala, L. L., Jiao, N., et al. (2013). Present and future global distributions of the marine Cyanobacteria *Prochlorococcus* and *Synechococcus*. *Proc. Natl. Acad. Sci. U.S.A.* 110, 9824–9829. doi: 10.1073/pnas.1307701110

Fontorbe, G., Frings, P. J., De La Rocha, C. L., Hendry, K. R., and Conley, D. J. (2016). A silicon depleted North Atlantic since the Palaeogene: evidence from sponge and radiolarian silicon isotopes. *Earth Planet. Sci. Lett.* 453, 67–77. doi: 10.1016/j.epsl.2016.08.006

Fontorbe, G., Frings, P. J., De La Rocha, C. L., Hendry, K. R., and Conley, D. J. (2017). Enrichment of dissolved silica in the deep Equatorial Pacific during the Eocene-Oligocene. *Paleoceanography* 32, 848–863. doi: 10.1002/2017PA003090

Frings, P. J., Clymans, W., and Conley, D. J. (2014). Amorphous silica transport in the Ganges basin: implications for Si delivery to the oceans. *Proc. Earth Planet. Sci.* 10, 271–274. doi: 10.1016/j.proeps.2014.08.059

Frings, P. J., Clymans, W., Fontorbe, G., De La Rocha, C. L., and Conley, D. J. (2016). The continental Si cycle and its impact on the ocean Si isotope budget. *Chem. Geol.* 425, 12–36. doi: 10.1016/j.chemgeo.2016.01.020

Frings, P. J., Clymans, W., Fontorbe, G., Gray, W., Govind, C., Conley, D. J., et al. (2015). Silicate weathering in the Ganges alluvial plain. *Earth Planet. Sci. Lett.* 427, 136–148. doi: 10.1016/j.epsl.2015.06.049

Geilert, S., Vroon, P. Z., and van Bergen, M. J. (2014). Silicon isotopes and trace elements in chert record early Archean basin evolution. *Chem. Geol.* 386, 133–142. doi: 10.1016/j.chemgeo.2014.07.027

Georg, R. B., West, A. J., Basu, A. R., and Halliday, A. N. (2009). Silicon fluxes and isotope composition of direct groundwater discharge into the Bay of Bengal and the effect on the global ocean silicon budget. *Earth Planet. Sci. Lett.* 283, 67–74. doi: 10.1016/j.epsl.2009.03.041

Gouretski, V., and Koltermann, K. P. (2004). WOCE global hydrographic climatology. *Berichte BSH* 35, 1–52.

Graham, L. E., and Wilcox, L. W. (2000). *Algae*. Upper Saddle River, NJ: Prentice-Hall.

Gunnarsson, I., and Arnórsson, S. (2000). Amorphous silica solubility and the thermodynamic properties of $H_4SiO_4^\circ$ in the range of 0° to 350°C at P_{sat}. *Geochim. Cosmochim. Acta* 64, 2295–2307. doi: 10.1016/S0016-7037(99)00426-3

Harper, H. E., and Knoll, A. H. (1975). Silica, diatoms, and Cenozoic radiolarian evolution. *Geology* 3, 175–177.

Hawkings, J. R., Wadham, J. L., Benning, L. G., Hendry, K. R., Tranter, M., Tedstone, A., et al. (2017). Ice sheets as a missing source of silica to the polar oceans. *Nat. Commun.* 8:14198. doi: 10.1038/ncomms14198

Heck, P. R., Huberty, J. M., Kita, N. T., Ushikubo, T., Kozdon, R., and Valley, J. W. (2011). SIMS analyses of silicon and oxygen isotope ratios for quartz from Archean and Paleoproterozoic banded iron formations. *Geochim. Cosmochim. Acta* 75, 5879–5891. doi: 10.1016/j.gca.2011.07.023

Hendry, K. R., and Brzezinski, M. A. (2014). Using silicon isotopes to understand the role of the Southern Ocean in modern and ancient biogeochemistry and climate *Q. Sci. Rev.* 89, 13–26. doi: 10.1016/j.quascirev.2014.01.019

Hendry, K. R., Gong, X., Knorr, G., Pike, J., and Hall, I. R. (2016). Deglacial diatom production in the tropical North Atlantic driven by enhanced silicic acid supply. *Earth Planet. Sci. Lett.* 438, 122–129. doi: 10.1016/j.epsl.2016.01.016

Hendry, K. R., and Robinson, L. F. (2012). The relationship between silicon isotope fractionation in sponges and silicic acid concentration: Modern and core-top studies of biogenic opal. *Geochim. Cosmochim. Acta* 81, 1–12. doi: 10.1016/j.gca.2011.12.010

Hildebrand, M. (2000). "Silicic acid transport and its control during cell wall silicification in diatoms," in *Biomineralization*, ed E. Bäuerlein (Weinheim: Springer), 171–188.

Hodson, M. J., White, P. J., Mean, A., and Broadley, M. R. (2005). Phylogenetic variation in the silicon composition of plants. *Ann. Bot.* 96, 1027–1046. doi: 10.1093/aob/mci255

Hori, K., and 49 co-authors. (2014). *Klebsormidium flaccidum* genome reveals primary factors for plant terrestrial adaptation. *Nat. Commun.* 5:3978. doi: 10.1038/ncomms4978

Hu, G. Y., Fan, C. F., Wan, D. F., Li, Y. H., and Chen, S. M. (2013). Geochemistry of bedded cherts in the cap carbonates in Three Gorges Region, Hubei Province, and its paleoenvironmental implications. *Acta Geol. Sin.* 87, 1469–1476. doi: 10.1016/j.palaeo.2016.10.004

Jessen, G. L., Lichtschlag, A., Ramette, A., Pantoja, S., Rossel, P. E., Schubert, C., et al. (2017). Hypoxia causes preservation of labile organic matter and changes seafloor microbial community composition (Black Sea). *Sci. Adv.* 3:e1601897. doi: 10.1126/sciadv.1601897

Jones, C., Nomosatryo, S., Crowe, S. A., Berrum, C. J., and Canfield, D. E. (2015). Iron oxides, divalent cations, silica, and the early earth phosphorus crisis. *Geology* 43, 135–138. doi: 10.1130/G36044.1

Kahn, A. S., Ruhl, H. A., and Smith, K. L. (2012). Temporal changes in deep-sea sponge populations are correlated to changes in surface climate and food supply. *Deep Sea Res. I* 70, 36–41. doi: 10.1016/j.dsr.2012.08.001

Katz, M. E., Finkel, Z. V., Grzebyk, D., Knoll, A. H., and Falkowski, P. G. (2004). Evolutionary trajectories and biogeochemical impacts of marine eukaryotic phytoplankton. *Annu. Rev. Ecol. Evol. Syst.* 35, 523–556. doi: 10.1146/annurev.ecolsys.35.112202.130137

Kidder, D. L., and Erwin, D. H. (2001). Secular distribution of biogenic silica through the Phanerozoic: comparison of silica-replaced fossils and bedded cherts at the series level. *J. Geol.* 109, 509–522. doi: 10.1086/320794

Kidder, D. L., and Tomescu, I. (2016). Biogenic chert and the Ordovician silica cycle. *Palaeogeogr. Palaeoclimatol. Palaeoecol.* 458, 29–38. doi: 10.1016/j.palaeo.2015.10.013

Kidder, D. L., and Worsley, T. R. (2010). Phanerozoic Large Igneous Provinces (LIPs), HEATT (Haline Euxinic Acidic Thermal Transgression) episodes, and mass extinctions. *Palaeogeogr. Palaeoclimatol. Palaeoecol.* 295, 162–191. doi: 10.1016/j.palaeo.2010.05.036

Klein, C. (2005). Some Precambrian banded iron-formations (BIFs) from around the world: their age, geologic setting, mineralogy, metamorphism, geochemistry, and origin. *Amer. Mineral.* 90, 1473–1499. doi: 10.2138/am.2005.1871

Knoll, A. H. (2003). Biomineralization and evolutionary history. *Rev. Mineral. Geochem.* 54, 329–356. doi: 10.2113/0540329

Knoll, A. H. (2017). Food for animal evolution. *Nature* 548, 528–530. doi: 10.1038/nature23539

Knoll, A. H., and Follows, M. J. (2016). A bottom-up perspective on ecosystem change in Mesozoic oceans. *Proc. R. Soc. B* 283:20161755. doi: 10.1098/rspb.2016.1755

Knoll, A. H., and Kotrc, B. (2015). "Protistan skeletons: a geologic history of evolution and constraint," in *Evolution of Lightweight Structures*, ed C. Hamm (Dordrecht: Springer), 1–16.

Konhauser, K. O., Amskolda, L., Lalondea, S. V., Posthb, N. R., Kapplerb, A., and Anbarc, A. (2007). Decoupling photochemical Fe(II) oxidation from shallow-water BIF deposition. *Earth Planet. Sci. Lett.* 258, 87–100. doi: 10.1016/j.epsl.2007.03.026

Konhauser, K. O., Jones, B., Phoenix, V. R., Ferris, G., and Renaut, R. W. (2004). The microbial role in hot spring silicification. *Ambio* 33, 552–558. doi: 10.1579/0044-7447-33.8.552

Kotrc, B., and Knoll, A. H. (2015). A morphospace of planktonic marine diatoms. I. Two views of disparity through time. *Paleobiology* 41, 45–67. doi: 10.1017/pab.2014.4

Kump, L. R. (2008). The rise of atmospheric oxygen. *Nature* 451, 277–278. doi: 10.1038/nature06587

Laruelle, G. G., Roubeix, V., Sferratore, A., Brodhern, B., Ciuffa, D., Conley, D. J., et al. (2009). Anthropogenic perturbations of the silicon cycle at the global scale: Key role of the land-ocean transition. *Glob. Biogeochem. Cycles* 23:GB4031. doi: 10.1029/2008GB003267

Lazarus, D., Barron, J., Renaudie, J., Diver, P., and Türke, A. (2014). Cenozoic planktonic marine diatom diversity and correlation to climate change. *PLoS ONE* 9:e84857. doi: 10.1371/journal.pone.0084857

Lazarus, D. B., Kotrc, B., Wulf, G., and Schmidt, D. N. (2009). Radiolarians decreased silicification as an evolutionary response to reduced Cenozoic ocean silica availability. *Proc. Natl. Acad. Sci. U.S.A.* 106, 9333–9338. doi: 10.1073/pnas.0812979106

Leadbeater, B. S. C., and Jones, W. C. (1984). Silicification of 'cell walls' of certain protistan flagellates [and Discussion]. *Proc. R. Soc. B* 304, 529–536. doi: 10.1098/rstb.1984.0044

Lenton, T. M., Crouch, M., Johnson, M., Pires, N., and Dolan, L. (2012). First plants cooled the Ordovician. *Nat. Geosci.* 5, 86–89. doi: 10.1038/ngeo1390

Lenton, T. M., and Daines, S. J. (2017). Biogeochemical transformations in the history of the ocean. *Ann. Rev. Mar. Sci.* 9, 31–58. doi: 10.1146/annurev-marine-010816-060521

Li, Y., Hou, K., Wan, D., Zhang, Z., and Yue, G. (2014). Precambrian banded iron formations in the North China Craton: silicon and oxygen isotopes and genetic implications. *Ore Geol. Rev.* 57, 299–307. doi: 10.1016/j.oregeorev.2013.09.011

Ma, J. F., and Yamaji, N. (2015). A cooperative system of silicon transport in plants. *Trends Plant Sci.* 20, 435–442. doi: 10.1016/j.tplants.2015.04.007

Ma, J. F., Yamaji, N., Mitani, N., Tamai, K., Konishi, S., Fujiwara, T., et al. (2007). An efflux transporter of silicon in rice. *Nature* 448, 209–212. doi: 10.1038/nature05964

Ma, J. F., Yamaji, N., Mitani, N., Xu, X.-Y., Su, Y.-H., McGrath, S. P., et al. (2008). Transporters of arsenite in rice and their role in arsenic accumulation in rice grain. *Proc. Natl. Acad. Sci. U.S.A.* 105, 9931–9935. doi: 10.1073/pnas.0802361105

Mackenzie, F. T., Garrels, R. M., Bricker, O. P., and Bickley, F. (1967). Silica in water: control by silica minerals. *Science* 155, 1404–1405. doi: 10.1126/science.155.3768.1404

Maldonado, M., Aguilar, R., Blanco, J., García, S., Serrano, A., and Punzón, A. (2015). Aggregated clumps of lithistid sponges: a singular, reef-like bathyal habitat with relevant paleontological connections. *PLoS ONE* 10:e0125378. doi: 10.1371/journal.pone.0125378

Maldonado, M., Carmona, M. C., and Cruzado, A. (1999). Decline in Mesozoic reef-building in sponges explained by silicon limitation. *Nature* 401, 785–788. doi: 10.1038/44560

Maliva, R. G., Knoll, A. H., and Siever, R. (1989). Secular change in chert distribution: a reflection of evolving biological participation in the silica cycle. *Palaios* 4, 519–532. doi: 10.2307/3514743

Maliva, R. G., Knoll, A. H., and Simonson, B. M. (2005). Secular change in the Precambrian silica cycle: insights from chert petrology. *GSA Bull.* 117, 835–845. doi: 10.1130/B25555.1

Marchetti, A., and Cassar, N. (2009). Diatom elemental and morphological changes in responseto iron limitation: a brief review with potentialpaleoceanographic applications. *Geobiology* 7, 419–431. doi: 10.1111/j.1472-4669.2009.00207.x

Marin-Carbonne, J., Robert, F., and Chaussidon, M. (2014). The silicon and oxygen isotope compositions of Precambrian cherts: a record of oceanic paleo-temperatures? *Precambrian Res.* 247, 223–234. doi: 10.1016/j.precamres.2014.03.016

Markovich, O., Steinera, E., Kourilb, Š., Tarkowski, P., Aharoni, A., and Elbaum, R. (2017). Silicon promotes cytokinin biosynthesis and delays senescence in Arabidopsis and Sorghum. *Plant Cell Environ.* 40, 1189–1196. doi: 10.1111/pce.12913

Marron, A. O., Alston, M. J., Heavens, D., Akam, M., Caccamo, M., Holland, P. W. H., et al. (2013). A family of diatom-like silicon transporters in the siliceous loricate choanoflagellates. *Proc. R. Soc. B* 280:20122543. doi: 10.1098/rspb.2012.2543

Marron, A. O., Ratcliffe, S., Wheeler, G. L., Goldstein, R. E., Nicole King, N., Not, F., et al. (2016). The evolution of silicon transport in eukaryotes. *Mol. Biol. Evol.* 33, 3226–3248. doi: 10.1093/molbev/msw209

McKenzie, N. R., Horton, B. K., Loomis, S. E., Stockli, D. F., Planavsky, N. J., and Cin-Ty, A. L. (2016). Continental arc volcanism as the principal driver of icehouse-greenhouse variability. *Science* 352, 444–447. doi: 10.1126/science.aad5787

Meckler, A. N., Sigman, D. M., Gibson, K. A., Francois, R., Martinez-Garcia, A., Jaccard, S. L., et al. (2013). Deglacial pulses of deep-ocean silicate into the subtropical North Atlantic Ocean. *Nature* 495, 495–498. doi: 10.1038/nature12006

Medlin, L. K., Kooistra, W. H., Gersonde, R., and Wellbrock, U. (1996). Evolution of the diatoms (Bacillariophyta). II. Nuclear-encoded small-subunit rRNA sequence comparisons confirm a paraphyletic origin for the centric diatoms. *Mol. Biol. Evol.* 13, 67–75. doi: 10.1093/oxfordjournals.molbev.a025571

Milligan, A. J., and Morel, F. M. M. (2002). A proton buffering role for silica in diatoms. *Science* 297, 1848–1850. doi: 10.1126/science.1074958

Misra, S., and Froelich, P. N. (2012). Lithium isotope history of Cenozoic seawater: changes in silicate weathering and reverse weathering. *Science* 335, 818–823. doi: 10.1126/science.1214697

Moore, T. C. (2008). Biogenic silica and chert in the Pacific Ocean. *Geology* 36, 975–978. doi: 10.1130/G25057A.1

Moulton, K. L., and Berner, R. A. (1988). Quantification of the effect of plants on weathering: studies in Iceland. *Geology* 26, 895–898.

Muttoni, G., and Kent, D. V. (2007). Widespread formation of cherts during the early Eocene climate optimum. *Palaeogeogr. Palaeoclimatol. Palaeoecol.* 253, 348–362. doi: 10.1016/j.palaeo.2007.06.008

Ohnemus, D. C., Rauschenberg, S., Krause, J. W., Brzezinski, M. A., Collier, J. L., Gerachi-Yee, J., et al. (2016). Silicon content of individual cells of *Synechococcus* from the North Atlantic Ocean. *Mar. Chem.* 187, 16–24. doi: 10.1016/j.marchem.2016.10.003

Pagani, M., Caldeira, K., Berner, R., and Beerling, D. J. (2009). The role of terrestrial plants in limiting atmospheric CO_2 decline over the past 24 million years. *Nature* 460, 85–89. doi: 10.1038/nature08133

Parfrey, L. W., Lahr, D. J. G., Knoll, A. H., and Katz, L. (2011). Estimating the timing of early eukaryotic diversification with multigene molecular clocks. *Proc. Natl. Acad. Sci. U.S.A.* 108, 13624–13629. doi: 10.1073/pnas.1110633108

Pogge von Strandmann, P. A. E., Desrochers, A., Murphy, M. J., Finlay, A. J., Selby, D., and Lenton, T. M. (2017). Global climate stabilisation by chemical weathering during the Hirnantian glaciation. *Geochem. Perspect. Lett.* 3, 230–237. doi: 10.7185/geochemlet.1726

Pogge von Strandmann, P. A. E., and Hendersen, G. (2015). The Li isotope response to mountain uplift. *Geology* 43, 67–70. doi: 10.1130/G36162.1

Pollard, R. T., Lucas, M. I., and Read, J. F. (2002). Physical controls on biogeochemical zonation in the Southern Ocean. *Deep Sea Res. II* 49, 3289–3305. doi: 10.1016/S0967-0645(02)00084-X

Pondaven, P., Gallinari, M., Chollet, S., Bucciarelli, E., Sarthou, G., Schultes, S., et al. (2007). Grazing-induced changes in cell wall silicification in a marine diatom. *Protist* 158, 21–28. doi: 10.1016/j.protis.2006.09.002

Porter, S. M., and Knoll, A. H. (2000). Testate amoebae in the Neoproterozoic Era: evidence from vase-shaped microfossils in the Chuar Group, Grand Canyon. *Paleobiology* 26, 360–385.

Quirk, J., Leake, J. R., Johnson, D. A., Taylor, L. L., Saccone, L., and Beerling, D. J. (2015). Constraining the role of early land plants in Palaeozoic weathering and global cooling. *Proc. R. Soc. B* 282:20151115. doi: 10.1098/rspb.2015.1115

Rabosky, D. L., and Sorhannus, U. (2009). Diversity dynamics of marine planktonic diatoms across the Cenozoic. *Nature* 457, 183–173. doi: 10.1038/nature07435

Racki, G., and Cordey, F. (2000). Radiolarian palaeoecology and radiolarites: is the present the key to the past? *Earth Sci. Rev.* 52, 83–120. doi: 10.1016/S0012-8252(00)00024-6

Rahman, S., Aller, R. C., and Cochran, J. K. (2016). Cosmogenic ^{32}Si as a tracer of biogenic silica burial and diagenesis: Major deltaic sinks in the silica cycle. *Geophys. Res. Lett.* 43, 7124–7132. doi: 10.1002/2016GL069929

Ramseyer, K., Amthor, J. E., Matter, A., Pettke, T., Wille, M., and Fallick, A. E. (2013). Primary silica precipitate at the Precambrian/Cambrian boundary in the south Oman salt basin, sultanate of Oman. *Mar. Petrol. Geol.* 39, 187–197. doi: 10.1016/j.marpetgeo.2012.08.006

Rasmussen, B., Krapež, B., Muhling, J. R., and Suvorova, A. (2015). Precipitation of iron silicate nanoparticles in early Precambrian oceans marks Earth's first iron age. *Geology* 43, 303–306. doi: 10.1130/G36309.1

Raven, J. A., and Waite, A. M. (2004). The evolution of silicification in diatoms: inescapable sinking and sinking as escape? *New Phytol.* 162, 45–61. doi: 10.1111/j.1469-8137.2004.01022.x

Reddy, T. R., Zheng, X. -Y., Roden, E. E., Beard, B. L., and Johnson, C. M. (2016). Silicon isotope fractionation during microbial reduction of Fe(III)–Si gels under Archean seawater conditions and implications for iron formation genesis. *Geochim. Cosmochim. Acta* 190, 85–99. doi: 10.1016/j.gca.2016.06.035

Renaudie, J. (2016). Quantifying the Cenozoic marine diatom deposition history: links to the C and Si cycles. *Biogeosciences* 13, 6003–6014. doi: 10.5194/bg-13-6003-2016

Rickaby, R. E. M. (2015). Goldilocks and the three inorganic equilibria: how Earth's chemistry and life coevolve to be nearly in tune. *Philos. Trans. R. Soc. A* 373:20140188. doi: 10.1098/rsta.2014.0188

Ritterbush, K. A., Rosas, S., Corsetti, F. A., Bottjer, D. J., and West, A. J. (2015). Andean sponges reveal long-term benthic ecosystem shifts following the end-Triassic mass extinction. *Palaeogeogr. Palaeoclimatol. Palaeoecol.* 420, 193–209. doi: 10.1016/j.palaeo.2014.12.002

Robert, F., and Chaussidon, M. (2006). A palaeotemperature curve for the Precambrian oceans based on silicon isotopes in cherts. *Nature* 443, 969–972. doi: 10.1038/nature05239

Sanchez-Baracaldoa, P., Raven, J. A., Pisani, D., and Knoll, A. H. (2017). Early photosynthetic eukaryotes inhabited low-salinity habitats. *Proc. Natl. Acad. Sci. U.S.A.* 114, E7737–E7745. doi: 10.1073/pnas.1620089114

Sanchez-Baracaldo, P. (2015). Origin of marine planktonic cyanobacteria. *Sci. Rep.* 5:17418. doi: 10.1038/srep17418

Sarmiento, J. L., Gruber, N., Brzezinski, M. A., and Dunne, J. P. (2004). High-latitude controls of thermocline nutrients and low latitude biological productivity. *Nature* 427, 56–60. doi: 10.1038/nature02127

Schneider, S. H., and Boston, P.J. (eds.). (1991). *Scientists on Gaia*. Massachusetts Institute of Technology, The MIT Press.

Schirrmeister, B. E., Sanchez-Baracaldo, P., and Wacey, D. (2016). Cyanobacterial evolution during the Precambrian. *Int. J. Astrobiology* 15, 187–204. doi: 10.1017/S1473550415000579

Schubert, J., Kidder, D. L., and Erwin, D. H. (1997). Silica-replaced fossils through the Phanerozoic. *Geology* 25, 1031–1034.

Schwartzman, D. W., and Volk, T. (1989). Biotic enhancement of weathering and the habitability of Earth. *Nature* 340, 457–460. doi: 10.1038/340457a0

Siever, R. (1991). "Silica in the oceans: biological-geochemical interplay," in *Scientists on Gaia,* eds S. H. Schneider and P. J. Boston (Cambridge, MA: MIT Press), 287–295.

Siever, R. (1992). The silica cycle in the Precambrian. *Geochim. Cosmochim. Acta* 56, 3265–3272. doi: 10.1016/0016-7037(92)90303-Z

Sims, P. A., Mann, D. G., and Medlin, L. K. (2006). Evolution of the diatoms: insights from fossil, biological and molecular data. *Phycologia* 45, 361–402. doi: 10.2216/05-22.1

Smith, J. M., and Szathmáry, E. (1995). *The Major Transitions in Evolution*. Oxford: Oxford University Press.

Sperling, E. A., Robinson, J. M., Pisani, D., and Peterson, K. J. (2010). Where's the glass? Biomarkers, molecular clocks, and microRNAs suggest a 200-Myr missing Precambrian fossil record of siliceous sponge spicules. *Geobiology* 8, 24–36. doi: 10.1111/j.1472-4669.2009.00225.x

Stefurak, E. J., Fischer, W. W., and Lowe, D. R. (2015). Texture-specific Si isotope variations in Barberton Greenstone Belt cherts record low temperature fractionations in early Archean seawater. *Geochim. Cosmochim. Acta* 150, 26–52. doi: 10.1016/j.gca.2014.11.014

Stefurak, E. J. T., Lowe, D. R., Zentner, D., and Fischer, W. W. (2014). Primary silica granules - A new mode of Paleoarchean sedimentation. *Geology* 42, 283–286. doi: 10.1130/G35187.1

Steinhoefel, G., Horn, I., and von Blanckenburg, F. (2009). Micro-scale tracing of Fe and Si isotope signatures in banded iron formation using femtosecond laser ablation. *Geochim. Cosmochim. Acta* 73, 5343–5360. doi: 10.1016/j.gca.2009.05.037

Steinhoefel, G., von Blanckenburg, F., Horn, I., Konhauser, K. O., Beukes, N. J., and Gutzmer, J. (2010). Deciphering formation processes of banded iron formations from the Transvaal and the Hamersley successions by combined Si and Fe isotope analysis using UV femtosecond laser ablation. *Geochim. Cosmochim. Acta* 74, 2677–2696. doi: 10.1016/j.gca.2010.01.028

Street-Perrott, F. A., and Barker, P. A. (2008). Biogenic silica: a neglected component of the coupled global continental biogeochemical cycles of carbon and silicon. *Earth Surf. Proc. Landf.* 33, 1436–1457. doi: 10.1002/esp.1712

Struyf, E., and Conley, D. J. (2012). Emerging understanding of the ecosystem silica buffer. *Biogeochemistry* 107, 9–18. doi: 10.1007/s10533-011-9590-2

Struyf, E., Smis, A., Van Damme, S., Garnier, J., Govers, G., Van Wesemae, B., et al. (2010). Historical land use change has lowered terrestrial silica mobilization. *Nat. Commun.* 1:129. doi: 10.1038/ncomms1128

Sunagawa, S., Coelho, L. P., Chaffron, S., Kultima, J. R., Labadie, K., Salazar, G., et al. (2015). Structure and function of the global ocean microbiome. *Science* 348:1261359. doi: 10.1126/science.1261359

Tang, T., Kisslinger, K., and Lee, C. (2014). Silicate deposition during decomposition of cyanobacteria may promote export of picophytoplankton to the deep ocean. *Nat. Commun.* 5:4143. doi: 10.1038/ncomms5143

Thamatrakoln, K., and Hildebrand, M. (2008). Silicon uptake in diatoms revisited: a model for saturable and nonsaturable uptake kinetics and the role of silicon transporters. *Plant Physiol.* 146, 1397–1407. doi: 10.1104/pp.107.107094

Tréguer, P. J., and De La Rocha, C. L. (2013). The world ocean silica cycle. *Ann. Rev. Mar. Sci.* 5, 477–501. doi: 10.1146/annurev-marine-121211-172346

Trembath-Reichert, E., Wilson, J. P., McGlynn, S. E., and Fischer, W. W. (2015). Four hundred million years of silica biomineralization in land plants. *Proc. Natl. Acad. Sci. U.S.A.* 112, 5449–5454. doi: 10.1073/pnas.1500289112

Uriz, M. -J. (2006). Mineral skeletogenesis in sponges. *Can. J. Zool.* 84, 322–356. doi: 10.1139/z06-032

Van Cappellen, P. (2003). Biomineralization and global biogeochemical cycles. *Rev. Mineral. Geochem.* 54, 357–381. doi: 10.2113/0540357

Van Cappellen, P., Dixit, S., and van Beusekom, J. (2002). Biogenic silica dissolution in the oceans: Reconciling experimental and field-based dissolution rates. *Glob. Biogechem. Cycles* 16:1075. doi: 10.1029/2001GB001431

van den Boorn, S. H., van Bergen, M. J., Nijman, W., and Vroon, P. Z. (2007). Dual role of seawater and hydrothermal fluids in Early Archean chert formation: evidence from silicon isotopes. *Geology* 35, 939–942. doi: 10.1130/G24096A.1

van den Boorn, S. H. J. M., van Bergen, M. J., Vroon, P. Z., de Vries, S. T., and Nijman, W. (2010). Silicon isotope and trace element constraints on the origin of ∼3.5 Ga cherts: implications for Early Archaean marine environments. *Geochim. Cosmochim. Acta* 74, 1077–1103. doi: 10.1016/j.gca.2009.09.009

Van de Poel, B., Cooper, E. D., Van Der Straeten, D., Chang, C., and Delwiche, C. F. (2016). Transcriptome profiling of the green alga *Spirogyra pratensis* (Charophyta) suggests an ancestral role for ethylene in cell wall metabolism, photosynthesis, and abiotic stress responses. *Plant Physiol.* 172, 533–545. doi: 10.1104/pp.16.00299

Vanneste, K., Sterck, L., Myburg, A. A., Van de Peer, Y., and Mizrachic, E. (2015). horsetails are ancient polyploids: evidence from *Equisetum giganteum*. *Plant Cell* 27, 1567–1578. doi: 10.1105/tpc.15.00157

van Tol, H. M., Irwin, A. J., and Finkel, Z. V. (2012). Macroevolutionary trends in silicoflagellate skeletal morphology: the costs and benefits of silicification. *Paleobiology* 38, 391–402. doi: 10.1666/11022.1

Walker, J. C. G., Hays, P. B., and Kasting, J. F. (1981). A negative feedback mechanism for the long-term stabilization of Earth's surface-temperature. *J. Geophys. Res. Oceans Atmosp.* 86, 9776–9782. doi: 10.1029/JC086iC10p09776

Wen, H., Fan, H., Tian, S., Wang, Q., and Hu, R. (2016). The formation conditions of the early Ediacaran cherts, South China. *Chem. Geol.* 430, 45–69. doi: 10.1016/j.chemgeo.2016.03.005

West, A. J., Galy, A., and Bickle, M. (2005). Tectonic and climatic controls on silicate weathering. *Earth Planet. Sci. Lett.* 235, 211–228. doi: 10.1016/j.epsl.2005.03.020

Wille, M., Sutton, J., Ellwood, M. J., Sambridge, M., Maher, W., Eggins, S., et al. (2010). Silicon isotopic fractionation in marine sponges: a new model for understanding silicon isotopic fractionation in sponges. *Earth Planet. Sci. Lett.* 292, 281–289. doi: 10.1016/j.epsl.2010.01.036

Yamada, K., Yoshikawa, S., Ichinomiya, M., Kuwata, A., Kamiya, M., and Ohki, K. (2014). Effects of silicon-limitation on growth and morphology of *Triparma laevis* NIES-2565 (Parmales, Heterokontophyta). *PLoS ONE* 9:e103289. doi: 10.1371/journal.pone.0103289

Yee, N., Phoenix, V. R., Konhauser, K. O., Benning, L. G., and Ferris, F. G. (2003). The effect of cyanobacteria on silica precipitation at neutral pH: Implications for bacterial silicification in geothermal hot springs. *Chem. Geol.* 199, 83–90. doi: 10.1016/S0009-2541(03)00120-7

Yool, A., and Tyrrell, T. (2005). Implications for the history of Cenozoic opal deposition from a quantitative model. *Palaeogeogr. Palaeoclimatol. Palaeoecol.* 218, 239–255. doi: 10.1016/j.palaeo.2004.12.017

Zheng, X. -Y., Beard, B. L., Reddy, T. R., Roden, E. E., and Johnson, C. M. (2016). Abiologic silicon isotope fractionation between aqueous Si and Fe(III)–Si gel in simulated Archean seawater: implications for Si isotope records in Precambrian sedimentary rocks. *Geochim. Cosmochim. Acta* 187, 102–122. doi: 10.1016/j.gca.2016.05.012

Conflict of Interest Statement: The authors declare that the research was conducted in the absence of any commercial or financial relationships that could be construed as a potential conflict of interest.

Copyright © 2017 Conley, Frings, Fontorbe, Clymans, Stadmark, Hendry, Marron and De La Rocha. This is an open-access article distributed under the terms of the Creative Commons Attribution License (CC BY). The use, distribution or reproduction in other forums is permitted, provided the original author(s) or licensor are credited and that the original publication in this journal is cited, in accordance with accepted academic practice. No use, distribution or reproduction is permitted which does not comply with these terms.

frontiers in Marine Science

ORIGINAL RESEARCH
published: 30 November 2017
doi: 10.3389/fmars.2017.00373

Assessing the Potential of Sponges (Porifera) as Indicators of Ocean Dissolved Si Concentrations

Belinda Alvarez, Patrick J. Frings†, Wim Clymans†, Guillaume Fontorbe and Daniel J. Conley*

Department of Geology, Lund University, Lund, Sweden

OPEN ACCESS

Edited by:
Brivaela Moriceau, Centre National de la Recherche Scientifique (CNRS), France

Reviewed by:
Sönke Hohn, Leibniz Centre for Tropical Marine Research (LG), Germany
Paco Cardenas, Uppsala University, Sweden

****Correspondence:***
Belinda Alvarez
belinda.alvarez@geol.lu.se

†Present Address:
Patrick J. Frings, Department of Geoscience, Swedish Museum of Natural History, Stockholm, Sweden and Earth Surface Geochemistry, GFZ German Research Centre for Geosciences, Potsdam, Germany
Wim Clymans, Earthwatch Institute (Europe), Oxford, United Kingdom

Specialty section:
This article was submitted to Marine Biogeochemistry, a section of the journal Frontiers in Marine Science

Received: *12 April 2017*
Accepted: *07 November 2017*
Published: *30 November 2017*

Citation:
Alvarez B, Frings PJ, Clymans W, Fontorbe G and Conley DJ (2017) Assessing the Potential of Sponges (Porifera) as Indicators of Ocean Dissolved Si Concentrations. Front. Mar. Sci. 4:373. doi: 10.3389/fmars.2017.00373

We explore the distribution of sponges along dissolved silica (dSi) concentration gradients to test whether sponge assemblages are related to dSi and to assess the validity of fossil sponges as a palaeoecological tool for inferring dSi concentrations of the past oceans. We extracted sponge records from the publically available Global Biodiversity Information Facility (GBIF) database and linked these records with ocean physiochemical data to evaluate if there is any correspondence between dSi concentrations of the waters sponges inhabit and their distribution. Over 320,000 records of Porifera were available, of which 62,360 met strict quality control criteria. Our analyses was limited to the taxonomic levels of family, order and class. Because dSi concentration is correlated with depth in the modern ocean, we also explored sponge taxa distributions as a function of depth. We observe that while some sponge taxa appear to have dSi preferences (e.g., class Hexactinellida occurs mostly at high dSi), the overall distribution of sponge orders and families along dSi gradients is not sufficiently differentiated to unambiguously relate dSi concentrations to sponge taxa assemblages. We also observe that sponge taxa tend to be similarly distributed along a depth gradient. In other words, both dSi and/or another variable that depth is a surrogate for, may play a role in controlling sponge spatial distribution and the challenge is to distinguish between the two. We conclude that inferences about palaeo-dSi concentrations drawn from the abundance of sponges in the stratigraphic records must be treated cautiously as these animals are adapted to a great range of dSi conditions and likely other underlying variables that are related to depth. Our analysis provides a quantification of the dSi ranges of common sponge taxa, expands on previous knowledge related to their bathymetry preferences and suggest that sponge taxa assemblages are not related to particular dSi conditions.

Keywords: sponge assemblages, palaeoecological indicators, spatial distribution, dissolved silica gradient, depth gradient, Si cycle

INTRODUCTION

Sponges are aquatic, sessile, benthic, and filter feeding organisms that belong to the animal phylum Porifera. Their body structure is simple, with different kinds of cells specialized in a variety of life functions and organized in different layers according to their function (Hooper and Van Soest, 2002; Van Soest et al., 2012; Maldonado, 2014). Their origins have been placed in the Cambrian

(Hooper and Van Soest, 2002; Xiao et al., 2005), or even before as suggested by the discovery of potential sponge biomarkers (Love et al., 2009; Yin et al., 2015; Gold et al., 2016).

Four classes of sponges are currently recognized: Calcarea, which includes species with calcareous skeletons; Hexactinellida, commonly known as glass sponges; Demospongiae, containing the majority of extant sponges; and the Homoscleromorpha (Hooper and Van Soest, 2002; Morrow and Cárdenas, 2015; Van Soest et al., 2017). The last three classes include species with siliceous skeletons cemented by organic components (i.e., a collagen-like protein, spongin), as well as species that lack a mineral (i.e., neither siliceous nor calcareous) skeleton and are constructed with spongin skeletons, occasionally reinforced with foreign inorganic elements (e.g., sand or remains of biogenic silica from other organisms, including sponges; Hooper and Van Soest, 2002).

Through complex enzymatic and metabolic processes (Wang et al., 2011a,b, 2012a), siliceous species of Hexactinellida, Demospongiae and Homoscleromorpha take up Si (predominantly present as silicic acid, H_4SiO_4 and conventionally referred to as dissolved silica; dSi) from their surrounding water to secrete individual structures known as spicules which provide skeletal support to the organic components of the sponge (Uriz et al., 2003). In some species of hexactinellids and demosponges, skeletal structures are massive and hypersilicified, with stony consistency and can form agglomerates and build reef-like formations (Conway et al., 2001; Uriz et al., 2003; Leys et al., 2004; Maldonado et al., 2015a,b) or "sponge grounds" (Klitgaard and Tendal, 2004). Sponges of these groups may be important players in the global silicon cycle due to their widespread occurrence and high preservation potential (Maldonado et al., 2005, 2010).

Silica uptake and silicification in sponges is regulated by the availability of dSi in the ambient water and dSi uptake conforms to enzymatic (Michalis-Menten) kinetics with maximal uptake rates occurring only above 100–200 μM dSi (Reincke and Barthel, 1997; Maldonado et al., 1999, 2011). These values are higher than typical concentrations in most of the modern ocean, suggesting sponge dSi uptake mechanisms evolved in higher dSi waters (Maldonado et al., 2015a) and dSi is a limiting factor for living sponges (Maldonado et al., 2011). Maldonado et al. (1999) also showed that secretion of certain spicule types is regulated by dSi thresholds and suggested that instances of these spicules in fossil sponges reflect dSi replete environments. Efficient mechanisms to utilize dSi have evolved in sponges (Müller et al., 2003; Schröder et al., 2004; Wang et al., 2012a,b) and involve the presence of silicatein, an enzyme that is able to control and catalyze the intracellular deposition of dSi from an unsaturated environment, as well as proteins that actively transport dSi across the cell membranes (Schröder et al., 2004; Marron et al., 2016).

Additional information about variations in the shape, or size of sponge spicules, or about disrupted spiculogenesis (shape changes, atrophies or other malformation of spicules) in relation to dSi concentration is scattered throughout the literature (Jørgensen, 1944; Hartman, 1958; Stone, 1970; Yourassowsky and Rasmont, 1984; Zea, 1987; Bavestrello et al., 1993; Rützler and Smith, 1993; Schönberg and Barthel, 1997; Mercurio et al., 2000; Valisano et al., 2012; Cárdenas and Rapp, 2013). Overall these studies show that the availability of dSi is a factor that can affect the morphology, composition or size of spicules in some species.

If spicule morphology and/or morphometrics are affected by dSi and given that these are the main underlying characters used for the classification of siliceous sponges (Hooper and Van Soest, 2002), some taxa or taxa assemblages may be characteristic of habitats with particular dSi conditions. These might conceivably have different adaptation mechanisms and therefore, differentially influence the ocean Si cycle. An essential first step to use sponges as indicators is recognizing and quantifying any causal relationship between modern sponge distributions and the underlying environmental drivers; this is the crucial first step in palaeoecological proxy development (e.g., Birks, 1995).

The spatial distribution of Porifera has been studied at local and regional scales and has been related to different environmental factors. Differences in sponge species composition between shallow and deep waters have been acknowledged for decades. De Laubenfels (1936) recognized that the spatial distribution of shallow water sponges is limited by strong environmental barriers (e.g., depth, light or temperature). More recently, the spatial distribution of marine sponges at local scales (e.g., 10 s of km; coral reefs, straits or gulfs) has been correlated to geomorphological features (Przeslawski et al., 2014), sediment properties, depth, distance to the coast, nutrient availability (including dSi), light penetration, hydrodynamics (Huang et al., 2011), deep sea currents (Cárdenas and Rapp, 2015), and biotic factors such as predation or competition for space (Huang et al., 2011; Pawlik et al., 2015; Slattery and Lesser, 2015). In general, these observations are replicated at regional or broader scales (e.g., >>100 km; seas or oceans). Here, sponge distributions have been related to depth, temperature and light availability (Vacelet, 1988; Finks and Keith Rigby, 2003; Leys et al., 2004; Downey et al., 2012), or to biogeographic regions (Hooper and Lévi, 1994; Van Soest, 1994; Van Soest et al., 2012) delimited by underlying abiotic drivers and characteristic marine biotas (e.g., Spalding et al., 2007). Interestingly, results from predictive models using physico-chemical environmental variables (Huang et al., 2011) and regional surveying (Howell et al., 2016) suggest that temperature, depth and nutrient status—including dSi—are major drivers controlling sponge distribution.

There is potential for sponge species composition and spicule morphology in the sedimentary record to yield insight into dSi at the time of their formation. The reconstruction of paleo-dSi is receiving increasing attention, partly motivated by the linkages between the long-term carbon and silicon biogeochemical cycles (Conley et al., 2000; Frings et al., 2016). To date, dSi reconstruction using sponges has been achieved by exploring morphometric relationships of fresh-water spicules through dSi gradients (Kratz et al., 1991). More recently, silicon isotope analysis of sponge spicules has exploited the observation that the fractionation of stable Si isotopes between ambient dSi and the biogenic Si in spicules is a function of dSi concentration in the surrounding environment (Hendry et al., 2010, 2011; Wille

et al., 2010; Hendry and Robinson, 2012; Fontorbe et al., 2016, 2017). The development of a complementary palaeoecological approach based on taxa assemblages could greatly extend the understanding of dSi changes in past and present oceans. By estimating the distributions of sponge taxa along a dSi gradient, particular species assemblages can be identified to provide insight into past Si dynamics in ocean and coastal environments.

In this work we explore the distribution of sponges along dSi gradients to test whether sponge assemblages are a function of dSi and to assess the validity of sponge taxonomy as a palaeoecological tool for inferring palaeo-concentrations of dSi. To achieve this we extracted and combined information from publically available oceanographic and biodiversity databases to evaluate the dSi conditions where sponges are found in the global ocean. Because dSi is correlated with depth in the modern ocean, we also explore taxa distributions as a function of depth. In general, we find that while there are hints of an assemblage-dSi relationship, sponges are not sufficiently differentiated as a function of dSi availability to clearly indicate specific dSi concentrations, a conclusion with implications for reconstructions of the ocean Si cycle.

MATERIALS AND METHODS

Data Sources

We used sponge records held in the Global Biodiversity Information Facility (GBIF) and a gridded climatology of ocean chemistry data, interpolated from measurements, from the World Ocean Circulation Experiment (WOCE) (Gouretski and Koltermann, 2004). This is available with a horizontal grid resolution of 0.5° and with 40 unevenly spaced vertical layers. GBIF is an international open data infrastructure and the world's largest biodiversity database, and provides a freely available, single point access to millions of biodiversity records (http://www.gbif.org/what-is-gbif). GBIF aggregates data from a variety of sources of variable extent, quality and taxonomic precision (see www.gbif.org for more information). WOCE is a global data resource of the US National Oceanic and Atmospheric Administration ultimately based on observations from ships, floats, drifters and satellites. We interrogated GBIF via the online portal (http://www.gbif.org/occurrence) and downloaded 323,953 georeferenced records of Porifera available in November 2016 (GBIF Occurrence Download: https://doi.org/10.15468/dl.viufhq). The taxonomic classification of species in these records follows that of the World Porifera Database (WPD, http://www.marinespecies.org/porifera/news.php?p=show&id=4893). Only records with an associated depth (143,275; 44%) were used in the analyses. Paleontological records and freshwater taxa included in the dataset were also removed (830 and 192 records, respectively). To validate the geolocation data of GBIF, we compared the water depth associated with each record with the ETOPO1 1 Arc-Minute Global Relief Model (Amante and Eakins, 2009). Because both datasets contain variable quality and resolution depth data, records that disagreed by more than 500 m were discarded. Agreement was taken as a sign of confidence in the depth data. This 500 m threshold was selected (rather arbitrarily) to allow for (i) the possibility of steep bathymetry at spatial scales below that of ETOPO1 and (ii) the inclusion of dredge samples, where only the trawl start or finish point is given. This quality control process lead to the exclusion of 5,190 (ca. 3.6%) of datapoints, which in some cases were in disagreement by $>$ 6000 m (see Supplementary Figure 1). In addition, any remaining records which were flagged within GBIF as having a "non-numeric" or "non-metric" depth in the original dataset (13,317 and 5,060, respectively) were removed, to avoid any conversion issues.

Information at the level of class and order, missing in some of the GBIF records although the lower taxonomic rank of family or genus was given, was added following the WPD. GBIF contains a mixture of reliable and unreliable taxonomic information (Van Soest et al., 2012), and includes records with taxonomic identifications derived from photographs and/or video-recordings, which e.g., Leys et al. (2004) have identified as a source of uncertainty. We assumed that the taxonomic identifications included in the GBIF records at the level of order and family are more accurate than those from lower levels (genera and species), which generally require a greater degree of taxonomic expertise. For this reason we limit our analyses to the level of family and above (order and class). Our analyses could be improved and extended to a higher taxonomic resolution with an increase in the reliability of taxonomic identifications of GBIF records.

The final dataset for this study included 62,360 discrete, globally distributed records (**Figure 1**). Of these, 2,905 are classified only as far as class, 890 only as far as order (31 different orders), 2086 to family level (128 different families), 24,525 to the level of genus (555 different genera) and the remainder (31,955) to species (2,758 different species) or subspecies. For comparison, the World Porifera Database (Van Soest et al., 2017) currently recognizes 32 extant orders, 149 extant families and 740 extant genera, implying we capture a large proportion of total global sponge biodiversity.

For each individual sponge observation in GBIF, ocean temperature, salinity and nutrient concentrations (nitrate, phosphate and dSi) were extracted from WOCE (Gouretski and Koltermann, 2004) from the box enclosing the recorded sponge location. A summary of the data, including counts, maxima, minima and averages for each variable on a taxa-by-taxa basis for each of the families represented in the data set is provided (Supplementary Table 1).

Effect of Sampling Techniques and Sampling Effort

dSi concentrations in ocean bottom waters and the locations of the sponge records from the dataset are shown in **Figure 1**. Most of the records examined are limited to shallow water collections where dSi is generally low, which we attempt to account for in our analysis (see below). However other sampling biases might also be present. For instance, deep sea habitats are usually sampled with trawls or dredges. These generally catch

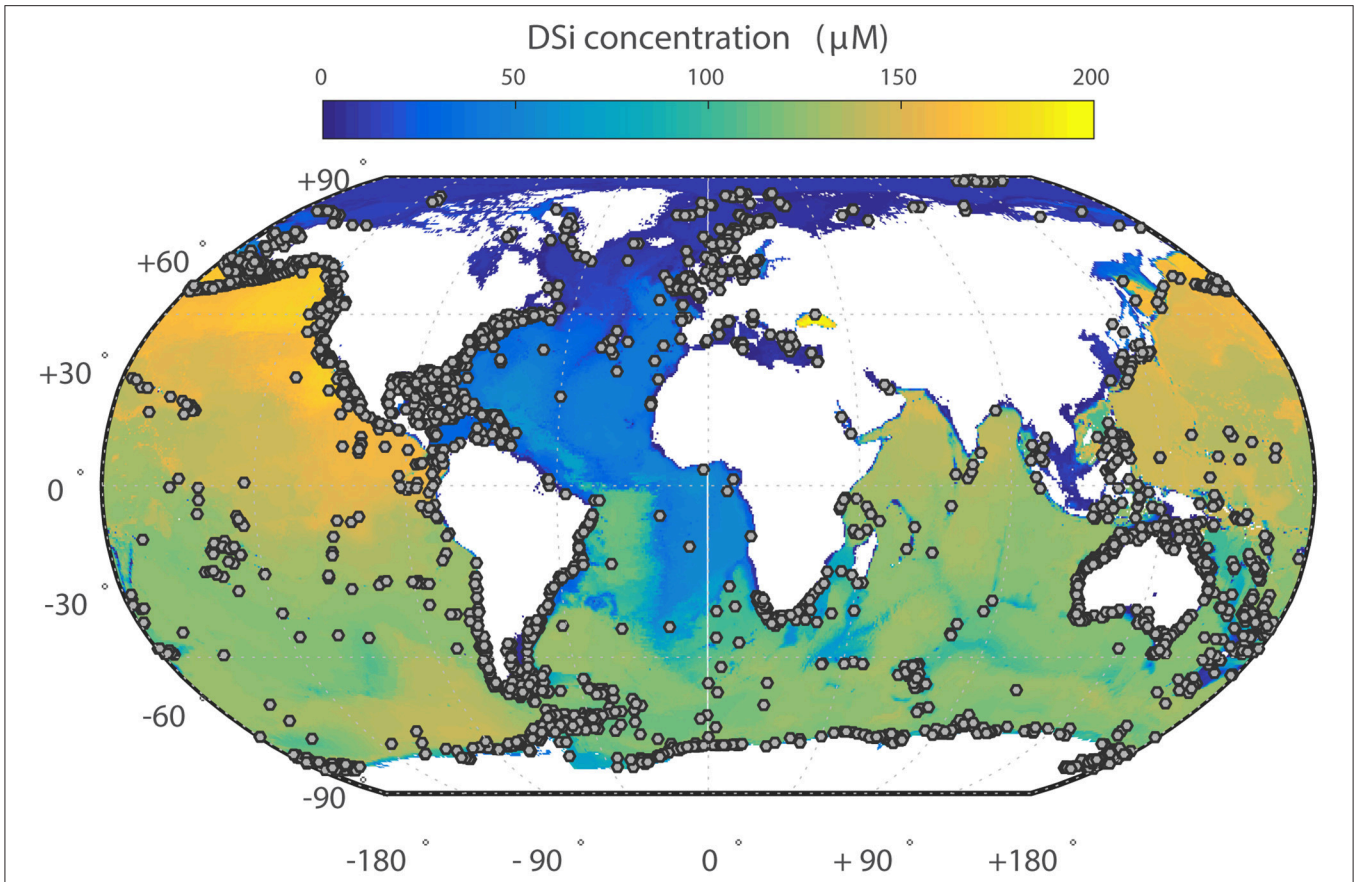

FIGURE 1 | Ocean dissolved silica concentrations in bottom waters (i.e., seafloor). Gray dots indicate the location of individual sponge records included in this manuscript from GBIF.

abundant, large or hard specimens, but groups represented by small or fragile individuals (e.g., Cladorhizidae and Calcarea) are often not recovered (Raff et al., 1994), and therefore might be underrepresented. At present, quantifying the scale and significance of this bias is not possible.

We investigated the impact of very intense sampling within small regions by first regarding the taxa as only present or absent for each box in the WOCE dataset, and calculating the global distribution along an environmental gradient using 20 equally spaced bins for each variable (shown for dSi in **Figure 2A**). The presence/absence aggregation made only a very minor difference to the distribution of taxa along environmental gradients (**Figure 2B**), so we proceed with the full (i.e., non-aggregated) dataset. To crudely address a sampling bias toward continental shelves and shallow water areas in GBIF records we normalized the taxa distributions to the total Porifera distribution (**Figure 2**) to obtain a suite of distributions that describe the relative importance of individual taxa to the total Porifera population along any given environmental gradient. This approach implicitly assumes that sampling and identification of the Porifera records is not biased toward one group of taxa and is not suitable for e.g., calibrating individual sponge taxa environmental preferences. However, the intent here is not to estimate the true distribution of sponge taxa in the global ocean, but rather to explore relative differences *among* taxa. In the Supplementary Table 1 we show a summary of the uncorrected data.

Violin Plots

For taxa that are abundant (more than 100 records in GBIF), violin plots of the normalized data as a function of underlying environmental gradients were created at different levels of taxonomic classification (class, order, and family) and form the basis of further discussion. Where applicable, we include sponge species (referred to as "lithistids" hereafter) with highly silicified skeletons that were previously classified in the polyphyletic order Lithistida (Pisera and Lévi, 2002) but are now divided among unrelated orders of the class Demospongiae (Cárdenas et al., 2012). In these plots, the width of the bars indicates the relative contribution of the taxa to the total of all sponge taxa recorded in GBIF at the corresponding value of the environmental variable; note these are further standardized to the maximum contribution of that taxa, so do not contain any useful information about the absolute abundance of any given taxa, which is not possible with the "presence-only" GBIF data.

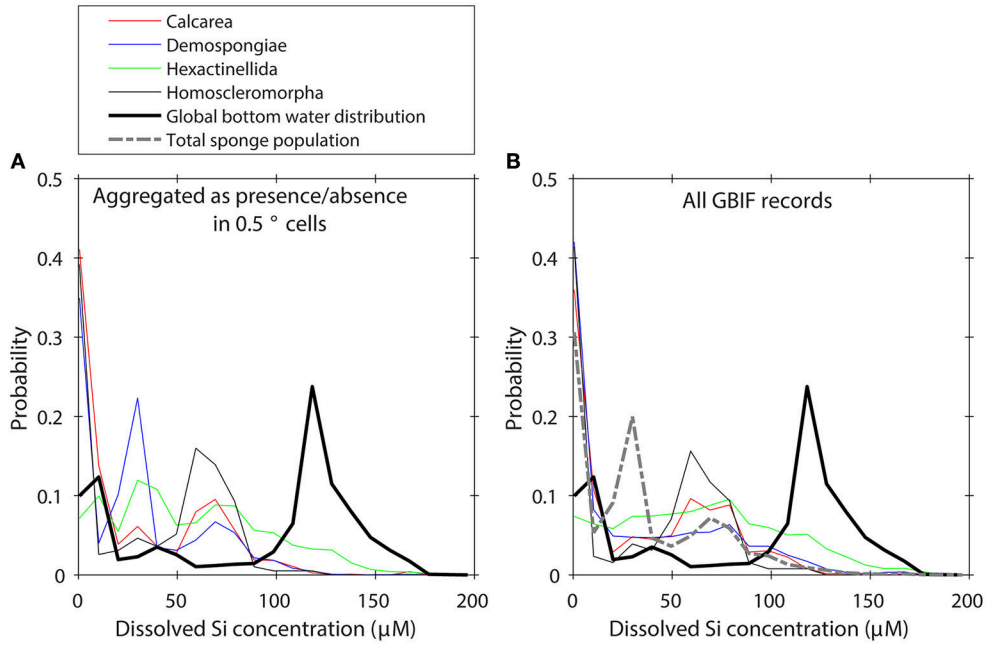

FIGURE 2 | (A) Global distribution of GBIF records aggregated as presence/absence values in 0.5° boxes of the WOCE dataset. **(B)** Global distribution of GBIF records without correction for sampling bias.

RESULTS

The relative frequency distribution of sponge taxa vs. dSi and depth is shown in **Figures 3–5**. At the level of class the Hexactinellida are found across broad ranges of dSi (0–180 µM; **Figure 3A**) and depth (0–6,000 m; **Figure 3B**). Sponges with calcareous skeletons show similar distributions but are a greater relative contributor to total sponge taxa at dSi <100 µM and < 3,000 m depth. The rest of the classes are also found in the same range, however their major contributions to the total are below 120 µM and shallower than 1,000 m for the siliceous classes Homosclerophorida and Demospongiae.

In our analysis, 19 of the 32 total sponge orders are represented within GBIF in at least 100 boxes of the WOCE dataset (**Figure 4**). A majority occur seem dominantly at dSi <50 µM, while other groups of demosponges (Tethyida, Suberitida Polymastiida and Haplosclerida), hexactinellids (Hexactinosa and Lyssacinosida), homosclerophorids and the Clathrinida are more evenly distributed along the dSi gradient. The hexactinellid order Amphidiscosida make their greatest contributions to sponge assemblages in environments with dSi>100 µM and the calcarean order Leucosolenida shows a bimodal distribution. **Figure 4B** shows the distribution of the same orders as a function of depth. A comparison between the two plots indicates that orders with relatively more frequent occurrences at higher dSi are also represented at depths greater than 2,000 m. The demosponge orders without siliceous skeletons (i.e., Dendroceratida, Verongiida –excluding some species (Ehrlich et al., 2010), and the Clionaida are not found in the GBIF database at depths greater than 1000 m. The distribution of lithistids along the depth gradient indicates this group is a relatively consistent contributor to total sponge assemblages at dSi below 50 µM and is not found at depths greater than 2,500 m.

At the highest level of taxonomic resolution that we consider, 43 families within Porifera occur in 100 or more WOCE boxes (for reference, there are 149 currently recognized families within Porifera; Van Soest et al., 2017). Their distributions follow similar tendencies to those shown at the level of order, with some families better represented at dSi<50 µM, some approximately equally represented along the gradient, some occurring at both high and low dSi and others more likely to be found at dSi>100 µM (**Figure 5A**). Distribution of these families along the depth gradient (**Figure 5B**) roughly tracks the dSi gradient. Families that occur at high dSi such as the Cladorhizidae, and Polymastiidae and all of the hexactinellids, are also likely to occur in deep waters. Non-siliceous sponges of the orders Verongiida, Dictyoceratida and Dendroceratida, with the exception of Spongiidae (see discussion below), are found within the group of taxa that occur at dSi <20 µM, together with the family Clionidae (usually sponges associated with calcium carbonate substrates) but also with families that have siliceous skeletons (i.e., Petrosiidae, Dictyonellidae and Callyspongiidae). These are only found at shallow depths (**Figures 5A,B**).

DISCUSSION

Our analysis provides a quantification of the dSi ranges of common sponge taxa and expands on previous knowledge

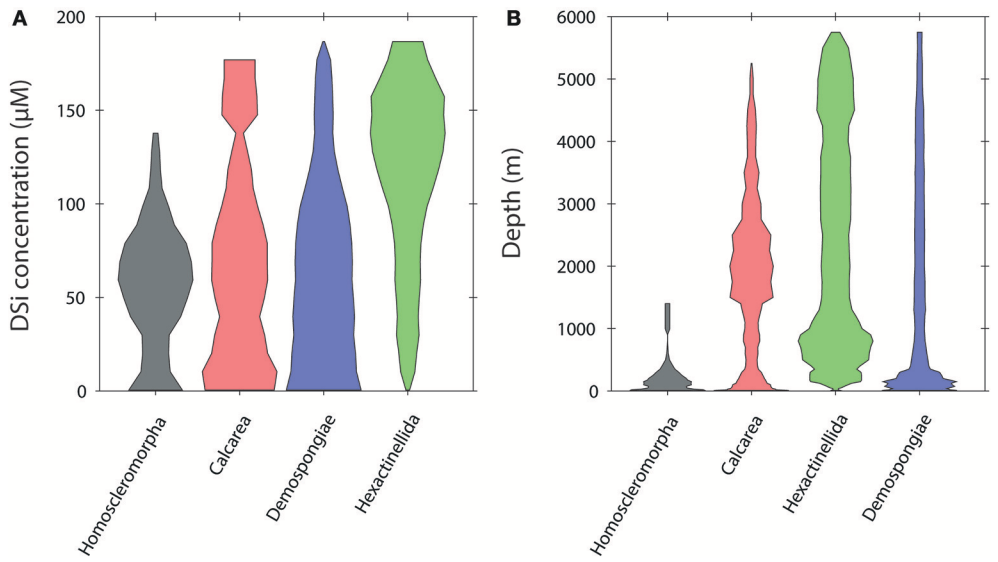

FIGURE 3 | Violin plots showing the distribution of the sponge classes in a dSi gradient **(A)** and a depth gradient **(B)**.

related to their bathymetry (Vacelet, 1988; Maldonado and Young, 1998; Rapp et al., 2011; Downey and Janussen, 2015; Hestetun et al., 2015). The distribution of sponge taxa along a depth gradient exhibits clear similarities to dSi, meaning the challenge is to distinguish between the two.

Below, we discuss the role of dSi availability, and the effects of other variables that might be indirectly influencing the patterns presented here. We also discuss how this data might contribute to clarifying the role of sponges in the ocean Si cycle in the geological past, and the usefulness of sponge assemblage data as a marine palaeoecological tool.

Effects of dSi Availability and Habitat Depth on Sponge Distributions

Depth is an important factor controlling sponge distribution (Vacelet, 1988; Huang et al., 2011; Howell et al., 2016), though it acts indirectly via its correlation with ecologically meaningful parameters (including dSi concentrations, but also light, food availability, temperature, etc.,). It is evident that either dSi, depth or both play a major role controlling the spatial distribution of sponge taxa (**Figures 3**–**5**). Our results confirm that the Porifera are not uniformly distributed along either a dSi or a depth gradient. Because the differentiation along the two gradients is similar, it is unclear whether dSi availability, habitat depth, or another unidentified factor (or combination of factors), is driving the spatial distributions of sponges. At least at regional scales, water depth acts as a surrogate variable for light penetration, temperature, and nutrient concentrations; these all are inter-correlated and could be influencing sponge distributions (Vacelet, 1988). Other depth-related factors such as food resources (i.e., particulate and dissolved matter), turbulence, spatial competition, and predation have been suggested as drivers of sponge community structure and distribution (Pawlik et al., 2015; Slattery and Lesser, 2015).

Bottom-water temperature and concentration of some nutrients have also been identified as important variables controlling sponge distribution at local scales (Huang et al., 2011; Howell et al., 2016). However, the distribution of sponges as a function of temperature, dissolved oxygen and nutrient (nitrate and phosphate) concentrations extracted from WOCE (see Supplementary Material) revealed that the distribution of sponge taxa along these gradients is not strongly differentiated, in contrast to the dSi and depth gradients. Although we cannot exclude these factors, the fact that habitat depth shows a similar sponge distribution pattern with dSi is suggestive of dSi availability being an important driver of the spatial distribution of some sponge groups, and implies that sponge distribution as a function of depth simply reflects the general relationship between depth and [Si] (see below; **Figure 6**). Unfortunately, we cannot strictly identify the direction of causality and rule out the possibility that depth is simply acting as a surrogate for another, as yet unidentified variable.

In general, ocean dSi correlates with depth (Sarmiento and Gruber, 2006), as biogenic silica produced by siliceous plankton at the surface progressively dissolves as it sinks through the water column (although this pattern is somewhat complicated by the marine overturning circulation that acts to mix water-masses of varying ages, and therefore accumulated dSi) and because of high diatom production due to upwelling. To further explore this issue, we have plotted dSi and depth for all families included in our dataset in **Figure 6**. This confirms the presence of a positive relationship between dSi and depth with a similar form to that for the whole ocean (**Figure 6**).

Sponge Assemblages along dSi And Depth Gradients

Our data show that either depth or dSi play major roles controlling the spatial distribution of some

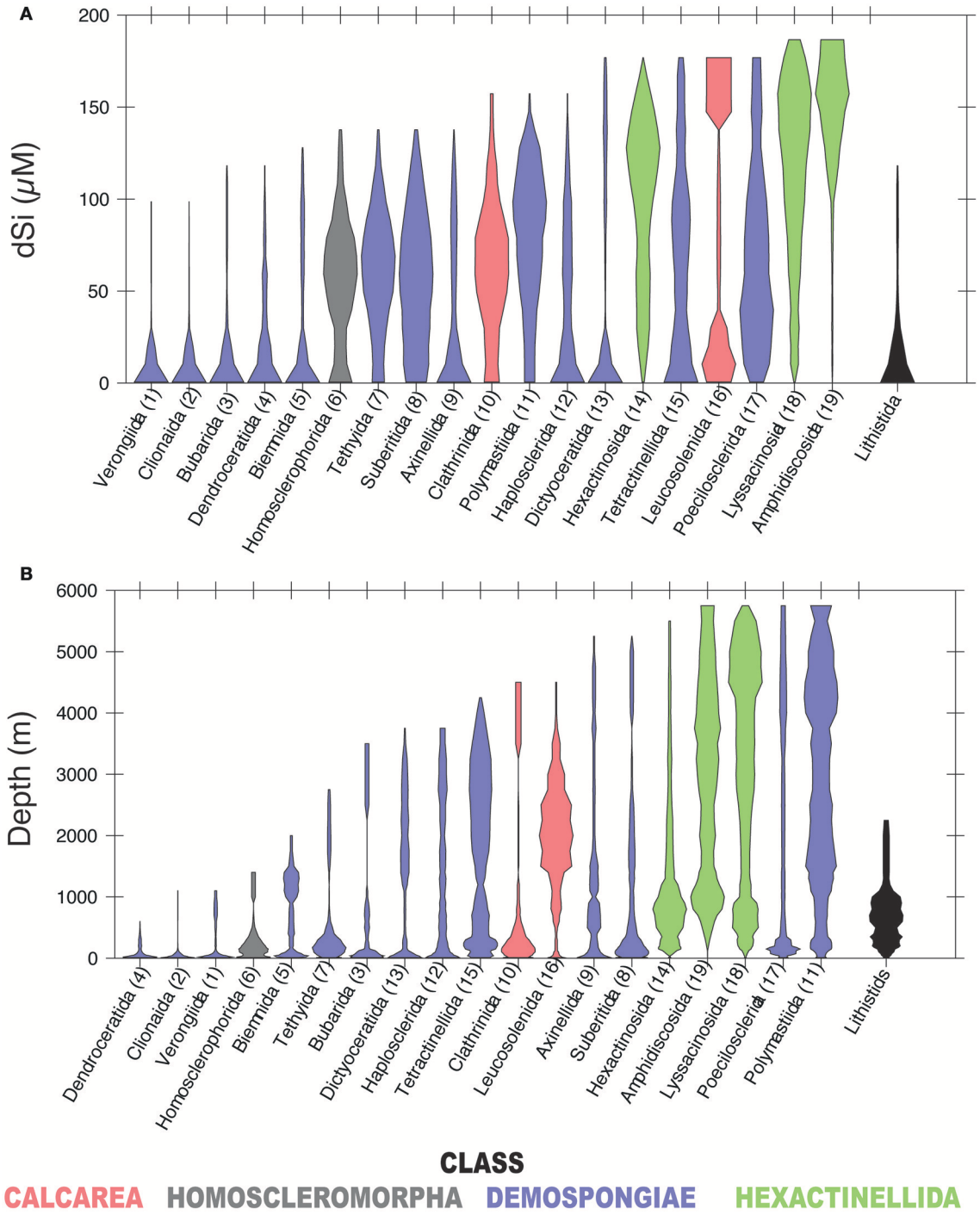

FIGURE 4 | Violin plots showing the distribution of sponge orders along the dSi gradient **(A)** and the depth gradient **(B)**. Only orders represented within GBIF in at least 100 boxes of WOCE dataset are shown. Numbers in parenthesis are codes given to each of the represented orders. Lithistids includes taxa assigned to this taxon by Pisera and Lévi (2002). Taxa with gray background include sponges without siliceous spicules. Color codes as in **Figure 3.**

taxa (**Figures 3–5**). Below we discuss which of those taxa might include species with different dSi uptake requirements and therefore could be indicative of dSi conditions.

Hexactinellida

Species of the order Hexactinosa (e.g., *Farrea occa, Aphrocallistes vastus* and *Heterochone calyx*) are known to construct hypersilicified skeletons and to form sponge reefs where

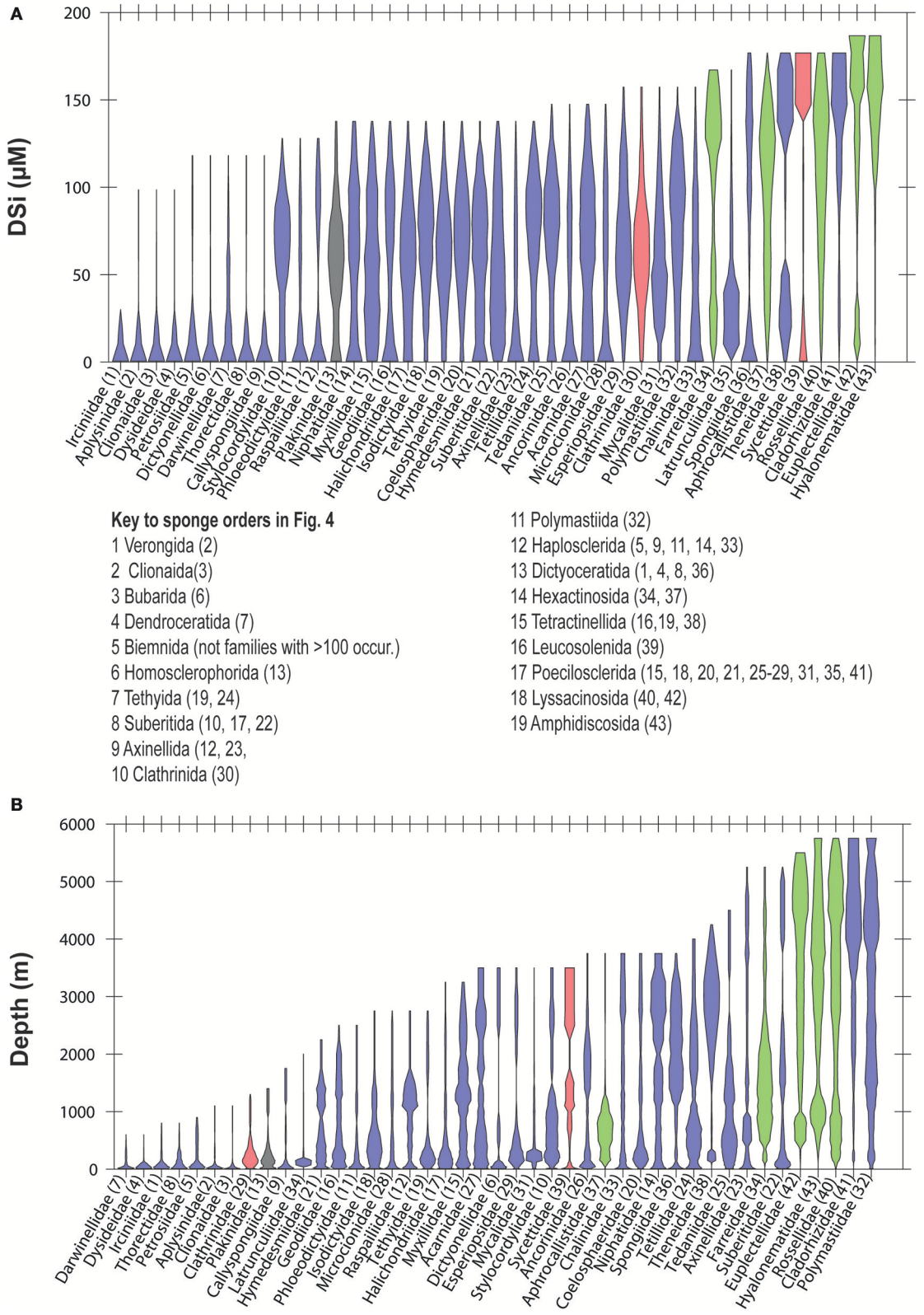

FIGURE 5 | Violin plots showing the distribution of sponge families in a dSi gradient **(A)** and a depth gradient **(B)**. Only families represented within GBIF in at least 100 boxes of WOCE dataset are shown. Numbers in parenthesis are codes given to each family. Taxa with gray background include sponges without siliceous spicules. A key to the orders represented in **Figure 4** is included. Color codes as in **Figure 3.**

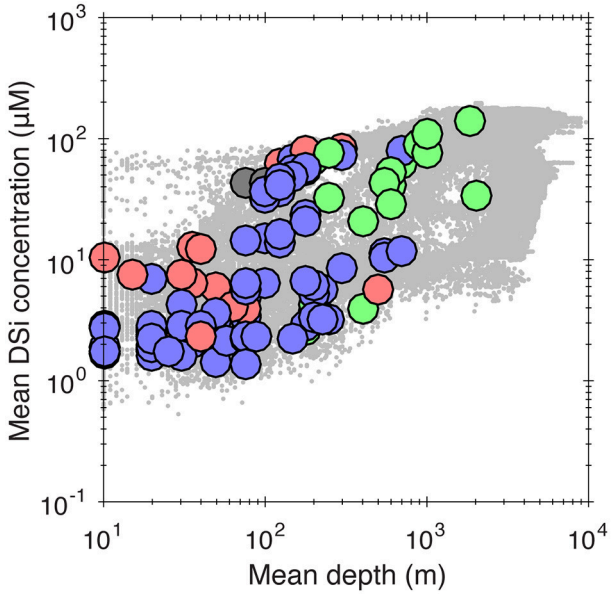

FIGURE 6 | Cross-plot of mean habitat depth and mean ambient dissolved Si concentrations for all sponge families in the GBIF database. See previous figures for key to colors. All taxa are included regardless of their abundance, unlike **Figures 3–5** where an occurrence criterion of 100 WOCE boxes is imposed. Data are aggregated at the presence/absence level for individual WOCE boxes. Gray dots in the background are ocean bottom water dSi concentrations (i.e., the same data as **Figure 1**).

dSi is reasonably high (ca. 40 µM), e.g., on the western coast of Canada (Leys et al., 2004; Conway et al., 2005; Whitney et al., 2005; Chu et al., 2011). The occurrence of these reef-building species is thought to be controlled by the combined action of particular oceanographic, geomorphological conditions and biotic factors, including dSi availability (Conway et al., 2005; Maldonado et al., 2015a). Hexactinosa (**Figure 4**) are important components of the sponge fauna at high dSi and depth together with species belonging to Amphidiscosida, Aulocalycoida, and Lyssacinosida (Rossellidae), which lack a dyctional (fused spicules in a 3D framework) skeleton suitable for reef formation but nevertheless have relatively more dSi per biomass unit than sponges from other sponge classes (Barthel, 1995).

Demospongiae

The families Cladorhizidae, and Polymastiidae are relatively more likely to be found in dSi rich waters (**Figure 5A**). These families have also a broad distribution range along depth gradients and are likely to be found in deep waters (>2,000 m) where dSi is also high. Whether or not the distribution of these taxa is driven by dSi or by depth remains to be answered. Detailed studies of dSi uptake mechanisms and rates of these sponge species, living in different dSi conditions will contribute to answer this question and to identify species that can be used as indicators of particular dSi ranges.

The remaining siliceous and non-siliceous demosponges are likely to be found in low dSi habitats, although some of those might occur at greater depths with high dSi. Some of Dictyoceratida families (i.e., Spongiidae), which lack siliceous skeletons, are likely to occur at high dSi and depth (**Figure 5**). This is an interesting observation because members of this group are conventionally thought to be found in tropical latitudes and shallow waters (Vacelet, 1988) and in some species the settlement of their larvae is affected by low temperatures, and light penetration (Maldonado, 2009). As far as we know, species of Spongiidae have not been reported from bathyal depths in the taxonomic literature. It is possible that these records might be misidentified, given that the taxonomy of these sponges is extremely difficult. However, until independent verification of these Dictyoceratida records we assume that their documentation in GBIF is correct, and therefore that other factors correlated to depth (including temperature, light penetration, nitrate or phosphate concentrations) are driving the occurrence of particular species of this group.

Lithistids

Sponges included in this polyphyletic (diverse phylogenetic affinities) group include species with articulated spicules called desmas, that form a rigid skeleton in most species (Pisera and Lévi, 2002). The majority (93%) of lithistid records are from the order Tetractinellida, and the most common families were Theonellidae (21%), Corallistidae (18%), and Scleritodermidae (17%). According to **Figure 4**, lithistid taxa are more likely to be found at <60 µM dSi, with the greatest relative frequency at <20 µM and <1,000 m. Some of them are known to build reef-like formations in habitats where dSi availability is low relative to that reported for the Hexactinosida reef-like builders (Maldonado et al., 2015a,b). Hypersilicified species lithistid (e.g., *Leiodermatium* spp) also cohabit with members of sponges without siliceous skeletons (i.e Dictyoceratida, Dendroceratida, and Verongiida) (Przeslawski et al., 2014, 2015) in relatively shallow habitats of northern Australia, with dSi concentrations <5 µM, exposed to strong tidal currents, high turbidity, and substantial sediment mobility (Przeslawski et al., 2011). As suggested by Maldonado et al. (2015b), some lithistid species seem to benefit from heavy sediment deposition, and patterns of local circulation that might deliver food and Si in pulses. It remains to be answered how these hypersilicified skeletons of lithistid species can develop in lower dSi and whether or not these species might have more efficient Si uptake systems than other taxa such as Hexactinosida which tend to be found in comparatively higher dSi (**Figures 4**, **5**).

Calcarea

The GBIF data shows that sponges of the class Calcarea are found in the depth gradient up to 5,000 m with peaks below 3,000 m. This confirms previous findings (Duplessis and Reiswig, 2000; Rapp et al., 2011) and suggest that the diversity of the group at abyssal depths is higher than previously thought, and that they are occasionally capable of growing in environments below carbonate mineral saturation.

Toward Quantification

There is a large body of literature that deals with methods to derive quantitative palaeoenvironmental reconstructions from (micro)fossil assemblages, in terrestrial, freshwater, and marine environments. As summarized in e.g., Telford and Birks (2005) or Juggins (2013), there is an increasing awareness of the limitations of these approaches, even in favorable situations. We have decided against a more quantitative approach for several reasons, including (i) GBIF data are compiled from disparate, unconnected sources with different sampling strategies, (ii) the higher end of the dSi gradient is poorly represented in the data, (iii) the data are "presence-only," rather than true species abundances, meaning taxa optima can not be easily defined, (iv) we have no independent model verification dataset, (v) variance-partitioning presumably will indicate a high degree of shared variance between depth and dSi, and (vi) the environmental calibration data has a hard-to-quantify noise component, being derived separately from the GBIF data at a lower spatial resolution.

In the future, a true sponge assemblage (with taxa abundances) and environmental variable dataset collected in a region or regions where dSi is decoupled from depth would be able to overcome some of these difficulties. Sponge silicon isotope ratios are becoming more widely used as a proxy for past-dSi concentrations (e.g., Fontorbe et al., 2017). Though not widely used, "mutual-range" approaches (Sinka and Atkinson, 1999), modern analog techniques (MAT; Lytle and Wahl, 2005), or artificial neural networks (Racca et al., 2007) may prove fruitful palaeoecological complements. Finally, lab- to field scale experiments carefully designed to extract the influence of dSi availability on sponge physiology and ecology, or approaches that seek to use individual spicule morphometrics (cf. Kratz et al., 1991) may also be part of the developing palaeo-dSi "toolbox."

Did dSi Control Sponge Distributions in the Past?

The evolution of the ocean Si cycle has received attention for many decades (e.g., Maliva et al., 1989; Kidder and Tomescu, 2016). The prevailing narrative (Maliva et al., 1989; Siever, 1991; Kidder and Tomescu, 2016) argues for two particularly important events. The first is a transition from a Precambrian ocean saturated with respect to dSi to a slightly undersaturated Mesozoic ocean. The second was a further decrease, sometime in the Cretaceous-Paleogene, in the dSi content of mean ocean water to a modern, dSi-deplete ocean. Both transitions are ascribed to biological innovations—the first to the evolution of silicification by radiolarians and sponges, and the second to the expansion of diatoms—and therefore biology's progressive ability to remove dSi from seawater. Superimposed on this long-term decline in ocean dSi, transient excursions in the ocean dSi inventory have been proposed in response to periods of extensive volcanism (particularly the emplacement of large igneous provinces, LIPs) (Ritterbush et al., 2014, 2015; Kidder and Tomescu, 2016), or orogenesis (e.g., Cermeño et al., 2015). One of the lines of evidence supporting these interpretations is a change in the sedimentary facies associated with sponges in the rock or sediment record (e.g., Kidder and Tomescu, 2016). The link between sponge abundances/distributions and dSi stems from the implicit assumption that siliceous sponges are unable to thrive at low dSi (e.g., Ritterbush et al., 2015; Kidder and Tomescu, 2016). Kidder and Tomescu (2016), for example, interpret an Ordovician retreat in sponges from lagoonal depositional environments toward deeper, shelf settings, as reflecting radiolarian driven dSi depletion of the surface ocean. After the mid-Ordovician, sponge fossils from peritidal and lagoonal facies are apparently rare in the fossil record (see Gammon et al., 2000) for a possible Eocene exception. Maliva et al. (1989) argue that sponges become quantitatively unimportant in the ocean Si cycle during the Cenozoic. To what extent are these putative changes in sponge abundance and distribution driven by dSi availability?

Our dataset shows that all sponge groups that are sufficiently sampled (i.e., >100 WOCE boxes, see Supplementary Table 1) are capable of growing in low dSi environments. Indeed, at least in some isolated instances, siliceous sponge taxa are capable of forming large reef-like aggregations at $<10\,\mu M$ dSi (Maldonado et al., 2015a,b). This implies that while any decline in dSi availability may have been a contributory factor to sponge exclusion from shallow water environments, other factors, perhaps related to the evolution, and ecology of sponge competitors should be taken into account. Therefore the presence of any given taxon cannot be in and of itself be indicative of the prevailing dSi concentrations.

For example, reef-building litihistid species, used as indicators of greater dSi availability in past environments (e.g., Corsetti et al., 2015; Ritterbush et al., 2015), are in our dataset more frequent $<20\,\mu M$ and $<$ 2,500 m. There is currently no evidence to suggest that they were unable to live in similar environments in the geological past (Pisera, 1997). The expansion of certain sponge groups after the Triassic-Jurassic extinction is more likely a consequence of a greater availability of suitable ecological niches vacated after the collapse of calcareous invertebrates in that period (Ritterbush et al., 2014, 2015).

Lastly it is important to mention that generally the majority of siliceous and non-siliceous sponges are not well represented in the fossil record as their skeletons are easily destroyed. Species with rigid skeletons, e.g., lithistids, some hexactinellids and fossil sponges with basal calcareous skeletons (i.e., Chaetetida and Stromatoporoidea) are more likely to be preserved, biasing the stratigraphic record (Pisera, 2006).

CONCLUSIONS

We show here that the distribution of sponges classified at the level of family is related to ambient dSi concentrations or habitat depth, or both. The distribution patterns along dSi concentrations or habitat depth indicate that the majority of taxa, including those in the class Calcarea without siliceous skeletons, occur in broad dSi (0–180 μM) and depth (0–~5,500 m) ranges. It also shows that the majority of demosponges without autochthonous siliceous skeletons are found at dSi $<20\,\mu M$ and shallow depths, but together with groups that

have skeletons made up of siliceous spicules. Demosponges with rigid siliceous skeletons and traditionally known as lithistids do not seem to be associated with deep environments rich in dSi indicating that these kind of sponges might have evolved particularly efficient mechanisms to incorporate and accumulate dSi in their skeletons. Hexactinellids on the other hand, also builders of strong and rigid siliceous skeletons are distributed along the dSi gradient but are more likely to be present in deep and silica-rich environments. The hexactinellids share this kind of environments with some demosponges evenly distributed along the dSi and depth gradient and mainly from the orders Cladorhizidae and Polymastiida.

The groups skewed to either low or high dSi might include species indicative of specific environmental Si conditions. As no unique or clear assemblage of taxa could be identified, additional information on Si uptake rates for possible indicative species is required to conclusively relate their spatial distribution to dSi levels. One might expect to see greater differentiation along environmental gradients if sponges are considered at the level of genera or even species, though we note that some genera (e.g., *Geodia*) are highly cosmopolitan. Similarly, studying dSi uptake mechanisms of sponge species occurring at a broad dSi and depth ranges could provide essential information on the adaptation potential of sponge taxa.

Links between the abundance of sponges in sedimentary records and the contemporary dSi concentrations should therefore be interpreted with caution, given these organisms are clearly adapted to live in a range of dSi concentrations and depth habitats, as seen in our results. Other biotic (e.g., competitive interactions) and abiotic factors (e.g., light penetration, temperature, nutrient and food availability), some of which are also related to depth, may be important factors in the distributions of modern sponges - and were probably equally important in palaeo-environments.

AUTHOR CONTRIBUTIONS

All authors listed have made a substantial, direct and intellectual contribution to the work, and approved it for publication. BA and PF are joint senior authors.

ACKNOWLEDGMENTS

This study was funded by a grant from the Knut and Alice Wallenberg Foundation to DC. Dmitry Schigel, GBIF and Merrick Ekins, Queensland Museum, provided valuable comments and suggestions related to the data downloaded from the GBIF portal. We thank all the suggestions and revisions of the reviewers.

SUPPLEMENTARY MATERIAL

The Supplementary Material for this article can be found online at: https://www.frontiersin.org/articles/10.3389/fmars.2017.00373/full#supplementary-material

REFERENCES

Amante, C., and Eakins, B. W. (2009). *Etopo1 1 Arc-Minute Global Relief Model: Procedures, Data Sources and Analysis*. NOAA Technical Memorandum NESDIS NGDC-24. Boulder, CO: National Geophysical Data Center, NOAA.

Barthel, D. (1995). Tissue composition of sponges from the Weddell Sea, Antarctica: not much meat on the bones. *Mar. Ecol. Prog. Ser.* 123, 149–153. doi: 10.3354/meps123149

Bavestrello, G., Bonito, M., and Sara, M. (1993). Silica content and spicular size variation during an annual cycle in *Chondrilla nucula* Schmidt (Porifera, Demospongiae) in the Ligurian Sea. *Sci. Mar.* 57, 421–425.

Birks, H. J. B. (1995). "Quantitative palaeoenvironmental reconstructions," in *Statistical Modelling of Quaternary Science Data*, eds D. Maddy and J. S. Brew (Cambridge, Quaternary Research Association), 161–254.

Cárdenas, P., Pérez, T., and Boury-Esnault, N. (2012). "Chapter two - sponge systematics facing new challenges," in *Advances in Marine Biology*, eds M. A. Becerro, M. J. Uriz, M. Maldonado, and X. Turon (London: Academic Press), 79–209.

Cárdenas, P., and Rapp, H. T. (2013). Disrupted spiculogenesis in deep-water Geodiidae (Porifera, Demospongiae) growing in shallow waters. *Invertebr. Biol.* 132, 173–194. doi: 10.1111/ivb.12027

Cárdenas, P., and Rapp, H. T. (2015). Demosponges from the Northern mid-atlantic ridge shed more light on the diversity and biogeography of North Atlantic deep-sea sponges. *J. Mar. Biol. Assoc. U.K.* 95, 1475–1516. doi: 10.1017/S0025315415000983

Cermeño, P., Falkowski, P. G., Romero, O. E., Schaller, M. F., and Vallina, S. M. (2015). Continental erosion and the Cenozoic rise of marine diatoms. *Proc. Natl. Acad. Sci. U.S.A.* 112, 4239–4244. doi: 10.1073/pnas.1412883112

Chu, J., Maldonado, M., Yahel, G., and Leys, S. (2011). Glass sponge reefs as a silicon sink. *Mar. Ecol. Prog. Ser.* 441, 1–14. doi: 10.3354/meps09381

Conley, D. J., Stålnacke, P., Pitkänen, H., and Wilander, A. (2000). The transport and retention of dissolved silicate by rivers in Sweden and Finland. *Limnol. Oceanogr.* 45, 1850–1853. doi: 10.4319/lo.2000.45.8.1850

Conway, K. W., Krautter, M., Barrie, J. V., and Neuweiler, M. (2001). Hexactinellid sponge reefs on the Canadian continental shelf: a unique "living fossil." *Geosci. Can.* 28, 71–78. Available online at: https://journals.lib.unb.ca/index.php/GC/article/view/4076

Conway, K. W., Krautter, M., Barrie, J. V., Whitney, F., Thomson, R. E., Reiswig, H., et al. (2005). *Sponge Reefs in the Queen Charlotte Basin, Canada: Controls on Distribution, Growth and Development* (Berlin: Springer-Verlag Berlin), 605–621.

Corsetti, F. A., Ritterbush, K. A., Bottjer, D. J., Greene, S., Ibarra, Y., Yager, J. A., et al. (2015). Investigating the paleoecological consequences of supercontinent breakup: sponges clean up in the early Jurassic. *Sediment. Rec.* 13, 4–10. Available online at: https://www.sepm.org/CM_Files/SedimentaryRecord/SedRecord13-2%235.pdf

De Laubenfels, M. W. (1936). A comparison of the shallow-water sponges near the Pacific end of the Panama Canal with those at the Caribbean end. *Proc. U.S. Natl. Mus.* 83, 441–464. doi: 10.5479/si.00963801.83-2993.441

Downey, R. V., Griffiths, H. J., Linse, K., and Janussen, D. (2012). Diversity and distribution patterns in high southern latitude sponges. *PLoS ONE* 7:e41672. doi: 10.1371/journal.pone.0041672

Downey, R. V., and Janussen, D. (2015). New insights into the abyssal sponge fauna of the Kurile–Kamchatka plain and trench region (Northwest Pacific). *Deep Sea Res. II Top. Stud. Oceanogr.* 111, 34–43. doi: 10.1016/j.dsr2.2014.08.010

Duplessis, K., and Reiswig, H. (2000). Description of a new deep-water calcareous sponge (*Porifera*: *Calcarea*) from Northern California. *Pac. Sci.* 54, 10–14. Available online at: http://hdl.handle.net/10125/1593

Ehrlich, H., Simon, P., Carrillo-Cabrera, W., Bazhenov, V. V., Botting, J. P., Ilan, M., et al. (2010). Insights into chemistry of biological materials: newly

discovered silica-aragonite-chitin biocomposites in demosponges. *Chem. Mat.* 22, 1462–1471. doi: 10.1021/cm9026607

Finks, R. M., and Keith Rigby, J. (2003). "Geographic and stratigraphic distribution," in *Treatise on Invertebrate Paleontology. Part E (Revised), Porifera,* Vol. 2, ed R. L. Kaesler (Boulder, CO; Lawrence, KS: The Geological Society of America & The University of Kansas), 275–296.

Fontorbe, G., Frings, P., De La Rocha, C. L., Hendry, K. R., and Conley, D. J. (2016). A silicon depleted North Atlantic since the Palaeogene: evidence from sponge and radiolarian silicon isotopes. *Earth Planet. Sci. Lett.* 453, 67–77. doi: 10.1016/j.epsl.2016.08.006

Fontorbe, G., Frings, P. J., De La Rocha, C. L., Hendry, K. R., Carstensen, J., and Conley, D. J. (2017). Enrichment of dissolved silica in the deep equatorial Pacific during the Eocene-Oligocene. *Paleoceanography* 32, 848–863. doi: 10.1002/2017PA003090

Frings, P. J., Clymans, W., Fontorbe, G., De La Rocha, C. L., and Conley, D. J. (2016). The continental Si cycle and its impact on the ocean Si isotope budget. *Chem. Geol.* 425, 12–36. doi: 10.1016/j.chemgeo.2016.01.020

Gammon, P. R., James, N. P., and Pisera, A. (2000). Eocene spiculites and spongolites in southwestern Australia: Not deep, not polar, but shallow and warm. *Geology* 28, 855–858. doi: 10.1130/0091-7613(2000)28<855:ESASIS>2.0.CO;2

Gold, D. A., Grabenstatter, J., de Mendoza, A., Riesgo, A., Ruiz-Trillo, I., and Summons, R. E. (2016). Sterol and genomic analyses validate the sponge biomarker hypothesis. *Proc. Natl. Acad. Sci. U.S.A.* 113, 2684–2689. doi: 10.1073/pnas.1512614113

Gouretski, V. V., and Koltermann, K. P. (2004). *WOCE Global Hydrographic Climatology. 35/2004.* Berichte des Bundesamtes fur Seeschifffahrt und Hydrographie.

Hartman, W., D (1958). Natural history of the marine sponges of southern new England. *Peabody Museum Nat. Hist.* 12, 1–155.

Hendry, K. R., Georg, R. B., Rickaby, R. E. M., Robinson, L. F., and Halliday, A. N. (2010). Deep ocean nutrients during the last glacial maximum deduced from sponge silicon isotopic compositions. *Earth Planet. Sci. Lett.* 292, 290–300. doi: 10.1016/j.epsl.2010.02.005

Hendry, K. R., Leng, M. J., Robinson, L. F., Sloane, H. J., Blusztjan, J., Rickaby, R. E. M., et al. (2011). Silicon isotopes in Antarctic sponges: an interlaboratory comparison. *Antarct. Sci.* 23, 34–42. doi: 10.1017/S0954102010000593

Hendry, K. R., and Robinson, L. F. (2012). The relationship between silicon isotope fractionation in sponges and silicic acid concentration: modern and core-top studies of biogenic opal. *Geochim. Cosmochim. Acta* 81, 1–12. doi: 10.1016/j.gca.2011.12.010

Hestetun, J. T., Fourt, M., Vacelet, J., Boury-Esnault, N., and Rapp, H. T. (2015). Cladorhizidae (*Porifera*, *Demospongiae*, *Poecilosclerida*) of the deep Atlantic collected during Ifremer cruises, with a biogeographic overview of the Atlantic species. *J. Mar. Biol. Assoc. U.K.* 95, 1311–1342. doi: 10.1017/S0025315413001100

Hooper, J. N. A., and Lévi, C. (1994). "Biogeography of Indo-west Pacific sponges: microcionidae, raspailiidae, axinellidaem," in *Sponges in Time and Space,* eds R. W. M. Van Soest, T. M. G. Van Kempen, and J. C. Braekman (Rotterdam: Balkema), 191–212.

Hooper, J. N. A., and Van Soest, R. W. M. (eds.). (2002). *Systema Porifera: A Guide to the Classification of Sponges*. New York, NY: Kluwer Academic/Plenum Publishers.

Howell, K.-L., Piechaud, N., Downie, A.-L., and Kenny, A. (2016). The distribution of deep-sea sponge aggregations in the North Atlantic and implications for their effective spatial management. *Deep Sea Res. I Oceanogr. Res. Pap.* 115(Suppl. C), 309–320. doi: 10.1016/j.dsr.2016.07.005

Huang, Z., Brooke, B., and Li, J. (2011). Performance of predictive models in marine benthic environments based on predictions of sponge distribution on the Australian continental shelf. *Ecol. Inform.* 6, 205–216. doi: 10.1016/j.ecoinf.2011.01.001

Jørgensen, C. B. (1944). *On the Spicule Formation of Spongilla lacustris (L.): The Dependence of the Spicule-Formation on the Content of Dissolved and Solid Silicic Acid of the Milieu*. København: E. Munksgaard (Bianco Lunos Bogtrykkeri).

Juggins, S. (2013). Quantitative reconstructions in palaeolimnology: new paradigm or sick science? *Quat. Sci. Rev.* 64, 20–32. doi: 10.1016/j.quascirev.2012.12.014

Kidder, D. L., and Tomescu, I. (2016). Biogenic chert and the Ordovician silica cycle. *Palaeogeogr. Palaeoclimatol. Palaeoecol.* 458, 29–38. doi: 10.1016/j.palaeo.2015.10.013

Klitgaard, A. B., and Tendal, O. S. (2004). Distribution and species composition of mass occurrences of large-sized sponges in the northeast Atlantic. *Prog. Oceanogr.* 61, 57–98. doi: 10.1016/j.pocean.2004.06.002

Kratz, T. K., Frost, T. M., Elias, J. E., and Cook, R. B. (1991). Reconstruction of a regional, 12,000-yr silica decline in lakes by means of fossil sponge spicules. *Limnol. Oceanogr.* 36, 1244–1249. doi: 10.4319/lo.1991.36.6.1244

Leys, S. P., Wilson, K., Holeton, C., Reiswig, H. M., Austin, W. C., and Tunnicliffe, V. (2004). Patterns of glass sponge (Porifera, Hexactinellida) distribution in coastal waters of British Columbia, Canada. *Mar. Ecol. Prog. Ser.* 283, 133–149. doi: 10.3354/meps283133

Love, G. D., Grosjean, E., Stalvies, C., Fike, D. A., Grotzinger, J. P., Bradley, A. S., et al. (2009). Fossil steroids record the appearance of demospongiae during the cryogenian period. *Nature* 457, 718–721. doi: 10.1038/nature07673

Lytle, D. E., and Wahl, E. R. (2005). Palaeoenvironmental reconstructions using the modern analogue technique: the effects of sample size and decision rules. *Holocene* 15, 554–566. doi: 10.1191/0959683605hl830rp

Maldonado, M. (2009). Embryonic development of verongid demosponges supports the independent acquisition of spongin skeletons as an alternative to the siliceous skeleton of sponges. *Biol. J. Linn. Soc.* 97, 427–447. doi: 10.1111/j.1095-8312.2009.01202.x

Maldonado, M. (2014). "Metazoans," in *The Tree of Life. Systematics and Evolution of the Living Organisms*, eds V. Pablo and R. Zardoya (Sunderland, MA: Sinauer), 182–205.

Maldonado, M., Aguilar, R., Bannister, R. J., Bell, J. J., Conway, K. W., Dayton, P. K., et al. (2015a). "Sponge grounds as key marine habitats: a synthetic review of types, structure, functional roles, and conservation concerns," in *Marine Animal Forests: The Ecology of Benthic Biodiversity Hotspots,* eds S. Rossi, L. Bramanti, A. Gori, and C. Orejas Saco del Valle (Cham: Springer International Publishing), 1–39.

Maldonado, M., Aguilar, R., Blanco, J., García, S., Serrano, A., and Punzón, A. (2015b). Aggregated clumps of lithistid sponges: a singular, reef-like bathyal habitat with relevant paleontological connections. *PLoS ONE* 10:e0125378. doi: 10.1371/journal.pone.0125378

Maldonado, M., Carmona, M. C., Uriz, M. J., and Cruzado, A. (1999). Decline in Mesozoic reef-building sponges explained by silicon limitation. *Nature* 401, 785–788. doi: 10.1038/44560

Maldonado, M., Carmona, M. C., Velásquez, Z., Puig, A., Cruzado, A., López, A., et al. (2005). Siliceous sponges as a silicon sink: an overlooked aspect of benthopelagic coupling in the marine silicon cycle. *Limnol. Oceanogr.* 50, 799–809. doi: 10.4319/lo.2005.50.3.0799

Maldonado, M., Navarro, L., Grasa, A., Gonzalez, A., and Vaquerizo, I. (2011). Silicon uptake by sponges: a twist to understanding nutrient cycling on continental margins. *Sci. Rep.* 1:30. doi: 10.1038/srep00030

Maldonado, M., Riesgo, A., Bucci, A., and Tzlerb, K.R. (2010). Revisiting silicon budgets at a tropical continental shelf: silica standing stocks in sponges surpass those in diatoms. *Limnol. Oceanogr.* 55, 2001–2010. doi: 10.4319/lo.2010.55.5.2001

Maldonado, M., and Young, C. M. (1998). Limits on the bathymetric distribution of keratose sponges: a field test in deep water. *Mar. Ecol. Prog. Ser.* 174, 123–139. doi: 10.3354/meps174123

Maliva, R. G., Knoll, A. H., and Siever, R. (1989). Secular change in chert distribution: a reflection of evolving biological participation in the silica cycle. *Palaios* 4, 519–532. doi: 10.2307/3514743

Marron, A. O., Ratcliffe, S., Wheeler, G. L., Goldstein, R. E., King, N., Not, F., et al. (2016). The evolution of silicon transport in Eukaryotes. *Mol. Biol. Evol.* 33, 3226–3248. doi: 10.1093/molbev/msw209

Mercurio, M., Corriero, G., Scalera Liaci, L., and Gaino, E. (2000). Silica content and spicule size variations in Pellina semitubulosa (*Porifera*: *Demospongiae*). *Mar. Biol.* 137, 87–92. doi: 10.1007/s002270000336

Morrow, C., and Cárdenas, P. (2015). Proposal for a revised classification of the *Demospongiae* (Porifera). *Front. Zool.* 12:7. doi: 10.1186/s12983-015-0099-8

Müller, W. E. G., Krasko, A., Le Pennec, G., and Schröder, H. C. (2003). Biochemistry and cell biology of silica formation in sponges. *Microsc. Res. Tech.* 62, 368–377. doi: 10.1002/jemt.10402

Pawlik, J. R., McMurray, S. E., Erwin, P., and Zea, S. (2015). No evidence for food limitation of Caribbean reef sponges: reply to slattery and lesser. *Mar. Ecol. Prog. Ser.* 527, 281–284. doi: 10.3354/meps11308

Pisera, A. (1997). Upper jurassic siliceous sponges from the swabian Alb: taxonomy and paleoecology. *Paleaeontologia Pol.* 57, 1–216.

Pisera, A. (2006). Palaeontology of sponges—a review. *Can. J. Zool.* 84, 242–261. doi: 10.1139/z05-169

Pisera, A., and Lévi, C. (2002). "Liithistid' Demospongiae," in *Systema Porifera. A Guide to the Classification of Sponges*, eds J. N. A. Hooper and R. W. M. Van Soest (New York, NY: Kluwer Academic/Plenum Publishers), 299–301.

Przeslawski, R., Alvarez, B., Battershill, C., and Smith, T. (2014). Sponge biodiversity and ecology of the Van Diemen rise and eastern Joseph Bonaparte Gulf, northern Australia. *Hydrobiologia* 730, 1–16. doi: 10.1007/s10750-013-1799-8

Przeslawski, R., Alvarez, B., Kool, J., Bridge, T., Caley, J., and Nichols, S. (2015). Implications of sponge biodiversity patterns for the management of a marine reserve in northern Australia. *PLoS ONE* 10:e0141813. doi: 10.1371/journal.pone.0141813

Przeslawski, R., Daniell, J., Anderson, T., Barrie, J. V., Heap, A., Hughes, M., et al. (2011). *Seabed Habitats and Hazards of the Joseph Bonaparte Gulf and Timor Sea, Northern Australia*. Geoscience Australia, Record 2011/40, 69.

Racca, J. M. J., Racca, R., Pienitz, R., and Prairie, Y. T. (2007). PaleoNet: new software for building, evaluating and applying neural network based transfer functions in paleoecology. *J. Paleolimnol.* 38, 467–472. doi: 10.1007/s10933-006-9082-x

Raff, A. R., Marshall, C. R., and Turbeville, J. M. (1994). Using DNA sequences to unravel the cambrian radiation of the animal phyla. *Annu. Rev. Ecol. Syst.* 25, 351–375. doi: 10.1146/annurev.es.25.110194.002031

Rapp, H. T., Janussen, D., and Tendal, O. S. (2011). Calcareous sponges from abyssal and bathyal depths in the Weddell Sea, Antarctica. *Deep Sea Res. II Top. Stud. Oceanogr.* 58, 58–67. doi: 10.1016/j.dsr2.2010.05.022

Reincke, T., and Barthel, D. (1997). Silica uptake kinetics of *Halichondria panicea* in Kiel Bight. *Mar. Biol.* 129, 591–593. doi: 10.1007/s002270050200

Ritterbush, K. A., Bottjer, D. J., Corsetti, F. A., and Rosas, S. (2014). New evidence on the role of siliceous sponges in ecology and sedimentary facies development in eastern panthalassa following the triassic–jurassic mass extinction. *Palaios* 29, 652–668. doi: 10.2110/palo.2013.121

Ritterbush, K. A., Rosas, S., Corsetti, F. A., Bottjer, D. J., and West, A. J. (2015). Andean sponges reveal long-term benthic ecosystem shifts following the end-Triassic mass extinction. *Palaeogeogr. Palaeoclimatol. Palaeoecol.* 420, 193–209. doi: 10.1016/j.palaeo.2014.12.002

Rützler, K., and Smith, K. P. (1993). The genus *Terpios* and new species in the *"Lobiceps"* complex. *Sci. Mar.* 57, 381–393.

Sarmiento, J. L., and Gruber, N. (2006). *Ocean Biogeochemical Dynamics.* Princeton, NJ: Princeton University Press.

Schönberg, C. H. L., and Barthel, D. (1997). Inorganic skeleton of the demosponge *Halichondria panicea*. seasonality in spicule production in the baltic sea. *Mar. Biol.* 130, 133–140. doi: 10.1007/s002270050232

Schröder, H. C., Perović-Ottstadt, S., Rothenberger, M., Wiens, M., Schwertner, H., Batel, R., et al. (2004). Silica transport in the demosponge *Suberites domuncula*: fluorescence emission analysis using the PDMPO probe and cloning of a potential transporter. *Biochem. J.* 381(Pt 3), 665–673. doi: 10.1042/BJ20040463

Siever, R. (1991). "Silica in the oceans: biological-geochemical interplay," in *Scientists on Gaia. Papers delivered at the American Geophysical Union's Annual Chapman Conference in March, 1988*, eds S. H. Schneider and J. B. Penelope (Cambridge, MA: MIT Press), 287–295.

Sinka, K. J., and Atkinson, T. C. (1999). A mutual climatic range method for reconstructing palaeoclimate from plant remains. *J. Geol. Soc. Lond.* 156, 381–396. doi: 10.1144/gsjgs.156.2.0381

Slattery, M., and Lesser, M. P. (2015). Trophic ecology of sponges from shallow to mesophotic depths (3 to 150 m): comment on Pawlik et al. (2015). *Mar. Ecol. Prog. Ser.* 527, 275–279. doi: 10.3354/meps11307

Spalding, M. D., Fox, H. E., Allen, G. R., Davidson, N., Ferdaña, Z. A., Finlayson, M., et al. (2007). Marine ecoregions of the world: a bioregionalization of coastal and shelf areas. *Bioscience* 57, 573–583. doi: 10.1641/B570707

Stone, A. R. (1970). Seasonal variations of spicule size in hymeniacidon perleve. *J. Mar. Biol. Assoc. U.K.* 50, 343–348. doi: 10.1017/S0025315400004562

Telford, R. J., and Birks, H. J. B. (2005). The secret assumption of transfer functions: problems with spatial autocorrelation in evaluating model performance. *Q. Sci. Rev.* 24, 2173–2179. doi: 10.1016/j.quascirev.2005.05.001

Uriz, M. J., Turon, X., Becerro, M., and Agell, G. (2003). Siliceous spicules and skeleton frameworks in sponges: origin, diversity, ultrastructural patterns, and biological functions. *Microsc. Res. Tech.* 62, 279–299. doi: 10.1002/jemt.10395

Vacelet, J. (1988). Indications de profounderur données par les Spongiaires dans les milieux benthiques actuels. *Géologie Méditerranéenne* 15, 13–26.

Valisano, L., Pozzolini, M., Giovine, M., and Cerrano, C. (2012). Biosilica deposition in the marine sponge Petrosia ficiformis (Poiret, 1789): the model of primmorphs reveals time dependence of spiculogenesis. *Hydrobiologia* 687, 259–273. doi: 10.1007/s10750-011-0987-7

Van Soest, R. W. M. (1994). "Demosponge distribution patterns," in S*ponges in Time and Space*, eds R. W. M. Van Soest, T. M. G. Van Kempen, and J. C. Braekman (Rotterdam: Balkema), 213–223.

Van Soest, R. W. M., Boury-Esnault, N., Hooper, J., Rützler, K., de Voogd, N. J., Alvarez, B., et al. (2017). *World Porifera Database.* Available online at: http://www.marinespecies.org/porifera. Last consulted on (Accessed Mar 23, 2017).

Van Soest, R. W. M., Boury-Esnault, N., Vacelet, J., Dohrmann, M., Erpenbeck, D., De Voogd, N. J., et al. (2012). Global diversity of sponges (Porifera). *PLoS ONE* 7:e35105. doi: 10.1371/journal.pone.0035105

Wang, X., Schloßmacher, U., Wiens, M., Batel, R., Schröder, H. C., and Müller, W. E. G. (2012a). Silicateins, silicatein interactors and cellular interplay in sponge skeletogenesis: formation of glass fiber-like spicules. *FEBS J.* 279, 1721–1736. doi: 10.1111/j.1742-4658.2012.08533.x

Wang, X., Schroder, H. C., Wang, K., Kaandorp, J. A., and Muller, W. E. G. (2012b). Genetic, biological and structural hierarchies during sponge spicule formation: from soft sol-gels to solid 3D silica composite structures. *Soft Matter* 8, 9501–9518. doi: 10.1039/c2sm25889g

Wang, X., Wiens, M., Schröder, H. C., Jochum, K. P., Schloßmacher, U., Götz, H., et al. (2011a). Circumferential spicule growth by pericellular silica deposition in the hexactinellid sponge Monorhaphis chuni. *J. Exp. Biol.* 214, 2047–2056. doi: 10.1242/jeb.056275

Wang, X., Wiens, M., Schröder, H. C., Schloßmacher, U., Pisignano, D., Jochum, K. P., et al. (2011b). Evagination of cells controls bio-silica formation and maturation during spicule formation in sponges. *PLoS ONE* 6:e20523. doi: 10.1371/journal.pone.0020523

Whitney, F., Conway, K., Thomson, R., Barrie, V., Krautter, M., and Mungov, G. (2005). Oceanographic habitat of sponge reefs on the Western Canadian continental Shelf. *Cont. Shelf Res.* 25, 211–226. doi: 10.1016/j.csr.2004.09.003

Wille, M., Sutton, J., Ellwood, M. J., Sambridge, M., Maher, W., Eggins, S., et al. (2010). Silicon isotopic fractionation in marine sponges: a new model for understanding silicon isotopic variations in sponges. *Earth Planet. Sci. Lett.* 292, 281–289. doi: 10.1016/j.epsl.2010.01.036

Xiao, S., Hu, J., Yuan, X., Parsley, R. L., and Cao, R. (2005). Articulated sponges from the lower cambrian hetang formation in southern Anhui, South China: their age and implications for the early evolution of sponges. *Palaeogeogr. Palaeoclimatol. Palaeoecol.* 220, 89–117. doi: 10.1016/j.palaeo.2002.02.001

Yin, Z., Zhu, M., Davidson, E. H., Bottjer, D. J., Zhao, F., and Tafforeau, P. (2015). Sponge grade body fossil with cellular resolution dating 60 Myr before the Cambrian. *Proc. Natl. Acad. Sci. U.S.A.* 112, E1453–E1460. doi: 10.1073/pnas.1414577112

Yourassowsky, C., and Rasmont, R. (1984). The differentiation of sclerocytes in fresh-water sponges grown in a silica-poor medium. *Differentiation* 25, 5–9. doi: 10.1111/j.1432-0436.1984.tb01330.x

Zea, S. (1987). *Esponjas del Caribe Colombiano.* Bogota: Editorial Catálogo Científico, 285.

Conflict of Interest Statement: The authors declare that the research was conducted in the absence of any commercial or financial relationships that could be construed as a potential conflict of interest.

Copyright © 2017 Alvarez, Frings, Clymans, Fontorbe and Conley. This is an open-access article distributed under the terms of the Creative Commons Attribution License (CC BY). The use, distribution or reproduction in other forums is permitted, provided the original author(s) or licensor are credited and that the original publication in this journal is cited, in accordance with accepted academic practice. No use, distribution or reproduction is permitted which does not comply with these terms.

frontiers in Marine Science

CORRECTION
published: 30 August 2017
doi: 10.3389/fmars.2017.00280

Corrigendum: Iron Availability Influences Silicon Isotope Fractionation in Two Southern Ocean Diatoms (*Proboscia inermis* and *Eucampia antarctica*) and a Coastal Diatom (*Thalassiosira pseudonana*)

Scott Meyerink[1]*, *Michael J. Ellwood*[1]*, *William A. Maher*[2] *and Robert Strzepek*[1]

[1] Research School of Earth Sciences, Australian National University, Canberra, ACT, Australia, [2] Ecochemistry Laboratory, Institute for Applied Ecology, University of Canberra, Canberra, ACT, Australia

Keywords: silicon isotopes, Southern Ocean, diatom, isotope fractionation, iron

A corrigendum on

Iron Availability Influences Silicon Isotope Fractionation in Two Southern Ocean Diatoms (*Proboscia inermis* and *Eucampia antarctica*) and a Coastal Diatom (*Thalassiosira pseudonana*) *by Meyerink, S., Ellwood, M. J., Maher, W. A., and Strzepek, R. (2017). Front. Mar. Sci. 4:217. doi: 10.3389/fmars.2017.00217*

OPEN ACCESS

Edited and reviewed by:
Brivaela Moriceau, Centre National de la Recherche Scientifique (CNRS), France

***Correspondence:**
Scott Meyerink
scott.meyerink@anu.edu.au
Michael J. Ellwood
michael.ellwood@anu.edu.au

Specialty section:
This article was submitted to Marine Biogeochemistry, a section of the journal Frontiers in Marine Science

Received: *16 August 2017*
Accepted: *17 August 2017*
Published: *30 August 2017*

Citation:
Meyerink S, Ellwood MJ, Maher WA and Strzepek R (2017) Corrigendum: Iron Availability Influences Silicon Isotope Fractionation in Two Southern Ocean Diatoms (Proboscia inermis and Eucampia antarctica) and a Coastal Diatom (Thalassiosira pseudonana). Front. Mar. Sci. 4:280. doi: 10.3389/fmars.2017.00280

In the original article, there was a mistake in **Table 1** as published. It seems that during the transcription of the data into **Table 1** an error occurred whereby three values from a different experiment were inadvertently added to the average silicon isotope data for iron-limited *Eucampia antarctica* experiment (*Eucampia antarctica* 4.4 nmol L^{-1} Fe; 40 nmol L^{-1} DFB). The corrected **Table 1** appears below. Note that the dataset used to generate Figure 2 was not in error. The authors apologize for this error and state that this does not change the scientific conclusions of the article in any way.

In the original article, the error in **Table 1** was translated through to a silicon isotope value quoted in the Abstract and the Results section of this manuscript. In the Abstract and in the Results section titled "Effects of Fe-Availability on Si Isotope Fractionation" the value of -1.57 ± 0.50‰ ($n = 11$) is in error as result of the error in **Table 1**. The correct value should be -1.82 ± 0.36‰ ($n = 8$).

A correction has been made to the Abstract and the following paragraph in the Results section titled "Effects of Fe-Availability on Si Isotope Fractionation":

Abstract: The fractionation of silicon (Si) isotopes was measured in two Southern Ocean diatoms (*Proboscia inermis* and *Eucampia antarctica*) and a coastal diatom (*Thalassiosira pseudonana*) that were grown under varying iron (Fe) concentrations. Varying Fe concentrations had no effect on the Si isotope enrichment factor (ε) in *T. pseudonana*, whilst *E. antarctica* and *P. inermis* exhibited significant variations in the value of ε between Fe-replete and Fe-limited conditions. Mean ε values in *P. inermis* and *E. antarctica* decreased from (± 1 SD) -1.11 ± 0.15‰ and -1.42 ± 0.41‰ (respectively) under Fe-replete conditions, to -1.38 ± 0.27‰ and -1.82 ± 0.36‰ (respectively) under Fe-limiting conditions. These variations likely arise from adaptations in diatoms arising from the nutrient status of their environment. *T. pseudonana* is a coastal clone typically accustomed to low Si but high Fe conditions whereas *E. antarctica* and *P. inermis* are typically accustomed to

TABLE 1 | Culture conditions, growth rates, Fe concentrations and Results from the Si isotope fractionation experiments for *Proboscia inermis*, *Eucampia Antarctica,* and *Thalassiosira pseudonana*.

Fe Treatment	Fe′ (pmol L^{-1})	Number of replicate cultures	μ (d^{-1})	PFD ($\mu E\ m^{-2}\ s^{-1}$)	*n*	$\delta^{30}Si_{NBS28}$ (per mil)	*f*	α	Fractionation factor (ε, ‰)	*P*
P. inermis										
58.3 nmol L^{-1} Fe; 10 μmol L^{-1} EDTA	3,369	3	0.35 ± 0.02	60	9	−0.55 ± 0.16	0.97 ± 0.06	0.9989 ± 0.0002	−1.11 ± 0.15	
4.4 nmol L^{-1} Fe; 80 nmol L^{-1} DFB	0.09	2	0.09 ± 0.02	60	5	−0.6 ± 0.23	0.68 ± 0.06	0.9986 ± 0.0003	−1.38 ± 0.27	0.08
E. antarctica										
58.3 nmol L^{-1} Fe; 10 μmol L^{-1} EDTA	3,369	4	0.32 ± 0.02	50	12	−0.65 ± 0.33	0.7 ± 0.02	0.9986 ± 0.0004	−1.42 ± 0.41	
4.4 nmol L^{-1} Fe; 40 nmol L^{-1} DFB	0.2	4	0.07 ± 0.01	50	8	−1.04 ± 0.32	0.72 ± 0.07	0.9982 ± 0.0004	−1.82 ± 0.36	0.04
T. pseudonana										
500 nmol L^{-1} Fe; 100 μmol L^{-1} EDTA	418	1	1.52*	133	3	0.09 ± 0.08	0.60	0.9994 ± 0.0001	−0.59 ± 0.11	
250 nmol L^{-1} Fe; 100 μmol L^{-1} EDTA	208	1	1.48*	133	3	0.13 ± 0.37	0.65	0.9995 ± 0.0005	−0.51 ± 0.46	0.8
80 nmol L^{-1} Fe; 100 μmol L^{-1} EDTA	67	1	0.85*	133	3	0.13 ± 0.08	0.67	0.9995 ± 0.0001	−0.51 ± 0.1	0.39
30 nmol L^{-1} Fe; 100 μmol L^{-1} EDTA	25	2	0.72 ± 0.01	133	6	−0.07 ± 0.08	0.87 ± 0.01	0.9993 ± 0.0001	−0.65 ± 0.08	0.42
Growth Media Si (Aquil replicates)					6	0.54 ± 0.13				
Growth Media Si (NaOH replicates)					3	0.53 ± 0.02				
Mean Growth Media Si (Aquil + NaOH replicates)					9	0.54 ± 0.11				

**Max growth rate from single culture, replicate cultures were Fe-replete. Because there was no difference in ε between replicate cultures, the value for ε is the mean of all cultures ± 1 SD. Fractionation factors were calculated from diatom silica as a function of f, where f is the fraction of the original $Si(OH)_4$ remaining in the system once diatoms were harvested. n is the number of measurements from cultures. All values presented as means ±1 SD. P-values are relative to Fe-replete (Fe+) conditions. For T. pseudonana, the Fe-replete concentration is equal to an Fe′ value of 418 pmol L^{-1}.*

High Si, High nitrate low Fe conditions. Growth induced variations in silicic acid ($Si(OH)_4$) uptake arising from Fe-limitation is the likely mechanism leading to Si-isotope variability in *E. antarctica* and *P. inermis*. The multiplicative effects of species diversity and resource limitation (e.g., Fe) on Si-isotope fractionation in diatoms can potentially alter the Si-isotope composition of diatom opal in diatomaceous sediments and sea surface $Si(OH)_4$. This work highlights the need for further in vitro studies into intracellular mechanisms involved in $Si(OH)_4$ uptake, and the associated pathways for Si-isotope fractionation in diatoms.

Effects of Fe-Availability on Si Isotope Fractionation: Mean values for ε varied between the Fe-replete and Fe-limited conditions for the two Southern Ocean diatoms (Table 2). While there was some variability in the values of ε for *E. antarctica*, there was a significant difference in ε ($p = 0.04$) between Fe-replete and Fe-limited conditions, with mean ε values being more negative for Fe-limited cultures (Fe-limited, $\varepsilon = -1.82 \pm 0.36‰$; Fe-replete, $\varepsilon = -1.40 \pm 0.41‰$) (**Table 1**). Mean ε values were also more negative for *P. inermis* cultured under Fe-limited conditions (Fe-limited, $\varepsilon = -1.38 \pm 0.27‰$; Fe-replete, $\varepsilon = -1.11 \pm 0.15‰$). Both Fe-replete and Fe-limited datasets for *P. inermis* exhibited a significant difference at the 90% confidence interval ($p = 0.08$), and removing outliers from both Fe-replete and Fe-limited data sets for *P. inermis* makes the difference more significant ($p = 0.04$).

The authors apologize for this error and state that this does not change the scientific conclusions of the article in any way.

Conflict of Interest Statement: The authors declare that the research was conducted in the absence of any commercial or financial relationships that could be construed as a potential conflict of interest.

Copyright © 2017 Meyerink, Ellwood, Maher and Strzepek. This is an open-access article distributed under the terms of the Creative Commons Attribution License (CC BY). The use, distribution or reproduction in other forums is permitted, provided the original author(s) or licensor are credited and that the original publication in this journal is cited, in accordance with accepted academic practice. No use, distribution or reproduction is permitted which does not comply with these terms.

frontiers in Marine Science

ORIGINAL RESEARCH
published: 07 July 2017
doi: 10.3389/fmars.2017.00217

Iron Availability Influences Silicon Isotope Fractionation in Two Southern Ocean Diatoms (*Proboscia inermis* and *Eucampia antarctica*) and a Coastal Diatom (*Thalassiosira pseudonana*)

Scott Meyerink[1]*, *Michael J. Ellwood*[1]*, *William A. Maher*[2] *and Robert Strzepek*[1]

[1] *Research School of Earth Sciences, Australian National University, Canberra, ACT, Australia,* [2] *Ecochemistry Laboratory, Institute for Applied Ecology, University of Canberra, Canberra, ACT, Australia*

OPEN ACCESS

Edited by:
Brivaela Moriceau, Centre National de la Recherche Scientifique, France

Reviewed by:
Damien Cardinal, Université Pierre et Marie Curie, France
Frank Dehairs, Vrije Universiteit Brussel, Belgium

***Correspondence:**
Scott Meyerink
scott.meyerink@anu.edu.au
Michael J. Ellwood
michael.ellwood@anu.edu.au

Specialty section:
This article was submitted to Marine Biogeochemistry, a section of the journal Frontiers in Marine Science

Received: *28 February 2017*
Accepted: *22 June 2017*
Published: *07 July 2017*

Citation:
Meyerink S, Ellwood MJ, Maher WA and Strzepek R (2017) Iron Availability Influences Silicon Isotope Fractionation in Two Southern Ocean Diatoms (Proboscia inermis and Eucampia antarctica) and a Coastal Diatom (Thalassiosira pseudonana). Front. Mar. Sci. 4:217. doi: 10.3389/fmars.2017.00217

The fractionation of silicon (Si) isotopes was measured in two Southern Ocean diatoms (*Proboscia inermis* and *Eucampia Antarctica*) and a coastal diatom (*Thalassiosira pseudonana*) that were grown under varying iron (Fe) concentrations. Varying Fe concentrations had no effect on the Si isotope enrichment factor (ε) in *T. pseudonana*, whilst *E. Antarctica* and *P. inermis* exhibited significant variations in the value of ε between Fe-replete and Fe-limited conditions. Mean ε values in *P. inermis* and *E. Antarctica* decreased from (± 1SD) −1.11 ± 0.15‰ and −1.42 ± 0.41 ‰ (respectively) under Fe-replete conditions, to −1.38 ± 0.27 ‰ and −1.57 ± 0.5 ‰ (respectively) under Fe-limiting conditions. These variations likely arise from adaptations in diatoms arising from the nutrient status of their environment. *T. pseudonana* is a coastal clone typically accustomed to low Si but high Fe conditions whereas *E. Antarctica* and *P. inermis* are typically accustomed to High Si, High nitrate low Fe conditions. Growth induced variations in silicic acid ($Si(OH)_4$) uptake arising from Fe-limitation is the likely mechanism leading to Si-isotope variability in *E. Antarctica* and *P. inermis*. The multiplicative effects of species diversity and resource limitation (e.g., Fe) on Si-isotope fractionation in diatoms can potentially alter the Si-isotope composition of diatom opal in diatamaceous sediments and sea surface $Si(OH)_4$. This work highlights the need for further *in vitro* studies into intracellular mechanisms involved in $Si(OH)_4$ uptake, and the associated pathways for Si-isotope fractionation in diatoms.

Keywords: silicon isotopes, Southern Ocean, diatom, isotope fractionation, iron

INTRODUCTION

Diatoms play a vital role in the biogeochemical cycles of carbon (C) and silicon (Si). They dominate the production of biogenic silica (BSi) in the ocean, and hence have a controlling influence on the marine Si cycle through the utilization of dissolved silicon [silicic acid, $Si(OH)_4$], which they use in the formation of their cell wall, or frustule (Nelson et al., 1995; Trèguer et al., 1995; Tréguer and De La Rocha, 2013). Diatoms make up a significant proportion of phytoplankton communities in

nutrient rich regions of the ocean such as the Southern Ocean, where they contribute significantly to the deep export of C and Si to ocean sediments (Smetacek, 1999; Kemp et al., 2000; Roca-Martí et al., 2017). BSi preservation rates can reach as high as 30% in some of these areas due to increased sedimentation rates of diatom produced opaline silica (McManus et al., 1995; Nelson et al., 1995; Ragueneau et al., 2000).While the accumulation of sedimentary BSi (or opal) presents a promising tool for reconstructing the degree of coupling between the Si and C cycles, indices based on the accumulation of sedimentary opal are often subject to winnowing and focusing of sediments, and the dissolution of opal at the sediment-water interface (De La Rocha et al., 1998; Ragueneau et al., 2000). Variations in the ratios of ^{30}Si to ^{28}Si (expressed as δ^{30}Si in ‰) in opaline sediments and in the $Si(OH)_4$ pool present in surface waters represents a promising tool in providing information on the marine Si cycle, and as such, has been used as a proxy for marine diatom production and $Si(OH)_4$ utilization in several palaeo-oceanographic studies (De La Rocha et al., 1998; Beucher et al., 2007; Pichevin et al., 2009; Ellwood et al., 2010; Rousseau et al., 2016); and in field studies (Varela et al., 2004; Cardinal et al., 2007; Beucher et al., 2011).

During Si uptake, diatoms discriminate against heavier isotopes, which changes the isotopic composition of both the diatom opal and the residual $Si(OH)_4$ pool (De La Rocha et al., 1997; Sutton et al., 2013). This results in a lighter isotope composition (^{28}Si or ^{29}Si vs. ^{30}Si) in the frustule, relative to its dissolved Si source. Although the exact mechanism of fractionation of silicon isotopes in diatoms is unknown, fractionation has been determined to resemble Rayleigh style fractionation kinetics under closed-system conditions, where the substrate [dissolved Si in the form of $Si(OH)_4$] is precipitated into the product, BSi (Criss and Criss, 1999). The isotope fractionation factor (α) for Rayleigh fractionation determines the rate of fractionation between the $Si(OH)_4$ and the Si-BSi product, and is calculated by the following equation (De La Rocha et al., 1997):

$$\alpha_{BSi-DSi} = \frac{\ln\left(1 - \left(\frac{(1+\delta^{30}Si_{acc}/1000)(1-f)}{(1+\delta^{30}Si_o/1000)}\right)\right)}{\ln f} \quad (1)$$

where $\alpha_{BSi—DSi}$ is the isotope fractionation factor between the $Si(OH)_4$ and the BSi product, f is the fractional depletion of $Si(OH)_4$ in the media and $\delta^{30}Si_{acc}$ and $\delta^{30}Si_o$ are the δ^{30}Si values of the accumulated BSi and of $Si(OH)_4$ in the media at $f = 1.0$ (respectively). Isotope fractionation is often described in terms of a per mil (‰) value such as the enrichment factor (ε). The relationship between α and ε can be described using the following equation:

$$\varepsilon(‰) = (\alpha - 1) \times 1000 \quad (2)$$

Estimates for Si isotope fractionation in diatoms under controlled laboratory conditions were initially found to be (expressed as ε in ‰), −1.1 ± 0.4 ‰ (average ± 1SD), with little variation between species (*Thalassiosira* sp., *Thalassiosira weissflogii* and *Skeletonema costatum*) (De La Rocha et al., 1997). Fractionation was also found to be independent of changes in temperature (12–22°C) (De La Rocha et al., 1997); Si quota, Si efflux and pCO_2 concentration in *T. weisflogii* (Milligan et al., 2004). While these studies focused mainly on temperate and sub-polar species of diatoms, they did not adequately represent the isotope composition of individual Polar and Southern Ocean diatoms, and further studies found an inter-species effect between the Southern Ocean diatoms *Fragilariopsis kergulensis* (−0.54 ± 0.09 ‰) and *Chaetoceros brevis* (−2.09 ± 0.09 ‰) (Sutton et al., 2013). While the reasons for the difference in isotopic composition of these species is unclear, Sutton et al. (2013) suggested that potential phylogenetic and morphological effects could play an important role in Si isotope fractionation.

Diatoms in the Southern Ocean experience rapid fluctuations in both physical and chemical conditions associated with the variations in sea ice extent, deep winter mixing and alterations in nutrient supply (Sackett et al., 2013). In the short term, these extremes in physico-chemical conditions can potentially influence Si isotope fractionation in diatoms through variations in cell morphology, growth rate and nutrient uptake rate (Hutchins and Bruland, 1998; Takeda, 1998; Brzezinski et al., 2002; Leynaert et al., 2004; Meyerink et al., 2017). Field studies show that Si isotopic fractionation by siliceous phytoplankton varies across the Antarctic Polar Frontal Zone (APFZ), and coincides with the presence of a strong northward gradient in $Si(OH)_4$ concentrations (Cardinal et al., 2007; Fripiat et al., 2011). Despite the large zonal variations in Si isotopic fractionation, there was no change among different size fractions, suggesting that the latitudinal variations in Si isotope fractionation in siliceous phytoplankton could be a direct result of nutrient availability, more than species composition (Cardinal et al., 2007). In order to decipher the effects both factors have on the surface Si isotope composition in the Southern Ocean, a better understanding of the effects nutrient availability has on Si isotope fractionation in diatoms is required.

Iron (Fe) availability affects the growth rate, Si uptake, cell morphology and BSi content in diatoms (Leynaert et al., 2004; Hoffmann et al., 2008; Marchetti and Cassar, 2009; Boutorh et al., 2016; Meyerink et al., 2017). These microscale effects can have far reaching consequences on the physico-chemical environment, particularly in the Southern Ocean. Fe-limited diatoms in Antarctic water take up more $Si(OH)_4$ relative to nitrate (NO_3^-), so that by the time surface waters reach the sub-Antarctic zone (SAZ), it is depleted in $Si(OH)_4$ relative to NO_3^- (Varela et al., 2004; Matsumoto et al., 2014). Alleviation of Fe-limitation in Antarctic waters may have potentially altered the $Si(OH)_4$: NO_3^- uptake ratio in diatoms during glacial times, and resulted in a "leakage" of silicic acid to sub-polar waters (Brzezinski et al., 2002; Matsumoto et al., 2002). Opaline sediments exhibit variations in their Si isotope composition from glacial times, and can potentially be a useful tool in resolving the mechanisms behind the glacial-interglacial transitions of the past (De La Rocha et al., 1998; Beucher et al., 2007; Pichevin et al., 2009; Ellwood et al., 2010; Rousseau et al., 2016). In order to quantitatively use δ^{30}Si to determine diatom production during these periods, a better understanding of how Fe-availability affects diatom δ^{30}Si composition is required; especially since it is thought that the supply of Fe to Southern Ocean waters was

higher during glacial periods (Martinez-Garcia et al., 2011). Here, the results of the fractionation of Si-isotopes in these diatoms under varying degrees of Fe-limitation are presented.

METHODS

Culture Conditions

The centric diatom *T. pseudonana* (Strain CS-20) was obtained from the Australian national algae culture collection in Hobart, Australia and maintained in *f/2* medium (CSIRO recipe) at 20°C under a continuous photon flux density (PFD) of 120–145 μE m^{-2} s^{-1}, before being transferred to Fe-replete Aquil medium (Price et al., 1988). Stock cultures of the Southern Ocean diatoms *P. inermis* and *E. Antarctica* were isolated from waters south of the Antarctic Polar Frontal Zone in December 2001 (Strzepek et al., 2011). The Southern Ocean diatoms have since been maintained in Fe-replete Aquil medium at a temperature of 3°C under a continuous photon flux density (PFD) of ∼35 μE m^{-2} s^{-1}. Cultures were acclimated to the different Fe concentrations in 28 mL polycarbonate vials for a minimum of three transfers (approximately 10–12 generations), before being transferred to 1 L polycarbonate bottles for experimental work. All cultures were grown in batches rather than under semi-continuous conditions to minimize contamination from trace metals. Average PFD's for cultures of *E. Antarctica*, *P. inermis,* and *T. pseudonana* were 45 μE m^{-2} s^{-1}, 60 μE m^{-2} s^{-1} and 133μE m^{-2} s^{-1} respectively (Sunda and Huntsman, 1997; Strzepek et al., 2012). Experimental temperatures were 20°C for *T. pseudonana* and 3°C for the Southern Ocean species.

Medium Preparation

Aquil medium was prepared using trace-metal ultra-clean techniques and enriched with the following nutrients; 10 μmol L^{-1} phosphate, 100 μmol $L^{-1}Si(OH)_4$, 300 μmol L^{-1} nitrate, 0.55 μg L^{-1} vitamin B_{12}, 0.5 μg L^{-1} Biotin and 100 μg L^{-1}thiamin. Basal medium and stock solutions were eluted through a column containing Toyopearl AF-chelate-650M (Tosohbioscience) ion-exchange resin to remove metal contaminants and filter sterilized (0.2 μm) (Price et al., 1988). Iron contamination of the basal medium was measured using high-resolution IC-PMS after pre-concentration (Ellwood et al., 2008) and found to be 0.56 ± 0.02 nmol L^{-1} ($n = 3$). Trace metal ion concentrations were controlled through the addition of a trace-metal ion buffer system, which used 10 and 100 μmol L^{-1} ethylene-diamine-tetra-acetic-acid (EDTA), as the chelating agent, for both Southern Ocean species and *T. pseudonana* (respectively). Trace metal concentrations were 7.91 nmol L^{-1} $ZnSO_4$, 1.98 nmol L^{-1} $CuSO_4$, 5 nmol L^{-1} $CoCl_2$, 22.8 nmol L^{-1} $MnCl_2$, 9.96 nmol L^{-1} Na_2SeO_3 and 100 nmol L^{-1} Na_2MoO_4 for media containing *P. inermis* and *E. Antarctica*; and 100 nmol L^{-1} $ZnSO_4$, 40 nmol L^{-1} $CuSO_4$, 40 nmol L^{-1} $CoCl_2$, 100 nmol L^{-1} $MnCl_2$, 10 nmol L^{-1} Na_2SeO_3 and 100 nmol L^{-1} Na_2MoO_4 for media containing *T. pseudonana*. Free ion concentrations were calculated using Visual MINTEQ, giving concentrations (expressed as –log free metal ion concentration = *p*Metal) of, *p*Cu 14.07, *p*Mn 8.18, *p*Zn 10.78 and *p*Co 11.09 for Aquil medium at a temperature of 3°C and a pH of 8.4 for Southern Ocean media, while *p*Metal values for *T. pseudonana* media were *p*Cu 13.65, *p*Mn 8.35, *p*Zn 10.72 and *p*Co 11.26 for Aquil medium at a temperature of 20°C and a pH of 8.1.

Measurement of Culture pH

Culture pH was measured by the change in absorbance of m-cresol purple in culture medium at specific wavelengths of 434, 578, and 730 nm respectively on a Varian Cary 1E UV-visible spectrophotometer with attached temperature controller (Clayton and Byrne, 1993; Yao et al., 2007). Measurements were made at 25°C and corrected for dye-induced changes in the pH. The pH was then adjusted to the culture temperature of 20°C using CO2SYS (http://cdiac.ornl.gov/oceans/co2rprt.html).

Iron Manipulation

T. pseudonana cultures were treated with a range of Fe concentrations varying from Fe limiting to Fe replete: from 30 through to 50, 80, 250, and 500 nmol L^{-1} of total dissolved Fe, equating to –log Fe^{3+} concentration (pFe) values of 20.59, 20.36, 20.16, 19.67, and 19.36 respectively. The Fe concentrations were selected to induce different degrees of limitation as defined by the reduction in growth rate from μmax. Inorganic Fe concentrations (Fe′) were calculated according to Sunda and Huntsman (2003) for a temperature of 20°C, a mean irradiance of 133 μE m^{-2} s^{-1} and a mean starting pH of 7.98. Fe′ values based on total dissolved Fe concentrations of 500, 250, 80, 50, and 30 nM equated to 0.42, 0.21, 0.07, 0.04, and 0.02 nM respectively (**Table 1**) (Sunda and Huntsman, 2003).

Southern Ocean cultures were treated differently to *T. pseudonana* cultures, and two competing ligands were used to induce Fe-limitation. This is because Southern Ocean diatoms are well adapted to iron limiting conditions over coastal isolates such as *T. pseudonana*. Iron replete media was prepared through the addition of a filter-sterilized FeEDTA complex (1:1.05[mol:mol]) to Aquil containing 10 μmol L^{-1} EDTA for a final concentration (including contamination) of 58.3 nmol L^{-1} of total dissolved Fe. Iron limited media was prepared by adding Fe pre-complexed with the terrestrial siderophore desferrioxamine B mesylate (DFB; Sigma Aldridge) to Aquil media containing 10 μMol L^{-1} EDTA for a final concentration of 4.4 nmol L^{-1}. Varying degrees of Fe limitation were induced in culture by increasing the amount of DFB in culture at concentrations of 40 and 80 nmol L^{-1} for *E. Antarctica* and *P. inermis* (respectively). The Fe′ concentration in the iron-replete media was calculated according to Sunda and Huntsman (2003) for a temperature of 3°C, a mean irradiance of 52 μE m^{-2} s^{-1} and a pH of 8.4. The overall conditional dissociation constant (K'_d) was calculated according to methods described by Strzepek et al. (2011) and represents the sum of the conditional stability constant in the dark (3.52×10^{-7}) and the conditional photo-dissociation constant ($K_{hv} = 2.17 \times 10^{-6}$) of EDTA at 3°C. The Fe′ concentration for FeDFB treatment was calculated according to the equation $[Fe'] = [FeDFB] / [L'] \times K^{cond}_{Fe'L}$; where $K^{cond}_{Fe'L} = 10^{11.8}$ (Maldonado et al., 2005). In the instance where total Fe exceeded the concentration of DFB bound Fe

TABLE 1 | Culture conditions, growth rates, Fe concentrations and Results from the Si isotope fractionation experiments for *Proboscia inermis*, *Eucampia antarctica* and *Thalassiosira pseudonana*.

Fe treatment	Fe' (pmol L^{-1})	Number of replicate cultures	μ (d^{-1})	PFD (μE m^{-2} s^{-1})	*n*	$\delta^{30}Si_{NBS28}$ (per mil)	*f*	α	Fractionation factor (ε, ‰)	*P*
P. inermis										
58.3 nmol L^{-1} Fe; 10 μmol L^{-1} EDTA	3369	3	0.35 ± 0.02	60	9	−0.55 ± 0.16	0.97 ± 0.06	0.9989 ± 0.0002	−1.11 ± 0.15	
4.4 nmol L^{-1} Fe; 80 nmol L^{-1} DFB	0.09	2	0.09 ± 0.02	60	5	−0.6 ± 0.23	0.68 ± 0.06	0.9986 ± 0.0003	−1.38 ± 0.27	0.08
E. Antarctica										
58.3 nmol L^{-1}Fe; 10 μmol L^{-1} EDTA	3369	4	0.32 ± 0.02	50	12	−0.65 ± 0.33	0.7 ± 0.02	0.9986 ± 0.0004	−1.42 ± 0.41	
4.4 nmol L^{-1} Fe; 40 nmol L^{-1} DFB	0.2	4	0.07 ± 0.01	50	11	−0.8 ± 0.48	0.72 ± 0.07	0.9984 ± 0.0005	−1.57 ± 0.5	0.04
T. pseudonana										
500 nmol L^{-1} Fe; 100 μmol L^{-1} EDTA	418	1	1.52*	133	3	0.09 ± 0.08	0.60	0.9994 ± 0.0001	−0.59 ± 0.11	
250 nmol L^{-1} Fe; 100 μmol L^{-1} EDTA	208	1	1.48*	133	3	0.13 ± 0.37	0.65	0.9995 ± 0.0005	−0.51 ± 0.46	0.8
80 nmol L^{-1} Fe; 100 μmol L^{-1} EDTA	67	1	0.85*	133	3	0.13 ± 0.08	0.67	0.9995 ± 0.0001	−0.51 ± 0.1	0.39
30 nmol L^{-1} Fe; 100 μmol L^{-1} EDTA	25	2	0.72 ± 0.01	133	6	−0.07 ± 0.08	0.87 ± 0.01	0.9993 ± 0.0001	−0.65 ± 0.08	0.42
Growth Media Si (Aquil replicates)					6	0.54 ± 0.13				
Growth Media Si (NaOH replicates)					3	0.53 ± 0.02				
Mean Growth Media Si (Aquil + NaOH replicates)					9	0.54 ± 0.11				

Fractionation factors were calculated from diatom silica as a function of f, where f is the fraction of the original $Si(OH)_4$ remaining in the system once diatoms were harvested. n is the number of measurements from cultures. All values presented as means ±1 SD. P-values are relative to Fe-replete (Fe+) conditions. For T. pseudonana, the Fe-replete concentration is equal to an Fe' value of 418 pmol L^{-1}.

**Maximum growth rate from single replicate culture. Because there was no difference in ε between replicate cultures, the value for ε is the mean of all cultures ±1 SD.*

(Fe_{tot} = 4.4 nmol L^{-1}; DFB = 4 nmol L^{-1}), we assumed a 0.1 nmol L^{-1} excess of DFB in the media and a 0.5 nmol L^{-1} excess of total Fe that was available for interaction with EDTA (**Table 1**).

Specific Growth Rate, Cell Counts and $Si(OH)_4$ Consumption

Growth rates were determined from in vivo chlorophyll *a* fluorescence using a Turner Designs model 10-AU Fluorometer. Specific growth rates of exponentially growing cultures were determined from linear regressions of ln *in vivo* fluorescence vs. time. Cell density (cells mL^{-1}) was determined by microscopy (Sedgewick-Rafter or Haemocytometer – brightline, Neubauer improved). Each sample was enumerated a minimum of three times resulting in a S.E between counts <11% for *P. inermis* and *E. Antarctica*, and <5% for *T. pseudonana*. Consumption of $Si(OH)_4$ in culture was obtained by measuring samples of culture media shortly after inoculation and at the exponential stage of growth (respectively), when cultures were harvested.

δ^{30}Si Determination of Diatom Silica

Once cultures were in their exponential phase of growth, 50–100 ml of cell culture was collected onto a 2 μm, 25 mm polycarbonate filter, rinsed with nutrient free Aquil, and washed into 3 mL Teflon bombs. Purification of the samples were done according to similar methods for sponge spicules by Wille et al. (2010). The samples were evaporated to dryness at 50°C in a drying oven overnight. To remove organics, samples were treated with 1 mL of 30% hydrogen-peroxide (H_2O_2) solution, and allowed to reflux for 24 h at 70°C on a hotplate. Following oxidation, the lids were removed, and the samples were left to evaporate to dryness before adding 2 ml of 0.5 M sodium hydroxide (NaOH) to dissolve the sediment. Samples were then left to reflux overnight again for 24 h at 50°C. The $Si(OH)_4$concentration within the sample digest was then measured colorimetrically (Strickland and Parsons, 1965). Sodium was removed from the samples using cation exchange columns to prevent any subsequent interference during isotope determination. Cation exchange columns consisted on 1 mL Dowex 50W-X8 cation exchange resin (200–400 mesh) with a 2.5 mL reservoir. Columns were cleaned with 0.5 mL 8% (w/w) hydrofluoric acid (HF) followed by 2.25 mL of deionized water. The resin with protonated by passing 2.25 mL of 4 mol L^{-1} HCl followed by 2.25 mL of deionized water. The columns were then loaded with 0.5 mL of sample, before being rinsed with 4 × 0.5 mL of deionized water. To minimize contamination, samples were collected in vials that were cleaned using 8% (w/w) HF, before being rinsed with deionized water. Samples for δ^{30}Si determination of the growth media were prepared by dissolving the sodium silicate standard used for nutrient enrichment in the growth medium to a concentration of 2 mmol L^{-1} in separate solutions of nutrient free Aquil and 0.5 M sodium hydroxide. These samples were then treated with the same column procedure as the cell samples prior to analysis.

Determination of δ^{30}Si of Diatom Silica

The δ^{30}Si composition of diatom silica was determined according to methods developed by Wille et al. (2010) using a multi-collector inductively coupled plasma mass spectrometer (MC-ICP-MS) (Finnigan Neptune, Germany) operating in dry plasma mode at medium-resolution (M/ΔM ∼2,000). An ESI-Apex nebulizer fitted with a Teflon inlet system and a demountable torch fitted with an alumina injector was used for sample introduction to minimize any background interference. A standard-sample-standard bracketing technique was used for data acquisition and reduction (Wille et al., 2010). The δ^{30}Si signal (based on the relative abundance of ^{30}Si to ^{28}Si (^{30}Si/^{28}Si) was calculated using the following formula:

$$\delta^{30}Si = \left[\left(\frac{R_{Sample}}{R_{Std}}\right) - 1\right] \times 1000 \quad (3)$$

Where R_{sample} is the ratio of ^{30}Si/^{28} Si of the sample and R_{Std} is the ^{30}Si/^{28}Si of the in-house standard developed from dissolution a diatomaceous sediment and purified (**Figure 1**). Measurements of sample blanks were made prior to each run to ensure that the combined blank and background was <1% of the total sample signal. Inter-laboratory NBS-28 and diatomite standards were prepared with each daily run, and were measured with every three samples (≤ 8 diatomite/NBS -28 standards per daily run).

δ^{30}Si and δ^{29}Si values relative to NBS-28 plotted on an mass-dependent fractionation line with a slope of 0.520 ± 0.009 and is consistent with the consensus slope of 0.511 obtained from inter-laboratory silicon standard measurements (Reynolds et al., 2007). The reproducibility of the δ^{30}Si signal measured for the NBS-28 standard (prepared in full and measured on 5 separate occasions) was 0.25 ± 0.04 ‰. Measurements of the "diatomite standard" produced a mean δ^{30}Si value of 1.29 ± 0.25 ‰ (2 SD, n = 33), and is in good agreement with inter-laboratory comparisons (δ^{30}Si = 1.27 ‰) (Reynolds et al., 2007).

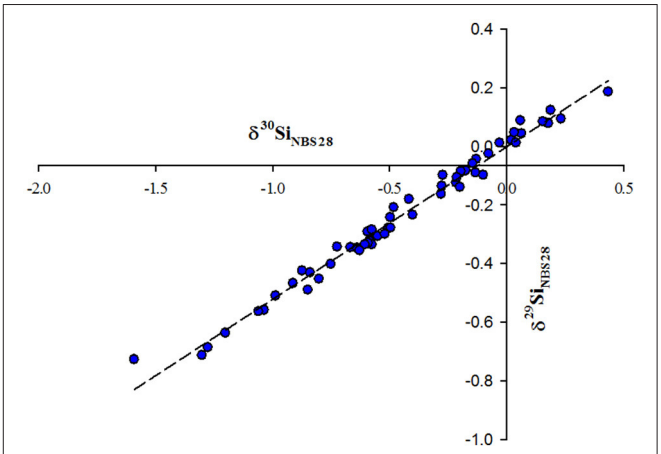

FIGURE 1 | Mass dependent fractionation of δ^{29}Si vs. δ^{30}Si for all diatom samples relative to NBS-28. Regression line represents δ^{29}Si = [0.520 ± 0.009].δ^{30}Si −0.002 ± 0.006, (r^2 = 0.99, n = 55 samples).

RESULTS

Growth rates between replicate cultures varied by <6 % (coefficient of variation, CV) and f was kept above a value of 0.6 in all cultures (**Table 1**). All values for ε are presented as means, ± 1 standard deviation (S.D.). *P. inermis*, *E. Antarctica* and *T. pseudonana* exhibited mean ε values of −1.11 ± 0.15 ‰, −1.42 ± 0.41 ‰ and −0.59 ± 0.11 ‰, respectively when grown under Fe-replete conditions (**Figure 2**). The mean ε values for *P. inermis* and *E. Antarctica* grown under Fe-replete conditions were not statistically different ($p > 0.05$) from the mean value of −1.1 ‰ obtained by De La Rocha et al. (1997); however, they were statistically different compared to the mean ε value for *T. pseudonana* ($p < 0.05$). Whilst a relatively low f compared to alternate studies (e.g., Sutton et al., 2013) may introduce an underestimation of the results (De La Rocha et al., 1997); the observation that *T. pseudonana* exhibited little variation in its isotope composition despite the range in f values suggests that this bias was insignificant (**Table 2**).

Effects of Fe-Availability on Si Isotope Fractionation

T. pseudonana displayed little variation in ε with decreasing Fe concentration (**Figure 2**). No clear trends were observed across the five Fe-conditions, with ε values ranging between 0.51 ± 0.46 ‰ and 0.75 ± 0.24 ‰. Comparisons of ε values between Fe-limited ($Fe' = 208$, 67, 42, and 25 pmol L^{-1}) and Fe-replete conditions ($Fe' = 418$ pmol L^{-1}) were not statistically significant (*ANOVA*, $p > 0.1$). Because of the statistical insignificance between these ε values, the mean was taken of all values (−0.61 ± 0.21 ‰) and compared against ε values obtained from two strains of *T. pseudonana* (CCMP1014 and CCCM58, −0.97 ± 0.14 and −0.88 ± 0.06 ‰, respectively) cultured under Fe-replete conditions by Sutton et al. (2013). We observed a difference ($p < 0.05$) between the ε in our strain (CS-20) and the two strains grown by Sutton et al. (2013) (**Table 2**).

Mean values for ε varied between the Fe-replete and Fe-limited conditions for the two Southern Ocean diatoms (**Table 2**). While there was some variability in the values of ε for *E. Antarctica*, there was a significant difference in ε ($p = 0.04$) between Fe-replete and Fe-limited conditions, with mean ε values being more negative for Fe-limited cultures (Fe-limited, ε = −1.57 ± 0.50 ‰; Fe-replete, ε = −1.40 ± 0.41 ‰) (**Table 1**). Mean ε values were also more negative for *P. inermis* cultured under Fe-limited conditions (Fe-limited, ε = −1.38 ± 0.27 ‰; Fe-replete, ε = −1.11 ± 0.15 ‰). Both Fe-replete and Fe-limited datasets for *P. inermis* exhibited a significant difference at the 90% confidence interval ($p = 0.08$), and removing outliers from both Fe-replete and Fe-limited data sets for *P. inermis* makes the difference more significant ($p = 0.04$).

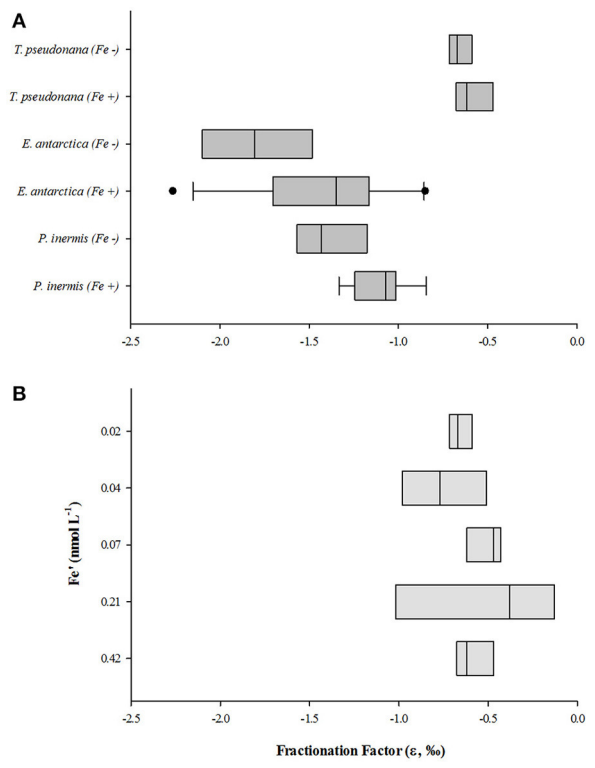

FIGURE 2 | Box and whisker plot displaying the effects of Fe-availability on *T. pseduonana*, *P. inermis* and *E. Antarctica*. **(A)** Represents comparisons between all species, **(B)** represents the variation in Si-isotope fractionation factor across multiple Fe-concentrations for *T. pseudonana*. Lines are median values, Boxes represent 1st and 3rd quartiles and dots represent outliers ($n \geq 3$).

DISCUSSION

This is the first study to specifically investigate the effects of Fe-limitation on Si-isotope fractionation in diatoms. Previous work has demonstrated that Fe-limitation can alter $Si(OH)_4$uptake kinetics, cell morphology and nutrient stoichiometry in diatoms (Hutchins and Bruland, 1998; Takeda, 1998; Brzezinski et al., 2002; Leynaert et al., 2004; Meyerink et al., 2017). Here, the processes by which Si isotopes are fractionated during diatom Si uptake and cell wall synthesis are explored and related back to mechanisms involving $Si(OH)_4$ uptake.

Fractionation of Si-Isotopes in Diatoms

Whilst little effect in the variability of the Si-isotope fractionation factor was observed in *T. pseudonana* in response to Fe-stress (**Figure 2B**), both Southern Ocean species exhibited a fractionation factor that was more negative under Fe-limitation (**Figure 2A**). Values for ε have been observed to vary under optimal growth conditions between diatom species (Sutton et al., 2013), so it is possible that there may be an inter-species effect when it comes to environmental controls on Si-isotope fractionation in diatoms. Sutton et al. (2013) demonstrated that Si-isotope fractionation can vary by as much as 1.5 ‰ between diatom species, enough to potentially confound palaeoceanographic interpretations utilizing δ^{30}Si from diatom opal to estimate the nutrient status of the surface ocean. In addition to interspecies effects, variations in the value for ε between individual diatom strains have been observed (Sutton et al., 2013). Silicon isotope fractionation independently measured in *T. weissflogii* across three seperate studies yielded

TABLE 2 | Comparison of Fe-replete, Si-isotope fractionation factors (ε, ‰) between this study and previous studies. *n* is the number of replicate cultures.

Species name	Strain/Isolation source	PFD ($\mu E\ m^{-2}\ s^{-1}$)	*n*	Temperature (°C)	μmax (day^{-1})	*f*	Fractionation factor (ε, ‰*)
This study							
P. inermis	ANARE V3 CLIVAR	60	3	3	0.35 ± 0.02	0.97 ± 0.06	−1.11 ± 0.15
E. Antarctica	ANARE V3 CLIVAR	50	4	3	0.32 ± 0.02	0.7 ± 0.02	−1.42 ± 0.41
*T. pseudonana**	**CS-20**	**133**	**6**	**20**	**1.52***	**0.77 ± 0.14**	**−0.61 ± 0.21**
Sutton et al., 2013							
T. pseudonana	**CCMP1014**	**200**	**4**	**18**	**1.30 ± 0.13**	**0.92 ± 0.005**	**−0.97 ± 0.14**
T. pseudonana	**CCCM58**	**200**	**4**	**18**	**1.34 ± 0.11**	**0.92 ± 0.007**	**−0.88 ± 0.06**
T. weissflogii	CCMP1010	200	3	18	0.66 ± 0.06	0.91 ± 0.15	−0.72 ± 0.04
P. glacialis	CCMP650	50	3	3	0.21 ± 0.01	0.91 ± 0.005	−1.15 ± 0.03
F. kerguelensis	LOHAFEX	90	4	3	0.22 ± 0.02	0.92 ± 0.007	−0.53 ± 0.11
F. kerguelensis	EIFEX	90	3	3	0.20 ± 0.02	0.9 ± 0.01	−0.56 ± 0.07
T. antarctica	CCMP982	30	3	3	0.19 ± 0.01	0.92 ± 0.001	−0.74 ± 0.05
C. brevis	CCMP164	90	4	3	0.36 ± 0.04	0.9 ± 0.01	−2.09 ± 0.09
T. nordenskioeldii	CCMP997	170	4	3	0.58 ± 0.01	0.92 ± 0.01	−1.21 ± 0.04
Milligan et al., 2004							
T. weissflogii	Coastal Strain	160	6	20	1.4 ± 0.05	0.88 ± 0.01	−1.58 ± 0.1
De La Rocha et al., 1997							
S. costatum	CCMP1332	99	4	15	No data reported	0.96 ± 0.03	−0.95 ± 0.4
T. weissflogii	Unknown source	99	4	15	No data reported	0.8 ± 0.08	−1.28 ± 0.46
Thalassiosira sp.	Isolate	99	5	15	No data reported	0.85 ± 0.03	−1.04 ± 0.42

*All values presented as means ±1 SD. μmax is the maximum growth rate per day. Inter-comparisons in ε between Thalassiosira pseudonana strains in this study and previous studies by Sutton et al. (2013) are highlighted in bold. *Maximum growth rate from single replicate culture. Because there was no difference in ε between replicate cultures, the value for ε is the mean of all cultures ±1 SD.*

ε values ranging between −0.72 ± 0.04 ‰ and −1.5 ± 0.1 ‰ (De La Rocha et al., 1997; Milligan et al., 2004; Sutton et al., 2013). Similar variations have also been observed for three *T. pseudonana* clones; −0.61 ± 0.21 ‰ measured in this study and −0.94 ± 0.14 ‰ and −0.88 ± 0.06 ‰ measured for two clones cultured by Sutton et al. (2013). Sutton et al. (2013) suggest that the differences in ε values for *T. weissflogii* can be attributable to the diatom being a coastal isolate rather than an open ocean isolate. There were remarkable similarities, however, in ε values between the two *T. pseudonana* strains (CCMP1014 and CCCM58) cultured by Sutton et al. (2013), even though CCMP1014 is an open ocean isolate from the (North Pacific Gyre; https://ncma.bigelow.org/) and CCCM58 is a coastal isolate (Moriches Bay, Long island, NY; http://www3.botany.ubc.ca/cccm/index.html). While it is possible that inherent differences between strains as a result of the growth conditions in their endemic environment, variations culturing conditions need to be ruled out first before this hypothesis can be invoked.

Potential Mechanisms Controlling Si Isotope Fractionation in Diatoms

Silicon-processing in diatoms is affected by Fe bioavailability (Meyerink et al., 2017) and hence can manifest to variations in the $\delta^{30}Si$ composition of diatom silica. Understanding how diatoms fractionate Si isotopes during uptake and bio-mineralization requires a thorough investigation into how diatoms take up $Si(OH)_4$ from the surrounding water column and use it in the formation of their cell frustules (Sutton et al., 2013; Meyerink et al., 2017). There are numerous intracellular pathways during the synthesis of biogenic silica in diatoms where fractionation of Si isotopes can potentially occur.

In diatoms, $Si(OH)_4$ uptake from the surrounding water column is typically characterized either by diffusion or Michaelis-Menten saturation kinetics (Hildebrand, 2008; Javaheri et al., 2014). At low ambient $Si(OH)_4$ concentrations, uptake is mainly a saturatable process ($\leq$10 μmol L^{-1}), and is facilitated by Si transporters (SITs) that are localized in cell membranes (Shrestha and Hildebrand, 2015). SITs are membrane bound proteins that actively take up $Si(OH)_4$and transport it across the outer cell membrane to the cell cytoplasm against a concentration gradient (Hildebrand, 2008). At higher ambient $Si(OH)_4$ concentrations ($\geq$30 μmol L^{-1}), diffusional uptake dominates Si acquisition with SITs playing more of a regulatory role (Thamatrakoln and Hildebrand, 2008; Shrestha and Hildebrand, 2015). Passive diffusion of $Si(OH)_4$ appears to be proportional to the permeability of the cell membrane and the concentration gradient across the cell membrane (Hildebrand, 2008; Javaheri et al., 2014). Once past the cell membrane, $Si(OH)_4$ is then transported intracellularly to the Si deposition vesicle (SDV) by as yet unknown transporters/compounds classified simply as "Si binding components" (Thamatrakoln and Hildebrand, 2008). Si binding components play an important role in setting the $Si(OH)_4$ concentration gradient across the cell membrane under scenarios where diffusional uptake dominates (Thamatrakoln and Hildebrand, 2008). Active transport involving SITs likely plays an important role in facilitating the transport of Si from

the cell cytoplasm into the SDV, as concentration gradients across the intracellular membrane separating the SDV from the cell cytoplasm are extremely high (Hildebrand, 2008). A new cell wall is created when the SDV is exocytosed at the M (mitosis) stage of the cell cycle. Cell wall formation during this stage is facilitated by silafins and long chain polyamines, which act as a "template" on to which the new cell wall is precipitated (Mock et al., 2008).

Fractionation of Si isotopes can potentially occur along any of these pathways. Milligan et al. (2004) explored where isotopic discrimination takes place within the cell by conducting a number of experiments where they varied the efflux:influx ratio of $Si(OH)_4$ into and out of the cell. They suggested that fractionation of Si isotopes occurs during the membrane transport step and not during Si polymerization, as Si isotope fractionation should scale linearly with the efflux:influx ratio. In addition, the relatively small Si isotope effect may also be evidence of discrimination at the transport level, as this does not necessitate the breaking or forming of chemical bonds (Milligan et al., 2004). If this is the case, fractionation of Si isotopes occurs either at the membrane/seawater interface, as $Si(OH)_4$ is taken up from the water column and transported to the cell cytoplasm, or, as Si is transported from the cell cytoplasm into the Silicon deposition vesicle.

Effects of Fe-Limitation on Si-Isotope Fractionation in Diatoms

Sutton et al. (2013) observed an inter-specific variation in mean ε values in Southern Ocean diatom species based on mono-culture *in-vitro* incubations. They argue that variability in diatom community composition could partly explain the observed variability in Southern Ocean Si-isotope fractionation factors. It is possible that variations in the Fe-status of certain regions in the Southern Ocean may contribute to variations in the apparent Si isotope fractionation factor. For example, Si isotope fractionation factors of diatom communities can potentially vary as a result of certain diatoms adapted to low Fe-conditions out competing other diatoms under Fe-limiting conditions. This may alter the $\delta^{30}Si_{DSi}$ composition of surface waters. While this scenario is hypothetical, it may contribute to some of the variability in the observed relationship between the mixed layer mean apparent fractionation factor ($\Delta^{30}Si = \delta^{30}Si_{DSi} - \delta^{30}Si_{BSi}$) and $Si(OH)_4$ concentration in the Southern Ocean and the seasonal variations in Si uptake:dissolution (Varela et al., 2004; Cardinal et al., 2007; Fripiat et al., 2012).

Silicon metabolism in diatoms is particularly sensitive to variations in Fe-supply and as such, variations in ε can potentially be dependent on Fe-induced physiological variations within the cell. A notable result from our study was the relative response in the Si isotope fractionation factor (ε) of *T. pseudonana* under Fe-limitation compared to *P. inermis* and *E. Antarctica*. *T. pseudonana* exhibited no variation in ε in response to Fe-limitation, and maintained a mean ε value of -0.61 ± 0.21 ‰ across all Fe′ concentrations. In contrast, we observed a negative response in Si isotope fractionation as a result of increased Fe-limitation in both Southern Ocean species (**Figure 2**). The reason behind this difference could lie in how Si is metabolized by Southern Ocean diatoms under Fe-stress.

Kinetic uptake experiments show diatoms decrease their $Si(OH)_4$ uptake rate under Fe-limitation (Franck et al., 2000; Leynaert et al., 2004; Meyerink et al., 2017). This is generally manifested by a reduction in the maximal $Si(OH)_4$ uptake rate (V_{Si-max}) and half saturation constant (K_{Si}). In addition, diatoms grown under Fe-limiting conditions generally exhibit reductions in their growth rate, and variations in their cell morphology. A recent study by Meyerink et al. (2017) investigated the effects of Fe availability on the $Si(OH)_4$ uptake kinetics of two Southern Ocean diatoms (*E. Antarctica* and *P. inermis*) and a coastal isolate (*T. pseudonana*). An interesting result from the study shows that when V_{Si-max} is normalized to cell surface area, it exhibits a linear relationship with cell growth rate. This relationship is independent of any variations in cell morphology or species. It is likely that this relationship can be explained by the fact that silicon uptake in the diatoms was under diffusion control, as they were acclimatized under high Si conditions. Under diffusion controlled uptake, the V_{Si-max} values reflect the realized $Si(OH)_4$ uptake rates in culture which at steady state cannot exceed cellular demands for $Si(OH)_4$ (Thamatrakoln and Hildebrand, 2008). In contrast, variations in K_{Si} in response to Fe availability exhibited no relationship with other cell parameters, however it was noticeably higher in value in the Southern Ocean species than the K_{Si} value for *T. pseudonana.* This is likely because the Southern Ocean diatoms are well adapted to growing under high Si conditions.

Diatoms with a high K_{Si} for $Si(OH)_4$ such as *E. Antarctica* and *P. inermis* ($\geq$10 μmol L^{-1}) (Meyerink et al., 2017) could possibly fractionate Si-isotopes differently to diatoms with a relatively low K_{Si} such as *T. pseudonana* because of their likely dependence on diffusional uptake of $Si(OH)_4$ at concentrations greater than 30 μmol L^{-1} (Thamatrakoln and Hildebrand, 2008). Under Fe-limitation, diatoms decrease their cellular growth rate, which results in a subsequent decrease in their maximal $Si(OH)_4$ uptake rate (V_{Si-max}) (Franck et al., 2000; Leynaert et al., 2004; Meyerink et al., 2017). This may result in a decrease in a diatoms specific affinity for $Si(OH)_4$ that can be maintained by a decrease in the K_{Si} (Franck et al., 2000; Leynaert et al., 2004; Meyerink et al., 2017). Previous studies suggest that diatoms maintain their affinity by altering their cell size (Leynaert et al., 2004); however, *E. Antarctica* exhibits a 2-fold decrease in K_{Si} when Fe-limited, which is concomitant with an increase in cell-size (Meyerink et al., 2017). It is therefore more likely that diatoms maintain their affinity for $Si(OH)_4$ by adjusting the point where diffusive transport takes over from active transport. Active transport persists at $Si(OH)_4$ concentrations greater than 30 μmol L^{-1} under Fe-limitation, and as a result, could possibly induce a decrease in the diatoms Si-isotope fractionation factor (Shrestha and Hildebrand, 2015). If this is correct, why do *E. Antarctica* and *P. inermis* exhibit a more negative response in ε when compared to *T. pseudonana*? It is possible that different genera of diatoms switch from active to diffusive transport at different $Si(OH)_4$ concentrations. While *T. pseudonana* does this at ~30 μmol L^{-1} under Fe-replete conditions (Shrestha and Hildebrand, 2015), this value could be higher for Southern Ocean diatoms. When

diatoms approached Fe-limiting conditions, such as in this study, *T. pseudonana* possibly remained under the threshold where active transport takes place, while *E. Antarctica* and *P. inermis* did not. If this is the case, then Si-isotope signatures may potentially be subject to the synergistic effects of species diversity and resource limitation.

CONCLUSIONS

This is the first culture study to investigate the effects of Fe-limitation on Si-isotope fractionation in diatoms. Whilst any effects arising from Fe-limitation on the value of ε were not evident in *T. pseudonana*, we observed that both Southern Ocean diatoms under Fe-limitation exhibit mean ε values that are 0.19–0.27‰ (within error) more negative compared to Fe-replete values. While this variation is likely not enough to have any significant effect on interpretations involving $\delta^{30}Si$ in diatomaceous opal or sea surface $Si(OH)_4$/BSi, the finding that the value for ε in the Southern Ocean species was prone to changes in the physico-chemical environment compared to that of the coastal species highlights the need to improve our understanding of how diatoms fractionate Si-isotopes during Si-uptake and frustule formation, and thus, warrants further investigation into the biochemical pathways in diatoms where Si-isotope fractionation can potentially occur.

AUTHOR CONTRIBUTIONS

SM and ME conceived of the research. SM undertook the experiments and SM and ME interpreted the results with contributions from WM and RS. SM wrote the manuscript with contributions from ME, WM, and RS.

ACKNOWLEDGMENTS

The Australian Research Council (DP130100679) and the Australian Antarctic Division (AAD Project 3120) are acknowledged for financial support of this work. The Authors would also like to thank two reviewers for their helpful comments.

REFERENCES

Beucher, C. P., Brzezinski, M. A., and Crosta, X. (2007). Silicic acid dynamics in the glacial sub-Antarctic: implications for the silicic acid leakage hypothesis. *Global Biogeochem. Cycles* 21:GB3015. doi: 10.1029/2006GB002746

Beucher, C. P., Brzezinski, M. A., and Jones, J. L. (2011). Mechanisms controlling silicon isotope distribution in the Eastern Equatorial Pacific. *Geochim. Cosmochim. Acta* 75, 4286–4294. doi: 10.1016/j.gca.2011.05.024

Boutorh, J., Moriceau, B., Gallinari, M., Ragueneau, O., and Bucciarelli, E. (2016). Effect of trace metal-limited growth on the postmortem dissolution of the marine diatom Pseudo-nitzschia delicatissima. *Global Biogeochem. Cycles* 30, 57–69. doi: 10.1002/2015GB005088

Brzezinski, M. A., Pride, C. J., Franck, V. M., Sigman, D. M., Sarmiento, J. L., Matsumoto, K., et al. (2002). A switch from $Si(OH)_4$ to NO_3^- depletion in the glacial Southern Ocean. *Geophys. Res. Lett.* 29, 5-1–5-4. doi: 10.1029/2001gl014349

Cardinal, D., Savoye, N., Trull, T. W., Dehairs, F., Kopczynska, E. E., Fripiat, F., et al. (2007). Silicon isotopes in spring Southern Ocean diatoms: large zonal changes despite homogeneity among size fractions. *Mar. Chem.* 106, 46–62. doi: 10.1016/j.marchem.2006.04.006

Clayton, T. D., and Byrne, R. H. (1993). Spectrophotometric seawater pH measurements: total hydrogen ion concentration scale calibration of m-cresol purple and at-sea results. *Deep Sea Res. Pt I* 40, 2115–2129. doi: 10.1016/0967-0637(93)90048-8

Criss, R. E., and Criss, R. (1999). *Principles of Stable Isotope Distribution*. New York, NY: Oxford University Press.

De La Rocha, C., Brzezinski, M., DeNiro, M., and Shemeshk, A. (1998). Silicon-isotope composition of diatoms as an indicator of past oceanic change. *Phys. Rev. Lett.* 77, 2041–2044.

De La Rocha, C. L., Brzezinski, M. A., and DeNiro, M. J. (1997). Fractionation of silicon isotopes by marine diatoms during biogenic silica formation. *Geochim. Cosmochim. Acta* 61, 5051–5056. doi: 10.1016/S0016-7037(97)00300-1

Ellwood, M. J., Boyd, P. W., and Sutton, P. (2008). Winter-time dissolved iron and nutrient distributions in the Subantarctic zone from 40-52S; 155-160E. *Geophys. Res. Lett.* 35:L11604. doi: 10.1029/2008gl033699

Ellwood, M. J., Wille, M., and Maher, W. (2010). Glacial silicic acid concentrations in the Southern Ocean. *Science* 330, 1088–1091. doi: 10.1126/science.1194614

Franck, V. M., Brzezinski, M. A., Coale, K. H., and Nelson, D. M. (2000). Iron and silicic acid concentrations regulate Si uptake north and south of the polar frontal zone in the pacific sector of the southern ocean. *Deep Sea Res. Pt II* 47, 3315–3338. doi: 10.1016/S0967-0645(00)00070-9

Fripiat, F., Cavagna, A.-J., Dehairs, F., Brauwere, A. D., André, L., and Cardinal, D. (2012). Processes controlling the Si-isotopic composition in the Southern Ocean and application for paleoceanography. *Biogeosciences* 9, 2443–2457. doi: 10.5194/bg-9-2443-2012

Fripiat, F., Cavagna, A.-J., Dehairs, F., Speich, S., Andre, L., and Cardinal, D. (2011). Silicon pool dynamics and biogenic silica export in the Southern Ocean inferred from Si-isotopes. *Ocean Sci.* 7, 533–547. doi: 10.5194/os-7-533-2011

Hildebrand, M. (2008). Diatoms, biomineralization processes, and genomics. *Chem. Rev.* 108, 4855–4874. doi: 10.1021/cr078253z

Hoffmann, L., Peeken, I., and Lochte, K. (2008). Iron, silicate, and light co-limitation of three Southern Ocean diatom species. *Polar Biol.* 31, 1067–1080. doi: 10.1007/s00300-008-0448-6

Hutchins, D. A., and Bruland, K. W. (1998). Iron-limited diatom growth and Si:N uptake ratios in a coastal upwelling regime. *Nature* 393, 561–564. doi: 10.1038/31203

Javaheri, N., Dries, R., and Kaandorp, J. (2014). Understanding the sub-cellular dynamics of silicon transportation and synthesis in diatoms using population-level data and computational optimization. *PLoS Comput. Biol.* 10:e1003687. doi: 10.1371/journal.pcbi.1003687

Kemp, A. E. S., Pike, J., Pearce, R. B., and Lange, C. B. (2000). The "Fall dump" – a new perspective on the role of a "shade flora" in the annual cycle of diatom production and export flux. *Deep Sea Res. Pt II* 47, 2129–2154. doi: 10.1016/S0967-0645(00)00019-9

Leynaert, A., Bucciarelli, E., Claquin, P., Dugdale, R. C., Martin-Jezequel, V., Pondaven, P., et al. (2004). Effect of iron deficiency on diatom cell size and silicic acid uptake kinetics. *Limnol. Oceanogr.* 49, 1134–1143. doi: 10.4319/lo.2004.49.4.1134

Maldonado, M. T., Strzepek, R. F., Sander, S., and Boyd, P. W. (2005). Acquisition of iron bound to strong organic complexes, with different Fe binding groups and photochemical reactivities, by plankton communities in Fe-limited subantarctic waters. *Global Biogeochem. Cycles* 19:GB4S23. doi: 10.1029/2005GB002481

Marchetti, A., and Cassar, N. (2009). Diatom elemental and morphological changes in response to iron limitation: a brief review with potential paleoceanographic applications. *Geobiology* 7, 419–431. doi: 10.1111/j.1472-4669.2009.00207.x

Martinez-Garcia, A., Rosell-Mele, A., Jaccard, S. L., Geibert, W., Sigman, D. M., and Haug, G. H. (2011). Southern Ocean dust-climate coupling over the past four million years. *Nature* 476, 312–315. doi: 10.1038/nature10310

Matsumoto, K., Chase, Z., and Kohfeld, K. (2014). Different mechanisms of silicic acid leakage and their biogeochemical consequences. *Paleoceanography* 29, 238–254. doi: 10.1002/2013PA002588

Matsumoto, K., Sarmiento, J. L., and Brzezinski, M. A. (2002). Silicic acid leakage from the southern ocean: a possible explanation for glacial atmospheric pCO2. *Global Biogeochem. Cycles* 16, 5–1. doi: 10.1029/2001GB001442

McManus, J., Hammond, D. E., Berelson, W. M., Kilgore, T. E., Demaster, D. J., Ragueneau, O. G., et al. (1995). Early diagenesis of biogenic opal: dissolution rates, kinetics, and paleoceanographic implications. *Deep Sea Res. Pt II* 42, 871–903. doi: 10.1016/0967-0645(95)00035-O

Meyerink, S. W., Ellwood, M. J., Maher, W. A., Price, G. D., and Strzepek, R. F. (2017). Effects of iron limitation on silicon uptake kinetics and elemental stoichiometry in two Southern Ocean diatoms, *Eucampia antarctica* and *Proboscia inermis*, and the temperate diatom *Thalassiosira pseudonana*. *Limnol. Oceanogr*. doi: 10.1002/lno.10578. [Epub ahead of print].

Milligan, A. J., Varela, D. E., Brzezinski, M. A., and Morel, F. M. M. (2004). Dynamics of silicon metabolism and silicon isotopic discrimination in a marine diatom as a function of pCO2. *Limnol. Oceanogr.* 49, 322–329. doi: 10.4319/lo.2004.49.2.0322

Mock, T., Samanta, M. P., Iverson, V., Berthiaume, C., Robison, M., Holtermann, K., et al. (2008). Whole-genome expression profiling of the marine diatom *Thalassiosira pseudonana* identifies genes involved in silicon bioprocesses. *Proc. Nat. Acad. Sci. U.S.A.* 105, 1579–1584. doi: 10.1073/pnas.0707946105

Nelson, D. M., Treguer, P., Brzezinski, M. A., Leynaert, A., and QuÈguiner, B. (1995). Production and dissolution of biogenic silica in the ocean: revised global estimates, comparison with regional data and relationship to biogenic sedimentation. *Global Biogeochem. Cycles* 9, 359–372. doi: 10.1029/95GB01070

Pichevin, L. E., Reynolds, B. C., Ganeshram, R. S., Cacho, I., Pena, L., Keefe, K., et al. (2009). Enhanced carbon pump inferred from relaxation of nutrient limitation in the glacial ocean. *Nature* 459, 1114–1117. doi: 10.1038/nature08101

Price, N. M., Harrison, G. I., Hering, J. G., Hudson, R. J., Nirel, P. M., Palenik, B., et al. (1988). Preparation and chemistry of the artificial algal culture medium Aquil. *Biol. Oceanogr.* 6, 443–461.

Ragueneau, O., Treguer, P., Leynaert, A., Anderson, R. F., Brzezinski, M. A., DeMaster, D. J., et al. (2000). A review of the Si cycle in the modern ocean: recent progress and missing gaps in the application of biogenic opal as a paleoproductivity proxy. *Glob. Planet. Change* 26, 317–365. doi: 10.1016/S0921-8181(00)00052-7

Reynolds, B. C., Aggarwal, J., André, L., Baxter, D., Beucher, C., Brzezinski, M. A., et al. (2007). An inter-laboratory comparison of Si isotope reference materials. *J. Anal. Atom. Spectrom.* 22, 561–568. doi: 10.1039/B616755A

Roca-Martí, M., Puigcorbé, V., Iversen, M. H., van der Loeff, M. R., Klaas, C., Cheah, W., et al. (2017). High Particulate organic carbon export during the decline of a vast diatom bloom in the Atlantic sector of the Southern Ocean. *Deep-Sea Res. Pt. II* 138, 102–115. doi: 10.1016/j.dsr2.2015.12.007

Rousseau, J., Ellwood, M. J., Bostock, H., and Neil, H. (2016). Estimates of late Quaternary mode and intermediate water silicic acid concentration in the Pacific Southern Ocean. *Earth Planet. Sci. Lett.* 439, 101–108. doi: 10.1016/j.epsl.2016.01.023

Sackett, O., Petrou, K., Reedy, B., De Grazia, A., Hill, R., Doblin, M., et al. (2013). Phenotypic plasticity of southern ocean diatoms: key to success in the sea ice habitat? *PLoS ONE* 8:e81185. doi: 10.1371/journal.pone.0081185

Shrestha, R. P., and Hildebrand, M. (2015). Evidence for a regulatory role of diatom silicon transporters in cellular silicon responses. *Eukaryot. Cell* 14, 29–40. doi: 10.1128/EC.00209-14

Smetacek, V. (1999). Diatoms and the ocean carbon cycle. *Protist* 150, 25–32. doi: 10.1016/S1434-4610(99)70006-4

Strickland, J. D. H., and Parsons, T. R. (1965). *A Manual of Sea Water Analysis*. Ottawa, ON: Fisheries Research Board of Canada.

Strzepek, R. F., Hunter, K. A., Frew, R. D., Harrison, P. J., and Boyd, P. W. (2012). Iron-light interactions differ in Southern Ocean phytoplankton. *Limnol. Oceanogr.* 57, 1182–1200. doi: 10.4319/lo.2012.57.4.1182

Strzepek, R. F., Maldonado, M. T., Hunter, K. A., Frew, R. D., and Boyd, P. W. (2011). Adaptive strategies by Southern Ocean phytoplankton to lessen iron limitation: Uptake of organically complexed iron and reduced cellular iron requirements. *Limnol. Oceanogr.* 56, 1983–2002. doi: 10.4319/lo.2011.56.6.1983

Sunda, W., and Huntsman, S. (2003). Effect of pH, light, and temperature on Fe-EDTA chelation and Fe hydrolysis in seawater. *Mar. Chem.* 84, 35–47. doi: 10.1016/S0304-4203(03)00101-4

Sunda, W. G., and Huntsman, S. A. (1997). Interrelated influence of iron, light and cell size on marine phytoplankton growth. *Nature* 390, 389–392. doi: 10.1038/37093

Sutton, J. N., Varela, D. E., Brzezinski, M. A., and Beucher, C. P. (2013). Species-dependent silicon isotope fractionation by marine diatoms. *Geochim. Cosmochim. Acta* 104, 300–309. doi: 10.1016/j.gca.2012.10.057

Takeda, S. (1998). Influence of iron availability on nutrient consumption ratio of diatoms in oceanic waters. *Nature* 393, 774–777. doi: 10.1038/31674

Thamatrakoln, K., and Hildebrand, M. (2008). Silicon uptake in diatoms revisited: a model for saturable and nonsaturable uptake kinetics and the role of silicon transporters. *Plant Physiol.* 146, 1397–1407. doi: 10.1104/pp.107.107094

Trèguer, P., Nelson, D. M., Van Bennekom, A. J., DeMaster, D. J., Leynaert, A., and Queguiner, B. (1995). The silica balance in the world ocean: a reestimate. *Science* 268:375. doi: 10.1126/science.268.5209.375

Tréguer, P. J., and De La Rocha, C. L. (2013). The world ocean silica cycle. *Ann. Rev. Mar. Sci.* 5, 477–501. doi: 10.1146/annurev-marine-121211-172346

Varela, D. E., Pride, C. J., and Brzezinski, M. A. (2004). Biological fractionation of silicon isotopes in Southern Ocean surface waters. *Global Biogeochem. Cycles* 18. doi: 10.1029/2003GB002140

Wille, M., Sutton, J., Ellwood, M. J., Sambridge, M., Maher, W., Eggins, S., et al. (2010). Silicon isotopic fractionation in marine sponges: A new model for understanding silicon isotopic variations in sponges. *Earth Planet. Sci. Lett.* 292, 281–289. doi: 10.1016/j.epsl.2010.01.036

Yao, W., Liu, X., and Byrne, R. H. (2007). Impurities in indicators used for spectrophotometric seawater pH measurements: assessment and remedies. *Mar. Chem.* 107, 167–172. doi: 10.1016/j.marchem.2007.06.012

Conflict of Interest Statement: The authors declare that the research was conducted in the absence of any commercial or financial relationships that could be construed as a potential conflict of interest.

Copyright © 2017 Meyerink, Ellwood, Maher and Strzepek. This is an open-access article distributed under the terms of the Creative Commons Attribution License (CC BY). The use, distribution or reproduction in other forums is permitted, provided the original author(s) or licensor are credited and that the original publication in this journal is cited, in accordance with accepted academic practice. No use, distribution or reproduction is permitted which does not comply with these terms.

Advantages of publishing in Frontiers

OPEN ACCESS
Articles are free to read for greatest visibility and readership

FAST PUBLICATION
Around 90 days from submission to decision

HIGH QUALITY PEER-REVIEW
Rigorous, collaborative, and constructive peer-review

TRANSPARENT PEER-REVIEW
Editors and reviewers acknowledged by name on published articles

Frontiers
Avenue du Tribunal-Fédéral 34
1005 Lausanne | Switzerland

Visit us: www.frontiersin.org
Contact us: info@frontiersin.org | +41 21 510 17 00

REPRODUCIBILITY OF RESEARCH
Support open data and methods to enhance research reproducibility

DIGITAL PUBLISHING
Articles designed for optimal readership across devices

FOLLOW US
@frontiersin

IMPACT METRICS
Advanced article metrics track visibility across digital media

EXTENSIVE PROMOTION
Marketing and promotion of impactful research

LOOP RESEARCH NETWORK
Our network increases your article's readership